DERMAL ABSORPTION MODELS IN TOXICOLOGY AND PHARMACOLOGY

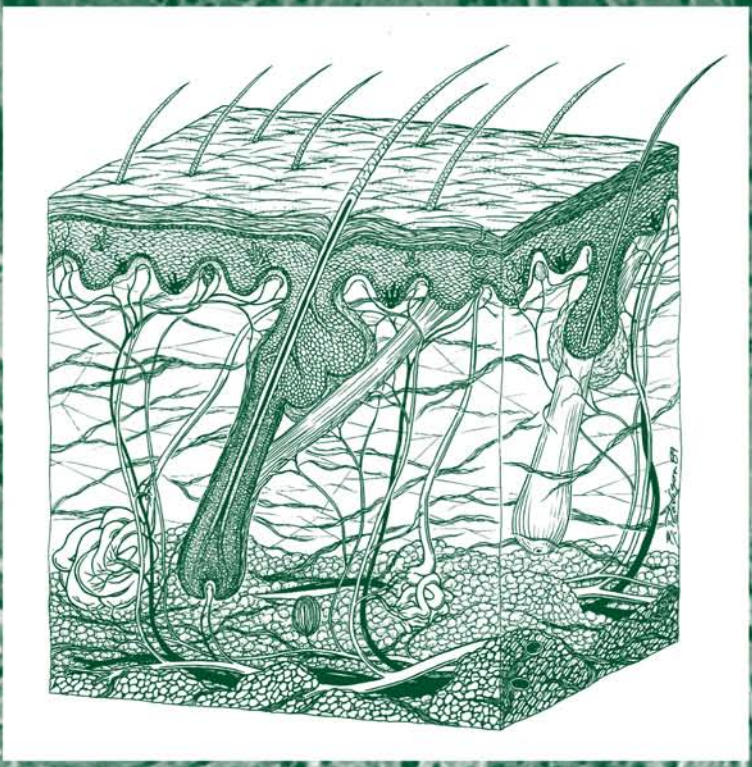

edited by

Jim E. Riviere

CRC Taylor & Francis
Taylor & Francis Group

DERMAL ABSORPTION MODELS IN TOXICOLOGY AND PHARMACOLOGY

DERMAL ABSORPTION MODELS IN TOXICOLOGY AND PHARMACOLOGY

Edited by

Jim E. Riviere

North Carolina State University
Raleigh, North Carolina

Taylor & Francis
Taylor & Francis Group
Boca Raton London New York

A CRC title, part of the Taylor & Francis imprint, a member of the
Taylor & Francis Group, the academic division of T&F Informa plc.

Published in 2006 by
CRC Press
Taylor & Francis Group
6000 Broken Sound Parkway NW, Suite 300
Boca Raton, FL 33487-2742

Printed in the United States of America on acid-free paper
10 9 8 7 6 5 4 3 2 1

International Standard Book Number-10: 0-415-70036-1 (Hardcover)
International Standard Book Number-13: 978-0-415-70036-8 (Hardcover)
Library of Congress Card Number 2005041842

Library of Congress Cataloging-in-Publication Data

Dermal absorption models in toxicology and pharmacology / edited by Jim E. Riviere.
p. ; cm.
Includes bibliographical references and index.
ISBN 0-415-70036-1 (alk. paper)
1. Dermatotoxicology--Mathematical models. 2. Dermatologic agents--Toxicology. 3. Health risk assessment. 4. Skin absorption. I. Riviere, J. Edmond (Jim Edmond)
[DNLM: 1. Skin Absorption. 2. Models, Theoretical. 3. Risk Assessment. 4. Toxicology--methods. WR 102 D4345 2005]

RL803.D445 2005
616.5--dc22 2005041842

T&F informa
Taylor & Francis Group
is the Academic Division of T&F Informa plc.

Visit the Taylor & Francis Web site at
http://www.taylorandfrancis.com

and the CRC Press Web site at
http://www.crcpress.com

Preface

Paradoxically, skin is both a primary barrier to systemic absorption of topically exposed chemicals and a portal to systemic delivery of transdermal medicaments. Knowledge of the factors that determine both extent and rate of chemical flux across the skin is an important component of both toxicology and pharmacology studies. The aim of this book is to provide current approaches and techniques by which dermal absorption may be quantitated utilizing end points relative to these two disciplines. There are a number of different experimental methods and mathematical modeling approaches in use today. Most are rooted in disciplines outside toxicology, yet their methods are applied to dermal absorption. This book serves as a bridge between general considerations in risk assessment and systemic toxicology texts.

The first four chapters introduce and overview both the structure and function of skin as well as the *in vitro* and *in vivo* experimental approaches available for assessing dermal absorption of drugs and chemicals. This is followed by mathematical or so-called *in silico* models to quantitating percutaneous absorption, including physiological-based pharmacokinetic modeling and quantitative structure–activity relationship methods. The next chapters deal with applications of these techniques to the risk assessment process. The remainder of the book discusses scenarios in which unique properties of the chemicals studied or the matrix in which they are exposed must be considered, including volatile compounds or dosing in soils. In many dermal absorption studies, unique properties of compounds or additives may alter a compound's absorption. These include vasoactive chemicals, the use of penetration enhancers, or exposure in complex chemical mixtures. The book wraps up with a comparative analysis of chemical permeability in human and animal skin.

This book reviews basic principles, presents in-depth discussions of the most widely used techniques, and offers select case studies of how these techniques have been applied under different scenarios. It serves as a concise introduction and review of the application of dermal absorption to problems in toxicology and pharmacology for both researchers in this field and graduate courses overviewing this area.

Jim E. Riviere

Editor

Jim E. Riviere, D.V.M., Ph.D., is the Burroughs Wellcome Fund Distinguished Professor of Pharmacology, and the director of the Center for Chemical Toxicology Research and Pharmacokinetics at North Carolina State University (NCSU) in Raleigh, North Carolina. He received his B.S. (summa cum laude) and M.S. degrees from Boston College and his D.V.M. and Ph.D. in pharmacology from Purdue University and is a fellow of the Academy of Toxicological Sciences. He is a member of Phi Beta Kappa, Phi Zeta, and Sigma Xi. Dr. Riviere is an elected member of the Institute of Medicine of the National Academies and serves on the Science Board of the U.S. Food and Drug Administration. His honors include the 1999 O. Max Gardner Award from the Board of Governors of the Consolidated University of North Carolina, the 1991 Ebert Prize from the American Pharmaceutical Association, and the Harvey W. Wiley Medal and FDA Commissioner's Special Citation. He is the editor of the *Journal of Veterinary Pharmacology and Therapeutics* and cofounder and codirector of the USDA Food Animal Residue Avoidance Databank (FARAD) program. He is past president of the Dermatotoxicology Specialty Section of the Society of Toxicology and is a member of the editorial board of *Toxicology and Applied Pharmacology* as well as *Skin Pharmacology and Physiology.* Dr. Riviere has had substantial extramural research support from both the government and the industry, totaling over $15 million in grants for which he was the principal investigator. He has published more than 380 full-length research papers and chapters. He holds five U.S. patents. Dr. Riviere has authored and edited 10 books on pharmacokinetics, toxicology, and food safety. His current research interests relate to risk assessment of chemical mixtures, absorption of drugs and chemicals across skin, and the food safety and pharmacokinetics of tissue residues in food-producing animals.

Contributors

Ronald E. Baynes
Department of Population Health and Pathobiology
Center for Chemical Toxicology Research and Pharmacokinetics
College of Veterinary Medicine
North Carolina State University
Raleigh, North Carolina

Keith R. Brain
Welsh School of Pharmacy
Cardiff University
Cardiff, United Kingdom

Robert L. Bronaugh
Office of Cosmetics and Colors
U.S. Food and Drug Administration
Laurel, Maryland

Annette L. Bunge
Chemical Engineering Department
Colorado School of Mines
Golden, Colorado

Rory Conolly
National Center for Computational Toxicology
U.S. Environmental Protection Agency
Research Triangle Park, North Carolina

Mark T.D. Cronin
School of Pharmacy and Chemistry
Liverpool John Moores University
Liverpool, England

Sheree E. Cross
Therapeutics Research Unit
School of Medicine
Princess Alexandra Hospital
University of Queensland
Brisbane, Australia

Richard H. Guy
Departments of Biopharmaceutical Sciences and Pharmaceutical Chemistry
University of California
San Francisco, California
and
Department of Pharmacy and Pharmacology
University of Bath
United Kingdom

Gerald B. Kasting
College of Pharmacy
The University of Cincinnati Medical Center
Cincinnati, Ohio

Jean-Paul Marty
Laboratoire de Dermopharmacologie
Université de Paris-Sud
Châtenay-Malabry, France

James N. McDougal
Department of Pharmacology and Toxicology
Wright State University School of Medicine
Dayton, Ohio

Babu M. Medi
Department of Pharmaceutical Sciences
College of Pharmacy
North Dakota State University
Fargo, North Dakota

Nancy A. Monteiro-Riviere
Department of Clinical Sciences
Center for Chemical Toxicology Research and Pharmacokinetics
College of Veterinary Medicine
North Carolina State University
Raleigh, North Carolina

Faqir Muhammad
Department of Physiology and Pharmacology
University of Agriculture
Faisalabad, Pakistan

Michael S. Roberts
Therapeutics Research Unit
School of Medicine
Princess Alexandra Hospital
University of Queensland
Brisbane, Australia

Jagdish Singh
Department of Pharmaceutical Sciences
North Dakota State University
Fargo, North Dakota

Somnath Singh
Department of Pharmacy Sciences
School of Pharmacy and Health Professions
Creighton University
Omaha, Nebraska

Gilles D. Touraille
Departments of Biopharmaceutical Sciences and Pharmaceutical Chemistry
University of California
San Francisco, California
and
Laboratoire de Dermopharmacologie
Université de Paris-Sud
Châtenay-Malabry, France

Brent E. Vecchia
Chemical Engineering Department
Colorado School of Mines
Golden, Colorado

Kenneth A. Walters
An-eX Analytical Services, Ltd.
Loughborough, United Kingdom

Xin-Rui Xia
Department of Population Health and Pathobiology
Center for Chemical Toxicology Research and Pharmacokinetics
College of Veterinary Medicine
North Carolina State University
Raleigh, North Carolina

Qiang Zhang
Division of Computational Biology
CIIT Centers for Health Research
Research Triangle Park, North Carolina

Yanan Zheng
Department of Biomedical Engineering
Purdue University
West Lafayette, Indiana

Contents

CHAPTER 1

Structure and Function of Skin

Nancy A. Monteiro-Riviere

CONTENTS

INTRODUCTION

This chapter describes how anatomical structures within the skin can contribute to and influence barrier function; it provides an overview of the structure and function of skin from a multifaceted perspective. The primary function of skin is to act as a barrier to the external environment. There has been a surge of interest in skin as a target organ partly because it is experimentally accessible, directly interfaces with

Table 1.1 Epidermal Thickness, Stratum Corneum Thickness, and Number of Cell Layers from the Back and Abdomen of Nine Species

Species	Area	Epidermal Thickness (μm)	Stratum Corneum Thickness (μm)	Number of Cell Layers
Cat	Back	12.97 ± 0.93	5.84 ± 1.02	1.28 ± 0.13
	Abdomen	23.36 ± 10.17	4.32 ± 0.95	2.06 ± 0.73
Cow	Back	36.76 ± 2.95	8.65 ± 1.17	2.22 ± 0.11
	Abdomen	27.41 ± 2.62	8.07 ± 0.56	2.39 ± 0.13
Dog	Back	21.16 ± 2.55	5.56 ± 0.85	1.89 ± 0.16
	Abdomen	22.47 ± 2.40	8.61 ± 1.92	2.33 ± 0.12
Horse	Back	33.59 ± 2.16	7.26 ± 1.04	2.50 ± 0.25
	Abdomen	29.11 ± 5.03	6.95 ± 1.07	2.89 ± 0.44
Monkey	Back	26.87 ± 3.14	12.05 ± 2.30	2.67 ± 0.24
	Abdomen	17.14 ± 2.22	5.33 ± 0.40	2.08 ± 0.08
Mouse	Back	13.32 ± 1.19	2.90 ± 0.12	1.75 ± 0.08
	Abdomen	9.73 ± 2.28	3.01 ± 0.30	1.75 ± 0.25
Pig	Back	51.89 ± 1.49	12.28 ± 0.72	3.94 ± 0.13
	Abdomen	46.76 ± 2.01	14.90 ± 1.91	4.47 ± 0.37
Rabbit	Back	10.85 ± 1.00	6.56 ± 0.37	1.22 ± 0.11
	Abdomen	15.14 ± 1.42	4.86 ± 0.79	1.50 ± 0.11
Rat	Back	21.66 ± 2.23	5.00 ± 0.85	1.83 ± 0.17
	Abdomen	11.58 ± 1.02	4.56 ± 0.61	1.44 ± 0.19

Note: Paraffin sections stained with hematoxylin and eosin; $n = 6$, mean ± SE.

Source: Modified from Monteiro-Riviere et al., *J. Invest. Dermatol.* 95:582–586, 1990.

the environment, and is an important route of entry for myriad environmental toxins. Developments in percutaneous absorption and dermal toxicology have considered how anatomical factors may affect the barrier function, thereby altering the rate of absorption. It is the purpose of this chapter to provide a basic understanding of the anatomy and function of skin so that studies in percutaneous penetration, metabolism, and cutaneous responses to specific chemicals can be better understood.

In general, the basic architecture of the integument is similar in most mammals. However, differences in the thickness of the epidermis and dermis in various regions of the body exist between species and within the same species (Table 1.1). In addition, the number of cell layers and the blood flow patterns between species and within species (body site differences) can differ. It is important to understand these variations in the skin for studies involving biopharmaceutics, dermatological formulations, cutaneous pharmacology, and dermatotoxicology (Monteiro-Riviere et al., 1990; Monteiro-Riviere, 1991).

Skin is usually thickest over the dorsal surface of the body and on the lateral surfaces of the limbs. It is thin on the ventral side of the body and medial surfaces of the limbs. In regions with a protective coat of hair, the epidermis is thin; in nonhairy skin, such as that of the mucocutaneous junctions, the epidermis is thicker. On the palmar and plantar surfaces, where considerable abrasive action occurs, the stratum corneum is usually the thickest. The epidermis may be smooth in some areas but has ridges or folds in other regions that reflect the contour of the underlying superficial dermal layer (Monteiro-Riviere, 1998).

FUNCTIONS OF SKIN

Numerous functions have been attributed to skin, the largest organ of the body. Skin can act as an environmental barrier protecting major organs, as a diffusion barrier that minimizes insensible water loss that would result in dehydration, and as a metabolic barrier that can metabolize a compound to more easily eliminate products after absorption has occurred. Skin can function in temperature regulation, in which blood vessels constrict to preserve heat and dilate to dissipate heat. Hair and fur act as insulation, whereas sweating facilitates heat loss by evaporation. The skin can serve as an immunological affector axis by having Langerhans cells process antigens and as an effector axis by setting up an inflammatory response to a foreign insult. It has a well-developed stroma, which supports all other organs. The skin has neurosensory properties by which receptors sense the modalities of touch, pain, and heat. In addition, the skin functions as an endocrine organ by synthesizing vitamin D and is a target for androgens that regulate sebum production and a target for insulin, which regulates carbohydrate and lipid metabolism. Skin possesses several sebaceous glands that secrete sebum, a complex mixture of lipids that function as antibacterial agents or as a water-repellent shield in many animals. The apocrine and eccrine sweat glands produce a secretion that contains scent and functions in territorial demarcation. The integument plays a role in metabolizing keratin, collagen, melanin, lipid, carbohydrate, and vitamin D as well as in respiration and in biotransformation of xenobiotics. Skin has many requirements to fulfill and is therefore a heterogeneous structure that contains many different cell types that will be discussed in detail.

RELEVANT ANATOMY AND PHYSIOLOGY

Anatomically, skin is comprised of two principal and distinct components: a stratified, avascular, outer cellular epidermis and an underlying dermis consisting of connective tissue with numerous cell types and special adnexial structures (Figure 1.1).

Epidermis

The epidermis is composed of keratinized stratified squamous epithelium derived from ectoderm, and it forms the outermost layer of the skin. Two primary cell types based on origin, the keratinocytes and nonkeratinocytes, comprise this layer. The classification of epidermal layers from the outer or external surface is as follows: stratum corneum (horny layer), stratum lucidum (clear layer), stratum granulosum (granular layer), stratum spinosum (spinous or prickle layer), and stratum basale (basal layer) (Figure 1.1, Figure 1.2, Figure 1.4). In addition to the keratinocytes, another population of cells exists; it is commonly known as the nonkeratinocytes and includes the melanocytes, Merkel cells (tactile epithelioid cells), and Langerhans cells (intraepidermal macrophages) that reside within the epidermis but do not participate in the process of keratinization (Figure 1.1). The epidermis is avascular and undergoes an orderly pattern of proliferation, differentiation, and keratinization

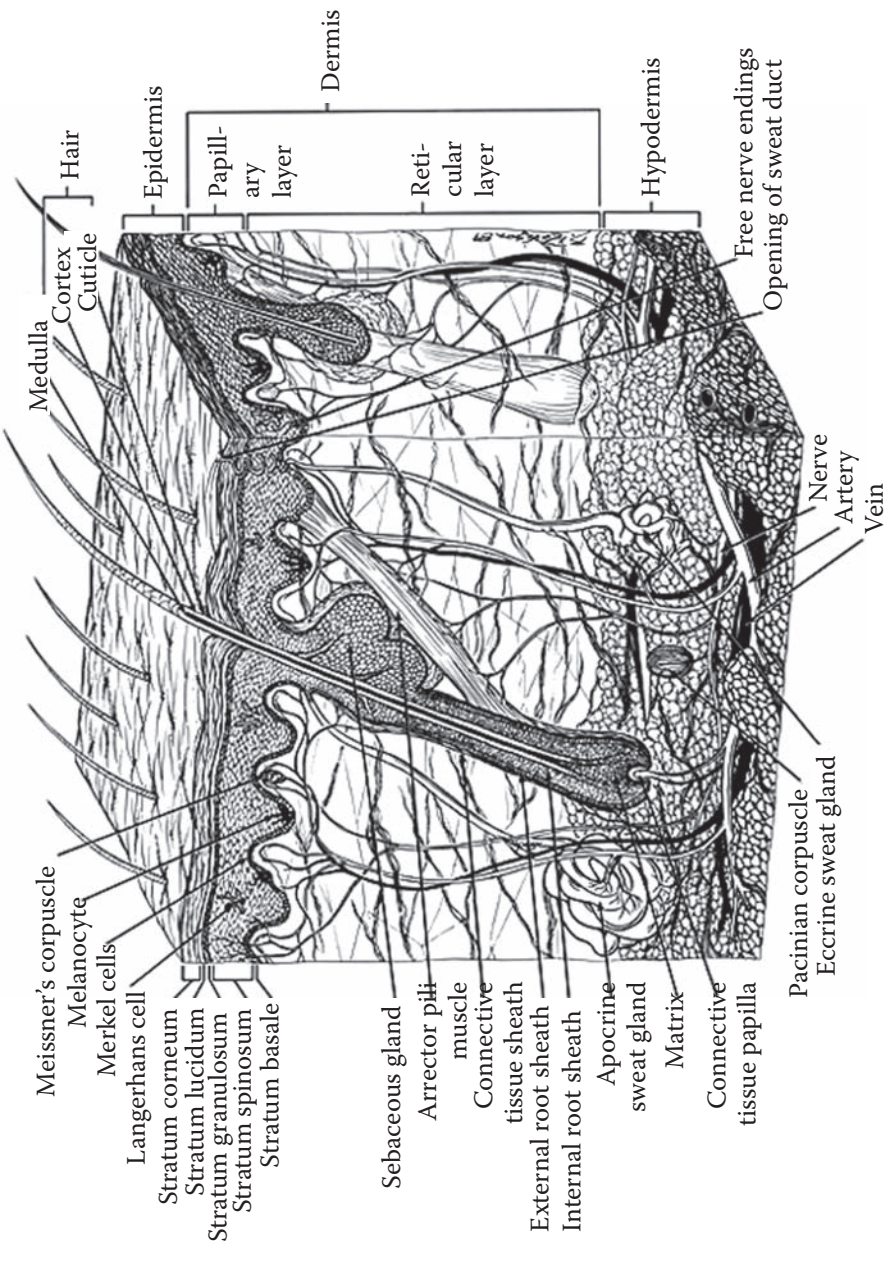

Figure 1.1
Schematic of mammalian skin. Depicts structures found in both animal (apocrine sweat glands) and human skin (eccrine sweat glands). (From Monteiro-Riviere, 1991.)

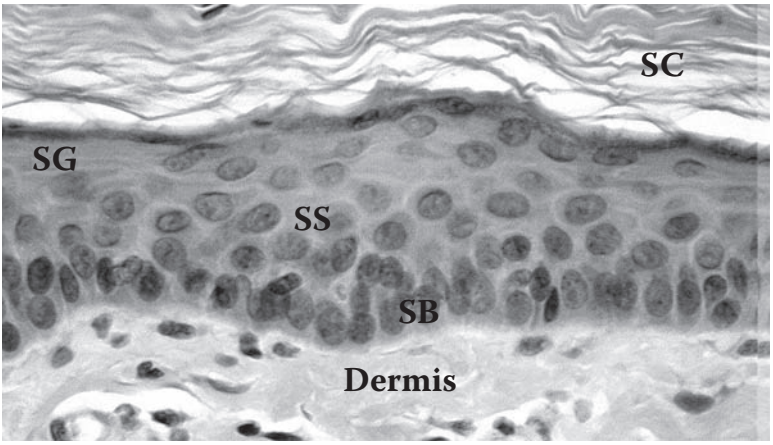

Figure 1.2 Light micrograph depicting the epidermal layers of skin. The stratum basale (SB), stratum spinosum (SS), stratum granulosum (SG), stratum corneum (SC) layers and dermis of skin. 500×

that as yet is not completely understood. Various skin appendages, such as hair, sweat and sebaceous glands, digital organs (hoof, claw, nail), feathers, horn, and glandular structures are all specializations of the epidermis (Figure 1.3). Beneath the epidermis is the dermis, or corium, which is of mesodermal origin and consists of dense irregular connective tissue. A thin basement membrane separates the epidermis from the dermis. Beneath the dermis is a layer of loose connective tissue commonly known as the hypodermis (subcutis); it consists of superficial fascia with elastic fibers and aids in binding the skin to the underlying fascia and skeletal muscle.

Layers of the Epidermis–Keratinocytes

Stratum Basale

The stratum basale, also known as the stratum germinativum, consists of a single layer of columnar or cuboidal cells that rests on the basal lamina (Figure 1.2, Figure 1.4). The cells are attached laterally to each other and to the overlying stratum spinosum cells by desmosomes and to the underlying basal lamina by hemidesmosomes (Breathnach, 1971; Selby, 1955, 1957; Wolff and Wolff-Schreiner, 1976). The nuclei of stratum basale cells are large and ovoid. These basal cells are functionally heterogeneous, and some act as stem cells, with the ability to divide and produce new cells, whereas others primarily serve to anchor the epidermis. The basal cells continuously undergo mitosis, which causes the daughter cells to be distally displaced, keeping the epidermis replenished as the stratum corneum cells are sloughed from the surface epidermis (Lavker and Sun, 1982, 1983). Depending on the region of the body, age, disease states, and other modulating factors, cell turnover and self-replacement in normal human skin are thought to take approximately 1 month. The mitotic rate increases after mechanical (tape stripping, incisions) or chemically induced injuries.

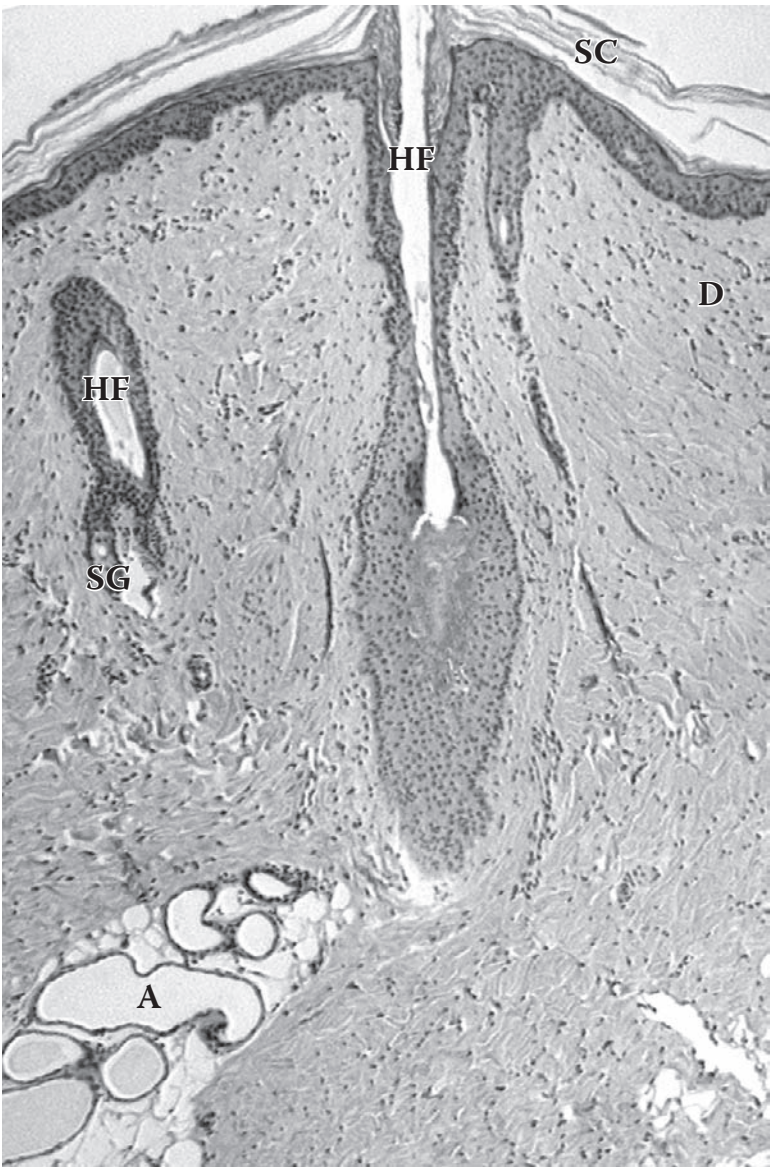

Figure 1.3 Light micrograph of pig skin depicting the stratum corneum (SC), hair follicle (HF), sebaceous glands (SG), apocrine glands (A), and dermis (D). 100×

Stratum Spinosum

The succeeding outer layer is the stratum spinosum, or "prickle cell layer"; it consists of several layers of irregular polyhedral cells (Figure 1.2, Figure 1.4). These cells are connected to adjacent stratum spinosum cells and to the stratum basale cells

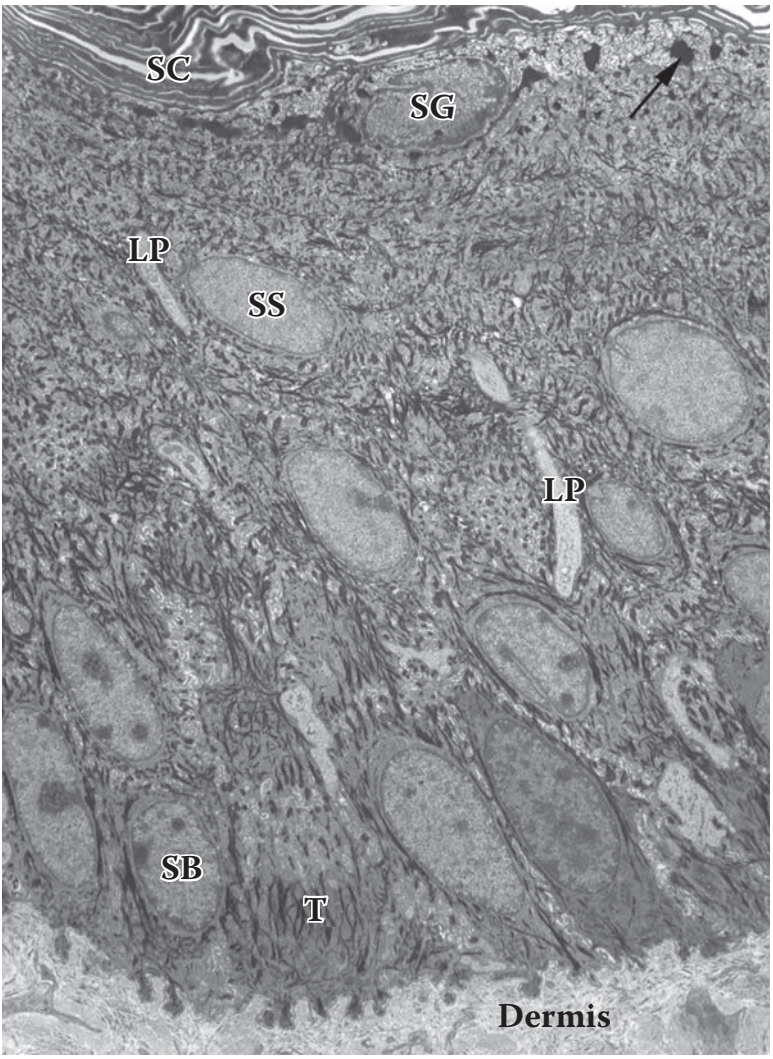

Figure 1.4 Transmission electron micrograph of the epidermal layers of skin. Note the stratum basale (SB), stratum spinosum (SS), stratum granulosum (SG), and stratum corneum (SC) layers. Langerhans' cell processes (LP) can be seen traversing through the intercellular space of the stratum spinosum layer. Note the keratohyalin granules (arrow) in the stratum granulosum layer, dermis, and numerous tonofilaments (T) throughout the layers. 3100×

below by desmosomes. The most notable characteristic feature of this layer is the numerous tonofilaments, differentiating this layer morphologically from the other cell layers. At times, this layer can possess large intercellular spaces caused by a shrinkage artifact during sample processing for light microscopic study. In the uppermost layers, small membrane-bound organelles known as lamellar granules

(Odland bodies, lamelated bodies, or membrane-coating granules) may sometimes be found; however, they are most prominent in the stratum granulosum.

Stratum Granulosum

The next layer is the stratum granulosum, which consists of several layers of flattened cells lying parallel to the epidermal–dermal junction that contain irregularly shaped, nonmembrane-bound, electron-dense keratohyalin granules (Figure 1.2, Figure 1.4). These granules contain profilaggrin, a structural protein and a precursor of filaggrin, and are believed to play a role in keratinization and barrier function. An archetypal feature of this layer is the presence of many lamellar granules. These granules are smaller than mitochondria and occur near the Golgi complex and smooth endoplasmic reticulum. They increase in number and size, move toward the cell membrane, and release their lipid contents by exocytosis into the intercellular space between the stratum granulosum and stratum corneum, thereby coating the cell membrane of the stratum corneum cells (Yardley and Summerly, 1981; Matolsty, 1976). The lamellar granules contain several types of lipid (ceramides, cholesterol, fatty acids, and small amounts of cholesteryl esters) and hydrolytic enzyme (acid phosphates, proteases, lipases, and glycosidases) (Downing, 1992; Swartzendruber et al., 1989). The content and mixture of lipids can vary between species and body site. These granules are the source of intercellular lipids that define the dermal absorption pathways.

Stratum Lucidum

The stratum lucidum is a thin, clear layer only found in specific areas of exceptionally thick skin, and it lacks hair (e.g., plantar and palmar surfaces). This layer appears as a translucent, homogeneous line between the stratum granulosum and stratum corneum and consists of several layers of fully keratinized, closely compacted, dense cells devoid of nuclei and cytoplasmic organelles. The cytoplasm contains eleidin, a protein that is similar to keratin but has a different staining affinity and protein-bound phospholipids.

Stratum Corneum

The stratum corneum is the outermost layer of the epidermis and consists of several layers of completely keratinized, dead cells that are constantly desquamated (Figure 1.1 to Figure 1.4). This layer does not contain nuclei or cytoplasmic organelles. The density of the stratum corneum cell layer can vary depending on how the filaments are packed. The most superficial layers of the stratum corneum that undergo constant desquamation are referred to as the *stratum disjunctum*.

The stratum corneum cell layers may vary in thickness from one body site to another. An interregional analysis was conducted in nine species to assess the variability in thickness and blood flow between body sites as well as the effect histologic techniques have on these metrics (Table 1.1). Such regional differences

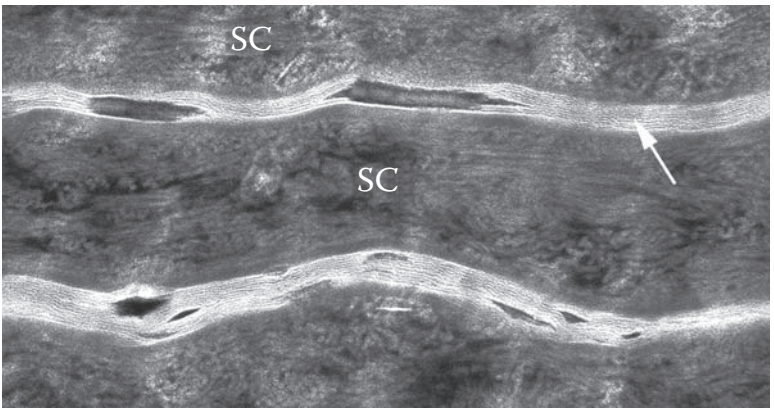

Figure 1.5 Transmission electron micrograph visualizing the lipid lamellae (arrow) between the stratum corneum (SC) cells. This region represents the pathway through which chemicals traverse through the stratum corneum barrier. 190,000×

may be important in topical percutaneous absorption as these may affect barrier function.

The intercellular substance derived from the lamellar granules is present between the stratum corneum cells and forms the intercellular lipid component of a complex stratum corneum barrier, which prevents both the penetration of substances from the environment and the loss of body fluids. Predominantly, it is the intercellular lipids, arranged into lamellar sheets, that constitute the epidermal permeability barrier (Elias, 1983) (Figure 1.5). Ruthenium tetroxide postfixation allows the visualization of these lipid lamellae at the ultrastructural layer (Swartzendruber, 1992). The number of lamellae may vary within the same tissue specimen. In some areas, a pattern of alternating electron-dense and electron-lucent bands represent the paired bilayers formed from fused lamellar granule disks, as postulated by Landmann (Landmann, 1986; Swartzendruber et al., 1987, 1989; Madison et al., 1987). Extraction of these epidermal lipids using organic solvents reduces barrier function (Monteiro-Riviere et al., 2001; Hadgraft, 2001).

These keratinized cells are surrounded by a plasma membrane and a thick submembranous layer that contains a protein, involucrin. This protein is synthesized in the stratum spinosum and cross-linked in the stratum granulosum by an enzyme that makes it highly stable. Involucrin provides structural support to the cell but does not regulate permeability.

Epidermal Nonkeratinocytes

Melanocytes

Melanocytes are located in the basal layer of the epidermis (Figure 1.1). They can be found in the external root sheath and hair matrix of hair follicles, in the sweat gland ducts, and in sebaceous glands. Melanocytes have dendritic processes that either extend between adjacent keratinocytes or run parallel to the dermal surface.

The melanocyte has a spherical nucleus and contains typical subcellular organelles. Their cytoplasm is clear except for pigment-containing ovoid granules referred to as *melanosomes*. The melanosomes impart color to skin and hair. Following melanogenesis, the melanosomes migrate to the tips of their dendritic processes, become pinched off, and then are phagocytized by the adjacent keratinocytes. Melanosomes are randomly distributed within the cytoplasm of the keratinocytes and sometimes localized over the nucleus, forming a caplike structure that protects the nucleus from ultraviolet radiation. Skin color is determined by the number, size, distribution, and degree of melanization of melanosomes.

Merkel Cells

Merkel cells, also referred to as tactile epithelioid cells, are located in the basal region of the epidermis in both hairless and hairy skin. Their long axis is usually parallel to the surface of the skin and thus perpendicular to the columnar basal epithelial cells above (Figure 1.1). Ultrastructurally, Merkel cells possess a lobulated and irregular nucleus with a clear cytoplasm, lack tonofilaments, and are connected to adjacent keratinocytes by desmosomes. These cells have a characteristic region of vacuolated cytoplasm near the dermis that has spherical electron-dense granules containing species-specific chemical mediators such as serotonin, serotonin-like substances, vasoactive intestinal polypeptide, peptide histidine-isoleucine, and substance P. Merkel cells are associated with axonal endings, and as the axon approaches the epidermis, it loses its myelin sheath and terminates as a flat meniscus on the basal aspect of the stratum basale cell. Merkel cells stimulate keratinocyte growth, act as slow-adapting mechanoreceptors for touch, and release trophic factors that attract nerve endings into the epidermis.

Langerhans Cells

Langerhans cells (intraepidermal macrophages) are dendritic cells located in the upper stratum spinosum layers and have long dendritic processes that traverse the intercellular space to the granular cell layer (Figure 1.1, Figure 1.4). They have been reported in adult pigs, cats, and dogs and are well characterized in rodents and humans. However, the specific phenotype (membrane receptors and antigens related to immune function) can vary between species. At the ultrastructural level, they have a clear cytoplasm containing organelles and an indented nucleus but lack tonofilaments and desmosomes. They are apparent in toluidine blue-stained sections embedded in epoxy and appear as dendritic clear cells in the suprabasal layers of the epidermis. A unique characteristic of this cell is distinctive rod- or racket-shaped granules within the cytoplasm called Langerhans (Birbeck) cell granules, which may function in antigen processing. Depending on the species, these granules can contain Langerin, a Ca^{2+}-dependent type II lectin.

Langerhans cells are derived from bone marrow and are functionally and immunologically related to the monocyte-macrophage series. They play a major role in the skin immune response because they are capable of presenting antigen to

lymphocytes and transporting them to the lymph node for activation. They are considered the initial receptors for cutaneous immune responses such as delayed-type hypersensitivity and to contact allergens and can play an initiating role in some forms of immune-mediated dermatologic reactions.

Keratinization

The process in which the epidermal cells differentiate and migrate upward to the surface epithelium is referred to as keratinization. This is designed to provide a constantly renewed protective surface to the epidermis. As the cells proceed through the terminal differentiation stage, many cellular degradation processes occur. The spinosum and granular layers have lost their proliferative potential and thus undergo a process of intracellular remodeling. As the cytoplasmic volume increases, tonofilaments, keratohyalin granules, and lamellar granules also become abundant.

Keratin is the structural protein abundantly synthesized by the keratinocytes and consists of many different molecular types. A loose network of keratins K5 and K14 are located within the basal cells. The active stratum spinosum cells secrete K1 and K10 and contain coarser filaments than those in the stratum basale. As the cells flatten, their cellular contents increase, the nuclei disintegrate, and the lamellar granules discharge their contents into the intercellular space coating the cells. The nucleus and other organelles disintegrate, and the flattened cells become filled by filaments and keratohyalin. This envelope consists of the precursor protein involucrin and the putative precursor protein cornifin-α/SPRR1 . The final product of this epidermal differentiation and keratinization process can be thought of as a stratum corneum envelope consisting of interlinked protein-rich cells containing a network of keratin filaments surrounded by a thicker plasma membrane coated by multilamellar lipid sheets. This forms the typical "brick-and-mortar" structure in which the lipid matrix acts as the mortar between the cellular bricks. This intercellular lipid mortar constitutes the primary barrier and paradoxically the pathway for penetration of topical drugs through skin.

Epidermal–Dermal Junction (Basement Membrane)

The basement membrane zone or epidermal–dermal junction is a thin extracellular matrix that separates the epidermis from the dermis. It is a highly specialized structure recognized with the light microscope as a thin, homogeneous band. Ultrastructurally, it can be divided into four component layers: (1) the cell membrane of the basal epithelial cell, which includes the hemidesmosomes; (2) the lamina lucida (lamina rara); (3) the lamina densa (basal lamina); and (4) the subbasal lamina (sublamina densa or reticular lamina), with a variety of fibrous structures (anchoring fibrils, dermal microfibril bundles, microthreadlike filaments) (Briggaman and Wheeler, 1975). The basement membrane has a complex molecular architecture with numerous components that play a key role in adhesion of the epidermis to the dermis. The macromolecules that are ubiquitous components of all basement membranes

include type IV collagen, laminin, entactin/nidogen, and heparan sulfate proteoglycans. Other basement membrane components, such as bullous pemphigoid antigen, epidermolysis bullosa acquisita, fibronectin, GB3 (Nicein, BM-600, epiligrin), L3d (type VII collagen), and 19DEJ-1 (Uncein) are limited in their distribution to the epithelial basement membrane of skin (Timpl et al., 1983; Woodley et al., 1984; Verrando et al., 1987; Fine et al., 1989; Rusenko et al., 1989; Briggaman, 1990).

The basal cell membrane of the epidermal–dermal junction is not always smooth. It may be irregular, forming fingerlike projections into the dermis. The basement membrane has several functions: It maintains epidermal–dermal adhesion, acts as a selective barrier between the epidermis and dermis by restricting some molecules and permitting the passage of others, influences cell behavior and wound healing, and serves as a target for both immunologic (bullous diseases) and nonimmunologic injury (friction- or chemically induced blisters). Pertinent to toxicology, the basement membrane is the target for specific vesicating agents such as *bis*(2-chloroethyl) sulfide and dichloro(2-chlorovinyl) arsine, which causes blisters on the skin after topical exposure (Monteiro-Riviere and Inman, 1995).

Dermis

The dermis or corium lies directly under the basement membrane and consists of dense irregular connective tissue with a feltwork of collagen, elastic, and reticular fibers embedded in an amorphous ground substance of mucopolysaccharides (Figure 1.1 to Figure 1.4). Predominant cell types of the dermis are fibroblasts, mast cells, and macrophages. In addition, plasma cells, chromatophores, fat cells, and extravasated leukocytes are often found in association with blood vessels, nerves, and lymphatics. Sweat glands, sebaceous glands, hair follicles, and arrector pili muscles are present within the dermis. Arbitrarily, the dermis can be divided into a superficial papillary layer that blends into a deep reticular layer. The papillary layer is thin and consists of loose connective tissue, which is in contact with the epidermis and conforms to the contour of the basal epithelial ridges and grooves. When it protrudes into the epidermis, it gives rise to the dermal papilla. When the epidermis invaginates into the dermis, epidermal pegs are formed. The reticular layer is a thicker layer made up of irregular dense connective tissue with fewer cells and more fibers.

Hypodermis

The hypodermis (subcutis) is a layer of loose connective tissue that lies beneath the dermis (Figure 1.1). It is not part of the skin but rather the superficial fascia, as seen in gross anatomical dissections. The hypodermis helps to anchor the dermis to the underlying muscle or bone. The loose arrangement of collagen and elastic fibers allows the skin flexibility and free movement over the underlying structures. In specific sites, large fat deposits may be found in the carpus, metacarpus, and digits, where they act as shock absorbers.

Appendageal Structures

Hair

Hair Shaft

Hairs are keratinized structures derived from epidermal invaginations and are found almost everywhere on the body surface except for specific body sites that include the palms, soles, and mucocutaneous junctions (Figure 1.1, Figure 1.3). The distal or free part of the hair above the surface of the skin is the hair shaft. The part within the follicle is the hair root, which has a terminal, hollow knob called the hair bulb, which is attached to a dermal papilla.

The hair shaft is composed of three layers: an outermost cuticle, a cortex of densely packed keratinized cells, and an innermost medulla of loose cuboidal or flattened cells. The cuticle is formed by a single layer of flat keratinized cells in which the free edges, which overlap like shingles on a roof, are directed toward the distal end of the shaft. The cortex consists of a layer of dense, compact, keratinized cells with their long axes parallel to the hair shaft. The medulla forms the center of the hair and is loosely filled with cuboidal or flattened cells. In the root, the medulla is solid, whereas in the shaft it contains air-filled spaces. The pattern of the surface of the cuticular cells, together with the cellular arrangement of the medulla, is characteristic for each species.

Hair Follicle

Hair and fur are important structures comprising skin and present as the most obvious distinguishing factor between species. They are also a prime target for many cosmetics and some pharmacologic preparations involved with stimulating hair growth. Finally, they are also a primary toxicologic target for chemotherapeutic drugs that target rapidly dividing cells. The hair follicle is embedded at an angle in the dermis, with the bulb sometimes extending as deep as the hypodermis (Figure 1.1, Figure 1.3). This fundamental anatomical arrangement is often ignored when dermatomed skin sections or epidermal membranes are employed in *in vitro* diffusion cell systems to assess dermal absorption. In these preparations, holes appear where the hair shafts once were (Grissom et al., 1987), making artifactual pathways for compound absorption.

The hair follicle consists of four major components: (1) internal root sheath (internal epithelial root sheath), (2) external root sheath (external epithelial root sheath), (3) dermal papilla, and (4) hair matrix. The cells covering the dermal papilla and composing most of the hair bulb are the hair matrix cells. These are comparable to stratum basale cells of regular epidermis except that they are more lipid deficient and produce harder keratin than their epidermal counterparts.

The innermost layer, next to the hair root, is the internal epithelial root sheath, which is composed of three layers: (1) internal root sheath cuticle, (2) middle granular epithelial layer (Huxley's layer), and (3) outer pale epithelial layer (Henle's

layer). The cuticle of the internal epithelial root sheath is formed by overlapping keratinized cells similar to those of the cuticle of the hair, except that the free edges are oriented in the opposite direction or toward the hair bulb. This arrangement results in a solid implantation of the hair root in the hair follicle. The granular epithelial layer is composed of one to three layers of cells rich in trichohyalin (keratohyalin in hair) granules. The pale epithelial layer is the outermost layer of the internal epithelial root sheath and is composed of a single layer of keratinized cells. Immediately below the opening of the sebaceous glands, the internal epithelial root sheath of the large follicles becomes corrugated, forming several circular or follicular folds. The sheath then becomes thinner, and the cells fuse, disintegrate, and become part of the sebum.

The external epithelial root sheath is composed of several layers of cells similar to the epidermis, with which it is continuous in the upper portion of the follicle. External to this layer is a homogeneous glassy membrane corresponding to the basal lamina of the epidermis. The entire epithelial root sheath (internal and external) is enclosed by a dermal root sheath composed of collagen and elastic fibers richly supplied by blood vessels and nerves, especially in the dermal papilla.

The dermal papilla of the hair follicle is the region of connective tissue directly underneath the hair matrix. The cells covering the dermal papilla and composing most of the hair bulb are the hair matrix cells. These are comparable to stratum basale cells of regular epidermis and give rise to the cells that keratinize to form the hair. They differ from the keratinocytes of the surface epidermis with respect to the type of keratin produced. The surface keratinocytes produce a “soft” form of keratin that passes through a keratohyalin phase. The cells containing soft keratin have a high lipid content and a low sulfur content and desquamate when they reach the surface of the epidermis. In contrast, the matrix cells of the hair follicle produce a “hard” keratin, which is also characteristic of horn and feather. The keratinocytes of the follicle do not go through a keratohyalin phase, do not desquamate, and have low lipid and high sulfur contents.

There are several different types of hair follicles in the domestic species. Primary hair follicles have a large diameter, are deeply rooted in the dermis, and usually associate with sebaceous and sweat glands as well as an arrector pili muscle. Secondary follicles are smaller in diameter than a primary follicle, and the root is nearer the surface. They may have a sebaceous gland but lack a sweat gland and an arrector pili muscle. Hairs from these follicles are secondary hair or underhairs. Secondary hairs lack a medulla. Simple follicles have only one hair emerging to the surface. Compound follicles are composed of clusters of several hair follicles located in the dermis. At the level of the sebaceous gland opening, the follicles fuse, and the various hairs emerge through one external orifice. Compound hair follicles usually have one primary hair follicle and several secondary hair follicles. In addition, sinus or tactile hair follicles of the head (e.g., the vibrissae [whiskers] of a cat) are highly specialized for tactile sense. They consist of large single follicles characterized by a blood-filled sinus between the inner and outer layers of the dermal root sheath.

Many structural differences exist in the arrangement of the hair follicles and hair follicle density among the domestic and laboratory animals. Pig and human hair

density is sparse compared to the rodent. Skin from the back of pigs and from the abdomen of humans has a density of 11 ± 1 hair follicles/cm^2 in comparison to the back of the rat with 289 ± 21, the mouse with 658 ± 38, and the hairless mouse with 75 ± 6 (Bronaugh et al., 1982). For a comprehensive review of hair follicle arrangement and microscopic anatomy of the integument in different domestic species, see Monteiro-Riviere, 1991, 1998.

Hair growth can vary from species to species, body site, and age of an individual. The process of keratinization is continuous in the surface epidermis; in the hair follicle, the matrix cells undergo periods of quiescence during which no mitotic activity occurs. Cyclic activity of the hair bulb accounts for the seasonal change in the hair coat of domestic animals. The hair cycle in which the cells of the hair bulb are mitotically active and growth occurs is called *anagen*. When the follicles go through a regressive stage and metabolic activity slows, it is referred to as *catagen*. In this phase, the base of the follicle migrates upward in the skin toward the epidermal surface. The hair follicle then enters *telogen*, a resting or quiescent phase in which growth stops, and the base of the bulb is at the level of the sebaceous canal. Following this phase, mitotic activity and keratinization start over again and a new hair is formed. As the new hair grows beneath the telogen follicle, it gradually pushes the old follicle upward toward the surface, where it is eventually shed. The hair cycle consists of intermittent mitotic activity and keratinization of the hair matrix cells and is controlled by several factors, including length of daily periods of light, ambient temperature, nutrition, and hormones, particularly estrogen, testosterone, adrenal steroids, and thyroid hormone (Monteiro-Riviere, 1998).

Of particular significance to toxicology is that a chemical with a mechanism of action that requires interaction with an active metabolic process may only exert toxicity when hair growth is in an active growth phase. Exposure at other times may not elicit any response. Many cytotoxic chemicals (e.g., cancer chemotherapeutic drugs and immunosuppressants such as cyclophosphamide) with a mechanism of action that is to kill dividing cells will produce hair loss (alopecia) as an unwanted side effect of nonselective activity.

Associated with most hair follicles are bundles of smooth muscle called the *arrector pili muscle*. This muscle attaches to the dermal root sheath of the hair follicle and extends toward the epidermis, where it connects to the papillary layer of the dermis. On contraction, this muscle not only erects the hairs but also plays a role in emptying the sebaceous glands.

Glands of the Skin

The excretory portion in the skin involves secretion from the sebaceous glands and the apocrine and eccrine sweat glands.

Sebaceous Glands

Sebaceous glands are usually found all over the body and are associated with hair follicles. Their density can vary between anatomical site and between individuals (Figure 1.1, Figure 1.3). They are evaginations of the epithelial lining,

and histologically are simple, branched, or compound alveolar glands containing a mass of epidermal cells enclosed by a connective tissue sheath. These cells move inward through mitotic activity and accumulate lipid droplets to release their secretory product, sebum, by the holocrine mode of secretion. Sebum, which is derived from the disintegration of these cells, contains antimicrobial lipids. The major lipids in the human sebaceous gland are squalene, cholesterol, cholesterol esters, wax esters, and triglycerides (Stewart, 1992). In lower mammals, the sebaceous glands can become specialized and are often associated with a pheromone-secreting role or can act as a waterproofing agent. Pig sebaceous glands are rudimentary. Sebaceous glands in humans are important because they have antifungal or antibacterial properties. The sebum that reaches the skin surface may contain free fatty acids with small amounts of mono- and diglycerides. Human sebum plays a major role during early adolescence in acne vulgaris and in the evaluation of antiacne drug candidates. It is thought that elderly people suffer from dry skin caused by low sebum secretion.

Sweat Glands — Sweat glands based on their morphologic and functional characteristics can be classified into apocrine or eccrine (merocrine). In domestic animals, the apocrine gland is extensively developed and found throughout most of the skin. However, in humans it is found only in specific body sites such as the axillary, pubic, and perianal regions. In humans, the eccrine (merocrine) glands are found over the entire body surface except for the lips, external ear canal, clitoris, and labia minora.

Apocrine Gland — The apocrine glands are simple saccular or tubular glands with a coiled secretory portion and a straight duct (simple coiled tubular glands) (Figure 1.1, Figure 1.3). The secretory portion has a large lumen lined with flattened cuboidal to low columnar epithelial cells, depending on the stage of their secretory activity. Most frequently, the duct penetrates the epidermis of the hair follicle just before it opens onto the surface of the skin. Myoepithelial cells are located at the secretory portion between the secretory cells and the basal lamina and are specialized smooth muscle cells that can contract and aid in moving the secretions toward the duct. The function of the apocrine glands is to produce a viscous secretion that contains a scent related to communications between species, probably as a sex attractant or as a territorial marker.

Eccrine Gland — Eccrine glands are simple tubular glands that open directly onto the surface of the skin and not into hair follicles (Figure 1.1). The duct of the eccrine sweat glands is comprised of two layers of cuboidal epithelium resting on the basal lamina and opens in a straight path onto the epidermal surface. The secretory portion is composed of cuboidal epithelium with dark and clear cells. Some workers postulate that the duct of these glands provides an alternate pathway for polar molecules, normally excluded by the stratum corneum, to be absorbed through skin. In addition, the secretory portion secretes isotonic fluid that is low in protein and similar to plasma in ionic composition and osmolarity. On passage down the duct, it becomes hypotonic, and reabsorption of sodium chloride, bicarbonate, lactate, and small

amounts of water occurs (Bijman, 1987; Quinton and Reddy, 1989). This gland is considered one of the major cutaneous appendages and plays a role in thermoregulation necessary for fluid and electrolyte homeostasis.

Blood Vessels, Lymph Vessels, and Nerves

The dermis is highly vascularized, providing direct access for distribution of compounds after passing through the epithelial barrier. The blood supply in the dermis is under complex, interacting neural and local humoral influences with a temperature-regulating function that can have an effect on distribution by altering blood supply to this area. The absorption of a chemical possessing vasoactive properties would be affected through its action on the dermal vasculature; vasoconstriction would retard absorption and increase the size of a dermal depot; vasodilation may enhance absorption and minimize any local dermal depot formation.

Terminal branches of the cutaneous arteries give rise to three plexuses: (1) the deep or subcutaneous plexus, which in turn gives off branches to the (2) middle or cutaneous plexus, which provides branches to make up the (3) superficial or subpapillary plexus. The superficial plexus, when present, also furnishes the capillary loops that extend into the dermal papillae (Ryan, 1991). Lymph capillaries arise in the superficial dermis and form a network that drains into a subcutaneous plexus. Small subcutaneous nerves give rise to a nerve plexus that pervades the dermis and sends small branches to the epidermis. Several types of endings are present: free afferent nerve endings in the epidermis and dermis (encircle hair follicles); free efferent endings in the hypodermis (at arrector pili muscles, glands, and blood vessels); nonencapsulated tactile corpuscles (Merkel cells); and encapsulated tactile (Meissner's) corpuscles.

Blood flow measurements in the skin using laser Doppler velocimetry at various sites in humans showed interindividual and spatial variations (Tur et al., 1983). The magnitude of cutaneous blood flow and epidermal thickness has been postulated to explain the regional differences in percutaneous absorption between body sites in humans and animals. A comprehensive study comparing the histologic thickness and laser Doppler blood flow measurements was conducted at five cutaneous sites (buttocks, ear, humeroscapular joint, thoracolumbar junction, and abdomen) in nine species (cat, cow, dog, horse, monkey, mouse, pig, rabbit, rat) to determine the correlation of blood flow and thickness. These studies suggested that laser Doppler velocimetry blood flow and skin thickness measurements did not correlate across species and body sites but are independent variables that must be evaluated separately in dermatology, pharmacology, and toxicology studies (Monteiro-Riviere et al., 1990).

CONCLUSION

As can be appreciated from this overview of the structure and function of skin, it is important to understand the basic aspects of skin anatomy and physiology to interpret the effects of exposure to occupational chemicals (solvents, corrosives, or

nanomaterials), environmental pollutants (pesticides and other organics), vesicant agents, cosmetics or dermatologics, or transdermal drugs that cross the cutaneous barrier. To properly study the dermatotoxicity of chemicals or the ability of a chemical to penetrate the stratum corneum barrier, a fundamental knowledge of skin microanatomy identifies the relevant structures that may interact with penetrating chemicals or particles.

REFERENCES

Bijman, J. (1987). Transport processes in the eccrine sweat gland, *Kidney Int*., 32, S109–S112.

Breathnach, A.S. (1971). *An Atlas of the Ultrastructure of Human Skin: Development, Differentiation, and Post-Natal Features*. London: Churchill Press.

Briggaman, R. and Wheeler, C.E. (1975). The epidermal-dermal junction, *J. Invest. Dermatol*., 65:71–84.

Briggaman, R.A. (1990). Epidermal-dermal junction: Structure, composition, function and disease relationships, *Prog. Dermatol*., 24:1–8.

Bronaugh, R.L., Stewart, R.F., and Congdon, E.R. (1982). Methods for *in vitro* percutaneous absorption studies. II. Animal models for human skin, *Toxicol. Appl. Pharmacol*., 62:481–488.

Downing, D.T. (1992). Lipid and protein structures in the permeability barrier of mammalian epidermis, *J. Lipid Res*., 33:301–313.

Elias, P.M. (1983). Epidermal lipids, barrier function, and desquamation, *J. Invest. Dermatol*., 80:44–49.

Fine, J.D., Horiguchi, Y., Jester, J., and Couchman, J.R. (1989). Detection and partial characterization of a midlamina lucida-hemidesmosome-associated antigen (19-DEJ-1) present within human skin, *J. Invest. Dermatol*., 92:825–830.

Grissom, R.E., Monteiro-Riviere, N.A., and Guthrie, F.E. (1987). A method for preparing mouse skin for assessing *in vitro* dermal penetration of xenobiotics, *Tox. Lett*., 36:251–258.

Hadgraft, J. (2001). Modulation of the barrier function of skin, *Skin Pharmacol. Appl. Skin Physiol*., 14(suppl 1):72–81.

Landmann, L. (1986). Epidermal permeability barrier: transformation of lamellar granule-disks into intercellular sheets by a membrane-fusion process, a freeze-fracture study, *J. Invest. Dermatol*., 87:202–209.

Lavker, R.M. and Sun, T.T. (1982). Heterogeneity in epidermal basal keratinocytes: morphological and functional correlations, *Science*, 215:1239–1241.

Lavker, R.M. and Sun, T.T. (1983). Epidermal stem cells, *J. Invest. Dermatol*., 81:121s–127s.

Madison, K.C., Swartzendruber, D.C., and Wertz, P.W. (1987). Presence of intact intercellular lipid lamellae in the upper layers of the stratum corneum, *J. Invest. Dermatol*., 88:714–718.

Matolsty, A.G. (1976). Keratinization, *J. Invest. Dermatol*., 67:20–25.

Monteiro-Riviere, N.A. (1991). Comparative anatomy, physiology, and biochemistry of mammalian skin, in D.W. Hobson (ed.), *Dermal and Ocular Toxicology: Fundamentals and Methods*, Boca Raton, FL: CRC Press, pp. 3–71.

Monteiro-Riviere, N.A. (1998). The integument, in H. Dieter-Dellman and J. Eurell (eds.), *Textbook of Veterinary Histology*, Media, PA: Williams and Wilkins, pp. 303–332.

Monteiro-Riviere, N.A., Bristol, D.G., Manning, T.O., Rogers, R.A., and Riviere, J.E. (1990). Interspecies and interregional analysis of the comparative histologic thickness and laser Doppler blood flow measurements at five cutaneous sites in nine species, *J. Invest. Dermatol.*, 95:582–586.

Monteiro-Riviere, N.A. and Inman, A.O. (1995). Indirect immunohistochemistry and immunoelectron microscopy distribution of eight epidermal-dermal junction epitopes in the pig and in isolated perfused skin treated with *bis*(2-chloroethyl) sulfide, *Toxicol. Pathol.*, 23:313–325.

Monteiro-Riviere, N.A., Inman, A.O., Mak, V., Wertz, P., and Riviere, J.E. (2001). Effect of selective lipid extraction from different body regions on epidermal barrier function, *Pharm. Res.*, 18:992–998.

Quinton, P.M. and Reddy, M.M. (1989). Cl^- conductance and acid secretion in the human sweat duct, *Ann. N. Y. Acad. Sci.*, 574:438–446.

Rusenko, K.W., Gammon, W.R., Fine, J.D., and Briggaman, R.A. (1989). The carboxyl-terminal domain of type VII collagen is present at the basement membrane in recessive dystrophic epidermolysis bullosa, *J. Invest. Dermatol.*, 92:623–627.

Ryan, T.J. (1991). Cutaneous circulation, in L.A. Goldsmith (ed.), *Physiology, Biochemistry, and Molecular Biology of the Skin*, 2nd ed., New York: Oxford University Press, pp. 1019–1084.

Selby, C. (1955). An electron microscopic study of the epidermis of mammalian skin in thin sections, *J. Biophys. Biochem. Cytol.,* 5:429.

Selby, C. (1957). An electron microscopic study of thin sections of human skin, *J. Invest. Dermatol.*, 29:131–149.

Stewart, M.E. (1992). Sebaceous gland lipids, *Semin. Dermatol.*, 11:100–105.

Swartzendruber, D.C. (1992). Studies of epidermal lipids using electron microscopy, *Semin. Dermatol.*, 11:157–161.

Swartzendruber, D.C., Wertz, P.W., Madison, K.C., and Downing, D.T. (1987). Evidence that the corneocyte has a chemically bound lipid envelope, *J. Invest. Dermatol.*, 88:709–713.

Swartzendruber, D.C., Wertz, P.W., Kitko, D.J., Madison, K.C., and Downing, D.T. (1989). Molecular models of the intercellular lipid lamellae in mammalian stratum corneum, *J. Invest. Dermatol.*, 92:251–257.

Timpl, R., Dziadek, M., Fujiwara, S., Nowack, H., and Wick, G. (1983). Nidogen: a new, self-aggregating basement membrane protein, *Eur. J. Biochem.*, 137:455–465.

Tur, E., Maibach, H.I., and Guy, R.H. (1983). Basal perfusion of the cutaneous microcirculation: Measurements as a function of anatomic position. *J. Invest. Dermatol.*, 81:442–446.

Verrando, P., Hsi, B.L., Yeh, C.J., Pisani, A., Serieys, N., and Ortonne, J.P. (1987). Monoclonal antibody GB3, a new probe for the study of human basement membranes and hemidesmosomes, *Exp. Cell Res.*, 170:116–128.

Wolff, K. and Wolff-Schreiner, E. (1976). Trends in electron microscopy of skin, *J. Invest. Dermatol.*, 67:39–57.

Woodley, D.T., Briggaman, R.A., O'Keffe, E.J., Inman, A.O., Queen, L.L., and Gammon, W.R. (1984). Identification of the skin basement-membrane autoantigen in epidermolysis bullosa acquisita, *N. Engl. J. Med.*, 310:1007–1013.

Yardley, H.J. and Summerly, R. (1981). Lipid composition and metabolism in normal and diseased epidermis, *Pharmacol. Ther.*, 13:357–383.

CHAPTER 2

In Vitro Diffusion Cell Studies

Robert L. Bronaugh

CONTENTS

INTRODUCTION

In vitro diffusion cell studies are frequently conducted to evaluate the skin absorption of chemical compounds. It may be the only ethical way of obtaining human skin absorption data for a potentially toxic compound. The *in vitro* system also permits the evaluation of skin metabolism if the viability of skin is maintained. Because the skin is isolated in the diffusion cell, there is no metabolic interference from enzymes in other parts of the body. A number of important decisions have to be made when conducting an *in vitro* absorption study, and this has led to some controversy regarding how a good study should be performed.

It is important to conduct a study in a way that most closely simulates normal exposure to the compound of interest. The length of exposure of a compound in contact with the skin is often assumed to be 24 h unless it is washed off more quickly, such as occurs with a shampoo or hair color. Because the vehicle can play a major role in determining the absorption rate, the vehicle used in the absorption study should be similar to that found in normal exposure conditions.

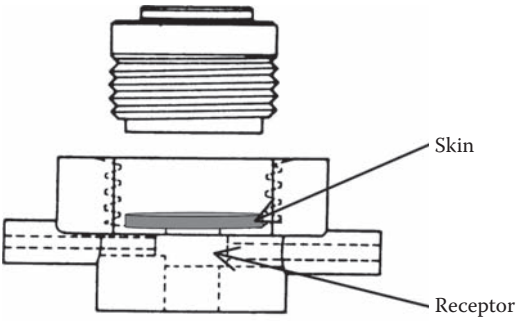

Figure 2.1 Cross-section of flow-through diffusion cell.

DESIGN OF DIFFUSION CELLS

Most studies today are conducted in one-chamber diffusion cells that hold receptor fluid beneath the skin. The top surface of the skin is exposed to the environment and is surrounded by a short wall. A tube extends upward from the receptor fluid for manual sample removal. The Franz cell is the most widely known cell of this type (Franz, 1975). A flow-through diffusion cell (Figure 2.1) is a modification of this design that should have a much smaller receptor fluid chamber to permit easy removal of contents with a moderate flow (1 to 2 ml/h) of receptor fluid (Bronaugh and Stewart, 1985). The continual replacement of the receptor fluid permits maintenance of skin viability when a physiological buffer is used (Collier et al., 1989). This diffusion cell also has the advantage of automatic sampling with the use of a fraction collector.

Special attention may be necessary in measuring the permeability of highly volatile compounds when the skin is not occluded to prevent evaporation. The short walls on the tops of some diffusion cells can protect the skin surface from air currents, and it has been suggested that this protection may be responsible for some differences observed between *in vivo* and *in vitro* results (Bronaugh and Maibach, 1985; Bronaugh et al., 1985).

A two-chamber diffusion cell has fluid on both sides of the skin and is used to apply a large (infinite) dose of test compound to one side of skin that will eventually result in a maximum, steady-state rate of absorption through skin. This information can be useful when infinite doses are applied to skin, such as in a transdermal delivery device.

PREPARATION OF SKIN

Because absorbed compounds are taken up by blood vessels in the papillary dermal tissue, most of the dermal tissue should be removed prior to assembling skin in a diffusion cell. This "split-thickness" preparation of skin is often prepared with a dermatome because it can be used for all types of skin, and the viability of skin can

be maintained (Bronaugh and Collier, 1991). Full-thickness skin (stratum corneum side up) is fixed to a Styrofoam block with hypodermic needles. The dermatome is pushed across the skin surface to prepare a layer of skin with much of the dermis removed. The dermatome is set to give a thickness of 200 to 500 μm. The thicker sections (greater than 350 μm) are needed with hairy skin to maintain an intact barrier (Bronaugh and Stewart, 1986). Separation of sparsely haired human skin at the epidermal–dermal junction can be achieved by immersing the skin in 60°C water for 1 min (Scheuplein, 1965; Bronaugh et al., 1981). All but the most stable enzymes are destroyed by this process.

Human skin is preferable for a safety evaluation, but pig skin is also used and may have barrier properties close to human skin for many compounds.

MEASUREMENT OF BARRIER INTEGRITY

It is necessary to measure the barrier integrity of skin once it is assembled in diffusion cells. This is particularly important after frozen storage of skin, which can result in damage (Bronaugh et al., 1986). A standard compound such as tritiated water is frequently used (Bronaugh et al., 1986; Dugard et al., 1984), but this procedure requires dosing the skin for 4 to 5 h for determination of the steady-state absorption of tritiated water. Bronaugh and coworkers (1986) developed a 20-min test for tritiated water absorption to give more rapid results without hydration of skin samples.

A short-term test that measures transepidermal water loss (TEWL) is also used to measure barrier integrity and has been mentioned specifically as an acceptable method by the European Union's Scientific Committee for Cosmetics and Non-Food Products (Scientific Committee, 2003). Measurement of TEWL from skin samples in diffusion cells appears to be a potentially convenient method that does not use radiolabeled material. However, some effort appears to be necessary to obtain consistent measurements, including the possible need for rooms with controlled environments for humidity and temperature (Benech-Kieffer et al., 1998). Some reports have found differences between skin permeability evaluations by tritiated water and TEWL methods (Chilcott et al., 2002).

RECEPTOR FLUID

In vitro skin absorption studies often differ in the receptor fluid used. A buffered saline solution may simply be used in a study with nonviable skin; however, a more physiological solution such as HEPES-buffered Hanks' balanced salt solution is required to maintain the viability of skin in the diffusion cells (Collier et al., 1989). The viability of skin can be maintained for at least 24 h based on glucose utilization of skin, histological evaluations, and the maintenance of estadiol and testosterone metabolism (Collier et al., 1989).

Modifications of the receptor fluid are sometimes made to facilitate the partitioning of lipophilic chemicals from skin into the receptor fluid to simulate the

in vivo absorption process. The addition of 3 to 5% bovine serum albumin is a mild, more physiological adjustment that can be useful but often does not provide sufficient lipid solubility to the receptor fluid (Bronaugh and Stewart, 1986). The use of surfactants (Bronaugh and Stewart, 1984) and organic solvents (Scott and Ramsey, 1987) provides increased lipid solubility but can damage the skin unless carefully used. The effectiveness of these harsher alternatives can vary with the test compound.

LIPOPHILIC COMPOUNDS: ARTIFICIAL RESERVOIR EFFECT

Because of the difficulty mentioned above in simulating the lipid solubility characteristics of blood, the receptor fluid absorption values obtained with lipophilic compounds should be viewed cautiously. If a substantial amount of absorbed lipophilic material remains in the skin at the end of a study, additional studies should be conducted to determine the "systemic" fate of this material. After removing unabsorbed material from the skin surface, it may be useful to continue to perfuse some diffusion cells with receptor fluid for an additional few days to determine if additional test material is collected. We call this an extended study. In an early study with musk xylol (Hood et al., 1996), receptor fluid levels of the compound doubled when the study was continued for an additional 48 h (Figure 2.2).

Some compounds appear to bind to skin during an absorption study and are therefore retained in a skin reservoir for reasons other than lipid solubility. Disperse Blue 1 appears to be an example of such a compound (Yourick et al., 2004). In the initial 24 h of the study, less than 0.2% of the applied dose penetrated into the receptor fluid, and most of the absorbed material remained in the skin (Figure 2.3). An extended study for an additional 48 h showed little additional penetration into

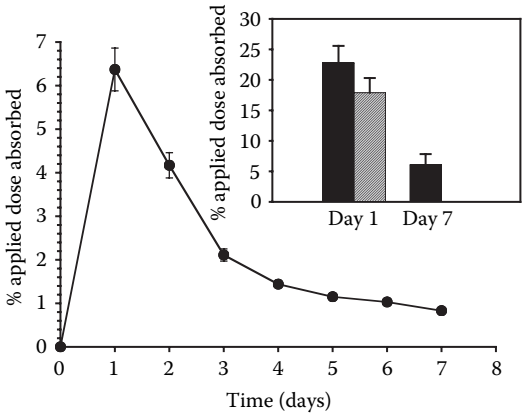

Figure 2.2 Time course of percutaneous absorption of musk xylol into the receptor fluid. Inset: Skin levels of musk xylol (solid bar, whole skin; grayed bar, stratum corneum). Values are the mean ± SE of determinations from four replicates with skin from each of two human subjects.

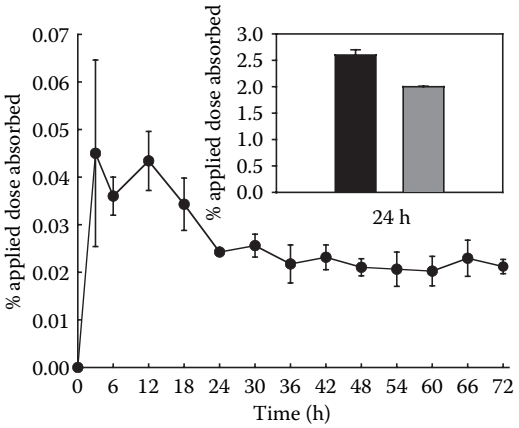

Figure 2.3 Time course of percutaneous absorption of Disperse Blue 1 into the receptor fluid. Inset: Skin levels of Disperse Blue 1 (solid bar, whole skin; grayed bar, stratum corneum). Values are the mean ± SE of determinations from three to four replicates with skin from each of two rats.

the receptor fluid. Therefore, the receptor fluid values alone may be good predictors of *in vivo* systemic absorption for this compound.

METABOLISM

Metabolism of compounds can occur as they are absorbed through the skin. For compounds that have pharmacological or toxicological actions on skin, biotransformation of absorbed material can be significant. Topically applied benzo[a]pyrene has been shown to be metabolized in skin to the metabolites responsible for its skin tumerogenic activity (Mukhtar et al., 1992). During an *in vitro* diffusion cell study with viable hairless guinea pig skin, metabolic conversion of benzo[a]pyrene to a metabolite of the ultimate carcinogen of this compound was observed in skin (Ng et al., 1992).

The activity of soluble enzymes such as esterase, acetyltransferase, and alcohol and aldehyde dehydrogenases has been shown to substantially metabolize substances applied to viable skin in diffusion cells. Benzocaine was shown to be metabolized to acetylbenzocaine during percutaneous absorption through viable hairless guinea pig skin in diffusion cells. At a dose approaching a topical anesthetic dose (0.2 mg/cm^2), 34% of absorbed benzocaine was metabolized by acetyltransferase in skin (Kraeling et al., 1996).

The absorption and metabolism of retinyl palmitate was examined after application in a volatile solvent (acetone) to viable human skin assembled in diffusion cells. Only a small amount (0.2%) of the applied retinyl palmitate that penetrated the skin was found in the receptor fluid at the end of the 24-h study. However, 18% of the applied dose of radioactivity was found in the skin, and 44% of this dose had been metabolized to retinol (Boehnlein et al., 1994).

Substantial metabolism of the hair dye ingredient 2-nitro-*p*-phenylenediamine (2NPPD) was observed during *in vitro* percutaneous absorption through viable rat and human skin (Yourick and Bronaugh, 2000). When 2NPPD was applied to human skin in a semipermanent hair dye formulation, 60% of the absorbed dye was metabolized to approximately equal amounts of N4-acetyl-2NPPD and triaminobenzene. Both metabolites may be more toxic than the parent compound. Acetyl CoA-dependent N-acetylation is important in the metabolic activation of arylamines to agents capable of damaging deoxyribonucleic acid (DNA) (Shinohara et al., 1986). It has been suggested that triaminobenzene may be responsible for the mutagenicity of 2NPPD (Nakao et al., 1991).

Total penetration of the sum of parent compound and metabolite(s) observed with viable skin may be similar to the penetration of the unmetabolized parent compound through nonviable skin. The primary barrier to skin absorption is often the nonliving stratum corneum layer on the surface of skin, and metabolism occurs after the rate-limiting step of penetration. The need to maintain viability of skin may be limited to instances when significant biotransformation of test compound in skin occurs. A safety assessment may inaccurately estimate either local or systemic toxicity of a compound if it fails to observe significant activation or detoxification of this material in skin.

REFERENCES

Benech-Kieffer, F., Wegrich, P., and Schaeffer, H., 1998, Transdermal water loss as an integrity test for skin barrier function *in vitro*: assay standardization, in *Perspectives in Percutaneous Penetration* (Eds. K.R. Brain, V.J. James, and K.A. Walters), STS Publishing, Cardiff, UK, Vol. 5B, pp. 125–128.

Boehnlein, J., Sakr, S., Lichtin, J.L., and Bronaugh, R.L., 1994, Characterization of esterase and alcohol dehydrogenase activity in skin. Metabolism of retinyl palmitate to retinol (vitamin A) in skin during percutaneous absorption, *Pharm. Res.*, 11:1155–1159.

Bronaugh, R.L. and Collier, S.W., 1991, Preparation of human and animal skin, in *In Vitro Percutaneous Absorption: Principles, Fundamentals, and Applications* (Eds. R. Bronaugh and H. Maibach), CRC Press, Boca Raton, FL, pp. 1–6.

Bronaugh, R.L., Congdon, E.R., and Scheuplein, R.J., 1981, The effect of cosmetic vehicles on the penetration of *N*-nitrosodiethanolamine through excised human skin, *J. Invest. Dermatol.*, 76:94–96.

Bronaugh, R.L. and Maibach, H.I., 1985, Percutaneous absorption of nitroaromatic compounds: *in vivo* and *in vitro* studies in the human and monkey, *J. Invest. Dermatol.*, 84:180–183.

Bronaugh, R.L. and Stewart, R.F., 1984, Methods for *in vitro* percutaneous absorption studies III: hydrophobic compounds, *J. Pharm. Sci.*, 73:1255–1258.

Bronaugh, R.L. and Stewart, R.F., 1985, Methods for *in vitro* percutaneous absorption studies IV: the flow-through diffusion cell, *J. Pharm. Sci.*, 74:64–67.

Bronaugh, R.L., and Stewart, R.F., 1986, Methods for *in vitro* percutaneous absorption studies VI: preparation of the barrier layer, *J. Pharm. Sci.*, 75:487–491.

Bronaugh, R.L., Stewart, R.F., and Simon, M., 1986, Methods for *in vitro* percutaneous absorption studies VII: use of excised human skin, *J. Pharm. Sci.*, 75:1094–1097.

Bronaugh, R.L., Stewart, R.F., Wester, R.C., Bucks, D., Maibach, H.I., and J. Anderson, 1985, Comparison of percutaneous absorption of fragrances by humans and monkeys, *Food Chem. Toxicol.*, 23:111–114.

Chilcott, R.P., Dalton, C.H., Emmanuel, A.J., Allen, C.E., and Bradley, S.T., 2002, Transepidermal water loss does not correlate with skin barrier function *in vitro, J. Invest. Dermatol.*, 118:871–875.

Collier, S.W., Sheikh, N.M., Sakr, A., Lichtin, J.L., Stewart, R.F., and Bronaugh, R.L., 1989, Maintenance of skin viability during *in vitro* percutaneous absorption/metabolism studies, *Toxicol. Appl. Pharmacol.*, 99:522–533.

Dugard, P.H., Walker, M., Mawdsley, J., and Scott, R.C., 1984, Absorption of some glycol ethers through human skin *in vitro*, *Environ. Health Perspect.*, 57:193–197.

Franz, T.J., 1975, On the relevance of *in vitro* data, *J. Invest. Dermatol.*, 64:190–195.

Hood, H.L., Wickett, R.R., and Bronaugh, R.L., 1996, The *in vitro* percutaneous absorption of the fragrance ingredient musk xylol, *Food Chem. Toxicol.*, 34:483–488.

Kraeling, M.E.K., Lipicky, R.J., and Bronaugh, R.L. 1996, Metabolism of benzocaine during percutaneous absorption in the hairless guinea pig: acetylbenzocaine formation and activity, *Skin Pharmacol.*, 9:221–230.

Mukhtar, H., Agarwal, R., and Bickers, D., 1992, Cutaneous metabolism of xenobiotics and steroid hormones, in *Pharmacology of the Skin* (Ed. H. Mukhtar), CRC Press, Boca Raton, FL, pp. 89–109.

Nakao, M., Goto, Y., Hiratsuka, A., and Watabe, T., 1991, Reductive metabolism of nitro-*p*-phenylenediamine by rat liver, *Chem. Pharm. Bull.*, 39:177–180.

Ng, K.M.E., Chu, I., Bronaugh, R.L., Franklin, C.A., and Somers, D.A., 1992, Percutaneous absorption and metabolism of pyrene, benzo[a]pyrene, and di(2-ethylhexyl) phthalate: comparison of *in vitro* and *in vivo* results in the hairless guinea pig, *Toxicol. Appl. Pharmacol.,* 115:216–223.

Scheuplein, R.J., 1965, Mechanism of percutaneous absorption I. Routes of penetration and the influence of solubility, *J. Invest. Dermatol.*, 45:334–346.

Scientific Committee on Cosmetic Products and Non-Food Products Intended for Consumers, 2003, Opinion concerning the basic criteria for the *in vitro* assessment of dermal absorption of cosmetic ingredients. Updated October 2003, available at: http://europa.eu.int/comm/health/ph_risk/committees/sccp/sccp_opinions_en.htm.

Scott, R.C. and Ramsey, J.D., 1987, Comparison of the *in vivo* and *in vitro* percutaneous absorption of a lipophilic molecule (Cypermethrin, a pyrethroid insecticide), *J. Invest. Dermatol.*, 89:142–146.

Shinohara, A., Saito, K., Tamazoe, Y., Kamataki, T., and Kato, R., 1986, Acetyl coenzyme A dependent activation of *N*-hydroxy derivatives of carcinogenic arylamines: Mechanism of activation, species difference, tissue distribution, and acetyl donor specificity, *Cancer Res.*, 46:4362–4370.

Yourick, J.J. and Bronaugh, R.L., 2000, Percutaneous penetration and metabolism of 2-nitro-*p*-phenylenediamine in human and fuzzy rat skin, *Toxicol. Appl. Pharmacol.*, 166:13–23.

Yourick, J.J., Koenig, M.L., Yourick, D.L., and Bronaugh, R.L., 2004, Fate of chemicals in skin after dermal application: does the *in vitro* skin reservoir affect the estimate of systemic absorption? *Toxicol. Appl. Pharmacol.*, 195:309–320.

CHAPTER 3

Perfused Skin Models

Jim E. Riviere

CONTENTS

INTRODUCTION

The primary models used in most dermal absorption studies fall under the rubric of *in vitro* or *in vivo* animal models. Most agree that *in vivo* human studies are optimal for predicting the absorption of topically applied chemicals in man. However, for highly toxic or carcinogenic chemicals, ethics preclude conducting such studies for routine risk analyses. Similar considerations apply to the humane use of animal surrogates. It is difficult to control many factors that might modulate percutaneous absorption when using intact animals. An important limitation is the inability to noninvasively sample the venous drainage of a topical application site to determine

the true cutaneous flux for use as an input into systemic risk assessment models. Similarly, extensive biopsies may not be taken to quantitate subtle, preclinical morphological or biochemical manifestations of dermatotoxicity. Simultaneously conducting both absorption and toxicity studies in the same preparation remains challenging.

The next step in the hierarchy of model systems is *in vitro* diffusion cell studies using human or animal skin. Although they have many advantages (as reviewed elsewhere in this text), there are limitations that may seriously detract from their usefulness. These include studies in which vasoactive compounds are used or the magnitude or distribution of cutaneous blood flow would affect the subsequent rate and extent of compound absorption or pattern of cutaneous distribution. Vascular changes could result from compound-induced cutaneous irritation where released inflammatory mediators could directly modulate vascular physiology. Some *in vitro* models are not optimal for studying the kinetics of cutaneous metabolism. An additional problem is availability of disease-free, fresh human skin from the same individual and body region. Variability in tissue sources may introduce an unacceptably high degree of intersample variation that could adversely affect experimental design. If the effects of chemical or physical pretreatment on subsequent chemical absorption are to be studied, ethical considerations may preclude performing these studies in humans.

Isolated perfused skin models, such as the isolated perfused porcine skin flap (IPPSF) developed in our laboratory, may be the "missing link" in the hierarchy of classic *in vitro* and *in vivo* models. Primary advantages of isolated perfused systems include the following:

- Presence of a functional skin microvascular system
- Metabolically viable epidermis and dermis
- Ease of continuously sampling venous perfusate
- Ability to conduct mass balance and metabolism studies
- Capability of simultaneously assessing transdermal chemical flux as well as biomarkers of cutaneous toxicity in the same chemical exposure
- Ability to conduct morphological evaluations at the end of a study in the same preparation that an absorption study was conducted
- Ease with which experimental conditions (temperature, humidity, perfusate flow, and composition) can be manipulated and controlled without concern for interference from systemic hormonal or neural feedback processes as is usually seen *in vivo*
- Availability of a large dosing surface area for human transdermal devices when raised on large species such as the pig
- Alternative humane animal model
- Relative low cost compared to either *in vivo* pig or *in vitro* bioengineered skin models

Isolated lung, liver, and kidney perfusions have been recognized for decades as important models for toxicology and pharmacology. Part of their acceptance relates to the ease of harvest because these organs are anatomically structured with "closed" vascular systems containing easily identifiable arterial inputs and venous outputs, both amenable to catheterizations with minimal expertise in surgery. In contrast, outside the possible exception of ears, skin does not possess such a closed vascular system.

Rabbit and pig ears have often been used as perfused skin systems to assess percutaneous absorption of topically applied compounds (Behrendt and Kampffmeyer, 1989; de Lange et al., 1992; Celesti et al., 1993; Chilcott et al., 2001). A fundamental problem with this approach is that the skin of the pinna is fundamentally different (hair density, adnexial structures) than other body sites as well as having a much greater degree of blood perfusion (Monteiro-Riviere et al., 1990; Monteiro-Riviere, Stinson, et al., 1993). The vasculature is specialized because of the unique thermoregulatory demands placed on this appendage. Auricular arteries perfuse a complex tissue bed consisting of skin, subcutaneous tissue, muscle, and cartilage. A comparative site study of methyl salicylate and VX absorption in swine showed significantly greater absorption from the ear compared to other body sites (Duncan et al., 2002). Thus, pig ear skin would be expected to be a suitable model for chemical absorption across human ear skin but not necessarily other body regions. These additional factors may outweigh the obvious economic benefits of obtaining ears from laboratory animals or from pigs in abattoirs. An *in vitro* study suggested that pig ear skin may be an appropriate model for preterm human infants (Sekkat et al., 2004). It must be cautioned that use of any skin from abattoirs must ensure that the skin is harvested from the carcass before any treatments (steaming, scalding, depilation) to remove surface microbes have been performed. These would damage the epidermal barrier.

Reports have sporadically appeared in the literature on perfused pieces of animal and human skin used in various studies (Feldberg and Paton, 1951; Kjaersgaard, 1954; Hiernickel, 1985; Kietzmann et al., 1991); however, none have ever been optimized or validated for percutaneous absorption studies. In contrast, a human–rat sandwich skin flap on athymic rats has been employed to study dermal absorption of various compounds (Krueger et al., 1985; Wojciechowski et al., 1987; Silcox et al., 1990). The IPPSF is the focus of the present chapter.

OVERVIEW OF METHOD

Surgical Preparation and Perfusion

The IPPSF is a single-pedicle, axial pattern, tubed skin flap created from the abdominal skin of weanling pigs. This anatomical site was selected because it is perfused by direct cutaneous arteries (superficial epigastric artery) and drained by their associated paired venous commitantes. This area of skin was also the site used in the *in situ* rat/human skin flap system (Krueger et al., 1985) as well as an isolated perfused human nontubed skin flap model (Kreidstein et al., 1991). This allows a tube of skin to be created with a sole vascular supply that may be cannulated and perfused *ex vivo*. The formation of a tubed flap allows the wound edges to be apposed, and after a short healing period of 2 days, the preparation only drains via the venous system. The IPPSF is fully described in the original publications describing its use (Riviere et al., 1986; Monteiro-Riviere et al., 1987; Riviere and Monteiro-Riviere, 1991). In addition, our group has developed an isolated perfused equine skin flap for use in assessing percutaneous absorption of chemicals across horse skin

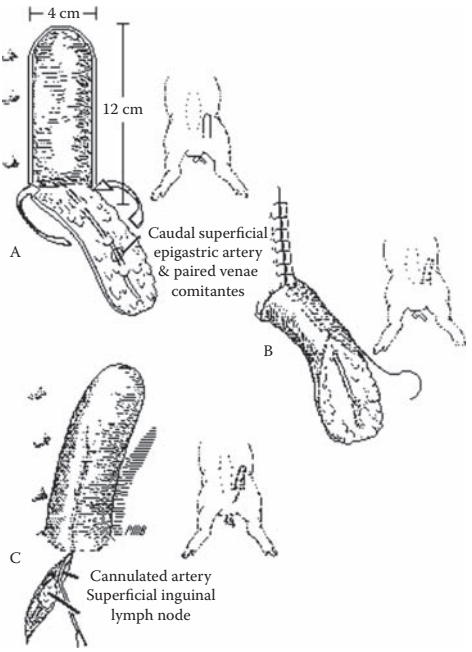

Figure 3.1 Two-stage surgical procedure used to create isolated perfused porcine skin flaps. A single-pedicle, axial pattern, tubed skin flap is created in stage 1 (A and B) and harvested 2 days later in the stage 2 (C) procedure.

(Bristol et al., 1991) and a perfused human tumor-bearing flap for use in anticancer drug targeting investigations (Vaden et al., 1993).

The IPPSF is created in a two-stage surgical procedure (Figure 3.1) (Bowman et al., 1991). Two flaps are created on each pig using the right and left caudal superficial epigastric arteries. Depending on the experimental design, this allows one flap to serve as a control for the other during perfusion studies to minimize interflap variability. In stage I surgery, conducted aseptically and under inhalational anesthesia, a 4 × 12 cm area of skin previously shown to be perfused by this artery is demarcated, excised, tubed, and allowed to remain on the pig. Two days later, a time found to be optimal based on morphological criteria (Monteiro-Riviere et al., 1987), the flap is excised, and the artery is cannulated in a simpler stage II procedure. Both flaps are then removed and placed in the isolated perfusion chambers described below. The small incision remaining on the pig is allowed to heal, and then the pig can be returned to its prior disposition (sale, other uses).

The isolated perfusion apparatus depicted in Figure 3.2 is a custom Plexiglas chamber designed to maintain the skin flap in a temperature- and humidity-regulated environment. Perfusion pressure, flow, pH, and temperature are set for desired conditions dictated by the experimental design and continuously monitored. The perfusion medium is a modified Krebs-Ringer bicarbonate buffer (pH 7.4, 350 mOsm/kg) containing albumin (45 g/L) and supplied with glucose (80 to 120 mg/dl) as the primary energy source. Albumin is added to provide the oncotic pressure required to maintain capillary patency as dictated by Starling's laws and

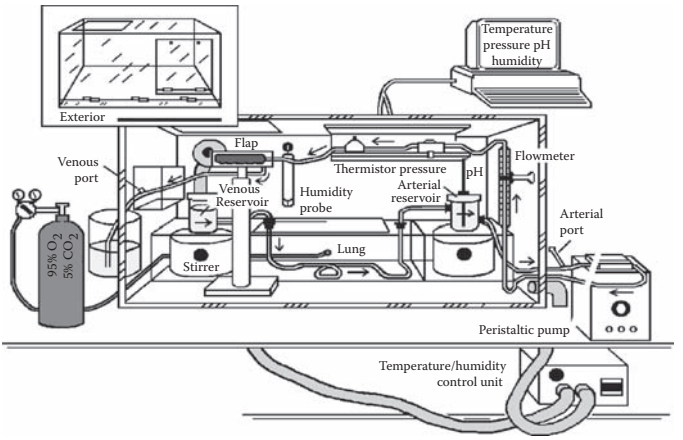

Figure 3.2 Temperature- and humidity-controlled chamber used to maintain IPPSF viability and environmental conditions throughout an experiment.

to facilitate the absorption of lipophilic penetrants that otherwise would not be soluble in a pure aqueous buffer system. Normal perfusate flow through the skin is maintained at 1 ml/min/flap (3 to 7 ml/min/100 g) with a mean arterial cannula pressure ranging from 30 to 70 mmHg. With this system, flaps may be maintained biochemically and morphologically viable for up to 24 h. Two experimental configurations are possible for flap perfusion: recirculating and nonrecirculating. For most studies, the single-pass nonrecirculating system is used. Our laboratory has perfused over 3000 IPPSFs, and several hundred more have also been independently perfused in nonacademic laboratories to which the technique has been transferred.

APPLICATIONS

There have been three types of studies conducted in the IPPSF: toxicology, percutaneous absorption (including biotransformation and pharmacokinetic modeling), and cutaneous drug distribution (drug administered by intraarterial infusion). The first two are discussed in this chapter.

Assessment of Flap Viability and Development of Biomarkers for Toxicity Assessment

Viability of the preparations are monitored in real time by assessing glucose utilization and perfusate pressure. During perfusion of a normal IPPSF, the most sensitive indicator of vascular function, and thus of vascular alterations in a dermatotoxicology experiment, is the parameter of vascular resistance calculated as perfusate pressure divided by flow. This parameter has also been used as an end point in pharmacological experiments assessing autonomic drug activity (Rogers and Riviere, 1994). Glucose utilization, calculated from the arterial–venous extraction ratio and perfusate flow, has been used as a marker of direct cutaneous toxicity of chemicals (King and

Monteiro-Riviere, 1990; King et al., 1992; Monteiro-Riviere, 1992; Srikrishna et al., 1992), with decreases in cumulative glucose utilization suggestive of direct chemical toxicity. However, glucose utilization may also be dependent on the extent of capillary perfusion because only cells that are perfused are capable of extracting glucose from the arterial perfusate (Rogers and Riviere, 1994). A decrease in glucose utilization is undoubtedly a manifestation of chemical activity; however, a chemically induced decrease in epidermal glucose utilization may be blunted by increased capillary perfusion. Independent markers of capillary perfusion (e.g., microspheres) would have utility in this area. Both vascular resistance and glucose utilization may also be altered secondary to a chemically induced release of inflammatory mediators.

Depending on the experimental design, a number of more specialized markers of viability, or loss thereof, may be assessed. We have assessed lactate production as a marker of epidermal glucose utilization and have observed decreased lactate production coexistent with decreased glucose utilization. Monitoring the release of inflammatory mediators into the perfusate as biomarkers for physical or chemically induced toxicity has proved of value for many chemical exposure scenarios. These have included prostaglandin E_2 (PGE_2), $PGF_{2\alpha}$, tumor necrosis factor α (TNF-α), and interleukins 1 and 8 as indicators of cutaneous inflammation (Monteiro-Riviere, 1992; Zhang et al., 1995a, 1995b). Prostaglandin fluxes changed with compounds that altered vascular resistance. These prostaglandin fluxes have been used as end points in pharmacologic intervention studies designed to block a cutaneous toxicant's effect by preexposure infusion of a specific antagonist. For example, to dissect the role of prostaglandins in sulfur mustard (HD)-induced cutaneous vesication, it was demonstrated that perfusion with the nonsteroidal anti-inflammatory drug (NSAID) indomethacin blunted both PGE_2 release and altered vascular resistance but did not completely prevent blister formation (Zhang et al., 1995b). Similarly, infusion of pyridostigmine bromide modulated interleukin 8, PGE_2, as well as TNF-α release after simultaneous exposure to topical irritants (Monteiro-Riviere et al., 2003).

The final markers of dermatotoxicity are the myriad morphological endpoints that may be assessed easily at the termination of an experiment. Specimens are routinely collected for light microscopy to evaluate skin viability and integrity (Monteiro-Riviere et al., 1987). These studies are pivotal in assessing the nature of the cutaneous toxicity produced (Monteiro-Riviere, 1992; Monteiro-Riviere at al., 2001). For a more specific insight into the mechanism of an observed effect, transmission electron microscopy may also be performed (Monteiro-Riviere et al., 1987, 2004; Monteiro-Riviere, 1990). These studies give a better indication of what is actually occurring within constitutive cells at a level before light microscopy or gross observations indicate an adverse effect. For greater insight, specialized morphological procedures may be conducted. These have included enzyme histochemistry to probe biochemical pathways affected by cutaneous toxicants (King et al., 1992; Srikrishna et al., 1992), immunohistochemistry and immunoelectron microscopy to study the specific molecular targets involved in vesication secondary to chemical alkylation (King et al., 1994; Monteiro-Riviere and Inman, 1995; Zhang, Peters, et al., 1995) or topical jet fuel exposure (Rhyne at al., 2002), and x-ray diffraction microscopy to probe pathways of metal penetration (Monteiro-Riviere et al., 1994b).

Although every one of the aforementioned biomarkers may be assessed in other skin models, the unique strength of the IPPSF is that all may be simultaneously evaluated in the same preparation. For example, we demonstrated the utility of the IPPSF to serve as a humane *in vitro* model for ultraviolet B phototoxicity (Monteiro-Riviere et al., 1994a). In these studies, physiological parameters such as vascular resistance, glucose utilization, and prostaglandin (PGE_2) efflux could be simultaneously evaluated in the same preparation as morphometric quantitation of pyknotic "sunburn" cells and estimation of epidermal growth fraction using histochemical staining for the proliferating cell nuclear antigen. In chemically induced dermatotoxicity, compound flux through the skin can simultaneously be determined in the same preparation that physiological and morphological end points are evaluated. Such studies have been conducted with paraquat (Srikrishna et al., 1992), lewisite (King et al., 1992), 2-chloroethyl methyl sulfide (King and Monteiro-Riviere, 1990), lidocaine delivered by iontophoresis (Monteiro-Riviere, 1990) and electroporation (Riviere, Monteiro-Riviere, et al., 1995), and recently with complex chemical mixtures.

The IPPSF model offers many unique advantages. First, it allows confirmation that cutaneous exposure to a penetrating molecule actually occurred. Second, it allows quantitation of this exposure and subsequent correlation to severity of toxicity observed. Finally, it would allow the development of linked toxicokinetic–toxicodynamic models to be developed, which should shed insight into the mechanisms of cutaneous toxicity.

Absorption Studies

The IPPSF has also been extensively utilized to quantitate the cutaneous penetration and absorption of topically applied compounds for which systemic exposure could result in toxicity. These studies can be conducted with varying degrees of experimental complexity depending on the nature of the penetrant and the precision desired. The simplest approach is to measure compound flux into the venous perfusate and express this as the percentage of applied dose absorbed. Figure 3.3 clearly illustrates how compounds with different absorption profiles can be easily distinguished. This method is accurate if most of the absorption is complete at the end of an experiment (e.g., venous fluxes are approaching background). The amount of penetrated chemical in the venous effluent may then be determined as the area under the curve (AUC) of the venous efflux profile. The compound remaining on the skin surface and within the skin can be easily assessed, especially if radiolabeled chemical was employed.

At the end of a topical treatment, samples in addition to perfusate may be collected to determine the amount and distribution of penetrated compound within tissues under the topical dosing site. The most precise technique available for this purpose is to take a core biopsy through the dosing site, snap freeze it in liquid nitrogen, and then cut serial sections to precisely localize chemical distribution within the skin as a function of penetration depth. In these studies, which are fully described in the literature (Riviere, Monteiro-Riviere, et al., 1992; Monteiro-Riviere, Inman, et al., 1993), the surface of the application site is first gently washed with a mild soap solution and then dried with gauze. Cellophane tape is then applied to

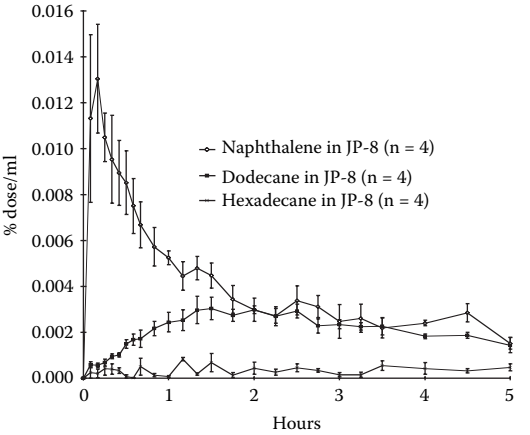

Figure 3.3 Typical IPPSF venous flux profile for a percutaneous absorption experiment (mean ± SD) depicting naphthalene, dodecane, and hexadecane absorption after topical dosing from JP-8 jet fuel.

"strip" the stratum corneum. A biopsy punch is used to take the core of tissue, which is then embedded in OCT compound, quenched in an isopentane well cooled by liquid nitrogen, and immediately stored at –80°C until it is sectioned in a cryostat. Each tissue section (representing a disk of skin containing radiolabeled compound) and the washes and tape strips are then combusted, and radioactivity is determined using liquid scintillation spectroscopy. The resulting data are a depth penetration profile for the compound under study. Although similar studies may be conducted *in vivo*, the advantage of the IPPSF is that these data are obtained in the same preparation that venous flux of the compound is determined, allowing the investigator to assess factors that modulate tissue penetration from absorption into the vasculature. For the compounds presented in Figure 3.3, a reverse pattern for tissue distribution was seen, suggesting that less naphthalene than dodecane was present in skin after exposure. This approach was utilized to assess the effect of various environmental exposure variables on the absorption of tetrachlorobiphenyl (TCB) (Qiao and Riviere, 2000). Finally, a technique was developed to assess the absorption of volatile compounds in this model (Riviere et al., 2000).

Percutaneous absorption in the IPPSF was correlated ($r^2 \approx 0.8$) to *in vivo* human absorption for five diverse compounds (Wester et al., 1998). The IPPSF estimate for absorption used was the amount absorbed into the perfusate plus the amounts penetrated into the skin. Comparative absorption values (% dose, mean ± SD) were as follows:

Table 3.1 IPPSF vs. Human Absorption

Compound	Human	IPPSF
Salicylic acid	6.5 ± 5	7.5 ± 2.6
Theophylline	16.9 ± 11.3	11.8 ± 3.8
2,4-Dimethylamine	1.1 ± 0.3	3.8 ± 0.6
Diethyl hexyl phthalic acid	1.8 ± 0.5	3.9 ± 2.4
ρ-Amino benzoic acid	11.5 ± 6.3	5.9 ± 3.7

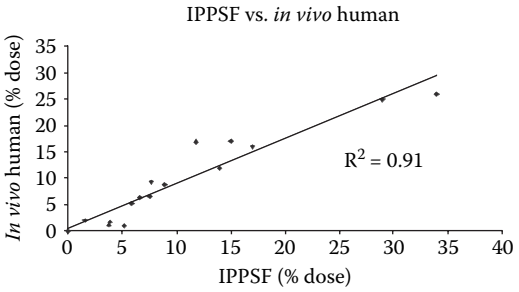

Figure 3.4 IPPSF-predicted vs. human availabilities for 16 compounds for which comparable experimental conditions (dose/unit area, vehicle) for both data sets were available.

A similar analysis of all available data in the IPPSF for which comparable (similar dose, vehicle) human dermal absorption data were also available is depicted in Figure 3.4. As can be seen, there is a high level of correlation ($R^2 = 0.91$) between absorption determined in IPPSFs compared to humans.

Dermatopharmacokinetic Studies

The greatest level of precision that may be achieved with this system is to apply pharmacokinetic models either to extrapolate to the *in vivo* situation or to quantitate the fate of the drug within the skin. These are especially adaptable to a system such as the IPPSF because venous drug efflux can be readily determined, which is the starting point for the analysis. If the goal of the study is to predict *in vivo* disposition, then one should view the IPPSF as a "living" infusion pump with output flux (venous efflux) that is actually the input into the systemic circulation. This approach allows one to use porcine skin data to model human skin penetration with human systemic pharmacokinetic data to avoid interspecies differences in systemic drug distribution, metabolism, or elimination. Second, this strategy allows prediction of the actual serum drug concentration–time profile that may be seen *in vivo*. This approach has been used to predict the *in vivo* disposition of a number of drugs, including arbutamine and luteinizing hormone-releasing hormone (Riviere, Williams, et al., 1992; Heit et al., 1993; Williams and Riviere, 1994). The systemic input may be either the observed IPPSF venous efflux profile or the pharmacokinetic simulation of this profile.

The second use of pharmacokinetic modeling is to predict the shape of the cutaneous efflux profile based on factors governing the absorption and distribution of the drug. Our group initiated these studies using drug infused into the arterial cannula by which arterial and venous extraction of the drug could be determined. This approach allowed the basic structure of our IPPSF model to be determined (Williams and Riviere, 1989a). The specific volumes of the extracellular and intracellular spaces were then validated using dual radiolabeled albumin and inulin infusions (Williams and Riviere, 1989b). The next step was to add a percutaneous absorption component (Williams et al., 1990; Carver et al., 1989). This approach allows conduction of an experiment over an 8-h period and use of the venous efflux

profile to determine the parameters of the pharmacokinetic model. If the venous efflux profiles demonstrated a peak or beginning of a plateau phase, then using the model parameters, the 8-h data may be extrapolated to extended time points. Such correlations ($r^2 \approx 0.9$) were determined between extrapolated IPPSF profiles and observed 6-day absorptions for a number of diverse compounds, further demonstrating both the utility of the IPPSF to predict percutaneous absorption in humans as well as the underlying similarity between pig and human skin (Riviere and Monteiro-Riviere, 1991). Because only the total fraction of a topically applied dose absorbed was predicted in these situations, *in vivo* pharmacokinetic data were not needed because a blood concentration–time profile was not available.

The only data used in these models are actual venous efflux profiles and the residual compound recovered at the end of an experiment (e.g., unabsorbed chemical bound to dosing device, skin surface wipes, and drug in the flap). The precision of such models may be greatly improved if the tissue penetration data described above (stratum corneum residues by tape strips, serial sections of biopsy cores) are also included in the data analysis. In addition, if other *in vitro* data such as stratum corneum partition coefficients and rates of evaporation are independently determined in porcine skin (Williams et al., 1994), more sophisticated models may be developed that can shed much greater insight into the mechanisms governing chemical absorption and penetration. Such models may also incorporate the fate of the vehicle used to apply the drug because it is widely acknowledged (but seldom modeled) that vehicle affects the rate and extent of penetration of many compounds (Williams and Riviere, 1995). This approach allows one to take into account penetrating chemical or vehicle interactions with stratum corneum lipids (e.g., enhancers such as Azone®) that could alter permeability to be directly incorporated into the analysis. The work has been extended to study the simultaneous absorption of multiple (more than two) penetrants so that a mechanistic approach to assessing exposure to chemical mixtures may be developed (Riviere et al., 1995). This approach is now applied to the complex absorption patterns seen in topical jet fuel exposure (Riviere et al., 1999). These and other complex mixture studies are fully reviewed in chapter 14 on chemical mixtures.

Absorption of toxic compounds that may alter their own absorption secondary to cutaneous toxicity of the penetrant has been studied using the chemical vesicant sulfur mustard (Riviere et al., 1995). In this model, absorption profiles could only be precisely described if the vascular compartment was modulated as a function of sulfur mustard in the skin. This was independently correlated to vascular volume/permeability using inulin infusions to measure vascular space.

The major limitation to all pharmacokinetic approaches such as these relate to the large data requirements needed to solve model parameters. A full solution for a multicompartment model requires a series of replicated experiments using a single chemical applied at different doses and experiments terminated at various time points. As mentioned, *in vitro* studies would be conducted to obtain specific biophysical parameter estimates. All data are simultaneously analyzed. For many compounds, specific components of the full model may not be required; thus, in reality the actual model fitted is simpler. Statistical algorithms are presently under development to select the optimum model for the specific compound studied and collapse the remainder of the model structure into a matrix from which individual rate parameters

cannot be extracted (Smith et al., 1995). This work has now resulted in the collapse of an equation that describes an IPPSF efflux profile to a three-parameter equation:

$$Y(t) = A(e^{-bt} - e^{-dt})$$

that adequately describes most IPPSF flux profiles (Riviere et al., 2001). This approach allows emphasis to be placed only on those compartments or processes that are important for the chemical studied, yet retains the general structure of the model for all compounds so that future extrapolations are facilitated.

Quantitative Structure–Activity Relationship (QSAR) IPPSF Models

As fully presented in chapter 7 on quantitative structure–activity relationship (QSAR) models in this book, a goal of much dermal absorption research is to be able to predict the absorption profile of a chemical solely based on physical chemical properties. The relationships identified in these analyses are expected to be different from those reported using *in vitro* diffusion cells because the IPPSF consists of different biological components in addition to an intact stratum corneum. The IPPSF, designed to predict *in vivo* absorption, also uses plasma surrogates as perfusate because oncotic pressure is required to maintain capillary perfusion. Although this could partially confound QSAR studies linked to permeability alone, it is more reflective of the *in vivo* end point modeled. It is important to realize that in this approach the model parameters are not steady-state permeability constants but rather pharmacokinetic descriptors (rate and extent) describing a perfusate concentration–flux profile as a function of dose.

IPPSF absorption data on nine chemicals (carbaryl, dimethylamine, methyl salicylate, paranitrophenol, pentachlorophenol, phenol, salicylic acid, sulfur mustard, and theophylline) were fit to the A,b,d model above using standard pharmacokinetic procedures. These compounds had molecular weights ranging from 94 to 390 and log K_{ow} from –0.7 to 9.2. Compounds selected had the same topically applied dose (40 μg/cm^2) applied in an ethanol vehicle under nonoccluded dosing conditions. All had the terminal phase of the perfusate flux profile discernible by hours, a factor that eliminated some slowly absorbed compounds. Although nine compounds are not optimal to fully define a QSAR relationship, these data are presented to illustrate the approach as well as shed light on the factors modulating absorption in the IPPSF.

Using multiple regression analysis (SAS, Cary, NC), the A,b,d parameters and the computed area under the perfusate curve reflecting total absorption were stepwise correlated to a large number of physicochemical parameters. Parameters selected were similar to those previously used to predict permeability through *in vitro* stratum corneum diffusion cells (Potts and Guy, 1992; Buchwold and Bodor, 2001; Sartorelli et al., 1998). Combinatorial regressions were run to confirm the necessity and overall significance of all five physicochemical parameters. The parameters selected were McGowan molecular volumes V_m; hydrogen-bonding energies (donor H-acidity and acceptor H-basicity); water solubilities; and s-polarizabilities (S-Pol) computed using Absolv® software. The results of this analysis are presented in Table 3.2. Correlation plots for the *b* and *d* rate constant regressions are shown in Figure 3.5.

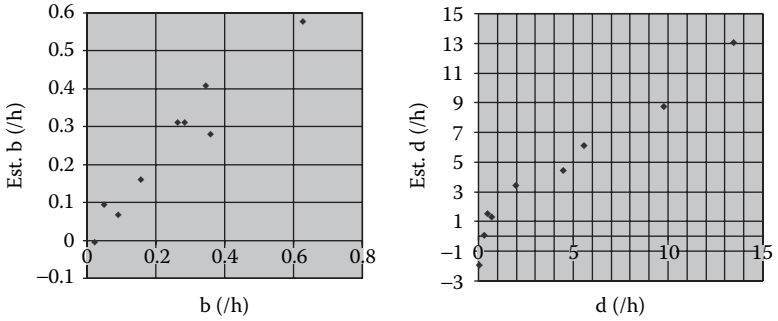

Figure 3.5 Correlation plots for the b and d rate constant estimates.

Table 3.2 IPPSF Absorption Parameters vs. Molecular Descriptors

	Intercept	H-acidity	H-basicity	V_m	S-Polarizability	H_2O Solubility	R^2
A (%D/h)	1.00522	–0.60136	–2.59481	–2.04362	2.57048	0.00765	0.9164
b (/h)	0.91228	–0.8142	–0.91053	–0.33453	0.33704	0.00331	0.9352
d (/h)	16.70476	–19.34336	–15.87366	–1.48847	2.31685	0.06775	0.9503

These data clearly demonstrate that IPPSF flux profiles can be characterized by five physical chemical parameters (H-acidity, H-basicity, V_m, S-Polarizability, and H_2O solubility). The correlation of the AUC of the IPPSF flux profile to these parameters was high (R^2 = 0.978), an important finding because AUC from skin would be the prime measure of systemic exposure in a toxicological risk assessment and could serve as the input function for a physiologically based pharmacokinetic model for a compound. The IPPSF efflux profile from skin reflected by its AUC has been previously used as the input profile for predicting *in vivo* human plasma–concentration time profiles after transdermal drug delivery (Riviere, Williams, et al., 1992).

Compared to such correlations based on stratum corneum permeability studies, IPPSF profiles may have additional parameters related to penetrant interactions with nonlipid components of the skin. Earlier exploratory analyses indicated that the d parameter in the above model was most closely correlated to $K_{o/w}$ (R^2 = 0.67), suggesting it is a parameter related to stratum corneum permeability. Note, however, that in a pharmacokinetic model, the epidermal permeability coefficient is not a single rate constant but rather would be a microconstant defined by the model's differential equations. This is a limitation of using the empirical A,b,d modeling approach.

This analysis suggests that the QSPR relationship for chemical percutaneous absorption in the biologically intact IPPSF requires five descriptors that are similar in nature to those previously used for *in vitro* models. Because all QSPR models utilize different chemicals and exposure conditions, it is hard to mechanistically compare these IPPSF results to earlier attempts. For example, molecular volume and hydrogen bond acidity and basicity were sufficient in the Potts and Guy (1995)

model. These terms are also present in the IPPSF model; however, polarizability and water solubility are also needed. Further comparisons would be too speculative as additional research using larger series of chemical analogues controlling for these properties would be required to make definitive statements. The data reported here indicate that IPPSF flux profiles for a diverse series of nine chemicals can be accurately predicted using a QSPR model containing H-acidity, H-basicity, V_m, S-Polarizability, and H_2O solubility.

Cutaneous Biotransformation

The final aspect of assessing percutaneous absorption is the role of cutaneous biotransformation. The IPPSF is ideally suited for this purpose and has been used to study metabolism of pesticides, drugs, and endogenous compounds (Bikle et al., 1994; Carver et al., 1990; Chang et al., 1994; Riviere et al., 1996). Specific pharmacokinetic models that incorporate IPPSF data and *in vivo* disposition have been constructed (Qiao et al., 1994; Qiao and Riviere, 1995). Increased absorption of pentacholorophenol (PCP)-associated label was detected after pretreatment with the cytochrome p450 inducer benzo[a]pyrene (Qiao and Riviere, 2002). Of note, both the perfusate flux and cutaneous distribution profiles were altered. These studies demonstrated a number of important features of percutaneous absorption of chemicals that are biotransformed during passage through the skin. The method of dose application significantly affects the metabolic profile observed in the venous efflux. Occlusion enhances the fraction of parathion metabolized to paranitrophenol in both the IPPSF and the *in vivo* pig. The mechanism of this effect has not been determined, although it illustrates the inherent complexity of skin relative to assessing the fate of chemicals applied on its surface. By constructing dermatopharmacokinetic models to address these phenomena, quantitative parameters describing absorption and cutaneous distribution independent of biotransformation may be used as experimental end points.

The primary implication of biotransformation to risk assessment is that commonly employed *in vitro* to *in vivo* extrapolation strategies are actually oversimplified because they assume all inputs from the skin to the general circulation are in the form of parent chemical. In reality, multiple inputs from the skin to systemic circulation, reflecting dermal biotransformation, may be required. This makes the extrapolation process more complex.

Percutaneous Absorption of Vasoactive Chemicals

One of the major advantages of using an isolated perfused tissue preparation is the presence of an intact vascular system with dermal microcirculation. This is important from the perspective of assessing the effect of altered blood flow on compound disposition as well as determining how a penetrating chemical's inherent vasoactivity affects its own fate. Blood flow effects on absorption are presented in chapter 13. Unlike other organ systems, the range of blood flow possible through mammalian skin is tremendous because of its role in thermoregulation. The primary impact of altered dermal perfusion on the disposition of penetrated chemical may be on the

surface area of the exchanging capillaries perfused, which determines the actual volume of dermis perfused and thus available for systemic absorption (Riviere and Williams, 1992; Williams and Riviere, 1995). Alternatively, changes in dermal perfusion resulting from modulation of arterial–venous shunt activity may completely bypass areas of skin or result in deeper dermal penetration, a phenomenon observed *in vivo* with piroxicam (Monteiro-Riviere, Inman, et al., 1993). Changes in dermal perfusion may be initiated by physiological homeostatic mechanisms, by exposure to vasoactive drugs, or secondarily by chemically induced irritation with concomitant release of vasoactive inflammatory mediators (e.g., prostaglandins). Using glucose utilization as a measurement of exchanging capillary perfusion, we have recently begun to map out the IPPSF vascular response to the infusion of vasoactive drugs in an attempt to experimentally define the pharmacodynamics of vasoactive drugs in this system for future integration into a comprehensive pharmacokinetic–pharmacodynamic model (Rogers and Riviere, 1994).

The impact of a drug's vasoactivity on its rate and extent of percutaneous absorption and distribution within skin can best be illustrated with IPPSF studies on the iontophoretic transdermal delivery of lidocaine coadministered with the vasodilator tolazoline or the vasoconstrictor norepinephrine (Riviere et al., 1991; Riviere, Monteiro-Riviere, et al., 1992). Coiontophoresis of both these compounds using *in vitro* diffusion cell systems resulted in essentially no effect on lidocaine flux. However, identical *in vivo* dosing conditions resulted in increased blood concentrations when tolazoline was present. Tolazoline enhanced and norepinephrine decreased lidocaine flux in IPPSF studies. When one examined the concentrations in the skin underlying these electrodes, the opposite pattern was seen. These vascular effects have now been incorporated into our dermatopharmacokinetic model (Williams and Riviere, 1993). These studies clearly demonstrated the importance of the microcirculation in determining the non-steady-state profile of drug delivery and dermal disposition. These data also suggest use of vasoactive compounds may confound results of a QSAR study such as discussed above.

CONCLUSION

The presentation here provides an overview of the uses of a perfused skin model such as the IPPSF in percutaneous absorption and dermatotoxicokinetic studies. One of its major advantages is that both absorption and toxicity may be assessed in the same preparation. The pharmacokinetic models developed are experimentally verifiable. The major limitations are centered on the cost of the preparation and the technical expertise required to successfully conduct the studies. The overall cost is significantly greater than *in vitr*o diffusion cell studies or *in vivo* rodent experiments, comparable to human skin equivalent and larger mammal (dog, pig, primate) *in vivo* work and much less expensive than human trials. However, cost alone is not a sufficient criterion. These studies are humane; more information may be gathered than is obtainable with either *in vitro* or *in vivo* work. Optimal benefit may be achieved if these studies serve as a bridge between *in vitro* human/animal and *in*

vivo animal work and the ultimate *in vivo* human exposure scenario. The further development of QSAR models would greatly facilitate this bridging.

REFERENCES

Behrendt, H. and Kampffmeyer, H.G., 1989, Absorption and ester cleavage or methyl salicylate by skin of single-pass perfused rabbit ears, *Xenobiotica*, 19:131–141.

Bikle, D.D., Halloran, B.P., and Riviere, J.E., 1994, Production of 1,25-dihydroxyvitamine D_3 by perfused pig skin, *J. Invest. Dermatol.,* 102:796–798.

Bowman, K.F., Monteiro-Riviere, N.A., and Riviere, J.E., 1991, Development of surgical techniques for preparation of *in vitro* isolated perfused porcine skin flaps for percutaneous absorption studies, *Am. J. Vet. Res.,* 25:75–82.

Bristol, D.G., Riviere, J.E., Monteiro-Riviere, N.A., Bowman, K.F., and Rogers, R.A., 1991, The isolated perfused equine skin flap: pPreparation and metabolic parameters, *Vet. Surg.,* 20:424–433.

Buchwald, P., and Bodor, N., 2001, A simple, predictive, structure-based skin permeability model, *J. Pharm. Pharmacol.,* 53, 1087–1098.

Carver, M.P., Levi, P.E., and Riviere, J.E., 1990, Parathion metabolism during percutaneous absorption in perfused porcine skin, *Pest. Biochem. Physiol.,* 38:245–254.

Carver, M.P., Williams, P.L., and Riviere, J.E., 1989, The isolated perfused porcine skin flap (IPPSF). III. Percutaneous absorption pharmacokinetics of organophosphates, steroids, benzoic acid and caffeine, *Toxicol. Appl. Pharmacol.,* 97:324–337.

Celesti, L., Murratzu, C., Valoti, M., Sgaragli, G., and Corti, P., 1993, The single-pass perfused rabbit ear as a model for studying percutaneous absorption of clonazepam, *Methods Find. Exp. Clin. Pharmacol.,* 15:49–56.

Chang, S.K., Williams, P.L., Dauterman, W.C., and Riviere, J.E., 1994, Percutaneous absorption, dermatopharmacokinetics, and related biotransformation studies of carbaryl, lindane, malathion and parathion in isolated perfused porcine skin, *Toxicology,* 91:269–280.

Chilcott, R.P., Jenner, J., Hotchkiss, S.A.M., and Rice, P., 2001, *In vitro* skin absorption and decontamination of sulphur mustard: comparison of human and pig-ear skin, *J. Appl. Toxicol.,* 21:279–283.

de Lange, J., van Eck, P., Elliott, G.R., de Kort, W.L.A.M., and Wolthius, O.L., 1992, The isolated blood-perfused pig ear: an inexpensive and animal saving model for skin penetration studies, *J. Pharmacol. Toxicol. Methods,* 27:71–77.

Duncan, E.J.S., Brown, A., Lundy, P., Sawyer, T.W., Hamilton, M., Hill, I., and Conley, J.D., 2002, Site-specific percutaneous absorption of methyl salicylate and VX in domestic swine, *J. Appl. Toxicol.,* 22:141–148.

Feldberg, W. and Paton, W.D.M., 1951, Release of histamine from skin and muscle in the cat by opium alkaloids and other histamine liberators, *J. Physiol.,* 114:490–509.

Heit, M., Williams, P., Jayes, F.L., Chang, S.K., and Riviere, J.E., 1993, Transdermal iontophoretic peptide delivery. *In vitro* and *in vivo* studies with luteinizing hormone releasing hormone (LHRH), *J. Pharm. Sci.,* 82:240–243.

Hiernickel, H., 1985, An improved method for *in vitro* perfusion of human skin, *Br. J. Dermatol.,* 112:299–305.

Kietzmann, M., Arens, D., Loscher, W., and Lubach, D., 1991, Studies on the percutaneous absorption of dexamethasone using a new *in vitro* model, the isolated perfused bovine udder, in *Prediction of Percutaneous Penetration* (R.C. Scott, R.H. Guy, J. Hadgraft, and H.E. Bodee, eds.), IBC Technical Services, London, pp. 519–526.

King, J.R. and Monteiro-Riviere, N.A., 1990, Cutaneous toxicity of 2-chloroethyl methyl sulfide in isolated perfused porcine skin, *Toxicol. Appl. Pharmacol.,* 104:167–179.

King, J.R., Peters, B.P., and Monteiro-Riviere, N.A., 1994, Matrix molecules of the epidermal basement membrane as targets for chemical vesication with lewisite, *Toxicol. Appl. Pharmacol.,* 126:164–173.

King, J.R., Riviere, J.E., and Monteiro-Riviere, N.A., 1992, Characterization of lewisite toxicity in isolated perfused skin, *Toxicol. Appl. Pharmacol.,* 116:189–201.

Kjaersgaard, A.R., 1954, Perfusion of isolated dog skin, *J. Invest. Dermatol.,* 22:135–141.

Kreidstein, M.L., Pang, C.Y., Levine, R.H., and Knowlton, R.J., 1991, The isolated perfused human skin flap: design, perfusion technique, metabolism and vascular reactivity, *Plast. Reconstr. Surg.,* 87:741–749.

Kreuger, G.G., Wojciechowski, Z.J., Burton, S.A., Gilhar, A., Huether, S.E., Leonard, L.G., Rohr, U.D., Petelenz, T.J., Higuchi, W.I., and Pershing, L.K., 1985, The development of a rat/human skin flap served by a defined and accessible vasculature on a congenitally athymic (nude) rat, *Fundam. Appl. Toxicol.,* 5:S112–S121.

Monteiro-Riviere, N.A., 1990, Altered epidermal morphology secondary to lidocaine iontophoresis: *in vivo* and *in vitro* studies in porcine skin, *Fundam. Appl. Toxicol.,* 15:174–185.

Monteiro-Riviere, N.A., 1992, Use of isolated perfused skin model in dermatotoxicology, *In Vitro Toxicol.,* 5:219–233.

Monteiro-Riviere, N.A., Baynes, R.E., and Riviere, J.E., 2003, Pyridostigmine bromide modulates topical irritant-induced cytokine release from human epidermal keratinocytes and isolated perfused porcine skin, *Toxicology,* 183:15–28.

Monteiro-Riviere, N.A., Bowman, K.F., Scheidt, V.J., and Riviere, J.E., 1987, The isolated perfused porcine skin flap (IPPSF): II. Ultrastructural and histological characterization of epidermal viability, *In Vitro Toxicol.,* 1:241–252.

Monteiro-Riviere, N.A., Bristol, D.G., Manning, T.O., Rogers, R.A., and Riviere, J.E., 1990, Interspecies and interegional analysis of the comparative histological thickness and laser Doppler blood flow measurements at five cutaneous sites in nine species, *J. Invest. Dermatol.,* 95:582–586.

Monteiro-Riviere, N.A. and Inman, A.O., 1995, Indirect immunohistochemistry and immunoelectron microscopy distribution of eight epidermal-dermal junction epitopes in the pig and in isolated perfused skin treated with *bis*(2-chloroethyl) sulfide, *Toxicol. Pathol.,* 23:313–325.

Monteiro-Riviere, N.A., Inman, A.O., and Riviere, J.E., 1994a, Development and characterization of a novel skin model for phototoxicology, *Photodermatol. Photoimmunol. Photomed.* 10:235–243.

Monteiro-Riviere, N.A., Inman, A.O., and Riviere, J.E., 1994b, Identification of the pathway of iontophoretic drug delivery: light and ultrastructural studies using mercuric chloride in pigs, *Pharm. Res.* 11:251–256.

Monteiro-Riviere, N.A., Inman, A.O., and Riviere, J.E., 2001, The effects of short-term high dose and low dose dermal exposure to jet A, JP-8, and JP-8 +100 jet fuels, *J. Appl. Toxicol.* 21:485–494.

Monteiro-Riviere N.A., Inman, A.O., and Riviere, J.E., 2004, Skin toxicity of jet fuels: ultrastructural studies and the effects of substance P, *Toxicol. Appl. Pharmacol.*, 195:339–347.

Monteiro-Riviere, N.A., Inman, A.O., Riviere, J.E., McNeill, S.C., and Francoeur, M.L., 1993, Topical penetration of piroxicam is dependent on the distribution of the local cutaneous vasculature, *Pharm. Res.,* 10:1326–1331.

Monteiro-Riviere, N.A., Stinson, A.W., and Calhoun, H.L., 1993, Integument, in *Textbook of Veterinary Histology*, 4th ed. (H.D. Dellmann, ed.), Lea and Febiger, Philadelphia, pp. 285–312.

Potts, R.O. and Guy, R.H., 1992, Predicting skin permeability, *Pharm. Res.,* 9:663–669.

Potts, R.O. and Guy, R.H., 1995, A predictive algorithm for skin permeability: the effects of molecular size and hydrogen bond activity, *Pharm. Res.,* 12:1628–1633.

Qiao, G.L. and Riviere, J.E., 1995, Significant effects of application site and occlusion on the pharmacokinetics of cutaneous penetration and biotransformation of parathion *in vivo* in swine, *J. Pharm. Sci.,* 84:425–432.

Qiao, G.L. and Riviere, J.E., 2000, Dermal absorption and tissue disposition of 3,3′,4,4′-tetrachlorobiphenyl (TCB) in an *ex vivo* pig model: assessing the impact of dermal exposure variables, *Int. J. Occup. Environ. Health,* 6:127–137.

Qiao, G.L. and Riviere, J.E., 2002, Systemic uptake and cutaneous disposition of pentachlorophenol in a sequential exposure scenario: effects of skin preexposure to benzo[a]pyrene, *J. Toxicol. Environ. Health, Part A*, 65:1307–1331.

Qiao, G.L., Williams, P.L., and Riviere, J.E., 1994, Percutaneous absorption, biotransformation and systemic disposition of parathion *in vivo* in swine. I. Comprehensive pharmacokinetic model, *Drug Metab. Dispos.,* 22:459–471.

Rhyne, B.N., Pirone, J.P., Riviere, J.E., and Monteiro-Riviere, N.A., 2002, The use of enzyme histochemistry in detecting cutaneous toxicity of three topically applied jet fuel mixtures, *Toxicol. Mechanisms Methods,* 12:17–34.

Riviere, J.E., Bowman, K.F., Monteiro-Riviere, N.A., Carver, M.P., and Dix, L.P., 1986, The isolated perfused porcine skin flap (IPPSF). I. A novel *in vitro* model for percutaneous absorption and cutaneous toxicology studies, *Fundam. Appl. Toxicol.,* 7:444–453.

Riviere, J.E., Brooks, J.D., and Qiao, G.L., 2000, Methods for assessing the percutaneous absorption of volatile chemicals in isolated perfused skin: studies with chloropentafluorobenzene (CPFB) and dichlorobenzene (DCB), *Toxicol. Methods,* 10:265–281.

Riviere, J.E., Brooks, J.D., Williams, P.L., McGowan, E., and Francoeur, M.L., 1996, Cutaneous metabolism of isosorbide dinitrate after transdermal administration in isolated perfused porcine skin, *Int. J. Pharm.,* 127:213–217.

Riviere J.E., Brooks, J.D., Williams, P.L., and Monteiro-Riviere, N.A., 1995, Toxicokinetics of topical sulfur-mustard penetration, disposition and vascular toxicity in isolated perfused porcine skin, *Toxicol. Appl. Pharmacol.*, 135:25–34.

Riviere, J.E. and Monteiro-Riviere, N.A., 1991, The isolated perfused porcine skin flap as an *in vitro* model for percutaneous absorption and cutaneous toxicology, *Crit. Rev. Toxicol.,* 21:329–344.

Riviere, J.E., Monteiro-Riviere, N.A., Brooks, J.D., Budsaba, K., and Smith, C.E. 1999. Dermal absorption and distribution of topically dosed jet fuels Jet A, JP-8, and JP-8(100), *Toxicol. Appl. Pharmacol.,* 160:60–75.

Riviere, J.E., Monteiro-Riviere, N.A., and Inman, A.O., 1992, Determination of lidocaine concentration in skin after transdermal iontophoresis: effects of vasoactive drugs, *Pharm. Res.,* 9:211–214.

Riviere, J.E., Monteiro-Riviere, N.A., Rogers, R.A., Bommannan, D., Tamada, J.A., and Potts, R.O., 1995, Pulsatile transdermal delivery of LHRH using electroporation. Drug delivery and skin toxicology, *J. Controlled Release,* 36:229–233.

Riviere, J.E., Sage, B.S., and Williams, P.L., 1991, The effects of vasoactive drugs on transdermal lidocaine iontophoresis, *J. Pharm. Sci.,* 80:615–620.

Riviere, J.E., Smith, C.E., Budsaba, K., Brooks, J.D., Olajos, E.J., Salem, H., and Monteiro-Riviere, N.A., 2001, Use of methyl salicylate as a simulant to predict the percutaneous absorption of sulfur mustard, *J. Appl. Toxicol.,* 21:91–99.

Riviere, J.E. and Williams, P.L., 1992, Pharmacokinetic implications of changing blood flow in skin, *J. Pharm. Sci.,* 81:601–602.

Riviere, J.E., Williams, P.L., Hillman, R., and Mishky, L., 1992, Quantitative prediction of transdermal iontophoretic delivery of arbutamine in humans using the *in vitro* isolated perfused porcine skin flap (IPPSF), *J. Pharm. Sci.,* 81:504–507.

Riviere, J.E., Williams, P.L., and Monteiro-Riviere, N.A., 1995, Mechanistically defined chemical mixtures (MDCM): a new experimental paradigm for risk assessment applied to skin, *Toxicologist,* 15:323–324.

Rogers, R.A. and Riviere, J.E., 1994, Pharmacologic modulation of cutaneous vascular resistance in the isolated perfused porcine skin flap (IPPSF), *J. Pharm. Sci.,* 83:1682–1689.

Sartorelli, P., Aprea, C., Cenni, A., Novelli, M.T., Orsi, D., Palmi, S., and Matteucci, G., 1998, Prediction of percutaneous absorption from physiochemical data: a model based on data of *in vitro* experiments, *Ann. Occup. Hyg.,* 42:267–276.

Sekkat, N., Kalia, Y.N., and Guy R.H., 2004, Porcine ear skin as a model for the assessment of transdermal drug delivery to premature neonates, *Pharm. Res.,* 21:1390–1397.

Silcox, G.D., Parry, G.E., Bunge, A.L., Pershing, L.K., and Pershing, D.W., 1990, Percutaneous absorption of benzoic acid across human skin. II. Prediction of an *in vivo*, skin-flap system using *in vitro* parameters, *Pharm. Res.,* 7:352–358.

Smith, C.E., Williams, P.L., and Riviere, J.E., 1995, Compartment model of skin transport. A dominant eigenvalue approach, *Proc. Biometric Sect., Am. Stat. Assoc.,* 449–454.

Srikrishna, V., Riviere, J.E., and Monteiro-Riviere, N.A., 1992, Cutaneous toxicity and absorption of paraquat in porcine skin, *Toxicol. Appl. Pharmacol.,* 115:89–97.

Vaden, S.L., Page, R.L., Peters, B.P., Cline, J.M., and Riviere, J.E., 1993, Development and characterization of an isolated and perfused tumor and skin preparation for evaluation of drug disposition, *Cancer Res.,* 53:101–105.

Wester, R.C., Melendres, J., Sedik, L., Maibach, H.I., and Riviere, J.E., 1998, Percutaneous absorption of salicylic acid, theophylline, 2,4-dimethylamine, diethyl hexylphthalic acid and ρ-aminobenzoic acid in the isolated perfused porcine skin flap compared to man, *Toxicol. Appl. Pharmacol.,* 151:159–165.

Williams, P.L., Brooks, J.D., Inman, A.I., Monteiro-Riviere, N.A., and Riviere, J.E., 1994, Determination of physiochemical properties of phenol, paranitrophenol, acetone and ethanol relevant to quantitating their percutaneous absorption in porcine skin, *Res. Commun. Chem. Pathol. Pharmacol.,* 83:61–75.

Williams, P.L., Carver, M.P., and Riviere, J.E., 1990, A physiologically relevant pharmacokinetic model of xenobiotic percutaneous absorption utilizing the isolated perfused porcine skin flap (IPPSF), *J. Pharm. Sci.,* 79:305–311.

Williams, P.L. and Riviere, J.E., 1989a, Definition of a physiologic pharmacokinetic model of cutaneous drug distribution using the isolated perfused porcine skin flap (IPPSF), *J. Pharm. Sci.,* 78:550–555.

Williams, P.L. and Riviere, J.E., 1989b, Estimation of physiological volumes in the isolated perfused porcine skin flap, *Res. Commun. Chem. Pathol. Pharmacol.,* 66:145–158.

Williams, P.L. and Riviere, J.E., 1993, A model describing transdermal iontophoretic delivery of lidocaine incorporating consideration of cutaneous microvascular state, *J. Pharm. Sci.,* 82:1080–1084.

Williams, P.L. and Riviere, J.E., 1994, A "full-space" method for predicting *in vivo* transdermal plasma drug profiles reflecting both cutaneous and systemic variability, *J. Pharm. Sci.,* 83:1062–1064.

Williams, P.L. and Riviere, J.E., 1995, A biophysically-based dermatopharmacokinetic compartment model for quantifying percutaneous penetration and absorption of topically applied agents. I. Theory, *J. Pharm. Sci.,* 84:599–608.

Wojciechowski, Z., Pershing, L.K., Huether, S., Leonard, L., Burton, S.A., Higuchi, W.I., and Krueger, G.G., 1987, An experimental skin sandwich flap on an independent vascular supply for the study of percutaneous absorption, *J. Invest. Dermatol.,* 88:439–446.

Zhang, A., Riviere, J.E., and Monteiro-Riviere, N.A., 1995a, Evaluation of protective effects of sodium thiosulfate, cysteine, niacinamide and indomethacin on sulfur mustard-treated isolated perfused porcine skin, *Chem.-Biol. Interact.,* 96:249–262.

Zhang, A., Riviere, J.E., and Monteiro-Riviere, N.A., 1995b, Topical sulfur mustard induces changes in prostaglandins and interleukin 1a in isolated perfused porcine skin, *In Vitro Toxicol.,* 8:149–158.

Zhang, A., Peters B.P., and Monteiro-Riviere, N.A., 1995, Assessment of sulfur mustard interaction with basement membrane components, *Cell Biol. Toxicol.* 11:89–101.

CHAPTER 4

In Vivo Models

Faqir Muhammad and Jim E. Riviere

CONTENTS

INTRODUCTION

As an outer protective covering of the body, the skin is in continuous contact with a variety of environmental and toxic substances, serving as a primary barrier to absorption and systemic exposure. Yet, transdermal drug delivery is also an intentional mode for skin contact with xenobiotics because of the numerous advantages inherent to this technique for the systemic administration of drugs. These include good patient compliance to a simple therapeutic regimen, increase in bioavailability

because of elimination of hepatic first-pass effect, controlled delivery of drugs with short biological half-lives, and avoidance of the risks and inconveniences of injection.

The determination of rate and extent of dermal absorption of drugs and chemicals remains a challenge for workers in this field. When does the skin function as a barrier, and when does it function as a portal of entry for topically applied chemicals? Different *in vitro* and *ex vivo* approaches have been documented (see other chapters in this text); however, *in vivo* percutaneous absorption serves as a standard for the validation of other absorption methods. This is because chemical and drug percutaneous absorption is influenced by a variety of biological (skin age, skin condition, anatomical site, skin metabolism, blood flow), physicochemical (hydration, drug–skin binding, temperature), and pharmaceutical factors (pK_a of drugs, viscosity and composition of vehicles) that are difficult to replicate with *in vitro* and *ex vivo* models. To account for the importance of these factors, *in vivo* methods are paramount because they assess the actual magnitude of percutaneous absorption of chemicals seen in the intact organism. In fact, many consider *in vivo* human models the "gold standard" against which other data are compared, followed by perfused skin and primate or swine skin models (Howes et al., 1996).

ANIMAL MODEL SELECTION

Numerous animal models have been developed for the prediction of dermal absorption in humans with variable degrees of correlations (Benfeldt, 1999; Kreilgaard, 2001; Wester and Maibach, 1992). The comparative biology of skin is discussed in chapter 1. Uncertainties in extrapolations between animals raise the need to determine the dermal absorption in multiple target species, including humans when possible. The available information on comparative penetration studies in human and laboratory rodents is complex and compound dependent. Rats provide a conservative alternative to humans because the percutaneous absorption of many chemicals is typically two- to fivefold higher than in humans (Bartek et al., 1972; Simon and Maibach, 1998; Johannes et al., 2000). This is acceptable if a toxicological risk assessment is conducted; however, rodent skin may not be a reasonable model to simulate the barrier properties of human skin (Kraeling et al., 1998) if prediction of precise transdermal flux is the goal of the research. Other animal models often employed include swine, rabbits, guinea pigs, dogs, and rhesus monkeys (Bartek et al., 1972; Reifenrath et al., 1984; Bronaugh et al., 1985, Wester and Maibach, 1989; Panchagnula et al., 1997; Hikima et al., 2002). All animal models may be appropriate for specific investigations, but the extrapolation of these results to humans must be made cautiously with this difference in permeability in mind.

Although the basic structure of skin is similar in most terrestrial mammals, between- and within-species differences exist in the thickness of the epidermis and dermis in various regions of the body (Monteiro-Riviere, 1991; Chapter 1, this volume). For example, in the pig, epidermal and stratum corneum thickness is almost twice that in cattle and horses. Stratum corneum thickness in sheep is similar to that in cattle, yet the epidermis in sheep is only half as thick. Other investigators have speculated that transappendagial transport of drugs across skin in cattle and sheep

may be more important than the transcellular or intercellular pathways as expected in humans and other animal species (Pitman and Rostas, 1982; Chen and Wilkinson, 1989). Skin appendages, including hair follicles, sweat glands, arrector pili muscles, and sebaceous glands, are more prevalent in certain body regions and vary dramatically across species. Extensive lanolin secretion in sheep may modify chemical absorption. Appendages may create aqueous channels that allow the passage of some small polar compounds into the skin (Riviere, 1990; Lauer et al., 1997). This hypothesis has not been vigorously tested across animal species.

Porcine skin is widely used in absorption studies because it is functionally and structurally similar to that of human skin (Monteiro-Riviere, 1991; Simon and Maibach, 2000). Swine are sparsely covered with hair like humans. The pigmentation characteristics and the vasculature of pigs are similar to those of humans (Monteiro-Riviere, 1996; Cole, 1990), as are stratum corneum lipid composition and biophysical properties, as well as epidermal turnover kinetics (approximately 30 days) (Morris et al., 1987; Sato et al., 1991; Monteiro-Riviere and Riviere, 1996). Taking these similarities into consideration, percutaneous absorption of toxic substances through porcine skin has often been shown to mimic absorption through human skin (Bartek et al., 1972; Reifenrath et al., 1984). Studies have demonstrated that the range of percutaneous absorption of carbaryl, lindane, malathion, and parathion in pig skin *in vivo* (Carver and Riviere, 1989) or *in vitro* (Chang et al., 1994) was similar to that observed in humans (Feldmann and Maibach, 1974). The permeability of hydrophilic chemicals (mannitol, water, and paraquat) and lipophilic chemicals (carbaryl, aldrin, and fluazifop-butyl) in porcine skin was compared with human abdominal skin and rat dorsal skin (Dick and Scott, 1992). This study also demonstrated that, for hydrophilic chemicals, pig ear skin and rat skin overestimated permeability in human skin. In a site comparison of methyl salicylate and VX absorption in swine, ear skin had significantly greater transdermal flux than other sites studied (Duncan et al., 2002). Although permeability was generally higher in animal skin than in human skin for the lipophilic chemicals, permeability of carbaryl in human and porcine skin was almost identical. Other *in vitro* studies have demonstrated similar permeability values in porcine and human skin for hydrophilic chemicals such as acetylsalicylic acid, urea (Bronaugh et al., 1982), and benzoic acid (Bhatti et al., 1988). Chapter 3 on perfused skin models should be consulted for further comparisons between human and porcine skin.

IN VIVO METHODS FOR ASSESSMENT OF DERMAL ABSORPTION

There are numerous approaches for assessing absorption *in vivo* in animals and humans. Although the common thread between them is their use in intact organisms, they do assess different components of the dermal absorption and penetration process. These are briefly introduced here in the context of what they are actually measuring and how a specific method's limitations may affect interpretation. Figure 4.1 illustrates the relationship between the fate of a compound within the skin and the *in vivo* methods discussed in this chapter. The primary developments in this area over recent years have been in response to developing more noninvasive

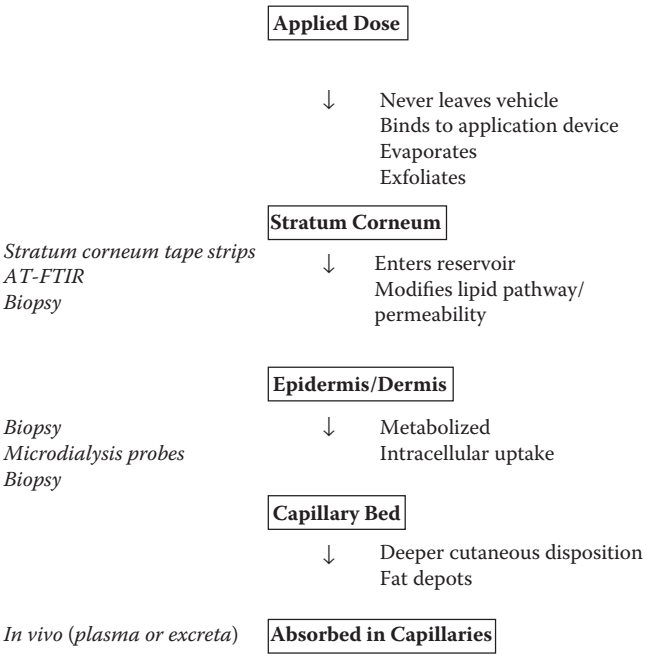

Figure 4.1 Fate of a topically applied compound in skin relative to *in vivo* methods used to assess absorption.

techniques, which are less stressful to animals undergoing these studies. This direction will continue into the future.

Mass Balance

A classic technique employed in pharmacology and toxicology disposition studies for all routes of administration is the mass balance approach (Riviere, 1999). Mass balance analysis accounts for all of the topically applied dose of the compound, whether it is in the formulation, associated with the skin surface, penetrated into the stratum corneum, distributed into the carcass, or absorbed into and excreted from the blood into urine and feces. In this context, total recovery of 90% of the applied dose is considered excellent recovery (Schaefer and Redelmeier, 1996). Mass balance studies are conducted by collecting all excreta after topical and parenteral administration. Data from a parenteral route such as intravenous dosing is required to correct for the fraction of absorbed compound appearing into the excreta collected if a precise estimate of bioavailability is to be determined and all routes of excretion are not collected (e.g., collection of urine and feces but not expired air) (Riviere, 1999). In such a study, absorption is calculated as follows:

$$\text{Absorption} = [\text{Urine} + \text{Feces}]_{\text{Topical}} \times \text{Dose}_{\text{iv}}/[\text{Urine} + \text{Feces}]_{\text{iv}} \times \text{Dose}_{\text{Topical}}$$

Instead, if blood samples alone are used to assess systemic absorption, then a similar approach is utilized by comparing total exposure by topical and intravenous administration. Total absorption in blood is assessed by determining the area under the curve (AUC) of the chemical concentration–time profiles using the sum of trapezoids or other curve integration techniques. Absorption is then calculated as

$$\text{Absorption} = \text{AUC}_{\text{Topical}} \times \text{Dose}_{\text{iv}}/\text{AUC}_{\text{iv}} \times \text{Dose}_{\text{Topical}}$$

Both of these approaches allow for assessment of systemic absorption by not conducting complete mass balance studies (e.g., expired air to catch absorbed compound metabolized to CO_2 or H_2O expired end products). *In vivo* dermal absorption studies not taking into account other routes of excretion must be interpreted with caution. One extension of this mass balance excretory analysis is to assess dermal absorption by only monitoring the primary excretory route for the compound studied. Dermal bioavailability has been assessed in exhaled breath using real-time ion trap mass spectrometry to track the uptake and elimination of compounds (e.g., trichloroethylene) from dermal exposure in humans and rats (Poet et al., 2000). A physiologically based pharmacokinetic model can be used to estimate the total bioavailability of compounds. The same approach was extended to determine the dermal uptake of volatile chemicals under non-steady-state conditions using real-time breath analysis in rats, monkeys, and humans (Thrall et al., 2000).

The mass balance approach was employed in the classical studies by Feldmann and Maibach (1969, 1970) that largely defined *in vivo* methodology up to the present. An interesting study illustrating this approach involved dermal penetration and absorption of ^{14}C-malathion in the Sprague-Dawley rat examined by three analytical techniques after topical application in different vehicles (Dary et al., 2001). This provides a basis for comparing *in vivo* data with other approaches. Tape-stripping followed by instant electronic autoradiography assessed the penetration of ^{14}C-malathion into the stratum corneum. Fourier transform infrared spectroscopy (FTIR) was used to identify malathion in skin sections. The absorption of ^{14}C-malathion was measured in various tissues and in the residual carcass using liquid scintillation counting. Penetration into the stratum corneum followed a linear trend. The capacity of the corneal reservoir for malathion was approximately 1% of the dermal dose; however, 6% of the dose was absorbed.

The mass balance approach was used to develop an *in vivo* animal model for skin penetration of topically applied drugs in hairless rats (Simonsen et al., 2002). Two drugs, ^{14}C-salicylic acid and ^{14}C-butyl salicylate were topically applied for the assessment of the model. Rapid and differentiated percutaneous absorption of both compounds was indicated by urinary excretion data. Total mass balance on the applied radioactivity was performed, and 90% recovery was achieved. Carver and Riviere (1989) conducted an extensive mass balance study with ^{14}C-labeled xenobiotics after topical and intravenous administration to pigs. These authors reported that dermal absorption of ^{14}C-benzoic acid, caffeine, malathion, parathion, progesterone, and testosterone was 25.7, 11.8, 5.2, 6.7, 16.2, and 8.8%, respectively, following topical administration to pigs.

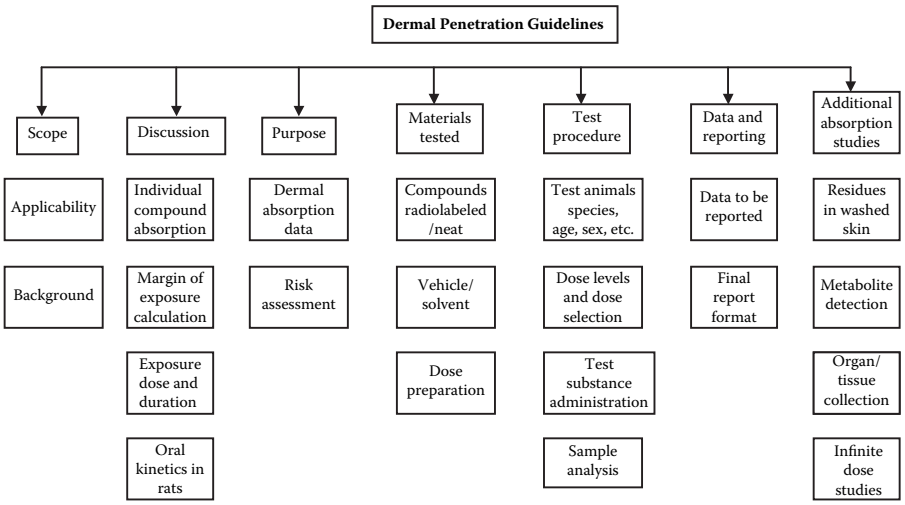

Figure 4.2 A schematic overview of EPA health effects test guidelines for dermal penetration studies.

The mass balance concept serves as the foundation of the Environmental Protection Agency (EPA) guidelines for assessing percutaneous absorption of chemicals (U.S. EPA, 1998). The combined use of the mass balance procedure coupled with detection and measurement of a substance in the stratum corneum and deeper layers of the skin may provide valuable information for exposure assessment. A schematic overview of the EPA Health Effects Test Guidelines for Dermal Penetration Studies is presented in Figure 4.2. A few points are highlighted:

1. *Scope*: These guidelines are according to the test requirements of the Federal Insecticide, Fungicide, and Rodenticide Act and the Toxic Substances Control Act.
2. *Discussion*: A risk assessment must be performed to determine the need for a dermal absorption study. The dermal absorption studies may be conducted for individual compounds having serious toxic effects after oral or nasal administration. Low-effect and no-effect doses from these studies can then be directly used for calculation of margin of exposure. The essential information on dermal exposure is gathered to determine doses and duration of exposure to be evaluated in dermal absorption studies. It is recommended that an oral kinetic study in rats be used to utilize the kinetic parameters in risk assessment. The dermal studies generate a "route-to-route" scaling factor for interpreting other systemic toxicology studies.
3. *Purpose*: The dermal absorption data enable EPA to make risk assessments when the oral or inhalation route determined the toxic effects in defined laboratory animal models yet the exposure to humans is expected by the dermal route. A complete kinetic analysis is essential to convert oral or inhalation low-effect and no-effect doses into dermal low-effect and no-effect doses. This allows for the calculation of margin of exposure or risk to predict systemic toxic effects that otherwise may not be tested practically by the dermal route. The rat is the preferred model because a large toxicology database exists in this species. The rat absorption

data are not intended to be used to estimate human dermal absorption; rather, they are intended to facilitate route-to-route scaling of rodent toxicology data generated by other routes of administration.

4. *Materials to be tested*: EPA prefers that a radiolabeled compound of known chemical purity be employed. Care must be taken that the radiolabel is integral to the compound and its major metabolites until excreted. If a sufficiently selective and sensitive analytical test for identification of the compound is available, then the labeled markers may not be required. The vehicle/solvent system used should mimic the field exposure scenario. It is advised that dilutions should be made with the field vehicle, always ensuring that sufficient quantities of radiolabel are present in each dose to allow sufficient sensitivity for detection in the samples analyzed. Finally, it is critical that the actual administered dose be known as this is the link to the other toxicology data. Preparation of the dose must ensure that the dosing area is both defined as well as restricted, and that significant quantities of applied dose are not lost into the dosing apparatus, which would reduce the dose available for absorption.
5. *Test procedure*: The study should be designed to cover the entire range of doses and durations of expected exposures for a wide variety of uses. The laboratory rat is the required species as these guidelines have been designed and validated for this species only. Again, it is important to stress that the rat is not intended as a model of absorption through the human skin but rather as a test system for dermal absorption for extrapolating to other routes of exposure in the rat. It is recommended that 24 male adult animals be used at each dose level. Four doses are recommended; three are required. It is advised that doses should be at log intervals and must be determined on the basis of quantity per unit area of exposed skin. The maximum dose volume should not exceed 10 $\mu l/cm^2$, and four animals per dose should be exposed for durations of 0.5, 1, 2, 4, 10, and 24 h in a full study. Animals are usually prepared by clipping the hairs from back and shoulders, and the area is wiped with acetone 24 h prior to dosing. The dose is applied to a measured area of the rat's skin of no less than 10 cm^2 for even spreading. The application area must be protected from dose loss, rubbing, or animal licking off the compound. Expired air, total urine, feces, blood, exposed skin, and selected organs should be collected. All samples are then analyzed to obtain a total material balance for each animal.
6. *Data and reporting*: It is stressed in these guidelines that the study report should include the method of determination of the limit of sensitivity, the actual quantity of test compound administered, the concentration of the test compound in tissue samples, mass balance totals for each animal, and determination of the percentage absorbed for each animal and for the group (mean). The quantity in the urine, cage wash, feces, expired air, blood, organs, and the remaining carcass is considered as absorbed, the quantity in/on the washed skin is considered as absorbable, and the quantity in skin wash and on the protective cover is considered as not absorbed. The final report format should contain a cover page, table of contents, and main body of the report, which should further contain summary, introduction, materials and methods, results, discussion, bibliography, and tables, figures, and appendices.
7. *Additional dermal absorption studies*: More specific studies may be necessary to clarify data collected during toxicity, metabolism, and kinetic studies of a compound. The guideline strongly recommends that the agency be consulted before performing such studies. For some compounds, the washed skin may retain more

material than was absorbed during the exposure period. In some cases, the difference between absorbed and retained material is sufficient to convert an acceptable risk into an unacceptable risk if all the retained quantity is considered as absorbed. When the specific metabolites of a compound are of toxicological concern, urine and fecal samples collected in the basic dermal absorption study may be analyzed for the production of these metabolites. If the toxic effect was originally identified with a route (e.g., oral), a blood/plasma kinetics study may be designed to generate data that can be used to compare with blood/plasma concentrations at effect and no-effect doses by the same route. It may be useful to determine test compound concentration in specific target tissues with time and dose following dermal absorption if a target organ for the toxic effect of the test compound has been identified. Finally, "infinite" dose studies may be conducted to address dermal absorption of test compounds in situations (e.g.. bathing, swimming) during which the individuals are exposed dermally to a constant concentration of a test chemical. However, these are difficult studies to conduct properly, making advance consultation with the agency advisable.

This guidance clearly illustrates EPA's preference to base regulatory decisions on *in vivo* rat studies. The rat has been selected not on its predictability to human *in vivo* absorption but rather on its ability to link to other exposure and toxicology data collected in this species. Dermal absorption data collected using procedures similar to those employed with inhalational or oral gavage studies in rats provide a basis for route-to-route extrapolations.

Note on the Use of Radioactivity in Biological Fluids

Measurement of radioactivity in biological fluids is the most commonly used indirect method for determination of percutaneous absorption of topically applied constituents. Because the absorbed concentration of chemical or drug following topical application is often low, many analytical techniques cannot detect the absorption. Use of radiotracers that can be easily detected in urine, feces, or plasma with standard liquid scintillation procedures solves this problem. Tritium (^{3}H) and ^{14}C are the most commonly used tracers in this methodology. The primary limitation of the technique is that it does not account for biotransformation of topically absorbed compound. Hence, the kinetic interpretation may be limited because the nature of the absorbed radioactivity is not clear (Bronaugh and Maibach, 1999). An alternate approach to characterize the metabolic profiles or to identify metabolites of topically applied radiolabeled compounds is to analyze the urine samples with more sensitive analytical techniques, such as two-dimensional thin-layer chromatography (Hui et al., 1998), gas chromatography–mass spectrometry, or high-performance liquid chromatography (HPLC) (Selim et al., 1995) to resolve parent compound and metabolites.

The radiotracer method has also been used in human subjects if the test compound is not toxic (Feldmann and Maibach, 1969, 1970, 1974). This approach was employed to assess percutaneous absorption of pesticides in swine (Qiao et al., 1994), in human testing of ultraviolet filters (Benech-Kieffer et al., 2003), and for determination of topical absorption of cosmetics (Malhotra et al., 2001) for clinical safety assessment.

Tape-Stripping

The penetration of a test chemical into the stratum corneum and elimination from the stratum corneum can provide dermatopharmacokinetic evidence of bioequivalence in a model test system (U.S. FDA, 1998). Sampling of stratum corneum *in vivo* using tape strips is a noninvasive method for studying the penetration of topically applied substances into the stratum corneum. The common analytical methods are then used to determine the amount of topically applied constituents removed with each tape strip, which is correlated to *in vivo* absorption. The penetration profiles can be determined by correlating the amount recovered from tape strips with the amount absorbed *in vivo* determined by mass balance studies. In the pivotal studies by Rougier et al. (1985) that defined this technique, a linear relation ($R^2 = 0.99$) was observed between the total penetration of theophylline, nicotinic acid, benzoic acid, and acetyl salicylic acid within 4 days and their concentrations in the stratum corneum reservoir after 30-min application to rats. This correlation found for these four molecules of different physicochemical characteristics suggests that partitioning into and diffusion from the stratum corneum is the driving process in dermal absorption. Numerous subsequent studies have confirmed these findings.

The amount of stratum corneum on removed strips can be derived from the density of the stratum corneum cells (corneocytes) on tape strips using laser scanning microscopy and classic microscopic techniques (Lindemann et al., 2003). A good correlation ($R^2 = 0.95$) had been shown between the amount of corneocytes determined with both microscopic techniques and the pseudoabsorption of corneocytes, a conventional method to determine the amount of stratum corneum on the tape strips. It had been concluded in an *in vivo* randomized clinical trial that neither the type of tape nor the site stripped significantly influenced the mass of stratum corneum removed (Bashir et al., 2001). The stripping method had shown concentrations of caffeine in human stratum corneum that were five times greater with emulsion than with acetone vehicle (Chambin-Remoussenard et al., 1993). This method had been tested for measuring dermal exposure to a multifunctional acrylate in human volunteers, and it was observed that first tape-stripping removed 94% of the theoretical quantity of deposited acrylate (Nylander-French, 2000). Lidocaine in different formulations had been applied on the forearm of six volunteers for 30 min (Padula et al., 2003). The stratum corneum was removed with 16 adhesive tape strips and was quantified for lidocaine using an HPLC method that resulted in 98% recovery of this topically applied drug.

Chemical contaminants may bind to and react with keratin proteins in the stratum corneum of the skin in occupational exposures under field conditions. The tape-stripping method was successfully applied for the removal and quantification of keratin from the stratum corneum for normalization of extracted amounts of naphthalene (marker hydrocarbon of jet fuel) from human volunteers experimentally exposed to JP-8 jet fuel (Chao and Nylander-French, 2004). Another study indicated that the naphthalene has a short retention time in the human stratum corneum, and that the tape-stripping method, if used within 20 min of the initial exposure, can be used to determine the amount of naphthalene initially in the stratum corneum following a single jet fuel exposure (Mattorano et al., 2004). These studies emphasized

the importance of reservoir effect of the stratum corneum for topically applied constituents for short periods of time as well as assessment of their *in vivo* percutaneous penetration. This tape-stripping method has become an important minimally invasive technique for assessing dermal absorption in humans.

Skin Surface Biopsy

The skin surface biopsy technique can be considered an additional method for percutaneous penetration studies. This simple and effective approach was initially introduced by Goldschmidt and Kligman in 1967 to study the stratum corneum and was later developed by Marks and Dawber (1971). It became possible to track the permeation of a compound through the stratum corneum by taking consecutive biopsies in the same area (Dykes et al., 1997). Skin surface biopsy alone does not provide any information regarding the amount of chemical permeated through various layers of skin and absorbed systemically but can be successfully combined with other analytical techniques, such as corneosurfametry (Pierard et al., 1994) and colorimetry (Zhai and Maibach, 1996), for quantitative determination with potential correlation to local skin effects.

Indirect Difference or Surface Disappearance Method

One may indirectly estimate dermal absorption by monitoring the disappearance of compound from the surface of skin. Such noninvasive methods have certain advantages, including low cost, use of small amounts of active drug or chemical, limited area for application, and ability to use on human skin *in vivo*. The drug is applied on the surface of skin and is recovered by washing with a suitable solvent at predetermined times. The amount of drug absorbed into the skin is evaluated by calculating the difference between the amount applied and the amount recovered. Evaporation of the dose would confound assessing absorption by this method. Finally, indirectly assessing absorption by loss of applied dose does not differentiate penetration of the dose into skin from systemic absorption of the dose through skin.

The percentage absorption of an ultraviolet blocker (benzophonone-3) through human skin 4 h after its application was calculated to be 35% of the applied dose (Fernandez et al., 2002). Similarly, the percutaneous absorption of caffeine in humans (Chambin-Remoussenard et al., 1993) and the enhancing effects of lipophilic vehicles on skin penetration of methyl nicotinate *in vivo* (Leopold and Lippold, 1995) were measured by the difference method. It is also possible to determine the disappearance of ^{14}C-labeled components from the surface of skin using appropriate procedures. Approximately 61 to 69% of the applied dose of ^{14}C-phenoxyethyl isobutyrate was recovered from the dressing and skin surface washing procedure performed after 6 h of exposure to rats (Api, 2004). The limitation of this technique using radioisotopes is that quenching effect of the skin may confound the recovery calculations. This approach may also be applied to skin biopsies.

Rosado and Rodrigues (2003) studied the differences in the permeation of two model permeants with hydrophilic (methylene blue) and with lipophilic (Sudan III) characteristics after skin pretreatment with the different solvents in human volunteers.

These authors placed a drop of adhesive glue on a glass slide, which was then placed over the skin and covered with a 200-g cylinder to apply constant pressure for 5 min. The glass slide was then removed quickly, and colorimetry was used to assess the resulting biopsy. They performed this procedure twice on each site. It was concluded that the combination of skin surface biopsy and colorimetry has the potential to obtain encouraging results, and that the methodology can be extended to the *in vivo* assessment of more complex formulations.

There are other published methods to assess the topical bioavailability *in vivo* using drug profiles at various depths into the stratum corneum. The cutaneous bioavailability of topically applied drugs has been estimated by serial tape-stripping (Kalia et al., 2001). The drug is extracted from the tapes and assayed by HPLC to determine the concentration profile as a function of the normalized position within the stratum corneum. These data can then be fitted to a solution of Fick's second law of diffusion to calculate characteristic membrane transport parameters. The AUC (integration of the concentration profile over the entire stratum corneum thickness) can provide an estimate of cutaneous bioavailability.

Microdialysis

Microdialysis has been shown to be a promising technique for assessment of *in vivo* dermal disposition (Simonsen et al., 2004; Mathy et al., 2003; Tegeder et al., 2002; Kreilgaard, 2001). This technique consists of a semipermeable membrane forming a thin hollow tube (0.2 to 0.5 mm diameter), which functionally resembles a blood vessel. The probe is implanted in the dermis of the skin via a guide cannula. The microdialysis fiber is perfused slowly at a rate of 0.1 to 5 μl/min with a physiological solution, which equilibrates with the extracellular fluid of the surrounding tissue. The exchange of substances occurs down concentration gradients according to Fick's second law of diffusion (Stahle, 2000), and the speed of equilibrium is proportional to the diffusion rate of the substance in the medium, the size of the gradient, and the surface area of the membrane. Because of the typically low cutoff values of microdialysis membranes, samples are protein free and readily analyzable without the need for further analytical purification (Kreilgaard, 2002).

Once the probe implantation has been done, pharmacokinetic profiles can be obtained from each sampling site for several days without further intervention (Lindberger et al., 1998). This technique is minimally invasive and only produces a minor reversible trauma by insertion of the guide cannula used for the implantation of the microdialysis probe (Groth and Serup, 1998). Substance recovery (the amount of substance in the dialysate) is an important parameter of this technique. The retrodialysis is the most prevalent experimental approach for recovery estimation in cutaneous microdialysis *in vivo*. This approach assesses the loss of the substance from the perfusate and relies on the assumption that net drug transport, through the microdialysis membrane from the perfusate into the surrounding tissues, equals the net drug transport from the tissues into the perfusate. To monitor recovery during the experiment, retrodialysis by a calibrator has successfully been applied to dermal drug delivery studies (Kreilgaard, 2001).

The trauma induced by insertion of the linear microdialysis probe in rat skin did not change skin permeability of drugs, blood flow or color, confirming the safety of this technique (Mathy et al., 2003). No significant physical damage after probe insertion was noticed. The probe depth neither influenced the trauma (Mathy et al., 2003) nor significantly influenced dialysate concentrations (Simonsen et al., 2004). An equilibration period of a minimum of 90 min in human skin and 30 min in rat skin after the insertion of probe is necessary to allow the effects of trauma to diminish (Groth, 1996). These studies validate the use of microdialysis in dermatopharmacokinetics studies after topical application of substances.

There are certain limitations and challenges involved in this technique. The microdialysis probe assesses chemical or drug absorption directly beneath the application site. Unlike other mass balance techniques, there is no assurance that all of the compound traversing the skin will be absorbed into the probe. A fraction of absorbed dose at any time point may be absorbed into the deeper vasculature or stay bound to dermal tissue. The most important limitation is the sampling of lipophilic substances because of the low relative recovery (Benfeldt and Groth, 1998). These limitations for sampling of highly lipophilic substances are related to the hydrophilic nature of the perfusate applied for microdialysis experiments and adherence of the substance to the microdialysis apparatus. One way to solve the low solubility of lipophilic substances is by the addition of solvents (e.g., polyethylene glycol, cyclodextrins, proteins, or lipids) to the perfusates (Khramov and Stenken, 1999). The analytical limitations can be overcome because of the recent introduction of the microbore/capillary liquid chromatographic methods and more sensitive detectors (e.g., mass spectrometers, biosensors, etc.). These additions have broadened the range of substances that can be sampled and analyzed by the microdialysis.

Microdialysis was employed to assess dermal barrier function when absorption of salicylic acid determined with cutaneous microdialysis in rats correlated well with transepidermal water loss and erythema (Benfeldt et al., 1999). Microdialysis sampling with two parallel probes in the dermis was demonstrated to be more sensitive than noninvasive measuring techniques in detecting significant barrier perturbation in skin following salicylic acid exposure (Benfeldt et al., 1999). This technique in combination with traditional techniques might give valuable information regarding the assessment of the penetration of drugs and other exogenous agents through the skin (Schnetz and Fartasch, 2001). The feasibility of cutaneous microdialysis as a method to study percutaneous absorption of methyl nicotinate through human skin was assessed both *in vitro* and *in vivo* and was suggested to be suitable for comparison of *in vivo* and *in vitro* data (Boelsma et al., 2000).

Microdialysis has also been used for topical bioavailability/bioequivalence studies. A correlation has been demonstrated between dermal AUC/C_{max} of topically applied tranilast in six different vehicles assessed with microdialysis and AUC/C_{max} from plasma concentration–time curves (Murakami, Yoshioka, Yumoto, et al., 1998). However, in another study, no correlation was found between dermal AUC/C_{max} and plasma AUC/C_{max} of salicylic acid applied in five different vehicles (Murakami, Yoshioka, Okamoto et al., 1998). These findings emphasize that plasma drug levels do not always correlate with dermal levels assessed by techniques such as microdialysis. The correlation or lack thereof is compound dependent secondary to their

dermal pharmacokinetic properties. The pharmacokinetic parameters assessed in human subjects demonstrated a significant increase in absorption rate and a decrease in lag time when lidocaine was applied in a microemulsion compared to octanol/water emulsion (Kreilgaard et al., 2001). The skin/plasma ratio of 8-methoxypsoralen was three to five orders of magnitude larger with topical route compared to oral route, emphasizing that the severe side effects observed after oral treatment could greatly be reduced with topical administration of drugs (Tegeder et al., 2002). The effectiveness and bioavailability of a number of bromocriptine (a dopamine agonist) gel formulations in rabbits concluded that transdermal delivery of this drug may be a promising alternative route for treatment compared to the oral route (Degim et al., 2003). A growing number of studies in the literature determined the cutaneous fluxes of a great number of drugs in animal and human subjects using microdialysis, supporting the potential of this technique for bioavailability studies.

Pharmacodynamic Responses

Assessing the skin's response to chemical exposure has often been used as an indirect method to indicate absorption has occurred. Pharmacodynamic models are among the conventional *in vivo* methods used to access the dermal absorption of topically applied drugs. The Draize test is a classic example of this approach (Draize et al., 1944). These models have limited utility in transcutaneous drug or chemical transport as they provide only a qualitative measure of dermal penetration. They do not give any indication of systemic exposure as the observed response may be within the skin. We have assessed the *in vivo* toxic effects of JP-8 jet fuel and its aliphatic hydrocarbons with the carbon chain length ranging from C9 to C16 in pigs after 4 days of repeated application (Muhammad et al., 2005). Erythema scores after 1 and 4 days of application of JP-8 and aliphatic hydrocarbons to pigs clearly demonstrated the differential *in vivo* response with varying carbon chain length of these hydrocarbons (Figure 4.3). The presence of erythema implies compound penetration into skin. However, the intensity of the response is a function of both individual hydrocarbon absorption as well as its own cytotoxic potency.

The combination of a pharmacodynamic model with a modern technique such as microdialysis is an attractive solution to assess pharmacokinetic/pharmacodyamic (PK/PD) relationships. Two separate studies supported this idea. Esterom Solution® is derived from the esterification of benzoylmethylecgonine (cocaine) and contains a mixture of components (McDonald and Lunte, 2003). This solution is intended to be a topical analgesic to relieve pain and increase the range of motion in patients with acute inflammation. A pharmacodynamic model can only provide information about the qualitative reduction in pain as a result of topical application of complete mixture. The dermal microdialysis analysis of this mixture revealed that the only component that penetrated the skin was hydroxypropyl benzoylecgonine (McDonald and Lunte, 2003). Thus, the analgesic activity of the Esterom Solution was caused by one component.

A second pharmacodynamic study showed a significant reduction in pain perception of prods with von Frey hairs during the application of two lidocaine formulations (microemulsion and 5% xylocaine), discernible from placebo treatment

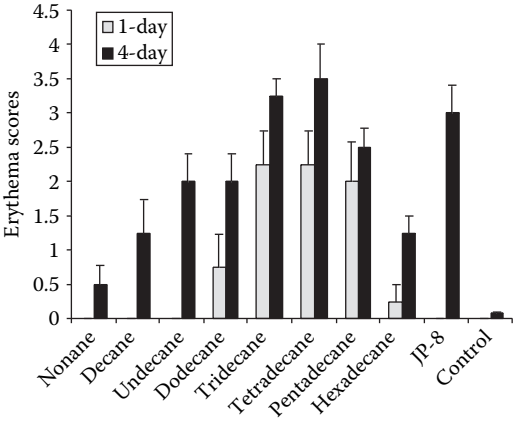

Figure 4.3 Erythema scores after 1 and 4 days of exposure to *in vivo* JP-8 or constituent aliphatic hydrocarbons (mean ± SEM). 0, no significant change; 1, very slight erythema; 2, slight, pale red in defined area; 3, moderate to severe, red in well-defined area; 4, severe, beet red in defined area. Note the differential *in vivo* response to increasing carbon chain length of hydrocarbons (C9 nonane to C16 hexadecane).

(Kreilgaard, 2001). The anesthetic effect of the two formulations indicated similar cutaneous absorption profiles of lidocaine from both formulations. However, a three-fold increase in apparent absorption rate and a significant decrease in lag time of lidocaine applied in microemulsion vehicle compared to 5% xylocaine were demonstrated with cutaneous microdialysis. This study illustrated that, compared to the pharmacodynamic model, the microdialysis technique has higher sensitivity and less variability to access bioequivalence of topically applied chemicals.

In contrast, a systemic pharmacodynamic end point may be used to infer that percutaneous absorption of a drug has occurred. This is commonly employed with the organophosphate pesticides, for which a decrease in acetylcholinesterase activity implies absorption of the topically applied compound. This approach was used to assess site-specific dermal absorption of the chemical warfare agent VX in swine (Duncan et al., 2002). Limitations to this approach include confounding of absorption with observable activity depending on factors governing the dose response relationship of the chemical with observable enzyme inhibition (e.g., different potencies for different compounds, lag time), lack of specificity, interference from other endogenous substances, and inability to detect parent drug from metabolites. Other similar "biomarkers" of systemic activity (e.g., altered cardiovascular activity, reduced pain response, cytokine release, etc.) may also be employed but share the same potential of confounding absorption with the nature of the pharmacokinetic/pharmacodynamic linkage (Riviere, 1999).

Attenuated Total Reflectance–Fourier Transform Infrared Spectroscopy

Attenuated total reflectance–Fourier transform infrared (ATR–FTIR) spectroscopy is an emergent physicochemical technique that is becoming a powerful tool for

obtaining structural information from cellular constituents of biological membranes. FTIR spectra reflect the complex chemical composition of the cells, with bands assigned to distinct functional groups or chemical substructures (Helm et al., 1991). This technique, which requires neither reagent nor sample preparation, is nondestructive, sensitive, and highly selective because of its ability to be a spectral fingerprint for molecular components (Franck et al., 1998). This technique has been demonstrated to be a convenient tool for pharmacotoxicological studies (Malins et al., 1996).

ATR–FTIR spectroscopy has been used to investigate chemical penetration kinetics in human stratum corneum and to elucidate the extent and mechanism of percutaneous penetration enhancement *in vivo* in human subjects (Pellet et al., 1997), a topic that is covered in chapter 12. There are some limitations in its application because the typical range of sampling depth with ATR–FTIR is 0.7 to 2.1 μm; however, it still has the advantage of utilizing *in vivo* samples. This limitation has been overcome by monitoring the amount of chemical in sequentially tape-stripped layers of the stratum corneum following exposure (Pirot et al., 1997). This improved technique has been further applied to evaluate and quantify stratum corneum uptake of volatile and nonvolatile solvents from the ventral forearms of human volunteers (Stinchcomb et al., 1999). Similarly, the concentration profiles of two model compounds of different lipophilicity and molecular size, 4-cyanophenol and cimetidine, were determined in the tape-stripped stratum corneum from human volunteers using ATR–FTIR spectroscopy (Tsai et al., 2003). The bioavailability of terbinafine in human stratum corneum from different topical formulations was determined with ATR–FTIR (Alberti et al., 2001). This technique has proved to be a useful tool for monitoring the percutaneous absorption of 4-hydroxybenzonitrile and to evaluate the sucrose oleate and sucrose laureate-induced biophysical changes in stratum corneum barrier function *in vivo* in human subjects (Ayala-Bravo et al., 2003).

A comparison of three noninvasive biophysical techniques—transepidermal water loss (TEWL), impedance spectroscopy (IS), and ATR–FTIR spectroscopy—was used to evaluate the effect of formulation excipients on stratum corneum *in vivo*. Two formulations, an ointment and an oil-in-water cream, were applied to the skin of human volunteers (Curdy et al., 2004). A simple tape-stripping protocol was also combined with these biophysical techniques to allow information to be derived across the entire stratum corneum. TEWL and IS only provided basic information regarding the effects of formulations on the skin barrier function, properly classified as a pharmacodynamic end point. However, ATR–FTIR showed the ability to track the diffusion of model compounds and to evaluate their concentration profiles within the stratum corneum, thus providing the mechanistic details necessary to explain the TEWL and IS results. These studies emphasized that ATR–FTIR spectroscopy can be successfully exploited as a reliable noninvasive tool to measure quantitatively and qualitatively the *in vivo* dermal uptake of drugs or chemicals.

Transepidermal Water Loss

TEWL is a noninvasive technique that assesses pharmacodynamic responses to topically applied drugs caused by disruption of skin barrier function as a result of

chemical insults. The principle is based on measuring the water vapor pressure gradient between the boundary layer of the skin surface and the ambient air at a temperature of approximately 20°C and 40% relative humidity. The increase in TEWL values is considered to correspond to the skin barrier disruption caused by chemical penetration. Modifications of TEWL because of repeated topical application of steroids or organic chemicals were studied on the forearms of healthy volunteers. It had been shown that the increase in TEWL was positively correlated with an increase in the percutaneous absorption of corticosteroids (Guillaume et al., 1981) and organic chemicals (Lotte et al., 1987). We observed an increase in TEWL at the 5-h and 24-h fabric and Hill Top occluded treatments with different jet fuel mixtures in pigs (Monteiro-Riviere et al., 2001). TEWL measurements with an evaporimeter provided a powerful noninvasive method for determining the efficiency of barrier functions of the skin (Kalia et al., 2000), although they are not useful for assessing the transport of other compounds besides water.

Confocal Microscopy

In skin research, drug and chemical targeting to various layers of skin is of great interest. For this purpose, various approaches have been tried. Confocal laser scanning microscopy has been employed to study the influence of permeant lipophilicity and vehicle composition on local chemical accumulation (Grams et al., 2003). In these studies, fluorescently labeled liposomes were applied on skin *in vivo*, and the penetration pathway and penetration depth of the lipophilic fluorescent label into the skin was visualized by confocal laser scanning microscopy (Van Kuijk-Meuwissen et al., 1998).

CONCLUSION

Percutaneous absorption of topically applied substances is important in the fields of dermatotoxicology of chemicals that pose a threat to human exposure and of dermatopharmacology of drugs used to treat local or systemic medical disorders. Direct measurements of percutaneous absorption of compounds in humans are often difficult because of ethical issues and lack of sensitive analytical techniques. Many alternate animal models have been developed for *in vivo* prediction of dermal absorption. It is generally agreed that *in vivo* animal models should mimic anatomical, physiological, and biochemical similarities to humans as closely as possible so that extrapolation errors can be minimized. However, direct measurements of dermal absorption in humans will remain the reference standard.

Advances of *in vivo* methods for dermal absorption studies have shown promising results. Microdialysis has been employed successfully for measuring dermal penetration of a wide variety of compounds. This technique has been used extensively in topical bioavailability and bioequivalence studies. The noninvasive techniques for percutaneous absorption studies such as tape-stripping, ATR–FTIR, and skin surface biopsies are also becoming popular because these can be used safely in humans. Regulatory bodies rely on mass balance approaches because all of the topically

applied dose can be accounted for, including dermal absorption, tissue retention, excretion, and recoveries. Systemic absorption after topical administration of drugs and chemicals can be measured by taking blood samples alone. This approach utilizes the comparison of AUCs and doses after topical and intravenous administration of compounds to correct for patterns of excretion. Such techniques will continue to be employed, with advances primarily related to the ever-increasing sensitivity of analytical and sampling methodology.

REFERENCES

Alberti, I., Kalia, Y.N., Naik, A., Bonny, J.D., and Guy, R.H., 2001, *In vivo* assessment of enhanced topical delivery of terbinafine to human stratum corneum, *J. Controlled Release*, 71, 319–327.

Api, A.M., 2004, Evaluation of the dermal subchronic toxicity of phenoxyethyl isobutyrate in the rat, *Food Chem. Toxicol.*, 42, 307–311.

Ayala-Bravo, H.A., Quintanar-Guerrero, D., Naik, A., Kalia, Y.N., Cornejo-Bravo, J.M., and Ganem-Quintanar, A., 2003, Effects of sucrose oleate and sucrose laureate on *in vivo* human stratum corneum permeability, *Pharm. Res.,* 20, 1267–1273.

Bartek, M.J., LaBudde, J.A., and Maibach, H.I., 1972, Skin permeability *in vivo*: comparison in rat, rabbit, pig and man, *J. Invest. Dermatol.,* 58, 114–123.

Bashir, S.J., Chew, A.L., Anigbogu, A., Dreher, F., and Maibach, H.I., 2001, Physical and physiological effects of stratum corneum tape-stripping, *Skin Res. Technol.,* 7, 40–48.

Benech-Kieffer, F., Meuling, W.J., Leclerc, C., Roza, L., Leclaire, J., and Nohynek, G., 2003, Percutaneous absorption of mexoryl SX in human volunteers: comparison with *in vitro* data, *Skin Pharmacol. Appl. Skin Physiol.,* 16, 343–355.

Benfeldt, E., 1999, *In vivo* microdialysis for the investigation of drug levels in the dermis and the effects of barrier perturbation on cutaneous drug penetration: studies in hairless rats and human subjects, *Acta Dermatol. Venereol. Suppl.,* 206, 7–54.

Benfeldt, E., Serup, J., and Menne, T., 1999, Effect of barrier perturbation on cutaneous salicylic acid penetration in human skin: *in vivo* pharmacokinetics using microdialysis and non-invasive quantification of barrier function, *Br. J. Dermatol.,* 140, 739–748.

Benfeldt, E. and Groth, L., 1998, Feasibility of measuring lipophilic or protein-bound drugs in the dermis by *in vivo* microdialysis after topical or systemic drug administration, *Acta Dermatol. Venereol.,* 78, 274–278.

Bhatti, A.S., Scott, R.C., and Dyer, A., 1988, *In vitro* percutaneous absorption: pig epidermal membrane as a model for human skin, *J. Pharm. Pharmacol.,* 40(Suppl), 45.

Boelsma, E., Anderson, C., Karlsson, A.M., and Ponec, M., 2000, Microdialysis technique as a method to study the percutaneous penetration of methyl nicotinate through excised human skin, reconstructed epidermis, and human skin in vivo, *Pharm. Res.,* 17, 141–147.

Bronaugh, R.L. and Maibach, H.I., 1999, *Percutaneous Absorption. Drugs—Cosmetics—Mechanisms—Methods,* New York: Dekker, pp. 215–227.

Bronaugh, R.L., Stewart, R.F., and Congdon, E.R., 1982, Methods for *in vitro* percutaneous absorption studies. II. Animal models for human skin, *Toxicol. Appl. Pharmacol.,* 62, 481–488.

Bronaugh, R.L., Stewart, R.F., Wester, R.C., Bucks, D., Mailbach, H.I., and Anderson, J., 1985, Comparison of percutaneous absorption of fragrances by humans and monkeys, *Food Chem. Toxicol.,* 23, 111–114.

Carver, M.P. and Riviere, J.E., 1989, Percutaneous absorption and excretion of xenobiotics after topical and intravenous administration to pigs, *Fundam. Appl. Toxicol.,* 13, 714–722.

Chambin-Remoussenard, O., Treffel, P., Bechtel, Y., and Agache, P., 1993, Surface recovery and stripping methods to quantify percutaneous absorption of caffeine in humans, *J. Pharm. Sci.,* 82, 1099–1101.

Chang, S.K., Dauterman, W.C., and Riviere, J.E., 1994, Percutaneous absorption of parathion and its metabolites, paraxon and *p*-nitrophenol, administered alone or in combination: *in vitro* flow-through diffusion cell studies, *Pestic. Biochem. Physiol.*, 48, 56–62.

Chao, Y.C. and Nylander-French, L.A., 2004, Determination of keratin protein in a tape stripped skin sample from jet fuel exposed skin, *Ann. Occup. Hyg.,* 48, 65–73.

Chen, E.H. and Wilkinson, P.K., 1989, Mechanism of transdermal penetration of avermectins through sheep skin, *Pharm. Res.,* 6(Suppl.), S108.

Cole, C.A., 1990, Animal models for sunscreens and photoprotection, in N.J. Lowe and N. A. Shaath (eds.), *Sunscreen: Development, Evaluation, and Regulatory Aspects*, New York: Dekker, pp. 447–457.

Curdy, C., Naik, A., Kalia, Y.N., Alberti, I., and Guy, R.H., 2004, Non-invasive assessment of the effect of formulation excipients on stratum corneum barrier function *in vivo*, *Int. J. Pharm.,* 27, 251–256.

Dary, C.C., Blancato, J.N., and Saleh, M.A., 2001, Chemomorphic analysis of malathion in skin layers of the rat: implications for the use of dermatopharmacokinetic tape-stripping in exposure assessment to pesticides, *Reg. Toxicol. Pharmacol.,* 34, 234–248.

Degim, I.T., Acarturk, F., Erdogan, D., and Demirez Lortlar, N., 2003, Transdermal administration of bromocriptine, *Biol. Pharm. Bull.*, 26, 501–505.

Dick, I.P. and Scott, R.C., 1992, Pig ear skin as an *in vitro* model for human skin permeability, *J. Pharm. Pharmacol.,* 44, 640–645.

Draize, J.H., Woodard, G., and Calvery, H.O., 1944, Methods for the study of irritation and toxicity of substances applied topically to the skin and mucous membranes, *J. Pharmacol. Exp. Ther.,* 82, 377–390.

Duncan E.J.S., Brown, A., Lundy, P., Sawyer, T.W., Hamilton, M., Hill, I., and Conley, J.D., 2002, Site-specific percutaneous absorption of methyl salicylate and VX in domestic swine, *J. Appl. Toxicol.,* 22, 141–148.

Dykes, P.J., Hill, S., and Marks, R., 1997, Pharmacokinetics of topically applied metronidazol in two different formulations, *Skin Pharmacol.*, 10, 28–33.

Feldmann, R.J. and Maibach, H.I., 1969, Percutaneous penetration of steroids in man, *J. Invest. Dermatol.,* 52, 89–94.

Feldmann, R.J. and Maibach, H.I., 1970, Absorption of some organic compounds through the skin of man, *J. Invest. Dermatol.,* 54, 399–404.

Feldmann, R.J. and Maibach, H.I., 1974, Percutaneous penetration of some pesticides and herbicides, *Toxicol. Appl. Pharmacol.,* 28, 126–132.

Fernandez, C., Nielloud, F., Fortune, R., Vian, L., and Marti-Mestres, G., 2002, Benzophonone-3: rapid prediction and evaluation using non-invasive methods of *in vivo* human penetration, *J. Pharm. Biomed. Anal.,* 28, 57–63.

Franck, P., Nabet, P., and Dousset, B., 1998, Applications of infrared spectroscopy to medical biology, *Cell Mol. Biol.*, 44, 273–275.

Goldschmidt, H. and Kligman, A.M., 1967, Exfoliative cytology of human horny layer, methods of cell removal and microscopic techniques, *Arch. Dermatol.,* 96, 572.

Grams, Y.Y., Alaruikka, S., Lashley, L., Caussin, J., Whitehead, L., and Bouwstra, J.A., 2003, Permeant lipophilicity and vehicle composition influence accumulation of dyes in hair follicles of human skin, *Eur. J. Pharm. Sci*., 18, 329–336.

Groth, L. and Serup, J., 1998, Cutaneous microdialysis in man: effects of needle insertion trauma and anaesthesia on skin perfusion, erythema and skin thickness, *Appl. Infrared Spectrosc. Med. Biol.,* 78, 5–9.

Groth, L., 1996, Cutaneous microdialysis. Methodology and validation, *Appl. Infrared Spectrosc. Med. Biol.* 197, 1–61.

Guillaume, J.C., De Rigal, J., Leveque, J.L., Galle, P., Touraine, R., and Dubertret, L., 1981, Study of the correlation between transepidermal water loss and percutaneous penetration of steroid, *Dermatologica,* 162, 380–390.

Helm, D., Labischinski, H., Schallehn, G., and Naumann, D., 1991, Classification and identification of bacteria by Fourier-transform infared spectroscopy, *J. Gen. Microbiol.,* 137, 69–79.

Hikima, T., Yamada, K., Kimura, T., Maibach, H.I., and Tojo, K., 2002, Comparison of skin distribution of hydrolytic activity for bioconversion of betaestradiol 17-acetate between man and several animals *in vitro*, *Eur. J. Pharm. Biopharm.,* 54, 155–160.

Howes, D., Guy, R., Hadgraft, J., Heylings, J., Hoeck, U., Kemper, F., Maibach, H., Marty, J.P., Merk, H., Parra, J., Rekkas, D., Rondelli, I., Schaefer, H., Tauber, U., and Verbiese, N., 1996, Methods for assessing percutaneous absorption: the report and recommendations of ECVAM workshop 13, *ATLA*, 24, 81–106.

Hui, X., Hewitt, P.G., Poblete, N., Maibach, H.I., Shainhouse, J.Z., and Wester, R.C., 1998, *In vivo* bioavailability and metabolism of topical diclofenac lotion in human volunteers, *Pharm. Res.,* 15, 1589–1595.

Johannes, J.M.V.D.S., Meuling, W.J.A., Elliott, G.R., Cnubben, N.H.P., and Hakkert, B.C., 2000, Comparative *in vitro in vivo* percutaneous absorption of the pesticide propoxur, *Toxicol. Sci.,* 58, 15–22.

Kalia, Y.N., Alberti, I., Naik, A., and Guy, R.H., 2001, Assessment of topical bioavailability *in vivo*: the importance of stratum corneum thickness, *Skin Pharmacol. Appl. Skin Physiol*., 14, 82–86.

Kalia, Y.N., Alberti, I., Sekkat, N., Curdy, C., Naik, A., and Guy, R.H., 2000, Normalization of stratum corneum barrier function and transepidermal water loss *in vivo*, *Pharm. Res*., 17, 1148–1150.

Khramov, A.N. and Stenken, J.A., 1999, Enhanced microdialysis recovery of some tricyclic antidepressants and structurally related drugs by cyclodextrin-mediated transport, *Analyst,* 124, 1027–1033.

Kraeling, M.E., Reddy, G., and Bronaugh, R.L., 1998, Percutaneous absorption of trinitrobenzene: animal models for human skin, *J. Appl. Toxicol*., 18, 387–392.

Kreilgaard, M., 2001, Dermal pharmacokinetic of microemulsion formulations determined by *in vivo* microdialysis*, Pharm. Res.,* 18, 367–373.

Kreilgaard, M., 2002, Assessment of cutaneous drug delivery using microdialysis, *Adv. Drug Delivery Rev.,* 55, 99–121.

Kreilgaard, M., Kemme, M.J., Burggraaf, J., Schoemaker, R.C., and Cohen, A.F., 2001, Influence of a microemulsion vehicle on cutaneous bioequivalence of a lipophilic model drug assessed by microdialysis and pharmacodynamics, *Pharm. Res.,* 18, 593–599.

Lauer, A.C., Elder, J.T., and Weiner, N.D., 1997, Evaluation of the hairless rat as a model for *in vivo* percutaneous absorption, *J. Pharm. Sci.,* 86, 13–18.

Leopold, C.S. and Lippold, B.C., 1995, Enhancing effects of lipophilic vehicles on skin penetration of methyl nicotinate *in vivo*, *J. Pharm. Sci.,* 84, 195–198.

Lindberger, M., Tomson, T., and Stahle, L., 1998, Validation of microdialysis sampling for subcutaneous extracellular valproic acid in humans, *Ther. Drug Monit.,* 20, 358–362.

Lindemann, U., Wilken, K., Weigmann, H.J., Schaefer, H., Sterry, W., and Lademann, J., 2003, Quantification of the horny layer using tape-stripping and microscopic techniques, *Biomed. Opt.,* 8, 601–607.

Lotte, C., Rougier, A., Wilson, D.R., and Maibach, H.I., 1987, *In vivo* relationship between transepidermal water loss and percutaneous penetration of some organic compounds in man: effect of anatomic site, *Arch Dermatol. Res.,* 279, 351–356.

Malhotra, B., Noveck, R., Behr, D., and Palmisano, M., 2001, Percutaneous absorption and pharmacokinetics of eflornithine HCl 13.9% cream in women with unwanted facial hair, *J. Clin. Pharmacol.,* 41, 972–978.

Malins, D.C., Polissar, N.L., and Gunselman, S.J., 1996, Progression of human breast cancers to the metastatic state is linked to hydroxyl radical-induced DNA damage, *Proc. Natl. Acad. Sci.,* 93, 2557–2562.

Marks, R. and Dawber, R.P.R., 1971, Skin surface biopsy: an improved technique for the examination of the horny layer, *Br. J. Dermatol.,* 84, 117–123.

Mathy, F.X., Denet, A.R., Vroman, B., Clarys, P., Barel, A., Verbeeck, R.K., and Preat, V., 2003, *In vivo* tolerance assessment of skin after insertion of subcutaneous and cutaneous microdialysis probes in the rat, *Skin Pharmacol. Appl. Skin Physiol.*, 16, 18–27.

Mattorano, D.A., Kupper, L.L., and Nylander-French, L.A., 2004, Estimating dermal exposure to jet fuel (naphthalene) using adhesive tape strip samples, *Ann. Occup. Hyg.*, 48, 139–146.

McDonald, S. and Lunte, C., 2003, Determination of the dermal penetration of esterom components using microdialysis sampling, *Pharm. Res.,* 20, 1827–1834.

Monteiro-Riviere, N.A., 1991, Comparative anatomy, physiology and biochemistry of mammalian skin, in D.W. Hobson, *Dermal and Ocular Toxicology: Fundamentals and Methods*, London: CRC Press, pp. 3–71.

Monteiro-Riviere, N.A., 1996, Anatomical factors affecting percutaneous absorption, in F.N. Marzulli and H.I. Maibach (eds.), *Dermatotoxicology,* 5th ed., Washington, D.C.: Taylor and Francis, pp. 3–17.

Monteiro-Riviere, N.A., Inman, A.O., and Riviere, J., 2001, Effects of short-term high dose and low dose dermal exposure to jet A, JP-8 and JP-8+100 jet fuels, *J. Appl. Toxicol.,* 21, 485–494.

Monteiro-Riviere, N.A. and Riviere, J.E., 1996, The pig as a model for cutaneous pharmacology and toxicology research, in M.E. Tumbleson and L.B. Schook (eds.), *Swine in Biomedical Research,* Vol. 2, New York: Plenum, pp. 425–458.

Morris, G.M., Rezvani, M., Hopewell, J.W., Franke, H., and Loeffler, M., 1987, Epidermal cell kinetics in pig skin, *Epithelia,* 1, 231–242.

Muhammad, F., Monteiro-Riviere, N.A., and Riviere, J.E., 2004, Comparative *in vivo* toxicity of JP-8 jet fuel and its individual hydrocarbon components: identification of tridecane and tetradecane as key constituents responsible for dermal irritation, *Toxicol. Pathol.,* 33, 258–266.

Murakami, T., Yoshioka, M., Okamoto, I., Yumoto, R., Higashi, Y., Okahara, K., and Yata, N., 1998, Effect of ointment bases on topical and transdermal delivery of salicylic acid in rats: evaluation by skin microdialysis, *J. Pharm. Pharmacol.,* 50, 55–61.

Murakami, T., Yoshioka, M., Yumoto, R., Higashi, Y., Shigeki, S., Ikuta, Y., and Yata, N., 1998, Topical delivery of keloid therapeutic drug, tranilast, by combined use of oleic acid and propylene glycol as a penetration enhancer: evaluation by skin microdialysis in rats, *J. Pharm. Pharmacol.,* 50, 49–54.

Nylander-French, L.A., 2000, A tape-stripping method for measuring dermal exposure to multifunctional acrylates, *Ann. Occup. Hyg.*, 44, 645–651.

Padula, C., Colombo, G., Nicoli, S., Catellani, P.L., Massimo, G., and Santi, P., 2003, Bioadhesive film for the transdermal delivery of lidocaine: *in vitro* and *in vivo* behavior, *J. Controlled Release,* 88, 277–285.

Panchagnula, R., Stemmer, K., and Ritschel, W.A., 1997, Animal models for transdermal drug delivery, *Methods Find. Exp. Clin. Pharmacol.,* 19, 335–341.

Pellet, M.A., Watkinson, A.C., Hadgraft, J., and Brain, K.R., 1997, Comparison of permeability data from traditional diffusion cell and ATR–FTIR spectroscopy. Part II. Determination of diffusional pathlengths in synthetic membranes and human stratum corneum, *Int. J. Pharm.*, 154, 217–227.

Pierard, G.E., Goffin, V., and Pierard-Franchimont, C., 1994, Corneosurfametry: a predictive assessment of the interaction of personal-care cleansing products with human stratum corneum, *Dermatology,* 189, 152–156.

Pirot, F., Kalia, Y.N., Stinchcomb, A.L., Keating, G., Bunge, A., and Guy, R.H., 1997, Characterization of the permeability barrier of human skin *in vivo*, *Proc. Natl. Acad. Sci.*, 94, 1562–1567.

Pitman, I.H. and Rostas, S.J., 1982, A comparison of frozen and reconstituted cattle and human skin as barriers to drug penetration, *J. Pharm. Sci.*, 71, 427–430.

Poet, T.S., Corley, R.A., Thrall, K.D., Edwards, J.A., Tranojo, H., Weitz, K.K., Hui, X., Maibach, H.I., and Wester, R.C., 2000, Assessment of the percutaneous absorption of trichloroethylene in rats and humans using MS/MS real-time breath analysis and physiologically based pharmacokinetic modeling, *Toxicol. Sci.,* 56, 61–72.

Qiao, G.L., Williams, P.L., and Riviere, J.E., 1994, Percutaneous absorption, biotransformation, and systemic disposition of parathion *in vivo* in swine. I. Comprehensive pharmacokinetic model, *Drug Metab. Disposition,* 22, 459–471.

Reifenrath, W.G., Chellquist, E.M., Shipwash, E.A., Jederberg, W.W., and Krueger, W.G., 1984, Percutaneous absorption in the hairless dog, weanling pig and grafted athymic nude mouse: evaluation of models for predicting skin penetration in man, *Br. J. Dermatol.,* 111(Suppl.), 27, 123–135.

Riviere, J.E., 1990, Biological factors in absorption and permeation, *Cosmetics Toiletries*, 105, 85–93.

Riviere, J.E., 1999, *Comparative Pharmacokinetics: Principles, Techniques, and Applications,* Ames, IA: Iowa State Press.

Rosado, C. and Rodrigues, L.M., 2003, Solvent effects in permeation assessed *in vivo* by skin surface biopsy, *BMC Dermatol.,* 3, 1–6.

Rougier, A., Dupuis, D., Lotte, C., and Roguet, R., 1985, The measurement of stratum corneum reservoir, a predictive method for *in vivo* percutaneous absorption studies: influence of application time, *J. Invest. Dermatol.*, 84, 66–68.

Sato, K., Sugibayashi, K., and Morimoto, Y., 1991, Species differences in percutaneous absorption of nicorandil, *J. Pharm. Sci.,* 80, 104–107.

Schaefer, H. and Redelmeier, T.E., 1996, *In vivo* measurement percutaneous absorption, in *Skin Barrier: Principles of Percutaneous Absorption,* Schaefer, H. and Redelmeier, T.E., (eds.), Basel, Switzerland: Karger, pp.118–128.

Schnetz, E. and Fartasch, M., 2001, Micordialysis for the evaluation of penetration through the human skin barrier: a promising tool for future research, *Eur. J. Pharm. Sci.,* 12, 165–174.

Selim, S., Hartnagel, R.E., Jr., Osimitz, T.G., Gabriel, K.L., and Schoenig, G.P., 1995, Absorption, metabolism, and excretion of *N,N*-diethyl-*m*-toluamide following dermal application to human volunteers, *Fundam. Appl. Toxicol.,* 25, 95–100.

Simon, G.A. and Maibach, H.I., 1998, Relevance of hairless mouse as an experimental model of percutaneous penetration in man, *Skin Pharmacol. Appl. Skin Physiol.*, 11, 80–86.

Simon, G.A. and Maibach, H.I., 1999, The pig as an experimental animal model of percutaneous permeation in man: qualitative and quantitative observations—an overview, *Skin Pharmacol. Appl. Skin Physiol.*, 13, 229–234.

Simonsen, L., Jorgensen, A., Benfeldt, E., and Groth, L. 2004. Differentiated *in vivo* skin penetration of salicylic compounds in hairless rats measured by cutaneous microdialysis, *Eur. J. Pharm. Sci.*, 21, 379–388.

Simonsen, L., Petersen, M.B., Benfeldt, E., and Serup, J., 2002, Development of an *in vivo* animal model for skin penetration in hairless rats assessed by mass balance, *Skin Pharmacol. Appl. Skin Physiol.,* 15, 414–424.

Stahle, L., 2000, On mathematical models of microdialysis: geometry, steady-state models, recovery and probe radius, *Adv. Drug Deliv. Rev.*, 45, 149–167.

Stinchcomb, A.L., Pirot, F., Touraille, G.D., Bunge, A.L., and Guy, R.H., 1999, Chemical uptake into human stratum corneum *in vivo* from volatile and nonvolatile solvents, *Pharm. Res.*, 16, 1288–1293.

Tegeder, I., Brautigam, L., Podda, M., Meier, S., Kaufmann, R., Geisslinger, G., and Grundmann-Kollmann, M., 2002, Time course of 8-methoxypsoralen concentrations in skin and plasma after topical and oral administration, *Clin. Pharmacol. Ther.,* 71, 153–161.

Thrall, K.D., Poet, T.S., Corley, R.A., Tanojo, H., Edwards, J.A., Weitz, K.K., Hui, X., Maibach, H.I., and Wester, R.C., 2000, A real-time *in vivo* method for studying the percutaneous absorption of volatile chemicals, *Int. J. Occup. Environ. Health,* 6, 96–103.

Tsai, J.C., Lin, C.Y., Sheu, H.M., Lo, Y.L., and Huang, Y.H., 2003, Noninvasive characterization of regional variation in drug transport into human stratum corneum *in vivo*, *Pharm. Res.*, 20, 632–638.

U.S. Department of Health and Human Services Food and Drug Administration Center for Drug Evaluation and Research, 1998, *Guidance for Industry: Topical Dermatological Drug Product NDAs and ANDAs*—In Vivo *Bioavailability, Bioequivalence,* In Vitro *Release, and Associated Studies,* pp. 1–19.

U.S. Environmental Protection Agency, 1998, *Health Effects Test Guidelines: OPPTS 870.7600 Dermal Penetration.*

Van Kuijk-Meuwissen, M.E., Mougin, L., Junginger, H.E., and Bouwstra, J.A., 1998, Application of vesicles to rat skin *in vivo*: a confocal laser scanning microscopy study, *J. Controlled Release,* 56, 189–196.

Wester, R.C. and Maibach, H.I., 1989, *In vivo* animal models for percutaneous absorption, in R.I. Bronaugh and H.I. Maibach (eds.), *Percutaneous Absorption*, 2nd ed., New York: Dekker, pp. 221–238.

Wester, R.C. and Maibach, H.I., 1992, Percutaneous absorption of drugs, *Clin. Pharmacokin.*, 23, 253–266.

Zhai, H. and Maibach, H.I., 1996, Effect of barrier creams: human skin *in vivo*, *Contact Dermatitis,* 35, 92–96.

CHAPTER 5

A Novel System Coefficient Approach for Systematic Assessment of Dermal Absorption from Chemical Mixtures

Xin-Rui Xia, Ronald E. Baynes, and Jim E. Riviere

CONTENTS

INTRODUCTION

Chemical mixtures have posed immense problems for human health as well as ecological systems. There are over 75,000 existing chemicals on the Toxic Substances Control Act inventory. Each year, an additional 2000 chemicals are added. Humans are exposed to thousands of chemical agents in various combinations every day in the home, the ambient environment, and the workplace. Skin is the largest organ protecting our body from exogenous toxins. Dermal absorption is one of the primary exposure routes in most environmental and occupational settings (Bronaugh and Maibach, 1999). Chemical exposure in these settings usually involves complex mixtures, not individual chemicals. However, the data used in most health risk assessments are based on individual chemicals because of lack of experimental data from chemical mixtures (U.S. Environmental Protection Agency [EPA], 2000, 2001).

Great efforts have been made to develop methods for quantitative assessments of dermal absorption. For risk assessment of chemical mixtures, many challenges are encountered: (1) lack of quantitative data for chemical mixtures because most of the data are measured with individual chemicals; (2) even for individual chemicals, only limited data acquired under comparable experimental conditions, and many data acquired under incomparable conditions are not useful for the urgent need for risk assessment of dermal absorption; (3) lack of fundamental methodology to handle thousands of chemicals and millions of their combinations. It is impossible to mechanistically study all of the chemicals and their combinations. This problem is likely to worsen with the increasing number of chemicals required to be evaluated.

The health risk assessment of chemical mixtures has become a research frontier. The congressional Commission on Risk Assessment and Risk Management recommended moving beyond individual chemical assessments and focusing on the broader issue of toxicity of chemical mixtures. The U.S. regulatory agencies (EPA, 2000; Agency for Toxic Substances and Disease Registry, 2001) proposed guidance for conducting health risk assessment of chemical mixtures. However, the guidelines are highly dependent on the available data; in most cases, experimental data from individual chemicals have to be used because of the lack of experimental data for chemical mixtures.

In this chapter, we introduce a novel system coefficient approach developed in our research center. The system coefficient approach uses a set of probe compounds to measure the molecular interaction strengths of a skin/chemical mixture system. A linear free-energy relationship (LFER, a thermodynamic principle) is used to dissect the complicated molecular interactions in the absorption system into basic molecular interaction forces, which can be parameterized and used to predict a free-energy-related property of the system, such as partition coefficients or permeability. In the system coefficient approach, a chemical mixture is treated as a medium composed of the major components and other minor or trace components. A set of system coefficients represents the relative molecular interaction strengths of the chemical mixture, and a set of solute descriptors represents the molecular interaction strengths of a chemical. A free-energy-related specific property is interactively correlated to the system coefficients of the chemical mixture and the solute descriptors of the chemicals, which can be used to provide quantitative predictions

systematically for each of the components regardless of the complexity of the chemical mixture.

METHOD DEVELOPMENT

In the system coefficient approach, a chemical mixture is treated as a composition of a medium and other minor or trace chemicals. The medium is composed of the major components that dominate the bulk physical-chemical properties; the minor or trace components will not significantly affect the bulk properties of the chemical mixture. When skin is exposed to the chemical mixture, the skin and the medium form an absorption system (skin/medium). The transport and distribution of a given chemical in the skin/medium system are governed by the relative molecular interaction strengths of the chemical with the skin and the medium, which can be parameterized with the system coefficient approach.

The system coefficient approach is based on Abraham's LFER, which is an application of the additive principle of the free-energy components in thermodynamics. The complicated molecular interactions in the skin and chemical mixture system are dissected into basic molecular forces. There are mainly four types of molecular forces for nonelectrolyte chemicals: London dispersion, hydrogen bonding, dipolarity/polarizability, and lone-pair electrons (Abraham, 1993b). The molecular interaction strengths of the chemical are described by five effective solute descriptors [R, π, α, β, V] because the hydrogen bonding needs two descriptors, hydrogen bonding acidity and basicity. The relative strengths of the molecular forces of the skin/medium system are described by a set of system coefficients: [*r, s, a, b, v*]. A free-energy-related specific property *SP* can be correlated with the solute descriptors of the chemical and the system coefficients of the skin/medium system via Abraham's LFER:

$$\text{Log } SP = c + r\text{R} + s\pi + a\alpha + b\beta + v\text{V} \tag{5.1}$$

The solute descriptors [R, π, α, β, V] are characteristic parameters of the chemical. Their values will not change when the chemical is transferred from one medium system to another. Each of the solute descriptors represents the relative strength of a specific type of molecular force of the chemical:

- Log *SP* is a specific free-energy-related property to be studied, such as partition coefficient or permeability.
- R is an excess molar refraction representing the molecular force of lone-pair electrons, which can be experimentally determined or calculated from refractive index.
- π is the effective dipolarity and polarizability of the chemical.
- α is the effective H-bond acidity, a summation of the acidity from all H-bonds of the chemical.
- β is the effective H-bond basicity, a summation of the basicity from all H-bonds of the chemical.
- V is the McGowan characteristic volume that represents London dispersion.

The system coefficients [*r, s, a, b, v*] are characteristic parameters of the skin/medium system. Their values will not change from one chemical to another. Each of the system coefficients represents the relative strength of a specific type of molecular force of the skin/medium system:

- *c* is a regression constant and can be treated as a system coefficient because it is related to the specific property of the system.
- *r* represents the tendency of the system to interact with the chemical through π* and n-electron pairs; usually, the *r* value is positive, but for phases that contain fluorine atoms, the *r* value can be negative.
- *s* represents the tendency of the system to interact with dipolar/polarizable chemicals.
- *a* is a measure of the H-bond basicity of the system, which describes the tendency of the system to interact with the H-bond acidity of the chemical.
- *b* is a measure of the H-bond acidity of the system, which describes the tendency of the system to interact with the H-bond basicity of the chemical.
- *v* is a combination of exothermic dispersion forces that make positive contributions; it mainly measures the hydrophobicity of the system.

The system coefficients are properties of the skin/chemical mixture system representing the relative molecular interaction strengths of the absorption system. They will not change with minor or trace chemicals in composition or proportion. Therefore, the system coefficients of the skin/chemical mixture system can be determined by using a set of probe compounds with known solute descriptors. The probe compounds are selected to cover a wide range of molecular interaction strengths. When a probe compound is added into the chemical mixture in trace concentration not affecting the system coefficients, the permeability of the probe compound through the skin is governed by the relative molecular interaction strengths of the compound with the skin and the medium of the chemical mixture. The skin permeability log k_p is determined for each of the probe compounds in the medium of the chemical mixture with conventional diffusion cell experiments. The log k_p value of a given compound can be scaled to the solute descriptors of the compound by the LFER equation (Equation 5.1). A LFER equation matrix can be generated from all of the probe compounds (e.g., 32 probe compounds):

$$\text{Log}\, k_p^n = c + rR^n + s\pi^n + a\alpha^n + b\beta^n + vV^n \qquad (n = 32) \tag{5.2}$$

The system coefficients of the skin/medium [*c, r, s, a, b, v*] can be obtained by multiple linear regression analysis of the LFER equation matrix (Equation 5.2). These system coefficients are properties of the skin/medium system. They will not change with minor or trace chemicals in composition or proportion.

Minor or Trace Chemicals

In the system coefficient approach, the minor or trace components do not affect the system coefficients. The physical-chemical behavior of the minor or trace chemical

in the skin/medium system is governed by the molecular interactions of the chemical with the skin and the medium. Once a robust set of system coefficients is obtained for the skin/medium system, the permeability can be predicted for any chemical of interest from the system coefficient of the skin/medium system and the solute descriptors of the chemical (Equation 5.1).

If the proportion of a chemical is so high that it will affect the system coefficients, then it becomes a major component. Its effects on the system coefficients and its permeability should be treated as major medium components.

Major Components

The medium is composed of the major components of the chemical mixture that determined the system coefficients of the skin/medium system. The permeability of a major component is also governed by the relative molecular interaction strengths of the major component with the skin and the medium of the chemical mixture. If a robust set of system coefficients is known, the permeability of a major component can also be predicted from the system coefficients and the solute descriptors of the component. However, the effective concentration should be used instead of the stoichiometric concentration for the major component. The effective concentration is a corrected concentration by fugacity as defined in physical chemistry. Because the major components determine the system coefficients, any change in the major components in proportion or composition will affect the system coefficients.

System Coefficients of Sufficient Similar Mixtures

When the major components change in composition or proportion, the system coefficients will be altered. Therefore, the changes in the system coefficients can be used to study the effects of the major components on the permeation properties of other components in the chemical mixture. If the chemical mixture has a small change in the medium, this change will be reflected in the system coefficients, that is, a small change will be introduced into the system coefficients: [Δc, Δr, Δs, Δa, Δb, Δv]. The changes in the system coefficients can be obtained by subtraction of the system coefficients of the chemical mixture from those after the change:

$$[\Delta c, \Delta r, \Delta s, \Delta a, \Delta b, \Delta v] = [c, r, s, a, b, v]_x - [c, r, s, a, b, v]_o$$

$$= [c_x - c_o, r_x - r_o, s_x - s_o, a_x - a_o, b_x - b_o, v_x - v_o]$$

or

$$[c, r, s, a, b, v]_x = [c_o + \Delta c, r_o + \Delta r, s_o + \Delta s, a_o + \Delta a, b_o + \Delta b, v_o + \Delta v] \quad (5.3)$$

where $[c, r, s, a, b, v]_o$ are the system coefficients of the original chemical mixture, $[c, r, s, a, b, v]_x$ are the system coefficients after the change of a major component

in the chemical mixture, and [Δc, Δr, Δs, Δa, Δb, Δv] are the changes in the system coefficients.

Note that the small change in the medium of the chemical mixture is a sufficiently similar mixture. Therefore, the system coefficients of the sufficiently similar mixture can be studied by the system coefficient approach. When system coefficients of the chemical mixture and those of the sufficiently similar mixtures are mapped over a range of interest by the system coefficient approach, the permeability of any chemical can be predicted for the chemical mixture in the given range.

Determination of the Solute Descriptors

The solute descriptors are required in the system coefficient approach. The solute descriptors can be found in Abraham's databases for many compounds. Commercial software (Absolv Pharma Algorithms, Ontario, Canada) is also available for estimating the values of the solute descriptors from the structure of the compounds. Experimental determination of the solute descriptors is best carried out through the use of multiple water/solvent partition coefficients (Abraham et al., 1999). However, it is difficult to determine the water/solvent partition coefficients using the traditional liquid–liquid extraction, which involves tedious manual operation, complicated sample handling, and emulsion problems.

The membrane-coated fiber technique has overcome these experimental difficulties. A membrane material coated onto a fiber is used as the absorption membrane to determine the membrane/solvent partition coefficients of chemicals. Multiple membrane/solvent systems can be calibrated with the probe compounds with known solute descriptors as follows. The partition coefficient of each probe compound in a given membrane/solvent system log $K_{m/s}$ is determined experimentally by the membrane-coated fiber technique. The log $K_{m/s}$ value of each probe compound is scaled to the solute descriptors of the compound with the LFER equation (Equation 5.1, where log SP = log $K_{m/s}$). A LFER equation matrix is generated from all of the probe compounds (Equation 5.2). The system coefficients of each membrane/solvent system can be obtained by multiple linear regression analysis of the LFER equation matrix.

Once the system coefficients of the multiple membrane/solvent systems are known, they can be used to determine the solute descriptors for any compounds of interest. For example, the partition coefficients of any chemical of interest are determined in 15 membrane/solvent systems (m = 15). The log $K_{m/s}$ value of a given membrane/solvent system can be scaled to the system coefficients via the LFER equation (Equation 5.1). A LFER equation matrix is generated from all of the membrane/solvent systems:

$$\log K^{m}_{m/s} = c_m + r_m R + s_m \pi + a_m \alpha + b_m \beta + v_m V \qquad m = 15 \tag{5.4}$$

In this regression, the system coefficients of the multiple membrane/solvent systems are known quantities; the solute descriptors [R, π, α, β, V] are the quantities

to be obtained by multiple linear regression analysis of the LFER equation matrix (Equation 5.4).

Effective Descriptors

It is noted that Abraham's solute descriptors do not represent a simple 1:1 interaction; rather, they represent the summation of specific types of interactions (Abraham, 1993a). For example, a compound may have several hydrogen bond groups; α represents the summation of the hydrogen bond acidity from all groups of the compound. Similarly, a system constant represents the summation of a specific type of interaction of the membrane/solvent system. For example, a represents the effective hydrogen bond basicity of the absorption system because it describes the molecular interaction strength of the system that interacts with the hydrogen bond acidity α of the chemicals. System coefficient b represents the effective hydrogen bond acidity because it describes the molecular interaction strength of the system that interacts with the hydrogen bond basicity β of the chemicals.

The skin permeability and the partition coefficients are free-energy-related quantities that can be modulated by the same set of solute descriptors of the chemicals. This offers a new strategy that the skin permeability does not have to be determined directly for all of the chemicals or chemical mixtures; rather, it can be predicted from the solute descriptors that can be determined via the measurement of their partition coefficients. The advantage of this strategy lies in the fact that the permeability measurement is affected by many experimental factors, and the experimental processes are difficult to be automated; the determination of the membrane/solvent partition coefficients can be highly automated with the membrane-coated fiber technique.

Selection of the Probe Compounds

The system coefficient approach uses a set of probe compounds to detect the molecular interaction strengths of the skin/chemical mixture system. The selection of the probe compounds is a critical step in development of the system coefficient approach.

1. The probe compounds should have reliable solute descriptors from reference handbooks or the literature.
2. The probe compounds should cover wide strength ranges of the different molecular interactions, which will eventually determine the application range of the system coefficients.
3. The probe compounds are added into the chemical mixture in trace concentrations not affecting the system coefficients. Analytical methods should be available for their quantitative analysis.
4. The probe compounds should be chemically stable; metabolism and specific biological interactions are negligible during the absorption processes.
5. Passive diffusion is the driving force in the absorption processes. When the absorption property is experimentally measured, it carries the molecular interaction information ready to be resolved by multiple linear regression analysis of the LFER equation matrix.

DETERMINATION OF THE SYSTEM COEFFICIENTS

Skin is a heterogeneous, multiple-layer organ. In a typical dermal absorption study, three biological levels are of main concern: stratum corneum, epidermis, and whole skin (Schaefer and Redelmeier, 1996). When the skin is exposed to a chemical mixture, the skin and the medium of the chemical mixture form an absorption system. For the three skin layers, three absorption systems could be generated for a given chemical mixture, which will provide abundant information on the three biological levels.

System Coefficients of the Stratum Corneum

The stratum corneum is composed of flat corneocytes embedded in a continuous intercellular lipid matrix. The intercellular lipid matrix is the main route for percutaneous absorption of many exogenous chemicals. However, it is difficult to use stratum corneum to conduct absorption experiments because of the hair follicles. Synthetic membranes, including lipid and silastic membranes, have been used to simulate the absorption properties of this lipidal layer.

The permeation coefficient of a given probe compound through a simulating membrane can be determined by diffusion cell experiments ($\log k_p$). The $\log k_p$ value can be scaled to the solute descriptors of the compound via the LFER equation (Equation 5.1, where $\log SP = \log k_p$). A LFER equation matrix is obtained from the permeation coefficient and the solute descriptors of all the probe compounds (Equation 5.2). The system coefficients of the membrane and the chemical mixture can be obtained by multiple linear regression analysis of the LFER equation matrix [$\log k_p$, R, π, α, β, V].

In the LFER equation (Equation 5.1), the specific property can be any free-energy-related quantity, such as partition coefficient or permeability. For a given absorption system, a set of the system coefficients can be obtained for each of the free-energy-related quantities. The system coefficients obtained from a specific property of the probe compounds can be used to predict the specific property for other compounds. A detailed example using polydimethylsiloxane (PDMS) membranes is described in the section on the system coefficients of PDMS/water (P/W) systems.

System Coefficients of Epidermis

Epidermis consists of the stratum corneum and adjacent viable layer. The system coefficients of the epidermis can be obtained by measuring the permeation coefficient of the probe compounds in the donor solution of the chemical mixtures using static Franz and flow-through diffusion cells. The $\log k_p$ value of a given probe compound is scaled to the solute descriptors of the compound via the LFER equation (Equation 5.1, where $\log SP = \log k_p$). A LFER equation matrix is generated from the permeation coefficients and the solute descriptors of all the probe compounds (Equation 5.2). The system coefficients of the epidermis and the chemical mixture can be obtained by multiple linear regression analysis of the LFER equation matrix [$\log k_p$, R, π, α, β, V]. The system coefficients of the epidermis would be different from

those of the stratum corneum even though the stratum corneum is the primary barrier layer. The contribution of the viable epidermal layer on the barrier can be described by the differences of the system coefficients between the epidermis and the stratum corneum.

It is noted that the system coefficients are not the properties of the epidermis itself; rather, they are properties of the absorption system composed of the epidermis and the medium of the chemical mixture. Only an absorption system has specific permeation properties that can be measured quantitatively by the system coefficients. This situation is also applied to the permeability measurement, that is, a given permeability of a chemical is for a specific absorption system consisting of the epidermis and the medium of the donor solution. The permeation coefficients of chemicals cannot simply be compared if they are measured in different media (e.g., water vs. ethanol). At a given dose concentration, different media could provide a significantly different driving force for the passive diffusion, which governs the absorption processes.

There are as yet no available example system coefficients obtained with the present approach. The LFER analysis has been used for skin permeation from compiled literature permeability data (Abraham et al., 1999). Large discrepancies are expected from the compiled literature data acquired in different laboratories with different protocols. It is difficult to systematically study the effects of experimental conditions on the system coefficients using compiled literature data (Moss et al., 2002).

System Coefficients of Skin

In practical applications, the effects of the whole skin on the systematic toxicology are the main concern. Although the absorption processes are much more complicated in the whole skin than those in the stratum corneum, passive diffusion is the driving force for many chemicals in this complicated biological system. Therefore, the system coefficient approach can be utilized to study the absorption processes of the chemicals in the whole skin. For some chemicals, their transport processes could be controlled by biological conversions (e.g., metabolism) or biological specific interactions (e.g., antibody–antigen interactions). These specific biological interactions are not considered in the system coefficient approach. For example, antibody–antigen interactions are structure dependent, which has not been considered in the system coefficient approach. Thus, the system coefficient approach can only provide accurate predictions when passive diffusion is the control mechanism. If the experimental observed permeation coefficient of a chemical is significantly different from the value predicted by the system coefficient approach, it reveals that biological specific interactions or metabolite conversions could occur during the absorption processes. Thus, the system coefficient approach can be used to detect possible biological specific interactions.

The effects of chemical mixture on a biological system could be synergistic, additive, or antagonistic. The system coefficient approach can quantitatively measure the additive contributions of chemical mixtures, which are governed by passive diffusion, nonspecific biological interactions. It also can be used to detect the existences

of the synergistic or antagonistic interactions by examining the deviations of the experimental observed values from the predicted ones by the system coefficient approach. The contributions of the specific interactions should be measured with special methodologies. The base values predicted by the system coefficient approach should be modified to account for the contributions of the specific interactions.

SYSTEM COEFFICIENTS OF THE POLYDIMETHYLSILOXANE/WATER SYSTEM

PDMS membranes have been widely used as a skin imitation membrane for dermal absorption studies (Moss et al ., 2002). A membrane-coated fiber technique has been developed in our center for quantitative analysis of the absorption kinetics and rapid determination of the partition coefficients of chemicals between the PDMS membrane and chemical mixtures (Xia et al., 2003). In the following sections, the system coefficient approach is demonstrated by measuring the partition coefficients of chemicals in the P/W systems.

Partition Coefficients

The chemical mixtures composed of 32 probe compounds were prepared in aqueous solutions. The partition coefficients of chemicals were determined by PDMS membrane-coated fibers. The partition coefficient can be obtained by equilibrium or regression methods. In the equilibrium method, the absorption amount $n°$ is determined at a predetermined equilibrium time. The partition coefficient of a chemical can be calculated from the equilibrium absorption amount $n°$ and the initial concentration C_o (Xia et al., 2003). The equilibrium absorption amount $n°$ can also be obtained by regression of the absorption data sampled before the equilibrium with a kinetic model. The absorption experiment time can be reduced considerably with the regression method (Xia et al., 2004).

System Coefficients

The system coefficients of the P/W system were obtained by using a set of probe compounds with known solute descriptors. The solute descriptors of the 32 probe compounds [R, π, α, β, V] are given in Table 5.1. The partition coefficient of a given probe compound (log $K_{P/W}$) was determined in the aqueous solutions using PDMS membrane-coated fibers. The log $K_{P/W}$ value of the compound was scaled to its solute descriptors via the LFER equation (Equation 5.1, where log SP = log $K_{P/W}$). A LFER equation matrix [log $K_{P/W}$; R, π, α, β, V] was generated from all of the probe compounds (n = 32, Table 5.1). The system coefficients of the P/W system were obtained by the multiple linear regression analysis of the LFER equation matrix:

$$\log K_{p/w} = 0.09 + 0.49\mathrm{R} - 1.11 - 2.36\alpha - 3.78 + 3.50\mathrm{V} \quad R^2 = 0.995 \qquad (5.5)$$

Table 5.1 Probe Compounds with Known Solute Descriptors and Determined Partition Coefficients

No.	Probe Compounds[a]	R	π	α	β	V	log $K_{P/W}$	log $K_{P/E50}$	log $K_{P/L10}$
1	Toluene	0.601	0.52	0	0.14	0.857	2.24	1.07	0.89
2	Chlorobenzene	0.718	0.65	0	0.07	0.839	2.40	1.00	0.90
3	Ethylbenzene	0.613	0.51	0	0.15	0.998	2.71	1.29	1.00
4	*p*-Xylene	0.613	0.52	0	0.16	0.998	2.76	1.34	1.01
5	Bromobenzene	0.882	0.73	0	0.09	0.891	2.51	1.00	0.77
6	Propylbenzene	0.604	0.5	0	0.15	1.139	3.14	1.52	1.00
7	4-Chlorotoluene	0.705	0.67	0	0.07	0.98	2.87	1.22	0.97
8	Phenol	0.805	0.89	0.60	0.3	0.775	−0.18	−0.53	−0.44
9	Benzonitrile	0.742	1.11	0	0.33	0.871	1.04	0.00	0.25
10	4-Fluorophenol	0.67	0.97	0.63	0.23	0.793	−0.28	−0.63	−1.93
11	Benzyl alcohol	0.803	0.87	0.33	0.56	0.916	−0.35	−0.56	−0.85
12	Iodobenzene	1.188	0.82	0	0.12	0.975	2.73	1.03	0.72
13	Phenyl acetate	0.661	1.13	0	0.54	1.073	0.86	0.06	−0.05
14	Acetophenone	0.818	1.01	0	0.48	1.014	1.04	−0.09	−0.09
15	*m*-Cresol	0.822	0.88	0.57	0.34	0.916	−0.03	−0.59	−0.83
16	Nitrobenzene	0.871	1.11	0	0.28	0.891	1.21	0.09	0.11
17	Methyl benzoate	0.733	0.85	0	0.46	1.073	1.65	0.27	0.23
18	4-Chloroanisole	0.838	0.86	0	0.24	1.038	2.37	0.77	0.60
19	Phenethyl alcohol	0.784	0.83	0.30	0.66	1.057	0.12	−0.49	−0.65
20	3-Methyl benzyl alcohol	0.815	0.9	0.33	0.59	1.057	0.17	−0.50	−0.77
21	4-Ethylphenol	0.80	0.9	0.55	0.36	1.057	0.60	−0.40	−0.61
22	3,5-Dimethylphenol	0.82	0.84	0.57	0.36	1.057	0.42	−0.52	−0.80
23	Ethylbenzoate	0.689	0.85	0	0.46	1.214	2.12	0.48	0.33
24	Methyl-2-methyl benzene	0.772	0.87	0	0.43	1.214	2.15	0.49	0.35
25	Naphthalene	1.36	0.92	0	0.2	1.085	2.83	1.03	0.76
26	3-Chlorophenol	0.909	1.06	0.69	0.15	0.898	0.31	−0.55	−0.28
27	4-Chloroaniline	1.06	1.13	0.30	0.31	0.939	0.84	−0.22	−0.91
28	4-Nitrotoluene	0.87	1.11	0	0.28	1.032	1.77	0.29	0.00
29	4-Chloroacetophen	0.955	1.09	0	0.44	1.136	1.64	0.10	−0.08
30	3-Bromophenol	1.06	1.15	0.70	0.16	0.95	0.46	−0.54	−1.23
31	1-Methyl naphthalene	1.344	0.90	0	0.20	1.226	3.26	1.26	0.81
32	Biphenyl	1.36	0.99	0	0.22	1.324	3.37	1.29	0.92

[a] The probe compounds were selected from the recommended compounds by Abraham (Poole et al., 1998).

The contributions from different types of molecular interactions are known from the values of the system coefficients. The contributions of lone pair electrons r, polarity/polarizability s, hydrogen bond basicity a, hydrogen bond acidity b, and hydrophobicity v of the P/W system were 0.49, −1.11, −2.36, −3.78, and 3.50, respectively. It indicates that lone-pair electron interaction r was not a significant factor in the partitioning process. The correlation of the lone-pair electron interaction r with the partition coefficient was loose ($R^2 = 0.43$). The dipolarity/polarizability interaction was also a weak factor in the partitioning process ($s = -1.11$) with a partial correlation coefficient R^2 of 0.77. The hydrogen bond basicity a, hydrogen bond acidity b, and hydrophobicity v of the P/W system were significant factors in the partition coefficients ($a = -2.36$, $b = -3.78$, and $v = 3.50$), with partial correlation coefficients R^2 of 0.98, 0.97, and 0.94, respectively.

MINOR OR TRACE COMPONENTS OF CHEMICAL MIXTURES

Quantitative assessment of the chemical exposures to multiple agents, particularly at low levels of exposure, is extremely difficult. The dose level for any individual chemical could be lower than the acceptable daily intake or reference dose levels. The potential health effects are a serious concern because we are exposed to low-dose chemical mixtures in diet, air, and water. Their combination toxic effects are unknown and could be additive, synergistic, or antagonistic. Our inability to predict whether agents will act in an additive, synergistic, or antagonistic fashion at concentrations encountered in our daily life creates a real problem for human health risk assessment. In most cases, toxicological effects cannot be observed in such low-dose exposures. The health risk assessment of the low-dose exposures is one of the challenges in chemical mixture scenarios.

The system coefficient approach could be a useful tool for quantitative assessment of the complicated low-dose exposures. Once a robust set of system coefficients is obtained for a given absorption system, the permeability of a minor or trace component can be predicted from the system coefficients and the solute descriptors of the component (Equation 5.1). The system coefficients of the absorption system are not altered by the minor or trace components in proportion or composition. Therefore, the prediction can be made for any minor and trace components regardless of the complexity of the chemical mixture. The exposure data obtained by the system coefficient approach are additive for different components of the chemical mixtures and can be readily used for quantitative assessment.

MAJOR COMPONENTS OF CHEMICAL MIXTURES

When the major components change in composition or proportion, the system coefficients will be altered. Therefore, the changes in the system coefficients can be used to study the changes of major components in the chemical mixture. If the chemical mixture has a small change in the medium, this change will be reflected in the system coefficients; that is, a small change will be introduced into the system

coefficients. The changes in the system coefficients can be obtained by subtraction of the system coefficients of the chemical mixture before the change from those after the change (Equation 5.3). This is another important application area of the system coefficient approach. It can be used to assess the matrix effects on dermal absorption processes quantitatively. The solvent and surfactant effects are used to demonstrate the applications of the system coefficient approach.

Solvent Effects

When ethanol was added into the aqueous solutions, the system coefficients were altered because the ethanol proportions were high enough to change the physiochemical properties of the medium. To study the solvent effects, the system coefficients were determined at different ethanol proportions. The system coefficients of a PDMS/ethanol–water system were obtained with the same procedures as those for the P/W system. For example, the partition coefficients of the PDMS/50% ethanol–water system (P/E50) were determined for all of the 32 probe compounds (Table 5.1). A new LFER equation matrix was generated from log $K_{P/E50}$ of a compound and its solute descriptors [log $K_{P/E50}$; R, π, α, β, V]. The respective system coefficients of the P/E50 system obtained by multiple regression analysis of the equation matrix were $[0.68, 0.31, -1.27, -1.53, -2.08, 1.35]_{P/E50}$, $R^2 = 0.991$. The solvent effects of 50% ethanol on the system coefficients can be obtained by subtraction of the system coefficients of the P/W system from the system coefficients of the P/E50 system:

$$[\Delta c, \Delta r, \Delta s, \Delta a, \Delta b, \Delta v]_{E50}$$

$$= [0.68, 0.31, -1.27, -1.53, -2.08, 1.35]_{P/E50} - [0.09, 0.49, -1.11, -2.36, -3.78, 3.50]_{P/W}$$

$$= [0.58, -0.18, -0.42, 0.83, 1.70, -2.15]_{E50}$$

The solvent effects of 50% ethanol on the system coefficients of the P/W system are shown in Figure 5.1. It shows that the hydrophobicity was regulated downward; that is, the contribution of the hydrophobicity to the partition coefficient was reduced by the addition of ethanol. This is theoretically expected because the addition of ethanol into the water solution will increase the hydrophobicity of the solution and consequently reduce the hydrophobicity difference between the PDMS and water solution. If the hydrophobicity of the solution and the PDMS membrane are the same, the hydrophobicity interactions of the compounds with the membrane and the solution will have no contribution to the partition coefficient. The contributions of hydrogen bond basicity Δa and acidity Δb are both increased. These observations revealed that hydrogen-bonding interactions became more important as the ethanol proportion increased. These results demonstrated that the system coefficient approach is not only quantitative but also qualitative; it allows the contributions of each type of molecular interaction to be analyzed. The system coefficient approach has high sensitivity in detecting the solvent effects. When the ethanol content

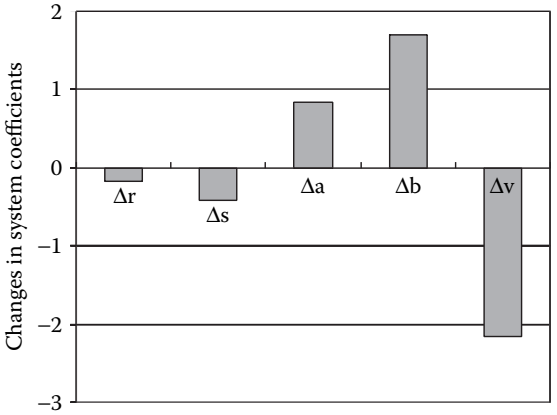

Figure 5.1 Solvent effects of 50% ethanol on the system coefficients.

increased from 0 to 50% (v/v), the system coefficients changed up to two orders of magnitude (Figure 5.1).

The contributions from different types of molecular interactions can be seen from the partial regression plots of the system coefficients. Figure 5.2 shows the partial regression plots of the PDMS/25% ethanol–water solution. The amplitudes of *y*-axis in a partial regression plot indicated the contribution of the system coefficient to the partition coefficient. It is shown that lone-pair electron interaction *r* was not a significant factor in the partitioning process. The range of the *y*-axis was 0.48. The widely scattered points revealed loose correlation of the partition coefficient with the lone-pair electron interactions ($R^2 = 0.27$). The dipolarity/polarizability interaction was also a weak factor in the partitioning process, with an amplitude of about 0.9 and a partial correlation coefficient of 0.72. The hydrogen bond basicity *a*, hydrogen bond acidity *b*, and hydrophobicity *v* of the P/W system were significant factors in the partition coefficients, with amplitudes of 2.0, 1.8, 1.0, respectively, and partial correlation coefficients R^2 of 0.96, 0.93, and 0.87, respectively.

Sodium Lauryl Sulfate Effects on Polydimethylsiloxane Absorption of Chemical Mixtures

The partition coefficients of the probe compounds were determined in solutions with different concentrations of sodium lauryl sulfate (SLS) surfactant. For example, the partition coefficients of the probe compounds in PDMS/10% SLS (P/L10) system are given in Table 5.1. The log $K_{P/L10}$ values of the probe compounds and their solute descriptors formed a new LFER equation matrix. The system coefficients of the P/L10 system were obtained by multiple linear regression analysis of the LFER equation matrix. The system coefficients of the P/L10 system were $[0.82, 0.25, -1.16, -1.93, -1.61, 0.86]_{P/L10}$ with a multiple linear regression coefficient R^2 of 0.89. When the P/W system was used as the reference system, the changes in system

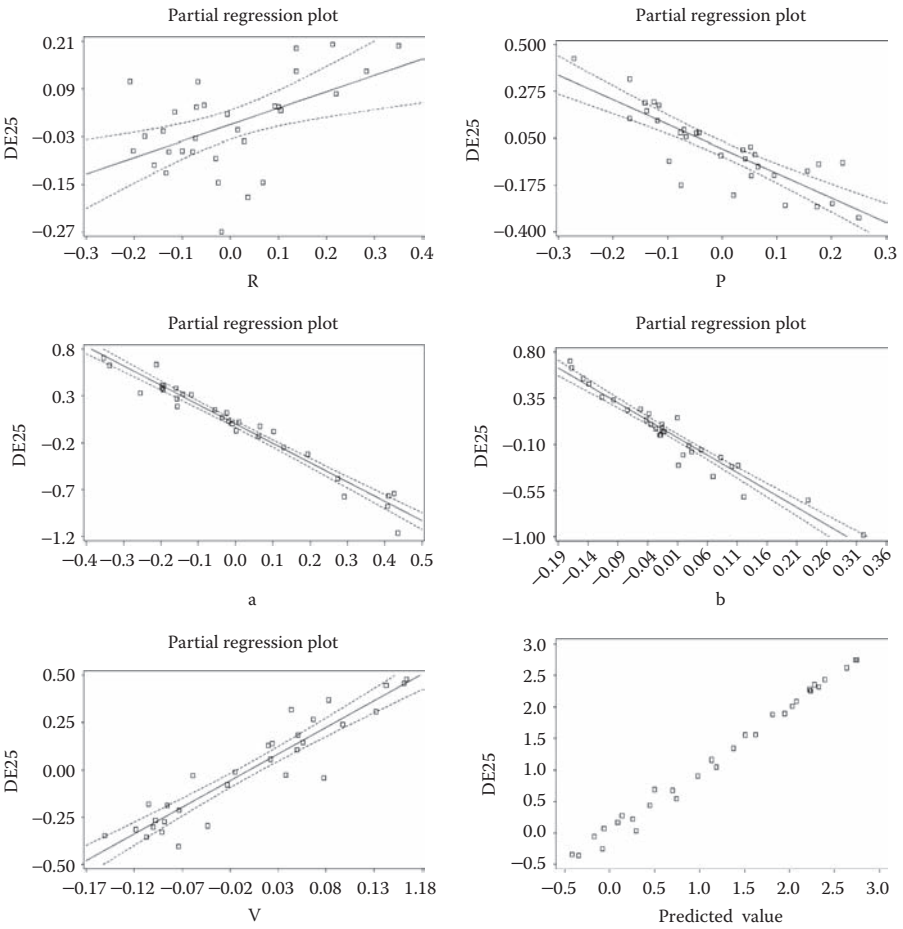

Figure 5.2 Contributions of the system coefficients to the partition coefficients.

coefficients caused by addition of 10% SLS into the P/W system were obtained as follows:

$$[\Delta c, \Delta r, \Delta s, \Delta a, \Delta b, \Delta v]_{L10}$$

$$= [0.82, 0.25, -1.16, -1.93, -1.61, 0.86]_{P/L10} - [0.09, 0.49, -1.11, -2.36, -3.78, 3.50]_{P/W}$$

$$= [0.73, -0.24, -0.05, 0.43, 2.17, -2.64]_{L10}$$

The surfactant effects of 10% SLS on the system coefficients of the P/W system are shown in Figure 5.3. The changes in system coefficients represent $[\Delta c, \Delta r, \Delta s, \Delta a, \Delta b, \Delta v]_{L10}$. Note that the effects of the SLS surfactant on the system coefficients were similar to the ethanol solvent effects. The system coefficients were altered by

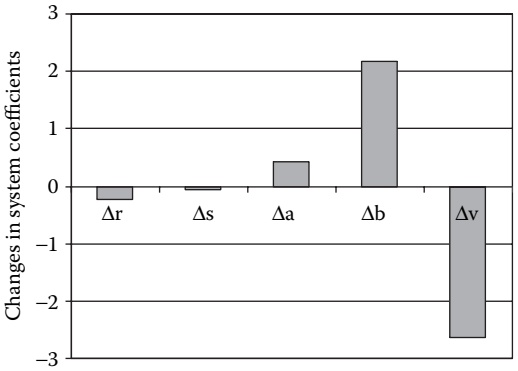

Figure 5.3 Surfactant effects of 10% SLS on the system coefficients.

more than two orders of magnitude when the SLS concentration changed from 0.1 to 10% (w/v). Hydrophobicity *v* and hydrogen bond acidity *b* were the main molecular interactions affected by SLS surfactant. Lone-pair electrons and dipolarity/polarizability were not significant molecular forces; hydrogen bond basicity of the system was not significantly affected by the addition of SLS surfactant (Δa; Figure 5.3).

ADVANTAGES OF THE SYSTEM COEFFICIENT APPROACH

The system coefficient approach can be used for any chemical mixtures regardless of complexity. This overcomes the toughest challenge in risk assessment of chemical mixtures, for which testing thousands of chemicals and millions of their combinations is formidable.

The system coefficient approach measures the mainstream of the chemical mixtures in which passive diffusion is the main transport mechanism. The biological conversions or specific interactions are events over the mainstream during the absorption processes. If the experimental observed values are significantly different from the predicted values, it indicates that some specific interactions occurred, and special techniques should be used to assess the specific biological interactions. The mainstream data should be corrected for the specific interactions.

The effects of chemical mixture on a biological system could be synergistic, additive, or antagonistic. The system coefficient approach provides a means for quantitative assessment of the additive contributions of the chemical mixtures. It also can be used to detect the existence of the synergistic or antagonistic interactions by examining the deviations of the experimental observed values from those predicted by the system coefficient approach.

The changes in the system coefficients can be used to quantitatively assess the solvent, formulation, and matrix effects. When system coefficients of the chemical mixture and those of the sufficiently similar mixtures are mapped over a range of interest by the system coefficient approach, the permeability of any chemical can be predicted for the chemical mixture in the given range.

The system coefficient approach seamlessly integrates the experimental techniques and theoretical model to systematically provide a means for quantitative assessment of dermal absorption from chemical mixtures. The required data can be determined using high-throughput, automatic instrumentation, not depending on compiled literature data. This not only overcomes the shortage of experimental data for chemical mixtures, but also significantly increases the prediction precision and accuracy.

The system coefficient approach is a thermodynamic principle-based experimental approach. It overcomes the trial-and-error weakness in the traditional empirical fitting approach. This significantly advances the fundamental methodology for risk assessment of dermal absorption from chemical mixtures.

Limitations of the System Coefficient Approach

Specific biological conversion and interactions are not considered in the system coefficient approach. Therefore, it cannot be used directly if specific chemical or biological interactions make significant contributions in the absorption processes. Special methods should be developed to assess the contribution of these specific chemical or biological interactions.

REFERENCES

Abraham, M.H. (1993a). Hydrogen bonding. 31. Construction of a scale of solute effective or summation hydrogen-bond basicity, *J. Phys. Org. Chem.,* 6, 660–684.

Abraham, M.H. (1993b). Scales of solute hydrogen-bonding: their construction and application to physicochemical and biochemical processes, *Chem. Soc. Rev.,* 22, 73–83.

Abraham, M.H., Chadha, H.S., Martins, F., Mitchell, R.C., Bradbury, M.W., and Gratton, J.A. (1999). Hydrogen bonding part 46. A review of the correlation and prediction of transport properties by an LFER method: physicochemical properties, brain penetration and skin permeability, *Pesticide Sci.,* 55, 78–88.

Agency for Toxic Substances and Disease Registry. (2001). *Guidance Manual for the Assessment of Joint Action of Chemical Mixtures,* Agency for Toxic Substances and Disease Registry, available at: http://www.atsdr.cdc.gov/interactionprofiles/ipga.html#bookmark01.

Bronaugh, R.L. and Maibach, H.I. (1999). *Percutaneous Absorption Drug—Cosmetics—Mechanisms—Methodology,* Basel, Switzerland: Dekker.

Environmental Protection Agency. (2000). *Supplementary Guidance for Conducting Health Risk Assessment of Chemical Mixtures,* EPA/630/R-00/002, Washington, D.C.: Environmental Protection Agency.

Environmental Protection Agency. (2001). *Risk Assessment Guidance for Superfund (RAGS), Volume 1: Human Health Evaluation Manual (Part E, Supplemental Guidance for Dermal Risk Assessment) Interim,* EPA/540/R/99/005, Washinton, D.C.: Environmental Protection Agency.

Moss, G.P., Dearden, J.C., Patel, H., and Cronin, M.T.D. (2002). Quantitative structure–permeability relationships (QSPRs) for dermal absorption, *Toxicol. In Vitro,* 16, 299–317.

Poole, C.F., Poole, S.K., and Abraham, M.H. (1998). Recommendations for the determination of selectivity in micellar electrokimetic chromatography, *J. Chromatogr. A.,* 798, 207–222.

Schaefer, H. and Redelmeier, T.E. (1996). *Skin Barrier: Principles of Dermal Permeation,* Basel, Switzerland: Karger.

Xia, X.R., Baynes, R.E., Monteiro-Riviere, N.A., Leidy, R.B., Shea, D., and Riviere, J.E. (2003). A novel *in-vitro* technique for studying dermal permeation with a membrane-coated fiber and gas chromatography / mass spectrometry. Part 1. Performances of the technique in studying chemical mixtures and determination of the permeation rates and partition coefficients of the chemical mixtures, *Pharm. Res.,* 20, 275–282.

Xia, X.R., Baynes, R.E., Monteiro-Riviere, N.A., and Riviere, J.E. (2004). A compartment model for the membrane-coated fiber technique used for determining the absorption parameters of chemicals into lipophilic membranes, *Pharm. Res.,* 21, 1345–1352.

CHAPTER 6

Biologically Based Pharmacokinetic and Pharmacodynamic Models of the Skin

James N. McDougal, Yanan Zheng, Qiang Zhang, and Rory Conolly

CONTENTS

INTRODUCTION

The ability to quantify the beneficial and toxic effects of chemicals in the skin is important for many reasons. The skin is a dynamic and complex organ that is directly exposed to the environment. It serves several important protective functions and is on the "front line" in the battle to keep hostile environments from disrupting the essential internal balance. This characteristic vulnerability to the local environment can be exploited pharmacologically but can cause concern when deleterious effects are considered. In both cases, it is the concentration of a compound or chemical inside the skin that interferes with normal skin structure and function in beneficial or deleterious ways. The effects produced by exogenous compounds are dependent on both the local concentration at the site of action in the skin and the potency of the compound. These components of the effect are classically separated into pharmacokinetic and pharmacodynamic processes. The pharmacokinetic process in the skin relates the external concentration *on* the skin to the target tissue dose or cellular dose *in* the skin. The pharmacodynamic process involves understanding the rela-

tionship between the target tissue dose and the local cellular or tissue response. Mathematical models (distinct from disease, organ system, or specific animal models) are useful tools for describing, understanding, and predicting these processes. Techniques for developing mathematical models for both of these processes have some characteristics in common, but because of their fundamental differences, they are addressed separately in this chapter after a discussion of the usefulness of skin models in general.

One might wonder why it is necessary to go to the trouble to develop quantitative models of biological processes in the skin. Why is it we cannot just be keen observers of the effects of chemicals? A main reason is that it is frequently not possible to observe or test every important mixture or formulation that might come into contact with the skin. It is much more cost-effective to use a mathematical model to describe the underlying "first principles" that apply to a wide range of mixtures or vehicle effects. With an understanding of the principles involved (i.e., thermodynamics, diffusion, blood flow, synergy, or protein–protein interactions), it is often possible to quantify pharmacokinetics or pharmacodynamics by extrapolation rather than by direct experimentation. Many biological processes are nonlinear (e.g., metabolism) or have positive or negative feedback mechanisms (e.g., cytokine release). Another main reason is that the awareness of the complexity of skin biology (from genomics and proteomics) is increasing at an astounding pace. As descriptions become more complicated, it becomes harder and harder to develop and maintain an intuitive understanding of the important parameters and their interactions. Models are useful because they allow us (and force us) to understand and mathematically describe the interactions (between exogenous chemicals and biological systems) that cause subsequent changes in homeostatic relationships that are considered either beneficial or deleterious.

Models are also useful because they can help us with experimental design of laboratory studies by predicting appropriate doses, exposure times, or sampling intervals. They can help us develop and test hypotheses about a disease or normal process or about actions of a specific biological component. A valid model is useful for interpolation within experimental parameters or extrapolation to situations that are difficult to observe experimentally. Ultimately, they can be used to improve the risk assessment process and assist in the design of prophylactic or therapeutic interventions.

BIOLOGICALLY BASED PHARMACOKINETIC MODELS

Pharmacokinetic models describe the biological processes of absorption, distribution, metabolism, and excretion of exogenous compounds. With the exception of absorption into and across the skin, absorption, distribution, metabolism, and elimination are essential processes that also occur with nutrients and endogenous compounds. Many of these processes can become nonlinear with increasingly higher exposure concentrations. Pulmonary absorption can be limited by respiratory rates. Metabolism can often show Michaelis-Menten or saturable kinetics. Distribution can be limited by the affinity of the chemical for a specific tissue or by blood flow.

Urinary and fecal elimination can be nonlinear because of active elimination processes. Biologically based pharmacokinetic models are useful for predicting these nonlinear behaviors because they are based on first principles instead of being strictly empirical.

Biologically based models have parameters that describe physiology, biochemistry, and physical chemistry. Physiological parameters include blood flow to an organ such as the liver, respiratory rates, urine flow, organ volumes, and body weights. These parameters are a characteristic of the particular organism studied, and the normal values describe physiology that is not dependent on the exogenous chemical modeled. Biochemical parameters, in contrast, describe the interaction of the physiology with the exogenous chemical modeled. Therefore, biochemical parameters are different with different chemicals. Examples of biochemical parameters are binding constants, partition coefficients, and metabolic rates. Physicochemical parameters are characteristics that are independent of the organism modeled. They reflect the properties of the chemical and examples are molecular weight and volatility. Taken together, these parameters can often describe the essential pharmacokinetic characteristics of the interaction of a biological organism with an exogenous chemical in ways that are useful.

One useful thing about pharmacokinetic models is that they are often used to extrapolate to other exposures. Target tissue doses from hypothetical exposure concentrations or exposure durations can often be predicted based on the physiological and biochemical parameters in the model. The only requirement is to change the exposure parameters to reflect the hypothetical exposure. They can also be used to extrapolate to other species based on updating the physiological parameters in the model with parameters of the new species of interest. This is sometimes the best way to attempt to relate laboratory animal studies to humans. One caveat is to check that the biochemical parameters updated are not qualitatively different. For example, serious errors may result from assuming that specific human blood proteins are quantitatively similar to rat blood proteins in their ability to bind exogenous chemicals.

Biologically based (sometimes called physiologically based pharmacokinetic models) have been used in toxicology and the pharmaceutical industry for a couple of decades, as described by several reviews (Andersen, 2003; Clewell et al., 1997; Krewski et al., 1994; Nestorov, 2003; Theil et al., 2003; Yang et al., 1995). In their simplest forms, these models maintain a mass balance for a specific chemical during the processes of absorption, distribution, metabolism, and elimination by estimating blood and tissue concentrations over the time of interest (Ramsey and Andersen, 1984). All of the perfused tissues in the body are lumped into compartments based on similar blood flow and affinity for the chemical of interest. Input from lung, gastrointestinal tract, skin, or directly into blood for intravenous dosing is included in the appropriate compartment. Losses caused by exhalation, metabolism, and urinary or fecal excretion are included. Blood flow and tissue/blood partition coefficients determine the concentrations of the chemical in the organ compartments over time. Figure 6.1 shows an example of a simple biologically based compartmental model with lumped compartments connected by blood flow.

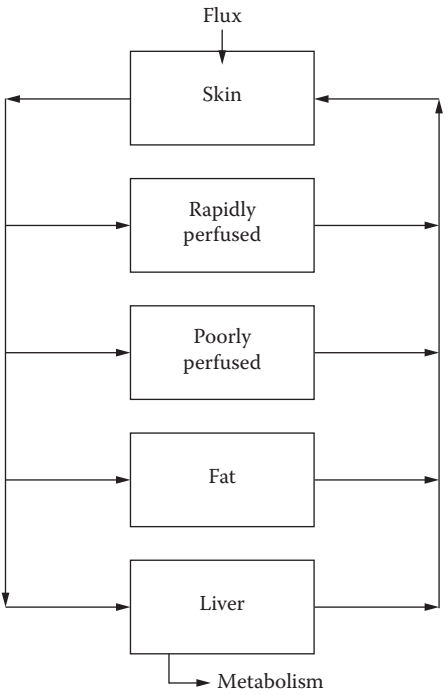

Figure 6.1 Schematic of a simple biologically based pharmacokinetic model showing five well-stirred compartments, each with arterial and venous blood flow signified by the arrows. Chemical flux is shown as an input to the skin compartment, and metabolism is shown as a loss from the liver compartment.

Compartments are chosen carefully in biologically based pharmacokinetic models. In contrast, compartments in traditional pharmacokinetic models are derived from the rate of drug elimination and usually have no physiological or anatomical reality (Gibaldi and Perrier, 1982). With biologically based models, all the perfused tissue is included in a compartment, but the major organs of storage, elimination, and absorption need to be included in the description as a specific compartment. The differential equation for a simple biologically based compartment (such as the fat compartment shown in Figure 6.1) is shown below:

$$V_{\mathrm{i}} \frac{dC_{\mathrm{i}}}{dt} = Q_{\mathrm{i}} C_b - Q_{\mathrm{i}} \frac{C_{\mathrm{i}}}{R_{\mathrm{i}/b}}$$

V_{i} is the volume of the compartment i; C_{i} is the concentration of chemical in compartment i; Q_{i} is the blood flow (arterial) to the compartment i; C_b is the concentration of chemical in the arterial blood; and $R_{i/b}$ is the partition coefficient for the chemical between the tissue and the blood. The concentration difference between the arterial blood and the tissue concentration, as normalized by the partition coefficient, is the driver for the amount of chemical in the tissue. The sum of the

flows times the concentration leaving each compartment is divided by the total cardiac output to estimate the concentration in the venous blood. See Ramsey and Andersen (1984) or McDougal (2004) for details of the equations.

Partition coefficients are an essential component of biologically based models. These coefficients, which are concentration ratios at equilibrium, provide the "chemical capacity" for each of the compartments and are important driving forces for absorption and distribution. See Gargas et al. (1989) for method of determination and background for volatile chemicals and Jepson et al. (1994) for method for nonvolatile chemicals. Equations for input rates, metabolism, tissue binding, and elimination are added to compartments if necessary. These details are not provided in this chapter so we can focus on the skin compartment but are available in excellent articles and reviews (Andersen, 2003; Bischoff et al., 1971; Clewell et al., 1997; Conolly, 2001; Gerlowski and Jain, 1983; Nestorov, 2003; Ramsey and Andersen, 1984). Many options are now available for solution of the simultaneous differential equations in these models, including acslXtreme® (Aegis Technologies Group, Inc.), Berkeley Madonna™ (University of California at Berkeley), and MATLAB® (The Math Works, Inc., Natick, MA).

The skin is frequently lumped into the poorly perfused compartment when skin absorption or toxicity is not of concern. When used as a separate compartment, biologically based skin compartments are usually connected to a whole-body pharmacokinetic model but can be used to describe *in vitro* diffusion cells (Bronaugh et al., 1994; McDougal and Jurgens-Whitehead, 2001) or isolated perfused skin (Williams et al., 1990). As part of a whole-body model, skin compartments can be used for parameter estimation or as the route of entry. When a biologically based model has been validated by another route and the surface area exposed and external skin concentration of chemicals are known, the model can be used to estimate flux or the permeability coefficient (Table 6.1).

Table 6.2 shows articles describing biologically based skin compartments used as an input to the whole-body model.

Skin compartments can be a simple, well-stirred compartment with diffusion or a more complex compartment, including some of the unique structural complexity of the skin. An important principle in biologically based modeling is to use the

Table 6.1 Models Using a Skin Compartment to Estimate Permeability Parameters

- Dermal absorption of chloroform by humans following bath water exposures (Corley et al., 2000)
- Penetration of 2,4,5,2′,4′,5′-hexachlorobiphenyl in young and adult rats (Fisher et al., 1989)
- Vehicle effects on the dermal absorption of halogenated methanes in rats (Jepson and McDougal, 1999)
- Dermal absorption of organic chemical vapors in rats (McDougal et al., 1986)
- Trichloroethylene in rats and humans (Poet, Corley, et al., 2000)
- Methyl chloroform in rats and humans (Poet, Thrall, et al., 2000)
- Perchloroethylene from a soil matrix in rats and humans (Poet et al., 2002)
- Aqueous toluene in rats using real-time breath analysis (Thrall and Woodstock, 2002)
- Dermal bioavailability of aqueous xylene in rats and humans (Thrall and Woodstock, 2003)

Table 6.2 Models with Skin Compartments Used as Input

- Plasma concentrations of benzoic acid after topical exposures based on diffusion cell measurements in hairless guinea pig (Bronaugh et al., 1994)
- Topical application of retinoic acid in humans (Clewell, Andersen et al., 1997)
- Dermal absorption of 2-butoxyethanol vapor in humans (Corley et al., 1997)
- Percutaneous absorption of clordecone in rats (Heatherington et al., 1998)
- Dermal dosing of 2,3,7,8-tetrabromodibenzo-*p*-dioxin (TBDD) in rats (Kedderis et al., 1993)
- Dermal absorption of *m*-xylene vapor in humans (Loizou et al., 1999)
- Dermal absorption of organic chemical vapors in the rat (McDougal et al., 1986)
- Chloroform breath levels in individuals exposed in showers by inhalation and dermal routes (McKone, 1993)
- Topical exposure to parathion in the swine (Qiao et al., 1994)
- Pentachlorophenol absorption from soil in the swine (Qiao et al., 1997)
- Dermal absorption of fluazifop-butyl through rat and human skin (Ramsey et al., 1994)
- Tetrachloroethylene in groundwater for a bathing and showering scenario (Rao and Brown, 1993)
- Distributed parameter physiologically based pharmacokinetic model for dermal exposure to volatile organic carbons (Roy et al., 1996)
- 2-Butoxyethanol disposition in rats following dermal exposure (Shyr et al., 1993)
- Salicylic acid at a dermal application site and in local underlying tissues below the site in rats (Singh and Roberts, 1993)
- Local tissue concentrations of bases and steroids in rats (Singh and Roberts 1994a)
- Deep-tissue penetration of lidocaine below a dermally applied site in rat (Singh and Roberts, 1994b)
- Xenobiotic absorption utilizing the isolated perfused porcine skin flap (Williams et al., 1990)

simplest model that works without being unnecessarily elaborate (Ramsey and Andersen, 1984). In all cases, the skin compartment includes a description of Fick's law to provide an input function (McDougal et al., 1986). The equation for a well-stirred skin compartment (as shown in Figure 6.1) is

$$V_{sk}\frac{dC_{sk}}{dt} = Q_{sk}\left(C_b - \frac{C_{sk}}{R_{sk/b}}\right) + P_{sk}A_{sk}\left(C_{sfc} - \frac{C_{sk}}{R_{sk/sfc}}\right)$$

New parameters are P_{sk}, which is the permeability coefficient (length/time), and A_{sk}, which is the skin exposure area (length^2). Blood flow and the partition coefficient for the skin relative to blood help describe the chemical that enters the skin from systemic circulation. The permeability/area product and the partition coefficient for skin relative to vehicle on the surface help in determining the input from the skin surface.

When necessary, the skin compartment can also be broken into well-stirred subcompartments to provide more detail about distribution and metabolism in the skin. This can be particularly important when pharmacokinetic models interface with pharmacodynamic models because of the complexity of the skin and localized effects of chemicals. Figure 6.2 shows an example of a skin compartment with multilayered subcompartments (Bookout et al., 1996).

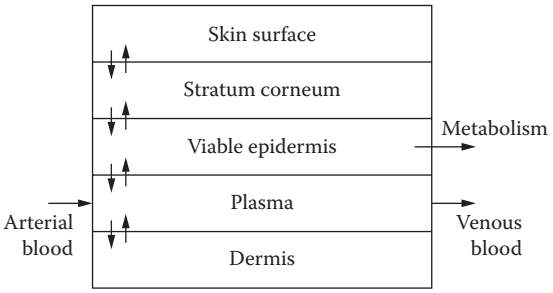

Figure 6.2 Schematic of a skin compartment with well-stirred subcompartments. The vertical arrows indicate movement of chemicals by diffusion. The surface subcompartment is in contact only with the rate-limiting barrier for most chemicals—the stratum corneum. The internal subcompartments gain and lose chemical from adjacent compartments. Loss from metabolism is only modeled in the viable epidermis. Both the viable epidermis and dermis are in contact with and can exchange chemical with the plasma.

A more detailed skin compartment with a parallel subcompartment to represent hair follicles and sweat glands could also be used if necessary (Bookout et al., 1997). See the original articles for detailed equations.

Skin compartments have physiological and biochemical parameters just like the whole-body models. In this case, the physiological parameters are blood flow to the skin and volumes and thicknesses for stratum corneum, viable epidermis, and dermis. Blood flow is available for laboratory animals (Manning et al., 1991; Monteiro-Riviere et al., 1990, 1991) and humans (Fagrell et al., 1977). Skin thickness is available for humans (Branchet et al., 1990; Odland, 1983) and laboratory animals (Grabau et al., 1995; Monteiro-Riviere et al., 1990). Biochemical parameters are metabolic constants, tissue partition coefficients, and tissue-binding parameters. They are available in the literature for many specific chemicals.

Absorption into the skin is the primary reason for having a separate skin compartment. A skin compartment based on Fick's law is a good tool for extrapolation to other skin exposure situations. Without a predictive model, it is necessary to do experiments at each of the concentrations of interest because of the nonlinear pharmacokinetics involved. The permeability coefficient is concentration independent (Scheuplein, 1977); therefore, it can be used to extrapolate from one exposure concentration to another. When the exposure concentration is doubled, the model predicts that the total amount of chemical absorbed would also double (Figure 6.3). This simulation is of an occluded exposure to an organic chemical in an aqueous vehicle. This figure shows that nearly all the chemical is absorbed from the water vehicle during 24 h.

Total chemical absorbed would include the chemical still in the skin and chemical already metabolized or eliminated; therefore, the nonlinearities in the system are not apparent at the level of total chemical absorbed. Although the total chemical absorbed over an extended time period can be predicted based on exposure concentration, the toxic or beneficial effects may not be directly related to exposure concentration because it is the tissue or blood concentration that determines the effect. Blood and tissue concentrations may more than double when the surface concentration is

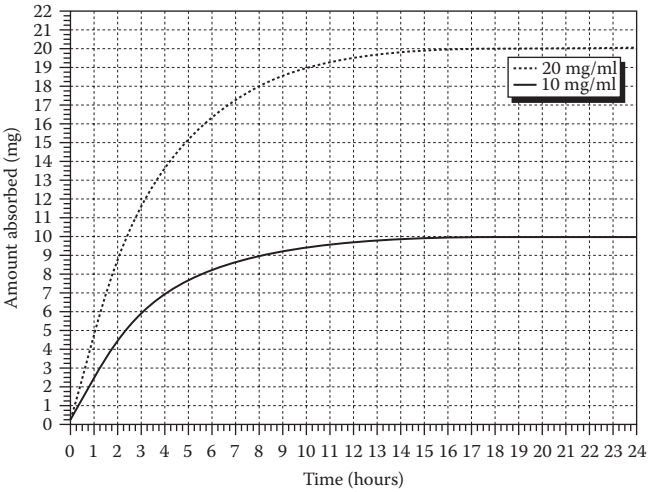

Figure 6.3 Total amount of chemical absorbed (including the amount in the skin) from a simulation in which the concentration in 1 ml of water is doubled from 10 to 20 mg/ml. Model parameters for the organic chemical (dibromomethane) are from Jepson and McDougal (1999).

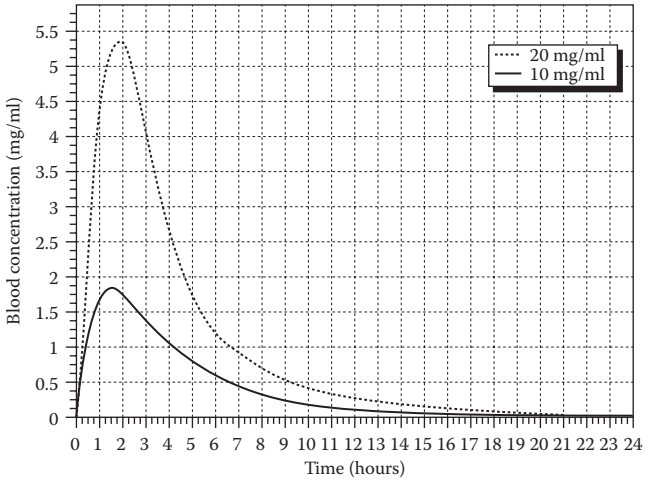

Figure 6.4 Simulation of the effect of doubling the exposure concentration of an organic chemical in 1 ml of water on the surface of the skin. Model parameters for the organic chemical (dibromomethane) are from Jepson and McDougal (1999).

doubled (Figure 6.4) because processes such as metabolism become saturated at the higher dose and therefore more parent chemical is present in the blood than would be expected if metabolism were not considered.

Predicted peak blood concentration at the low dose is about 1.8 mg/ml, and peak blood concentration at the doubled dose is about 5.5 mg/ml. This figure shows that

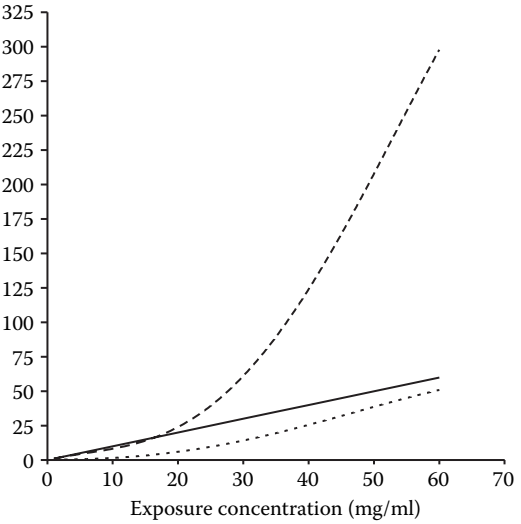

Figure 6.5 Some of the nonlinearities involved with skin penetration over a range of exposure concentrations with the same vehicle volume. The solid line is total chemical absorbed (mg). The short dashed line is peak blood concentration (mg/ml). The long dashed line is area under the blood curve (mg/ml-h). The same exposure (organic chemical in aqueous solution) and model parameters as Figure 6.3 were used.

the blood concentrations peak at about 1 to 2 h because the concentration of chemical in the water vehicle on the surface decreases as absorption occurs. Doubling the exposure concentration results in a threefold increase in peak blood concentration. Figure 6.5 shows that many pharmacokinetic parameters are nonlinear with penetration of chemicals through the skin. Peak blood concentration (mg/ml) may be responsible for a therapeutic or toxic effect with a chemical that acts at receptors or one that has its primary effect in the membrane, such as anesthetics. Peak blood concentration increases slowly at low exposure concentrations because saturable metabolism removes a larger portion of the total chemical absorbed. At higher exposure concentrations, the amount metabolized can become negligible compared to the total absorbed dose, and the peak blood concentration becomes more linearly related to exposure concentration. The area under the curve in the blood or tissue may directly relate to the therapeutic or toxic effect when both concentration and duration are involved (Jarabek, 1995). Area under the curve shows a nonlinear relationship with exposure concentration. A biologically based pharmacokinetic model (which incorporates distribution from the blood, metabolism, and elimination) is a good way to accurately describe the nonlinear relationship between tissue dose and exposure concentration.

Without a model, percentage absorbed is often the only means available to try to extrapolate to other exposure conditions, but as described here, this measurement has limited usefulness. Percentage of chemical absorbed has historically been used as a measurement of chemical absorption from a variety of *in vivo* and *in vitro* situations (Brain et al., 1995; Bronaugh et al., 1982; Feldmann and Maibach, 1970;

Moody and Ritter, 1992; Wester et al., 1993). It describes a first-order relationship between mass of chemical in contact with the skin and penetration, but penetration is often a nonlinear function of applied dose. Percentage of dose absorbed can be used to predict total absorption for a different chemical concentration over the same surface area as long as exposure time is equivalent, such as the percentage absorbed at 24 h for both the original and the doubled dermal dose in Figure 6.3, which is nearly 100%. The percentage absorbed at 1 h would be about 25%. Percentage absorbed is dependent on exposure time; therefore, it is not possible to accurately extrapolate to other exposure times.

Chemicals may end up on the skin as solids, liquids, or mixtures (the simplest is one chemical in a vehicle composed of a single chemical). Concentration and volume applied adequately describe liquids and mixtures but not solids. The universal description of the amount on the surface is surface density (mass per surface area), although not all experimental exposures are described that way. Any particular surface density will either be less than the amount that would completely cover the exposure area or in excess of that amount. If the mass on the surface is more than the amount that just completely covers it (often called a monolayer), not all of the applied dose is available for absorption into the skin. Most percentages absorbed reported in the literature are much less than 100% because many times the mass on the skin is in excess of a monolayer. When excess chemical on the skin is included in the calculation of percentage absorbed, obviously the measured percentage absorption would decrease. For percentage absorbed to be predictive, the absorption must be experimentally measured over the exact surface density, time, and concentration that are of interest. It is not possible to extrapolate surface density because concentration difference is the driving force, not mass, and it is not possible to extrapolate to other exposure times because the percentage absorbed measurement is time dependent. These problems are overcome, preferably, by using a biologically based skin compartment.

Pharmacokinetic models are designed to accurately describe the processes of absorption, distribution, metabolism, and elimination. All of these processes can be defined from the perspective of the skin and mathematically described. A big advantage of biologically based pharmacokinetic models is that they can explicitly describe the concentration of chemical in layers of the skin depending on where the chemical has its toxic or beneficial effects. This is both useful and necessary when connecting a pharmacokinetic skin model to a pharmacodynamic skin model, therefore providing the ability to relate surface concentration to effect in the skin. Metabolism in the epidermis, dermis, or a specific appendage could also be included in the model to provide local concentrations of metabolites that might be biologically active. Another pharmacokinetic process that is important in the skin is elimination. The skin concentration will be decreased by blood flow from the skin (depending on solubility of the chemical in the blood) as the chemical is distributed to other parts of the body. Another potential route of elimination of volatile chemicals is evaporation from the surface of the skin or from the outer layers. Evaporation can have a big impact on the target tissue dose of volatile chemicals (Boman and Maibach, 2000; Guy and Hadgraft, 1984). Unlike most organs, the skin can lose chemical by “sloughing” the outer layers of the stratum corneum in a process called *desquamation*. This might

only be important for chemicals that are lipophilic or ones that bind to skin proteins (Reddy et al., 2000). Pharmacokinetic skin models in their simplest form are useful when the skin is the route of exposure, but using more complete skin models provides the potential to predict pharmacokinetics accurately and ultimately the chemical concentration in the skin.

The ability to extrapolate from an experimental species to a species of interest is a demonstrated capability of biologically based models (Andersen, 2003) that can be relevant to skin compartments if the physiological parameters (skin thickness and blood flow) and the biochemical parameters (skin/vehicle partition coefficients and metabolic constants) are changed to the species of interest (Bogdanffy et al., 2001). As described, an important capability of a validated skin exposure model is the ability to extrapolate to other exposure parameters (concentration, area, and times) for the same exposure compound. Often, the exposure parameters are constant during an exposure, but with small amounts of chemical, the exposure area and concentration both can decrease as the chemical is absorbed or evaporated. Biologically based skin models can be used to describe the concentration on the surface and the exposure area dynamically to simulate chemical exposures to small amounts of chemical (McDougal and Jurgens-Whitehead, 2001). Limited studies with biologically based models have shown that it may be possible to use these models to extrapolate between vehicles for one chemical. Jepson and McDougal (1999) showed that, although the flux from pure chemical, aqueous, and oil solutions varies over a hundredfold, the permeability can be predicted with an accuracy of about twofold by taking into account the skin/vehicle partition coefficient.

The use of biologically based skin models has allowed important contributions to science, including the ability to determine internal doses, extrapolate between species, and improve risk assessments (Table 6.1 and Table 6.2). Most of these models address systemic toxicity from skin exposures, but one of the most important, but mostly unexplored, uses of these models is to address local beneficial or deleterious effects in the skin. The relationship between the skin tissue dose and the response in the skin is the next boundary that can be expanded using biologically based models. Computational systems biology is an important and growing field that has come about because of advances in experimental techniques, advanced software, and analytical methods. The potential for biologically based pharmacodynamic models in the systems biology arena is described next.

BIOLOGICALLY BASED PHARMACODYNAMIC MODELS

Pharmacodynamic models have much more breadth than pharmacokinetic models because of the scope of the types of processes that are represented. Instead of primarily describing chemical interactions with biological systems, these dynamic mathematical models focus on describing the biological systems themselves so that their perturbation by beneficial or toxic chemicals can be understood. The spectrum of regulatory, metabolic, and homeostatic processes that could be affected by exogenous chemicals is large. Each of these processes may have unique characteristics, stimuli, or checks and balances, but the fundamental principles in these biological

systems, such as protein–protein interactions, secretion, molecular transport, and gene expression, can be mathematically described. Computational systems biology has become popular as a means to understand and assimilate increasingly detailed and complex scientific information as related in recent reviews (Ge et al., 2003; Ideker et al., 2001; Kitano, 2002). This new information has become available because of tremendous technological advancement in scientific tools and techniques that allows high-throughput gene and protein sequencing, characterization and measurement of messenger ribonucleic acid (RNA) and protein expression levels, and manipulation of biological systems (such as knockout mice and small interfering RNA). Whether called pharmacodynamic, computational biology, or systems biology, these models address biological systems using essentially the same approach.

The first part of the approach is an attempt to understand the biological system of interest by systematically perturbing it with biochemical, genetic, or physiological stimuli and monitoring the change in the output of the system. The change may be in gene or protein expression or metabolic or biochemical reactions. The magnitude and the temporal aspects of the responses are important to capture because they relate to the magnitude and timing of the stimulus. Second, a mathematical model is developed that describes both the "normal" function and the perturbed state. It is not necessary to model every component of the system, only those that are directly involved with the response are required. As with pharmacokinetic models, unnecessarily complicated pharmacodynamic models can be more of a hindrance than a help in understanding the system. The third aspect of the approach is the combination of the modeling with further experimentation in an attempt to refine and validate the model. This involves perturbing the biological system with different stimuli, predicting the outcome with the model, and comparing the model output with the experimental observations in an iterative process. Dynamic models may have varying degrees of complexity or sophistication, but they will have many characteristics in common; that is, they are based on first principles and a quantitative understanding of biological relationships.

The usefulness of biologically based pharmacodynamic models is similar to the usefulness of biologically based pharmacokinetic models. Pharmacodynamic models are often developed to predict the level of activation of the system based on a specific stimulus or mixed stimuli, but they also can be used to generate hypotheses that can be experimentally tested. A good model can provide insight into mechanisms and provide verification of biological issues at various levels. Pharmacokinetic and systems biology models are making important contributions to both quantitative and qualitative understanding of biological phenomena. These models have been applied to topics ranging from basic gene expression regulation to more complicated disease progression (Table 6.3).

The complexity of a biological model can vary depending on how many biological details the model contains. As more biochemical and functional details are experimentally resolved, they will probably be continuously incorporated into models. As a result, although large-scale simulations become possible, they also impose a series of challenges related to model viability and reusability. These problems can be minimized by using an object-oriented instead of a procedural approach to build complex models from scratch or extend existing models. Modules, which are functionally

Table 6.3 Examples of Biologically Based Models That Illustrate the Scope of Their Utility

- *Gene regulatory network*: Spatial and temporal expression patterns of *Drosophila* segment polarity genes (Albert and Othmer, 2003)
- *Signal transduction*: MAPK cascade (Bhalla et al., 2002)
- *Biological rhythm*: Circadian rhythm (Smolen et al., 2001)
- *Cell cycle*: Eukaryotic cell cycle (Tyson and Novak, 2001)
- *Neuronal firing*: Spike-frequency adaptation (Benda and Herz, 2003)
- *Metabolic network*: Metabolic model of *Helicobacter pylori* 26695 (Schilling et al., 2002)
- *Tumor progression*: Markov modeling of melanoma progression (Wanek et al., 1994)
- *Disease pathogenesis*: Alzheimer's disease (Hasselmo, 1997)
- *Neural transmission*: Synaptic transmission failures (Goldman, 2004)

independent units, can be built in advance and used as building blocks for large models that specify the connections between different modules. The granularity (level of detail) of modules is likely dependent on the nature of the model in question. For instance, to simulate a gene transcription event initiated from the cell membrane, it is reasonable to model the processes of signal propagation in the cytoplasm, RNA transcription in the nucleus, and protein synthesis again separately in the cytoplasm as individual modules rather than model them as a whole. Programs describing the functions of organelles or cell types in the skin could exist as individual modules as well. Thus, to simulate a cellular function that depends on coordinated operations between distinct organelles, these modular programs simply need to be invoked or included in the main model program. One could also envision modules for each of the numerous cell types in the skin, such as keratinocytes, Merkel cells, melanocytes, hair follicles, and so on or modules for the functionally and anatomically distinct layers in the epidermis. Besides avoidance of repeated coding, another advantage of this approach is that the modeler does not have to be concerned with the biological details encapsulated in each functional module. The modeler who uses the module only needs to deal with the module interface that describes the input and output signals. Update of modules themselves will not affect their usage because their implementation details are hidden from the users.

Built to reflect the biological system, a pharmacodynamic model usually consists of various entities or components and relations describing the interactions between these entities. With the exception of homology modeling (Al Lazikani et al., 2001; Burley and Bonanno, 2002) and ligand docking (Glen and Allen, 2003), the majority of cellular modeling is conducted at the molecular level at which biochemical reactions take place. The molecular species can be any measurable molecule both inside and outside the cell. This would include proteins, carbohydrates, fatty acids, nucleic acids, amino acids, ions, and so on. The concentrations of these molecular species, which are the state variables in the model, change or remain static with time as reactions involving these molecules take place. The core ability of a model is to capture these concentration changes under physiological or perturbed conditions. Many types of biochemical reaction govern the dynamics of molecular species. Enzymatic reactions, invariably involving at least one protein species as the enzyme, can drive the syntheses and degradation of molecules and state transitions such as phosphorylation and methylation. Molecular interactions involving no enzymes

include protein–protein interaction, protein–deoxyribonucleic acid interaction, ligand binding, and the like. In addition, molecular events occurring in the cell are often compartmentalized. For instance, gene transcription occurs in the nucleus, whereas protein kinase activation usually takes place in the cytoplasm. With this consideration, translocation of molecules between different compartments is also a determinant affecting the concentrations of molecules. At a higher level, the state variables can be cell numbers, dendritic length, organ weights, and so on. Accordingly, cellular events affecting these state variables will include proliferation, differentiation, cell death, or migration, which can also be modeled mathematically.

Model topology, that is, the interconnections between various components in the model as a whole, and the kinetic parameters associated with each connection determine the dynamics of the model. Interactions between components in the model can be either stimulatory or inhibitory. Series of interactions arranged in the form of loops can function as either positive or negative feedback. These feedback loops, depending on the parameter values, can display nonlinear dynamic behaviors such as oscillation and bistability (Bhalla et al., 2002; Hoffmann et al., 2002). These various features can in turn modulate the response of the system to input signals, making complex dose responses such as switchlike or nonmonotonic ones possible.

Determining the level of detail to include in a model is not an easy task. There can be a tendency to incorporate much more detail than is necessary because the relationships and interactions are known. An appropriate model would only include components that are involved in the behaviors that the model is designed to predict. For example, a model of inflammation in the skin would only need to include the components involved with cytokine signaling, chemokine activation, and cell damage. Most important, the model parameters should reflect the experimental data available. Large numbers of unnecessary variables with estimated rather than measured parameters will reduce the ability of the model to predict accurately and will restrict it to being descriptive. Also, a bloated model including every minor detail is not only unnecessary, but also poses a challenge to available computing resources because large models tend to run with much less efficiency. To circumvent such problems, modules contained in large models can be simplified, whenever possible, with mathematical expressions that depict the same dynamic properties as the modules do. Components related to processes that have only minor impact on the behavior modeled can be eliminated. The “principle of parsimony” dictates that the best model is the simplest one that adequately describes the system without unnecessary assumptions (d’Auvergne and Gooley, 2003; Forster, 2000).

A pharmacodynamic model can be developed in a variety of ways. Among these, kinetic models characterize the progression of biological processes with kinetic rate laws. This approach is most commonly used to model biochemical reaction systems such as signal transduction and metabolic pathways. One of the limitations of the kinetic approach is the scarcity of measured kinetic rate parameters available to support the parameter estimations. In contrast, Boolean models have been proposed that disregard all the detailed kinetic information and view biological phenomena as existing in binary states governed by logical operations. The Boolean method is particularly suitable for modeling gene regulatory networks, for which the regulatory relationships between the genes are of more interest rather than the details of how

each gene is activated (Huang, 1999). It has also been applied to protein regulatory networks (Huang and Ingber, 2000).

Either kinetic models or Boolean models can be constructed with a deterministic or a stochastic approach. A deterministic model describes the system as "doomed" to a certain behavior with a given input; a stochastic model allows variability that more closely resembles the fluctuations and uncertainty encountered in the real biological system. An example of the deterministic approach is to use a set of ordinary differential equations (ODEs) to model the progression of the system with time, whereas a stochastic model can be developed by assuming certain probabilistic distribution of the parameters in the ODEs (e.g., intracellular protein levels). Additional stochastic approaches include Gillespie's Monte Carlo method (Gillespie, 1977), Markov chain (Kim, 2002), and others (Lee et al., 2003; Morton-Firth et al., 1999). Although deterministic models are more widely used because they are easier to manipulate, more attention is paid to stochastic models. Advances in computer technology (running a stochastic model is generally more time consuming than a deterministic model) and the increased appreciation of the randomness of biological systems are making these models more common.

Spatial consideration is another important aspect of computational modeling. As described in the section on biologically based pharmacokinetic models, compartmentalization has been used to account for spatial constraints in pharmacokinetic models. The same approach can be used for pharmacodynamic modeling. For example, cellular-level models are usually compartmentalized to extracellular and intracellular space as well as different cellular organelles. Such models assume these compartments are "well mixed" such that diffusion can be ignored. In contrast, the "spatial-temporal" model, at the cost of increased complexity, takes diffusion into account and therefore is especially suitable for situations in which geometry is an important factor (e.g., for models of skin layers). Because every method has its own advantages and disadvantages, hybrid models usually provide more flexibility to suit particular needs. For example, stochasticity can appear in parts of an otherwise deterministic model to gain desired randomness while controlling the model complexity, and a spatial-temporal model may also be combined with a simple compartmental model to describe a system in which certain compartments are diffusion constrained.

After the model is formulated, parameterization is the next challenging step of pharmacodynamic modeling. Initial parameter values can be derived from direct kinetic measurements, indirect experimental observations, or existing mathematical models. Model simulations starting with these initial parameter values can then be fitted to available experimental data to optimize parameter estimations. Parameter fitting can be done through a variety of general optimization routines, such as the conjugate gradient, Newton method, and genetic algorithms (Chong and Zak, 2001). However, the power of these tools is compromised by the problem that limited data are available to estimate a large number of parameters. Therefore, manual data fitting has been widely used either alone or as a supplement to the automatic approaches. Manual fitting not only greatly improves the quality of parameter optimization, but also provides qualitative insight about how individual parameters contribute to the fitness of the model. Sensitivity analysis (Saltelli et al., 2000) is a good tool to

provide a systematic way to quantify the relative impact of the parameters. A sensitivity analysis allows the modeler to focus on the experimental determination of the most crucial elements of the biological system modeled (Cho et al., 2003). Nonlinear analysis for ODE-based models (Jordan and Smith, 1999) is another useful tool to characterize model behaviors within a parameter space. Because nonlinear properties such as the thresholding effect and bistability are commonly found in biological systems, nonlinear analyses provide stringent and straightforward mathematical explanations for the emergence of these phenomena (Tyson and Novak, 2001).

The final step of pharmacodynamic modeling is model validation. In general, model validation is performed with experimental data that are not used for initial development of the model. As mentioned in the introduction, one power of modeling is generation of hypotheses that can be tested experimentally. Model-driven experimental design of new experiments can be used to validate the model predictions. In most cases, the initial model is not good enough to capture all aspects of the real system. Inconsistencies may occur and will lead to refinement of model structure with incorporation of new parameters. The resulting newer model can be further tested with newer experimental data. Therefore, in practice, pharmacodynamic modeling can be viewed as an iterative process during which the model accuracy is continuously improved.

Many models have been developed that address dynamic processes in the skin. A thorough literature search results in hundreds of mathematical or systems biology models in the skin. Many of these relate to skin absorption and thermoregulation. Here, we briefly describe two models simulating signal transduction.

A model of keratinocyte growth factor (KGF) signaling as it relates to wound healing has been developed (Wearing and Sherratt, 2000). KGF is secreted by dermal fibroblasts and acts only on epidermal keratinocytes. This model incorporates diffusion of KGF from the dermis across the basal lamina to the epidermis. It describes KGF concentration in both the dermis and epidermis and the number of free and bound KGF receptors per cell. Production of KGF is substantially upregulated after injury and reaches a saturation level. The equations in the signaling model include a partial differential equation and three ODEs that address diffusion, production, dermal–epidermal interaction, decay, internalization, binding, and dissociation. Another part of the model describes the rate of change in basal keratinocyte density as it would relate to reepithelialization caused by the processes of migration, mitosis, and cell loss. The authors used this model to predict that the large upregulation of KGF after wound healing extends the KGF signal range beyond what is necessary for wound closure. They suggested that the large upregulation may have an unknown role distinct from wound closure.

Resat and coauthors (2003) have developed an integrated model of epidermal growth factor (EGF) receptor signal transduction and endocytosis. Signaling pathways for the receptor have been well characterized, but the phenomenon of EGF receptor trafficking (endocytosis and movement among cellular compartments) has not been previously described. The authors used a probability-weighted dynamic Monte Carlo simulation to address hundreds of endocytic compartments and

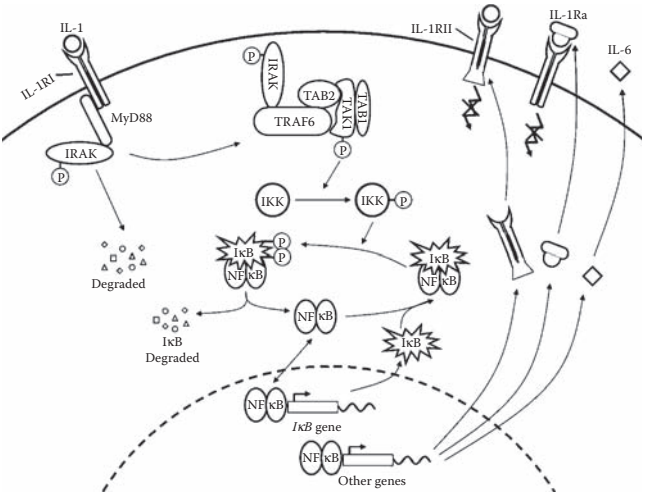

Figure 6.6 The major biochemical events of the IL-1 signaling pathway in keratinocytes. Receptors on the cell surface are shown at the top with the associated ligands, and the nucleus is at the bottom.

thousands (~13,000) of reactions that occur over a broad spatiotemporal range. These stochastic simulations adequately describe responses of the HMEC cell line 184A1 to both EGF and transforming growth factor α (TGF-α) and provide insights into dynamic mechanisms involved in EGF receptor trafficking. This model shows that large-scale simulations of the dynamics of signaling networks are possible.

We have developed a preliminary kinetic model of the interleukin 1 (IL-1)-stimulated intracellular signaling pathway in epidermal keratinocytes as an initial effort toward the pharmacodynamic modeling of the skin. On exposure to external stimuli, such as chemical irritants, the skin secretes various cytokines and chemokines and evokes a cascade of events in the subcutaneous tissue. Therefore, the pharmacodynamic process of the skin primarily involves the responses of the skin cells to these endogenous proteins. Among them, one of central importance is IL-1, a proinflammatory cytokine that mediates the host defense activities of the skin. The model captures the series of biochemical events initiated from IL-1α binding to IL-1 receptor (type I) on the cell surface that activates the transcriptional factor nuclear factor (NFκ-B) and leads to production of a responsive protein, IL-6, as illustrated in Figure 6.6.

The model takes into account two important autocrine regulatory loops of the system: the induction of a decoy IL-1 receptor (IL-1RII) and IL-1 receptor antagonist (IL-1Ra) by IL-1 signaling. The expressed IL-1RII and IL-1Ra compete with the normal receptor and ligands and serve as negative-feedback regulations.

Using a deterministic approach, the model describes the system with a set of ODEs assembled from reaction rate laws and divides it into three compartments: nucleus, cytosol, and extracellular space. A sample equation for the rate of change in concentration of the NFκB inhibitor protein IκB follows:

$$\frac{d[I\kappa B]}{dt} = -k_{f1}[I\kappa Kp][I\kappa B] + k_{b1}[I\kappa Kp - I\kappa B] - k_{f2}[NF\kappa B][I\kappa B] + k_{b2}[I\kappa B - NF\kappa B]$$

$$- k_{f3}[I\kappa B] + k_{f4}[I\kappa Bt] - k_{f5}[I\kappa B] + k_{b5}[I\kappa B_n]/r$$

where the brackets denote the concentration of the correspondent protein (except for [IκBt], which represents the IB gene transcript); k_{fi} and k_{bi} are forward and backward reaction rate terms, respectively; and r is the cytosol-to-nucleus volume ratio. The cytosolic IκB concentration decreases by binding to IκKp (net forward reaction rate $k_{f1}[I\kappa Kp][I\kappa B] - k_{b1}[I\kappa Kp - I\kappa B]$) and to NF-κB (net forward reaction rate $k_{f2}[NF\kappa B][I\kappa B] - k_{b2}[I\kappa B - NF\kappa B]$), its constitutive degradation ($k_{f3}[I\kappa B]$), as well as translocation to the nucleus ($k_{f5}[I\kappa B] - k_{b5}[I\kappa B_n]/r$). [IκB] increases as it is synthesized from IκB mRNA ($k_{f4}[I\kappa Bt]$).

The model predicts the time course of secreted IL-6 at different doses of IL-1 shown in Figure 6.7.

As demonstrated, the changes in the stimulus level not only alter the overall amount of IL-6 production, but also its dynamic shape. Although a high IL-1 dose sustains IL-6 production for a long period of time, a low dose produces more of a spikelike behavior. As opposed to a linear model, in which the output should change proportionally with the input level, such behavior is typical for a highly nonlinear system with negative-feedback loops, such as this model. Because prolonged inflammatory responses can be harmful to tissue, the bell-shaped dynamics will be more desirable, thus emphasizing the importance of the autocrine regulatory mechanisms (of decoy IL-1 receptor and antagonist) in the pharmacodynamic process of the skin. Another interesting observation from the model is that the temporal behavior of the upstream transcriptional factor NF-κB activation differs tremendously from that of IL-6 (Figure 6.8).

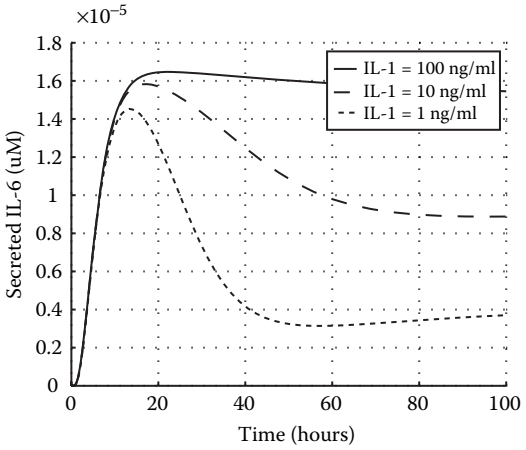

Figure 6.7 Simulated time courses of IL-6 secretion at different doses of IL-1.

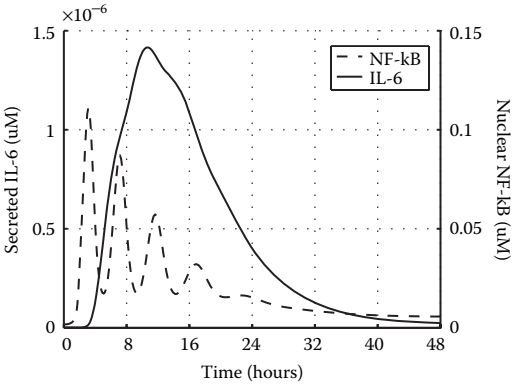

Figure 6.8 Simulated time courses of IL-6 secretion and NF-B activation at 1 pg/ml of IL-1.

At low doses of IL-1, NF-κB yields an oscillatory rather than spikelike response because of the IκB–NF-κB feedback existing in the generic NF-κB signaling module (Hoffmann et al., 2002). The events downstream of NF-κB, namely the IL-6 gene transcription, protein synthesis, and transportation, thus serve as a signal integrator to convert oscillations to a smooth final output. This suggests that measuring a cellular response by detecting extracellular protein secretion alone may not be sufficient for pharmacodynamic studies: Intracellular proteins have to be examined to properly reflect the actual dynamics of the signaling pathway. Taken together, the above analyses have demonstrated an example of applying systems biology modeling to provide insights to the pharmacodynamics of the skin. Understanding the relationship between chemical concentration in the skin from the pharmacokinetic model and the IL-1 concentration in the pharmacodynamic model will allow the prediction of the IL-6 response based on the concentration of chemical on the skin surface.

CONCLUSION

In summary, biologically based pharmacokinetic and pharmacodynamic models have tremendous potential to help solve problems in the skin. These models are especially useful for predicting pharmacokinetics and system responses that are nonlinear because they are based on first principles. They can also help design experiments and develop and test hypotheses. Ultimately, these models can be used to improve risk assessments or develop prophylactic or therapeutic approaches.

ACKNOWLEDGMENTS

We gratefully acknowledge support from the Air Force Office of Scientific Research (AFOSR/NL) and a Wright State University Major Collaboration grant.

REFERENCES

Albert, R. and Othmer, H.G., 2003, The topology of the regulatory interactions predicts the expression pattern of the segment polarity genes in *Drosophila melanogaster*, *J. Theor. Biol*., 223, 1–18.

Al Lazikani, B., Jung, J., Xiang, Z., and Honig, B., 2001, Protein structure prediction, *Curr. Opin. Chem. Biol*., 5, 51–56.

Andersen, M.E., 2003, Toxicokinetic modeling and its applications in chemical risk assessment, *Toxicol. Lett*., 138, 9–27.

Benda, J. and Herz, A.V., 2003, A universal model for spike-frequency adaptation, *Neural Comput*., 15, 2523–2564.

Bhalla, U.S., Ram, P.T., and Iyengar, R., 2002, MAP kinase phosphatase as a locus of flexibility in a mitogen-activated protein kinase signaling network, *Science*, 297, 1018–1023.

Bischoff, K.B., Dedrick, R.L., Zaharko, D.S., and Longstreth, J.A., 1971, Methotrexate pharmacokinetics, *J. Pharm. Sci*., 60, 1128–1133.

Bogdanffy, M.S., Plowchalk, D.R., Sarangapani, R., Starr, T.B., and Andersen, M.E., 2001, Mode-of-action-based dosimeters for interspecies extrapolation of vinyl acetate inhalation risk, *Inhal. Toxicol*., 13, 377–396.

Boman, A. and Maibach, H.I., 2000, Influence of evaporation and solvent mixtures on the absorption of toluene and *n*-butanol in human skin *in vitro*, *Ann. Occup. Hyg*, 44, 125–135.

Bookout, R.L., Jr., McDaniel, C.R., Quinn, D.W., and McDougal, J.N., 1996, Multilayered dermal subcompartments for modeling chemical absorption, *SAR QSAR. Environ. Res*., 5, 133–150.

Bookout, R.L., Jr., Quinn, D.W., and McDougal, J.N., 1997, Parallel dermal subcompartments for modeling chemical absorption, *SAR QSAR. Environ. Res*., 7, 259–279.

Brain, K.R., James, V.J., Dressler, W.E., Howes, D., Kelling, C., and Gettings, S.D., 1995, Percutaneous penetration of dimethylnitrosamine through human skin *in vitro*: application from cosmetic vehicles, *Food Chem. Toxicol*., 33, 315–322.

Branchet, M.C., Boisnic, S., Frances, C., and Robert, A.M., 1990, Skin thickness changes in normal aging skin, *Gerontology*, 36, 28–35.

Bronaugh, R.L., Collier, S.W., Macpherson, S.E., and Kraeling, M.E., 1994, Influence of metabolism in skin on dosimetry after topical exposure, *Environ. Health Perspect*., 102(Suppl. 11), 71–74.

Bronaugh, R.L., Stewart, R.F., Congdon, E.R., and Giles, A.L., Jr., 1982, Methods for *in vitro* percutaneous absorption studies, I. Comparison with *in vivo* results, *Toxicol. Appl. Pharmacol*., 62, 474–480.

Burley, S.K. and Bonanno, J.B., 2002, Structuring the universe of proteins, *Annu. Rev. Genomics Hum. Genet*., 3, 243–262.

Cho, K.H., Shin, S.Y., Lee, H.W., and Wolkenhauer, O., 2003, Investigations into the analysis and modeling of the TNF α-mediated NF-κ B-signaling pathway, *Genome Res*., 13, 2413–2422.

Chong, E.K.P. and Zak, S.H., 2001, *An Introduction to Optimization*, 2nd ed., New York: Wiley.

Clewell, H.J., III, Andersen, M.E., Wills, R.J., and Latriano, L., 1997, A physiologically based pharmacokinetic model for retinoic acid and its metabolites, *J. Am. Acad. Dermatol*., 36(Pt. 2), S77–S85.

Clewell, H.J., III, Gentry, P.R., and Gearhart, J.M., 1997, Investigation of the potential impact of benchmark dose and pharmacokinetic modeling in noncancer risk assessment, *J. Toxicol. Environ. Health*, 52, 475–515.

Conolly, R.B., 2001, Biologically motivated quantitative models and the mixture toxicity problem, *Toxicol. Sci.*, 63, 1–2.

Corley, R.A., Gordon, S.M., and Wallace, L.A., 2000, Physiologically based pharmacokinetic modeling of the temperature-dependent dermal absorption of chloroform by humans following bath water exposures, *Toxicol. Sci.*, 53, 13–23.

Corley, R.A., Markham, D.A., Banks, C., Delorme, P., Masterman, A., and Houle, J.M., 1997, Physiologically based pharmacokinetics and the dermal absorption of 2-butoxyethanol vapor by humans, *Fundam. Appl. Toxicol.*, 39, 120–130.

d'Auvergne, E.J. and Gooley, P.R., 2003, The use of model selection in the model-free analysis of protein dynamics, *J. Biomol. NMR*, 25, 25–39.

Fagrell, B., Fronek, A., and Intaglietta, M., 1977, A microscope-television system for studying flow velocity in human skin capillaries, *Am. J. Physiol.*, 233, H318–H321.

Feldmann, R.J. and Maibach, H.I., 1970, Absorption of some organic compounds through the skin in man, *J. Invest. Dermatol.*, 54, 399–404.

Fisher, H.L., Shah, P.V., Sumler, M.R., and Hall, L.L., 1989, *In vivo* and *in vitro* dermal penetration of 2,4,5,2′,4′,5′-hexachlorobiphenyl in young and adult rats, *Environ. Res.*, 50, 120–139.

Forster, M.R., 2000, Key concepts in model selection: performance and generalizability, *J. Math. Psychol.*, 44, 205–231.

Gargas, M.L., Burgess, R.J., Voisard, D.E., Cason, G.H., and Andersen, M.E., 1989, Partition coefficients of low-molecular-weight volatile chemicals in various liquids and tissues, *Toxicol. Appl. Pharmacol.*, 98, 87–99.

Ge, H., Walhout, A.J., and Vidal, M., 2003, Integrating "omic" information: a bridge between genomics and systems biology, *Trends Genet.*, 19, 551–560.

Gerlowski, L.E. and Jain, R.K., 1983, Physiologically based pharmacokinetic modeling: principles and applications, *J. Pharm. Sci.*, 72, 1103–1127.

Gibaldi, M. and Perrier, D., 1982, One-compartment model, in M. Gibaldi and D. Perrier (eds.), *Pharmacokinetics*, 2nd ed., Vol. 15, New York: Dekker, pp. 1–43.

Gillespie, D.T., 1977, Exact stochastic simulation of coupled chemical reactions, *J. Phys. Chem.*, 81, 2340–2361.

Glen, R.C. and Allen, S.C., 2003, Ligand-protein docking: cancer research at the interface between biology and chemistry, *Curr. Med. Chem.*, 10, 763–767.

Goldman, M.S., 2004, Enhancement of information transmission efficiency by synaptic failures, *Neural Comput.*, 16, 1137–1162.

Grabau, J.H., Dong, L., Mattie, D.R., Jepson, G.W., and McDougal, J.N., 1995, *Comparison of Anatomical Characteristics of the Skin for Several Laboratory Animals*, AL/OE-TR-1995-066, Wright-Patterson AFB, OH: Toxicology Division, Armstrong Laboratory.

Guy, R.H. and Hadgraft, J., 1984, A theoretical description of the effects of volatility and substantivity on percutaneous absorption, *Int. J. Pharm.*, 18, 139–147.

Hasselmo, M.E., 1997, A computational model of the progression of Alzheimer's disease, *MD Comput.*, 14, 181–191.

Heatherington, A.C., Fisher, H.L., Sumler, M.R., Waller, C.L., Shah, P.V., and Hall, L.L., 1998, Percutaneous absorption and disposition of [14C]chlordecone in young and adult female rats, *Environ. Res.*, 79, 138–155.

Hoffmann, A., Levchenko, A., Scott, M.L., and Baltimore, D., 2002, The IkappaB-NF-kappaB signaling module: temporal control and selective gene activation, *Science*, 298, 1241–1245.

Huang, S., 1999, Gene expression profiling, genetic networks, and cellular states: an integrating concept for tumorigenesis and drug discovery, *J. Mol. Med.*, 77, 469–480.

Huang, S. and Ingber, D.E., 2000, Shape-dependent control of cell growth, differentiation, and apoptosis: switching between attractors in cell regulatory networks, *Exp. Cell Res.*, 261, 91–103.

Ideker, T., Galitski, T., and Hood, L., 2001, A new approach to decoding life: systems biology, *Annu. Rev. Genomics Hum. Genet.*, 2, 343–372.

Jarabek, A.M., 1995, The application of dosimetry models to identify key processes and parameters for default dose-response assessment approaches, *Toxicol. Lett.*, 79, 171–184.

Jepson, G.W., Hoover, D.K., Black, R.K., McCafferty, J.D., Mahle, D.A., and Gearhart, J.M., 1994, A partition coefficient determination method for nonvolatile chemicals in biological tissues, *Fundam. Appl. Toxicol.*, 22, 519–524.

Jepson, G.W. and McDougal, J.N., 1999, Predicting vehicle effects on the dermal absorption of halogenated methanes using physiologically based modeling, *Toxicol. Sci.*, 48, 180–188.

Jordan, D.W. and Smith, P., 1999, *Nonlinear Ordinary Differential Equations*, 3rd ed., Oxford, U.K.: Clarendon Press.

Kedderis, L.B., Mills, J.J., Andersen, M.E., and Birnbaum, L.S., 1993, A physiologically based pharmacokinetic model for 2,3,7,8-tetrabromodibenzo-*p*-dioxin (TBDD) in the rat: tissue distribution and CYP1A induction, *Toxicol. Appl. Pharmacol.*, 121, 87–98.

Kim S., Li, H., Dougherty, E.R., Cao, N.W., Chen, Y.D., Bittner, M., and Suh, E.B., 2002, Can Markov chain models mimic biological regulation?, *J. Biol. Syst.*, 10, 337–357.

Kitano, H., 2002, Systems biology: a brief overview, *Science*, 295, 1662–1664.

Krewski, D., Withey, J.R., Ku, L.F., and Andersen, M.E., 1994, Applications of physiologic pharmacokinetic modeling in carcinogenic risk assessment, *Environ. Health Perspect.*, 102(Suppl. 11), 37–50.

Lee, K.H., Dinner, A.R., Tu, C., Campi, G., Raychaudhuri, S., Varma, R., Sims, T.N., Burack, W.R., Wu, H., Wang, J., Kanagawa, O., Markiewicz, M., Allen, P.M., Dustin, M.L., Chakraborty, A.K., and Shaw, A.S., 2003, The immunological synapse balances T cell receptor signaling and degradation, *Science*, 302, 1218–1222.

Loizou, G.D., Jones, K., Akrill, P., Dyne, D., and Cocker, J., 1999, Estimation of the dermal absorption of *m*-xylene vapor in humans using breath sampling and physiologically based pharmacokinetic analysis, *Toxicol. Sci.*, 48, 170–179.

Manning, T.O., Monteiro-Riviere, N.A., Bristol, D.G., and Riviere, J.E., 1991, Cutaneous laser Doppler velocimetry in nine animal species, *Am. J. Vet. Res.*, 52, 1960–1964.

McDougal, J.N., 2004, Physiologically based pharmacokinetic modeling, in H. Zhai and H. Maibach (eds.), *Dermatotoxicology*, 6th ed., Boca Raton, FL: CRC Press, pp. 590–619.

McDougal, J.N., Jepson, G.W., Clewell, H.J., III, MacNaughton, M.G., and Andersen, M.E., 1986, A physiological pharmacokinetic model for dermal absorption of vapors in the rat, *Toxicol. Appl. Pharmacol.*, 85, 286–294.

McDougal, J.N. and Jurgens-Whitehead, J.L., 2001, Short-term dermal absorption and penetration of chemicals from aqueous solutions: theory and experiment, *Risk Anal.*, 21, 719–726.

McKone, T.E., 1993, Linking a PBPK model for chloroform with measured breath concentrations in showers: implications for dermal exposure models, *J. Expo. Anal. Environ. Epidemiol.*, 3, 339–365.

Monteiro-Riviere, N.A., Banks, Y.B., and Birnbaum, L.S., 1991, Laser Doppler measurements of cutaneous blood flow in ageing mice and rats, *Toxicol. Lett.*, 57, 329–338.

Monteiro-Riviere, N.A., Bristol, D.G., Manning, T.O., Rogers, R.A., and Riviere, J.E., 1990, Interspecies and interregional analysis of the comparative histologic thickness and laser doppler blood flow measurements at five cutaneous sites in nine species, *J. Invest. Dermatol.*, 95, 582–586.

Moody, R.P. and Ritter, L., 1992, An automated *in vitro* dermal absorption procedure: II. comparative *in vivo* and *in vitro* dermal absorption of the herbicide fenoxaprop-ethyl in rats, *Toxicol. In Vitro*, 6, 53–59.

Morton-Firth, C.J., Shimizu, T.S., and Bray, D., 1999, A free-energy-based stochastic simulation of the Tar receptor complex, *J. Mol. Biol.*, 286, 1059–1074.

Nestorov, I., 2003, Whole body pharmacokinetic models, *Clin. Pharmacokinet.*, 42, 883–908.

Odland, G.F., 1983, Structure of the skin, in L. B. Goldsmith (ed.), *Biochemistry and Physiology of the Skin*, Vol. 1, Oxford, U.K.: Oxford University Press, pp. 3–63.

Poet, T.S., Corley, R.A., Thrall, K.D., Edwards, J.A., Tanojo, H., Weitz, K.K., Hui, X., Maibach, H.I., and Wester, R.C., 2000a, Assessment of the percutaneous absorption of trichloroethylene in rats and humans using MS/MS real-time breath analysis and physiologically based pharmacokinetic modeling, *Toxicol. Sci.*, 56, 61–72.

Poet, T.S., Thrall, K.D., Corley, R.A., Hui, X., Edwards, J.A., Weitz, K.K., Maibach, H.I., and Wester, R.C., 2000b, Utility of real time breath analysis and physiologically based pharmacokinetic modeling to determine the percutaneous absorption of methyl chloroform in rats and humans, *Toxicol. Sci.*, 54, 42–51.

Poet, T.S., Weitz, K.K., Gies, R.A., Edwards, J.A., Thrall, K.D., Corley, R.A., Tanojo, H., Hui, X., Maibach, H.I., and Wester, R.C., 2002, PBPK modeling of the percutaneous absorption of perchloroethylene from a soil matrix in rats and humans, *Toxicol. Sci.*, 67, 17–31.

Qiao, G.L., Brooks, J.D., and Riviere, J.E., 1997, Pentachlorophenol dermal absorption and disposition from soil in swine: effects of occlusion and skin microorganism inhibition, *Toxicol. Appl. Pharmacol.,* 147, 234–246.

Qiao, G.L., Williams, P.L., and Riviere, J.E., 1994, Percutaneous absorption, biotransformation, and systemic disposition of parathion *in vivo* in swine. I. Comprehensive pharmacokinetic model, *Drug Metab. Dispos.*, 22, 459–471.

Ramsey, J.C. and Andersen, M.E., 1984, A physiologically based description of the inhalation pharmacokinetics of styrene in rats and humans, *Toxicol. Appl. Pharmacol.*, 73, 159–175.

Ramsey, J.D., Woollen, B.H., Auton, T.R., and Scott, R.C., 1994, The predictive accuracy of *in vitro* measurements for the dermal absorption of a lipophilic penetrant (fluazifop-butyl) through rat and human skin, *Fundam. Appl. Toxicol.*, 23, 230–236.

Rao, H.V. and Brown, D.R., 1993, A physiologically based pharmacokinetic assessment of tetrachloroethylene in groundwater for a bathing and showering determination, *Risk Anal.*, 13, 37–49.

Reddy, M.B., Guy, R.H., and Bunge, A.L., 2000, Does epidermal turnover reduce percutaneous penetration? *Pharm. Res.*, 17, 1414–1419.

Resat, H., Ewald, J.A., Dixon, D.A., and Wiley, H.S., 2003, An integrated model of epidermal growth factor receptor trafficking and signal transduction, *Biophys. J.*, 85, 730–743.

Roy, A., Weisel, C.P., Lioy, P.J., and Georgopoulos, P.G., 1996, A distributed parameter physiologically-based pharmacokinetic model for dermal and inhalation exposure to volatile organic compounds, *Risk Anal*., 16, 147–160.

Saltelli, A., Chan, K., and Scott, E.M., 2000, *Sensitivity Analysis,* New York: Wiley.

Scheuplein, R.J., 1977, Permeability of the skin, in D. Lee (ed.), *Handbook of Physiology: Reactions to Environmental Agents*, Bethesda, MD: American Physiological Society, pp. 299–322.

Schilling, C.H., Covert, M.W., Famili, I., Church, G.M., Edwards, J.S., and Palsson, B.O., 2002, Genome-scale metabolic model of *Helicobacter pylori* 26695, *J. Bacteriol*., 184, 4582–4593.

Shyr, L.J., Sabourin, P.J., Medinsky, M.A., Birnbaum, L.S., and Henderson, R.F., 1993, Physiologically based modeling of 2-butoxyethanol disposition in rats following different routes of exposure, *Environ. Res*., 63, 202–218.

Singh, P. and Roberts, M.S., 1993, Dermal and underlying tissue pharmacokinetics of salicylic acid after topical application, *J. Pharmacokinet. Biopharm*., 21, 337–373.

Singh, P. and Roberts, M.S., 1994a, Deep tissue penetration of bases and steroids after dermal application in rat, *J. Pharm. Pharmacol*., 46, 956–964.

Singh, P. and Roberts, M.S., 1994b, Dermal and underlying tissue pharmacokinetics of lidocaine after topical application, *J. Pharm. Sci*., 83, 774–782.

Smolen, P., Baxter, D.A., and Byrne, J.H., 2001, Modeling circadian oscillations with interlocking positive and negative feedback loops, *J. Neurosci*., 21, 6644–6656.

Theil, F.P., Guentert, T.W., Haddad, S., and Poulin, P., 2003, Utility of physiologically based pharmacokinetic models to drug development and rational drug discovery candidate selection, *Toxicol. Lett*., 138, 29–49.

Thrall, K. and Woodstock, A., 2003, Evaluation of the dermal bioavailability of aqueous xylene in F344 rats and human volunteers, *J. Toxicol. Environ. Health A*, 66, 1267–1281.

Thrall, K.D. and Woodstock, A.D., 2002, Evaluation of the dermal absorption of aqueous toluene in F344 rats using real-time breath analysis and physiologically based pharmacokinetic modeling, *J. Toxicol. Environ. Health A*, 65, 2087–2100.

Tyson, J.J. and Novak, B., 2001, Regulation of the eukaryotic cell cycle: molecular antagonism, hysteresis, and irreversible transitions, *J. Theor. Biol*., 210, 249–263.

Wanek, L.A., Elashoff, R.M., Goradia, T.M., Morton, D.L., and Cochran, A.J., 1994, Application of multistage Markov modeling to malignant melanoma progression, *Cancer*, 73, 336–343.

Wearing, H.J. and Sherratt, J.A., 2000, Keratinocyte growth factor signalling: a mathematical model of dermal–epidermal interaction in epidermal wound healing, *Math. Biosci*., 165, 41–62.

Wester, R.C., Maibach, H.I., Sedik, L., Melendres, J., and Wade, M., 1993, Percutaneous absorption of PCBs from soil: *in vivo* rhesus monkey, *in vitro* human skin, and binding to powdered human stratum corneum, *J. Toxicol. Environ. Health*, 39, 375–382.

Williams, P.L., Carver, M.P., and Riviere, J.E., 1990, A physiologically relevant pharmacokinetic model of xenobiotic percutaneous absorption utilizing the isolated perfused porcine skin flap, *J. Pharm. Sci*., 79, 305–311.

Yang, R.S., el Masri, H.A., Thomas, R.S., Constan, A.A., and Tessari, J.D., 1995, The application of physiologically based pharmacokinetic/pharmacodynamic (PBPK/PD) modeling for exploring risk assessment approaches of chemical mixtures, *Toxicol. Lett*., 79, 193–200.

CHAPTER 7

The Prediction of Skin Permeability Using Quantitative Structure–Activity Relationship Methods

Mark T.D. Cronin

CONTENTS

INTRODUCTION

It is accepted that the assessment of skin permeability of a chemical is required for a number of reasons, including risk assessment and topical delivery. The measurement of skin permeability is a time-consuming and difficult process and, when put in the context of the vast numbers of chemicals that may come into contact with the skin, is costly. Because of these factors, there has been interest for a considerable time in the ability to "predict" the ability of a compound to cross the skin from its physicochemical characteristics.

The formalization of the relationship between the biological activity and physicochemical or structural properties for a series of compounds is termed the development of a quantitative structure–activity relationship (QSAR) (Cronin, 2004). QSARs have been applied to model many different biological activities (such as pharmacological and pesticide activity, toxicity); physicochemical properties; pharmacokinetic attributes (absorption, distribution, metabolism and excretion); and the ability of compounds to cross membranes. The advantages of QSARs include the fact that they provide a model that is able to predict the chosen activity for compounds that are untested if the chemical structure is known. This has great potential in rationalizing product development in that the properties of potential lead compounds can, in theory, be known prior even to their synthesis. Thus, this may lead to more efficient product discovery, reducing costs and animal usage (Dearden and Cronin, 2004). Another general benefit of QSAR development is insight provided into mechanisms of actions and stimulating thought into their consideration and interpretation. Another area in which QSARs are already in use and will see increasing use (especially regarding predicting skin permeability) is for risk assessment by regulatory agencies. It is envisaged that the use of QSARs by regulatory agencies will be to fill data gaps and prioritize chemicals for testing and for classification and labeling purposes (Cronin, Jaworska, et al., 2003; Cronin, Walker, et al., 2003)

This aims of this chapter are first to describe what a QSAR is and give some pointers to successful development, then to review briefly QSARs currently available for skin permeability, and last to highlight the limitations of current models and make recommendations to allow for the appropriate application of QSARs.

QUANTITATIVE STRUCTURE–ACTIVITY RELATIONSHIPS

As noted, QSARs describe the relationship between the biological activity and physicochemical or structural properties of some compounds. That biological activity and chemical structure were intimately related was noted as long ago as the 1850s, and the expression QSAR became widely used in the early 1960s. Since then, an immense wealth of methods for the development of QSARs has been established, which is well beyond the scope of this chapter; the chapter concentrates on those applicable to skin permeability. For details on the historical aspects of QSARs, refer to the articles by Kubinyi (2002) and Schultz, Cronin et al. (2003). For a starting point into the complexity of QSARs, the reader is referred to (Cronin and Livingstone, 2004b),

which provides a didactic description of the methods, pitfalls, and some of the potential applications.

Essentially, there are three parts to any QSAR (1) the activity or property to be modeled, (2) some descriptors of the physicochemical properties or structural attributes of the molecules, and (3) a statistical technique to form the relationship between structure and activity. To comprehend how these three parts of a QSAR are relevant to the prediction of skin permeability, each is described briefly below.

The Activity or Property to Be Modeled

Any coherent activity or property data relating to a series of compounds can be modeled; the potential sources of data for use in QSAR are well described elsewhere (Cronin, 2005; Kaiser, 2004). Usually, these "activity" data may be considered as either a biological effect (such as a pharmacological activity or toxicity) or a physicochemical property (such as a partition coefficient, melting point, etc.). Although skin permeability data are derived from biological tissues, to consider them as biological effects is not necessarily correct. A biological effect implies some type of interaction between a chemical and a cell (or its components) that produces a defined response (i.e., disruption of cell function, inhibition of an enzyme, differential gene expression, etc.). Assuming the passage of a molecule across the skin barrier is as a result of passive diffusion, there is no interaction of the molecule with a biological structure. Thus, in this regard, skin permeability as a result of passive diffusion should be considered akin to a physicochemical property of the molecule. Although this is a minor point, it suggests that the QSAR modeling of skin permeability can be achieved in an empirical manner.

There is an overused saying, "garbage in, garbage out." Although this is clichéd and ugly English, the saying holds true for all modeling (including biological, chemical, and physical effects). To predict any quantity successfully, high-quality data and an understanding of what controls the phenomenon are required. Regarding QSAR activity or property data, a number of workers have made suggestions concerning what constitutes "high quality" (Cronin, 2005; Cronin and Schultz, 2003). The factors that would identify a data set as containing high-quality data include the same laboratory as the source of the measured values (ideally by the same worker), using a well-defined and consistent protocol (preferably to Organisation for Economic Co-operation and Development [OECD] or International Organisation for Standardization guideline specification). Further, the work should be performed to good laboratory practice (GLP) standards. All these criteria are markers of high-quality data. It must be appreciated that when data sets are "diluted" (i.e., they become compilations of literature values), the quality of the data set is almost always reduced. Although this does not preclude the use of these data from modeling, the effects on QSARs and the modelers' expectations must be tempered (see Cronin, 2005, and Cronin and Schultz, 2003, for a fuller discussion of this issue). This somewhat subtle, and often-overlooked point, has proved to be important in the QSAR modeling of historical skin permeability data (see the section on the Flynn data set).

Physicochemical Properties and Structural Descriptors of the Molecules

There are a huge number of descriptors of a molecule that may be used in a QSAR analysis or computational approach to predict a biological event. There are a number of good reviews of such descriptors (Dearden, 1990; Livingstone, 2000, 2003; Cronin and Livingstone, 2004a; Fisk et al., 2004; Netzeva, 2004; Schüürmann, 2004; Todeschini and Consonni, 2000), and only a taste of the descriptors and their potential use can be given here. Generally, the compounds in a QSAR analysis are described either by their "classical" physicochemical properties or by some form of structural property. These can be summarized into four general groups of descriptors: (1) hydrophobic properties, (2) electronic properties, (3) steric (size and shape) properties, and (4) structural and topological properties. The most frequently used descriptors in all aspects of QSAR are those assessing the hydrophobicity of a compound. The most commonly used measure of hydrophobicity is the octanol–water partition coefficient *P*, normally used in its logarithmic form (log *P*). There are a large number of algorithms for the calculation of log *P*, the majority of useful ones are summarized by Cronin and Livingstone (2004a).

The electronic properties of a molecule include physical aspects of its chemistry, such as its ability to accept and donate hydrogen bond, ionization, dipole moment, as well as those calculated from a knowledge of electron distribution. Of the last, molecular orbital properties are easily calculated and widely used; these include atomic charge, superdelocalizability, and energies of electrons in specific molecular orbitals. The calculation and use of electronic descriptors, molecular orbital properties in particular, were well reviewed by Schüürmann (2004).

The steric attributes of a molecule include its size and shape. Molecular size or bulk is easily assessed from properties such as molecular weight, volume, or surface area. A summary of parameters for molecular bulk is provided by Livingstone (2000). Molecular shape is much more difficult to parameterize, and there is no single descriptor capable of doing so (Patel and Cronin, 2001b). Different aspects of molecular shape, such as chirality, linearity, and branching, are often addressed individually (Livingstone, 2003).

The final set of descriptors (topological indices and structural properties) is often considered a subset of steric properties. This is probably because many of them parameterize molecular bulk. To think of them as purely parameters of bulk is not wholly correct, however, as some do describe molecular branching, linearity, and the presence of rings and other structural fragments, among other molecular properties. The most commonly used topological indices are the so-called molecular connectivities. Although easy to calculate and apply, these indices do suffer the drawback of lacking any true physicochemical interpretation (Netzeva, 2004).

As alluded to above, there are literally hundreds of descriptors of molecular structure available for use in a QSAR (cf. Livingstone, 2003; Todeschini and Consonni, 2000). The problem faced by the QSAR developer (and user) is which to consider for the modeling of a particular endpoint. There are no hard-and-fast rules, but the following general conditions can be applied to most QSARs: First, the aim should always be to use the fewest number of descriptors in a QSAR as possible.

Second, descriptors should ideally be chosen that can be related to the putative mechanism of action or effect; that is, they should be interpretable ensuring transparency of the model.

Thus, for the modeling of skin penetration, it is usually considered preferable to use descriptors that may be related to the capability of a molecule to cross the stratum corneum. This typically relates to hydrophobic and steric properties of a molecule, but other commonly utilized descriptors include those for hydrogen bonding, ionization, and aqueous solubility. Such properties may be related directly to capability of a molecule to cross a membrane such as the skin (Moss et al., 2002).

A Statistical Technique to Form the Relationship between Structure and Activity

A typical QSAR data set will constitute a series of biological data (such as measurements of the ability of a molecule to cross the skin) and a matrix of one (or usually more) descriptors of the molecules. A statistical technique is required to relate the two data sets and therefore create some form of algorithm for the prediction of the biological effect. A large number of statistical techniques are available for modeling purposes, ranging from regression analysis through to more multivariate approaches, such as partial least squares, principal component analysis, and artificial neural networks. The range of statistical techniques that may be utilized in the computational modeling of toxicity were well described by Livingstone (1995, 2004).

There are a large number of caveats when using any statistical approach for modeling. A useful "beginners" guide to building QSARs is provided by Livingstone (2004). Generally, the simpler the statistical approach that may be used, the better it is considered. A number of workers have proposed that it is better to use a simple approach to predict biological activity at the expense of losing statistical fit, than a more complex method with potentially greater statistical fit (cf. Cronin and Schultz, 2003). This chapter considers regression analysis as the method for QSAR development as it is most applicable to the modeling of skin permeability. Workers interested in the topic of computational modeling of biological activity are strongly recommended, however, to familiarize themselves with other techniques.

Regression analysis is a simple statistical technique that relates the dependent variable (i.e., the biological activity or effect) to one or more independent variables (the physicochemical or structural properties) (van de Waterbeemd, 1995). Regression analysis has a number of advantages in QSAR as it is simple to perform (it is available in nearly all, if not all, commercial statistical packages), and it provides a clear, unambiguous, and transparent model. Regression-based QSARs can be communicated easily and unequivocally, and a number of diagnostic techniques can be applied to it. It should be again stressed that regression analysis is not appropriate for all QSAR models, and QSAR developers should be aware of other statistical techniques and their associated strengths and weaknesses (cf. Cronin et al., 2002, for introduction to the comparison of methods). In QSAR modeling, regression analysis usually takes the form of

$$BA = a\ \text{Property}_1 + b\ \text{Property}_2 \ldots + c\ \text{Property}_n + \text{Constant} \qquad (7.1)$$

where: *BA* is the biological activity (or effect) to be modeled, and Property_1, and so on are the physicochemical or structural properties to be modeled.

In theory, any number of properties can be included, although for practical purposes most valid regression-based QSARs would be based on three or fewer properties. The QSAR can also be assessed in terms of the goodness of fit (or statistical fit) of the model or its predictivity, that is, a real case scenario of making predictions for compounds not included in the training set. The statistics commonly associated with the goodness of fit of a regression-based QSAR are the squared multiple correlation coefficient adjusted for degrees of freedom R^2; the cross-validated (leave-one-out) multiple correlation coefficient R^2_{CV}; the standard error of the fit *s*, and the *F* statistic. Further, *t* values and associated probabilities *p* should be available for individual variables in the regression analysis, and the number of compounds used in the model *n* should be reported (for further details on these statistical measures, cf. Livingstone, 1995, 2004). To assess the predictivity of a computational model for biological activity, some form of external validation is required (Golbraikh and Tropsha, 2002). External validation usually involves the prediction of the activity of compounds not considered in the development of the model.

QUANTITATIVE STRUCTURE–ACTIVITY RELATIONSHIPS OF SKIN PERMEABILITY: MODELING PERMEABILITY COEFFICIENTS

The development of QSARs for any endpoint requires biological effect data to model. Without these data, no modeling is possible. The limitations of the data to be modeled (both biological and physicochemical) must be appreciated by both the model developer and user. Criteria have been established to classify data for QSAR analysis according to their quality (Cronin, 2005; Cronin and Schultz, 2003). For some biological effects, large coherent databases have been specifically created for the development of products and possibly QSAR modeling. Unfortunately, this has not been the case in the area of skin permeability, and the enthusiastic QSAR modeler is left with historical literature data unless the modeler has a personal source of in-house data to model.

The Flynn Data Set

To assess the types of data that may be used for QSAR analysis of skin permeability, refer to the reviews of Geinoz et al. (2004), Moss et al. (2002), and Vecchia and Bunge (2004b). There has been a wide variety of types of skin permeability data used for QSAR modeling. However, most data sets tend to be relatively "small" for QSAR development, typically between 5 and 20 compounds. In addition, it must be pointed out that most usable data were published from the 1960s to the 1980s. Because of the small number of individual data in data sets, it is appropriate to

attempt to combine data into a larger data set. This was performed by Flynn (1990) for the permeability coefficients of 94 compounds through human skin *in vitro*.

In terms of skin permeability data for QSAR analysis, it is true to say that the science has not moved on significantly since the publication in 1990 of what is now universally known as the Flynn data set (Flynn, 1990). The Flynn data set is summarized in Table 7.1. For the purposes of this chapter, QSARs for the Flynn data set are reviewed; refer elsewhere (Geinoz et al., 2004; Moss et al., 2002; Vecchia and Bunge, 2003a, 2003b) for further details and more complete reviews of the use of QSARs in this area (which goes beyond the scope of this chapter). The Flynn data set is a compilation of skin permeability coefficients K_p for 94 compounds with a significant range of physicochemical properties. The data have been brought together from at least 15 publications and are characterized by lacking consistency in the protocols. Such lack of consistency in the data contained within the database is associated with considerable interlaboratory variation in data. Such variation in the data ultimately leads to variability in the QSARs developed and is demonstrated by a lack of statistical fit in the resultant model.

The first and probably most often cited skin permeability QSAR developed from the Flynn data set was that from Potts and Guy (1992). They developed the following model:

$$\text{Log } K_p = 0.71 \text{ log } P - 0.0061 \text{ MW} - 6.3 \tag{7.2}$$

where $n = 93$, and $R^2 = 0.67$ (no other statistics were provided by Potts and Guy, 1992).

Since the seminal publication of Potts and Guy (1992), more accurate log P data have become available, and a more thorough QSAR analysis is warranted. Regression analysis of the complete Flynn data set (as recorded in Table 7.1) was performed using the MINITAB statistical software (version 13.1). This provides the following QSAR (note this includes all 94 compounds listed by Flynn):

$$\text{log } K_p = 0.599 \text{ log } P - 0.00557 \text{ MW} - 2.64 \tag{7.3}$$

$$n = 94,\ s = 0.794,\ R^2 = 0.641,\ F = 84.1$$

$$t \text{ value log } P = 10.7;\ p > .0001$$

$$t \text{ value MW} = -9.81;\ p > .0001$$

At this point, it should be noted that the statistics mentioned here are for illustrative purposes only. Such statistics describe the goodness of fit of an equation (e.g., R^2, s); its significance (e.g., F); and the significance of individual variables. For a more thorough statistical assessment, a wide variety of other statistical measures can be applied; these were well described by Eriksson et al. (2003). The other statistical measures are likely to be those required for formal "validation" of a QSAR, frameworks for which were described in detail by Worth et al. (2004a, 2004b).

Table 7.1 Summary of the Flynn Data Set (Flynn, 1990) and Other Published Data

Name	Log K_p	Log P	MW
Aldosterone	–5.52	1.08	360.44
	–4.24[a]		
Amobarbital	–2.64	2.07	226.27
Atropine	–5.07	1.83	289.37
	–4.12[b]		
Barbital	–3.95	0.65	184.19
Benzyl alcohol	–2.22	1.10	108.14
4-Bromophenol	–1.44	2.59	173.00
2,3-Butanediol	–4.40	–0.92	90.12
Butyric acid	–3.00	0.79	88.10
n-Butanol	–2.60	0.88	74.12
2-Butanone	–2.35	0.29	72.10
Butobarbital	–3.71	1.73	212.24
4-Chlorocresol	–1.26	3.10	142.58
2-Chlorophenol	–1.48	2.15	128.55
4-Chlorophenol	–1.44	2.39	128.55
Chloroxylenol	–1.28	3.48	156.61
Chlorpheniramine	–2.66	3.38	274.80
Codeine	–4.31	1.19	299.30
Cortexolone[c]	–4.13	3.25	346.46
Cortexone[c]	–3.35	2.88	330.45
Corticosterone	–4.22	1.94	346.46
	–3.52[a]		
Cortisone[c]	–5.00	1.47	360.44
2-Cresol	–1.80	1.95	108.14
3-Cresol	–1.82	1.96	108.14
4-Cresol	–1.75	1.94	108.14
n-Decanol	–1.10	4.57	158.28
2,4-Dichlorophenol	–1.22	3.06	163.00
Diethylcarbamazine	–3.89	0.37	199.29
Digitoxin[c]	–4.89	2.83	764.94
Ephedrine	–2.22	1.13	165.23
Estradiol	–3.52	4.01	272.39
	–2.28[d]		
	–2.40[a]		
Estriol	–4.40	2.45	288.38
Estrone	–2.44	3.13	270.37
Ethanol	–3.10	–0.31	46.06
2-Ethoxy ethanol	–3.60	–0.32	90.12
Ethyl benzene	0.08	3.15	106.16
Ethyl ether	–1.80	0.89	74.12
4-Ethyl phenol	–1.46	2.47	122.16
Etorphine	–2.44	1.47	409.52
Fentanyl	–2.25	3.89	336.47
	–2.00[d]		
Fluocinonide	–2.77	3.19	494.55
Heptanoic acid	–1.70	2.41	130.18
n-Heptanol	–1.50	2.72	116.20
Hexanoic acid	–1.85	1.92	116.16
n-Hexanol	–1.89	2.03	102.17

(continued)

Table 7.1 (Continued) Summary of the Flynn Data Set (Flynn, 1990) and Other Published Data

Name	Log K_p	Log P	MW
Hydrocortisone	–5.52	1.61	362.46
	–3.93[d]		
	–3.64[a]		
[Hydrocortisone-21-yl]-*N,N*dimethyl succinamate[c]	–4.17	2.03	489.6
[Hydrocortisone-21-yl]-hemipimelate[c]	–2.75	3.26	504.6
[Hydrocortisone-21-yl]-hemisuccinate[c]	–3.20	1.89	462.5
[Hydrocortisone-21-yl]-hexanoate[c]	–1.75	4.48	460.6
[Hydrocortisone-21-yl]-hydroxy hexanoate[c]	–3.04	2.79	476.6
[Hydrocortisone-21-yl]-octanoate[c]	–1.21	5.49	488.7
[Hydrocortisone-21-yl]-pimelamate[c]	–3.05	2.31	503.6
[Hydrocortisone-21-yl]-propionate[c]	–2.47	2.80	418.5
[Hydrocortisone-21-yl]-succinamate[c]	–4.59	1.43	461.6
Hydromorphone	–4.82	0.21	285.3
Hydroxypregnenolone[c]	–3.22	3.71	330.45
17α-Hydroxyprogesterone[c]	–3.22	3.17	330.46
Isoquinoline	–1.78	2.08	129.16
Meperidine	–2.43	2.45	247.33
Methanol	–3.30	–0.77	32.04
Methyl-[hydrocortisone-21-yl]-succinate[c]	–3.68	2.58	476.6
Methyl-[hydrocortisone-21-yl]-pimelate[c]	–2.27	3.70	518.6
Methyl-4-hydroxy benzoate	–2.04	1.96	152.14
Morphine	–5.03	0.76	287.35
2-Naphthol	–1.55	2.70	144.16
Naproxen	–3.40	3.34	230.26
	–2.54[b]		
Nicotine	–1.71	1.87	162.23
	–2.48[b]		
Nitroglycerine	–1.96	1.62	227.09
3-Nitrophenol	–2.25	2.00	139.11
4-Nitrophenol	–2.25	1.94	139.11
n-Nitrosodiethanolamine	–5.22	–1.51	134.13
n-Nonanol	–1.22	3.77	144.26
Octanoic acid	–1.60	2.11	144.21
n-Octanol	–1.28	3.00	130.23
Ouabain	–6.11	–2.00	584.64
Pentanoic acid	–2.70	1.39	102.13
n-Pentanol	–2.22	1.56	88.14
Phenobarbital	–3.34	1.47	232.23
Phenol	–2.09	1.47	94.11
Pregnenolone[c]	–2.82	4.22	316.47
Progesterone[c]	–2.82	3.87	314.46
n-Propanol	–2.85	0.25	60.09
Resorcinol	–3.62	0.80	110.11
Salicylic acid	–2.20	2.26	138.12
	–1.86[b]		
Scopolamine	–4.30	0.26	303.35
Styrene	–0.19	2.95	104.15
Sucrose	–5.28	–3.70	342.29
Sulfentanyl	–1.92	3.95	387.5

(continued)

Table 7.1 (Continued) Summary of the Flynn Data Set (Flynn, 1990) and Other Published Data

Name	Log K_p	Log P	MW
Testosterone	–3.40	3.32	288.42
	–2.66[a]		
Thymol	–1.28	3.30	150.22
Toluene	0.00	2.73	92.14
2,4,6-Trichlorophenol	–1.23	3.69	197.44
Water	–3.30	–1.38	18.01
3,4-Xylenol	–1.44	2.35	122.17

Note: Permeability coefficients K_p, octanol–water partition coefficients P, and molecular weight (MW) for 94 compounds listed by Flynn (1990).

[a] New permeability coefficient taken from Johnson et al. (1995).
[b] New permeability coefficient taken from Degim et al. (1998).
[c] Duplicate value reported by Flynn (1990).
[d] K_p for this compound was not included in Equation 7.5.

A further assessment of the quality of a QSAR can be made in terms of which compounds (if any) are poorly predicted by the model or do not fit it well. These compounds are commonly termed *outliers*, and a number of techniques exist to identify them (Eriksson et al., 2003). There are a number of reasons for the occurrence of outliers (Cronin and Schultz, 2003). In aquatic ecotoxicology, outliers are frequently associated with chemicals acting by a different mechanism of toxic action, and much has been learned from their analysis (cf. Lipnick, 1991). Another reason for the occurrence of outliers is the creation of an insignificant model that is simply not predictive. Also, outliers may result from the use of poor (i.e., low-quality) or erroneous data in a model.

The treatment of outliers has sparked controversy among QSAR developers for decades. The most simplistic approach is simply to remove outliers and pretend they do not exist. This is not good modeling, however. It is now recognized that the complete data set to be modeled should be reported, as well as any outliers. The removal of outliers should be performed on a rational basis according to the reasons outlined above (i.e., compounds acting by a different mechanism of action, poor quality data, etc.). In the prediction of a "nonspecific" process such as skin permeation (as compared to acute toxicity), we may be able to assume a general passive diffusion process through the membrane. Therefore, if any outliers are present from a model, it should be logical to check the quality of the data. Specifically regarding the modeling of a data set such as compiled by Flynn, we should be cautious of the quality of the data because it is a compilation from different sources.

One of the simplest methods of identifying outliers from a multiple regression analysis is the use of the standard residual. This provides a measure of how well or poorly a compound is predicted by that model. Again, it should be stressed that this is a simple statistic and is internal to the model; that is, the prediction is made for the compound already in the model. More severe methods for the identification of outliers are available (Eriksson et al., 2003; Tropsha et al., 2003). The sign on the standard residual also indicates if a compound is over- or underpredicted by a model. Examination of the standard residuals (which are provided automatically by most

statistical software) from Equation 7.3 shows some interesting trends. A number of compounds are shown to be outliers (full results are not included here); these include the steroids, sucrose, atropine, etorphine, and so on. The fact that there are outliers to the Potts and Guy equation has been recognized by a number of workers (for a full discussion, see Moss et al., 2002). To ensure consistency, Degim et al. (1998) and Johnson et al. (1995) have remeasured the skin permeability values for a number of these compounds. As shown in Table 7.1, the remeasured values are significantly different from the original published data. Reanalysis of the complete data set with the new (and presumably more accurate) data results in development of the following model:

$$\log K_p = 0.603 \log P - 0.00528 \text{ MW} - 2.64 \tag{7.4}$$

$$n = 94,\ s = 0.676,\ R^2 = 0.704,\ F = 112$$

$$t \text{ value log } P = 12.6;\ p > .000$$

$$t \text{ value MW} = -10.9;\ p > .000$$

Further analysis of the standard residuals from Equation 7.4 shows that the steroids remain as significant outliers. Again, this is almost certainly a result of the poor quality of the original data. This issue has been discussed by Cronin et al. (1999) and notably by Abraham et al. (1997). Many authors are of the opinion that these data should be removed because of these concerns over data quality, and the QSAR should be recalculated. Other workers (see the discussion in Geinoz et al., 2004) have taken a different view and reanalyzed the data using more descriptors. Some descriptors appear to be useful (such as those associated with large numbers of carbon atoms; Dearden et al., 2000), but this is likely to be a spurious correlation as these will uniquely identify the steroids in this data set and through the modeling process will account for the error in the original measurements.

In this analysis, 19 compounds have been removed because of their association with steroid-type structures and if there are no new data (these are noted in Table 7.1). Their removal results in the following QSAR:

$$\log K_p = 0.613 \log P - 0.00575 \text{ MW} - 2.54 \tag{7.5}$$

$$n = 75,\ s = 0.631,\ R^2 = 0.749,\ F = 112$$

$$t \text{ value log P} = 12.6;\ p > .000$$

$$t \text{ value MW} = -8.57;\ p > .000$$

Some compounds remain outliers (e.g., sucrose), although the model is not developed further.

Reanalysis and improvement of the Potts and Guy Equation 7.2 has been performed. Through reanalysis of the data, Equation 7.3 confirms the validity of the model published by Potts and Guy. This has been improved in terms of statistical quality (e.g., goodness of fit, etc.) through the use of improved data (Equation 7.4) and the removal of suspected poor-quality data (Equation 7.5). Importantly, the coefficients on the descriptors and the constant in the model do not change from Equation 7.2 to Equation 7.5. This is a good indicator of the stability of the model. Also, although the statistical fit of the model is not perfect (75% of the variance of the data is explained by Equation 7.5), it is realistic in terms of the data being modeled, that is, a diverse set of values with considerable interlaboratory error. The standard error of about 0.65 log units is acceptable and relates well to the error that may be expected from experimental measurement.

Mechanistic Interpretation of the Potts and Guy Model

In addition to the assessment of statistical criteria and predictivity, the ability to interpret a QSAR from a mechanistic point of view is essential to determine the relevance and applicability of the model (Worth et al., 2004a, 2004b). Mechanistic interpretation of a QSAR is normally achieved by the ability to place some physiological relevance to the model. The Potts and Guy equation can be simplified to the following:

$$\log K_p = \text{Hydrophobicity} - \text{Molecular size} + \text{Constant} \tag{7.6}$$

The two properties included in this model can be interpreted easily. Partition into the skin is strongly related to lipophilicity and hence hydrophobicity. Diffusion through the skin is related to the size of the molecule.

In terms of the descriptors used in the prediction of skin permeability coefficients, the octanol–water partition coefficient P is a well-established measure of hydrophobicity (Dearden, 1990). There is a variety of algorithms to calculate log P, including Web-based programs and the KOWWIN software, which is part of the EPISuite utility. EPISuite is available free from the U.S. Environmental Protection Agency (see Cronin and Livingstone, 2004b, for more details; EPISuite can be downloaded from http://www.epa.gov/oppt/exposure/docs/episuite.htm). Molecular size is well modeled by molecular weight, which of course is fundamental and trivial to calculate.

The issue of the appropriate term to describe molecular size has often been raised. Although molecular weight is a simple and fundamental term, it provides only a gross estimate of molecular bulk. Potts and Guy (1992) and other workers have discussed the possibility of using a molecular volume term. To address this issue, Patel and Cronin (2001a) investigated 17 steric properties in QSAR based on Equation 7.6 for skin permeability coefficients. The steric properties considered included gross estimates of molecular bulk, volume, topology, and shape. The findings suggested that there is little difference in the use of alternative descriptors for molecular size and that molecular weight could be used with confidence. The only caveat to this problem may be for compounds with low molecular weight and high

density. However, the currently available data are limited in terms of such compounds; therefore, this hypothesis has yet to be explored.

Beyond the Flynn Data Set: Other Sources of Data for Modeling

Since the publication of the Flynn data set, there have been a number of efforts to extend and expand it in terms of the number of chemicals and the coverage of the compounds. Such efforts have also allowed for the quality of such data to be established. An excellent and comprehensive review of the data available was provided by Vecchia and Bunge (2003b). The same authors (Vecchia and Bunge, 2003a) also provided an excellent resource for modeling in terms of a data set of validated values relating to skin permeability parameters. The reader is well advised to start with these two references before investigating the literature for any further data.

Another excellent resource is provided by the University of Newcastle (England) via the EDETOX Web site (http://www.ncl.ac.uk/edetox/). The on-line database contains data that have been produced by *in vitro* and *in vivo* percutaneous penetration studies. These have been compiled from the published literature, and data generated during the EDETOX project have also been entered. The database has allowed for the formation of a QSAR based on the formalism of Equation 7.6. The equation is of good statistical quality and has extended the data set from 94 chemicals published by Flynn to over 140 (Fitzpatrick et al., 2004). Again, there is no significant difference in the coefficients on the variables and constants, which further confirms the stability and versatility of this approach to modeling skin permeability coefficients.

Other Modeling Approaches

There are many other approaches to the modeling of skin permeability data (permeability coefficients and others). It is beyond the scope and purpose of this chapter to review fully these approaches; refer to the recent articles by Geinoz et al. (2004), Moss et al. (2002), and Vecchia and Bunge (2003a) for further details. Although in no way a comprehensive review, the following discussion is of notable other approaches used to model skin permeability.

General linear free-energy relationships (LFERs) or linear solvation-energy relationships have been developed by Abrahams and coworkers for a number of years. The philosophy and approach was well described by Abraham et al. (1999). Briefly, the general LFER is

$$\text{Property} = e\text{E} + s\text{S} + a\text{A} + b\text{B} + v\text{V} + \text{Constant} \tag{7.7}$$

where Property is the effect to be predicted (i.e., skin permeability coefficient); E is the solute excess molar refractivity; S is the solute dipolarity/polarizability; A and B are the overall or summation hydrogen bonding acidity and basicity, respectively; and V is the McGowan characteristic volume.

LFER is suitable to be applied to the problem of predicting skin permeability coefficients. Abraham and Martins (2004) summarized their previous work and then

described the analysis of a data set of 119 compounds. Importantly, in the new work they standardized the data set for temperature (i.e., 37°C) and for the effects of ionization. Both these factors are important and until now had been relatively overlooked in the modeling of skin permeability coefficients. Abraham and Martins (2004) reported that correcting for temperature and accounting for ionization greatly improved the statistical fit of the model and its predictive capability. The general LFER equation reported for skin permeability coefficients is

$$\text{Log } K_p = -0.106\ \text{E} - 0.473\ \text{S} - 0.473\ \text{A} - 3.00\ \text{B} + 2.30\ \text{V} - 5.27 \quad (7.8)$$

$$n = 119,\ R^2 = 0.832,\ s = 0.461,\ F = 112$$

The t values for variables were not given.

Clearly, the statistical fit (in terms of R^2 and s) is improved over Equation 7.2 to Equation 7.5. However, this may be because of the improvement brought about by the adjustment for temperature and corrections for ionization. In terms of mechanistic interpretation, the terms E, S, A, B, and V have been clearly defined and are related strongly to chemical and physiological phenomena (Abrahams et al., 1999; Abrahams and Martins, 2004). However, the LFER lacks the simplicity of the Potts and Guy approach as (for the most accurate application) the parameters require experimental determination from chromatography. This limits its use as a predictive technique from structure.

A simpler approach to the prediction of permeability coefficients was provided by Buchwald and Bodor (2001). This involved only two parameters, namely, the effective van der Waals molecular volume (Ve) and the hydrogen bonding N parameter. These parameters gave the following model:

$$\text{Log } K_p = 0.0128\ \text{Ve} - 0.492\ \text{N} - 5.94 \quad (7.9)$$

$$n = 98,\ R^2 = 0.72,\ s = 0.62,\ F = 124$$

The t values for variables were not given.

The statistical fit for Equation 7.9 is similar to that for Equations 7.4 and 7.5 and is realistic for the quality and precision of the data modeled. Whether the user will find any advantage in using this model over Equation 7.8 is a decision the user will have to make from personal analysis, philosophy of model development, and the intended use. In reviewing this work, Geinoz et al. (2004) observed that although the two parameters Ve and N are not interrelated in terms of physicochemical meaning, they are strongly intercorrelated statistically ($r = 0.92$). Highly correlated variables are not normally acceptable in regression-based QSAR.

Among the many other works in this area, some studies have been attempted on skin permeability measurements other than the permeability coefficient. Skin permeability coefficients are usually utilized in QSAR modeling because they provide steady-state constants with the possibility of varying across a large number of orders of magnitude (the limitations of this type of data are described in the section

"Limitations of Quantitative Structure–Activity Relationship Models for Skin Permeability"). Some work has been performed on percentage absorbed data that may be more applicable to risk assessment. For instance, Roy et al. (1998) modeled the percentage of the applied dose of polycyclic aromatic hydrocarbons that penetrated rat skin *in vitro* after 24 h (PADA) using log *P* and a second term for molecular size, Shadow 6 Area (SHDW6):

$$\text{PADA} = -14.7 \log P - 22.0\ \text{SHDW6} + 111.9 \tag{7.10}$$

$$n = 60,\ R^2 = 0.64,\ s = 7.7,\ F = 54$$

The *t* values for variables were not given.

This equation is unusual in that it has a negative coefficient with log *P*. Moss et al. (2002) rationalized this as the downslope of a parabolic, or biphasic, relationship with log P. In an attempt to provide a more mechanistically interpretable model, Gute et al. (1999) reanalyzed the data set and developed the following model:

$$\text{PADA} = -0.3\ \text{MW} + 90.6 \tag{7.11}$$

$$n = 60,\ R^2 = 0.67,\ s = 7.4,\ F = 120$$

The *t* values for variables were not given.

EXPERT SYSTEMS

A large and increasing number of expert systems are available in predictive toxicology. Expert systems have been defined as "any formalised system, not necessarily computer-based, which enables a user to obtain rational predictions about the toxicity of chemicals" (Dearden et al., 1997, p. 224). It is again beyond the scope of this chapter to review in detail expert systems, and the reader is referred to the comprehensive reviews of Combes and Rodford (2004) and Dearden et al. (1997) as well as many of the chapters in Helma's work (2005). It should be emphasized, however, that most expert systems are designed to calculate physicochemical properties (e.g., log *P*, aqueous solubility, etc.) or to assist in the risk assessment process by the calculation of toxicities rather than predict skin permeability. The advantage of an expert system is that, as a (normally) computer-based program, it allows that user to enter a chemical structure (normally in a simple manner) and quickly and efficiently obtain some prediction of effect or property.

One expert system for the prediction of skin permeability is available. This is the Dermal Permeability Coefficient Program (DERMWIN). This program is freely available from the U.S. Environmental Protection Agency through the EPISuite software and can be downloaded from http://www.epa.gov/oppt/exposure/docs/episuite.htm. DERMWIN estimates the dermal permeability coefficient K_p and the dermally absorbed dose per event (DA_{event}) of organic compounds. As explained in the section "Quantitative Structure–Activity Relationships," and is

typical with expert systems, DERMWIN requires only a chemical structure to estimate K_p. Structures are entered into DERMWIN through the Simplified Molecular Input Line Entry System (SMILES) notation. SMILES is a simple-to-learn system for describing molecular structure. An excellent online tutorial is available for novices (see http://www.daylight.com/dayhtml/smiles/smiles-intro.html), and the notation is also well described by Kaiser (2004). The EPISuite software also has the capability to provide SMILES notations automatically from the Chemical Abstract Service (CAS) Registry numbers for more than 103,000 compounds.

DERMWIN estimates a log P value for every SMILES string using the KOWWIN program. DERMWIN also automatically retrieves experimental log P values from a database containing more than 13,200 measured values. When a match is made in the database, the experimental log P value is retrieved and used to predict K_p rather than the estimated value. The calculation of molecular weight is trivial and is easy to obtain from a knowledge of the SMILES string.

DERMWIN uses a version of the Potts and Guy (1992) general estimation equation to predict K_p for all structures:

$$\log K_p = 0.71 \log P - 0.0061 \text{ MW} - 2.72 \tag{7.12}$$

In addition to the K_p estimation from the general estimation equation, DERMWIN makes K_p estimates for the alcohol, phenol, and steroid chemical classes using the following class-specific equations:

(Aliphatic) Alcohols:

$$\log K_p = 0.544 \log \text{P} - 2.88 \tag{7.13}$$

The aliphatic alcohol equation applies to any structure (except steroid types) containing the –OH functional group connected to an aliphatic carbon.

Phenols:

$$\log K_p = 2.39 \log P - 0.39(\log P)^2 - 5.2 \tag{7.14}$$

The phenol equation applies to any structure containing the –OH functional group connected to an aromatic carbon.

Steroids:

$$\log K_p = 1.01 \log P - 5.33 \tag{7.15}$$

DERMWIN also uses two methods to estimate the DA_{event}. The first method is the steady-state approach using the following adapted equation of Fick's first law:

$$\text{DA}_{\text{event}} \text{ (mg/cm}^2\text{-event)} = K_p \times C_{\text{w}} \times t_{\text{event}} \tag{7.16}$$

where C_{w} is the concentration of the chemical in water (mg/cm^3), and t_{event} is the duration of the event (h/event).

The second method is based on the K_p prediction from the general estimation equation.

LIMITATIONS OF QUANTITATIVE STRUCTURE–ACTIVITY RELATIONSHIP MODELS FOR SKIN PERMEABILITY

There are a number of limitations to the current models for the prediction of the skin permeation of chemicals. These relate mainly to the modeling processes that are appropriate and available to us and to the issues with data.

Data Availability and Quality

It is true to say that a QSAR developer will never admit to having sufficient high-quality data to model. So saying, it is fundamental to the modeling process, and current models are limited in terms of the quality of data available. This problem data quality is gradually being rectified by work such as that of Vecchia and Bunge (2003a, 2003b) and the EDETOX project.

Although the current numbers of chemicals for which reliable skin permeability coefficients are available is relatively large (i.e., over 100), this is still small in comparison with the total number of compounds that may enter the environment or to which a human may be exposed. This may limit the applicability of a model, particularly in terms of its lack of chemical heterogeneity. For instance, the Flynn data set is developed mainly from common drugs or common organic compounds. A further issue is the number of compounds actually required for a successful QSAR model (Schultz et al., 2003). If we may assume that a Potts and Guy (1992) approach (Equation 7.6; i.e., using only two parameters for hydrophobicity and molecular size) is appropriate, then, fortunately, a data set of over 100 compounds well exceeds the number of compounds required to make a statistically significant regression-based QSAR.

Endpoint to Be Predicted

QSAR will work best for steady-state permeability coefficients from an aqueous vehicle at infinite dose. Such permeability coefficients may be reasonably well predicted but are relatively limited in their use for risk assessment, for instance.

Data Modeling by Nonexperts

By its nature, QSAR is a multidisciplinary activity that requires expertise in biology, chemistry, and statistics. It is true to say that most QSAR modelers are experts in only one of these fields and will miss subtleties (if not basic knowledge) in other areas. Even a biologist (such as myself) may be specialized in one area (toxicology in my case) and may lack the knowledge to model data and understand other endpoints sufficiently (it is true that I have faced a steep learning curve in coming to grips with skin permeability data). The converse is also true; an expert in skin

penetration processes may wish to develop a QSAR but may not be familiar with its limitations, the caveats, and its rules to be followed. Finally, a user of a model may not be trained in the endpoint predicted or the modeling process and therefore may use the model in an inappropriate manner. Thus, QSAR development and use should be performed preferably by a team of experts spanning the appropriate depth of knowledge in the endpoint modeled, the appreciation of the physicochemical properties, and the statistical technique (and its limitations) applied.

Formulations and Vehicle Effects

As stated, currently available QSARs are available only for permeability coefficients from aqueous vehicles. This limits their usefulness in terms of the assessment of mixtures and the like. Currently, little is known about the quantitative effect of penetration enhancers, formulations, and different solvents (Moss et al., 2002). This means that predictions from aqueous vehicles cannot be extrapolated to predict the effects of other solvents or formulations. This is a severe limitation in the applicability of QSARs in skin permeability.

RECOMMENDATIONS FOR THE USE OF QUANTITATIVE STRUCTURE–ACTIVITY RELATIONSHIPS TO PREDICT SKIN PERMEABILITY COEFFICIENTS

For successful model development, a large data set of high-quality data is required. The efforts to obtain, assess, and "validate" skin permeability data as described in this chapter should be encouraged. Only those data deemed to be high quality should be used for modeling. Ideally, some assessment of the chemical space of the current data should be made and is where we are lacking knowledge.

Although a number of skin permeability measurements can be used, it is highly likely that modeling will be best with skin permeability coefficients. For successful modeling and to ensure high-quality data, the data must be standardized. This means that only permeability coefficients measured at infinite dose and in aqueous solution will be modeled successfully. In addition, it has been shown that data should be adjusted for temperature and corrected for ionization.

Skin permeability data for QSAR modeling should be treated as passive diffusion data and modeled in an empirical manner. Ideally, this means that QSAR development should commence with descriptors that reflect the process modeled. Thus, descriptors for partitioning (i.e., log P) and molecular size (e.g., molecular weight or similar) are recommended. Much has been made of the relevance of properties such as hydrogen bonding in QSAR for skin permeability. However, its exact role is uncertain and, as yet, unquantified, so it should be treated with caution.

All QSAR development should consider and abide by the guidance on good practice in modeling (cf. Livingstone, 2004). Of the statistical techniques available, regression analysis is simplistic but has many advantages. More multivariate methods run the risk of overfitting the data and "hiding" problems in the data and model.

Finally, the QSAR developer should be pragmatic and aware of the intended use for a model. A QSAR may only provide a "rough estimate" of skin penetration or even a qualitative assessment (e.g., high/low). If this is sufficient for the required purpose, then no further modeling necessary. Thus, as well as the intricacies of the modeling process, the QSAR developer should always bear in mind the likely application of the model.

CONCLUSION

QSARs allow for the prediction of biological activities and effects, including the skin permeability coefficient. Careful use of historical data, such as those reported by Flynn (1990) and Vecchia and Bunge (2003a, 2003b), will assist in the development of QSARs for human skin permeability coefficients from *in vitro* measurements. The most successful QSARs for K_p have been based on the approach taken by Potts and Guy (1992), namely, regression analysis based on two descriptors for hydrophobicity and molecular size. There are a number of limitations to these QSARs, however; namely, they are developed from a data set with limited chemical heterogeneity and are based on measurements from infinite dose in aqueous solution. Despite this, with an appreciation of the limitations of the models and careful and appropriate use, QSARs may be applied successfully for the prediction of K_p.

REFERENCES

Abraham, M.H., Chadha, H.S., Martins, F., Mitchell, R.C., Bradbury, M.W., and Gratton, J.A. (1999). Hydrogen bonding. Part 46. A review of the correlation and prediction of transport properties by an LFER method: physicochemical properties, brain penetration, and skin permeability, *Pesticide Science*, 55, 78–88.

Abraham, M.H. and Martins, F. (2004). Human skin permeation and partition: general linear free-energy relationship analyses, *Journal of Pharmaceutical Sciences*, 93, 1508–1523.

Abraham, M.H., Martins, F., and Mitchell, R.C. (1997). Algorithms for skin permeability using hydrogen bond descriptors: the problem of steroids, *Journal of Pharmacy and Pharmacology*, 49, 858–865.

Buchwald, P. and Bodor, N. (2001). A simple, predictive, structure-based skin permeability model, *Journal of Pharmacy and Pharmacology*, 53, 1087–1098.

Combes, R.D. and Rodford, R.A. (2004). The use of expert systems for toxicity prediction: illustrated with reference to the DEREK program, in M.T.D. Cronin and D.J. Livingstone (eds.), *Predicting Chemical Toxicity and Fate*, Boca Raton, FL: CRC Press, pp. 193–204.

Cronin, M.T.D. (2004). Predicting chemical toxicity and fate in humans and the environment—an introduction, in M.T.D. Cronin and D.J. Livingstone (eds.), *Predicting Chemical Toxicity and Fate*, Boca Raton, FL: CRC Press, pp. 3–13.

Cronin, M.T.D. (2005). Toxicological information for use in predictive modelling: quality, sources, and databases, in C. Helma (ed.), *Predictive Toxicology*, New York: Dekker, pp. 93–133.

Cronin, M.T.D., Aptula, A.O., Duffy, J.C., Netzeva, T.I., Rowe, P.H., Valkova, I.V., and Schultz, T.W. (2002). Comparative assessment of methods to develop QSARs for the prediction of the toxicity of phenols to *Tetrahymena pyriformis*, *Chemosphere*, 49, 1201–1221.

Cronin, M.T.D., Dearden, J.C., Moss, G.P., and Murray-Dickson, G. (1999). Investigation of the mechanism of flux across human skin *in vitro* by quantitative structure-permeability relationships, *European Journal of Pharmaceutical Sciences*, 7, 325–330.

Cronin, M.T.D., Jaworska, J.S., Walker, J.D., Comber, M.H.I., Watts, C.D., and Worth, A.P. (2003). Use of QSARs in international decision-making frameworks to predict health effects of chemical substances, *Environmental Health Perspectives*, 111, 1391–1401.

Cronin, M.T.D. and Livingstone, D.J. (2004a). Calculation of physicochemical properties, in M.T.D. Cronin and D.J. Livingstone (eds.), *Predicting Chemical Toxicity and Fate*, Boca Raton, FL: CRC Press, pp. 31–40.

Cronin, M.T.D. and Livingstone, D.J. (eds.). (2004b). *Predicting Chemical Toxicity and Fate*, Boca Raton, FL: CRC Press.

Cronin, M.T.D. and Schultz, T.W. (2003). Pitfalls in QSAR, *Journal of Molecular Structure (Theochem)*, 622, 39–51.

Cronin, M.T.D., Walker, J.D., Jaworska, J.S., Comber, M.H.I., Watts, C.D., and Worth, A.P. (2003). Use of QSARs in international decision-making frameworks to predict ecologic effects and environmental fate of chemical substances, *Environmental Health Perspectives*, 111, 1376–1390.

Dearden, J.C. (1990). Physico-chemical descriptors, in W. Karcher and J. Devillers (eds.), *Practical Applications of Quantitative Structure–Activity Relationships (QSAR) in Environmental Chemistry and Toxicology*, Brussels: EEC, pp. 25–59

Dearden, J.C., Barratt, M.D., Benigni, R., Bristol, D.W., Combes, R.D., Cronin, M.T.D., Judson, P.M., Payne, M.P., Richard, A.M., Tichy, M., Worth, A.P., and Yourick, J.J. (1997). The development and validation of expert systems for predicting toxicity. The report and recommendations of an ECVAM/ECB workshop (ECVAM workshop 24), *ATLA*, 25, 223–252.

Dearden, J.C. and Cronin, M.T.D. (2005). Quantitative structure–activity relationships and drug design, in J.C. Smith (ed.), *Introduction to the Principles of Drug Design and Action,* 4th ed., Amsterdam: Harwood, in press.

Dearden, J.C., Cronin, M.T.D., Patel, H., and Raevsky, O.A. (2000). QSAR prediction of human skin permeability coefficients, *Journal of Pharmacy and Pharmacology*, 52(S), 221.

Degim, I.T., Pugh, W.J., and Hadgraft, J. (1998). Skin permeability data: anomalous results, *International Journal of Pharmaceutics*, 170, 129–133.

Eriksson, L., Jaworska, J., Worth A.P., Cronin, M.T.D., McDowell, R.M., and Gramatica, P. (2003). Methods for reliability and uncertainty assessment and applicability evaluations of classification-, regression-based and QSARs, *Environmental Health Perspectives*, 111, 1361–1375.

Fisk, P.R., McLaughlin, L., and Wildey, R.J. (2004). Good practice in physicochemical property prediction, in M.T.D. Cronin and D.J. Livingstone (eds.), *Predicting Chemical Toxicity and Fate*, Boca Raton, FL: CRC Press, pp. 41–59.

Fitzpatrick, D., Corish, J., and Hayes, B. (2004). Modeling skin permaeability in risk assessment — the future, *Chemosphere*, 55, 1309–1314.

Flynn, G.L. (1990). Physicochemical determinants of skin absorption, in T.R. Gerrity and C.J. Henry (eds.), *Principles of Route-to-Route Extrapolation for Risk Assessment*, New York: Elsevier, pp. 93–127.

Geinoz, S., Guy, R.H., Testa, B., and Carrupt, P.-A. (2004). Quantitative structure–permeation relationships (QSPeRs) to predict skin permeation: a critical evaluation, *Pharmaceutical Research*, 21, 83–92.

Golbraikh, A. and Tropsha, A. (2002). Beware of q2! *Journal of Molecular Graphics and Modelling*, 20, 269–276.

Gute, C.D., Grunwald, G.D., and Basak, S.C. (1999). Prediction of the dermal penetration of polycyclic aromatic hydrocarbons (PAHs): a hierarchical QSAR approach, *SAR and QSAR in Environmental Research*, 10, 1–15.

Helma, C. (ed.). (2005). *Predictive Toxicology*, New York: Dekker.

Johnson, M.E., Blankschtein, D., and Langer, R. (1995). Permeation of steroids through skin, *Journal of Pharmaceutical Sciences*, 84, 1144–1146.

Kaiser, K.L.E. (2004). Toxicity data sources, in M.T.D. Cronin and D.J. Livingstone (eds.), *Predicting Chemical Toxicity and Fate*, Boca Raton, FL: CRC Press, pp. 17–29.

Kubinyi, H. (2002). From narcosis to hyperspace: the history of QSAR, *Quantative Structure–Activity Relationships,* 21, 348–356.

Lipnick, R.L. (1991). Outliers, their origin and use in the classification of molecular mechanisms of toxicity, *Science of the Total Environment*, 109/110, 131–154.

Livingstone, D.J. (1995). *Data Analysis for Chemists: Applications to QSAR and Chemical Product Design*, Oxford, UK: Oxford University Press.

Livingstone, D.J. (2000). The characterisation of chemical structures using molecular properties—a survey, *Journal of Chemical Information and Computer Sciences*, 40, 195–209.

Livingstone, D.J. (2003). Theoretical property predictions, *Current Topics in Medicinal Chemistry*, 3, 1171–1192.

Livingstone, D.J. (2004). Building QSAR models—a practical guide, in M.T.D. Cronin and D.J. Livingstone (eds.), *Predicting Chemical Toxicity and Fate*, Boca Raton, FL: CRC Press, pp. 151–170.

Moss, G.P., Dearden, J.C., Patel, H., and Cronin, M.T.D. (2002). Quantitative structure–permeability relationships (QSPRs) for percutaneous absorption, *Toxicology in Vitro,* 16, 299–317.

Netzeva, T.I. (2004). Whole molecule and atom-based topological descriptors, in M.T.D. Cronin and D.J. Livingstone (eds.), *Predicting Chemical Toxicity and Fate*, Boca Raton, FL: CRC Press, pp. 61–83.

Patel, H., Cronin, M.T.D. (2001a). Determination of the optimal physico-chemical parameters to use in a QSAR-approach to predict skin permeation rate. Final Report. CEFIC-LRI Project No. NMALRI-A2.2UNJM-0007. June 2001, available at http://www.staff.livjm.ac.uk/phamcron/qsar/CEFIC/cefic_intro.htm or from the author m.t.cronin@livjm.ac.uk.

Patel, H. and Cronin, M.T.D. (2001b). A novel index for the description of molecular linearity, *Journal of Chemical Information and Computer Sciences*, 41, 1228–1236.

Potts, R.O. and Guy, R.H. (1992). Predicting skin permeability, *Pharmaceutical Research,* 9, 663–669.

Roy, T.A., Krueger, A.J., Mackerer, C.R., Neil, W., Arroyo, A.M., and Yang, J.J. (1998). SAR models for estimating the percutaneous absorption of polynuclear aromatic hydrocarbons, *SAR and QSAR in Environmental Research*, 9, 171–185.

Schultz, T.W., Cronin, M.T.D., Walker, J.D., and Aptula, A.O. (2003). Quantitative structure–activity relationships (QSARs) in toxicology: a historical perspective, *Journal of Molecular Structure (Theochem)*, 622, 1–22.

Schultz, T.W., Netzeva, T.I., and Cronin, M.T.D. (2003). Selection of data sets for QSARs: analyses of *Tetrahymena* toxicity from aromatic compounds, *SAR and QSAR in the Environmental Sciences*, 14, 59–81.

Schüürmann, G. (2004). Quantum chemical descriptors in structure–activity relationships—calculation, interpretation and comparison of methods, in M.T.D. Cronin and D.J. Livingstone (eds.), *Predicting Chemical Toxicity and Fate*, Boca Raton, FL: CRC Press, pp. 85–149.

Todeschini, R. and Consonni, V. (eds.). (2000). *Handbook of Molecular Descriptors (Methods and Principles in Medicinal Chemistry)*, Weinheim: Wiley-VCH.

Tropsha, A., Gramatica, P., and Gombar, V. K. (2003). The importance of being earnest: validation is the absolute essential for successful application and interpretation of QSPR models, *QSAR and Combinatorial Sciences*, 22, 69–77.

van de Waterbeemd, H. (ed.). (1995). *Chemometric Methods in Molecular Design*, Weinheim, Germany: VCH.

Vecchia, B.E. and Bunge, A.L. (2003a). Partitioning of chemicals into skin: results and predictions, in R.H. Guy and J. Hadgraft (eds.), *Transdermal Drug Delivery*, 2nd ed., New York: Dekker, 143–198.

Vecchia, B.E. and Bunge, A.L. (2003b). Skin absorption databases and predictive equations, in R.H. Guy and J. Hadgraft (eds.), *Transdermal Drug Delivery*, 2nd ed., New York: Dekker, pp. 57–141.

Worth, A.P., Cronin, M.T.D., and van Leeuwen, C.J. (2004a). A framework for promoting the acceptance and regulatory use of (quantitative) structure–activity relationships, in M.T.D. Cronin and D.J. Livingstone (eds.), *Predicting Chemical Toxicity and Fate*, Boca Raton, FL: CRC Press, pp. 429–440.

Worth, A.P., Hartung, T., and van Leeuwen, C.J. (2004b). The role of the European Centre for the Validation of Alternative Methods (ECVAM) in the validation of (Q)SARs, *SAR and QSAR in Environmental Research*, 15, 345–358.

CHAPTER 8

How Dermal Absorption Estimates Are Used in Risk Assessment

Kenneth A. Walters and Keith R. Brain

CONTENTS

INTRODUCTION

There is an increasing demand for quantitative data on the rates of penetration and permeation of a diverse range of chemical entities in human skin as such data can be used to estimate the potential systemic load following accidental or deliberate exposure. These estimates may also be useful for toxicological and risk assessment purposes when the implications of the everyday use of a wide range of potentially harmful materials in the agrochemical, chemical, cosmetic, household, and pharmaceutical sectors may be determined and appropriate steps taken to minimize any possible risk. The development of suitable experimental methods and protocols has been driven largely by regulatory and safety bodies and the perceived need for

improved data on the permeability of the skin to xenobiotics. For example, the U.S. Environmental Protection Agency (EPA) is currently addressing the issue of the dermal absorption testing of 80 compounds designated by the Occupational Safety and Health Administration (OSHA) and the Interagency Testing Committee (ITC) as worthy of particular interest (*Federal Register*, 1996; Walker et al., 1996). Updated guidelines also appear on a regular basis (see, for example, EPA, 2003).

Although toxicological issues are perhaps the most important factors, it is also clear that increasing the depth and breadth of the database on skin penetration and permeation will improve understanding of the mechanisms of this process and lead to more reliable methods for prediction of any potential hazard (Geinoz et al., 2004). The need for relevant data produced under reproducible and reliable conditions (see, for example, Beck et al., 2000) has led to an increase in both the development and the standardization of *in vitro* and *in vivo* test procedures. As detailed earlier in chapter 2, there have been numerous recommendations on *in vitro* and *in vivo* methodologies, and many of these have been collated as guidelines by both regulatory bodies and committees of interested parties. Perhaps the most widely known of these guidelines are those produced following a U.S. Food and Drug Administration/American Association of Pharmaceutical Scientists (FDA/AAPS) workshop on the performance of *in vitro* skin penetration studies (Skelly et al., 1987). However, more recent publications also contain useful and updated information (Table 8.1). These include the European Centre for the Validation of Alternative Methods (ECVAM) workshop report "Methods for Assessing Percutaneous Absorption" (Howes et al., 1996), documents from the European Centre for Ecotoxicology and Toxicology of Chemicals (ECETOC, 1993) and the European Cosmetic Toiletry and Perfumery Association (COLIPA) (Diembeck et al., 1999), the final monograph from the Scientific Committee on Cosmetic Products and Non-Food Products intended for Consumers (SCCNFP, 2000), the European Commission Health and Consumer Protection Directorate-General Guidance Document on Dermal Absorption (Sanco/222/2000 rev. 6, 2002), and information from the National Occupational Research Agenda Dermal Exposure Research Program Description (NORA DERP) program.

Determination of the risk associated with environmental and occupational exposure to chemicals such as pesticides necessarily involves a range of assumptions regarding contact with contaminated air, soil, or water. In addition, the potential for

Table 8.1 Protocols and Guidelines for *In Vitro* Skin Penetration and Permeation Studies

Date	Organization or Author	Type	Reference
1987	FDA/AAPS	Guideline	Skelly et al., 1987
1991	Bronaugh and Collier	Protocol	Bronaugh and Collier, 1991
1993	ECETOC	Protocol	ECETOC, 1993
1996	ECVAM	Protocol	Howes et al., 1996
1999	COLIPA	Guideline	Diembeck et al., 1999
2000	SCCNFP	Guideline	SCCNFP, 2000
2004	Organization for Economic Cooperation and Development	Protocol	OECD, 2005

exposure via different routes (inhalation, oral, dermal) leads to complex paradigms that must be resolved (Schneider et al., 1999; Ross et al., 2001). Four years ago, the European Community funded the RISKOFDERM project designed to improve risk assessment for occupational dermal exposure to chemicals. A consortium of interested parties was established, and their main aim was to develop a conceptual model for dermal risk assessment for regulatory purposes. A further goal was to design a computer-compatible tool kit that would enable simple assessment of dermal exposure risk (Oppl et al., 2003; Schuhmacher-Wolz et al., 2003). The project is nearing completion, and the tool kit is presently available for downloading (Eurofins, 2003). The tool kit, however, is only capable of providing an approximate measure of exposure and risk and, as such, may be useful to determine safe exposure durations or the need for supply and use of personal protective equipment. However, more accurate determinants for dermal risk assessment are required, one of which, human skin absorption, can be derived from data generated during measurements of human skin permeation *in vitro*. An international workshop specifically dedicated to Methods to Determine Dermal Permeation for Human Risk Assessment, was sponsored by the European Chemical Industry Council (CEFIC), which was recently held in Utrecht.

DERMAL RISK ASSESSMENT

Risk assessment has been defined as "the process by which the probability that a harmful effect may occur [is determined]" (Gettings et al., 1998). There are four steps involved in risk assessment: hazard assessment, dose response assessment, exposure assessment, and risk characterization. It is evident that before any assessment can be made it is necessary to determine whether the compound under investigation is indeed harmful following systemic exposure (hazard); this is usually determined from 90-day oral dosing studies in laboratory rodents. These studies provide a no observed adverse effect level (NOAEL), following oral or intravenous administration, which may be subsequently used, in combination with exposure assessment and skin permeability data, to assess dermal safety margins. Although the NOAEL is obtained from a pragmatic experimental procedure performed using established and validated protocols, the assessment of exposure and determination of skin permeability often leads to values that can be somewhat variable depending on the models and methods used (Schneider et al., 1999; McDougal and Boeniger, 2002; Marquart et al., 2003; van de Sandt, 2004).

There has been considerable progress in standardization of *in vitro* skin permeation experimentation (as described in the introduction), but some important parameters require further discussion. As an example, a range of additives may be included in the receptor solution used during *in vitro* skin permeation experiments, and these can have significant effects on the amount of test compound that is determined as permeated (Figure 8.1) (Cross et al., 2003; Stinchcomb et al., 2004). It is important, therefore, that the protocols used to determine the amount of skin permeation are designed carefully and with due respect to the intended use of the generated data. With this in mind, the following examples describe some effects

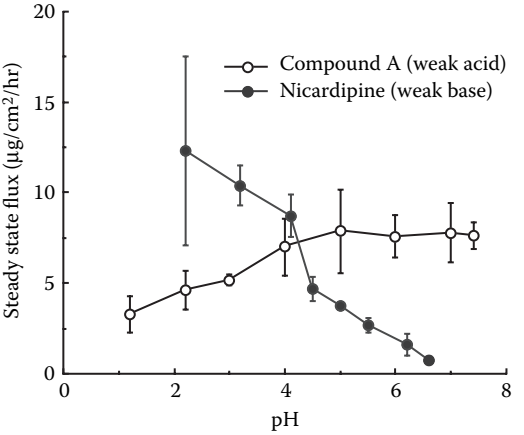

Figure 8.1 The effect of receptor fluid pH on the flux of a weak acid (pK_a 2.60) and a weak base (pK_a 5.68) across human skin *in vitro*. Skin permeation of the weak acid increased with increasing pH, whereas that for the base decreased. (Data from Kou, J.H., Roy, S.D., Du, J., and Fujiki, J., *Pharm. Res.,* 10, 986–990M 1883.)

of varying experimental procedures on the data generated. These examples are discussed in approximate experimental chronological order. More complete information is available elsewhere in this volume and in several comprehensive reviews (e.g., Brain et al., 2002).

The formulation in which the test compound is applied to the skin should always be identical to the final "in-use" product. It is pointless, for example, to develop a margin-of-safety factor for a compound that is formulated for use in an aqueous-based gel based on skin permeation data of the test compound applied in an ethanolic solution. Cumulative permeation of the compound will probably be totally different over set exposure periods, and the margin of safety may be completely over- or underestimated. In addition, limitations of analytical sensitivity may sometimes require the use of radiolabeled test materials.

The use of radiolabeled permeants is attractive because this greatly simplifies sample analysis, particularly for mass balance experiments. Although guidelines for the choice and use of radiolabels in permeation experiments are provided by COLIPA (Diembeck et al., 1999), not all problems are addressed. It is essential that radiolabeled materials be homogeneously mixed with nonlabeled permeant. When a radiolabel is used to evaluate a formulated product, it is highly desirable that the radiolabel is incorporated in the same way, and at the same stage of manufacture, as the cold permeant. However, this may only be possible for formulations in which the exact constituents and method of manufacture can be reproduced. A less-rigorous alternative is to manufacture a small quantity of labeled formulation and attempt to blend this thoroughly with a larger quantity of cold formulation. If the test formulation is a marketed product with an exact manufacturing process and ingredients that are unknown, incorporation of the label in these ways is impossible, limiting the options to spiking the market formulation with radiolabel dissolved in the most appropriate solvent to minimize the possibility of modification of the release rate. In all cases,

it is essential to demonstrate the homogeneity of distribution of the label in the final formulation. However, it must be appreciated that, in complex formulations containing discrete phases, homogeneous distribution at a (sub)microscopic level may not be achievable by spiking, and that solvent used to incorporate a label may significantly alter the performance of a formulation.

The greatest problem in the use of radiolabeled material is probably the potential lack of specificity. Radiolabeled test compounds will always contain some level of impurities (usually of smaller molecular weight), and tritium exchange is a more significant phenomenon than often appreciated. It is necessary to demonstrate that the integrity of the permeant is maintained during the experiment, and that scintillation counts attributed to permeation of the target molecule are not caused by impurities, degradation, exchange, or metabolism. This can be achieved by chromatographic separation of the analyte before counting, although this removes a major advantage of the radiolabeled approach.

The manner in which a test substance is applied to the skin surface can be a major determinant of its subsequent penetration and absorption. Several factors must be considered when selecting a suitable application procedure, including: the nature of the vehicle, the permeant concentration, the amount of vehicle applied, the mechanism of application, the exposure time, and the method for removing an applied vehicle (if required). Many of these issues may be intrinsic to the purpose of the study. For example, risk assessment involving the study of the skin permeation of an ingredient in a commercially available product should be performed with the material in the formulation as it is marketed or used and with an application regime that mimics as closely as possible the in-use situation (see, for example, Brain et al., 1995; Walters, Brain, Howes, et al., 1997).

There are two common methods of applying substances to the skin. The infinite dose technique involves application of a sufficient amount of permeant to make any changes in donor concentration over the experimental time frame caused by diffusion or evaporation negligible (i.e., the dose is effectively infinite). On the other hand, finite dose techniques (Franz, 1978) are designed to model in-use conditions and involve application of a dose that may show marked depletion during an experiment. Depletion occurs when the proportion of the test compound entering the membrane, or evaporating, is large relative to the amount applied (Anissimov and Roberts, 2001; Rogers and McDougal, 2002; Saiyasombati and Kasting, 2003). Alternatively, the test compound may be removed from the skin surface during, for example, the simulation of a rinsing or washing procedure. With finite dosing, the permeation profile may exhibit the characteristic plateauing effect that accompanies donor depletion (Figure 8.2), whereas infinite dosing usually generates typical Barrer-type diffusion profiles. It is obvious that, in most cases, infinite dosing will lead to an overestimate of cumulative permeation relative to finite dosing. Direct comparisons of finite and infinite dose applications are relatively rare, but the predicted effects have been investigated (Franz et al., 1993; Walters, Brain, Dressler, et al., 1997; Wester et al., 1998).

Another important consideration in the determination of skin permeation is the absolute amount of test compound or formulation to apply to the skin surface. There are conflicting reports regarding the effect of dose level on the degree of permeation

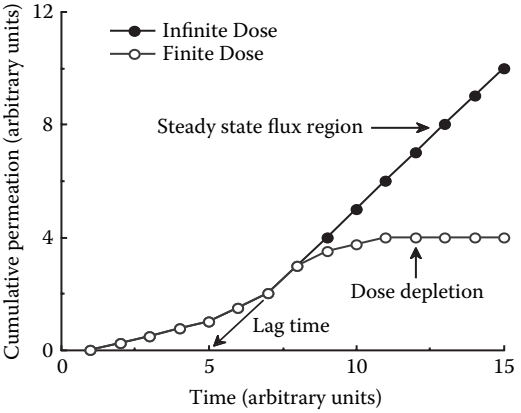

Figure 8.2 Sample cumulative permeation patterns following finite and infinite dosing regimes. With infinite dose permeation normally reaches a steady-state flux region, from which it is possible to calculate permeability coefficients and diffusional lag times. In finite dosing, the permeation profile normally exhibits a plateauing effect as a result of donor depletion.

through skin. For example, increased dose concentration did not produce proportional increases in the flux of ibuprofen or flurbiprofen across human skin *in vitro* when deposited as a thin film from acetone (Akhter and Barry, 1985). Three concentrations of each drug were applied in 50 μl of solvent, and the authors concluded that, as the acetone evaporated from the skin surface, the thermodynamic activity of the drugs increased until saturation was reached, at which concentration maximum flux would be expected. When all of the solvent had evaporated, leaving a plug of solid drug with poor dissolution properties, the flux dropped in all cases. The effect of volume on the permeation of minoxidil from ethanol was linear between 10 and 50 μl (Tata et al., 1995), but it was concluded that it was the total drug loading, rather than the application volume, that was important. Note that this is only the case for a volatile vehicle that evaporates rapidly from the skin surface. In practice, the actual skin permeation of volatile compounds, such as dimethylnitrosamine (Figure 8.3) and 2-phenoxy-ethanol, is significantly reduced by evaporation (Brain et al., 1995; Roper et al., 1997). Other literature covers the theories of finite dosing (Kubota and Yamada, 1990; Seta et al., 1992; Anissimov and Roberts, 2001), thickness of the application vehicle (Addicks et al., 1988; Walker et al., 1991), and contact time effects (Ferry et al., 1990).

Because risk is principally a function of usage or exposure, any form of assessment should only be based on experimental protocols that reproduce demographic use of the product in question. In dermal risk assessment, it is important that any estimation of skin absorption take into consideration the likely amount, extent, and duration of exposure that would occur in use (see, for example, Barlow et al., 2001). These parameters are readily controlled during *in vitro* experiments, and certainly the amount of product applied has been the subject of considerable guidance. There are several published recommendations on both the expression of dose levels and the specific quantities involved. The FDA/AAPS guidelines (Skelly et al., 1987)

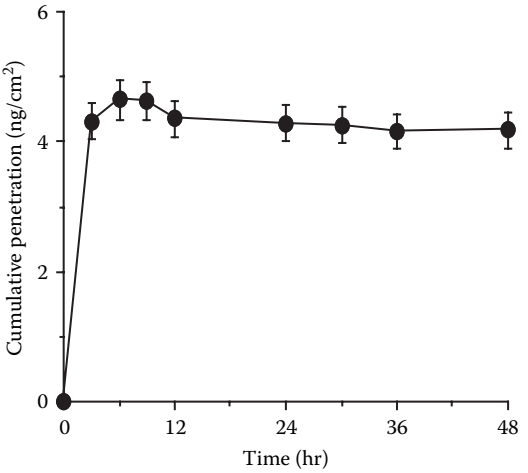

Figure 8.3 Permeation profile for dimethylnitrosamine (DMN) across human skin *in vitro*. DMN was applied at finite dose levels in an oil-in-water emulsion vehicle. Note that permeation was significantly reduced by evaporation following 6 h of exposure. (From Brain, K.R., Walters, K.A., James, V.J., Dressler, W.E., Howes, D., Kelling, C.K., Moloney, S.J., and Gettings, S.D., *Food Chem. Toxicol.,* 33, 315–322, 1995. Used with permission.)

suggested a universal application weight of approximately 5 mg/cm^2 of formulation. COLIPA (Diembeck et al., 1999) proposed 5μl/cm^2 for liquid formulations and 2 mg/cm^2 for semisolid formulations (or 5 mg/cm^2 if these are compared to a liquid). Distribution of accurately measured amounts of such small quantities of semisolid formulations as an even film over the surface of skin membranes presents considerable practical challenges (Addicks et al., 1988). Semisolid materials can be applied and spread with a small spatula coated with preweighed formulation. The precise weight applied is determined by difference, and all test materials should be applied by the same operator.

Furthermore, other factors that determine the degree of potential consumer exposure, such as end product use, should be considered during *in vitro* skin permeation determinations. This is especially true when determining the duration of the experiment. Although some workers have extended the duration of *in vitro* experiments to 120 h (Akhter and Barry, 1985), it is recommended that they are restricted to 24 h (Diembeck et al., 1999) or 48 h (Howes et al., 1996). It has been suggested that 48 h may be too short to establish a steady-state flux from an infinite dose, leading to misinterpretation of the data (Potts and Guy, 1994), and the ECVAM report (Howes et al., 1996) suggested that experiments may be extended to 72 h (in the presence of antimicrobial agents) in such cases. Based on electrical resistance measurements and permeation parameters, human epidermal membranes were shown to retain integrity for up to 5 days provided that they were supported on suitable nonrate-limiting membranes (Peck et al., 1993). In the absence of the filter membrane support, tissue integrity was compromised by the physical stress accompanying

sample withdrawal and skin washing. Investigators should, however, be aware of the possibility of barrier degradation over extended time frames.

Sample intervals should be of an appropriate frequency to allow realistic assessment of such parameters as lag time and steady-state, or pseudo-steady-state, flux (if possible) (Anissimov and Roberts, 1999). For a compound with unknown permeation characteristics, samples should ideally be taken at 2 h intervals for the duration of the experiment. Early samples (1 to 4 h) may be important in identifying cells in which the barrier is compromised, showing anomalously high early permeability.

There is a high intra- and intersubject variability in human skin permeability (Southwell et al., 1984; Williams et al., 1992; Kasting et al., 1994), and a large number of replicates for each dosage regimen is recommended. The most widely quoted recommendation for numbers of replicates in *in vitro* studies on human skin is 12 per test group (Skelly et al., 1987), and any comparative studies should also use matched skin samples distributed through the test groups. In addition, prior to determination of the permeation of the test compound, each sample of skin may be tested for barrier integrity. Skin integrity can be addressed in a qualitative manner by simple visual examination of specimens or, more quantitatively, by measurement of transepidermal water loss (Benech-Kieffer et al., 1997) or the flux of marker compounds, such as tritiated water (Hood et al., 1996) or sucrose (Pendlington et al., 1997). The generally accepted upper limit of the permeability coefficient for water diffusion through human skin is 2.5×10^{-3} cm/h (Bronaugh et al., 1986). Samples showing particularly high permeability are often rejected as outliers with questionable barrier integrity but may actually represent the real population spread if their distribution is indeed log-normal (Williams et al., 1992; Roper et al., 2004).

Prolonged skin exposure to the test product is not always appropriate in dermal risk assessment. For example, leave-on cosmetics (creams, lotions) have a greater potential to deliver the test compounds to the skin than do rinse-off products (because most of the chemical is invariably rinsed away). A rinse-off product is one designed to be applied to the hair or body in diluted or undiluted form for a short period of time (less than 1 h) followed by thorough rinsing. Examples of such products include shampoos, cleansers, hair conditioners, hair dyes, and depilatories. A leave-on product is one that is intended to be applied to the skin and left in place for a long enough period to achieve the desired benefit. Examples include hand and body lotions, sunscreen products, and antiperspirants. There are several examples in the literature that describe the ability to carry out and evaluate the influence of rinse-off and leave-on procedures during *in vitro* skin permeation experiments (see, e.g., Walters, Brain, Howes et al., 1995, 2002; Walters, Brain, Dressler et al., 1997).

In contrast, estimation of exposure from the use of hair care products presents a different set of considerations relative to skin care products (Dressler, 1998). In particular, the assumptions for the calculation of percutaneous absorption for hair dyes are unique to these types of products. Factors that should be considered include the sporadic use of the product, consequential scalp exposure to the dye material, the nature of the dye itself (permanent; semipermanent), and alterations in potential bioavailability caused by desquamation.

The formation of the stratum corneum is a terminal differentiation process that leads eventually to desquamation of the outermost cells. In humans, epidermal turnover rates can vary somewhat (Roberts and Marks, 1980; Finlay et al., 1982; Egelrud, 2000), but on average one cornified cell layer is shed each day, leading to complete turnover of the stratum corneum every 2 to 4 weeks. It is important therefore to consider the effect that desquamation may have on the absorption of compounds through the skin. This is particularly significant when considering what should be included in the "absorbed dose" when using data derived from *in vitro* skin permeation studies. A complete study should analyze not simply the amount of test compound appearing in the receptor phase over time, but also the distribution of material through the various skin layers at the end of the experiment. Residual surface material should also be removed and quantified together with analysis of material in the stratum corneum (using tape strips) and the viable epidermis. This not only enables the experimenter to determine whether a reservoir of test compound exists in the stratum corneum but also allows a full mass balance calculation that accounts for all of the test material applied.

Preliminary algorithmic attempts suggested that desquamation, together with other factors (Figure 8.4), would significantly reduce the total systemic load of a lipophilic permeant following dermal exposure (Howes et al., 1997). More recent analyses have confirmed both theoretically and practically that desquamation may significantly reduce the absorption of applied substances for highly lipophilic and high molecular weight compounds (Reddy et al., 2000; O'Connor et al., 2004). Data obtained experimentally using polycyclic musks and rat skin *in vivo* confirmed this observation for lipophilic materials (Ford et al., 1999), and desquamation was also observed to slightly increase the percutaneous absorption of *N*-methyl-2-pyrrolidone across rat skin (Payan et al., 2003). Yourick and colleagues (2004) reported studies on the fate of several compounds following dermal application. Of the three compounds studied [dihydroxyacetone, DHA; 7-(2H-naphtho[1,2-d]triazol-2-yl)-3-phenylcoumarin, 7NTPC; disperse blue 1, DB1], two (DHA and DB1) formed epidermal reservoirs, and the authors concluded that the amount remaining in the skin should not be considered as absorbed material. On the other hand, the data for 7NTPC indicated that this material was spread throughout the epidermis and dermis and as such could not be justifiably excluded from the total absorbed dose without further experimentation.

These equivocal data suggest that no universal rule can presently be established regarding the total absorbed dose for use in calculating safety margins in dermal risk assessment. Data must be generated for each compound, and the results should be carefully analyzed before assessing risk.

EXAMPLES OF THE USE OF *IN VITRO* SKIN PENETRATION DATA IN DERMAL RISK ASSESSMENT

The determination of the potential risk associated with chemical use and dermal exposure to environmental contaminants is often based on an evaluation of *in vivo* and *in vitro* dermal absorption in the rat together with *in vitro* evaluation using

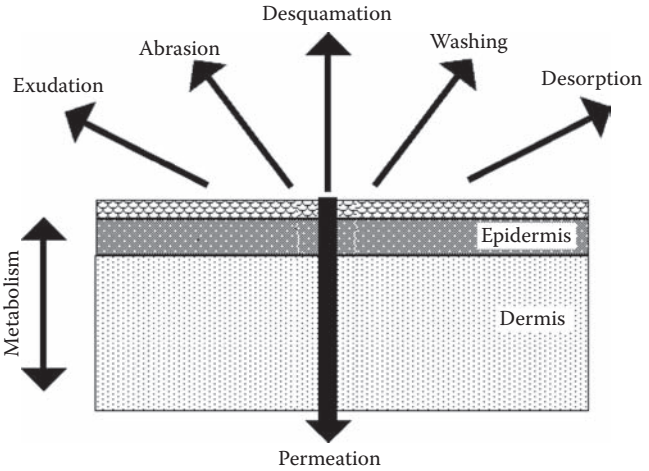

Figure 8.4 Competing processes that can significantly modify the degree to which materials present in the stratum corneum are subsequently absorbed. (From Howes, D., Watkinson, A.C., and Brain, K.R. (1997). A more complete approach to the modeling of dermal risk assessment, in K.R. Brain, V.J. James, and K.A. Walters (eds.), *Perspectives in Percutaneous Penetration,* Vol. 5b, Cardiff, U.K.: STS Publishing, pp. 68–69. (Used with permission.)

human skin (Scott et al., 1993; van Ravenzwaay and Leibold, 2004). In this way, human *in vivo* absorption is estimated based on three measured determinants:

$$\%\ \text{human } in\ vivo \text{ absorption} = \frac{(\%\ \text{rat dermal } in\ vivo) \times (\text{abs. rate human } in\ vitro)}{(\text{abs. rate rat } in\ vitro)}$$

However, the European Union Cosmetics Directive targeted the prohibition of animal testing of finished cosmetic products and cosmetic ingredients. The generation of margins of safety for cosmetic ingredients is therefore solely dependent on *in vitro* evaluation. Although human skin is the most suitable membrane, it is not readily available, and pig skin is therefore often used as a surrogate (Steiling et al., 2001) because it shows some similarity in permeation characteristics (Table 8.2).

Examples of the complexity of dermal risk assessments for environmental contaminants and cosmetic ingredients and the use of parameters derived from *in vitro* skin permeation experiments are given next.

Environmental Contaminants

There are many variables involved in the risk assessment of environmental and occupational chemicals such as pesticides. In an occupational setting, for example, dermal exposure to pesticides often occurs when the pesticide is present in a formulation, which may contain other potentially harmful materials and will certainly contain materials that can affect the barrier function of the skin (Riviere et al., 2001; chapter 14, this volume). Molecular size of the permeant can play a significant role

Table 8.2 Observed Permeability of Several Compounds through the Skin of Pigs and Humans, Measured Using *In Vivo* Techniques

Permeant	% Applied Dose Absorbed	
	Human	Pig
Acetylcysteine	2.4	6.0
Butter yellow	21.6	41.9
Caffeine	47.6	32.4
Cortisone	3.4	4.1
DDT	10.4	43.4
Haloprogin	11.0	19.7
Lindane	9.3	37.6
Malathion	8.2	15.5
Parathion	9.7	14.5
Testosterone	13.2	29.4

Source: Walters, K.A. and Roberts, M.S., Veterinary applications of skin penetration enhancers, in K.A. Walters and J. Hadgraft (eds.), *Pharmaceutical Skin Penetration Enhancement*, New York: Dekker, 1993, pp. 345–364. (Used with permission.)

in the permeation and maximum flux of a compound across the skin (Magnusson et al., 2004). Skin surface loading and unloading rates, mass balance transfer from contaminated soil and water to skin, area and site of exposure, skin decontamination procedures, and the use of personal protective clothing will all affect the rate and extent of skin absorption and subsequent systemic load (Wester and Maibach, 1999; Phillips and Garrod, 2001; McDougal and Jurgens-Whitehead, 2001; Navidi and Bunge, 2002; Riley et al., 2004). In view of these variables, the EPA commissioned and published a comprehensive report on skin absorption and factors affecting the dermal uptake process (EPA, 1992). A stepwise dermal exposure assessment process was defined that included the identification of contaminated media; the identification of chemical contaminants and determination of their concentrations; the identification of activities resulting in dermal exposure; and quantification of exposed skin area, contact rate, exposure time, exposure frequency, and exposure duration. Included within the assessment process was the determination and evaluation of dermal absorption values. An update to this document (EPA, 2001) has identified several crucial factors that are important in defining more accurate determinants of risk associated with dermal exposure.

The challenge in determining the dermal absorption values most relevant to factor into a risk assessment process for environmental contaminants is to define the most relevant parameter (i.e., flux, permeability coefficient, percentage absorption, or total systemic load). For example, when using *in vitro* techniques to determine potential dermal absorption of a contaminant in water (in which it will probably be present at low concentrations), the most common model would use an infinite dose aqueous application. This will allow the determination of flux and the calculation of a permeability coefficient. However, from such an experiment, the percentage absorption value will be practically meaningless. The total systemic load will be dependent on many other factors, such as concentration and solubility of contaminant within the medium, pH of the medium (and thus the degree of ionization of the contaminant),

duration of exposure, frequency of exposure, area of exposure, temperature, and so on. In this instance, therefore, the most appropriate *in vitro* diffusion parameter to use for risk assessment would be the permeability coefficient. The permeability coefficient, derived from the measured skin flux at steady state, is independent of concentration of the contaminant and the area of application. Thus, with a known permeability coefficient for a particular contaminant in a particular medium, if the concentration of the contaminant in the medium is known, then the flux per unit area can be determined. The flux data can be used to calculate the amount of contaminant absorbed per unit area per event (e.g., swimming, bathing), and the overall daily systemic load, or dermally absorbed dose (DAD, mg/kg/day), can be estimated from (EPA, 1992) the following:

$$\mathrm{DAD} = \frac{\mathrm{DA}_{\mathrm{event}} \times \mathrm{EV} \times \mathrm{ED} \times \mathrm{EF} \times \mathrm{A}}{\mathrm{BW} \times \mathrm{AT}}$$

where $\mathrm{DA}_{\mathrm{event}}$ is the absorbed dose per event (mg/cm^2/event, which is calculated from the equation $\mathrm{DA}_{\mathrm{event}} = K_p \times C_{\mathrm{w}} \times t_{\mathrm{event}}$, in which K_p is the permeability coefficient, C_{w} is the concentration of contaminant in water, and t_{event} is the duration of exposure per event); A is the skin contact surface area (cm^2); EV is the event frequency (events/day); EF is the exposure frequency (days/year); ED is the exposure duration (years); BW is body weight (70 kg for adults, 15 kg for children); AT is the averaging time in days (for noncarcinogenic effects, AT = ED; for carcinogenic effects, AT = 25,550 days).

The updated guidance document (EPA, 2001) includes refinements to the above equation to account for the potential bioavailability of contaminants in the stratum corneum when exposure has ended and variable exposure times. Furthermore, the newer document discusses, in depth, the use of mathematical predictions of the permeability coefficient in dermal risk assessment. It is important to appreciate that the permeability coefficient should be determined experimentally using, ideally, a donor phase that mimics as closely as possible the existing environmental conditions. The use of permeability coefficients predicted from theoretically derived equations adds a further uncertainty to the overall risk calculation. Although it has been suggested that the dermal permeability estimates are the most uncertain of the parameters in the dermal dose computation (EPA, 1992), it could be argued, given the refinement of *in vitro* techniques and the correlation between *in vitro* and *in vivo* measurements of human skin (Franz, 1978; Wester et al., 1992; van de Sandt et al., 2000; Cnubben et al., 2002; Zobrist et al., 2003; Colombo et al., 2003), that these measurements are the least assumptive and the most accurate of all the parameters used.

Soil contamination presents further complexities in dermal risk assessment (see Chapter 11, this volume). Briefly, additional factors involved in the estimation of risk include soil type (and particle size) and loading rate; skin–soil adherence (Holmes et al., 1999), which can vary according to body site; area of exposure (fraction of body area exposed is limited by clothing); and climate. The equation used to determine the dermally absorbed dose from soil contact is the same as that

used for water (above), although the derivation of the absorbed dose per event (DA_{event}) is slightly different and takes into account an adherence factor for soil onto skin (AF):

$$DA_{event} = C_{soil} \times CF \times AF \times ABS_d$$

where C_{soil} is the concentration of contaminant in the soil, CF is a conversion factor equivalent to 10^{-6} kg/mg, and ABS_d is the dermal absorption fraction.

Note that, in this equation, exposure time is not factored, and this will lead to a measure of uncertainty. At present, the dermal absorption fraction (ABS_d), which is measured experimentally and believed to be related to the adherence factor (Duff and Kissel, 1996), is the preferred determinant for skin absorption from soil. More research into the assessment of flux and permeability coefficients, including soil–skin partitioning, is required.

Cosmetics

In many respects, risk assessment for components of cosmetic formulations is a more straightforward task than that for environmental contaminants (Yourick and Bronaugh, 1999). Exposure periods and amounts applied to the skin can be readily defined, and the concentration of the substance in question in the product is usually known. There is also a reasonably accurate measure of the frequency of application, which can be established by demographic studies. The studies described below illustrate the use of experimentally derived *in vitro* skin permeation data in generating margins of safety for two commonly used cosmetic types, sunscreen agents and hair dyes.

Sunscreen Agent: Octyl Salicylate

Ultraviolet radiation causes sunburn, premature aging of skin, and skin cancer, and there is a considerable body of evidence that suggests that actinic keratosis, basal cell and squamous skin cancer, malignant melanoma, and cutaneous lupus erythematosis are exacerbated or triggered by sun exposure (Naylor and Farmer, 1997; Ting et al., 2003). An understanding of the potential for human systemic exposure is an integral part of the safety assessment of sunscreen actives used in consumer products (Hayden et al., 1998; Federal Register, 1999). The available data on the skin permeation of sunscreen actives has been reviewed (Walters et al., 1999).

The *in vitro* human skin permeation of a commonly used sunscreen active, octyl salicylate (2-ethylhexyl salicylate) was determined from two vehicles (an oil-in-water emulsion and a hydroalcoholic formulation) that were representative of typical commercial sunscreen products (Walters, Brain, Howes, et al., 1997). Human abdominal skin that was obtained at autopsy was heat separated to yield epidermal membranes (comprising stratum corneum and viable epidermis) and mounted in glass horizontal-type diffusion cells. Receptor phase solutions consisted of phosphate-buffered saline, pH 7.4, containing 6% Volpo N20 to ensure sink conditions. A finite dose of the oil-in-water emulsion formulation (5 mg/cm^2) and hydroalcoholic

Table 8.3 Permeation and Recovery Data for Octyl Salicylate After Application as Finite Doses *In Vitro* in Typical Sunscreen Vehicles

Parameter	Hydroalcoholic Lotion	Oil-in-Water Emulsion
Total permeated at 48 h	1.58 ± 0.25 μg/cm^2	1.58 ± 0.36 μg/cm^2
Total percentage[a] absorption at 48 h	0.59 ± 0.09	0.65 ± 0.16
Recovery in wash (%)	36.21 ± 5.98	36.66 ± 5.31
Recovery in skin (%)	32.77 ± 4.74	17.18 ± 1.28
Total recovery (%)	69.57 ± 6.84	54.50 ± 5.47

[a] All percentage values are percentage applied dose.

Data from Walters, K.A., Brain, K.R., Howes, D., James, V.J., Kraus, A.L., Teetsel, N.M., Toulon, M., Watkinson, A.C., and Gettings, S.D., *Food Chem. Toxicol.,* 35, 1219–1225, 1997. Data are means ± SE.

lotion (5 μl/cm^2) was applied to the skin surface. Permeation of ^{14}C-labeled material was determined by analysis of samples taken from the receptor phase at intervals over 48 h. The data clearly showed that the percutaneous penetration of octyl salicylate from these typical sunscreen vehicles was low (<1% over 48 h) (Table 8.3). The cumulative percutaneous penetration of ^{14}C-labeled material was similar in each case (1.58 μg/cm^2 over 48 h), although the amount of applied material remaining in the skin at 48 was slightly higher for the hydroalcoholic solution (32.8%) than the oil-in-water emulsion (17.2%).

Because it might reasonably be expected that vehicles of this type would have a greater influence on the cumulative amount of permeant appearing in the receptor phase, these data reflect the importance of the use of final formulations (rather than simple solutions) in the risk assessment of substances intended for topical exposure. However, these data should also be interpreted cautiously. The amount of ^{14}C-labeled material recovered from the skin *in vitro* may be an overestimate of the quantity of octyl salicylate remaining within the stratum corneum or epidermis, under userlike conditions, because the surface rinsing procedure used here was not particularly rigorous. Moreover, sunscreen products are typically formulated to provide a high degree of skin substantivity (i.e., the sunscreen active is delivered preferentially to the skin surface, where it remains in or on the upper layers of the stratum corneum). Nonetheless, based on the determination of the percutaneous penetration of octyl salicylate under the *in vitro* conditions described here, predicted *in vivo* human exposure may be calculated based on the following assumptions:

Typical adult body weight	60 kg
Average amount of sunscreen applied per day	16 g
Maximum allowable concentration in sunscreen products	5%
Maximum (*in vitro*) percutaneous absorption	0.65%

Human exposure may be calculated as

$$\frac{16\text{ g} \times 0.65\% \times 5\%}{60\text{ kg}} = 0.087\text{ mg/kg}$$

Using the results of toxicology studies conducted *in vivo* (Cosmetic, Toiletry, and Fragrance Association [CTFA], unpublished data, 1994), which demonstrated

an NOAEL of 250 mg/kg, a margin of safety (i.e., the ratio of the lowest dose resulting in no observable toxicity to the estimated human dose) may be calculated as follows:

$$\frac{250\ \text{mg/kg}}{0.087\ \text{mg/kg}} = 2{,}900$$

Hair Dyes: 2-nitro-4-aminodiphenylamine and N-1-(2-Hydroxyethyl)-2-nitro-p-phenylenediamine

Human poisoning by hair dyes is extremely rare and has only been reported following oral ingestion (Suliman et al., 1983; Nohynek et al., 2004). Although there have been reports that suggested a link between hair dye use and bladder cancer in both users and hair care professionals (Gago-Dominquez et al., 2001; Czene et al., 2003), conservative risk assessments and genotoxicity studies suggested that there is no, or negligible, cancer risk to consumers for ingredients that were found to be positive in rodent oral carcinogenicity studies (Haws et al., 1994; La Vecchia and Tavani, 1995; Holly et al., 1998; Kirkland and Marzin, 2003; Andrew et al., 2004).

It is well known that the actives used in hair dye formulations can penetrate into and permeate across the skin (Dressler, 1998; Yourick and Bronaugh, 2000). The rate and total cumulative amount of dye that has been shown to be absorbed, however, is variable and also dependent on the study protocol. When similar protocols have been used, in inter- and intralaboratory studies variability is considerably reduced (Beck et al., 2000). Calculation of safety margins for hair dyes using *in vitro* skin permeation data is somewhat more complex than that illustrated above for a sunscreen agent. Whereas a typical sunscreen agent is applied as a leave-on product over a large area of the body, hair dye products are applied to the hair over a relatively small (but certainly an area rich in hair follicles) area of skin and remain in place for a short period of time. Thus, to determine the potential systemic load using *in vitro* skin permeation measurements, the experiments should follow as closely as possible the in-use scenario.

Although it has been calculated that the amount of a hair dye product typically applied to the hair is of the order of 100 mg/cm^2 of formulation, the assumption is usually made that the amount of formulation coming into contact with the underlying skin is approximately 10 mg/cm^2. Formulations containing 2-nitro-4-aminodiphenylamine (HC Red No. 1; containing 1% w/w dye) and *N*-1-(2-hydroxyethyl)-2-nitro-*p*-phenylenediamine (HC Red No. 3; containing 1.5% w/w dye) were applied to epidermal membranes derived from human abdominal or breast skin *in vitro* at a dose level of 10 mg/cm^2. The applied formulations were rinsed off the skin following 30 min of exposure, and permeation of any residual dye was followed over a 48 h time period. At the end of the experimental period, the epidermal membranes were removed from the diffusion cells, and the amount of dye in the stratum corneum and residual epidermis was determined. Measurement of the various phases (30-min rinse, terminal rinse, stratum corneum, residual epidermis, and receptor fluid) allowed complete dose accountability (mass balance). The collective data were

Table 8.4 Calculated Margins of Safety for Hair Dyes: HC Red No. 1 and HC Red No. 3

Determinant	HC Red No. 1, 1.0% Dye	HC Red No. 3, 1.5% Dye
Cumulative mass penetrated at 24 h (μg/cm^2) (24 h receptor fluid value)	1.51	0.17
Typical human body weight (kg)	60	60
Typical scalp surface area (cm^2)	600	600
Percutaneous permeation (μg/kg/day) (24 h Receptor fluid value × Scalp area/Body weight)	15.1	1.70
Amount in skin (μg/cm^2) (48 h Stratum corneum + Residual epidermis values)	0.37	1.48
Potential systemic exposure per application (μg/kg/applied) (Receptor fluid value + Epidermal amount × Scalp area/Body weight	18.8	16.5
Use frequency (days)	15	15
Average daily systemic exposure (μg/kg/day) (assuming all epidermal amounts become bioavailable)	1.25	1.10
No observed adverse effect level (NOAEL; mg/kg/day)	8	125
Margin of Safety 1 (NOAEL/systemic exposure dose) (using 24 h receptor fluid value)	530	73,529
Margin of Safety 2 (NOAEL/systemic exposure dose) (using 24 h receptor fluid value and total epidermal levels averaged over 15 day use interval)	6400	113,630

Courtesy of Dr. W.E. Dressler. Safety margins were calculated based on a single 24 h exposure or averaged over a 15 day use interval.

subsequently used to generate margin of safety values for the two dye substances. Margins of safety either were based on simple 24 h exposure receptor solution values or were averaged over a 15 day use interval period (Table 8.4). Quite clearly, when frequency of use is included, the margins of safety increase considerably (W.E. Dressler, 2004, personal communication).

CONCLUSION

The foregoing discussion indicates that choice of an appropriate experimental model (one based on anticipated environmental exposure conditions or exposure during accidental or deliberate product use) is probably the most important aspect of the design of *in vitro* skin penetration studies for risk assessment and will have a direct impact on the applicability of resultant data for use in environmental contaminants and cosmetic risk assessment. Careful consideration of individual protocol elements will greatly enhance the quality of results, their usefulness in the prediction of skin penetration *in vivo*, and the assessment of risk following actual human exposure.

The selection of finite or infinite dose conditions is an important factor, and as illustrated above, these considerations are chosen for different reasons and provide different information on skin penetration. Experiments performed at infinite doses serve to characterize a compound in terms of steady-state absorption rate, permeability coefficient, and lag time and as such are useful in determining the risks

associated with exposure to environmental water contaminants. The information gathered from infinite dose experiments is especially useful in enabling comparisons between materials for which actual skin penetration data exist and other materials with similar physicochemical properties for which there are no data.

Anticipated human exposure conditions should always dictate the choice of *in vitro* exposure conditions and the interpretation of the data obtained. Thus, for cosmetics and soil-borne contaminants, the skin is normally exposed to small amounts of vehicle. In these cases, finite-dose applications are more relevant to human exposure assessment, especially for those materials that may be present at low levels or as trace contaminants in soil or cosmetic formulations. Typically, such materials will be deposited at low levels on the skin following exposure.

In summary, useful information on the prediction of skin penetration of environmental contaminants and cosmetic ingredients can be obtained from estimates using mathematical models based on physicochemical properties, determined using *in vitro* methods. We have attempted to describe the utility of percutaneous penetration experiments conducted *in vitro* and described some key experimental design considerations. However, even data obtained under *in vitro* finite-dose experimental conditions should be interpreted cautiously. For example, permeant volatility can complicate the conduct and interpretation of such experiments. In normal use, the deposited material is often reduced by mechanical processes (e.g., abrasion by clothing, perspiration, sebum secretion) and normal activities (e.g., washing, bathing, skin cleansing), which are difficult to reproduce using *in vitro* models. Each of these factors should be carefully considered when using the data generated from skin penetration experiments for actual risk assessment purposes.

REFERENCES

Addicks, W.J., Flynn, G.L., Weiner, N., and Chiang, C.-M. (1988). Drug transport from thin applications of topical dosage forms: development of methodology, *Pharmaceutical Research,* 5, 377–382.

Akhter, S.A. and Barry, B.W. (1985). Absorption through human skin of ibuprofen and flurbiprofen: effect of dose variation, deposited drug films, occlusion and the penetration enhancer *N*-methyl-2-pyrrolidone, *Journal of Pharmacy and Pharmacology,* 37, 27–37.

Andrew, A.S., Schned, A.R., Heaney, J.A., and Karagas, M.R. (2004). Bladder cancer risk and personal hair dye use, *International Journal of Cancer,* 109, 581–586.

Anissimov, Y.G. and Roberts, M.S. (1999). Diffusion modeling of percutaneous absorption kinetics: 1. Effects of flow rate, receptor sampling rate, and viable epidermal resistance for a constant donor concentration, *Journal of Pharmaceutical Sciences,* 88, 1201–1209.

Anissimov, Y.G. and Roberts, M.S. (2001). Diffusion modeling of percutaneous absorption kinetics: 2. Finite vehicle volume and solvent deposited solids, *Journal of Pharmaceutical Sciences,* 90, 504–520.

Barlow, S.M., Sullivan, F.M. and Lines, J. (2001). Risk assessment of the use of deltamethrin on bednets for the prevention of malaria, *Food and Chemical Toxicology,* 39, 407–422.

Beck, H., Brain, K., Dressler, W., Grabarz, R., Green, D., Howes, D., Kitchiner, L., Pendlington, R., Python, M., Schroder, K., Sharma, R., Steiling, W., Sugimoto, K., Walters, K., and Watkinson, A. (2000). An interlaboratory/interspecies comparison of percutaneous penetration of ^{14}C-*p*-phenylenediamine (PPD) from a hair dye formulation *in vitro*, in K.R. Brain and K.A.Walters (eds.), *Perspectives in Percutaneous Penetration,* Vol. 7a, Cardiff, U.K.: STS Publishing, p. 27 .

Benech-Kieffer, F., Wegrich, P., and Schaefer, H. (1997). Transepidermal water loss as an integrity test for skin barrier function *in vitro*: assay standardization, in K.R. Brain, V.J. James, and K.A. Walters (eds.), *Perspectives in Percutaneous Penetration,* Vol. 5a, Cardiff, U.K.: STS Publishing p. 56.

Brain, K.R., Brain, S., Green, D.M., Walters, K.A., Watkinson, A.C., Alcasey, S., Blackburn, K., Brock, W., Burdick, J., Davis, D., Dressler, W., Driedger, A., Fung, W., Gettings, S., Mann, S., Re, T., and Rios-Blanco, M. (2002). Penetration and distribution of diethanolamine through human skin *in vitro* after application from cosmetic vehicles under in-use conditions, in K.R. Brain and K.A. Walters (eds.), *Perspectives in Percutaneous Penetration,* Vol. 8a, Cardiff, U.K.: STS Publishing, p. 101.

Brain, K.R., Walters, K.A., James, V.J., Dressler, W.E., Howes, D., Kelling, C.K., Moloney, S.J., and Gettings, S.D. (1995). Percutaneous penetration of dimethylnitrosamine through human skin *in vitro*: application from cosmetic vehicles, *Food and Chemical Toxicology,* 33, 315–322.

Brain, K.R., Walters, K.A., and Watkinson, A.C. (2002). Methods for studying percutaneous absorption, in K.A. Walters (ed.), *Dermatological and Transdermal Formulations*, New York: Dekker, pp. 197–269.

Bronaugh, R.L. and Collier, S.W. (1991). Protocol for *in vitro* percutaneous absorption studies, in R.L. Bronaugh and H.I. Maibach (eds.), In Vitro *Percutaneous Absorption: Principles, Fundamentals, and Applications,* Boca Raton, FL: CRC Press, pp. 237–241.

Bronaugh, R.L., Stewart, R.F., and Simon, M. (1986). Methods for *in vitro* percutaneous absorption studies VII: use of excised human skin, *Journal of Pharmaceutical Sciences,* 75, 1094–1097.

Cnubben, N.H., Elliott, G.R., Hakkert, B.C. Meuling, W.J., and van de Sandt, J.J. (2002). Comparative *in vitro–in vivo* percutaneous absorption of the fungicide ortho-phenylphenol, *Regulatory Toxicology and Pharmacology,* 35, 198–208.

Colombo, G., Zucchi, A., Allegra, F., Colombo, P., Zani, F., and Santi, P. (2003). *In vitro* and *in vivo* study of 5-methoxypsoralen skin concentration after topical application, *Skin Pharmacology and Applied Skin Physiology,* 16, 130–136.

Cross, S.E., Anissimov, Y.G., Magnusson, B.M., and Roberts, M.S. (2003). Bovine-serum-albumin-containing receptor phase better predicts transdermal absorption parameters for lipophilic compounds, *Journal of Investigative Dermatology,* 120, 589–591.

Czene, K., Tiikkaja, S., and Hemminki, K. (2003). Cancer risks in hairdressers: assessment of carcinogenicity of hair dyes and gels, *International Journal of Cancer,* 105, 108–112.

Diembeck, W., Beck, H., Benech-Kieffer, F., Courtellemont, P., Dupuis, J., Lovell, W., Paye, M., Spengler, J., and Steiling, W. (1999). Test guidelines for *in vitro* assessment of dermal absorption and percutaneous penetration of cosmetic ingredients, *Food and Chemical Toxicology,* 37, 191–205.

Dressler, W.E. (1998). Percutaneous absorption of hair dyes, in M.S. Roberts and K.A. Walters (eds.), *Dermal Absorption and Toxicity Assessment*, New York: Dekker, pp. 489–536.

Duff, R.M. and Kissel, J.C. (1996). Effect of soil loading on dermal absorption efficiency from contaminated soils, *Journal of Toxicology and Environmental Health,* 48, 93–106.

European Centre for Ecotoxicology and Toxicology of Chemicals. (1993). *Percutaneous Absorption*, Monograph No. 20, Brussels: European Centre for Ecotoxicology and Toxicology of Chemicals.

Egelrud, T. (2000). Desquamation, in M. Loden and H.I. Maibach (eds.), *Dry Skin and Moisturizers,* Boca Raton, FL: CRC Press, pp. 109–117.

Enviromental Protection Agency. (1992). *Dermal Exposure Assessment: Principles and Applications,* USEPA/600/8-91/011B EPA, Washington, D.C.

Environmental Protection Agency. (2001). *Risk Assessment Guidance for Superfund (RAGS), Volume 1: Human Health Evaluation Manual (Part E, Supplemental Guidance for Dermal Risk Assessment) Interim,* EPA/540/R/99/005. Available at: www.epa.gov/superfund/programs/risk/ragse/index.htm.

Environmental Protection Agency. (2003). *Updated Dermal Exposure Assessment Guidance*, Philadelphia: U.S. Environmental Protection Agency, Region 3. Available at: www.epa.gov/reg3hwmd/risk/dermalag.htm.

Eurofins (2003). RISKOFDERM: Risk assessment for occupational dermalexposure of chemicals. Available at: www.eurofins.com/services/Research_and_Development/occupational_hygiene/riskofderm.asp.

Federal Register. (1996, April 3). Requests for Proposals for Enforceable Consent Agreements; Dermal Absorption Rate Testing of 80 OHSA Chemicals; Solicitation of Interested Parties; Text of Protocol, Vol. 61, No. 65.

Federal Register. (1999, May 21). Sunscreen Drug Products for Over-the-Counter Human Use; Final Monograph, Vol. 64, 27666.

Ferry, J.J., Shepard, J.H., and Szpunar, G.L. (1990). Relationship between contact time of applied dose and percutaneous absorption of minoxidil from a topical solution, *Journal of Pharmaceutical Sciences,* 79, 483–486.

Finlay, A.Y., Marshall, R.J., and Marks, R. (1982). A fluorescent photographic photometric technique to assess stratum corneum turnover rate and barrier function *in vivo*, *British Journal of Dermatology,* 107, 35–42.

Ford, R.A., Hawkins, D.R., Schwarzenbach, R., and Api, A.M. (1999). The systemic exposure to the polycyclic musks, AHTN and HHCB, under conditions of use as fragrance ingredients: evidence of lack of complete absorption from a skin reservoir, *Toxicology Letters,* 111, 133–142.

Franz, T.J. (1978). The finite dose technique as a valid *in vitro* model for the study of percutaneous absorption in man, *Current Problems in Dermatology,* 7, 58–68.

Franz, T.J., Lehman, P.A., Franz, S.F., North-Root, H., Demetrulias, J.L., Kelling, C.K., Moloney, S.J., and Gettings, S.D. (1993). Percutaneous penetration of *N*-nitrosodiethanolamine through human skin (*in vitro*): comparison of finite and infinite dose applications from cosmetic vehicles. *Fundamental and Applied Toxicology,* 21, 213–221.

Gago-Dominguez, M., Castelao, J.E., Yuan, J.M., Yu, M.C., and Ross, R.K. (2001). Use of permanent hair dyes and bladder-cancer risk. *International Journal of Cancer,* 94, 903–906.

Geinoz, S., Guy, R.H., Testa, B., and Carrupt, P.-A. (2004). Quantitative structure–permeation relationships (QSPeRs) to predict skin permeation: a critical evaluation, *Pharmaceutical Research,* 21, 83–92.

Gettings, S.D., Howes, D., and Walters, K.A. (1998). Experimental design considerations and use of *in vitro* skin penetration data in cosmetic risk assessment, in M.S. Roberts and K.A. Walters (eds.), *Dermal Absorption and Toxicity Assessment*, New York: Dekker, pp. 459–487.

Haws, L.C., Jackson, B.A., Turnbull, D., and Dressler, W.E. (1994). Two approaches for assessing human safety of disperse blue 1, *Regulatory Toxicology and Pharmacology,* 19, 80–96.

Hayden, C.G.J., Benson, H.A.E., and Roberts, M.S. (1998). Sunscreens: toxicological aspects, in M.S. Roberts and K.A. Walters (eds.), *Dermal Absorption and Toxicity Assessment*, New York: Dekker, pp. 537–599.

Holly, E.A., Lele, C. and Bracci, P.M. (1998). Hair-color products and risk for non-Hodgkins lymphoma: a population-based study in the San Francisco bay area, *American Journal of Public Health,* 88, 1767–1773.

Holmes, K.K., Shirai, J.H., Richter, K.Y., and Kissel, J.C. (1999). Field measurement of dermal soil loadings in occupational and recreational activities, *Environmental Research,* 80, 148–157.

Hood, H.L., Wickett, R.R., and Bronaugh, R.L. (1996). *In vitro* percutaneous absorption of the fragrance ingredient musk xylol, *Food and Chemical Toxicology,* 34, 483–488.

Howes, D., Guy, R., Hadgraft, J., Heylings, J., Hoeck, F., Maibach, H., Marty, J-P., Merk, H., Parra, J., Rekkas, D., Rondelli, I., Schaefer, H., Täuber, U., and Verbiese, N. (1996). Methods for assessing percutaneous absorption, ECVAM Workshop Report 13, *ALTA,* 24, 81–106.

Howes, D., Watkinson, A.C., and Brain, K.R. (1997). A more complete approach to the modeling of dermal risk assessment, in K.R. Brain, V.J. James, and K.A. Walters (eds.), *Perspectives in Percutaneous Penetration,* Vol. 5b, Cardiff, U.K.: STS Publishing, pp. 68–69.

Kasting, G.B., Filloon, T.G., Francis, W.R., and Meredith, M.P. (1994). Improving the sensitivity of *in vitro* skin penetration experiments, *Pharmaceutical Research,* 11, 1747–1754.

Kirkland, D. and Marzin, D. (2003). An assessment of the genotoxicity of 2-hydroxy-1,4-naphthoquinone, the natural dye ingredient of henna, *Mutation Research,* 537, 183–199.

Kou, J.H., Roy, S.D., Du, J., and Fujiki, J. (1993). Effect of receiver fluid pH on *in vitro* skin flux of weakly ionizable drugs, *Pharmaceutical Research,* 10, 986–990.

Kubota, K. and Yamada, T. (1990). Finite dose percutaneous drug absorption: theory and its application to *in vitro* timolol permeation, *Journal of Pharmaceutical Sciences,* 79, 1015–1019.

La Vecchia, C. and Tavani, A. (1995). Epidemiological evidence on hair dyes and the risk of cancer in humans, *European Journal of Cancer Prevention,* 4, 31–43.

Magnusson, B.M., Anissimov, Y.G., Cross, S.E., and Roberts, M.S. (2004). Molecular size as the main determinant of solute maximum flux across the skin, *Journal of Investigative Dermatology,* 122, 993–999.

Marquart, J., Brouwer, D.H., Gijsbers, J.H., Links, I.H., Warren, N., and van Hemmen, J.J. (2003). Determinants of dermal exposure relevant for exposure modeling in regulatory risk assessment, *Annals of Occupational Hygiene,* 47, 599–607.

McDougal, J.N. and Boeniger, M.F. (2002). Methods for assessing risks of dermal exposures in the workplace, *Critical Reviews in Toxicology,* 32, 291–327.

McDougal, J.N. and Jurgens-Whitehead, J.L. (2001). Short-term dermal absorption and penetration of chemicals from aqueous solutions: theory and experiment, *Risk Analysis,* 21, 719–726.

Navidi, W.C. and Bunge, A.L. (2002). Uncertainty in measurements of dermal absorption of pesticides, *Risk Analysis,* 22, 1175–1182.

Naylor, M.F. and Farmer, K.C. (1997). The case for sunscreens. A review of their use in preventing actinic damage and neoplasia, *Archives of Dermatology,* 133, 1146–1154.

Nohynek, G.J., Fautz, R., Benech-Kieffer, F., and Toutain, H. (2004). Toxicity and human health risk of hair dyes, *Food and Chemical Toxicology,* 42, 517–543.

O'Connor, J., Cage, S., and Fong, L. (2004). *In vitro* skin absorption—can it be used in isolation for risk assessment purposes? In K.R. Brain and K.A. Walters (eds.), *Perspectives in Percutaneous Penetration,* Vol. 9a, Cardiff, U.K.: STS Publishing, p. 92.

Oppl, R., Kalberlah, F., Evans, P.G., and Hemmen, J.J. (2003). A toolkit for dermal risk assessment and management: an overview, *Annals of Occupational Hygiene,* 47, 629–640.

Payan, J.P., Boudry, I., Beydon, D., Fabry, J.P., Grandclaude, M.C., Ferrari, E., and Andre, J.C. (2003). Toxicokinetics and metabolism of *N*-[(14)C]*N*-methyl-2-pyrrolidone in male Spraque-Dawley rats: *in vivo* and *in vitro* percutaneous absorption. *Drug Metabolism and Disposition,* 31, 659–669.

Peck, K.D., Ghanem, A.H., Higuchi, W.I., and Srinivasan, V. (1993). Improved stability of the human epidermal membrane during successive permeability experiments, *International Journal of Pharmaceutics*, 98, 141–147.

Pendlington, R.U., Sanders, D.J., Cooper, K.J., Howes, D., and Lovell, W.W. (1997). The use of sucrose as a standard penetrant in *in vitro* percutaneous penetration experiments, in K.R. Brain, V.J. James, and K.A. Walters (eds.), *Perspectives in Percutaneous Penetration,* Vol. 5a, Cardiff, U.K.: STS Publishing, p. 55.

Phillips, A.M. and Garrod, A.N. (2001). Assessment of dermal exposure—empirical models and indicative distributions, *Applied Occupational and Environmental Hygiene,* 16, 323–328.

Potts, R.O. and Guy, R.H. (1994). Drug transport across the skin and the attainment of steady-state fluxes, *Proceedings of the International Symposium on Controlled Release of Bioactive Materials,* 21, 162–163.

Reddy, M.B., Guy, R.H., and Bunge, A.L. (2000). Does epidermal turnover reduce percutaneous penetration? *Pharmaceutical Research,* 17, 1414–1419.

Riley, W.J., McKone, T.E., and Cohen Hubal, E.A. (2004). Estimating contaminant dose for intermittent dermal contact: model development, testing, and application, *Risk Analysis,* 24, 73–85.

Riviere, J.E., Qiao, G., Baynes, R.E., Brooks, J.D., and Mumtaz, M. (2001). Mixture component effects on the *in vitro* dermal absorption of pentachlorophenol, *Archives of Toxicology,* 75, 329–334.

Roberts, D. and Marks, R. (1980). The determination of regional and age variations in the rate of desquamation: a comparison of four techniques, *Journal of Investigative Dermatology,* 74, 13–16.

Rogers, J.V. and McDougal, J.N. (2002). Improved method for *in vitro* assessment of dermal toxicity for volatile organic chemicals, *Toxicology Letters,* 135, 125–135.

Roper, C.S., Crow, L.F., and Madden, S. (2004). Should we use a barrier integrity test for skin barrier function of human skin in skin penetration studies? In K.R. Brain and K.A. Walters (eds.), *Perspectives in Percutaneous Penetration,* Vol. 9a, Cardiff, U.K.: STS Publishing, p. 69.

Roper, C.S., Howes, D., Blain, P.G., and Williams, F.M. (1997). Percutaneous penetration of 2-phenoxyethanol through rat and human skin, *Food and Chemical Toxicology,* 35, 1009–1016.

Ross, J.H., Driver, J.H., Cochran, R.C., Thongsinthusak, T., and Krieger, R.I. (2001). Could pesticide toxicology studies be more relevant to occupational risk assessment? *Annals of Occupational Hygiene,* 45(Suppl. 1), S5–S17.

Saiyasombati, P. and Kasting, G.B. (2003). Two-stage kinetic analysis of fragrance evaporation and absorption from skin, *International Journal of Cosmetic Science,* 25, 235–243.

Scientific Committee on Cosmetic Products and Non-Food Products. (2000) Annex 10—guidelines for *in vitro* methods to assess percutaneous absorption of cosmetic ingredients, in *Notes of Guidance for Testing of Cosmetic Ingredients for Their Safety Evaluation*, Monograph SCCNFP/1321/00, EC, Brussels, Belgium, pp. 77–85.

Schneider, T., Vermeulen, R., Brouwer, D.H., Cherrie, J.W., Kromhout, H., and Fogh, C.L. (1999). Conceptual model for assessment for dermal exposure. *Occupational and Environmental Medicine*. 56, 765–773.

Schuhmacher-Wolz, U., Kalberlah, F., Oppl, R., and Hemmen, J.J. (2003). A toolkit for dermal risk assessment: toxicological approach for hazard characterization, *Annals of Occupational Hygiene,* 47, 641–652.

Scott, R.C., Carmichael, N.G., Huckles, K.R., Needham, D., and Savage, T. (1993). Methods for measuring dermal penetration of pesticides, *Food and Chemical Toxicology,* 31, 523–529.

Seta, A.H., Higuchi, W.I., Borsadia, S., Behl, C.R., and Malick, A.W. (1992). Physical model approach to understanding finite dose transport and uptake of hydrocortisone in hairless guinea pig skin, *International Journal of Pharmaceutics,* 81, 89–99.

Skelly, J.P., Shah, V.P., Maibach, H.I., Guy, R.H., Wester, R.C., Flynn, G., and Yacobi, A. (1987). FDA and AAPS report of the workshop on principles and practices of *in vitro* percutaneous penetration studies: relevance to bioavailability and bioequivalence. *Pharmaceutical Research,* 4, 265–267.

Southwell, J.D., Barry, B.W., and Woodford, R. (1984). Variations in permeability of human skin within and between specimens, *International Journal of Pharmaceutics,* 18, 299–309.

Steiling, W., Kreutz, J., and Hofer, H. (2001). Percutaneous penetration/dermal absorption of hair dyes *in vitro*. *Toxicology* In Vitro, 15, 565–570.

Stinchcomb, A.L., Valiveti, S., Hammell, D.C., and Ramsey, D.R. (2004). Human skin permeation of Δ^8-tetrahydrocannabinol, cannabidiol and cannabinol, *Journal of Pharmacy and Pharmacology,* 56, 291–297.

Suliman, S.M., Homeida, M., and Aboud, O.I. (1983). Paraphenylenediamine induced acute tubular necrosis following hair dye ingestion, *Human Toxicology,* 2, 633–635.

Tata, S., Flynn, G.L., and Weiner, N.D. (1995). Penetration of minoxidil from ethanol/propylene glycol solutions: effect of application volume and occlusion, *Journal of Pharmaceutical Sciences,* 84, 688–691.

Ting, W.W., Vest, C.D., and Sontheimer, R. (2003). Practical and experimental consideration of sun protection in dermatology, *International Journal of Dermatology,* 42, 505–513.

van de Sandt, J.J.M. (2004). *In vitro* predictions of skin absorption: robustness and critical factors, in K.R. Brain and K.A. Walters (eds.), *Perspectives in Percutaneous Penetration,* Vol. 9a, Cardiff, U.K:. STS Publishing, p. 7.

van de Sandt, J.J., Meuling, W.J., Elliott, G.R., Cnubben, N.H., and Hakkert, B.C. (2000). Comparative *in vitro–in vivo* percutaneous absorption of the pesticide propoxur, *Toxicological Sciences,* 58, 15–22.

van Ravenzwaay, B. and Leibold, E. (2004). The significance of *in vitro* rat skin absorption studies to human risk assessment, *Toxicology* In Vitro, 18, 219–225.

Walker, J.D., Whittaker, C., and McDougal, J.N. (1996). Role of the TSCA interagency testing committee in meeting the U.S. government data needs: designating chemicals for percutaneous absorption rate testing, in F.N. Marzulli and H.I. Maibach (eds.), *Dermatotoxicology*, 5th ed., Washington, D.C.: Taylor and Francis, pp. 371–381.

Walker, M., Chambers, L.A., Holingsbee, D.A., and Hadgraft, J. (1991). Significance of vehicle thickness to skin penetration of halcinonide, *International Journal of Pharmaceutics,* 70, 167–172.

Walters, K.A., Brain, K.R., Howes, D., James, V.J., Kraus, A.L., Teetsel, N.M., Toulon, M., Watkinson, A.C., and Gettings, S.D. (1997). Percutaneous penetration of octyl salicylate from representative sunscreen formulations through human skin *in vitro*. *Food and Chemical Toxicology,* 35, 1219–1225.

Walters, K.A., Brain, K.R., Dressler, W.E., Green, D.M., Howes, D., James, V.J., Kelling, C.K., Watkinson, A.C., and Gettings, S.D. (1997). Percutaneous penetration of *N*-nitroso-*N*-methyldodecylamine through human skin *in vitro*: application from cosmetic vehicles, *Food and Chemical Toxicology,* 35, 705–712.

Walters, K.A., Gettings, S.D., and Roberts, M.S. (1999). Percutaneous absorption of sunscreens, in R.L. Bronaugh and H.I. Maibach (eds.), *Percutaneous Absorption,* 3rd ed., New York: Dekker, pp. 861–877.

Walters, K.A. and Roberts, M.S. (1993). Veterinary applications of skin penetration enhancers, in K.A. Walters and J. Hadgraft (eds.), *Pharmaceutical Skin Penetration Enhancement*, New York: Dekker, pp. 345–364.

Wester, R.C., Hui, X., Hartway, T., Maibach, H.I., Bell, K., Schell, M.J., Northington, D.J., Strong, P., and Culver, B.D. (1998). *In vivo* percutaneous absorption of boric acid, borax, and disodium octaborate tetrahydrate in humans compared to *in vitro* absorption in human skin from infinite and finite doses, *Toxicological Sciences,* 45, 42–51.

Wester, R.C. and Maibach, H.I. (1999). Dermal decontamination and percutaneous absorption, in R.L. Bronaugh and H.I. Maibach (eds.), *Percutaneous Absorption,* 3rd ed., New York: Dekker, pp. 241–254.

Wester, R.C., Maibach, H.I., Melendres, J., Sedik, L., Knaak, J., and Wang, R. (1992). *In vivo* and *in vitro* percutaneous absorption and skin evaporation of isofenphos in man, *Fundamental and Applied Toxicology,* 19, 521–526.

Williams, A.C., Cornwell, P.A., and Barry, B.W. (1992). On the non-Gaussian distribution of human skin permeabilities, *International Journal of Pharmaceutics,* 86, 69–77.

Yourick, J.J. and Bronaugh, R.L. (1999). Percutaneous penetration as it relates to the safety evaluation of cosmetic ingredients, in R.L. Bronaugh and H.I. Maibach (eds.), *Percutaneous Absorption,* 3rd ed., New York: Dekker, pp. 659–671.

Yourick, J.J. and Bronaugh, R.L. (2000). Percutaneous penetration and metabolism of 2-nitro-*p*-phenylenediamine in human and fuzzy rat skin, *Toxicology and Applied Pharmacology,* 166, 13–23.

Yourick, J.J., Koenig, M.L., Yourick, D.L., and Bronaugh, R.L. (2004). Fate of chemicals in skin after dermal application: does the *in vitro* skin reservoir affect the estimate of systemic absorption? *Toxicology and Applied Pharmacology,* 195, 309–320.

Zobrist, R.H., Quan, D., Thomas, H.M., Stanworth, S., and Sanders, S.W. (2003). Pharmacokinetics and metabolism of transdermal oxybutynin: *in vitro* and *in vivo* performance of a novel delivery system, *Pharmaceutical Research,* 20, 103–109.

CHAPTER 9

Gulf War Syndrome: Risk Assessment Case Study

Ronald E. Baynes

CONTENTS

INTRODUCTION

Veterans of the Persian Gulf War in 1991 were diagnosed with a variety of illnesses following their return to their homeland. This poorly defined syndrome was associated not only with 10% of U.S. veterans (80,000), but also with soldiers from other allied nations who participated in the conflict. Although the etiology of the illness has been difficult to confirm, recent independent research has led scientists to consider that the syndrome may be associated with exposure to chemical or microbiological agents during the Persian Gulf War conflict. The purpose of this chapter is to assess the dermal absorption of the several chemical agents (e.g., pesticides) veterans were exposed to during the Persian Gulf War. The data described in this assessment were generated from experimental topical application of relevant mix-

tures to an isolated porcine skin flap model. This validated skin model (Wester et al., 1998) not only allows for mimicking topical exposure in Gulf War veterans, but also arterial infusion of drugs to mimic blood levels of drugs that the veterans were self-medicating with during the conflict.

The reader should also be aware that the soldier's skin was in most cases exposed either simultaneously or sequentially to more than one chemical. Veterans were also exposed to petroleum byproducts such as polyaromatic hydrocarbons (such as benzo[a]pyrene) and heavy metals during the burning of oil fields in Kuwait (Madany and Raveendran, 1992). This complicates any toxicological risk assessment exercise as little is known about how these various classes of hazardous chemicals influence the dermal absorption of each other.

EXPOSURE ASSESSMENT OF RELEVANT CHEMICALS

Pesticide Exposure

Recent reports (Abou-Donia et al., 1996; Petersdorf et al., 1996) have confirmed that soldiers may have been exposed to one or more of the pesticides listed in Table 9.1 via the dermal route. The Federal Supply System and the Armed Forces Pest Management Board identified a total of 21 different major pesticides used by U.S. forces during Operations Desert Shield and Storm (Fricker et al., 2000). Table 9.1 provides a list of several of these pesticides selected from five pyrethroids, five organophosphates, four carbamates, one insect repellent, and one organochlorine; the remaining pesticides were rodenticides.

Some veterans were exposed to these pesticides by intentional application, but because many exposures were accidental, it has been difficult to assess pesticide exposure accurately and therefore a topical dose in exposed veterans. Permethrin was intentionally impregnated into the soldier's uniform fabric at a concentration of 0.125 mg/cm^2 to help control insect infestation while in the dessert. This pyrethroid insecticide consists of four different isomers (Figure 9.1), with the *cis* isomer more toxic than the *trans* isomer. Permethrin is a large molecule (MW = 391.3) and has a log octanol–water partition coefficient of 6.5, which suggests that it could readily partition from the uniform into the lipophilic stratum corneum layer of the soldier's skin. With a transfer rate of 0.49% per day of permethrin from the fabric to skin, the daily dose was estimated to be 6.8×10^{-5} mg/kg/day (National Research Council

Table 9.1 List of Major Pesticides to Which Veterans Were Potentially Exposed via the Skin

Pyrethrins	Organophosphates	Carbamates	Repellents
Allethrin/resmethrin	Azamethiphos	Bendiocarb	DEET
Cypermethrin	Chlorpyrifos	Carbaryl	
d-Phenothrin	Diazinon	Methomyl	
Pyrethrin	Dichlorvos	Propoxur	
Permethrin	Malathion		

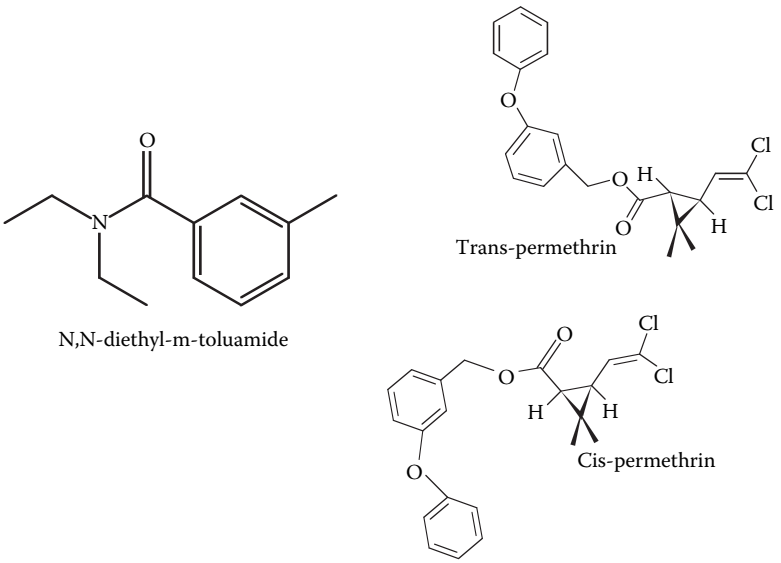

Figure 9.1 Chemical structures for DEET and permethrin.

[NRC], 1994). However, as is fully described in subsequent paragraphs, this large molecule does not readily penetrate into the skin or is taken up into the bloodstream to result in systemic toxicity. Permethrin has a large oral median lethal dose (LD_{50}) in female rats of 3801 mg/kg and dermal LD_{50} above 5000 mg/kg in rabbits (U.S. Environmental Protection Agency [EPA], 1986), demonstrating that it is a relatively safe pesticide by oral and dermal routes. The regulatory status of permethrin indicates that it is a moderately to practically nontoxic pesticide in American EPA toxicity class II or III, depending on the formulation. There is significant evidence of its safety, as demonstrated by the fact that permethrin is often the active ingredient in antilice formulations used to treat scalp lice in children. We know that the skin in children tends to be thinner than that of the adult; therefore, its approval for use as a medication in such a sensitive subpopulation further supports the general lack of concern if humans are exposed to this pesticide by the dermal route.

Veterans also intentionally applied liberal amounts of the insect repellent DEET (*N,N*-diethyl-*m*-toluamide) to their skin surface. This repellent can cause acute severe neurotoxicity when applied in such large quantities. Compared to permethrin, DEET is a smaller molecule (MW = 191.27) and a smaller log octanol–water partition coefficient of 1.69. These features tend to favor significantly greater transdermal flux of DEET (63.2 $\mu g/cm^2/h$) (Ross and Shah, 2000). The oral LD_{50} in rats is 2170 to 3664 mg/kg; its dermal LD_{50} is 5000 mg/kg in the same species, and it is in toxicity category III (U.S. EPA, 1998).

During their deployment, veterans were exposed to a variety of organophosphate insecticides to protect them against insect-borne diseases. Although these exposures were primarily limited to surroundings and not directly applied to the skin, there

was some concern that accidental exposure, especially to chlorpyrifos, was not uncommon. However, there is limited information about veteran's exposure levels, and these chemicals are not addressed in this chapter.

Chemical Warfare Agents

The two major classes of chemical warfare agents include mustard and the nerve agent sarin (Reuter, 1999). The fact that these chemicals can be harmful via any route of exposure at low doses makes them effective chemical warfare agents. The nerve agents are all fluorine- or cyanide-containing organophosphates, but they can be as much as 10^3 to 10^4 times more potent than the most potent commercially available organophosphate. Late in fall 1991, the Department of Defense (DoD) concluded that it was likely that U.S. soldiers had unknowingly destroyed sarin- and cyclosarin-filled rockets in a March 1991 demolition at Khamisiyah, Iraq (Feussner, 2001). This demolition resulted in smoke plumes that drifted several miles to where military personnel were most likely exposed to low levels of chemical warfare agents via dermal or inhalation routes. On the basis of exposure modeling performed thus far, the degree of exposure of U.S. troops located within the path of the sarin plume is believed to be quite low over a period of several hours (Central Intelligence Agency [CIA] and DoD, 1997). Although no acute cholinergic effects were reported by the 20,000 troops within the 50-km radius, low-level exposures could have occurred with no health effects. Unfortunately, the well-known terrorist attack in Matsumoto, Japan in 1994 with sarin vapor at intermediate to high levels resulted in 600 people developing acute symptoms, and 7 people dying (Morita et al., 1995). The release of diluted sarin vapor in the Tokyo subway system a year later by terrorists resulted in 1000 symptomatic people, 12 of whom subsequently died (Woodall, 1997).

Mustard is the classical vessicant/skin-blistering agent that was first used by the Germans in World War I and more recently by the Iraqis during the Iraq–Iran war. This alkylating agent interacts with cellular deoxyribonucleic acid (DNA) and can result in classical skin lesions such as blisters (Monteiro-Riviere and Inman, 1997); it is also known to cause cancer (Heston, 1950). Mustard is fat soluble, which means that it readily absorbs across most membranes, including skin (Riviere et al., 1995). Although there is limited evidence that veterans were exposed to sulfur mustard during the Persian Gulf War conflict, there are still a significant number of veterans who believed they were exposed to mustard (Stuart et al., 2003). Therefore, for this reason and the possibility that service men and women could be exposed to this agent in future conflicts warrants that sulfur mustard be included in mixture studies of chemicals relevant to the Gulf War exposure scenario.

Prophylactic Agents and Other Medications

Veterans were also exposed to a variety of over-the-counter (for example, nonsteroidal antiinflammatory drugs [NSAIDS]) and prescription drugs (such as antibiotics), vaccines, and a prophylactic, pyridostigmine bromide (PB) for nerve agent exposure. Although many of these drugs were administered orally and not topically, their presence in the bloodstream could have a significant effect on the dermal

absorption of the hazardous chemicals previously described. PB is not really a nerve agent antidote but rather a pretreatment medication that binds reversibly to acetylcholinesterase, thus preventing irreversible binding of nerve agents such as sarin. PB has a quaternary amine structure that makes it almost impossible for PB molecules to cross the blood–brain barrier and cause central nervous system (CNS) effects. When a military commander determined that nerve agents were a threat, service members took a 30-mg tablet every 8 h for a maximum of 14 days (Keller et al., 1991). Because compliance was believed to be greater than 99% among service personnel, PB exposure can be accurately assessed for Gulf War veterans. A population pharmacokinetics-pharmacodynamics study of 60 individuals, however, determined that PB kinetics was weight and gender dependent (Marino et al., 1998). Average peak plasma concentration was 25 ng/ml and could be as high as 50 ng/ml. Interestingly, a mean plasma concentration of 7.7 ng/ml was needed to obtain 10% inhibition of acetylcholinesterase activity; therefore, the mean level of inhibition was greater than 10% throughout the study. However, 30% of the individuals were below this 10% level during trough time, demonstrating population variability.

Jet Fuels

Gulf War veterans were exposed to military jet fuels JP-8 or JP-8(100) in their working or living environment. During the refueling and maintenance of military aircraft, veterans were exposed by inhalation and dermal routes to these fuels, which are really complex mixtures of aliphatic and aromatic hydrocarbons and performance additives unique to military jet fuels (Zeiger and Smith, 1998). The aliphatic component makes up 80–90% of the jet fuel mixture, and the aromatic component makes up about 17%. These fuels are known to primarily cause irritant dermatitis (Monteiro-Riviere et al., 2001, 2004) and significant neurological effect (Pliel et al., 2000) and can also cause immune, hepatic, and respiratory effects (Harris et al., 2000; Robledo et al., 2000). Recent estimates of dermal exposure to jet fuels suggested that service personnel exposure could result in significantly less hydrocarbon absorption than if exposure was by inhalation (McDougal et al., 2000). However, it is difficult to compare routes as more of the volatile fraction of jet fuels is available for systemic absorption via inhalation than via the dermal route. The skin also has the potential to retain more of the nonvolatile fraction, such as aliphatic hydrocarbons (Riviere et al., 1999; Baynes et al., 2001), which is believed to be primarily responsible for the occupational irritant dermatitis observed in service personnel working around military aircraft (Chou et al., 2002).

PERMETHRIN ABSORPTION FOLLOWING SINGLE CHEMICAL AND MIXTURE EXPOSURE

The molecular weight and structure of permethrin suggest limited dermal absorption. However, dermal absorption studies with rodent skin demonstrated significant dermal absorption of permethrin. For example, the literature reported as much 63.8% absorption in 8 h in mice *in vivo* (Shah et al., 1981) and 49 to 57% in 72 h in rats (Shah et al.,

1987a). *In vivo* studies in rhesus monkeys have demonstrated 14 to 28% absorption of *cis* and *trans* isomers in the forehead and 5 to 12% of both isomers in the forearm (Sidon et al., 1988). It should be noted that many of these studies measured radioactivity in excretory biological samples and therefore did not differentiate between permethrin and its metabolites. This argument has been supported by *in vitro* and *ex vivo* studies, which demonstrated that absorption in perfused rabbit, human, and pig skin was less than 2% (Franz et al., 1996; Bast and Kampffmeyer, 1996; Baynes et al., 1997).

These data are consistent with why there is minimal concern about dermal exposure to permethrin and why its has such widespread agronomic use as well as common application to children's scalps for lice treatment. Therefore, there was little or no concern about causing permethrin toxicity in soldiers who wore permethrin-impregnated military uniforms. Application of fabric impregnated with permethrin to the backs of rabbits resulted in a 3.2% migration to the skin surface, with 2% of the impregnant being absorbed and 1.2% remaining on the skin surface after 7 days of continuous skin contact (Snodgrass, 1992).

Permethrin absorption could have been influenced by the presence of other additives present in any given pesticide formulation and any other chemical that may have been present on the skin of the veterans before or after they dressed with the permethrin-impregnated uniforms. Commercial pesticides are often formulated with several important performance additives, such as surfactants and solvent vehicles (Seaman, 1990), and the effect of these formulation additives on pesticide absorption has been reported in our laboratory (Baynes and Riviere, 1998).

However, in the Persian Gulf theater, these mixture interactions may have been more important for exposures to chlorpyrifos and other pesticides that were applied to premises and encampments as a liquid formulation rather than permethrin, which was impregnated in the service men's uniforms. In the absence of formulation additives, the only other factors that would have influenced permethrin absorption in skin would have been dermal occlusion associated with the wearing of uniforms or environmental conditions in the desert during the conflict. Although little is known about occlusive effects of the service men and women's uniforms on permethrin absorption, it has been demonstrated that fabric occlusion does not alter permethrin disposition, but complete occlusion with cellophane can significantly increase permethrin absorption by two- to fourfold (Riviere et al., 2002).

Unfortunately, the skin of many service men and women wearing these permethrin-impregnated uniforms was exposed simultaneously to the insect repellent DEET and accidentally to jet fuel splashes and possibly a nerve agent. DEET was originally thought to enhance the dermal absorption of drugs and pesticides by acting as a cosolvent (Windheuser et al., 1982). For example, DEET can significantly increase 2,4-dichlorophenoxyacetic acid (2,4-D) absorption and significantly decrease lag time (Pont et al., 2004). However, my laboratory and others have recently discovered that the complete unexpected and opposite effect can occur with simultaneous exposure to insecticides and repellent (Baynes and Riviere, 1998; Baynes et al., 1997; Moody et al., 1987; Baynes et al., 2002). These studies described significant inhibition of representative carbamate, organophosphate, and pyrethroid absorption in the presence of DEET (Figure 9.2). It is safe to assume that the presence

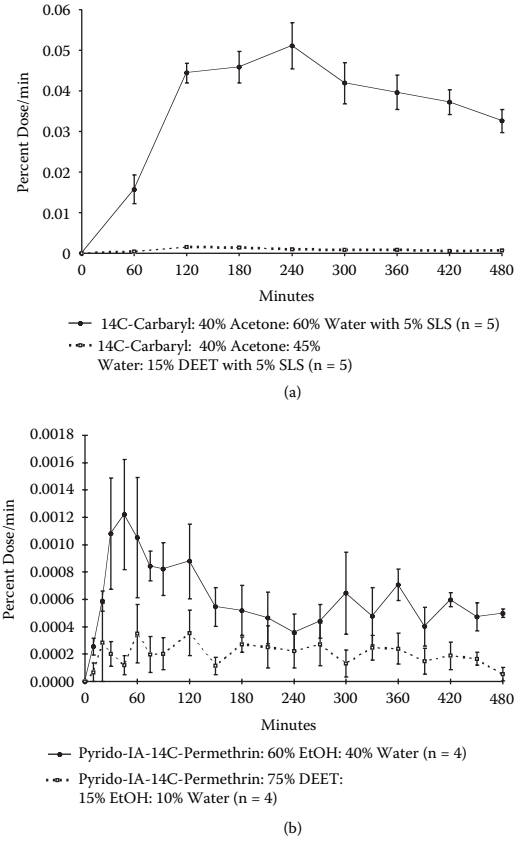

Figure 9.2 Inhibiting effects of DEET on the dermal absorption of (a) carbaryl and (b) permethrin.

of DEET in these topical mixtures effectively reduced the log stratum corneum–vehicle partition coefficient, leading to retention of permethrin in the vehicle or surface compartment of the exposed skin.

However, be aware that, in spite of these surface effects, DEET enhanced permethrin depot formation in fat as well as the skin surface. Further stratum corneum partitioning studies demonstrated that permethrin was least likely to partition into the stratum corneum when DEET was present. These observations are unique in that DEET readily diffuses into the skin, and in spite of it small molecular weight of 191.3 and log octanol–water partition coefficient of 1.69, it has the capacity to retain pesticide levels in the skin layers. Although DEET may enhance this retention of pesticides in the skin layers and probably preclude acute toxicoses, this skin depot is available for dermal absorption albeit by a slow diffusion process across the skin.

In a similar series of experiments, our laboratory demonstrated that topical exposure to a nerve agent stimulant, diisopropyl fluorophosphate (DFP), more than doubled permethrin absorption (Baynes et al., 2002). This significant effect on

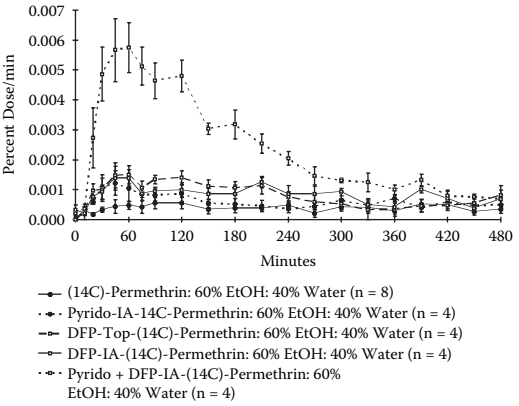

Figure 9.3 Influence of topical DFP, intra-arterial pyridostigmine (Pyrido), or both permethrin absorption in aqueous mixtures.

permethrin absorption (Figure 9.3) occurred irrespective of whether these were aqueous or nonaqueous mixtures applied to the skin surface.

The mechanism behind this enhanced effect on dermal absorption is at the moment difficult to dissect as DFP does not alter stratum corneum lipids or proteins (Potts et al., 1989). In an effort to simulate the effects of systemic DFP on permethrin absorption, the skin flap model was perfused with subtoxic doses of DFP; again, the data strongly suggested that if a nerve agent is present in the bloodstream, then this can also lead to enhanced permethrin absorption (Baynes et al., 2002). It is quite possible that nerve agents such as DFP and sarin increase acetylcholine levels in the skin by binding to acetylcholinesterases. As a consequence, the many muscarinic receptors in neuronal and nonneuronal cells in the skin (Grando et al., 1993; Haberberger and Bodenbenner, 2000) will respond to increased acetylcholine levels and result in smooth muscle relaxation in the skin microvasculature and vasodilation. Theoretically, increased skin vasodilation should increase solute transport across skin; however, there are numerous shunts in the skin microvasculature that, on vasodilation, will not necessarily increase but decrease blood flow (Riviere and Williams, 1992). My laboratory demonstrated similar DFP effects in Bronaugh's *in vitro* flow-through diffusion cell system, which utilizes skin sections lacking an intact microvasculature. These observations may not be sufficient evidence to totally rule out DFP interactions with muscarinic receptors in the microvasculature, but they strongly support a DFP-induced biochemical alteration in keratinocytes that increased solute permeability.

Service men and women working on the flight line in the U.S. Air Force were exposed daily to the military jet fuel JP-8. My recently concluded studies with Riviere et al. (2002) demonstrated that JP-8 significantly increased permethrin absorption in skin by twofold and skin penetration by threefold. This dermal enhancer effect of JP-8 is not surprising as these jet fuels contain aliphatic and aromatic components as well as performance additives that by themselves or as a mixture can alter dermal permeability. In separate studies, JP-8 fuel additives were

observed to interact synergistically to increase or decrease dermal absorption and dermal deposition of aliphatic and aromatic components of jet fuel (Baynes et al., 2000; Baynes, 2001). These additives in military jet fuel perform as icing inhibitors (for example, diethylene glycol monomethyl ether [DIEGME]), antistatic compounds for conductivity (for example, Octel's Stadis450), and corrosive inhibitors (such as 8Q21) (White, 1999). However, the physicochemical properties of these additives suggest that they could influence permethrin absorption as we observed additive effects on the dermal absorption of aliphatic and aromatic components of jet fuel. What is not clear from these studies is whether the additives or the aromatic and aliphatic components played a major role in enhanced permethrin absorption or whether there was a synergistic interaction here as well.

Beyond the pure physicochemical interactions described, there is increasing evidence that jet fuels themselves can alter skin structure, and it is probably by this additional mechanism that may be associated with increased dermal absorption of permethrin. These chemical-induced modifications in skin structure have been demonstrated by increased transepidermal water loss and significant dermatotoxicity at the macroscopic and molecular levels in skin (Monteiro-Riviere et al., 2001, 2004; McDougal and Rogers, 2004). It is therefore no surprise that chronic exposure to these mixtures of solvents can enhance jet fuel hydrocarbon absorption (Muhammad et al., 2004). This is characteristic for chronic dermal exposures to solvents and strongly suggests that military personnel are more likely to absorb hazardous chemicals across their skin if they are chronically exposed to jet fuels or solvent-related chemicals.

Finally, service men and women were simultaneously taking oral doses of PB when there was imminent threat of nerve agent attack. Previous rodent studies demonstrated that PB can reduce permethrin uptake into the CNS by as much as 30% (Buchholz et al., 1997). Surprisingly, the presence of this prophylactic agent in either the porcine skin flap perfusate or porcine skin diffusion cell perfusate significantly increased permethrin absorption by as much as 1.36- to 3.82-fold (Baynes et al., 2002). When the porcine skin flap was then perfused with a mixture of PB plus DFP to mimic simultaneous nerve agent and prophylactic exposure, permethrin absorption was significantly increased 6-fold (Figure 9.3). This significant PB- or PB plus DFP-induced modulation of permethrin absorption in skin could be related to changes in membrane integrity in the vascular endothelium as well as epidermal corneocytes. Other investigators have demonstrated that PB or nerve agents can increase blood–brain barrier permeability (Abou-Donia et al., 2001; Grauer et al., 2001). In essence, the presence of PB or DFP in the skin microvasculature most likely resulted in local or keratinocyte cytotoxicity (Monteiro et al., 2003), although it is possible that these chemicals could have altered the neurohumoral pathway in skin. Its also possible for DFP to act as a metabolic (esterase) inhibitor in skin and thereby increase parent drug absorption, as demonstrated in rat skin (Bando et al., 1997). However, our study did not demonstrate this interaction with permethrin in porcine skin.

It was, however, surprising that the skin-blistering agent sulfur mustard decreased dermal absorption and penetration of permethrin (Riviere et al., 2002). It is safe to assume that this interaction is based on the disposition of sulfur mustard in skin and

its ability to alter normal anatomy and physiology of skin. Sulfur mustard is rapidly absorbed across the skin within 1 h, and a significant proportion of the dose is readily evaporated from the skin surface (Riviere et al., 1995). Sulfur mustard causes severe cutaneous injury, as characterized by epidermal–dermal separation (King and Monteiro-Riviere, 1990). My laboratory and others have utilized *in vivo* and *ex vivo* skin models to demonstrate sulfur mustard-induced microvesicles or gross blisters in a dose dependent response (Zhang et al., 1995); numerous other *in vitro* studies have demonstrated sulfur mustard-induced cytotoxicity in epidermal cells (Ray et al., 1990). Although these cellular changes would suggest increased solute permeability, it clearly does not apply to permethrin; however, it may be applied to solutes that are more water soluble (such as DEET), which are able to diffuse across the blister space. It is also possible that the blisters interrupt solute diffusion into the microcapillaries. It is also possible that sulfur mustard may have reacted directly with permethrin, thereby reducing its permeability (Riviere et al., 2002).

DEET ABSORPTION FOLLOWING SINGLE CHEMICAL AND MIXTURE EXPOSURE

Compared to permethrin, the molecular weight and lipophilicty of DEET suggest that it should be more readily absorbed across skin. This repellent is more readily absorbed across rodent skin than either porcine or human skin. About 6% of a topical dose of commercially formulated DEET (15% in ethanol) was absorbed across human skin within 8 h (Selim et al., 1995). Our laboratory also reported about 3% dose absorption in porcine skin within this same time period; however, absorption in mice skin ranged from 10 to 21% of the dose (Baynes et al., 1997). These data highlight the potential problem of overestimating the risk of DEET in humans if rodent data are used in dermal risk assessment.

There are limited reports of chemical mixture effects on DEET absorption across skin. A recent publication suggested that the formulation additives in various sunscreen products may significantly enhance DEET absorption (Ross et al., 2004). The authors also noted that one of these preparations indicated safe pediatric use. Formulation additives can also reduce DEET permeation in skin simply by altering the skin–vehicle partition coefficient (Ross and Shah, 2000). In this study, the solvents ethanol and propylene glycol increased solubilization of DEET in the vehicle and resulted in DEET preferring to remain in the vehicle than diffuse into skin, thus reducing skin permeation.

These thermodynamic interactions are operative when one considers which other solutes the Gulf War veterans were exposed to while administering DEET topically as an insect repellent. My laboratory reported that coexposure to low-level sulfur mustard, PB, and the nerve agent DFP significantly modulated the dermal absorption of DEET in porcine skin flaps (Riviere et al., 2003). Arterial infusion with PB or DFP resulted in minimal and insignificant increase in DEET absorption, but when they were combined, they produced a 2.24-fold increase in DEET absorption. It is also worth noting that sulfur mustard significantly increased DEET absorption almost 2-fold when the porcine skin flaps were not infused with PB (Figure 9.4). Stated

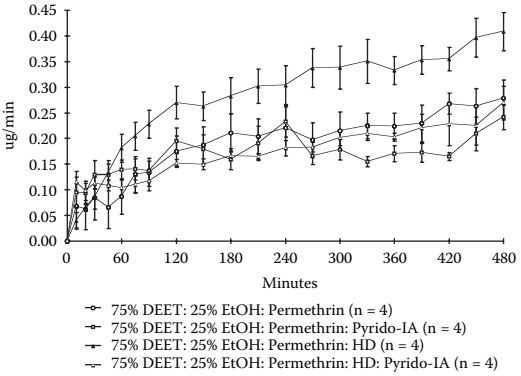

Figure 9.4 The influence of topical sulfur mustard (HD) and intra-arterial pyridostigmine infusion on DEET absorption.

differently, the presence of the nerve agent prophylactic (PB) could significantly reduce DEET absorption in skin exposed to a vesicating agent such as sulfur mustard. These two observations strongly suggest that the presence of prophylactic drugs or toxic agents in the cutaneous circulation could significantly influence DEET absorption in the skin of soldiers similarly exposed. Recall that sulfur mustard had the opposite effects on permethrin absorption, but it was not clear whether PB played a significant role on permethrin absorption when sulfur mustard was simultaneously applied to the skin.

Assuming that significant levels of permethrin were transferred from the military uniform to the skin, this insecticide did not appear to influence DEET absorption in the porcine skin flaps but appeared to blunt DEET absorption in porcine skin sections and silastic membranes. This blunting effect apparently occurred on the skin surface or stratum corneum as it was also observed in silastic membranes. It is quite conceivable that this physicochemical interaction on the skin surface had to have been overcome by the diffusion of DFP or PB from the cutaneous capillaries for these agents to enhance DEET penetration from the surface.

In an attempt to determine whether skin hydration or moisture levels on the skin had an impact on DEET absorption under the above conditions, water was added to the formulations or occluded the exposed skin surface after topical exposure. Reducing the ethanol concentration in the topical formulation from 25 and 15% by adding water had no significant effect on DEET absorption in porcine skin flaps. Not surprisingly, complete surface and fabric occlusion increased its DEET absorption to almost threefold when the skin was exposed to all of the above mixture components.

These studies also determined that these various exposure conditions resulted in a wide range of DEET absorption (13 to 68 $\mu g/cm^2$) within 8 h of dermal exposure. It should be noted that DEET absorption ranged from 13 to 16 $\mu g/cm^2$ irrespective of whether it is either 7.5 or 75% DEET in a binary ethanol mixture. In effect, DEET transdermal flux is a zero-order kinetic process with a flux of 2.0 $\mu g/cm^2/h$. This transdermal flux was also observed in human skin exposed to either neat or 15% DEET (Selim et al., 1995) and demonstrates that DEET flux is saturated

through *in vivo* skin. In effect, human exposure to increasing levels of DEET will not significantly increase transdermal flux but rather the observed synergistic interactions with the mixtures described above that can significantly increase DEET flux and ultimately systemic levels of DEET in the body.

CONCLUSION

The question that often arises from these series of dermal absorption studies is whether there is sufficient dermal absorption of permethrin, DEET, nerve agent, vessicant, or jet fuels to have adverse health effect on service people in the Persian Gulf theater. Nerve agents and vessicants require only small-dose exposures to cause severe adverse effects, including death. Although chemical mixtures could modulate the dermal absorption of these highly toxic agents, this may not translate into significant change in health effects as only a small dose is required to produce an adverse outcome. Jet fuels can cause local dermatological effects as has been well documented in the literature. However, there have been limited studies that have assessed the systemic toxicity of military jet fuels following dermal exposure. The limited available studies suggest that dermal exposure to military jet fuels will not cause any adverse systemic toxicity. McDougal et al. (2000) further determined from *in vitro* dermal absorption studies that human hands will have to be exposed for about 20 min on a daily basis for there to be significant absorption of these components that will result in systemic adverse effects.

The primary focus of this chapter was to demonstrate that chemical mixtures can influence the dermal disposition of permethrin and DEET, which were frequently used in the Persian Gulf War and were deemed relatively nontoxic. However, DEET and permethrin can potentially cause adverse effects if significant levels are absorbed across the skin into the bloodstream. The no-observed-adverse-effect-level (NOAEL) for permethrin is 5 mg/kg/day and the maximum permitted intake (MPI) of 3.0 mg/day for a 60-kg person is based on hepatic effects in laboratory animals following chronic feeding studies (U.S. EPA, 1986). The daily dose from military uniform transfer to a soldier's skin was estimated to be 6.8×10^{-5} mg/kg/day, and it is clear that this dermal daily dose should not result in significant health effects. This assessment is based on the assumption that dermal bioavailability (<2%) is significantly less than oral bioavailability (~70%) and a reference dose (RfD) of 5.0×10^{-2} mg/kg/day, which is significantly greater than the estimated dermal dose in veterans wearing permethrin-impregnated uniforms. The RfD was based on above NOAEL from chronic toxicity studies and a safety factor of 100. This assessment will also be true if one considers the enhancement effect (one- to sixfold) associated with mixture interactions summarized in Figure 9.5.

The studies described in this chapter clearly demonstrated that dermal absorption of DEET and permethrin can be significantly increased in soldiers if they were simultaneously exposed to other topical agents or had other chemicals in the blood vessels supplying blood to the skin. The enhancing effects of PB, DFP, and PB plus DFP on permethrin absorption as summarized in Figure 9.5 were surprising observations, although the mechanism of enhanced absorption may be associated with

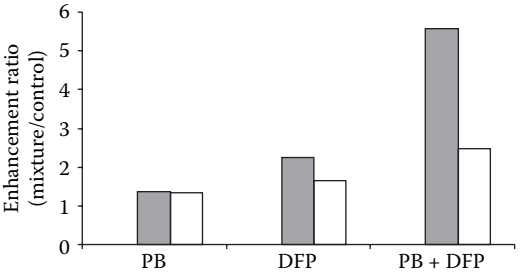

Figure 9.5 The dermal enhancement effects of pyridostigmine bromide (PB), DFP, or both on the absorption of permethrin in aqueous and nonaqueous mixtures.

known anticholinesterase activity (Baynes et al., 2002). It is difficult to assess at this stage whether these mixture effects could have resulted in sufficiently high enough blood concentrations to result in acute DEET- or permethrin-induced effects in the nervous system.

DEET, in particular, is a major concern because it has caused acute severe neurological symptoms and even death in humans following topical exposure. A NOAEL of 100 mg/kg/day (RfD = 1 mg/kg/day) was determined by the U.S. EPA (1998) and was based on systemic effects in female rats following a 2-year chronic study. Although the oral RfD of DEET is greater than the oral RfD of permethrin, it does not follow that humans can be exposed to larger doses of DEET by any route without effect. As indicated earlier, the rate and extent of DEET transport across human skin will be significantly greater than that for permethrin and consequently sufficiently high blood concentrations to cause an acute DEET-related toxicosis than a permethrin-related toxicity. On the other hand, the reader needs to be aware that permethrin is more likely than DEET to reside in the stratum corneum because of its significantly greater octanol–water partition coefficients (6.5 vs. 1.7) and then be absorbed into the bloodstream at later time points. This stratum corneum persistence supports the local dermal irritant effects that have been sporadically reported in the literature (McKillop et al., 1987; Dorman and Beasley, 1991).

In environmental conditions similar to those experienced by the soldiers in the Iraqi desert, the skin will be exposed to a variety of topical formulations that are not considered hazardous to human health. For example, the active ingredients in sunscreens not only influence DEET absorption but also can influence the herbicide 2,4-D (Pont et al., 2004) and probably numerous other hazardous materials not described in this chapter or listed by the U.S. military as being present in the Persian Gulf War theater of operation. In essence, the complex nature of this exposure scenario during this conflict could also reflect occupational exposure in agricultural or industrial settings. For this reason, the lessons learned from these exposures could be applicable to related exposures in civilian life as well as future conflicts. That is, a multifold increase in dermal absorption can occur with chemical mixtures irrespective of whether they are applied topically or systemically. Further research is required to (1) understand the underlying mechanism(s) enhancing chemical absorption in skin following systemic exposure and (2) determine whether these mixture effects can be predicted from known mechanistic interactions.

REFERENCES

Abou-Donia, M.B., Khan, W.A., Suliman, H.B., and Abdel-Rehman, A.A. (2001). Sarin-induced increase in blood–brain barrier (BBB) permeability is augmented by coexposure with stress, pyridostigmine bromide (PB), DEET, and permethrin in rats, *Conference on Illness Among Gulf War Veterans: A Decade of Scientific Research*, Alexandria, VA, January 24–26, 2001, p. 140.

Abou-Donia, M.B., Wilmarth, K.R., Jensen, K.F., Oehme, F.W., and Kurt, T.L. (1996). Neurotoxicity resulting from coexposure to pyridostigmine bromide, DEET, and permethrin, *J. Toxicol. Environ. Health*, 48, 35–56.

Bando, H., Mohri, S., Yamashita, F., Takakura, Y., and Hashida, M.J. (1997). Effects of skin metabolism on percutaneous penetration of lipophilic drugs, *Pharm. Sci.,* 86, 759–761.

Bast, G.E. and Kampffmeyer, H.G. (1996). No effect of albumin on the dermal absorption rate of hydrocortisone 21-butyrate, permethrin or diflunisal in the isolated, single-pass perfused rabbit ear, *Skin Pharmacol*., 9, 327–333.

Baynes, R.E., Brooks, J.D., Budsaba, K., Smith, C., and Riviere, J.E. (2001). Mixture effects of JP-8 additives on the dermal disposition of jet fuel components, *Toxicol. Appl. Pharmacol.,* 175, 269–281.

Baynes, R.E., Brooks, J.D., and Riviere, J.E. (2000). Membrane transport of naphthalene and dodecane in jet fuel mixtures, *Toxicol. Indust. Health,* 16(6), 225–238.

Baynes, R.E., Halling, K.B., and Riviere, J.E. (1997). The influence of diethyl-*m*-toluamide (DEET) on percutaneous absorption of permethrin and carbaryl, *Toxicol. Appl. Pharmacol*., 144**,** 332–339.

Baynes, R.E., Monteiro-Riviere, N.A., and Riviere, J.E. (2002). Pyridostigmine bromide modulates the dermal disposition of [14C]permethrin, *Toxicol. Appl. Pharmacol*., 181, 164–173.

Baynes, R.E. and Riviere, J.E. (1998). Influence of inert ingredients in pesticide formulations on dermal absorption of carbaryl, *Am. J. Vet. Res*., 59, 168–175.

Buchholz, B.A., Pawley, N.H., Vogel, J.S., and Mauthe, R.J. (1997). Pyrethroid decrease in central nervous system from nerve agent pretreatment, *J. Appl. Toxicol.,* 17**,** 231–234.

Central Intelligence Agency and Department of Defense (CIA-DoD). (1997). *Modeling the Chemical Warfare Agent Release at Khamisiyah Pit*, Washington, D.C.: CIA-DoD.

Chou, C.C., Riviere, J.E., and Monteiro-Riviere, N.A. (2002). Differential relationship between the carbon chain length of jet fuel aliphatic hydrocarbons and their ability to induce cytotoxicity versus interleukin-8 release in human epidermal keratinocytes, *Toxicol. Sci*., 2002, 69, 226–233.

Dorman, D.C. and Beasley, V.R. (1991). Neurotoxicology of pyrethrin and the pyrethroid insecticides, *Vet. Hum. Toxicol*., 33, 238–243.

Feussner, J.R. (2001, January 24–26). Gulf War illnesses research: science, policy, and politics, in *Conference on Illnesses Among Gulf War Veterans: A Decade of Scientific Research,* Alexandria, VA, pp. 11–14.

Franz, T.J., Lehman, P.A., Franz, S.F., and Guin, J.D. (1996). Comparative percutaneous absorption of lindane and permethrin, *Arch. Dermatol.,* 132, 901–905.

Fricker, R.D., Reardon, E., Spektor, D.M., Cotton, S.K., Hawes-Dawson, J., Pace, J.E., and Hosek, S.D. (2000). Rand Publication Series. *Pesticide Use During the Gulf War: A Survey of Gulf War Veterans*. Rand Publications, Santa Monica, CA, chapter 1, pp. 1–5, MR–1018/12–OSD.

Grando, S.A., Kist, D.A., Qi, M., and Dahl, M.V. (1993). Human keratinocytes synthesize, secrete, and degrade acetylcholine, *J Invest. Dermatol*., 101, 32–36.

Grauer, E., Ben Nathan, D., Lustig, S., Kobiler, D., Kapon, J., and Danenberg, H.D. (2001). Viral neuroinvasion as a marker for BBB integrity following exposure to cholinesterase inhibitors, *Life Sci*., 68**,** 985–990.

Haberberger, R.V. and Bodenbenner, M. (2000). Immunohistochemical localization of muscarinic receptors (M2) in the rat skin, *Cell Tissue Res*., 300**,** 389–396.

Harris, D.T., Sakiestewa, D., Robledo, R.F., Young, R.S., and Witten, M. (2000). Effects of short-term JP-8 jet fuel exposure on cell-mediated immunity, *Toxicol. Ind. Health*, 16, 78–84.

Heston, W.E. (1950). Carcinogenic action of the mustards, *J. Natl. Cancer Inst*., 11, 415–423.

Heymann, E., Hoppe, W., Krusselmann, A., and Tschoetschel, C. (1993). Organophosphate sensitive and insensitive carboxylesterases in human skin, *Chem. Biol. Interact*., 87**,** 217–226.

Keeler, J.R., Hurst, C.G., and Dunn, M.A. (1991). Pyrostigmine used as a nerve agent pretreatment under wartime conditions, *J. Am. Med. Assoc.,* 266(5), 693–695.

King, R. and Monteiro-Riviere, N.A. (1990). Cutaneous toxicity of 2-chloroethyl methyl sulfide in isolated perfused porcine skin, *Toxicol. Appl. Pharmacol*., 104, 167–179.

Madany, I.M. and Raveendran, E. (1992). Polycyclic aromatic hydrocarbons, nickel and vanadium in air particulate matter in Bahrain during the burning of oil fields in Kuwait, *Sci. Total Environ*., 116, 281–289.

Marino, M.T., Schuster, B.G., Brueckner, R.P., Lin, E., Kaminskis, A., and Lasseter, K.C. (1998). Population pharmacokinetics and pharmacodynamics of pyridostigmine bromide for prophylaxis against nerve agents in humans, *J. Clin. Pharmacol*., 38, 227–235.

McDougal, J.N., Pollard, D.L., Weisman, W., Garrett, C.M., and Miller, T.E. (2000). Assessment of skin absorption and penetration of JP-8 jet fuel and its components, *Toxicol. Sci.,* 55, 247–255.

McDougal, J.N. and Rogers, J.V. (2004). Local and systemic toxicity of JP-8 from cutaneous exposures, *Toxicol. Lett*., 149, 301–308.

McKillop, C.M., Brock, J.A., Oliver, G.J., and Rhodes, C. (1987). A quantitative assessment of pyrethroid-induced paraesthesia in the guinea-pig flank model, *Toxicol. Lett*. 36, 1–7.

Monteiro-Riviere, N.A., Baynes, R.E., and Riviere, J.E. (2003). Pyridostigmine bromide modulates topical irritant-induced cytokine release from human epidermal keratinocytes and isolated perfused porcine skin, *Toxicology* 183, 15–28.

Monteiro-Riviere, N.A. and Inman, A.O. (1997). Ultrastructural characterization of sulfur mustard-induced vesication in isolated perfused porcine skin, *Microsc. Res. Tech.*, 37, 229–241.

Monteiro-Riviere, N., Inman, A., and Riviere, J. (2001). Effects of short-term high-dose and low-dose dermal exposure to Jet A, JP-8 and JP-8 + 100 jet fuels, *J. Appl. Toxicol.*, 21, 485–494.

Monteiro-Riviere, N.A., Inman, A.O., and Riviere, J.E. (2004). Skin toxicity of jet fuels: ultrastructural studies and the effects of substance P, *Toxicol. Appl. Pharmacol*., 195, 339–347.

Moody, R.P., Riedel, D., Ritter, L., and Franklin, C.A. (1987). The effect of DEET (*N,N*,-diethyl-*m*-toluamide) on dermal persistence and absorption of the insecticide fenitrothion in rats and monkeys, *J. Toxicol. Environ. Health,* 22, 471–480.

Morita, H., Yanagisawa, N., Nakajima, T., Shimizu, M., Hirabayashi, H., Okudera, H., Nohara, M., Midorikawa, Y., and Mimura, S. (1995). Sarin poisoning in Matsumoto, Japan, *Lancet*, 346, 290–293.

Muhammad, F., Monteiro-Riviere, N.A**.,** Baynes, R.E., and Riviere, J.E. (2005). Effect of *in vivo* jet fuel exposure on subsequent *in vitro* dermal absorption of individual aromatic and aliphatic hydrocarbon fuel constituents, *J. Toxicol. Environ. Health*, in press.

National Research Council, Committee on Toxicology. (1994). *Health Effects of Permethrin-Impregnated Army Battle-Dress Uniforms*, Washington, D.C.: National Academy Press.

Petersdorf, R.G., Page, W.F., and Thaul, S. (1996). *Interactions of Drugs, Biologics, and Chemicals in U.S. Military Forces*, National Academy Press, Washington, D.C.

Pleil, J.D., Smith, L.B., and Zelnick, S.D. (2000). Personal exposure to JP-8 jet fuel vapors and exhaust at Air Force bases, *Environ. Health Perspect.,* 108, 183–192.

Pont, A.R., Charron, A.R., and Brand, R.M. (2004). Active ingredients in sunscreens act as topical penetration enhancers for the herbicide 2,4-dichlorophenoxyacetic acid, *Toxicol. Appl. Pharmacol*., 195, 348–354.

Potts, R.O., McNeill, S.C., Desbonnet, C.R., and Wakshull, E. (1989). Transdermal drug transport and metabolism. II. The role of competing kinetic events, *Pharm. Res.,* 6, 119–124.

Ray, R., Legere, R.H.., and Broomfield, C.A. (1990). Membrane composition and fluidity changes due to alkylating agents*, J. Cell Biol.,* 3, 73A.

Reuter, S. (1999). Hazards of chemical weapons release during war: new perspectives, *Environ. Health. Perspect*., 107, 985–990.

Riviere, J.E., Baynes, R.E., Brooks, J.D., Yeatts, J.L., and Monteiro-Riviere, N.A. (2003). Percutaneous absorption of topical *N,N*-diethyl-*m*-toluamide (DEET): effects of exposure variables and coadministered toxicants, *J. Toxicol. Environ. Health A,* 66, 133–151.

Riviere, J.E., Brooks, J.D., Williams, P.L., and Monteiro-Riviere, N.A. (1995). Toxicokinetics of topical sulfur mustard penetration, disposition, and vascular toxicity in isolated perfused porcine skin, *Toxicol. Appl. Pharmacol*., 135, 25–34.

Riviere, J.E., Brooks, J.D., Monteiro-Riviere, N.A., Budsaba, K., and Smith, C.E. (1999). Dermal absorption and distribution of topically dosed jet fuels Jet-A, JP-8, and JP-8(100)*, Toxicol. Appl. Pharmacol.,* 160, 60–75.

Riviere, J.E., Monteiro-Riviere, N.A., and Baynes, R.E. (2002). Gulf War related exposure factors influencing topical absorption of 14C-permethrin, *Toxicol. Lett.,* 135, 61–71.

Riviere, J.E. and Williams, P.L. (1992). Pharmacokinetic implications of changing blood flow in skin, *J. Pharm. Sci*., 81, 601–602.

Robledo, R.F., Young, R.S., Lantz, R.C., and Witten, M.L. (2000). Short-term pulmonary response to inhaled JP-8 jet fuel aerosol in mice, *Toxicol. Pathol*., 28, 656–663.

Ross, J.S. and Shah, J.C. (2000). Reduction in skin permeation of *N,N*-diethyl-*m*-toluamide (DEET) by altering the skin/vehicle partition coefficient, *J. Controlled Release*, 67, 211–221.

Ross, E.A., Savage, K.A., Utley, L.J., and Tebbett, I.R. (2004). Insect repellant interactions: sunscreens enhance DEET (*N,N*-diethyl-*m*-toluamide) absorption, *Drug Metab. Dispos*., 32, 783–785.

Seaman, D. (1990). Trends in the formulation of pesticides, *Pestic. Sci*., 29, 437–449.

Selim, S., Hartnagel, R.E., Jr., Osimitz, T.G., Gabriel, K.L., and Schoenig, G.P. (1995). Absorption, metabolism, and excretion of *N,N*-diethyl-*m*-toluamide following dermal application to human volunteers, *Fundam. Appl. Toxicol*., 25, 95–100.

Shah, P.V., Monroe, R.J., and Guthrie, F.E. (1981). Comparative rates of dermal penetration of insecticides in mice, *Toxicol. Appl. Pharmacol*., 59(3), 414–423.

Shah, P.V., Fisher, H.L., Sumler, M.R., Monroe, R.J., Chernoff, N., and Hall, L.L. (1987). Comparison of the penetration of 14 pesticides through the skin of young and adult rats, *J. Toxicol. Environ. Health*, 21(3), 353–366.

Sidon, E.W., Moody, R.P., and Franklin, C.A. (1988). Percutaneous absorption of cis- and trans-permethrin in rhesus monkeys and rats: anatomic site and interspecies variation, *J. Toxicol. Environ. Health*, 23(2), 207–216.

Snodgrass, H.L. (1992). Permethrin transfer from treated cloth to the skin surface: potential for exposure in humans, *J. Toxicol. Environ. Health*, 35, 91–105.

Stuart, J.A., Ursano, R.J., Fullerton, C.S., Norwood, A.E., and Murray, K. (2003). Belief in exposure to terrorist agents: reported exposure to nerve or mustard gas by Gulf War veterans, *J. Nerv. Ment. Dis.,* 191, 431–436.

U.S. Environmental Protection Agency. (1986, April 16). *Federal Register* 51, 12885, Washington, D.C.: U.S. Government Printing Office.

U.S. Environmental Protection Agency. (1998, September). *Reregistration Eligibility Decision (RED) DEET,* EPA738-R-98-010.

Wester, R.C., Melendres, J., Sedik, L., Maibach, H., and Riviere, J.E. (1998). Percutaneous absorption of salicylic acid, theophylline, 2,4-dimethylamine, diethyl hexyl phthalic acid, and *p*-aminobenzoic acid in the isolated perfused porcine skin flap compared to man *in vivo*, *Toxicol. Appl. Pharmacol.* 151, 159–165.

White, R.D. (1999). Refining and blending of aviation turbine fuels, *Drugs Chem. Toxicol.*, 22, 143–153.

Windheuser, J.J., Haslam, J.L., Caldwell, L., and Shaffer, R.D. (1982). The use of *N,N*-diethyl-*m*-toluamide to enhance dermal and transdermal delivery of drugs, *J. Pharm. Sci.*, 71, 1211–1213.

Woodall, J. (1997). Tokyo subway gas attack, *Lancet*, 350, 296.

Zhang, Z., Riviere, J.E., and Monteiro-Riviere, N.A. (1995). Evaluation of protective effects of sodium thiosulfate, cysteine, niacinamide and indomethacin on sulfur mustard-treated isolated perfused porcine skin, *Chem. Biol. Interact.,* 96, 249–262.

Zeiger, E. and Smith, L. (1998). The first international conference on the environmental health and safety of jet fuel, *Environ. Health Perspect.* 106, 763–764.

CHAPTER 10

Estimating the Absorption of Volatile Compounds Applied to Skin

Gerald B. Kasting

CONTENTS

INTRODUCTION

Although considerable progress has been made toward estimating the steady-state absorption rates of organic compounds applied to skin as aqueous solutions (Kasting et al., 1992; Potts and Guy, 1992; Wilschut et al., 1995; Johnson et al., 1997), less is known regarding the absorption of chemicals through skin under other conditions.

In particular, the absorption of compounds, either volatile or nonvolatile, applied to skin neat or from volatile solvents is poorly understood. The problem is of great importance in risk assessment for both environmental and occupational chemical hazards, health and personal care products, and chemical warfare agents. This chapter focuses on the skin absorption of volatile chemicals, using fine fragrance ingredients as an example. These materials have been the subject of recent investigations in my laboratory (Kasting and Saiyasombati, 2001, 2003a, 2003b, 2004a, 2004b).

For fine fragrances as well as many other fragranced consumer products, the chief concern in risk assessment is usually the potential for eliciting allergic contact dermatitis, otherwise known as skin sensitization (Robinson et al., 2000; Basketter, 1998; Kimber et al., 1999). The risk is usually assessed using a variety of tools, including structural-alert computer programs (Sanderson and Earnshaw, 1991), animal skin sensitization databases (Basketter et al., 2000), and human repeat insult patch tests (Basketter, 1998). Few, if any, additional animal studies are conducted on cosmetic products or ingredients given the zero animal use guidelines that have been adopted by the cosmetic and personal care industries. Consequently, there is a clear need to make accurate predictions from *in silico* models prior to exposing human subjects via a human repeat insult patch test (HRIPT) or a product introduction onto the market.

A second aspect of risk assessment for fragranced products concerns systemic levels achieved by a combination of dermal absorption and inhalation. The hazards associated with each ingredient are carefully evaluated and controlled by a combination of exposure assessment plus intrinsic toxicity assessment (Gerberick and Robinson, 2000). Because most absorption occurs via the dermal route (caused by high dilution of the vapor into room air), skin absorption provides the link between these two areas. Absorption models should therefore attempt to answer the questions, What fraction of a topically applied dose will be absorbed? and How rapidly will this occur?

For fragrance ingredients, a conservative but widely used approach is to assume 100% absorption (Robinson et al., 2000). There appear to be no widely used guidelines regarding absorption rates.

The method described in this chapter represents a step toward tightening the risk assessment process for volatile compounds. It is simple to use and has been calibrated for fragrance ingredients (Kasting and Saiyasombati, 2001, 2003a, 2003b, 2004a, 2004b). Based on these data and the analysis described below, the method allows the estimation of percentage absorption and absorption rate to within a factor of two for commonly encountered fragrance ingredients. Research is under way to refine the method and extend its range of use to other chemical classes (Bhatt and Kasting, 2003).

METHOD

The simple model depicted in Figure 10.1 is chosen to represent the disposition of a volatile compound, or mixture of compounds, applied to skin. Each ingredient is assumed to dissolve into the lipids of the skin surface and outer stratum corneum

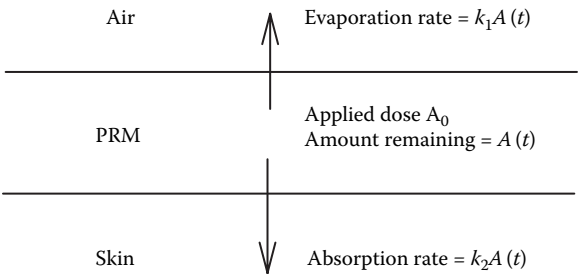

Figure 10.1 Simple model for the disposition of volatile compounds applied to skin. (Adapted from Kasting, G.B. and Saiyasombati, P. *Int. J. Cosmet. Sci.*, 23, 49–58, 2001.)

(SC) and , consequently, to evaporate and absorb at rates proportional to its fraction of saturation in these lipids (Kasting and Saiyasombati, 2001). The evaporation rate (ER) and absorption rate (AR) are given by

$$\text{ER}(\%\text{ of dose/h}) = \frac{100k_1}{k_1 + k_2} e^{-(k_1+k_2)t} \tag{10.1}$$

$$\text{AR}(\%\text{ of dose/h}) = \frac{100k_2}{k_1 + k_2} e^{-(k_1+k_2)t} \tag{10.2}$$

where

$$k_1 = k_1^v \cdot P_{vpr} / (K_{oct} S_w)_r \tag{10.3}$$

$$k_2 = k_2^T \cdot MW_r^{-2.7} \tag{10.4}$$

In Equation 10.3 and Equation 10.4, P_{vp} is vapor pressure in torr, K_{oct} is the octanol–water partition coefficient, S_w is water solubility (g L^{-1}), and MW is molecular weight. All properties are calculated at skin temperature, usually taken to be 30 to 32°C. The subscript r indicates that the property has been divided by a characteristic value; thus, $P_{vpr} = P_{vp}/1$ torr, $(K_{oct}\, S_w)_r = K_{oct}\, S_w/(1000$ g $L^{-1})$, and $MW_r = MW/100$ Da. Estimated values for k_1^v and k_2^T are shown in Table 10.2. The integrated forms of Equation 10.1 and Equation 10.2 yield the cumulative amounts evaporated and absorbed at time t hours postdose:

$$\%\text{ evap}(t) = \frac{100k_1}{k_1 + k_2}\left[1 - e^{-(k_1+k_2)t}\right] \tag{10.5}$$

$$\%\text{ abs}(t) = \frac{100k_2}{k_1 + k_2}\left[1 - e^{-(k_1+k_2)t}\right] \tag{10.6}$$

After a long time ($t \rightarrow \infty$), Equation 10.5 and Equation 10.6 yield

$$\%\,\text{evap}(\infty) = \frac{100 x_r}{k + x_r} \tag{10.7}$$

$$\%\,\text{abs}(\infty) = \frac{100 k}{k + x_r} \tag{10.8}$$

where $k = k_2^T / k_1^v$ and $x_r = P_{vpr} MW_r^{2.7} / (K_{oct} S_w)_r$. Using the parameters in Table 10.2, Equation 10.7 was shown to correlate the cumulative evaporation data from a controlled human forearm evaporation study involving 11- and 12-component fragrance mixtures (Vuilleumier et al., 1995) with r^2 values of 0.80 and 0.73, respectively (Saiyasombati and Kasting, 2003b). The compounds tested and their physical properties are shown in Table 10.1, and the correlations are shown in Figure 10.2. The corresponding estimated percentage absorption, calculated as % abs(∞) = 100 – % evap(∞), is shown in Figure 10.3.

Based on the results in Figure 10.2 and Figure 10.3, Equation 10.7 and Equation 10.8 tend to overpredict evaporation and underpredict absorption of the highly volatile "top note" ingredients linalool (I), dihydromyrcenol (II), and 10-undecanal (III), for which $x_r \geq 0.5$. This deficiency can be largely corrected by the following empirical modification, which may be proposed for risk assessment purposes:

$$\%\,\text{evap}(\infty) = \frac{100 x_r - 15 x_r^2}{0.165 + x_r} \quad ; \qquad 0 < x_r < 1 \tag{10.9}$$

$$\%\,\text{abs}(\infty) = \frac{16.5 + 15 x_r^2}{0.165 + x_r} \quad ; \qquad 0 < x_r < 1 \tag{10.10}$$

Smooth curves calculated from Equation 10.9 and Equation 10.10 are shown on Figure 10.2 and Figure 10.3. The root mean square (rms) deviation of Equation 10.10 from the estimated percentage absorption values is 11% for both fragrance vectors. The maximum underprediction of absorption (31% calculated vs. 55% observed) occurs for 10-undecanal (III) when incorporated in the fixed fragrance, Vector B. The maximum overprediction (68% calculated vs. 45% observed) occurs for *cis*-7-*p*-menthanol (VIII) when incorporated in the unfixed fragrance, Vector A. These values support the contention that Equation 10.10 estimates absorption to within a factor of two for fragrance ingredients applied to skin under conditions comparable to those in Vuilleumier et al. (1995). Thus, Equation 10.10 is the central equation in this report.

Table 10.1 Fragrance Raw Materials Studied in Vuilleumier et al. (1995)

ID	Compound	MW (Da)	P^{a}_{vp}(torr)	log K^{a}_{oct}	S^{a}_{w}(g/L)	x_r Eq. 4	f^{b}_{evap} Vector A	f^{b}_{evap} Vector B
I	Linalool	154	0.13	2.55	2.3	0.52	0.681 ± 0.004	0.575 ± 0.015
II	Dihydromyrcenol	156	0.19	3.03	0.76	0.79	0.735 ± 0.016	0.658 ± 0.022
III	10-Undecanal	170	0.093	4.05	0.072	0.48	0.594 ± 0.004	0.452 ± 0.061
IV	Citronellol	156	0.028	3.25	0.46	0.11	0.500 ± 0.004	0.412 ± 0.007
V	2-Phenyl-1-ethanol	122	0.039	1.36	35	0.08	0.260 ± 0.003	0.186 ± 0.020
VI	(E)-Cinnamic alcohol	134	0.0050	1.95	8.5	0.01	0.039 ± 0.004	0.037 ± 0.006
VII	α-Damascone	192	0.032	3.62	0.19[c]	0.28	0.712 ± 0.007	0.570 ± 0.028
VIII	*cis*-7-*p*-Menthanol	156	0.019	3.33	0.38	0.08	0.545 ± 0.014	0.469 ± 0.054
IX	2,2,2-Trichloro-1-phenylethylacetate	268	0.0029	4.05	0.072[c]	0.08	0.422 ± 0.004	0.405 ± 0.032
X	MPCC[d]	192	0.010	3.87	0.11	0.07	0.330 ± 0.005	0.237 ± 0.022
XI	(E)-2-Benzylideneoctanal	216	0.00088	4.85	0.011[c]	0.01	0.069 ± 0.007[e]	0.043 ± 0.007[e]
XII	15-Pentadecanolide	240	0.00010	5.35	0.0034[c]	0.001	NA[f]	0.066 ± 0.010[e]

[a] For sources of physical properties, see Kasting and Saiyasombati (2001).
[b] Experimental fraction of dose evaporated extrapolated to $t \rightarrow \infty$ (except for XI and XII) (Kasting and Saiyasombati, 2001).
[c] Estimated value, corrected as in Kasting and Saiyasombati (2001).
[d] 3-(4-Methyl-3-pentenyl)-3-cyclohexene-1-carbaldehyde + 4-(4-methyl-3-pentenyl)-3-cyclohexene-1-carbaldehyde.
[e] 0 to 7.25 h only.
[f] This ingredient (a musk fixative) was included in Vector B, but not in Vector A.

Source: Adapted from Saiyasombati, P. and Kasting, G.B., *Int. J. Cosmet. Sci.*, 25, 235–243, 2003.

Table 10.2 Regression Parameters (Mean ± SD, 20 Determinations per Vector) for Fit of Equation 10.3 to Equation 10.6 to Fragrance Evaporation Data in Vuilleumier et al. (1995)

Parameter	Units	Vector A	Vector B
k_1^v	h^{-1}	14.5 ± 10.5	9.1 ± 8.9
k_2^T	h^{-1}	1.9 ± 0.6	1.5 ± 0.5
Regression statistics (Cumulative fits)			
n		143	132
s		0.13	0.16
r^2		0.7960	0.7333

Source: Adapted from Saiyasombati, P. and Kasting, G.B., *Int. J. Cosmet. Sci.*, 25, 235–243, 2003.

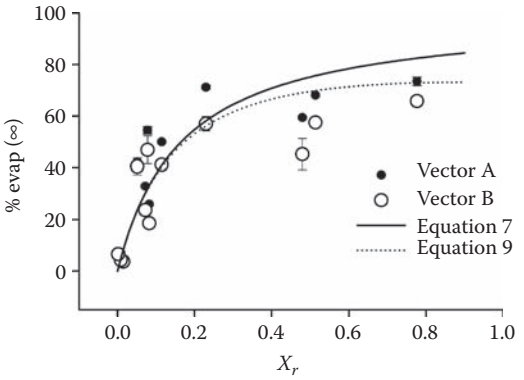

Figure 10.2 Cumulative evaporation of fragrance ingredients described from a human volar forearm (Vuilleumier et al., 1995), extrapolated to infinite time (Kasting and Saiyasombati, 2001). The value of k in Equation 10.7 was calculated as k = 1.5/9.1 = 0.165 (Table 1, Vector B).

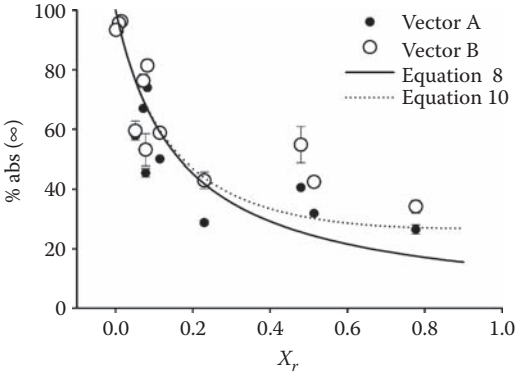

Figure 10.3 Calculated cumulative absorption of fragrance ingredients from a human volar forearm (Vuilleumier et al., 1995), extrapolated to infinite time. The results were calculated from the data in Figure 10.2 by assuming %abs(∞) = 100 – %evap(∞).

MODEL ASSUMPTIONS AND RATIONALE

The model represented by Equation 10.1 to Equation 10.10 is a highly simplified representation of the disposition of volatile chemicals on skin, yet it captures the major features of the data in Vuilleumier et al. (1995) and several related investigations (Kasting and Saiyasombati, 2001, 2003a, 2004a, 2004b). The distinguishing feature of this model versus other kinetic models that can readily correlate rate profiles (see, for example, Guy et al., 1982; Guy and Hadgraft, 1983) is the physical properties dependence contained in Equation 10.3 and Equation 10.4. This section reviews the rationale behind these choices and the assumptions made in the derivation of Equation 10.1 to Equation 10.4. The latter are as follows:

1. The total chemical dose to the skin falls within the small dose limit in which nearly first-order absorption is often observed (Kasting and Saiyasombati, 2001; Kasting, 2001). An upper limit to this range may be taken as 100 μg cm^{-2} (Kasting, 2001), although it may be higher for highly volatile solvents such as ethanol.
2. Compounds evaporate and absorb independently of one another and do not bind irreversibly to skin.
3. The absorptive flux J_{skin} is a fraction of the maximum flux J_{max}. The latter is directly proportional to lipid solubility and inversely related to molecular weight (Kasting et al., 1992). Thus,

$$\begin{aligned} J_{\text{skin}} &= \frac{c_{lip}(t)}{S_{lip}} J_{\max} \\ &= \frac{c_{lip}(t)}{S_{lip}} \cdot \left[\text{const.} \cdot S_{lip} \cdot MW^{-b} \right] \\ &= \text{const.} \cdot c_{lip}(t) \cdot MW^{-b} \end{aligned} \tag{10.11}$$

   In Equation 10.11, $c_{lip}(t)$ is the concentration of the compound in the SC lipid phase at time t, S_{lip} is its solubility in these lipids (taken to be the product of water solubility S_w and octanol–water partition coefficient K_{oct}), and b is a positive exponent with a value of about 2.7 (Kasting and Saiyasombati, 2001). The value of b was estimated based on an analysis of the Flynn skin permeability database (Johnson et al., 1997), which represents steady-state permeabilities obtained with hydrated human skin *in vitro*. It is possible that a somewhat higher value of b may apply for volatile disposition on air-dried skin if it is more size selective than hydrated skin. Such a refinement has not been attempted here.
4. The evaporative flux J_{evap} is given by a Henry's law like expression, with the SC lipids as the relevant solvent. Thus,

$$J_{\text{evap}} = \text{const.} \cdot f(v) \cdot c_{lip}(t) \cdot P_{vp} / S_{lip} \tag{10.12}$$

5. where $f(v)$ is an airflow function, P_{vp} is vapor pressure, and S_{lip} is estimated as $K_{oct} \cdot S_w$. An analogous expression has been used to estimate the evaporation rates of pesticides from soil (Lyman et al., 1982), in which the relevant solvent is the soil organic fraction.

Temperature Dependence

Skin permeability, as well as evaporation rate, are strong functions of temperature. Equation 10.3 and Equation 10.4 are written with this in mind. The values of k_2^T in Table 10.1 apply to skin at a temperature of 30°C; an Arrhenius correction to these values for other temperatures is suggested in Kasting and Saiyasombati (2001). The temperature dependence of evaporation rate, on the other hand, occurs through the variation of P_{vp} with temperature, a dependence that is easily approximated and factored into Equation 10.3. Thus, the model calculations can readily be extended to exposure scenarios involving a range of skin temperatures.

Airflow Dependence

Intuitively, one expects that evaporative loss from the skin will be directly related to the wind velocity or airflow over the skin surface. That this is so has been demonstrated in my laboratory (Saiyasombati and Kasting, 2003a, 2004a) using methods similar to those employed in Vuilleumier et al. (1995). A picture of the test apparatus employed in Saiyasombati and Kasting (2004a) is shown in Figure 10.4, and a plot of the airflow dependence obtained for evaporation of a model fragrance ingredient, benzyl alcohol, is shown in Figure 10.5 (open circles). In this section, we relate these laboratory results to those in Vuilleumier et al. (1995) and establish a basis for the use of Equation 10.10 as a plausible absorption estimate for unoccluded skin sites on broad body surfaces (torso, arm, leg) exposed to relatively still air indoors. Adjustments for more permeable skin sites (face, postauricular, underarm) are discussed in the next section.

The data in Figure 10.2 and Figure 10.3 (on which the present model was calibrated) were generated on human volar forearm using a dose cell similar to that shown in Figure 10.4 and an airflow of 5 L h^{-1} or 83 ml min^{-1} (Vuilleumier et al., 1995). These conditions may be equated to those in Saiyasombati and Kasting (2004a) (Figure 10.5, open circles) at comparable airflows on the basis of a similar cell design and experimental method. From the physical properties of benzyl alcohol at 30°C reported in Saiyasombati and Kasting (2003a) (P_{vp} = 0.0847 torr, MW = 108.1 Da, log K_{oct} = 1.1, S_w = 44.7 g L^{-1}), a value of k_1^v = (10.5 ± 2.2) h^{-1} at v = 83 ml min^{-1} may be calculated for the *in vivo* benzyl alcohol evaporation data in Figure 10.5, which is comparable to the range k_1^v = 9.1 to 14.5 h^{-1} found in Table 10.1.

Additional studies with benzyl alcohol applied to cadaver skin *in vitro* demonstrated a similar airflow dependence to that shown *in vivo* Saiyasombati and Kasting (2003a). The results are shown as solid circles in Figure 10.5. The evaporation rates *in vitro* and *in vivo* were found to vary in direct proportion to the airflow and inversely with the volume of the dose cell, which was about eightfold higher *in vivo* (Saiyasombati and Kasting, 2004a); thus, the *in vitro* airflow corresponding to 83 ml^{-1} *in vivo* was about 10 to 15 ml min^{-1}. This may be seen by comparing the evaporation profiles in Figure 10.5.

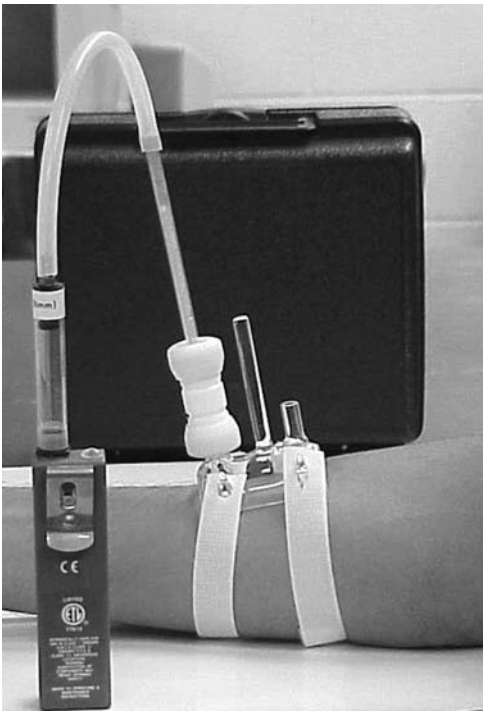

Figure 10.4 Apparatus for trapping volatiles from a human forearm *in vivo* (Saiyasombati and Kasting, 2004a).

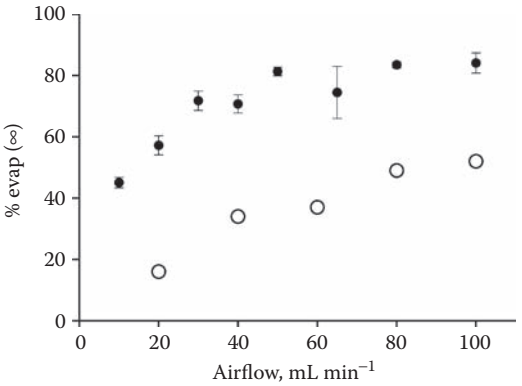

Figure 10.5 Cumulative percentage of benzyl alcohol evaporated from human skin as a function of airflow in the collection cell. •, *in vitro*, 2.25 h postdose (Saiyasombati and Kasting, 2003a); *in vivo*, 2 h postdose (Saiyasombati and Kasting, 2004a).

Finally, recent work in my laboratory with another test permeant, (*N,N*)-diethyl-*m*-toluamide (the mosquito repellant DEET), has established a relationship between DEET disposition on skin *in vitro* (Bhatt and Kasting, 2003) and in several human *in vivo* studies (Feldmann and Maibach, 1970; Spencer et al., 1979; Selim et al., 1995). The best comparison to the *in vitro* results is a clinical study in which ^{14}C-DEET was applied to the forearm of test subjects, and the dose site was subsequently covered with a perforated aluminum dome (Selim et al., 1995). The dose was removed after 8 h, and urinary excretion of radioactivity was determined over 128 h. This comparison suggests that the *in vitro* airflow corresponding to the perforated dome exposure *in vivo* is about 20 ml min^{-1} (G.B. Kasting and V. Bhatt, 2004, unpublished data). The combination of this result with the earlier finding that the data in Vuilleumier et al. (1995) correspond to approximately 10 ml min^{-1} *in vitro* forms the basis for proposing the use of Equation 10.9 and Equation 10.10 for risk assessment. The perforated dome study (Selim et al., 1995) conservatively approximated still room air, and an additional small safety margin is provided by the fact that the conditions in Selim et al. (1995) evidently correspond to a higher *in vitro* airflow than do those in Vuilleumier et al. (1995).

Influence of Skin Site and Occlusion

To maintain consistent safety factors, it is both reasonable and appropriate to modify Equation 10.9 and Equation 10.10 for exposures involving highly permeable skin sites or high degrees of occlusion. The following modifications are suggested based on literature data (Feldmann and Maibach, 1967; Maibach et al., 1971; Scheuplein and Blank, 1971; Wester et al., 1984; Rougier et al., 1988; Schwindt et al., 1998; Guy and Maibach, 1984) on site-to-site variations in skin permeability.

Skin Site

Postauricular and facial skin have been found to be two- to sixfold more permeable than broad body surfaces, including forearm (Feldmann and Maibach, 1967; Maibach et al., 1971; Scheuplein and Blank, 1971; Rougier et al., 1988; Guy and Maibach, 1984). Underarm, genitalia, and other mucosal surfaces are even more permeable (Feldmann and Maibach, 1967; Maibach et al., 1971; Guy and Maibach, 1984). For the last sites, it is recommended that Equation 10.9 and Equation 10.10 be replaced with a 100% absorption estimate in the absence of additional data. This conservative estimate is made in light not only of increased skin permeability, but also of the relatively high occlusion of these sites under clothing. For postauricular and facial skin, a substitute for Equation 10.10 based on a threefold higher value of the absorption rate constant k_2^T may be suggested:

$$\%\text{Abs}(\infty) = \frac{49.5 + 15x_r^2}{0.495 + x_r} \quad ; \quad 0 < x_r < 1 \tag{10.13}$$

Occlusion

Fully occluded sites do not allow evaporation and furthermore lead to hydrated skin and higher skin temperatures. A 100% absorption estimate must be applied for long-term occluded exposures to skin-permeable compounds such as fragrance ingredients, pesticides, and volatile organic solvents. Rates of absorption may be estimated using available methods for nonvolatile compounds (Kasting et al., 1992; Potts and Guy, 1992; Wilschut et al., 1995; Johnson et al., 1997). For example, the Potts-Guy equation (Potts and Guy, 1992) has been shown to satisfactorily describe the absorption of fragrance ingredients from aqueous solution (Hostynek, 1997).

LIMITATIONS OF MODEL

The method described in this chapter represents a first attempt to quantitatively relate the skin disposition of volatile chemicals to their physical properties and to environmental conditions, including variable temperature and airflow over the skin surface. The relationships were developed for fragrance ingredients; however, it is likely they can be extended to include other important classes of compounds such as noncorrosive industrial solvents, pesticides, herbicides, and (noncorrosive) chemical warfare agents. Drawing the comparison to steady-state skin permeability models in which much more is known, it is evident that considerable experience must be gained with the use of such models before widespread acceptance may be expected. Areas for further attention are outlined next.

Dose Dependence

Equation 10.1 to Equation 10.10 were developed within the low-dose limit in which the applied compound(s) dissolve rapidly into the SC lipids. If the lipid volume is taken to be V_{lip}, then $c_{lip}(0) = \text{Dose}/V_{lip}$. Substitution of this relationship into Equation 10.11 and Equation 10.12 leads directly to Equation 10.1 to Equation 10.4. However, the SC lipid volume is small (100 to 150 $\mu g\ cm^{-2}$), and only a fraction of this volume can be immediately accessed by a topically applied permeant. Appropriate incorporation of a solubility limit, such that $c_{lip}(0) \leq S_{lip}$, would provide upper bounds to both the evaporation rate (Equation 10.1) and absorption rate (Equation 10.2) without changing their relative values. The key is establishing the accessible lipid volume and confirming or improving on the octanol solubility model. This problem has been discussed elsewhere (Kasting, 2001).

Ingredient Interactions

The present model assumes that ingredients diffuse and evaporate independently, whereas thermodynamic and mass transport considerations dictate that interactions must occur in concentrated mixtures (Cussler, 1997). Careful analysis of the evaporation rates in Vuilleumier et al. (1995) shows this to be the case: The musk ingredient, compound XII in Table 10.2, depressed the initial evaporation rates of

the fragrance top notes in a complex mixture (Saiyasombati and Kasting, 2003b). My group attempted to account for these interactions using activity coefficients calculated from a (universal quasichemical functional activity coefficient) UNIFAC/UNIQUAC approach (Reid et al., 1987) but were unable to obtain any improvements to a unit activity assumption in the context of one- and two-compartment kinetic models (Saiyasombati and Kasting, 2003b). The subject is worth revisiting in a true diffusion–evaporation model.

Kinetic Profiles

Equation 10.1 and Equation 10.2 lead to simple, exponential decays without time lags for both evaporation and absorption rates. There is experimental evidence to support more protracted decay curves and, of course, a diffusive time lag for absorption (Saiyasombati and Kasting, 2003a, 2003b). These features can be accommodated using two-compartment kinetic models that explicitly consider a vehicle layer (Saiyasombati and Kasting, 2003a, 2003b). However, the impact of this refinement on cumulative evaporation and absorption calculations is minimal, and the parameter assignments are not unique. A more promising direction is to use a diffusion model for the SC rather than a well-stirred compartment. This approach can account for both absorption time lag and curvature in semilogarithmic plots of absorption and evaporation rates using fewer undetermined parameters (G.B. Kasting and V. Bhatt, 2004, unpublished observations). It is the direction of the current research in our laboratory.

Physical Properties Dependence

Whether compartmental or diffusion models are employed, relationships analogous to Equation 10.3 and Equation 10.4 must be developed and confirmed to have predictive capabilities. Equation 10.3 stems directly from steady-state skin permeability relationships (cf. Equation 10.12), whereas Equation 10.4 is derived from Henry's law using octanol to represent the SC lipids (cf. Equation 10.11). Both of these relationships have room for improvement. An empirical modification, Equation 10.9 and Equation 10.10, to the physical properties relationship implied by Equation 10.3 and Equation 10.4 was suggested in this report to better correlate the data in Vuilleumier et al. (1995). Physically based modifications are needed.

CONCLUSION

A simple kinetic model for the disposition of volatile chemicals applied to skin has been developed and calibrated for fragrance ingredients and mixtures. The model allows the estimation of the percentage of each ingredient evaporated and absorbed as a function of time to within a factor of two. Suggestions for extension and refinement of the approach are provided.

ACKNOWLEDGMENT

This work was supported by grant R01 OH007529 from the National Institute for Occupational Safety and Health, a branch of the U.S. Centers for Disease Control and Prevention.

REFERENCES

Basketter, D.A. (1998). Skin sensitization: Risk assessment, *Int. J. Cosmet. Sci.*, 20, 141–150.

Basketter, D.A., Blaikie, L., Dearman, R.J., Kimber, I., Ryan, C.A., Gerberick, G.F., Harvery, P., Evans, P., White, I.R., and Rycroft, R.J.G. (2000). Use of the local lymph node assay for the estimation of relative contact allergenic potential, *Contact Dermatitis*, 42, 344–348.

Bhatt, V. and Kasting, G.B. (2003, November). A model for estimating the absorption and evaporation rates of DEET from human skin, paper presented at the American Association of Pharmaceutical Scientists National Meeting, Salt Lake City, UT.

Cussler, E.L. (1997). *Diffusion: Mass Transfer in Fluid Systems*, Cambridge, U.K.: Cambridge University Press, pp. 50–78.

Feldmann, R.J. and Maibach, H.I. (1967). Regional variations in percutaneous penetration of 14C-cortisol in man, *J. Invest. Dermatol.*, 48, 181–183.

Feldmann, R.J. and Maibach, H.I. (1970). Absorption of some organic compounds through the skin in man, *J. Invest. Dermatol.*, 54, 399–404.

Gerberick, G.F. and Robinson, M.K. (2000). A skin sensitization risk assessment approach for evaluation of new ingredients and products, *Am. J. Contact Dermatitis*, 11, 65–73.

Guy, R.A. and Hadgraft, J. (1983). Physicochemical interpretation of the pharmacokinetics of percutaneous absorption, *J. Pharm. Biopharm.*, 11, 189–203.

Guy, R.A., Hadgraft, J., and Maibach, H.I. (1982). A pharmacokinetic model for percutaneous absorption, *Int. J. Pharm.*, 11, 119–129.

Guy, R.H. and Maibach, H.I. (1984). Correction factors for determining body exposure from forearm percutaneous absorption data, *J. Appl. Toxicol.*, 4, 26–28.

Hostynek, J.J. (1997). Safeguards in the use of fragrance chemicals, *Cosmet. Toilet.*, 112, 47–54.

Johnson, M.E., Blankschtein, D., and Langer, R. (1997). Evaluation of solute permeation through the stratum corneum: lateral bilayer diffusion as the primary transport mechanism, *J. Pharm. Sci.*, 86, 1162–1172.

Kasting, G.B. (2001). Kinetics of finite dose absorption. 1. Vanillylnonanamide, *J. Pharm. Sci.*, 90, 202–212.

Kasting, G.B. and Saiyasombati, P. (2001). A physico-chemical properties based model for estimating evaporation and absorption rates of perfumes from skin, *Int. J. Cosmet. Sci.*, 23, 49–58.

Kasting, G.B., Smith, R.L., and Anderson, B.D. (1992). Prodrugs for dermal delivery: solubility, molecular size, and functional group effects, in *Prodrugs: Topical and Ocular Drug Delivery* (K.B. Sloan, ed.), New York: Dekker, pp. 117–161.

Kimber, I., Gerberick, G.F., and Basketter, D.A. (1999). Thresholds in contact sensitization: theoretical and practical considerations, *Food Chem. Toxicol.*, 37, 553–560.

Lyman, W.J., Reehl, W.F., and Rosenblatt, D.H., eds. (1982). *Handbook of Chemical Property Estimation*, New York: McGraw-Hill, pp. 16-25 to 16-27.

Maibach, H.I., Feldmann, R.J., Milby, T.H., and Serat, W.F. (1971). Regional variations in percutaneous penetration in man, *Arch. Environ. Health*., 23, 208–211.

Potts, R.O. and Guy, R.H. (1992). Predicting skin permeability, *Pharm. Res*., 9, 663–669.

Reid, R.C., Prausnitz, J.M., and Poling, B.E., eds. (1987). *The Properties of Liquids and Gases*, New York: McGraw-Hill.

Robinson, M.K., Gerberick, G.F., Ryan, C.A., McNamee, P., White, I., and Basketter, D.A. (2000). The importance of exposure estimation in the assessment of skin sensitization risk, *Contact Dermatitis,* 42, 251–259.

Rougier, A., Lotte, C., Corcuff, P., and Maibach, H.I. (1988). Relationship between skin permeability and corneocyte size according to anatomic site, age, and sex in man, *J. Soc. Cosmet. Chem*., 39, 15–26.

Saiyasombati, P. and Kasting, G.B. (2003a). Disposition of benzyl alcohol following topical application to human skin *in vitro, J. Pharm. Sci*., 92, 2128–2139.

Saiyasombati, P. and Kasting, G.B. (2003b). Two-stage kinetic analysis of fragrance evaporation and absorption from skin, *Int. J. Cosmet. Sci*., 25, 235–243.

Saiyasombati, P. and Kasting, G.B. (2004a). Evaporation of benzyl alcohol from human skin *in vivo, J. Pharm. Sci*., 93, 515–520.

Saiyasombati, P. and Kasting, G.B. (2004b). Prediction of fragrance headspace concentrations from physicochemical properties, *Perfumer Flavorist*, 29, 38–47.

Sanderson, D.M. and Earnshaw, C.G. (1991). Computer prediction of possible toxic action from chemical structure; the DEREK system, *Human Exp. Toxicol*., 10, 261–273.

Scheuplein, R.J. and Blank, I.H. (1971). Permeability of the skin, *Physiol. Rev.*, 51, 702–747.

Schwindt, D.A., Wilhelm, K.-P., and Maibach, H.I. (1998). Water diffusion characteristics of human stratum corneum at different anatomical sites *in vivo, J. Invest. Dermatol*., 111, 385–389.

Selim, S., Hartnagel, R.E., Osimitz, T.G., Gabriel, K.L., and Schoenig, G.P. (1995). Absorption, metabolism, and excretion of *N,N*-diethyl-*m*-toluamide following dermal application to human volunteers, *Fundam. Appl. Toxicol*., 25, 95–100.

Spencer, T.S., Hill, J.A., Feldmann, R.J., and Maibach, H.I. (1979). Evaporation of diethyltoluamide from human skin *in vivo* and *in vitro, J. Invest. Dermatol*., 72, 317–319.

Vuilleumier, C., Flament, I., and Sauvegrain, P. (1995). Headspace analysis study of evaporation rate of perfume ingredients applied onto skin, *Int. J. Cosmet. Sci*., 17, 61–76.

Wester, R.C., Maibach, H.I., and Bucks, D.A.W. (1984). *In vivo* percutaneous absorption of paraquat from hand, leg, and forearm of humans, *J. Toxicol. Environ. Health*, 14, 759–762.

Wilschut, A., ten Berge, W.F., Robinson, P.J., and McKone, T.E. (1995). Estimating skin permeation. The validation of five mathematical skin penetration models, *Chemosphere*, 30, 1275–1296.

CHAPTER 11

Modeling Dermal Absorption from Soils and Powders Using Stratum Corneum Tape-Stripping *In Vivo*

Annette L. Bunge, Gilles D. Touraille, Jean-Paul Marty, and Richard H. Guy

CONTENTS

INTRODUCTION

The skin is a complex organ that is the major interface between humans and their environment. The skin's primary function is to restrict passive water loss from the body. It is the outermost 10 to 15 μm thick layer of the skin, the stratum corneum (SC), which provides this barrier function. The SC is composed of dead keratinized cells (corneocytes) embedded in a matrix of lipids, a structure that has been represented as a brick-and-mortar wall (Schaefer and Redelmeier, 1996). However, the SC is not totally impermeable, of course, and chemicals with appropriate physicochemical properties can be absorbed in amounts sufficient to provoke both local and systemic pharmacological and toxic effects (Guy, 1996).

The local and systemic bioavailability of topically applied chemicals depends on the kinetics and extent of the percutaneous absorption process. *In vivo*

experiments are the most relevant to evaluate the penetration of a drug and its distribution within the body. The uptake of chemical into the SC is an estimate of the amount available to permeate the deeper layers of the skin (Schaefer and Redelmeier, 1996) and enter the body. Recently, the method of infrared (IR) spectroscopy has been applied creatively to the question of skin barrier function and percutaneous transport (Bommannan et al., 1990; Clancy et al., 1994; Jadoul et al., 1995; Knutson et al., 1985, 1987; Mak et al., 1990; Margarida et al., 1995; Pellett et al., 1997; Potts and Francoeur, 1992). Using attenuated total reflectance (ATR), furthermore, IR evaluation of absorbed chemicals within the skin can be performed *in vivo* in humans (Higo et al., 1993; Mak et al., 1990). In particular, in combination with sequential tape-stripping, ATR-IR has been used to determine a chemical's concentration profile across the SC, and the subsequent analysis of these data, using the appropriate solution to Fick's second law of diffusion, has permitted diffusion and partitioning parameters to be deduced (Pirot et al., 1997).

The objective of the work described here was to examine whether a similar approach can be used to assess chemical uptake into the skin *in vivo* from contaminated soil. It is now well recognized that human skin contact with contaminated soil can represent an important route of exposure to toxic compounds in occupational, environmental, and recreational settings. Data on the dermal uptake of chemicals from soil, especially *in vivo,* are limited, however, and those that do exist may underrepresent the true risk. This is because the amount of soil applied to skin in these experiments (1) greatly exceeds the mass of soil adhering to skin during a typical exposure (U.S. Environmental Protection Agency, 2001) and (2) may have provided multiple soil layers that do not contribute equally to dermal absorption (Bunge and Parks, 1998).

Using 4-cyanophenol (CP) as a model compound, ATR-IR has been applied following an approach published by Pirot et al. (1997). The SC distribution profile of the chemical following its relatively short-term contact, via contaminated soil, with the skin has been determined and used to obtain diffusion and partitioning parameters. In addition, the results have permitted the hypothesis that a significant mass transfer resistance exists across the soil–skin interface, reducing thereby the rate and extent of chemical absorption following short-term contact.

MATERIALS AND METHODS

In vivo studies, which had received ethical approval, were conducted on healthy volunteers. The subjects, aged 25 to 35 years, had no history of dermatological disease. All experiments were conducted on the ventral forearms of the volunteers. The soil was a clay loam from Fort Collins, Colorado, with an organic carbon fraction of 0.011 (Choate, 2002). Only the sieve fraction 250 μm or less was used, which had a particle size distribution (by weight) of 36.2% at 125 to 250 μm, 38.5% at 63 to 125 μm, 14.9% at 38 to 63 μm, 4.6% at 25 to 38 μm, and 5.8% below 25 μm. Analytical-grade CP was purchased from Aldrich Chemical (Milwaukee, WI). The selection of this chemical was based on its relatively good absorption across human skin (Higo et al., 1993; Mak et al., 1990; Pellett et al., 1997; Pirot et al., 1997) and

its intense C≡N stretching absorbance at 2230 cm^{-1}, a region of the IR spectrum at which the SC is quite transparent (Higo et al., 1993; Potts et al., 1991). Soil was contaminated with CP dissolved in ethanol:water solutions (90:10). Typically, the initial slurry consisted of 10 ml ethanol–water and 5 g soil. The mixture was completely dried overnight and was then shaken vigorously for 30 min to disintegrate any residual clumps of soil. The exact amount of CP on the contaminated soil was determined by extracting small, carefully weighed aliquots (20 mg) with acetonitrile for 24 h followed by ultraviolet (UV) spectroscopy. The amount of CP in the soil (~0.05 g/g soil) was large enough that a white residue of the chemical was visible on the soil particles when viewed under the microscope. In other words, more CP was added than was required to saturate the soil. This was confirmed in a subsequent independent study of the CP solubility limit of this soil (Chen et al., 2004).

The neat contaminated soil or neat powdered CP was distributed within an 8 × 2 cm delimiting card frame attached to the skin surface with a nonocclusive transparent dressing (10 × 12 cm, Tegaderm 1626, 3M Company, St. Paul, MN). The mass of soil or neat solid chemical applied to the skin surface was much greater than that required to provide at least a single layer of tightly packed particles. Experiments were conducted at short (45 min) and longer (either 120 or 180 min) durations on opposite forearms. From previous *in vivo* studies, the lag time for CP penetration through the SC was known to be between 30 and 45 min (Pirot et al., 1997; Reddy et al., 2002; Stinchcomb et al., 1999). Because the time to reach steady state is approximately 2.5 times the lag time, experiments conducted at the longer durations were expected to be at steady state. At the end of the specified exposure, the soil or neat chemical was removed. Two different cleaning procedures were used. For subjects A through D, the skin was cleaned gently using dry cotton swabs and compressed air. For subjects E through I, the skin was cleaned using water-moistened cotton swabs.

At the end of the application period, the CP concentration profile across the SC was determined. This required determination of the chemical's level as a function of position within the barrier. To probe the SC at different depths, the application site was tape stripped (Scotch, 3M Company) up to 20 times. The tapes of fixed area (19 cm^2) were weighed before and after stripping to determine the mass of SC removed by each strip. Knowing the density of the SC (1 g cm^{-3}; Higo et al., 1993), the average SC thickness adhering to each strip is the SC weight per stripped area divided by the density. It was therefore possible from the cumulative mass of SC removed by n tape strips to determine the average depth into the SC (x) up to that point (Kalia et al., 1996). Transepidermal water loss (TEWL) was measured (ServoMed Evaporimeter EPI, ServoMed AB, Stockholm, Sweden) following each set of four tape strips. In subjects A through D, TEWL measurements were made on the application site as it was tape stripped for CP determination. Because cleaning the skin with water would have altered these TEWL measurements, compressed air was used instead to clean the soil from the site. In subjects E through I, the TEWL measurements were made on skin adjacent to the application site, thereby allowing the soil to be cleaned off with water. Linear regressions of $[TEWL]^{-1}$ vs. x were derived. As described by Kalia et al. (1996), the SC thickness L can be deduced

from the zero intercept of $[TEWL]^{-1}$ plotted as a function of x. Data from different subjects could then be presented on a common scale of normalized SC depth (x/L).

The concentration of CP in the SC removed by each tape was determined by ATR-IR using a Nicolet 520 Fourier transform IR spectrophotometer (Nicolet, CA) equipped with a liquid nitrogen-cooled mercury-cadmium-telluride detector and an ATR accessory (7×1 cm^2) consisting of a trapezoidal ZnSe crystal at 45° (Spectratech, Stamford, CT). The CP was detected by its absorbance at 2230 cm^{-1}. Tapes, adhesive side down, were applied to the crystal and pressed firmly using a gripper device (Spectratech) to maximize contact between tape and crystal and hence improve the reproducibility of the measurement. The method was calibrated by spiking tapes, which had been used to strip uncontaminated SC, with known amounts of CP (10-μl aliquots in ethanol spread evenly over areas of 7×1 cm^2) to give the following calibration curve:

$$\log PA = 1.0627 \log [CP] - 2.8682; \; PA > 0.01243 \tag{11.1}$$

where PA was the measured peak area, and [CP] was the amount (in nmol cm^{-2}) of CP in a tape. The calibration was repeated in quadruplicate, with the limit of detection set at 10 times the absorbance at 2230 cm^{-1} from a blank tape (i.e., on the order of 8 nmol cm^{-2}). Equation 11.1 varied insignificantly over the course of the experiments. The concentration of CP in a tape strip (C) was calculated by dividing [CP] by the average thickness of the SC on that tape. In calculations of C as a function of position x within the SC, the concentration of the nth tape strip C_n is located at position $(x_n + x_{n-1})/2$ where x_n is the cumulative thickness of SC removed by n tape strips.

THEORY

Assuming a chemical that comes into contact with the skin equilibrates quickly between the vehicle and the SC and that the SC controls mass transfer through the skin, then the resulting concentration of the chemical in the SC, as a function of time and position x, is given by the appropriate solution to Fick's second law of diffusion (Crank, 1975). The typical boundary conditions applicable in skin absorption experiments are (1) that the SC is initially free of chemical (i.e., at $t = 0$, $C = 0$ for $0 < x < L$); (2) that the chemical concentration in the surface layer of the SC (C_o) is equal to a concentration in equilibrium C_{eq} with the concentration in the vehicle C_v (i.e., at $x = 0$, $C = C_o = C_{eq} = K_{sc/v} C_v$ for $t \geq 0$, where $K_{sc/v}$ is the SC–vehicle partition coefficient); and (3) that the viable epidermis acts as a sink for chemical that has permeated the SC (i.e., at $x = L$, $C = 0$ for $t \geq 0$, where L is the apparent thickness of the SC). Under these conditions, the concentration profile is given by (Crank, 1975)

$$C = C_{eq} \left\{ 1 - \frac{x}{L} - \frac{2}{\pi} \sum_{n=1}^{\infty} \frac{\sin\left(\pi n x / L\right)}{n} \exp\left(\frac{-n^2 \pi^2 t_{\exp}}{6 t_{lag}} \right) \right\} \tag{11.2}$$

where t_{lag} is the lag time through the SC and is related to the apparent diffusion coefficient of the chemical in this membrane (D) as $t_{lag} = L^2/(6D)$.

Equation 11.2 has been used to fit the unsteady-state concentration profile of CP across human SC following exposure to a saturated solution of chemical (Pirot et al., 1997), and the surface concentration and the diffusion coefficient parameters ($C_o = C_{eq}$ and D/L^2) were estimated. These values could then be substituted back into Equation 11.2 and the profile recalculated (i.e., predicted) at different times. A comparison of predicted and experimental results has demonstrated the predictive capabilities of Equation 11.2 (Pirot et al., 1997).

In this work, the vehicle for CP was either soil or neat powder, for which an additional mass transfer resistance (i.e., the slow transfer of chemical from soil to SC) may exist. If this resistance is sufficiently large, it may have a discernible effect on overall dermal penetration. This scenario was addressed by McCarley and Bunge (1998), who introduced into the simple model described above a vehicle mass transfer resistance factor α that modifies the solution to Fick's second law as follows:

$$C = C_{eq}\left\{\frac{\alpha}{1+\alpha}\left(1-\frac{x}{L}\right) - 2\alpha\sum_{n=1}^{\infty}\frac{\alpha\,\sin\left(\lambda_n x/L\right)+\lambda_n\cos\left(\lambda_n x/L\right)}{\lambda_n\left(\alpha^2+\alpha+\lambda_n^2\right)}\exp\left(\frac{-\lambda_n^2 t}{6t_{lag}}\right)\right\} \tag{11.3}$$

in which the eigenvalues λ_n satisfy the identity: $\alpha \tan \lambda_n + \lambda_n = 0$. Equation 11.3 was developed assuming (1) that the SC is initially free of chemical, (2) that the transport of chemical from the soil vehicle into the SC is described by a first-order mass transfer coefficient, and (3) that the concentration of the absorbing chemical at the innermost layer of the SC is zero.

The parameter $\alpha = k_o L/D$ is the ratio of the rate of chemical transfer from the soil to the SC (a process that can be characterized by a mass transfer coefficient k_o, which has units of cm s^{-1}) to the rate of mass transport through the SC (i.e., D/L). Thus, when $\alpha > 1$, the SC resistance is most important; on the other hand, for $\alpha < 1$, mass transfer from the soil to the SC limits the dermal absorption rate. When the mass transfer resistance from the vehicle is insignificant, the concentration of chemical on the skin surface (i.e., C_o) is equal to C_{eq} (see Equation 11.2). By comparison, when the mass transfer resistance within the vehicle is not small relative to that in the SC (i.e., α is not very large), then at steady state C_o is reduced relative to C_{eq} as specified by Equation 11.3. That is,

$$C_o = \left(\frac{\alpha}{1+\alpha}\right)C_{eq} \tag{11.4}$$

Furthermore, as illustrated in Figure 11.1, which is constructed from Equation 11.3, it takes some time for C at $x = 0$ to reach C_o. The time required for C to equal C_o decreases as the relative significance of the vehicle mass transfer resistance decreases

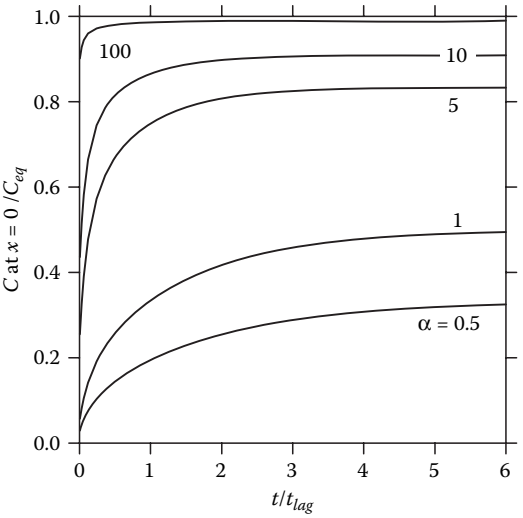

Figure 11.1 Normalized chemical concentration at the surface of the SC plotted as a function of dimensionless time when the mass transfer rate from the vehicle relative to that in the SC varies from small to large (α = 0.5 to 100).

(i.e., as α increases). In the limit of very large α, C is immediately equal to C_o consistent with Equation 11.2.

When α is not very large, the additional time required for C at $x = 0$ to reach C_o increases the lag time $t_{lag,v}$ relative to the lag time through the SC alone t_{lag} as follows (McCarley and Bunge, 1998):

$$t_{lag,v} = \left(\frac{3+\alpha}{1+\alpha}\right) t_{lag} \tag{11.5}$$

Notably, a mass transfer resistance within the vehicle can only increase the lag time by a factor of three.

As long as concentration within the vehicle does not change and clearance from the SC does not affect mass transfer across the barrier (that is, the deeper skin layers and the uptake into the cutaneous circulation are rapid compared to penetration through the SC), the steady-state flux J_{ss} through the SC is given by

$$J_{ss} = \frac{C_o D}{L} = \frac{C_o L}{6 t_{lag}} \tag{11.6}$$

Hence, using Equation 11.6 we can estimate J_{ss} knowing C_o and t_{lag}.

RESULTS AND DISCUSSION

Figure 11.2 shows the concentration profile of CP from subjects A through D after applying contaminated soil for 45 and 180 min. The curves were calculated using t_{lag} and C_o derived from best-fit regressions of Equation 11.2 to the measured data for each subject and each application time. The calculated values of t_{lag} and C_o for each subject, summarized in Table 11.1, were determined by minimizing the sum of the residual squared (SRS) between experimental and model-simulated tape-stripping concentrations. It is common for the first few tape strips to be more variable than the later tape strips because of the presence of some residual chemical at the surface of the skin. This was especially the case for subjects A through D, for whom the application site was cleaned without the use of any water. Some investigators have then excluded the first one or few tape strips in their data analysis (Shah et al., 1998). For subjects A, C, and D, the amount of CP on the first one or two tape strips appeared to be disproportionately large relative to the other tape strips, which is consistent with incomplete cleaning of the skin surface. For these subjects, best-fit regressions were completed that did and did not include these data (indicated in Figure 11.2 by dashed and solid curves, respectively).

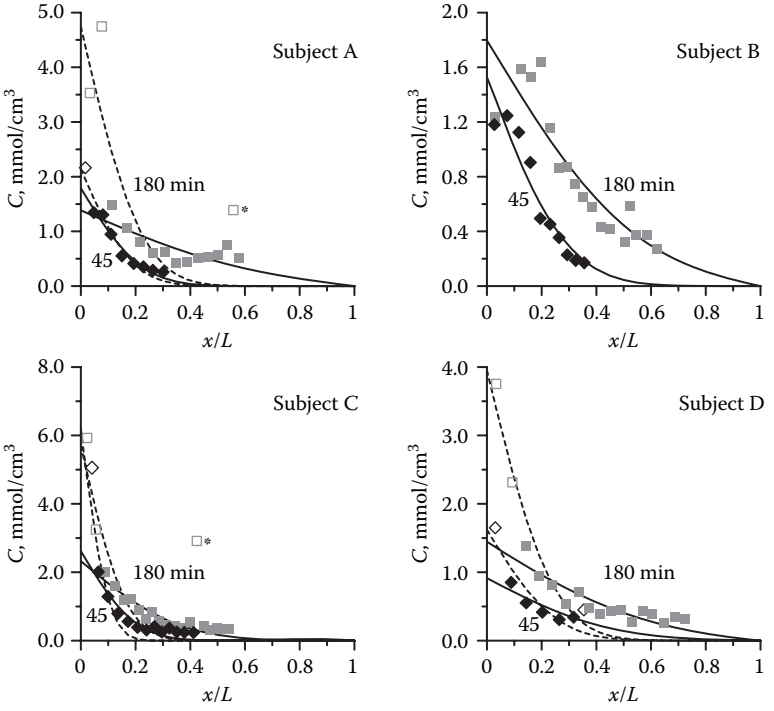

Figure 11.2 Concentration profiles after contaminated soil was applied for 45 min (diamonds) and 180 min (squares). Curves were derived by data regression to Equation 11.2 assuming the lag time was different for the two application times. Dashed curves were developed using all data points except those designated by an asterisk; solid curves were developed using only the data designated by solid symbols.

Table 11.1 Apparent Lag Times t_{lag} and Surface Concentrations C_o Determined by Best-Fit Regression of Equation 11.2 to Tape Strip Data Collected After Application of Contaminated Soil for 45 and 180 Min

	45-min Application Time				180-min Application Time			
Subject	L (μm)	C_o (mmol/cm^3)	t_{lag} (h)	Tape Strips Excluded[a]	L (μm)	C_o (mmol/cm^3)	t_{lag} (h)	Tape Strips Excluded[a]
A	10.6	2.14	11.3	None	8.7	4.74	33.1	14
		1.79	8.23	1		1.38	3.84	1, 2, 14
B	16.2	1.53	4.74	None	16.9	1.80	5.33	None
C	12.6	6.19	41.6	None	13.3	5.71	60.2	15
		2.62	10.2	1		2.33	12.9	1, 2, 15
D	8.4	1.62	6.50	None	8.1	3.95	27.7	None
		0.91	2.04	1		1.45	4.67	1, 2
E	18.0	0.30	1.19	None	14.8	0.37	0.42	None
F	12.5[b]	0.29	1.06	None	12.5[b]	0.49	6.79	None
						0.29	1.46	1

Note: Calculations assumed that t_{lag} could be different for the two application times.

[a] Tape strip number counted in order of application for each time (i.e., 1 is the first strip).
[b] Thickness measured at only one location.

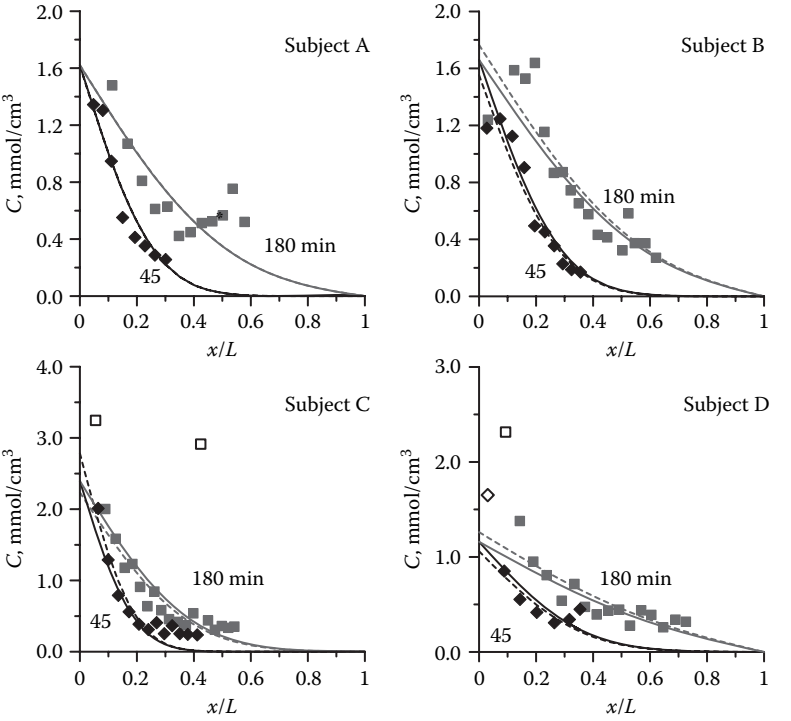

Figure 11.3 Concentration profiles after contaminated soil was applied for 45 min (diamonds) and 180 min (squares). Curves were derived by data regression to Equation 11.2 using the data points designated by solid symbols and assuming the lag time was the same for the two application times. Results are shown for regressions in which it was assumed that the surface concentrations C_o for the two application times were either the same (solid curves) or different (dashed curves).

Figure 11.3 presents the same data as Figure 11.2 but with best-fit regressions derived under the assumption that t_{lag} should be the same for both application times in a single subject. The regression procedure used here excluded the elevated values in the first one or two tape strips and assumed that C_o either was or was not the same for the two application times (designated by the solid and dashed curves, respectively). In these regressions, the data for each application time were weighted equally by minimizing the sum of the average sum of the residual squared (SRS) for each application time. Best-fit values of t_{lag} and C_o for the curves shown in Figure 11.3 are listed in Table 11.2 along with values calculated by regression including the first one or two tape strips. As seen from Figure 11.3 and Table 11.2, regression results derived assuming C_o was and was not the same for the two application times produced similar results.

For comparison, results from previous studies of CP absorption into human skin *in vivo* and *in vitro* are summarized in Table 11.3. Except for one study of pure powder, the results listed in Table 11.3 were measured from saturated aqueous solutions. The thermodynamic activity of CP (and driving force for dermal absorption) in a saturated aqueous solution is the same as for pure CP powder and for soil

Table 11.2 **Apparent Lag Times t_{lag} and Surface Concentrations C_o Determined by Best-Fit Regression of Equation 11.2 to Tape Strip Data Collected After Application of Contaminated Soil for 45 and 180 Min**

	Different C_o						
	C_o (mmol/cm^3)			Same C_o		Tape Strips Excluded[a]	
Subject	45 min	180 min	t_{lag} (h)	C_o (mmol/cm^3)	t_{lag} (h)	45 min	180 min
A	2.51	4.29	23.3	3.15	10.8	None	14
	1.62	1.62	6.11	1.62	6.10	1	1, 2, 14
B	1.55	1.77	5.03	1.66	4.98	None	None
C	6.53	5.43	50.1	5.84	50.2	None	15
	2.78	2.24	11.7	2.40	11.4	1	1, 2, 15
D	2.12	3.54	19.2	2.62	15.4	None	None
	1.06	1.26	3.24	1.16	3.24	1	1, 2
E	0.29	0.37	0.94	0.35	1.61	None	None
F	0.34	0.40	2.49	0.37	2.58	None	None
	0.29	0.29	1.06	0.29	1.04	None	1

Note: Calculations assumed that t_{lag} was the same for the two application times.

[a] Tape strip number counted in order of application (i.e., 1 is the first strip).

contaminated with more CP than required to saturate the soil's organic matter. Significantly, in experiments from a saturated aqueous solution, C_o varied from about 0.6 to 2.5 mmol cm^{-3}, with an average value of about 1 mmol cm^{-3}. These are smaller than C_o in the soil experiments of subjects A through D when data from all tape strips were used, supporting the premise that cleaning of the skin surface was incomplete in these subjects.

When the amount of CP on the first one or two tape strips is elevated, the curvature of the concentration profile is more pronounced than it should be. As a result, t_{lag} estimated from the best-fit regression including all the data was larger than t_{lag} calculated without the first one or two tape strips. However, even when the first one or two tape strips were not included in the analysis, the t_{lag} values for subjects A through D were 7- to 20-fold larger than the value of about 0.5 h determined for CP absorption from saturated water (see Table 11.3). If mass transfer from contaminated soil is much slower than mass transfer from a saturated aqueous solution, then the lag time would increase by at most a factor of three (see Equation 11.5). Furthermore, if mass transfer limitations in the soil contributed significantly, then for the estimated values of t_{lag}, C_o should be larger after an application time of 180 min compared to 45 min (Figure 11.1), a fact that is not supported by the data from subjects A through D (see Table 11.2). Thus, for these subjects there is little evidence that mass transfer of CP from the contaminated soil was slower than transfer through skin, and the larger-than-expected values for t_{lag} must have another cause.

Equation 11.2 will describe the amount of chemical on tape strips provided the stripping procedure occurs immediately and rapidly following removal of chemical from the skin surface. If the tape-stripping procedure is slow relative to chemical diffusion, taking longer than about 0.2 times the lag time for chemical to diffuse through the SC (t_{lag}), then the concentration of chemical in the SC continues to change as specified by Fick's second law (Reddy et al., 2002).

In the experiments on subjects A through D, TEWL measurements were performed after every fourth tape strip. Given that it required about 20 sec, on average, to remove each tape strip, and that each TEWL measurement took about 3 min, then the total duration of the SC removal process (including the time necessary to clean the surface postexposure) approached 30 min, which represents a significant fraction of t_{lag}. It follows that changes in the CP profile during the tape-stripping procedure were likely. Therefore, to describe the final distribution observed in this case, it would be necessary to solve Fick's second law at different times in the stripping process taking into account the amount of SC already removed and the amount that remains. The boundary conditions at the surface of the remaining SC would now be different from that used to derive Equation 11.2; of course, since there is no chemical replacement because the exposure has ended. An analytical solution of this problem is not possible, and the mathematical treatment requires numerical methods and knowledge of the time course of the tape strip collection, which was not recorded. This hypothesis could, however, explain the larger than expected values of t_{lag} calculated for subjects A to D.

The effect of slow tape-stripping is illustrated in Figure 11.4, which was taken from Reddy et al. (2002). In this experiment, CP was applied to skin in a saturated aqueous solution for 1 h, after which the site was tape stripped 30 times in less than

Table 11.3 Previously Reported Surface Concentrations C_o, Lag Times t_{lag}, and Steady-State Fluxes J_{ss} After Application of Saturated Water or Pure Powder CP to Human Skin *In Vivo* and *In Vitro*[a]

Reference	Type of Experiment[b]	n[c]	L (μm)	C_o (mmol/cm^3)	t_{lag} (h)	J_{ss} (μg cm^{-2} h^{-1})
Pirot et al., 1997	*In vivo*, SW	3	15[d]	1.54 ± 0.56[e]	0.54 ± 0.10[f]	83 ± 18
Reddy et al., 2002[g]	*In vivo*, SW	3	10.2 ± 1.5[h]	0.98 ± 0.07	0.52 ± 0.08	38 ± 4.4
Stinchcomb et al., 1999[i]	*In vivo*, SW	2	5.0/10.8[h]	2.52/0.63	0.2/0.18	126/75
Romonchuk and Bunge, 2004[j]	*In vitro*, SW	12	—	—	—	168 ± 33
Romonchuk and Bunge, 2004[j]	*In vitro*, PP	12	—	—	—	12 ± 6

[a] Unless noted otherwise, data are listed as mean ± standard deviation.
[b] SW, saturated water; PP, pure powder.
[c] Number of subjects except in the *in vitro* experiments, which were replicates from one subject.
[d] Thickness of SC was assumed to be 15 μm.
[e] Average and standard deviation of three subjects after 15- and 60-min application times (i.e., includes six measurements).
[f] Average and standard deviation of three subjects after a 15-min application time.
[g] After a 60-min application, skin was tape stripped either immediately or after waiting 60 min. C_o was determined from the immediate tape strip data; t_{lag} was calculated from the tape strip data collected after a 60-min delay.
[h] Calculated from the total amount of SC removed by all tape strips. This tends to underestimate the SC thickness compared to the TEWL method used in this study.
[i] C_o and t_{lag} were deduced from an unsteady-state analysis of the average concentration of the combined tape strips from each of three application times: 1, 5, and 15 min. Of the four subjects studied, data for two were outside the unsteady-state period and are not included here. Parameter values for the remaining two subjects are listed.
[j] Also available in Romonchuk and Bunge, 2003.

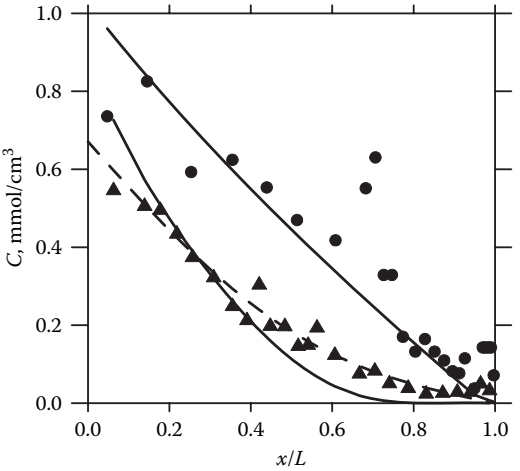

Figure 11.4 Concentration of CP as a function of relative position within the SC after a 60-min application of a saturated aqueous solution and tape strip removal of the SC that took either 1 h (triangles) or less than 6 min (circles) to complete. The dashed curve, calculated by regressing Equation 11.2 to the data represented by the triangles, corresponds to C_o = 0.67 mmol cm^{-3} and t_{lag} = 1.58 h. The two solid curves, calculated by regressing all of the data to a mathematical model that accounted for CP diffusion while the tape-stripping proceeded, corresponds to C_o = 1.0 mmol cm^{-3} and t_{lag} = 0.67 h. This figure is taken from Reddy et al. (2002), which also provides details of the calculations that include diffusion while tape-stripping.

6 min or over a period of 1 h. As expected from the results summarized in Table 11.3, the 1-h application time was long enough to achieve steady state, as indicated by a linear concentration profile when tape-stripping was fast (i.e., the circles in Figure 11.4). However, when the time to tape strip was about two times t_{lag}, the concentration profile looks nonlinear (i.e., the triangles in Figure 11.4). If Equation 11.2 is regressed to the data from the slow tape strip procedure, then the calculated value for t_{lag} is approximately threefold larger than its actual value. Because the time course of the tape strip collection was known in this experiment, the solution of Fick's second law accounting for diffusion during the slow tape-stripping procedure, which is shown in Figure 11.4 as the solid curve, was used to obtain values for C_o and t_{lag} (1.0 mmol cm^{-3} and 0.67 h, respectively) that were comparable to results from other studies (Reddy et al., 2002).

In a second series of experiments conducted on subjects E and F, the TEWL measurements were completed separately on skin adjacent to the site of soil application. As a result, the application site could be cleaned more thoroughly using small amounts of water, and tape strip collection was rapid. The concentration profiles for subjects E and F are presented in Figure 11.5 and Figure 11.6. The curves shown in Figure 11.5 were derived by best-fit regression to Equation 11.2 allowing both t_{lag} and C_o to be different for the two application times. The curves in Figure 11.6 were calculated assuming t_{lag} was the same for both application times and that C_o was and was not the same. Table 11.1 and Table 11.2 list the numerical values for t_{lag} and C_o used to generate the curves shown in Figure 11.5 and Figure 11.6 for subjects E and F.

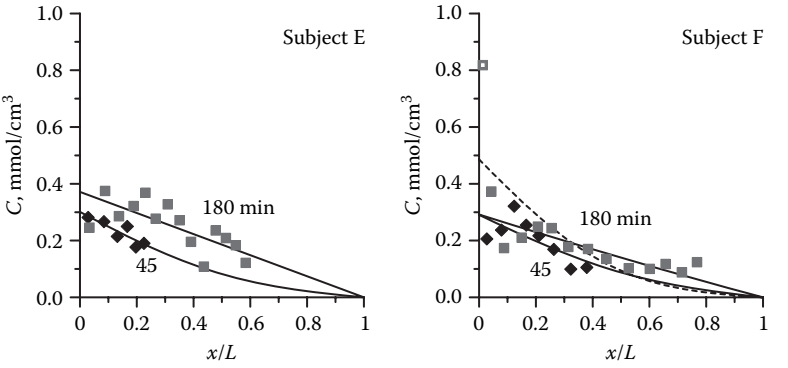

Figure 11.5 Concentration profiles after contaminated soil was applied for 45 min (diamonds) and 180 min (squares). Curves were derived by data regression to Equation 11.2 assuming the lag time was different for the two application times. Solid curves were derived from the data designated by solid symbols; the dashed curve for subject F following application of CP for 180 min was developed from the data designated by solid squares and the open square for the point at very small x/L.

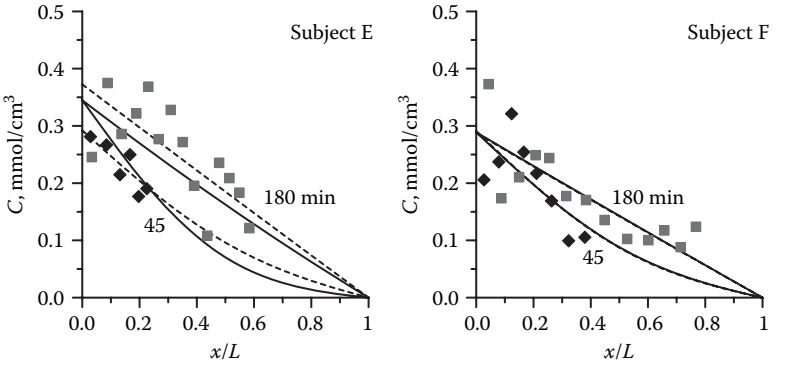

Figure 11.6 Concentration profiles after contaminated soil was applied for 45 min (diamonds) and 180 min (squares). Curves were derived by data regression to Equation 11.2 using the data points designated by solid symbols and assuming the lag time was the same for the two application times. Results are shown for regressions in which it was assumed that the surface concentrations C_o for the two application times were the same (solid curves) or different (dashed curves). For subject F, the dashed and solid curves are coincident.

For subjects E and F, the first two tape strips did not appear to be elevated compared to the amount of chemical on the other tape strips, except for the 180-min application time on subject F. This is consistent with the improved surface-cleaning procedure compared with that used for subjects A through D. Values of C_o measured in subjects E and F were three to five times smaller than those determined in subjects A through D even when the first one or two tape strips from subjects A through D were excluded. Interestingly, values of C_o calculated for subjects E and F were smaller than from saturated water by a factor of about three.

The calculated values of t_{lag} for subjects E and F were smaller than for subjects A through D but larger than observed from saturated water by a factor of about two. If a mass transfer limitation in the soil were the cause for this increased t_{lag}, then from Equation 11.5 we would estimate that $\alpha \approx 1$. If so, then we would expect $C_o = C_{eq}/2$, which is a little larger than was experimentally observed assuming that $C_o = C_{eq}$ in the saturated water experiments. Based on experiments from saturated water, t_{lag} is 0.5 h, meaning that t/t_{lag} is 1.5 and 6, respectively, for 45- and 180-min application times. As shown in Figure 11.1, C_o from a 45-min application time would be only slightly smaller (by about 20%) than that from the 180-min application time. This difference is small enough that it would be difficult to discern experimentally.

Estimates of steady-state flux calculated from Equation 11.6 should use t_{lag} for diffusion through the SC not including any mass transfer resistance from the vehicle. Based on previous measurements from saturated water, we estimate that t_{lag} is approximately 35 min (i.e., 0.58 h). Using this value and estimates for C_o, we have calculated J_{ss} for the six subjects studied here. The results are shown in Table 11.4.

For subjects A through D, the average value for J_{ss} was 71 μg cm^{-2} h^{-1}, a value similar to that from saturated water (see Table 11.3). This is rather surprising given recent *in vitro* experiments in which the flux from pure powder (with an average particle diameter of 50 μm) was 12 ± 6 μg cm^{-2} h^{-1}, compared with 168 ± 33 μg cm^{-2} h^{-1} for saturated water (Table 11.3). In these *in vitro* experiments, J_{ss} was measured first for the pure powder, and then, after replacing the powder with saturated water, J_{ss} was determined for water (Romonchuk and Bunge, 2003, 2004). Because the CP concentration in the contaminated soil studied here was larger than the soil's solubility limit, we might expect dermal absorption from this matrix to be similar to CP powder. Values of J_{ss} estimated for subject E and subject F (21 and 12 μg cm^{-2} h^{-1}, respectively) are consistent with the *in vitro* experiments from CP powder listed in Table 11.3.

The results of tape-stripping experiments following application of CP powder for 45 and 120 min are presented in Figure 11.7. Because the data scatter was large, a best-fit regression analysis was not performed. Unlike the *in vitro* powder experiments summarized in Table 11.3, CP particle size was not controlled in this study, and this may explain some of the variability. Even then, it is apparent that C_o is comparable to that observed from soil for subjects E and F. Except for subject H, C_o was essentially the same for the 45- and 120-min application times.

Based on the estimated values for C_o and t_{lag} for contaminated soil measured in subjects E and F and the results shown in Figure 11.7 for powders, it is tempting to conclude that the rates of CP mass transfer from this heavily contaminated soil and from the CP powder are similar to CP penetration rates for skin (i.e., $\alpha \approx 1$). However, results from experiments comparing CP penetration through silicone rubber (i.e., polydimethylsiloxane) membranes from powders and saturated water are inconsistent with this conclusion. Specifically, the steady-sate flux of CP from pure powder (with an average diameter of about 50 μm) was approximately 90% of that measured from saturated water (Romonchuk and Bunge, 2003, 2004). Furthermore, in recent experiments using the same soil contaminated with 0.03 g CP/g soil (which is larger than the CP solubility limit of ~ 0.003 g/g for this soil; Chen et al., 2004), CP flux was the same as from pure powders until absorption into the silicone membrane

Table 11.4 Apparent Steady-State Flux J_{ss} Across Skin Calculated Using Equation 11.5 Assuming that C_o Was the Same for the 45- and 180-min Application Times When Determined by Data Regression to Equation 11.2 and Using t_{lag} Listed

Subject	Average L (μm)	C_o (mmol/cm^3)	t_{lag}[b] (h)	J_{ss} (μg cm^{-2} h^{-1})	Tape Strips Excluded[a]	
					45 min	180 min
A	9.65	1.62	0.58	53	1	1, 2, 14
B	16.6	1.66	0.58	93	None	None
C	13.0	2.40	0.58	106	1	1, 2, 15
D	8.3	1.16	0.58	33	1	1, 2
E	16.4	0.35	1.56[c]	7.5	None	None
	16.4	0.35	0.58	21	None	None
F	12.5	0.29	1.04[c]	6.9	None	1
	12.5	0.29	0.58	12	None	1

[a] Tape strip number counted in order of application (i.e., 1 is the first strip).
[b] Unless specified otherwise, t_{lag} is 35 min (0.58 h), which was measured in experiments from saturated water.
[c] Values of t_{lag} determined by regression to Equation 11.2 assuming t_{lag} and C_o were the same for both application times.

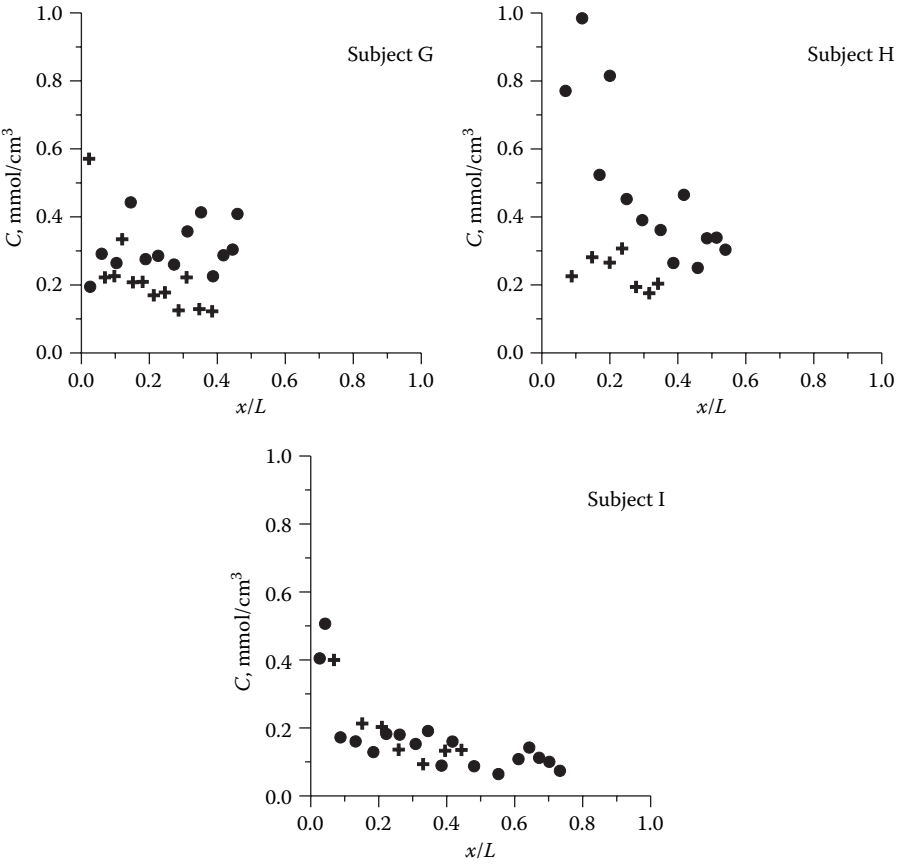

Figure 11.7 Concentration profiles after application of powdered CP for 45 min (crosses) and 120 min (circles).

significantly depleted the amount of CP (Deglin et al., 2004). These results suggest that the mass transfer parameter for these silicone rubber membranes α_{SR} could not be smaller than approximately 10 (see Figure 11.1). The mass transfer parameter for the SC (α) is related to α_{SR} as follows:

$$\alpha = \alpha_{SR} \frac{D_{SR}}{L_{SR}} \frac{L}{D} = \alpha_{SR} \frac{D_{SR}}{L_{SR}} \frac{6t_{lag}}{L} \tag{11.7}$$

where D_{SR} is the diffusion coefficient for CP in silicone rubber (approximately 0.001 $cm^2\ h^{-1}$; McCarley and Bunge, 2003), and L_{SR} is the membrane thickness (~350 μm). For L = 15 μm and t_{lag} = 35 min, it is estimated that $\alpha \approx 670$, which means that mass transfer through skin should be much slower than mass transfer from the powder (or soil) to skin. Stated differently, if α were 1 for CP transfer from soil or powder to skin (as speculated above), then α_{SR} would be ~ 1/670 = 0.0015. This

should cause the ratio of steady-state fluxes through silicone rubber from powders and water to be about 0.0015 [$= \alpha_{SR}/(1 + \alpha_{SR})$]. Clearly, this was not the case, casting doubt on the hypothesis that slow transfer rates from the soil and powder in this study caused the differences in dermal absorption of CP from contaminated soil and water.

An alternate explanation is that only a fraction of the skin surface actually touches a particle, even when solid particles completely cover the skin surface. As a result, only a fraction of the skin surface can equilibrate with respect to the *saturated* solution, and the transport is reduced compared to the saturated aqueous solution, which is in intimate contact with the entire exposed surface. If CP penetrates the SC through the intercellular lipid bilayers surrounding the nearly impermeable keratinized skin cells (i.e., the keratinocytes), then only the area where the intercellular lipids are exposed to the skin surface would be available for chemical penetration. Typically, intercellular lipids are reported to account for about 10% of the SC mass (Johnson et al., 1997). Ignoring density differences of the lipids and keratinocytes and assuming simplistically that the fraction of intercellular lipids on the SC surface is the same as the volume fraction within the SC, then only about 10% of the skin surface would be available for chemical absorption. Compared with the heterogeneous permeability of the SC, the silicone rubber membranes are homogeneous, permitting transfer through the entire membrane surface and thus a larger flux than observed for skin.

One other explanation is that either solubility or diffusion of CP in skin is affected significantly when skin is completely hydrated as compared to partially hydrated (that is, the skin surface is covered in water rather than left open to air). Based on the results from subjects E and F, we would estimate that the ratio of CP diffusion and partitioning into the partially hydrated SC are each reduced by a factor of about three compared with fully hydrated SC. As a result, steady-state flux across the fully hydrated SC would be about an order of magnitude greater than that across the partially hydrated SC. Although this possibility cannot be discounted, of the handful of studies that examined hydration, effects of two- to fourfold are more typical. Furthermore, the effect of increased hydration is reported to be diminished for more hydrophilic compounds such as hydrocortisone (Bucks et al., 1991). This is significant because log $K_{o/w}$ for CP (1.60) is similar to hydrocortisone (1.61).

If either of these last two explanations is the source of the reduced flux from a saturated soil or pure powder compared with saturated water, then the larger lag time calculated for subjects E and F (i.e., 1.56 and 1.04 h, respectively) would represent diffusion through the SC. As a result, flux through the SC should be calculated using these values of t_{lag} rather than 0.58 h estimated for CP absorption from saturated water. When calculated this way, J_{ss} is approximately 7 $\mu g\ cm^{-2}\ h^{-1}$, which is about 1/10th of J_{ss} determined from saturated water. This is similar to the *in vitro* results summarized in Table 11.3 for pure powder and saturated water. These data are also consistent results observed *in vitro* with hairless mouse skin and for cellulosic membranes (Touraille et al., 1998, 2005): The steady-state fluxes of CP measured from saturated soil and pure powders are approximately an order of magnitude smaller than those from an aqueous saturated solution.

For the heavily contaminated soil studied here, there is approximately 1 mg of CP cm^{-2} in the soil particles that would directly contact the skin surface, estimated to be approximately 2 mg of soil per square centimeter (Duff and Kissel, 1996). This is enough CP that the concentration in the soil layer in contact with skin would not change during the experiment. If the amount of CP on the soil relative to the flux across the skin or membrane were smaller, then absorption would reduce CP concentration and the flux. However, because a nonvolatile chemical such as CP can only transfer to skin from particles in direct contact with the skin surface, increasing the amount of applied soil above that required to cover the skin surface completely with a single layer has little effect. Although not shown here, this has been observed for CP-contaminated soils applied to silicone rubber membranes (Deglin et al., 2004).

CONCLUSION

Dermal absorption to chemically contaminated soil has been studied *in vivo* through human skin with CP as a model chemical. Using a simple solution to Fick's second law of diffusion, the surface concentration of CP (C_o) and the lag time of CP through human skin t_{lag} are estimated. When the vehicle is not in intimate contact with the skin, as might occur with soil, a vehicle-side resistance could be expected. Compared to a saturated aqueous solution, t_{lag} was larger, and the steady-state flux and C_o were smaller from a saturated soil. The steady-state flux values determined by *in vitro* methods for this saturated soil and pure powder were similar. This is consistent with the *in vivo* tape strip result that C_o was the same for the saturated soil and pure powder as long as the skin surface was cleaned well at the end of the exposure. Although these findings could be consistent with a vehicle-side mass transfer resistance, experiments comparing CP absorption from pure powder and saturated aqueous solution in human skin *in vitro* and across silicone rubber membranes suggest otherwise. It seems likely that, for the heavily contaminated soil studied here, the SC was the rate-limiting factor to the absorption of CP. Meanwhile, the data confirm results already observed *in vitro* with hairless mouse skin and a cellulosic membrane: The steady-state fluxes of CP measured from saturated soil and pure powders are approximately an order of magnitude smaller than those from an aqueous saturated solution.

ACKNOWLEDGMENTS

This work was supported in part by the National Institute of Environmental Health Sciences (ES06825), the U.S. Environmental Protection Agency (CR824053, R826684, R830131), and the U.S. Air Force Office of Scientific Research (F49620-95-1-021).

NOTATION

C	Concentration of diffusing solute in the SC
C_{eq}	Concentration of diffusing solute in the SC in equilibrium with the vehicle $= K_{sc/v}C_v$
C_o	Surface concentration of diffusing solute in the SC (i.e., C at $x = 0$)
C_v	Concentration of diffusing solute in the vehicle
[CP]	Amount of CP in a tape (nmol cm^{-2})
D	Effective diffusion coefficient of the absorbing chemical in the SC
D_{SR}	Diffusion coefficient of the absorbing chemical in the silicone rubber membrane
J_{ss}	Steady-state flux
k_o	Mass transfer coefficient describing the rate of chemical transfer from the soil to the SC
$K_{sc/v}$	Equilibrium partition coefficient between the SC and vehicle for the absorbing chemical
L	Effective thickness of the SC
L_{SR}	Thickness of the silicone rubber membranes
PA	Peak area in the Fourier transform infrared measurement
SC	Stratum corneum
TEWL	Transepidermal water loss
t	time
t_{lag}	Lag time for diffusion across the SC
$t_{lag,v}$	Lag time for transfer from a vehicle to the SC combined with diffusion across the SC
x	Position within the SC

GREEK

α	Ratio of the rates of chemical transfer from the soil to the SC and through the SC $= k_oL/D$
α_{SR}	Ratio of the rates of chemical transfer from the soil to the silicone rubber membrane and through silicone rubber membrane $= k_oL_{SR}/D_{SR}$
λ_n	Eigenvalues satisfying the identity that $\alpha \tan \lambda_n + \lambda_n = 0$

REFERENCES

Bommannan, D., Potts, R.O., and Guy, R.H. (1990). Examination of stratum corneum barrier function *in vivo* by infrared spectroscopy, *J. Invest. Dermatol.,* 95**:**403–408.

Bucks, D., Guy, R., and Maibach, H. (1991). Effects of occlusion, in R.L. Bronaugh and Maibach, H.I. (eds.), *In Vitro Percutaneous Absorption: Principles, Fundamentals, and Applications*, Boca Raton, FL: CRC Press, pp. 85–114.

Bunge, A.L. and Parks, J.M. (1998). Soil contamination: theoretical descriptions, in M.S. Roberts and K.S. Walters (eds.), *Dermal Absorption and Toxicity Assessment*, New York: Dekker, pp. 669–696.

Chen, C.-P., Macalady, D.L., and Bunge, A.L. (2004). Soil solubility and soil-water partitioning of PAH contaminated soils determined by solid phase sorption, in preparation.

Choate, L.M. (2002). The effect of variations in soil organic matter with particle size on organic contaminate sorption and its relationship to dermal exposure, Ph.D. thesis, Colorado School of Mines, Golden.

Clancy, M.J., Corish, J., and Corrigan, O.I. (1994). A comparison of the effects of electrical current and penetration enhancers on the properties of human skin using spectroscopic (FTIR) and calorimetric (DSC) methods, *Int. J. Pharm.,* 105**:**47–56.

Crank, J. (1975). *The Mathematics of Diffusion,* Oxford, U.K.: Oxford Science Publication.

Deglin, S.E., Macalady, D.L., and Bunge, A.L. (2004). In K.R. Brain and K.A. Walters (eds.), *Perspectives in Percutaneous Penetration*, Vol. 9a, La Grande Motte, France: STS Publishing, p. 87.

Duff, R.M. and Kissel, J.C. (1996). Effect of soil loading on dermal absorption efficiency from contaminated soil, *J. Toxicol. Env. Health,* 48**:**93–106.

Guy, R.H. (1996). Current status and future prospects of transdermal drug delivery, *Pharm. Res.,* 13**:**1765–1769.

Higo, N., Naik, A., Bommannan, D.B., Potts, R.O., and Guy, R.H. (1993). Validation of reflectance infrared spectroscopy as a quantitative method to measure percutaneous absorption *in vivo*, *Pharm. Res.,* 10**:**1500–1506.

Jadoul, A., Hanchard, C., Thysman, S., and Preat, V. (1995). Quantification and localization of fentanyl and TRH delivered by iontophoresis in the skin, *Int. J. Pharm.,* 120**:**221–228.

Johnson, M.E., Blankschtein, D., and Langer, R. (1997). Evaluation of solute permeation through the stratum corneum: Lateral bilayer diffusion as the primary transport mechanism, *J. Pharm. Sci.,* 86**:**1162–1172.

Kalia, Y.N., Pirot, F., and Guy, R.H. (1996). Homogeneous transport in a heterogeneous membrane: water diffusion across human stratum corneum *in vivo*, *Biophys. J.,* 71**:**2692–2700.

Knutson, K., Krill, S.L., Lambert, W.J., and Higuchi, W.I. (1987). Physicochemical aspects of transdermal permeation, *J. Controlled Release,* 6**:**59–74.

Knutson, K., Potts, R.O., Guzek, D.B., Golden, G.M., McKie, J.E., Lambert, W.J., and Higuchi, W.I. (1985). Macro- and molecular physical-chemical considerations in understanding drug transport in the stratum corneum, *J. Controlled Release,* 2**:**67–87.

Mak, V.H., Potts, R.O., and Guy, R.H. (1990). Percutaneous penetration enhancement *in vivo* measured by attenuated total reflectance infrared spectroscopy, *Pharm. Res.,* 7**:**835–841.

Margarida, A., Tralhao, L., Watkinson, A.C., Brain, K.R., Hadgraft, J., and Armstrong, N.A. (1995). Use of ATR-FTIR spectroscopy to study the diffusion of ethanol through glycerogelatin films, *Pharm. Res.,* 12**:**572–575.

McCarley, K.D. and Bunge, A.L. (1998). Physiologically relevant one-compartment pharmacokinetic models for skin. 1. Development of models, *J. Pharm. Sci.,* 87**:**470–481.

McCarley, K.D. and Bunge, A.L. (2003). Absorption into silicone rubber membranes from powders and aqueous solutions, *Int. J. Pharm.,* 250**:**169–180.

Pellett, M.A., Watkinson, A.C., Hadgraft, J., and Brain, K.R. (1997). Comparison of permeability data from traditional diffusion cells and ATR-FTIR spectroscopy. Part II. Determination of diffusional pathlengths in synthetic membranes and human stratum corneum, *Int. J. Pharm.,* 154**:**217–227.

Pirot, F., Kalia, Y.N., Stinchcomb, A.L., Keating, G., Bunge, A., and Guy, R.H. (1997). Characterization of the permeability barrier of human skin *in vivo*, *Proc. Nat. Acad. Sci. USA,* 94**:**1562–1567.

Potts, R.O. and Francoeur, M.L. (1992). Physical methods for studying stratum corneum lipids, *Semin. Dermatol.,* 11**:**129–138.

Potts, R.O., Golden, G.M., Francoeur, M.L., Mak, V.H.W., and Guy, R.H. (1991). Mechanism and enhancement of solute transport across the stratum corneum, *J. Controlled Release,* 15**:**249–260.

Reddy, M.B., Stinchcomb, A.L., Guy, R.H., and Bunge, A.L. (2002). Determining dermal absorption parameters *in vivo* from tape-stripping data, *Pharm. Res.,* 19**:**292–297.

Romonchuk, W.J. and Bunge, A.L. (2003). Absorption of 4-cyanophenol from powder and saturated aqueous solution into silicone rubber membranes and human skin, *AAPS PharmSci,* 5(S1)**:**Abstract T2179, available at: http://www.aapspharmsci.org/.

Romonchuk, W.J. and Bunge, A.L. (2004). Absorption of 4-cyanophenol and methyl paraben from powder and saturated aqueous solution into silicone rubber membranes and human skin, unpublished data.

Schaefer, H. and Redelmeier, T.E. (1996). *Skin Barrier—Principles of Percutaneous Absorption,* Basel, Switzerland: Karger.

Shah, V.P., Flynn, G.L., Yacobi, A., Maibach, H.I., Bon, C., Fleischer, N.M., Franz, T.J., Kaplan, S.A., Kawamoto, J., Lesko, L.J., Marty, J.-P., Pershing, L.K., Schaefer, H., Sequeira, J.A., Shrivastave, S.P., Wilkins, J., and Williams, R.L. (1998). Bioequivalence of topical dermatological dosage forms—methods of evaluation of bioequivalence, *Pharm. Res.,* 15**:**167–171.

Stinchcomb, A.L., Pirot, F., Touraille, G.D., Bunge, A.L., and Guy, R.H. (1999). Chemical uptake into human stratum corneum *in vivo* from volatile and non-volatile solvents, *Pharm. Res.,* 16**:**1288–1293.

Touraille, G.D., Arnold, S.M., Bunge, A.L., Marty, J.-P., and Guy, R.H. (1998). Uptake of 4-cyanophenol from soils, water and pure solids, in K.R. Brain and Walters, K.A. (eds.), *Perspectives in Percutaneous Penetration*, Cardiff, U.K.: STS Publishing, pp. 92.

Touraille, G.D., McCarley, K.D., Bunge, A.L., Marty, J.-P., and Guy, R.H. (2005). Percutaneous absorption of 4-cyanophenol from freshly contaminated soil *in vitro*: effects of soil loadings and contamination concentration, *Environ. Sci. Technol.*, 39(10):3723–3731.

U.S. Environmental Protection Agency. (2001). *Risk Assessment Guidance for Superfund, Volume I: Human Health Evaluation Manual (Part E, Supplemental Guidance for Dermal Risk Assessment), Interim Guidance*, EPA/540/R/99/005, Washington, D.C.: Office of Emergency and Remedial Response.

CHAPTER 12

Assessing Efficacy of Penetration Enhancers

Babu M. Medi, Somnath Singh, and Jagdish Singh

CONTENTS

INTRODUCTION

Topical and transdermal delivery systems offer many advantages over other systems, including avoidance of gastric degradation, first-pass liver metabolism, and improved patient compliance. However, the major limitation of these delivery systems is that skin is highly impermeable to hydrophilic and macromolecular drugs, which is mainly attributed to the excellent barrier property of stratum corneum (SC). The successful transdermal formulation of a drug depends on the skin permeation rate of the drug to attain therapeutic drug level. As many of the drugs lack ideal physicochemical properties for percutaneous absorption, penetration enhancers are promising in the development of transdermal formulations. Penetration enhancers are chemical compounds that can reversibly alter the permeability of the skin, primarily by interacting with the constituents of the skin. Numerous chemicals have been investigated as percutaneous penetration enhancers. Advances in understanding of the makeup and function of SC resulted in testing a diverse range of compounds for their efficacy as percutaneous penetration enhancers. The goal of using penetration enhancers is to ensure that the drugs are delivered at a required rate from the transdermal formulations. The selection of an enhancer for a transdermal product should be based on its efficacy, lack of toxicity, and compatibility with other components of the transdermal system. This chapter focuses on the methods available to assess the efficacy of skin penetration enhancers along with a review of percutaneous absorption studies done so far using different classes of penetration enhancers.

ADVANTAGES AND LIMITATIONS OF PENETRATION ENHANCERS

Formulation of poorly penetrating drugs using penetration enhancers is a fairly common practice in transdermal drug delivery research. Percutaneous penetration enhancers help in accelerating the rate of transport of the otherwise impermeable/weakly permeable drugs across or into the skin. An ideal penetration enhancer should promote the penetration of drugs across the skin barrier in a predictable way without any irreversible effects on the skin barrier properties. It should be pharmacologically inert, odorless, colorless, nontoxic, nonirritating, nonallergenic, and compatible with most drugs and excipients. It should reversibly reduce the diffusional barrier of SC without damaging viable cells. The onset and duration of the enhancer effect should be predictable, reproducible, and reversible. Furthermore, it should be pharmaceutically and cosmetically acceptable. No single penetration enhancer can meet all the desirable properties of an ideal enhancer. Thus, it might be helpful to use a combination of penetration enhancers depending on the need of the situation. In addition, the effect of these enhancers on the properties of drug, such as the solubility of the drug in the delivery vehicle, should be considered carefully. Toxicity and skin irritation limit the practical application of many penetration enhancers in transdermal/topical drug delivery systems. Thus, the investigation continues for safe, effective, and generically useful penetration enhancers.

METHODS TO ASSESS THE EFFICACY OF PENETRATION ENHANCERS

Permeation Studies

In vitro permeation of potential drug candidates through skin is performed as a primary method to assess the efficacy of an enhancer. The *in vitro* method warrants the use of viable human or animal skin assembled in flow-through or static diffusion cells to get a good approximation (Bronaugh, 1998). Skin from the pig and monkey generally approximates the permeability of human skin (Wester and Maibach, 1989; Bhatia and Singh, 1996). Histological characteristics of pig and human skin are comparable with respect to epidermal thickness and composition, pelage density (Montagna and Yun, 1964), lipid content (Gray and Yardley, 1989), and general morphology (Meyer et al., 1978; Monteiro-Riviere, 1986). Carefully designed and conducted *in vitro* percutaneous absorption experiments can be good predictors of *in vivo* absorption (Bronaugh, 1989). The ability of static and flow-through systems to measure *in vitro* percutaneous absorption of chemicals was reported to be similar (Hughes et al., 1993; Clowes et al., 1994). Different types of diffusion cells were reported in the literature for this purpose (Brain et al., 2002). A wide range of molecules of varying molecular weights and polarities were tested for their percutaneous penetration and to assess the effects of enhancers on polar and nonpolar routes of SC (Barry, 1987).

Although percutaneous penetration results obtained *in vivo* in human volunteers are the most appropriate, it is not always ethically or practically feasible. Therefore, *in vivo* percutaneous absorption measurements are done using several animal models even though there is lack of good animal models for human skin (Priborsky and Muhlbachova, 1990). For this reason, a well-designed *in vitro* permeation experiment with human skin may be preferable to an *in vivo* animal study (Bronaugh, 1998). For extensive information on the animal models used in percutaneous absorption studies, refer to previous reviews (Wester and Maibach, 1999; Brain et al., 2002). Cutaneous microdialysis is used to determine the transdermal transport of drugs *in vivo* by implanting microdialysis probes in the dermis (Ault et al., 1992; Hegemann et al., 1995; McDonald and Lunte, 2003). This method can be used to demonstrate the kinetics of the transport of topically applied drugs from the skin surface to the dermis.

Diffraction Studies

The primary diffusion barrier of the SC is caused by the intercellular lipid domains located between the corneocytes. Investigation of the physical properties and molecular structure of these lipid domains is an important step in understanding the percutaneous absorption, which gives an insight into the effects of the penetration enhancers on SC lipids. X-ray and electron diffraction studies using small- and wide-angle are the most direct and powerful tools for acquiring this structural information for SC.

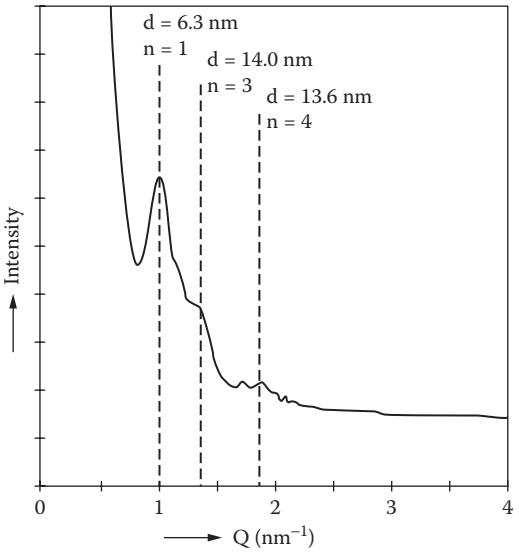

Figure 12.1 Small-angle x-ray scattergram obtained from 20 to 40% hydrated stratum corneum; d, unit cell repeat distance; n, order of reflection. (Reprinted from Cornwell, P.A., Barry, B.W. Bouwstra, J.A., and Gooris, G.S., *Int. J. Pharm.*, 127:9–26, 1996, with permission from Elsevier.)

The interference caused by an object in the path of waves results in diffraction. The x-rays incident on the sample interact with the electron clouds present in the molecules of the sample and are scattered onto a detector, which gives an imprint of the intensities and positions of the scattered x-rays. Therefore, the x-ray diffraction (XRD) pattern is dependent on the molecular geometry and electron density of the sample. Small-angle x-ray diffraction (SAXD) and wide-angle x-ray diffraction (WAXD) have been used to study the structure of SC (White et al., 1988; Bouwstra et al., 1994; Marjukka Suhonen et al., 1999). Structural features with large repeat distances of 50 to 150 Å can be obtained using SAXD, and structural features with small repeat distances of 3 to 10 Å can be obtained using WAXD (Bouwstra et al., 1997). The diffraction studies can be useful in conjunction with permeation and other techniques to understand the effects of penetration enhancers on the SC structure (Ribaud et al., 1994; Schreiner et al., 2000). For example Cornwell et al., (1996) demonstrated the effects of propylene glycol (PG) alone or in combination with terpenes (Figure 12.1 and Figure 12.2) on human SC. A typical diffraction spectrum consists of a plot of reflected intensities versus the scattering angle θ (theta) or 2θ. In Figure 12.1 and Figure 12.2, the scattering intensities were plotted against the scattering vector Q, calculated using the formula $Q = (4\pi \sin \theta)/\lambda$, where λ is the wavelength of the x-rays (usually 1.54 Å).

SAXD and WAXD have provided the lamellar and lateral lipid organization in the SC. However, these techniques require large quantities of the SC for sample preparation; therefore, they cannot provide any information regarding the local structural information on the lipids. Electron diffraction can be used to obtain the

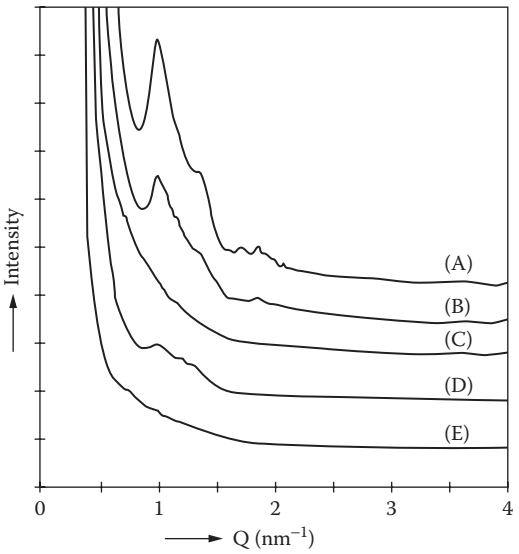

Figure 12.2 Small-angle x-ray scattergrams obtained from (A) untreated 20 to 40% hydrated stratum corneum and stratum corneum treated with (B) propylene glycol, (C) *d*-limonene saturated in propylene glycol, (D) nerolido 190% w/w in propylene glycol, and (E) 1-8-cineole saturated in propylene glycol. (Reprinted from Cornwell, P.A., Barry, B.W. Bouwstra, J.A., and Gooris, G.S., *Int. J. Pharm.*, 127:9–26, 1996, with permission from Elsevier.)

local structural information on variations in the lateral packing of the lipids (Pilgram et al., 1998, 1999). Electron diffraction allows determination of the three-dimensional structures of macromolecules. Electrons are scattered strongly by their interaction with the charges of electrons and nuclei and have been used to study the molecules in the gas phase on surfaces and in thin films. Recent advances in electron diffraction techniques allow it to be useful for studying solid samples. The major advantage of this technique is that it requires a small sample, several million times smaller than that required for XRD studies. Thus, XRD and electron diffraction studies can provide useful information on the effects of penetration enhancers on the SC.

Spectroscopic Studies

Spectroscopic techniques are among the most widely used to study the effects of penetration enhancers on the SC. Infrared (IR) spectroscopy, especially Fourier transform IR (FTIR), has been used extensively to study the structure of SC *in vitro*. IR spectroscopy deals with the interaction between a molecule and radiation from the IR region of the electromagnetic spectrum (IR region = 10,000 to 400 cm^{-1}, with the most useful region for functional analysis 4000 to 400 cm^{-1}). IR radiation causes the excitation of the vibrations of covalent bonds within that molecule. These vibrations include the stretching and bending modes. FTIR spectroscopy provides

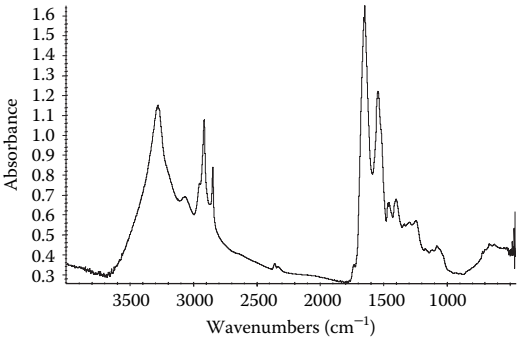

Figure 12.3 FTIR spectrum (500 to 4000 cm^{-1}) of untreated porcine SC.

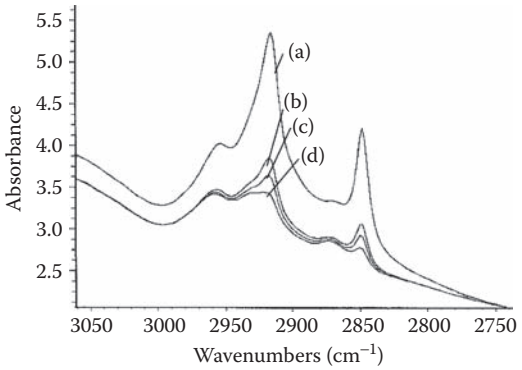

Figure 12.4 FTIR spectrum (2750 to 3050 cm^{-1}) of porcine stratum corneum treated with chloroform:methanol (2:1) for various time intervals: (a) control, (b) 10 min, (c) 20 min, (d) 40 min. (Data from Rastogi and Singh, 2001.)

information on the vibrational modes of the absorbing species and probes the structure at molecular level.

For the study of lipid biophysics, the peaks caused by C–H stretching vibrations are of particular interest. These absorbances occur around 2848 and 2915 cm^{-1} for symmetric and asymmetric C–H stretching vibrations, respectively. The changes in the amount of SC lipids have been related to the C–H stretching absorbance intensity (Goates and Knutson, 1994; Bhatia and Singh, 1998a; Levang et al., 1999; Rastogi and Singh, 2002). The SC lipid extraction leads to a decrease in the C–H stretching absorbance intensity. This was demonstrated by the removal of extracellular SC lipids by chloroform:methanol extraction, which leads to a dramatic decrease (>95%) in the intensity of C–H stretching peaks (Casal and Mantsch, 1984) and increases SC permeability by several orders of magnitude (Scheuplein and Ross, 1974). Representative FTIR spectrum of control porcine SC is shown in Figure 12.3. Figure 12.4 shows the FTIR spectrum (2750 to 3050 cm^{-1}) of porcine SC treated with chloroform:methanol (2:1) for different time periods. Table 12.1 shows the percentage decrease in symmetric and asymmetric C–H stretching absorbance peak

Table 12.1 Changes in Symmetric and Asymmetric C-H Stretching Absorbance Peak Areas of the Stratum Corneum After Treatment with Chloroform:Methanol (2:1)

	Peak Area (mean ± SD, n = 3)					
	Asymmetric			Symmetric		
Treatment Time (Min)	Control	Treatment	% Decrease	Control	Treatment	% Decrease
10	6.48 ± 0.41	2.08 ± 0.60	68.11	2.20 ± 0.54	0.71 ± 0.30	65.95
20	6.46 ± 0.50	1.69 ± 1.22	74.65	2.50 ± 0.24	0.57 ± 0.22	77.31
40	6.09 ± 0.21	1.12 ± 0.94	75.94	2.36 ± 0.62	0.23 ± 0.10	89.94

Note: Data from Rastogi and Singh (2001). % decrease = 100 – [(Absorbance peak area due to treatment/Absorbance peak area due to control) × 100].

areas of the porcine SC after treatment with C:M (2:1) for different time periods. The treatment resulted in the decrease of C–H symmetric and asymmetric peaks associated with an increase in the transport of hydrophilic solutes through porcine skin (Rastogi and Singh, 2001).

Appearance of peaks near 1654 and 1546 cm^{-1} are caused by C=O stretching and N–H bending, which are characteristic of the SC protein absorbances. Proteins play a crucial role in the structural assembly of the intercellular lipid lamellae of SC (Lazo et al., 1995). Hence, the changes in the C=O stretching and N–H bending peaks suggest disturbances in the SC barrier.

Furthermore, attenuated total reflectance (ATR)-IR spectroscopy was useful for *in vivo* SC observations (Bommannan et al., 1990). It can be used to measure the water content in human SC (Potts et al., 1985; Edwardson et al., 1991). The method is used to measure the percutaneous absorption of drugs in addition to monitoring the effects of enhancers on the SC *in vivo* (Higo et al., 1993; Pirot et al., 1997). Electron spin resonance spectroscopy (ESR) can be used *in vitro* for studying the effects of penetration enhancer on SC (Rehfeld et al., 1990), and it is demonstrated to be useful for evaluating the fluidity of SC (Alonso et al., 1995; Kawasaki et al., 1997; Mizushima et al., 2000).

Raman spectroscopy was also reported to be useful for studying the molecular nature of human SC (Williams et al., 1992a). Recently, Raman microspectroscopy is being used to characterize the lipid domains of SC (Percot and Lafleur, 2001). Combined with confocal microscopy, it is useful as a noninvasive *in vivo* optical method to measure molecular concentration profiles in the skin (Caspers et al., 2001), which allows measuring percutaneous absorption along with detailed information about the molecular composition of the skin with high spatial resolution (Caspers et al., 2003).

Proton magnetic resonance spectroscopy and ^{13}C nuclear magnetic resonance (NMR) spectroscopy have been reported to study the nature of water in human SC (Foreman, 1976; Yamamura and Tezuka, 1989; Jokura et al., 1995). The ^{2}H-NMR data are useful to study dynamic structural disorder of the intercellular lamellar lipid structure in the SC (Bezema et al., 1996). For further information on the use of NMR for investigating SC structure, refer to the review by Abraham et al. (1997).

Thermal Analysis

Temperature-induced changes in the SC can provide valuable information regarding its structure. Thermal techniques, differential scanning calorimetry (DSC), and thermogravimetric analysis (TGA) can be used to monitor the changes in the SC structure induced by penetration enhancers. DSC is a dynamic comparison method in which the difference in energy inputs into a substance and a reference standard is measured as a function of temperature while both the substance and reference standard are subjected to a controlled temperature program. DSC measures the amount of energy (heat) absorbed or released by a sample as it is heated, cooled, or held at a constant temperature. Sensitive calorimetry can reveal small enthalpy changes from the transitions of the monolayers, such as melting and solid–solid transitions. DSC has been used previously to study lipid and protein transitions in a variety of biological and synthetic systems (Golden et al., 1986, 1987). Typically, four transitions are observed in the DSC thermal profile of human SC between 25 and 105°C (Figure 12.5). The transitions occur near 35, 65, 80, and 105°C, each representing different components of SC.

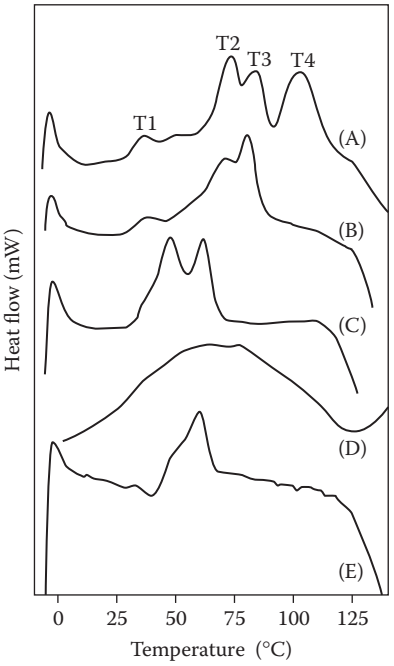

Figure 12.5 DSC traces of (A) untreated 20 to 40% hydrated stratum corneum and stratum corneum treated with (B) propylene glycol, (C) *d*-limonene saturated in propylene glycol, (D) nerolidol 90% w/w in propylene glycol, and (E) l-8-cineole saturated in propylene glycol. Endothermic transitions appear as peaks. (Reprinted from Cornwell, P.A., Barry, B.W. Bouwstra, J.A., and Gooris, G.S., *Int. J. Pharm.*, 127:9–26, with permission from Elsevier.)

DSC thermograms of SC are shown in Figure 12.5. Endotherm T1 is related to the melting of lipids from the sebaceous gland or cholesterol side-chain motion, T2 is attributed to the transition of lipid chain within the bilayer structure along with nonpolar lipids, T3 is caused by dissociation of lipid polar groups or protein-lipid associations, and T4 is ascribed to intracellular keratin denaturation (Barry, 1987). Changes in the transition peak areas (phase transition enthalpy, ΔH) and transition melting temperatures T_m were noted for the DSC endotherms of SC treated with different penetration enhancers (Barry, 1987; Lambert et al., 1989; Leopold and Lippold, 1995; Vaddi et al., 2002). The changes in SC induced by some terpene enhancers along with PG are shown in Figure 12.5. As these changes in DSC endotherm represent the disorder in the SC structure, DSC serves as an important technique to assess the effects of penetration enhancer on SC.

TGA measures the change in mass as a function of temperature. The TGA can be used to analyze deabsorption and decomposition behavior of a sample. It has been used to determine the SC water content by monitoring the change of weight and temperature (Liron, Wright, et al., 1994). The water vapor absorption and desorption kinetics were monitored in porcine SC (Liron, Clewell, et al., 1994).

Microscopic Studies

Understanding the mechanism involved with the enhancing properties of the penetration enhancers and the effects of these substances on skin structure is of prime importance in developing novel transdermal therapeutic systems. Different microscopic techniques can be useful for achieving the above-stated goals. Light microscopy combined with the staining techniques can reveal microscopic changes in skin structure. Light microscopy examines the structure of the cells in the skin and provides direct visual evidence of any anatomical changes (Monteiro-Riviere, 1991; Singh and Singh, 2001). Skin is anatomically divided into two principal components, the outer epidermis and the underlying dermis. By light microscopic study, the structure-to-function relationship can be overviewed (Roberts and Walters, 1998).

Transmission electron microscopy (TEM) is the most efficient way to visualize the effects of penetration enhancers on ultrastructure of the SC (Bentley et al., 1997; Bhatia et al., 1997). In contrast to light microscopy, TEM uses a beam of electrons in place of a beam of light. The samples must be prepared to a thickness that allows the transmission of electrons. By propelling electrons at a thin sample and detecting those transmitted through it, a map of the local densities of the sample can be obtained. The magnification that can be achieved with TEM is on the order of several hundreds of thousands depending on the type of instrument used. The resolution obtained with TEM images is several orders of magnitude better than that of a light micrograph because the wavelength of electrons is much smaller than that of light. Because of the high spatial resolution, TEM is often employed to determine the detailed crystallography of materials as a complementary tool to conventional crystallographic methods such as XRD. This approach was investigated to characterize the ultrastructure of SC and the effects of penetration enhancer treatment on lipid lamellar packing of SC (Marjukka Suhonen et al., 1999; Ponec et al., 2000). Images obtained with a TEM are two-dimensional sections of the material under study.

The scanning electron microscope (SEM) can be used to obtain a three-dimensional image of the sample. SEM is one of the most versatile and widely used tools of modern science as it allows the study of both morphology and composition of biological and physical materials. By directing an electron beam across a specimen, high-resolution images of the morphology or topography of a specimen can be obtained. Warner et al. (2003) showed the disruptions in human SC ultrastructure by hydration using TEM and SEM. The ultrastructure of the intercellular spaces of SC can be studied by freeze-fracture electron microscopy, field emission SEM, and confocal laser scanning microscopy (Corcuff et al., 2001). Confocal laser scanning microscopy (LSM) has been used for monitoring percutaneous absorption using penetration enhancers and the pathways of transport using fluorescent compounds (Mitragotri et al., 1995; Van Kuijk-Meuwissen et al., 1998; Cladera et al., 2003). Fluorescence microscopy can be utilized for qualitative localization of fluorescence-labeled compounds within different layers of the skin (Wong et al., 2003).

Atomic force microscopy (AFM), also called scanning force microscopy (SFM), can be used for mapping the surface of biological samples to obtain three-dimensional images. The AFM utilizes a sharp probe moving over the surface of a sample. The ability of AFM to image at atomic resolution, combined with its ability to image a wide variety of samples under a wide variety of conditions, has created a great deal of interest in applying it to the study of biological structures. AFM provides insight into the molecular architecture of the SC. The resolution obtained with AFM allows imaging of the molecular architecture of the SC (Chen and Wiedmann, 1996). The morphological parameters of individual corneocytes, such as the volume, average thickness, and real surface area, can be measured using AFM (Kashibuchi et al., 2002). In conclusion, microscopic techniques provide powerful tools to monitor the effects of penetration enhancers on SC at the microscopic level.

Other Techniques

The quantification of drug transport enhancement by penetration enhancers can be accomplished either by directly determining the drug fluxes or by measuring the pharmacodynamic response. For example, Barry et al. (1984) used vasoconstrictor assays (skin-blanching assay) by scoring the degree of pallor induced by a test steroid to assess the efficacy of penetration enhancers on topical bioavailability. Thus, monitoring pharmacodynamic response following transdermal delivery provides an indirect method of assessing the efficacy of penetration enhancers. Autoradiographic techniques were shown to be a useful method for detecting the localization of radioactive material in different layers of the skin (Bidmon et al., 1990; Fabin and Touitou, 1991).

Transepidermal water loss (TEWL) can be considered a determinant indicative of the functional state of the cutaneous barrier (Wilson and Maibach, 1982; Maibach et al., 1984; Rougier et al., 1989) and provides a method for assessing macroscopic changes in the barrier properties of the SC (Abrams et al., 1993). Biophysical investigations suggest that the SC lipid domains are the primary barrier to both water loss and the penetration of compounds through the skin (Van Duzee, 1971; Kalia et al., 2001). Therefore, measurement of TEWL is a relevant parameter for the

prediction of the percutaneous penetration of substances (Lotte et al., 1987; Levang et al., 1999). Skin irritation tends to reduce the efficiency of SC barrier function and results in an increase in TEWL. This sometimes is associated with a decrease in skin water content (Wilhelm et al., 1989) and an increase in skin temperature (Grice et al., 1971). Hence, measurement of skin capacitance or skin hydration and skin temperature may also be used to assess the effects of penetration enhancers on skin barrier and irritation (Thiele and Malten, 1973; Serban et al., 1981; Singh and Singh, 2004) along with TEWL (Mizushima et al., 2000; Alberti et al., 2001).

PENETRATION ENHANCERS

Penetration enhancers are the substances that increase the permeability of the skin without severe irritation or damage to its structure and reversibly remove the barrier resistance of the SC (Barry, 1987). The information obtained from infrared, thermal, and fluorescence spectroscopic examinations of the SC and its components suggests that permeation of solutes through the SC improved by penetration enhancer is associated with alterations involving the hydrocarbon chains of the SC lipid components. The data obtained from electron microscopy and XRD reveal that the disordering of the lamellar packing is also an important mechanism for increased permeation of drugs induced by penetration enhancers (Marjukka Suhonen et al., 1999). Several classes of penetration enhancers have been reported to enhance the transdermal transport of drugs. This section describes some of the enhancers that have shown great promise for use in transdermal systems.

Fatty Acids

Fatty acids and fatty acid esters have been known to increase percutaneous penetration of a variety of molecules. The use of saturated and unsaturated fatty acid enhancers for drug permeation enhancement is of interest in topical and transdermal drug delivery systems research (Aungst, 1994). Structurally, fatty acids consist of an aliphatic hydrocarbon chain and a terminal carboxy group. Fatty acids could differ in their chain length and in the number, position, and configuration of the double bonds and have branching and other substituents. It has been reported that variations of octadecenoic acids with respect to number of double bonds and *cis*/*trans* configuration of isomers show differences in their penetration-enhancing effect on naloxane flux through human skin (Aungst et al., 1986; Tanojo et al., 1998). The *cis* isomers of octadecenoic acid were effective permeation enhancers, whereas the corresponding *trans* isomers had less or no enhancing effect on the salicylic acid flux (Golden et al., 1987). The nature of the solvent used along with fatty acids also plays an important role in the interactions between the fatty acids and the intercellular lipids in the SC (Wang et al., 2004). The chemical structure of fatty acids (such as chain length, polarity, and level of unsaturation) and their interaction with SC has been reviewed (Kanikkannan et al., 2000).

In Vitro *Studies*

The effects of fatty acids on skin structure, especially the SC, have been evaluated by using FTIR, TGA, and DSC. Although the mechanism by which fatty acids enhance the permeation of drugs through the skin is not clearly understood, oleic acid can interact with SC lipids and disrupt their structures, increasing their fluidity and consequently increasing the flux (Barry, 1991). Studies showed that oleic acid provides a pathway of diminished resistance for drug transport by disrupting the intercellular lipid domain of the SC (Jiang and Zhou, 2003) or coexisting as pools in the ordered SC lipid structure (lipid phase separation) (Williams and Barry, 1992b). Selective perturbation of the intercellular lipid bilayer in the SC appears to be the major route of enhancing activity of the fatty acids (Golden et al., 1987).

In a similar study using differential thermal analysis (DTA), the perturbation effects of fatty acids on the SC were studied (Tanojo et al., 1994). Thermal behavior of the SC revealed that saturated fatty acids easily mix with the skin lipids and monounsaturated fatty acids to form a separate domain containing mostly pure fatty acids within the SC lipids. Polyunsaturated fatty acids also formed separate domains. but the extent of thermal transition was more than that showed by saturated fatty acids and less than monounsaturated fatty acids. In a recent investigation, SEMs of the skin treated with 10% oleic acid in ethanolic solution showed generation of pores on the surface of epidermal corneocytes (Touitou et al., 2002).

A number of fatty acids have been tested for their efficacy to promote percutaneous permeation of a variety of drugs. Table 12.2 summarizes findings of the in vitro percutaneous absorption studies using fatty acids.

In Vivo *Efficacy and Toxicity*

In vivo studies have shown the efficacy of fatty acids as potential skin penetration enhancers. Percutaneous absorption of dihydroergotamine was enhanced (208-fold)

Table 12.2 Summary of *In Vitro* Percutaneous Absorption of Drugs Using Fatty Acids as Penetration Enhancer

Drug	Concentration of Fatty Acid	Vehicle Membrane	Enhancement Ratio (ER)	Reference
Naloxone	10% Heptanoic acid in PG	Human	29.00	Aungst et al., 1986
	10% Capric acid in PG		117.00	
	10% Lauric acid in PG		147.00	
	10% Stearic acid in PG		14.00	
	10% Palmitoleic acid in PG		38.00	Aungst, 1989
	10% Palmitelaidic acid		28.00	
Testosterone	0.5 *M* capric acid in PG	Human	3.60	Aungst et al., 1990

(continued)

Table 12.2 (continued) Summary of *In Vitro* Percutaneous Absorption of Drugs Using Fatty Acids as Penetration Enhancer

Drug	Concentration of Fatty Acid	Vehicle Membrane	Enhancement Ratio (ER)	Reference
Naloxone			31.00	
Benzoic acid			1.50	
Indomethacin			47.00	
5-fluorouracil			66.00	
Methotrexate			1.30	
Testosterone	0.5 *M* lauric acid in PG	Human	5.50	Aungst et al., 1990
Naloxone			38.00	
Benzoic acid			1.30	
Indomethacin			102.00	
5-fluorouracil			58.00	
Methotrexate			1.40	
Ketoprofen	10% Caproic acid in PG	Rat	24.00	Kim et al., 1993
	10% Capric acid in PG		26.50	
	10% Lauric acid in PG		45.60	
	10% Myristic acid in PG		13.40	
	10% Stearic acid in PG		7.40	
Corticosterone	Linoleic acid	Human	8.40	Johnson et al., 1996
5-fluorouracil	10% Oleic acid in EtOH	Porcine	4.00	Gao and Singh, 1997
	10% Oleic acid in PG		14.50	
Luteinizing hormone releasing hormone (LHRH)	10% Lauric acid in EtOH	Porcine	1.66	Bhatia and Singh, 1998b
	10% Palmitic acid in EtOH		3.70	
	10% Oleic acid in EtOH		2.30	
	10% Linoleic acid in EtOH		4.10	
	10% Linolenic acid in EtOH		4.87	
Piroxicam	Linolenic acid in Poloxamer 407 gel	Rat	1.76	Shin et al., 2000
Aspalatone	5% linolenic acid in PG	Hairless mouse	132.00	Gwak and Chun, 2001
Salbutamol	0.1 *M* Oleic acid	Artificial membrane	2.20	Nolan et al., 2003

Note: ER, a ratio of the skin permeability coefficient or the flux for skin exposed to fatty acids vs. a control value for skin not exposed to fatty acids; PG, propylene glycol; EtOH, ethanol.

by oleic acid in rabbits (Niazy, 1991), and the blanching intensity of the model drug betamethasone 17-benzoate was higher in humans (Bach and Lippold, 1998). Other studies have shown oleic acid in PG-enhanced penetration of nicardipine and ketorolac acid in rhesus monkeys (Yu et al., 1988), azidothymidine in rats (Seki et al., 1989), and piroxicam in rabbits (Hsu et al., 1991). Only a slight increase in the *in vivo* skin uptake of flurbiprofen in rats after treatment with linolenic, linoleic, and oleic acids was reported (Fang et al., 2003b) in rats. Oleic acid was shown to enhance the permeation of model hydrophilic (methylene blue) and lipophilic (Sudan III) dyes using a combination of skin surface biopsy with calorimetry in human volunteers (Rosado and Rodrigues, 2003). Oleic acid was demonstrated *in vivo* in human SC using attenuated total reflectance IR spectroscopy to cause a significant shift in the frequency of the C–H asymmetric stretching absorbance. These changes were implicated in the increased lipid chain disorder and thereby increase in the drug transport across the SC (Mak et al., 1990).

Enhanced epidermal proliferation has been observed by several investigators (Xu and Chien, 1991; Fang et al., 2003b). In yet another toxicological study, fatty acids showed no epidermal tissue damage, but oleic acid induced mild skin irritation and inflammatory cells by enhancing cytokine production (Boelsma et al., 1996). Oleic acid was also shown to cause a reduction in epidermal Langerhans' cell population and create pores on the surface of epidermal corneocytes (Touitou et al., 2002). Increased neutrophils and lymphocytes in the epidermis/dermis (inflammatory cell infiltration) was observed with oleic acid treatment (Fang et al., 2003b). Fatty acids (linoleic, linolenic, and oleic acids) were shown to increase the TEWL in rats (Fang et al., 2003b). Among all the fatty acids, oleic acid is the most effective and widely studied as a percutaneous penetration enhancer. However, it is reported to cause erythema and edema when applied to rabbit skin (Aungst, 1989).

Terpenes

Natural products are receiving considerable interest in the pharmaceutical industry, and terpenes may provide a series of relatively safe and clinically acceptable penetration enhancers for drugs. Terpenes are widely found in plants as constituents of essential oils and are designated by their chemical structure, made up of isoprene units [CH_2=C(CH_3)–CH=CH_2]. Terpenes are represented by the general formula $(C_5H_8)_n$. However, some of the terpenes may contain oxygen in addition to carbon and hydrogen; these are called terpenoids. Terpenes are classified according to the number of isoprene units (Table 12.3).

In Vitro *Efficacy of Terpenes*

Terpenes are widely used chemical penetration "enhancers" (Williams and Barry, 1991b; Barry and Williams, 1993). Structural formulas of terpenes used as penetration enhancers are presented in Figure 12.6. Terpenes are of low cutaneous irritancy, provide excellent enhancement ability, and appear to be promising candidates for pharmaceutical formulations (El-Kattan et al., 2001; Gao and Singh, 1998; Zhao and Singh, 1999). Table 12.4 lists the *in vitro* percutaneous absorption enhancement of drugs using terpenes.

Table 12.3 Classification of Terpene Hydrocarbons

Terpenes	Number of Isoprene Units	Examples
Monoterpenes	2	Pinene, nerol, citral, camphor, menthol, limonene, borneol
Sesquiterpenes	3	Santonin, gossypol, periplanone, nerolidol, farnesol
Diterpenes	4	Phytol, vitamin A_1
Triterpenes	6	Squalene
Tetraterpenes	8	Carotene (provitamin A_1)

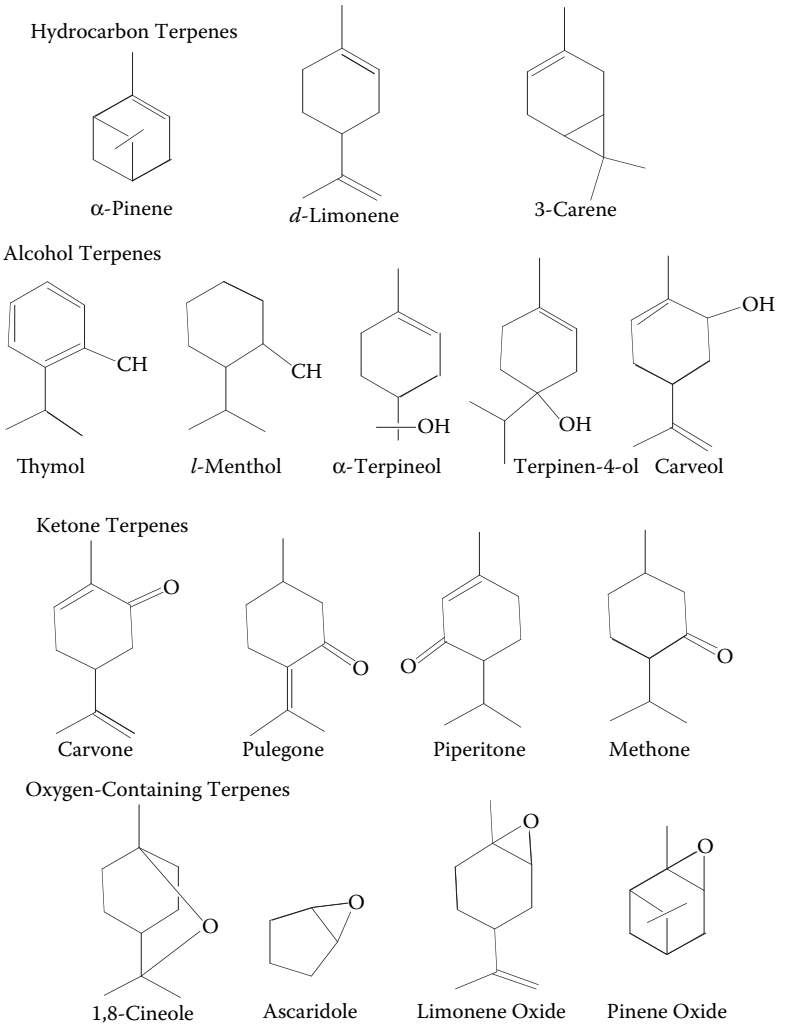

Figure 12.6 Structural formulas of some terpenes used as penetration enhancers.

Table 12.4 ***In Vitro*** **Percutaneous Absorption of Drugs Using Terpenes as a Skin Penetration Enhancer**

Drug	Terpene/Vehicle	Membrane	Enhancement Ratio (ER)	Reference
Caffeine	0.4 *M* Neomenthol/PG	Mouse	13	Godwin and Michniak, 1999
	0.4 *M* Geraniol/PG	Mouse	16	Godwin and Michniak, 1999
Carbamazepine	2 % w/w Fenchone/HPC gel	Hairless mouse	1.5	El-Kattan et al., 2001
	2 % w/w Thymol/HPC gel	Hairless mouse	4.2	El-Kattan et al., 2001
	2 % w/w Limonene/HPC gel	Hairless mouse	6.6	El-Kattan et al., 2001
	2 % w/w Nerolidol/HPC gel	Hairless mouse	7.5	El-Kattan et al., 2001
Curcumin	5% β-Myrcene/E-CP buffer	Rat	1.5	Fang et al., 2003a
	5% Eugenol/E-CP buffer	Rat	3.5	Fang et al., 2003a
	5% Menthol/E-CP buffer	Rat	2.8	Fang et al., 2003a
	5% Cineole/E-CP buffer	Rat	3.2	Fang et al., 2003a
	5% Terpineol/E-CP buffer	Rat	6.3	Fang et al., 2003a
	5% Carveol/E-CP buffer	Rat	5.8	Fang et al., 2003a
	5% Farnesol/E-CP buffer	Rat	3.4	Fang et al., 2003a
	5% Nerolidol/E-CP buffer	Rat	5.1	Fang et al., 2003a
5-Fluorouracil	5% Cineole/50% ethanol	Porcine	92	Gao and Singh, 1997
	5% Carvone/50% ethanol	Porcine	154	Gao and Singh, 1997
Hydrocortisone	0.4 *M* Terpinen-4-ol/PG	Mouse	3.9	Godwin and Michniak, 1999
	0.4 *M* α-Terpineol/PG	Mouse	5.0	Godwin and Michniak, 1999
	2 % w/w Fenchone/HPC gel	Hairless mouse	7.8	El-Kattan et al., 2001
	2 % w/w Thymol/HPC gel	Hairless mouse	10.5	El-Kattan et al., 2001
	2 % w/w Limonene/HPC gel	Hairless mouse	28.0	El-Kattan et al., 2001
	2 % w/w Nerolidol/HPC gel	Hairless mouse	32.7	El-Kattan et al., 2001
	2 % w/w Terpinen-4-ol/HPC gel	Hairless mouse	11.3	El-Kattan et al., 2000
	2 % w/w Verbenone/HPC gel	Hairless mouse	11.5	El-Kattan et al., 2000
	2 % w/w Carvone/HPC gel	Hairless mouse	13.1	El-Kattan et al., 2000
	2 % w/w Menthone/HPC gel	Hairless mouse	18.7	El-Kattan et al., 2000

(continued)

Table 12.4 (continued) ***In Vitro*** **Percutaneous Absorption of Drugs Using Terpenes as a Skin Penetration Enhancer**

Drug	Terpene/Vehicle	Membrane	Enhancement Ratio (ER)	Reference
	2 % w/w α-Terpineol/HPC gel	Hairless mouse	13.3	El-Kattan et al., 2000
	2 % w/w Cineole/HPC gel	Hairless mouse	14.5	El-Kattan et al., 2000
	2 % w/w Geraniol/HPC gel	Hairless mouse	16.9	El-Kattan et al., 2000
	2 % w/w Cymene/HPC gel	Hairless mouse	22.9	El-Kattan et al., 2000
LHRH	5% Thymol/ethanol	Porcine	2.4	Bhatia and Singh, 1999
	5% Cineole/ethanol	Porcine	2.2	Bhatia and Singh, 1999
	5% Carvone/ethanol	Porcine	3.8	Bhatia and Singh, 1999
	5% Limonene/ethanol	Porcine	4.7	Bhatia and Singh, 1999
	10% Thymol/ethanol	Porcine	2.4	Bhatia and Singh, 1999
	10% Cineole/ethanol	Porcine	2.1	Bhatia and Singh, 1999
	10% Carvone/ethanol	Porcine	3.5	Bhatia and Singh, 1999
	10% Limonene/ethanol	Porcine	4.4	Bhatia and Singh, 1999
Nicardipine	2% w/w Carvone/HPC gel	Rat	3.5	Krishnaiah et al., 2003
	4% w/w Carvone/HPC gel	Rat	5.8	Krishnaiah et al., 2003
	8% w/w Carvone/HPC gel	Rat	7.6	Krishnaiah et al., 2003
	12% w/w Carvone/HPC gel	Rat	7.9	Krishnaiah et al., 2003
	2 % w/w Fenchone/HPC gel	Hairless mouse	17.9	El-Kattan et al., 2001
	2 % w/w Thymol/HPC gel	Hairless mouse	18.2	El-Kattan et al., 2001
	2 % w/w Limonene/HPC gel	Hairless mouse	60.0	El-Kattan et al., 2001
	2 % w/w Nerolidol/HPC gel	Hairless mouse	134.8	El-Kattan et al., 2001
Propranolol	1% Menthol/hydroalcohol (60:40)	Hairless mice	904	Kunta et al., 1997
	1% Carveol/hydroalcohol (60:40)	Hairless mice	1156	Kunta et al., 1997
	1% Limonene/hydroalcohol (60:40)	Hairless mice	319	Kunta et al., 1997
	1% Linalool/hydroalcohol (60:40)	Hairless mice	178	Kunta et al., 1997

(continued)

Table 12.4 (continued) ***In Vitro*** **Percutaneous Absorption of Drugs Using Terpenes as a Skin Penetration Enhancer**

Drug	Terpene/Vehicle	Membrane	Enhancement Ratio (ER)	Reference
	5% Menthol/hydroalcohol (60:40)	Hairless mice	904	Kunta et al., 1997
	5% Carveol/hydroalcohol (60:40)	Hairless mice	1252	Kunta et al., 1997
	5% Limonene/hydroalcohol (60:40)	Hairless mice	304	Kunta et al., 1997
	5% Linalool/hydroalcohol (60:40)	Hairless mice	1141	Kunta et al., 1997
	10% Menthol/hydroalcohol (60:40)	Hairless mice	852	Kunta et al., 1997
	10% Carveol/hydroalcohol (60:40)	Hairless mice	1393	Kunta et al., 1997
	10% Limonene/hydroalcohol (60:40)	Hairless mice	311	Kunta et al., 1997
	10% Linalool/ hydroalcohol (60:40)	Hairless mice	1267	Kunta et al., 1997
Tamoxifen	5% Menthone/50% PG	Porcine	1.9	Zhao and Singh, 2000
	5% Eugenol/50% PG	Porcine	17.3	Zhao and Singh, 2000
	5% Limonene/50% PG	Porcine	25.3	Zhao and Singh, 2000
	5% Carvone/50% ethanol	Porcine	244	Gao and Singh, 1998
	5% Cineole/50% ethanol	Porcine	51	Gao and Singh, 1998
	5% Menthol/50% ethanol	Porcine	4	Gao and Singh, 1998
	5% Thymol/50% ethanol	Porcine	17	Gao and Singh, 1998
	1% Menthone/50% ethanol	Porcine	2.0	Zhao et al., 2001
	2% Menthone/50% ethanol	Porcine	5.4	Zhao et al., 2001
	3% Menthone/50% ethanol	Porcine	15.4	Zhao et al., 2001
	5% Menthone/50% ethanol	Porcine	33.1	Zhao et al., 2001
	2% w/w Fenchone/HPC gel	Hairless mouse	0.6	El-Kattan et al., 2001
	2% w/w Thymol/HPC gel	Hairless mouse	1.4	El-Kattan et al., 2001
	2% w/w Limonene/HPC gel	Hairless mouse	1.6	El-Kattan et al., 2001

(continued)

Table 12.4 (continued) *In Vitro* Percutaneous Absorption of Drugs Using Terpenes as a Skin Penetration Enhancer

Drug	Terpene/Vehicle	Membrane	Enhancement Ratio (ER)	Reference
	2% w/w Nerolidol/HPC gel	Hairless mouse	1.7	El-Kattan et al., 2001
Triamcinolone acetonide	0.4 *M* α-Terpineol/PG	Mouse	2.5	Godwin and Michniak, 1999
	0.4 *M* Carvone/PG	Mouse	1.7	Godwin and Michniak, 1999

Note: E-CP buffer, ethanol:citrate phosphate buffer (25:75); pH 7.4, 50% PG, 50% propylene glycol in water; HPC, hydroxypropyl cellulose; LHRH, leuteinizing hormone releasing hormone.

Limonene increased the skin permeation of hydrophilic (Obata et al., 1990; Ohara et al., 1995) and lipophilic (Okabe et al., 1992) solutes. Terpenes (for example, carvone, 1,8-cineole, and thymol) enhanced the percutaneous absorption of 5-fluorouracil either by increasing the SC lipid fluidity or by perturbing the barrier integrity of the SC (Gao and Singh, 1997, 1998). Lipophilicities of enhancers are considered to affect their enhancing activities (El-Kattan 2000a, 2000b, 2001). In a group of ketone or epoxide terpenes, a linear relationship was observed between enhancement ratios for 5-fluorouracil permeation and logarithms of their octanol–water partition coefficients (Williams and Barry, 1991a). The concentration of terpenes in the barrier partly determined the extent of lipid disruption and hence drug diffusivity.

The penetration-enhancing activities of monoterpenes, sesquiterpenes, and diterpenes were evaluated. Terpenes with relatively high lipophilic index exhibited absorption-promoting effects; however, extremely high lipophilicity led to lower enhancing activities (Takayama et al., 1991). It was suggested that the difference in percutaneous absorption enhancing efficiency of terpenes arose from the difference in their thermodynamic activities in the vehicle (Obata et al., 1993).

Synergistic effects of terpenes in combination with ethanol on the percutaneous absorption enhancement have been investigated (Obata et al., 1991; Gao and Singh, 1998; Zhao and Singh, 1998). At higher concentrations of ethanol, the percutaneous absorption enhancement effects of lipophilic terpenes were greater in comparison to hydrophilic terpenes. An aqueous vehicle containing menthol and ethanol showed a marked percutaneous absorption enhancement on hydrophilic and lipophilic drugs (Kobayashi et al., 1993). Zhao et al. (2001) found significantly ($p < .05$) greater enhancement of tamoxifen flux through porcine skin with increasing concentration of menthone. However, skin damage induced by lower menthone concentrations (e.g., 1 and 2%) was reversible to a greater extent than higher concentrations (e.g., 3 and 5%). Many have found a synergistic effect of terpenes with PG on the percutaneous absorption enhancement (Williams and Barry, 1989; Zhao and Singh, 2000). It is generally accepted that PG used with enhancers accumulates in the tissue and increases the partitioning of the drugs because of high affinity of drugs for the solvent (Barry, 1987, 1991).

Patents exist for the use of carvone and eugenol as skin penetration enhancers (Leonard et al., 1989a, 1989b). Camphor and eucalyptus oil as a vehicle containing

50% ethanol increased the total flux of nicotine through the hairless mouse skin (Nuwayser et al., 1988). The greater permeability enhancement of leuprolide acetate through nude mouse, snake, and cadaver skin has been reported with a nonirritating formulation containing ethanol, menthol, camphor, methyl salicylate, and urea (Lu et al., 1992).

In Vivo *Efficacy and Dermal Toxicity of Terpenes Used as Penetration Enhancers*

There are few studies on the *in vivo* efficacy and irritancy of terpenes used as an enhancer in percutaneous absorption. The percutaneous absorption-promoting effect and skin irritancy of cyclic monoterpenes were investigated in rats and with rabbits, respectively (Okabe et al., 1990). Plasma concentration of the drug (ketoprofen) markedly increased with the addition of the hydrocarbons of cyclic monoterpenes such as trans-*p*-methane and *d*-limonene. Irritancy of cyclic monoterpenes in rabbits was evaluated using the Draize scoring method. No skin irritation was observed when ethanol-containing hydrocarbons of cyclic monoterpenes (trans-*p*-menthane and *d*-limonene) were applied to dorsal skin.

Fang et al. (2003a, 2003b) reported the effect of terpenes on *in vivo* percutaneous absorption and dermal toxicity in rats. The back area of rat was treated with a transdermal patch containing terpene enhancers (β-myrcene, eugenol, menthol, cineole, terpineol, carveol, farnesol, and nerolidol) for various length of time before applying transdermal patches containing curcumin. After specified time points, curcumin transdermal patches were removed, and the amount of curcumin transported and TEWL were determined. Dermal toxicity was evaluated by histological examination of a skin sample from the patch application site. The skin reservoir of curcumin after topical application of curcumin hydrogel–based transdermal patches was significantly higher ($p < .5$) for all the enhancer-treated groups than for the control. TEWL values were also significantly increased ($p < .05$) by all enhancers. Also, morphological alterations of the skin structure increased in the following order (Fang et al., 2002): nontreated group < eugenol < terpineol < carveol.

Terpenes are good penetration enhancers based on the their *in vitro and in vivo* percutaneous absorption studies. There cannot be a generalized rule for their relative efficiency. The physicochemical properties of drug can influence the penetration-enhancing efficiency of terpenes. Therefore, they should be screened for their use with a particular drug before making a final decision. There are insufficient human data on their safety. Hence, further *in vivo* skin irritation and dermatotoxicity studies with terpenes are warranted.

Azone

Azone® (1-dodecylazacycloheptan-2-one, laurocapram), along with its derivatives are probably the most widely investigated penetration enhancers and are effective at low concentrations for both lipophilic and hydrophilic drugs but suffer from toxicity problems. Azone is a hybrid of a cyclic amide with an alkyl sulfoxide, and its chemical structure has a long alkyl chain and a lactam group (Williams and Barry,

1992b; Hadgraft et al., 1993). It is often used by researchers because of its increased percutaneous absorption-enhancing ability, which also makes it a useful agent for comparison with new enhancers. It is thought to exert its penetration effects by interacting with the intercellular lipid of the SC and causing an increase in "fluidity" of the azone. The effects of the lipid bilayer (Julian et al., 1996) are considered to be partially because of its C12 alkyl chain, which helps it insert among the acyl chain of lipids in the bilayers of the intercorneocyte space (López-Castellano et al., 2000). The enhanced fluidity is thought to facilitate the diffusion of the drug molecules through the hydrocarbon region of the bilayer.

In Vitro *Efficacy*

Numerous *in vitro* studies have been reported looking into the enhancement efficiency and the mechanism involved with azone and its analogues. FTIR investigations have shown that azone is distributed homogeneously in SC and increases SC fluidity (Harrison et al., 1996). DTA and DSC studies revealed the effect of azone and its analogues on lowering the phase transition temperatures of the SC lipids (Bouwstra et al., 1989; Lambert et al., 1989). XRD studies have shown the disordering of lipid lamellae in human SC (Bouwstra et al., 1992).

The flux enhancement and the toxicity of azone and its derivatives with the hydrocarbon chain lengths from C2 to C16 were investigated. The *in vitro* cytotoxicity as well as the flux increased from C2 to C8, then remained constant from C8 to C14, and subsequently decreased with increasing alkyl chain length. This shows that, with these compounds, a parallelism exists between skin cell toxicity and penetration-enhancing capacity (Ponec et al., 1989). The *in vitro* percutaneous absorption enhancement of different drugs with Azone is presented in Table 12.5.

In Vivo *Efficacy and Toxicity*

Pure Azone is poorly absorbed in humans, and the small amount of azone absorbed is cleared rapidly by the kidneys (Wiechers et al., 1987). Azone is usually used in combination with a solvent (Table 12.5). An extensive review covering the entire *in vivo* and clinical studies with azone as a percutaneous penetration enhancer has been published (Hadgraft et al., 1993). The percutaneous absorption of 2′,3′-dideoxyinosine in rats was higher when the skin was pretreated with azone (Mukherji et al., 1994). Enhanced percutaneous absorption of methotrexate was shown using azone in combination with PG (Chatterjee et al., 1997). The disposition and metabolic profile of azone was also reported *in vivo* in animals and humans (Wiechers et al., 1990).

There have been several studies looking into the toxicity potential of azone and its analogues. Contrasting reports were published, some reporting that azone is a moderate irritant (Lashmar et al., 1989) and others reporting that it is not irritating (Barry and Bennet, 1987). Recently, it was shown to exert moderate skin irritation and enhance the TEWL values in rats (Fang et al., 2003a). The skin irritation caused by azone may be the prime reason for not using it as a penetration enhancer in transdermal systems.

Table 12.5 Summary of *In Vitro* Percutaneous Absorption of Drugs Using Azone as a Penetration Enhancer

Drug	Concentration of Azone/Vehicle	Membrane	Enhancement Ratio (ER)	Reference
Acyclovir	0.1 *M* in PG	Hairless mouse	41.00	Okamoto et al., 1990
	0.1 *M* in ET	Hairless mouse	19.00	Okamoto et al., 1990
	0.1 *M* in IPA	Hairless mouse	4.00	Okamoto et al., 1990
	0.1 *M* in IPM	Hairless mouse	2.00	Okamoto et al., 1990
Benazepril	3% Azone	Hairless mouse	67.70	Tenjarla et al., 1999
Buspirone HCl	2.5% in 50:50 (v/v) ethanol/water	Human	27.30	Meidan et al., 2003
Clonazepam	5% in carbomer gel containing PG/ET	Human	2.86	Puglia et al., 2001
Difluoromethyl ornithine	10% Azone	Porcine	1.30	McCullough et al., 1985
Estradiol	2% in PG	Human	1.40	Goodman and Barry, 1988
	3% Azone	Human	1.30	Goodman and Barry, 1988
5-Fluorouracil	1.8% Azone	Hairless mouse	80.00	Stoughton, 1982
	2% in PG	Hairless mouse	130.00	Bond and Barry, 1988
	2% in PG	Human	20.00	Bond and Barry, 1988
	3% Azone	Human	8.00	Goodman and Barry, 1988
	1% Azone	Rat	6.70	Lopez et al., 2000
	5% Azone	Rat	195.00	Lopez et al., 2000
Hydrocortisone	5% in PG	Hairless mouse	45.00	Mirejovsky and Takruri, 1986
	3% Azone	Hairless mouse	22.00	Tenjarla et al., 1999
Ibuprofen	5% Azone	Hairless rat	3.00	Ito et al., 1988
Indomethacin	3% Azone	Hairless rat	9.00	Sugibayashi et al., 1988
	6% in PG	Rat	5.00	Ogiso et al., 1986
Indomethacin calcium	6% Azone	Rat	2.00	Ogiso et al., 1986
Insulin	0.1% in PG	Porcine	14.00	Priborsky et al., 1987
Isoproterenol	1% in PG	Human	8.00	Patel and Vasavada, 1988
Ketoprofen	5% Azone	Rat	30.30	Wu et al., 2001
Lorazepam	5% in carbomer gel containing PG/ET	Human	3.16	Puglia et al., 2001

(continued)

Table 12.5 (continued) Summary of *In Vitro* Percutaneous Absorption of Drugs Using Azone as a Penetration Enhancer

Drug	Concentration of Azone/Vehicle	Membrane	Enhancement Ratio (ER)	Reference
Methotrexate	3% in Phosphate buffer	Hairless mouse	~1000.00	Chatterjee et al., 1997
	3% in IPA	Hairless mouse	~3000.00	Chatterjee et al., 1997
	1% in PG	Hairless mouse	~6000.00	Chatterjee et al., 1997
Naproxen	3% in ET	Human	3.00	Degim et al., 1999

Note: ER, a ratio of the skin permeability coefficient or the flux for skin exposed to azone vs. a control value for skin not exposed to azone; PG, propylene glycol; ET, ethanol; IPA, isopropanol; IPM, isopropyl myristate.

Pyrrolidones

The most-studied analogues of naturally occurring pyrrolidone carboxylic acid are 2-pyrrolidone and *N*-methyl-pyrrolidone (NMP). It has been shown that 2-pyrrolidone increases the permeability by enhancing the diffusivity through polar routes of the skin (Southwell and Barry, 1983). Consequently, these enhancers are most active with hydrophilic rather than lipophilic molecules. Aungst et al. (1986) studied a series of pyrrolidones and their effect on the *in vitro* percutaneous absorption of naloxone. In a different study, a combination of pyrrolidones greatly enhanced 5-fluorouracil absorption (Sasaki et al., 1990b). Table 12.6 presents a summary of *in vitro* percutaneous absorption enhancement of different drugs by pyrrolidones.

NMP was shown to enhance the percutaneous absorption of mefenamic acid and bupranolol *in vivo* in rabbits (Naito et al., 1985; Ogiso et al., 2001). In humans, NMP and 2-pyrrolidone were shown to cause skin irritation while increasing the bioavailability of betamethasone-17-benzoate (Barry et al., 1984; Bennet et al., 1985). Even though they are effective, the skin irritation prevents the widespread use of these agents in transdermal systems (Sasaki et al., 1990a).

Miscellaneous

Many other categories of compounds, such as sulfoxides, alcohols, glycols, and surface active agents, have been tested as percutaneous penetration enhancers. Dimethyl sulfoxide (DMSO) has been widely investigated as a percutaneous penetration enhancer for a wide range of drugs (Astley and Levine, 1976; Hwang and Danti, 1983; Aungst et al., 1986; Kurihara-Bergstrom et al., 1987; Yoshike et al., 1993; De Rosa et al., 2000). Even though DMSO was shown to be an effective percutaneous penetration enhancer, the toxicity problems associated with its use prevented the widespread use of DMSO in transdermal systems (Lashmar et al., 1989; Al-Saidan et al., 1987; Kurihara-Bergstrom et al., 1987; Sjogren and Anderson, 2000).

Decylmethyl sulfoxide (DCMS) has been shown to be an effective enhancer for hydrophilic and ionized molecules (Choi et al., 1990; 1991). It has been found that

Table 12.6 Summary of *In Vitro* Percutaneous Absorption of Drugs Using Pyrrolidones as a Penetration Enhancer

Drug	Concentration of Azone/Vehicle	Membrane	Enhancement Ratio (ER)	Reference
Bupranolol	15% NMP in a gel formulation	Rabbit	3.66	Ogiso et al., 2001
5-Fluorouracil	2 *mM* NMP + LP in IPM	Rat	32.50	Sasaki et al., 1990b
Hydrocortisone	100% NMP	Human	8.70	Barry and Bennet, 1987
	100% 2-Pyrrolidone	Human	95.00	Barry and Bennet, 1987
Indomethacin	2 *mM* NMP in water	Rat	2.70	Sasaki et al., 1990c
	2 *mM* HP in water	Rat	34.2	Sasaki et al., 1990c
	2 *mM* LP in water	Rat	152.00	Sasaki et al., 1990c
	2% NMP in 55% ET	Hairless rat	1.26	Ogiso et al., 1995
	10% NMP in 55% ET	Hairless rat	1.51	Ogiso et al., 1995
Leutinizing hormone releasing hormone	100% 2-Pyrrolidone (skin pretreated for 2 h)	Porcine	2.31	Bhatia and Singh, 1997
Mannitol	100% 2-Pyrrolidone	Human	448.00	Barry and Bennet, 1987
	100% NMP	Human	256.00	Barry and Bennet, 1987
Metronidazole	5% NMP	Human	2.70	Hoelgaard et al., 1988
	5% NMP in IPM	Human	3.80	Hoelgaard et al., 1988
Naloxone	10% NMP in PG	Human	1.10	Aungst et al., 1986
	N-Hydroxyethyl pyrrolidone		1.10	
	N-Cyclohexyl pyrrolidone		2.10	
	N-Dimethylamino-propyl pyrrolidone		2.40	
	N-Cocoalkyl pyrrolidone		34.50	
	N-Tallowalkyl pyrrolidone		24.00	
Progesterone	100% 2-Pyrrolidone	Human	22.60	Barry and Bennet, 1987
	100% NMP	Human	17.50	Barry and Bennet, 1987

Note: ER, a ratio of the skin permeability coefficient or the flux for skin exposed to pyrrolidones vs. a control value for skin not exposed to pyrrolidones; NMP, *N*-methyl-2-pyrrolidone; LP, 1-lauryl-2-pyrrolidone; IPM, isopropyl myristate; HP, 1-hexyl-2-pyrrolidone; ET, ethanol; PG, propylene glycol.

somatostatin analogue permeated both human and mouse skin, with a clinically significant flux, when administered topically with DCMS (Weber et al., 1987). DCMS enhanced 35-fold and 75-fold *in vitro* percutaneous absorption of 5-fluorouracil (Goodman and Barry, 1988) and azidothymidine (Wearley and Chien, 1990), respectively, through human skin. It has also increased the permeation of several drugs through hairless mouse skin (Choi et al., 1991). It has been demonstrated in clinical studies that DCMS present in tetracycline topical lotion for treatment of acne vulgaris is safe and nonirritating (Frank, 1976; Smith et al., 1976; Wechsler et al., 1978). Urea is a good penetration enhancer that induced no discernible change in the histological appearance of the skin and caused no skin irritation in nude mice (Lashmar et al., 1989).

Alcohols such as ethanol and isopropanol are frequently used as a part of the solvent system in transdermal preparations. The ethanol–water system alone or in combination with other solvents enhanced the absorption of drugs (Berner et al., 1989; Pershing et al., 1990; Kim et al., 1996; Vaddi et al., 2003). Other alcohols, including lauryl and linolenyl alcohols, were also investigated (Aungst et al., 1986). Enhanced percutaneous penetration was reported with surfactants, mainly sodium lauryl sulfate (Wilhelm et al., 1991; Riviere et al., 2001). However, sodium lauryl sulfate is known to cause skin irritation and barrier perturbation (Van der Valk and Maibach, 1989). PG showed enhancement of 5-fluorourail and estradiol (Goodman and Barry, 1988). In combination with other enhancers, PG showed a synergistic activity (Barry and Bennet, 1987; Priborsky et al., 1987; Komata et al., 1992; Yamane et al., 1995; Chatterjee et al., 1997; Gwak and Chun, 2002). Other categories of compounds tested for percutaneous absorption enhancement include alkanes (Hori et al., 1992) and alkyl esters (Catz and Friend, 1989; Rastogi and Singh, 2002).

CONCLUSION

Percutaneous penetration enhancers offer a way to enhance the rate of transport of the drugs through skin. Many chemicals have been investigated for their skin penetration–enhancing properties. Understanding of the mechanisms and efficacy of different classes of enhancers along with their toxicological profiles is important for their clinical use. Several techniques have been described to study the mechanism of action of penetration enhancers. Rapid advances in analytical and microscopic techniques allowed deducing some of the effects of these enhancers. Despite their effectiveness, the widespread use of many of the enhancers in transdermal/topical pharmaceutical systems is precluded because of their toxicological effects. With all this scientific information available, it can be seen that there still is great need for understanding the mechanism involved, improving the existing penetration enhancers, and synthesizing new molecules, which would display the ideal characteristics of an enhancer.

REFERENCES

Abraham, W., Kitson, N., Bloom, M., and Thewalt, J.L. (1997). Investigation of membrane structure and dynamics by deuterium NMR: application to stratum corneum, in R.O. Potts and R.H. Guy (eds.), *Mechanisms of Transdermal Drug Delivery*, New York: Dekker, pp. 163–198.

Abrams, K., Harvell, J.D., Shriner, D., Wertz, P., Maibach, H., Maibach, H.I., and Rehfeld, S.J. (1993). Effect of organic solvents on *in vitro* human skin water barrier function, *J. Invest. Dermatol.*, 101:609–613.

Alberti, I., Kalia, Y.N., Naik, A., Bonny, J.D., and Guy, R.H. (2001). *In vivo* assessment of enhanced topical delivery of terbinafine to human stratum corneum, *J. Controlled Release*, 71:319–327.

Alonso, A., Meirelles, N.C., and Tabak, M. (1995). Effect of hydration upon the fluidity of intercellular membranes of stratum corneum: an EPR study, *Biochim. Biophys. Acta*, 1237:6–15.

Al-Saidan, S.M., Selkirk, A.B., and Winfield, A.J. (1987). Effect of dimethylsulfoxide concentration on the permeability of neonatal rat stratum corneum to alkanols, *J. Invest. Dermatol.*, 89:426–429.

Astley J.P. and Levine, M. (1976). Effect of dimethyl sulfoxide on permeability of human skin *in vitro, J. Pharm. Sci.*, 65:210–215.

Ault, J.M., Lunte, C.E., Meltzer, N.M., and Riley, C.M. (1992). Microdialysis sampling for the investigation of dermal drug transport, *Pharm. Res.*, 9:1256–1261.

Aungst, B.J. (1989). Structure/effect studies of fatty acid isomers as skin penetration enhancers and skin irritants, *Pharm. Res.*, 6:244–247.

Aungst, B.J. (1994). Fatty acids as skin permeation enhancers, in D.S. Hsieh (ed.), *Percutaneous Penetration Enhancers*, Basel, Switzerland: Dekker, pp. 277–285.

Aungst, B.J., Blake, J.A., and Hussain, M.A. (1990). Contributions of drug solubilization, partitioning, barrier disruption, and solvent permeation to the enhancement of skin permeation of various compounds with fatty acids and amines, *Pharm Res.*, 7:712–718.

Aungst, B.J., Rogers, N.J., and Shefter, E. (1986). Enhancement of naloxone penetration through human skin *in vitro* using fatty acids, fatty alcohols, surfactants, sulfoxides and amides, *Int. J. Pharm.,* 33:225–234.

Bach, M. and Lippold, B.C. (1998). Influence of penetration enhancers on the blanching intensity of betamethasone 17-benzoate, *Int. J. Pharm.*, 168:97–108.

Barry, B.W. (1991). The LPP theory of permeation, in R.L. Bronaugh and H.I. Maibach (eds.), In Vitro *Percutaneous Absorption: Principles, Fundamentals and Applications*, Boca Raton, FL: CRC Press, pp. 165–183.

Barry, B.W. (1987). Mode of action of penetration enhancers in human skin, *J. Controlled Release*, 6:85–97.

Barry, B.W. and Bennett, S.L. (1987). Effect of penetration enhancers on the permeation of mannitol, hydrocortisone and progesterone through human skin, *J. Pharm. Pharmacol.*, 39:535–546.

Barry, B.W., Southwell, D., and Woodford, R. (1984). Optimization of bioavailability of topical steroids: penetration enhancers under occlusion, *J. Invest. Dermatol.*, 82:49–52.

Barry, B.W. and Williams, A.C. (1993). Terpenes as skin penetration enhancers, in K.A. Walters and J. Hadgraft (eds.), *Pharmaceutical Skin Penetration Enhancement,* New York: Dekker, pp. 95–111 .

Bennett, S.L., Barry, B.W., and Woodford, R. (1985). Optimization of bioavailability of topical steroids: non-occluded penetration enhancers under thermodynamic control, *J. Pharm. Pharmacol.*, 37:298–304.

Bentley, M.V., Vianna, R.F., Wilson, S., and Collett, J.H. (1997). Characterization of the influence of some cyclodextrins on the stratum corneum from the hairless mouse, *J. Pharm. Pharmacol.*, 49:397–402.

Berner, B., Mazzenga, G.C., Otte, J.H., Steffens, R.J., Juang, R.H., and Ebert, C.D. (1989). Ethanol:water mutually enhanced transdermal therapeutic system II: skin permeation of ethanol and nitroglycerin, *J. Pharm. Sci.*, 78:402–407.

Bezema, F.R., Marttin, E., Roemelé, P.E.H., Brussee, J., Boddé H.E., and de Groot, H.J.M. (1996). ^{2}H NMR evidence for dynamic disorder in human skin induced by the penetration enhancer Azone, *Spectrochim. Acta Part A: Mol. Spectrosc.*, 52:785–791.

Bhatia, K.S., Gao, S., Freeman, T.P., and Singh, J. (1997). Effect of penetration enhancers and iontophoresis on the ultrastructure and cholecystokinin-8 permeability through porcine skin, *J. Pharm. Sci.*, 86:1011–1015.

Bhatia K.S. and Singh, J. (1996). Pig ear skin as a model for predicting percutaneous absorption for humans, *Pharm. Sci.*, 2:275–276.

Bhatia, K.S. and Singh, J. (1997). Effect of dimethylacetamide and 2-pyrrolidone on the iontophoretic permeability of LHRH through porcine skin, *Drug Dev. Ind. Pharm.*, 23:1215–1218.

Bhatia, K.S. and Singh J. (1998a). Mechanism of transport enhancement of LHRH through porcine epidermis by terpenes and iontophoresis: permeability and lipid extraction studies, *Pharm Res.*, 15:1857–1862.

Bhatia, K.S. and Singh, J. (1998b). Synergistic effect of iontophoresis and a series of fatty acids on LHRH permeability through porcine skin, *J. Pharm. Sci.*, 87:462–469.

Bhatia, K.S. and Singh, J. (1999). Effect of linolenic acid/ethanol or limonene/ethanol and iontophoresis on the *in vitro* percutaneous absorption of LHRH and ultrastructure of human epidermis, *Int. J. Pharm.*, 180:235–250.

Bidmon, H., Pitts, J.D., Solomon, H.F., Bondi, V., and Stumpf, W.E. (1990). Estradiol distribution and penetration in rat skin after topical application, studies by high resolution autoradiography, *Histochemistry*, 95:43–54.

Boelsma, E., Tanojo, H., Boddé, H.E., and Ponec, M. (1996). Assessment of the potential irritancy of oleic acid on human skin: evaluation *in vitro* and *in vivo*, *Toxicol.* In Vitro, 10:729–742.

Bommannan, D., Potts, R.O., and Guy, R.H. (1990). Examination of stratum corneum barrier function *in vivo* by infrared spectroscopy, *J. Invest. Dermatol.*, 95:403–408.

Bond, J.R. and Barry, B.W. (1988). Hairless mouse skin is limited as a model for assessing the effects of penetration enhancers in human skin, *J. Invest. Dermatol.*, 90:810–813.

Bouwstra, J.A., Gooris, G.S., Brussee, J., Salomons-de Vries, M.A., and Bras, W. (1992). The influence of alkyl-azones on the ordering of the lamellae in human stratum corneum, *Int. J. Pharm.*, 79:141–148.

Bouwstra, J.A., Gooris, G.S., van der Spek, J.A., Lavrijsen, S., and Bras, W. (1994). The lipid and protein structure of mouse stratum corneum: a wide and small angle diffraction study, *Biochim. Biophys. Acta.*, 1212:183–192.

Bouwstra, J.A., Gooris, G.S., and White, S.H. (1997). X-ray analysis of the stratum corneum and its lipids, in R.O. Potts and R.H. Guy (eds.), *Mechanisms of Transdermal Drug Delivery*, New York: Dekker, pp. 41–86.

Bouwstra, J.A., Peschier, L.J.C., Brussee, J., and Boddé, H.E. (1989). Effect of *N*-alkyl-azocycloheptan-2-ones including Azone on the thermal behaviour of human stratum corneum, *Int. J. Pharm.*, 52:1–90.

Brain, K.R., Walters, K.A., Watkinson, A.C., (2002). Methods for studying percutaneous absorption, in K.A. Walters (ed.), *Dermatological and Transdermal Formulations*, New York: Dekker, pp. 197–269.

Bronaugh, R.L. (1989). Determination of percutaneous absorption by *in vitro* techniques, in R.L. Brounaugh and H.I. Maibach (eds.), *Percutaneous Absorption, Mechanisms—Methodology—Drug Delivery*, New York: Dekker, pp. 239–258.

Bronaugh, R.L. (1998). Current issues in the *in vitro* measurement of percutaneous absorption, in M.S. Roberts and K.A. Walters (eds.), *Dermal Absorption and Toxicity Assessments*, New York: Dekker, pp. 155–160.

Casal, H.L. and Mantsch, H.H. (1984). Polymeric phase behaviour of phospholipid membranes studied by infrared spectroscopy, *Biochim. Biophys. Acta*, 779:381–401.

Caspers P.J., Lucassen, G.W., Carter, E.A., Bruining, H.A., and Puppels, G.J. (2001). *In vivo* confocal Raman microspectroscopy of the skin: noninvasive determination of molecular concentration profiles, *J. Invest. Dermatol.*, 6:434–442.

Caspers, P.J., Lucassen, G.W., and Puppels, G.J. (2003). Combined *in vivo* confocal Raman spectroscopy and confocal microscopy of human skin, *Biophys. J.*, 85:572–580.

Catz, P. and Friend, D.R. (1989). Alkyl esters as skin permeation enhancers for indomethacin, *Int. J. Pharm.*, 55:17–23.

Chatterjee, D.J., Li, W.Y., and Koda, R.T. (1997). Effect of vehicles and penetration enhancers on the *in vitro* and *in vivo* percutaneous absorption of methotrexate and edatrexate through hairless mouse skin, *Pharm. Res.*, 14:1058–1065.

Chen, Y.L. and Wiedmann, T.S. (1996). Human stratum corneum lipids have a distorted orthorhombic packing at the surface of cohesive failure, *J. Invest. Dermatol.*, 107:15–19.

Choi, H.K., Flynn, G.L., and Amidon, G.L. (1990). Transdermal delivery of bioactive peptides: the effect of *n*-decylmethyl sulfoxide, pH, and inhibitors on enkephalin metabolism and transport, *Pharm. Res.*, 7:1099–1106.

Choi, H.K., Flynn, G.L., and Amidon, G.L. (1991). Some general influences of *n*-decylmethyl sulfoxide on the permeation of drugs across hairless mouse skin, *J. Invest. Dermatol.*, 96:822–826.

Cladera, J., O'Shea, P., Hadgraft, J., and Valenta, C. (2003). Influence of molecular dipoles on human skin permeability: use of 6-ketocholestanol to enhance the transdermal delivery of bacitracin, *J. Pharm. Sci.*, 92:1018–1027.

Clowes, H.M., Scott, R.C., and Heylings, J.R. (1994). Skin absorption: flow through or static diffusion cells, *Toxicol.* In Vitro, 8:827–830.

Corcuff, P., Fiat, F., and Minondo, A.M. (2001). Ultrastructure of the human stratum corneum, *Skin Pharmacol. Appl. Skin Physiol.*, 14:4–9.

Cornwell, P.A., Barry, B.W. Bouwstra, J.A., and Gooris, G.S. (1996). Modes of action of terpene penetration enhancers in human skin; differential scanning calorimetry, small-angle x-ray diffraction and enhancer uptake studies, *Int. J. Pharm.*, 127:9–26.

Degim, I.T., Uslu, A., Hadgraft, J., Atay, T., Akay, C., and Cevheroglu, S. (1999). The effects of Azone and capsaicin on the permeation of naproxen through human skin, *Int. J. Pharm.*, 179:1–134.

De Rosa, F.S., Marchetti, J.M., Thomazini, J.A., Tedesco, A.C., and Bentley, M.V. (2000). A vehicle for photodynamic therapy of skin cancer: influence of dimethylsulphoxide on 5-aminolevulinic acid *in vitro* cutaneous permeation and *in vivo* protoporphyrin IX accumulation determined by confocal microscopy, *J. Controlled Release*, 65:359–366.

Edwardson, P.A., Walker, M., Gardner, R.S., and Jacques, E. (1991). The use of FT-IR for the determination of stratum corneum hydration *in vitro* and *in vivo*, *J. Pharm. Biomed. Anal.*, 9:1089–1094.

El-Kattan, A.F., Asbill, C.S., Kim, N., and Michniak, B.B. (2001). The effects of terpene enhancers on the percutaneous permeation of drugs with different lipophilicities, *Int. J. Pharm.*, 215:229–240.

El-Kattan, A.F., Asbill, C.S., and Michniak, B.B. (2000). The effect of terpene enhancer lipophilicity on the percutaneous permeation of hydrocortisone formulated in HPMC gel systems, *Int. J. Pharm.*, 198:179–189.

Fabin, B. and Touitou, E. (1991). Localization of lipophilic molecules penetrating rat skin *in vivo* by quantitative autoradiography, *Int. J. Pharm.*, 74:59–65.

Fang, J.Y., Hung, C.F., Chiu, H.C., Wang, J.J., and Chan, T.F. (2003a). Efficacy and irritancy of enhancers on the *in vitro* and *in vivo* percutaneous absorption of curcumin, *J. Pharm. Pharmacol.*, 55:593–601.

Fang, J.Y., Hwang, T.L., Fang, C.L., and Chiu, H.C. (2003b). *In vitro* and *in vivo* evaluations of the efficacy and safety of skin permeation enhancers using flurbiprofen as a model drug, *Int. J. Pharm.*, 255:153–166.

Fang, J.Y., Leu, Y.L., Wang, Y.Y., and Tsai, Y.H. (2002). *In vitro* topical application and *in vivo* pharmacodynamic evaluation of nonivamide hydrogels using Wistar rat as an animal model, *Eur. J. Pharm. Sci.*, 15:417–423.

Foreman, M.I. (1976). A proton magnetic resonance study of water in human stratum corneum, *Biochim. Biophys. Acta*, 437:599–603.

Frank, S.B. (1976). Topical treatment of acne with a tetracycline preparations: results of a multi-group study, *Cutis*, 17:539–545.

Gao, S. and Singh, J. (1997). Mechanism of transdermal transport of 5-fluorouracil by terpenes: carvone, 1,8-cineole and thymol, *Int. J. Pharm.*, 154:67–77.

Gao, S. and Singh, J. (1998). In vitro percutaneous absorption enhancement of a lipophilic drug tamoxifen by terpenes, *J. Controlled Release*, 51:193–199.

Goates, C.Y. and Knutson, K. (1994). Enhanced permeation of polar compounds through human epidermis. I. Permeability and membrane structural change in the presence of short-chain alcohols, *Biochim. Biophys. Acta*, 1195:169–179.

Godwin, D.A. and Michniak, B.B. (1999). Influence of drug lipophilicity on terpenes as transdermal penetration enhancers, *Drug Dev. Ind. Pharm.*, 25:905–915.

Golden, G.M., Guzek, D.B., Harris, R.R., McKie, J.E., and Potts, R.O. (1986). Lipid thermotropic transitions in human stratum corneum, *J. Invest. Dermatol.*, 86:255–259.

Golden G.M., Guzek, D.B., Kennedy, A.H., McKie, J.E., and Potts, R.O. (1987). Stratum corneum lipid phase transitions and water barrier properties, *Biochemistry*, 26:2382–2388.

Golden, G.M., McKie, J.E., and Potts, R.O. (1987). Role of stratum corneum lipid fluidity in transdermal drug flux, *J. Pharm. Sci.*, 76:25–28.

Goodman, M. and Barry, B.W. (1988). Action of penetration enhancers on human skin as assessed by the permeation of model drugs 5-fluorouracil and estradiol. I. Infinite dose technique, *J. Invest. Dermatol.*, 91:323–327.

Gray, G.M. and Yardley, H.J. (1989). Lipid composition of cells isolated from pig, human, and rat epidermis, *J. Lipid Res.*, 16:434.

Grice, K., Sattar, H., Sharratt, M., and Baker, H. (1971). Skin temperature and transepidermal water loss, *J. Invest. Dermatol.*, 57:108–110.

Gwak, H.S. and Chun, I.K. (2001). Effect of vehicles and enhancers on the *in vitro* skin penetration of aspalatone and its enzymatic degradation across rat skins, *Arch. Pharm. Res.*, 24:572–577.

Gwak, H.S. and Chun, I.K. (2002). Effect of vehicles and penetration enhancers on the *in vitro* percutaneous absorption of tenoxicam through hairless mouse skin, *Int. J. Pharm.*, 236:57–64.

Hadgraft, J., Williams, D.G., and Allan, G. (1993). Azone: mechanisms of action and clinical effect, in K.A. Walters and J. Hadgraft (eds.), *Pharmaceutical Skin Penetration Enhancement*, New York: Dekker, pp. 175–197.

Harrison, J.E., Watkinson, A.C. Green, D.M., Hadgraft, J., and Brain, K. (1996). The relative effect of Azone and Transcutol on permeant diffusivity and solubility in human stratum corneum, *Pharm. Res.*, 13:542–546.

Hegemann, L., Forstinger, C., Partsch, B., Lagler, I., Krotz, S., and Wolff, K. (1995). Microdialysis in cutaneous pharmacology: kinetic analysis of transdermally delivered nicotine, *J. Invest. Dermatol.*, 104:839–843.

Higo, N., Naik, A., Bommannan, D.B., Potts, R.O., and Guy, R.H. (1993). Validation of reflectance infrared spectroscopy as a quantitative method to measure percutaneous absorption *in vivo*, *Pharm Res.*, 10:1500–1506.

Hoelgaard, A., Møllgaard, B., and Baker, E. (1988). Vehicle effect on topical drug delivery. IV. Effect of *N*-methylpyrrolidone and polar lipids on percutaneous drug transport, *Int. J. Pharm.*, 43:233–240.

Hori, M., Maibach, H.I., and Guy, R.H. (1992). Enhancement of propranolol hydrochloride and diazepam skin absorption *in vitro*. II: Drug, vehicle, and enhancer penetration kinetics, *J. Pharm. Sci.*, 81:330–333.

Hsu, L.R., Tsai, Y.H., and Huang, Y.B. (1991). The effect of pretreatment by penetration enhancers on the *in vivo* percutaneous absorption of piroxicam from its gel form in rabbits, *Int. J. Pharm.*, 71:193–200.

Hughes, M.F., Shrivastava, S.P., Fisher, H.L., and Hall, L.L. (1993). Comparative *in vitro* percutaneous absorption of *p*-substituted phenols through rat skin using static and flow-through diffusion systems, *Toxicol.* In Vitro, 7:221–227.

Hwang, C.C. and Danti, A.G. (1983). Percutaneous absorption of flufenamic acid in rabbits: effect of dimethyl sulfoxide and various nonionic surface-active agents, *J. Pharm. Sci.*, 72:857–860.

Ito, Y., Ogiso, T., and Iwaki, M. (1988). Thermodynamic study on enhancement of percutaneous penetration of drugs by Azone, *J. Pharmacobiodyn.*, 11:749–757.

Jiang, S.J. and Zhou, X.J. (2003). Examination of the mechanism of oleic acid-induced percutaneous penetration enhancement: an ultrastructural study, *Biol. Pharm. Bull.*, 26:66–68.

Johnson, M.E., Mitragotri, S., Patel, A., Blankschtein, D., and Langer, R. (1996). Synergistic effects of chemical enhancers and therapeutic ultrasound on transdermal drug delivery, *J. Pharm. Sci.*, 85:670–679.

Jokura, Y., Ishikawa, S., Tokuda, H., and Imokawa, G. (1995). Molecular analysis of elastic properties of the stratum corneum by solid-state ^{13}C-nuclear magnetic resonance spectroscopy, *J. Invest. Dermatol.*, 104:806–812.

Julian, E., Harrison, P.W., Groundwater, K.R., and Hadgraft, J. (1996). Azone® induced fluidity in human stratum corneum. A Fourier transform infrared spectroscopy investigation using the perdeuterated analogue, *J. Controlled Release*, 41:283–290.

Kalia, Y.N., Alberti, I., Sekkat, N., Curdy, C., Naik, A., and Guy, R.H. (2001). Normalization of stratum corneum barrier function and transepidermal water loss *in vivo*, *Pharm. Res.*, 17:1148–1150.

Kanikkannan, N., Kandimalla, K., Lamba, S.S., and Singh, M. (2000). Structure–activity relationship of chemical penetration enhancers in transdermal drug delivery, *Curr. Med. Chem.*, 7:593–608.

Kashibuchi, N., Hirai, Y., O'Goshi, K., and Tagami, H. (2002). Three-dimensional analyses of individual corneocytes with atomic force microscope: morphological changes related to age, location and to the pathologic skin conditions, *Skin Res. Technol.*, 8:203–211.

Kawasaki, Y., Quan, D., Sakamoto, K., and Maibach, H.I. (1997). Electron resonance studies on the influence of anionic surfactants on human skin, *Dermatology*, 194:238–242.

Kim, C.K., Kim, J.J., Chi, S.C., and Shim, C.K. (1993). Effect of fatty acids and urea on the penetration of ketoprofen through rat skin, *Int. J. Pharm.*, 99:109–118.

Kim, D.D., Kim, J.L., and Chien, Y.W. (1996). Mutual hairless rat skin permeation-enhancing effect of ethanol/water system and oleic acid, *J. Pharm. Sci.*, 85:1191–1195.

Kobayashi, D., Matsuzawa, T., Sugibayashi, K., Morimoto, Y., Kobayashi, M., and Kimura, M. (1993). Feasibility of use of several cardiovascular agents in transdermal therapeutic systems with 1-menthol-ethanol system on hairless rat and human skin, *Biol. Pharm. Bull.*, 16:254–258.

Komata, Y., Inaoka, M., Kaneko, A., and Fujie, T. (1992). *In vitro* percutaneous absorption of thiamine disulfide from a mixture of propylene glycol and fatty acid, *J. Pharm. Sci.*, 81:744–746.

Krishnaiah, Y.S.R., Satyanarayana, V., and Bhaskar, P. (2003). Enhanced percutaneous permeability of nicardipine hydrochloride by carvone across the rat abdominal skin, *Drug Dev. Ind. Pharm.*, 29:191–202.

Kunta, J.R., Goskonda, V.R., Brotherton, H.O., Khan, M.A., and Reddy, I.K. (1997). Effect of menthol and related terpenes on the percutaneous absorption of propranolol across excised hairless mouse skin, *J. Pharm. Sci.*, 86:1369–1373.

Kurihara-Bergstrom, T., Flynn, G.L., and Higuchi, W.I. (1987). Physicochemical study of percutaneous absorption enhancement by dimethyl sulfoxide: dimethyl sulfoxide mediation of vidarabine (ara-A). Permeation of hairless mouse skin, *J. Invest. Dermatol.*, 89:274–280.

Lambert; W.J., Higuchi, W.I., Knutson, K., and Krill, S.L. (1989). Dose-dependent enhancement effects of azone on skin permeability, *Pharm. Res.*, 6:798–803.

Lashmar, U.T., Hadgraft, J., and Thomas, N. (1989). Topical application of penetration enhancers to the skin of nude mice: a histopathological study, *J. Pharm. Pharmacol.*, 41:118–122.

Lazo, N.D., Maine, J.G., and Downing, D.T. (1995). Lipids are covalently attached to corneocyte protein envelopes existing predominantly as β-sheets: a solid state nuclear magnetic resonance study, *J. Invest. Dermatol.*, 105:301–313.

Leonard, T.W., Mikula, K.K., and Schlesinger, M.S. (1989a). Carvone enhancement of transdermal drug delivery, U.S. Patent 4888360.

Leonard, T.W., Mikula, K.K., and Schlesinger, M.S. (1989b). Eugenol enhancement of transdermal drug delivery, U.S. Patent 4888362.

Leopold, C.S. and Lippold, B.C. (1995). An attempt to clarify the mechanism of the penetration enhancing effects of lipophilic vehicles with differential scanning calorimetry (DSC), *J. Pharm. Pharmacol.*, 47:276–281.

Levang, A.K., Zhao, K., and Singh, J. (1999). Effect of ethanol/propylene glycol on the *in vitro* percutaneous absorption of aspirin, biophysical changes and macroscopic barrier properties of the skin, *Int. J. Pharm.*, 181:255–263.

Liron, Z., Clewell, H.J., and McDougal, J.N. (1994a). Kinetics of water vapor sorption in porcine stratum corneum, *J. Pharm. Sci.*, 83:692–698.

Liron, Z., Wright, R.L., and McDougal, J.N. (1994b). Water diffusivity in porcine stratum corneum measured by a thermal gravimetric analysis technique, *J. Pharm. Sci.*, 83:457–462.

Lopez, A., Llinares, F., Cortell, C., and Herraez, M. (2000). Comparative enhancer effects of Span20 with Tween20 and Azone on the *in vitro* percutaneous penetration of compounds with different lipophilicities, *Int. J. Pharm.*, 202:133–140.

López-Castellano, C., Cortell-Ivars, G., López-Carballo and Herráez-Domínguez, M. (2000). The influence of Span®20 on stratum corneum lipids in Langmuir monolayers: comparison with Azone®, *Int. J. Pharm.*, 203:245–253.

Lotte, C., Rougier, A., Wilson, D.R., and Maibach, H.I. (1987). *In vivo* relationships between transepidermal water loss and percutaneous penetration of some organic compounds in man: effect of anatomic site, *Arch. Dermatol. Res.*, 279:351–356.

Lu, M.Y., Lee, D., and Rao, G.S. (1992). Percutaneous absorption enhancement of leuprolide, *Pharm. Res.*, 9:1575–1579.

Maibach, H.I., Bronaugh, R., Guy, R., Turr, E., Wilson, D., Jacques, S., and Chaing, D. (1984). Noninvasive techniques for determining skin function, in V.A. Drill and P. Lazar (eds.), *Cutaneous Toxicity*, New York: Raven Press, pp. 63–97.

Mak, V.H., Potts, R.O., and Guy, R.H. (1990). Percutaneous penetration enhancement *in vivo* measured by attenuated total reflectance infrared spectroscopy, *Pharm. Res.*, 7:835–841.

Marjukka Suhonen, T., Bouwstra, J,A., and Urtti, A. (1999). Chemical enhancement of percutaneous absorption in relation to stratum corneum structural alterations, *J. Controlled Release*, 59:149–161.

McCullough, J.L., Peckham, P., Klein, J., Weinstein, G.D., and Jenkins, J.J. (1985). Regulation of epidermal proliferation in mouse epidermis by combination of difluoromethyl ornithine (DFMO) and methylglyoxal bis(guanylhydrazone) (MGBG), *J. Invest. Dermatol.*, 85:518–521.

McDonald, S. and Lunte, C. (2003). Determination of the dermal penetration of esterom components using microdialysis sampling, *Pharm. Res.*, 20:1827–1834.

Meidan, V.M., Al-Khalili, M., and Michniak, B.B. (2003). Enhanced iontophoretic delivery of buspirone hydrochloride across human skin using chemical enhancers, *Int. J. Pharm.*, 264:73–83.

Meyer, W., Schwarz, R., and Neurand, K. (1978). The skin of domestic mammals as a model for the human skin, with reference to the domestic pig, *Curr. Probl. Dermatol.*, 7:39.

Mirejovsky, D. and Takruri, H. (1986). Dermal penetration enhancement profile of hexamethylenelauramide and its homologues: *in vitro* versus *in vivo* behavior of enhancers in the penetration of hydrocortisone, *J. Pharm. Sci.*, 75:1089–1093.

Mitragotri, S., Edwards, D.A., Blankschtein, D., and Langer, R. (1995). A mechanistic study of ultrasonically-enhanced transdermal drug delivery, *J. Pharm. Sci.*, 84:697–706.

Mizushima, J., Kawasaki, Y., Tabohashi, T., Kitano, T., Sakamoto, K., Kawashima, M., Cooke, R., and Maibach, H.I. (2000). Effect of surfactants on human stratum corneum: electron paramagnetic resonance study, *Int. J. Pharm.*, 197:193–202.

Montagna, W. and Yun, J.S. (1964). The skin of domestic pig, *J. Invest. Dermatol.*, 43:11.

Monteiro-Riviere, N.A. (1986). Ultrastructural evaluation of porcine integument, in M.E. Tumbleson (ed.), *Swine in Biomedical Research*, New York: Plenum, pp. 641–655.

Monteiro-Riviere, N.A. (1991). Comparative anatomy, physiology, and biochemistry of mammalian skin, in D.W. Hobson (ed.), *Dermal and Ocular Toxicology: Fundamental and Methods*, Boston: CRC Press, pp. 3–72.

Mukherji, E., Millenbaugh, L.S., and Au, J.S. (1994). Percutaneous absorption of 2′,3′-dideoxyinosine in rats, *Pharm. Res.*, 11:809–815.

Naito, S.I., Nakamori, S. Awataguchi, M. Nakajima, T., and Tominaga, H. (1985). Observations on and pharmacokinetic discussion of percutaneous absorption of mefenamic acid, *Int. J. Pharm.*, 24:127–147.

Niazy, E.M. (1991). Influence of oleic acid and other permeation promoters on transdermal delivery of dihydroergotamine through rabbit skin, *Int. J. Pharm.*, 67:97–100.

Nolan, L.M., Corish, J. Corrigan, O.I., and Fitzpatrick, D. (2003). Iontophoretic and chemical enhancement of drug delivery. Part I: across artificial membranes. *Int. J. Pharm.*, 257:41–55.

Nuwayser, E.S., Gay, M.H. De Roo, D.J., and Blaskivich, P.D. (1988). Transdermal nicotine—an aid to smoking cessation, *Proc. Int. Symp. Controlled Release Bioact. Mater.*, 15:213–214.

Obata, Y., Takayama, K., Machida, Y., and Nagai, T. (1991). Combined effect of cyclic monoterpenes and ethanol on percutaneous absorption of diclofenac sodium, *Drug Des. Discov.*, 8:137–144.

Obata, Y., Takayama, K., Maitani, Y., Machida, Y., and Nagai, T. (1993). Effect of pretreatment of skin with cyclic monoterpenes on permeation of diclofenac in hairless rat, *Biol. Pharm. Bull.*, 16:312–314.

Obata, Y., Takayama, K., Maitani, Y., Okabe, H., and Nagai, T. (1990). Effect of cyclic monoterpenes on percutaneous absorption in the case of a water-soluble drug (diclofenac sodium), *Drug Des. Deliv.*, 6:319–328.

Ogiso, T., Hata, T., Iwaki, M., and Tanino, T. (2001). Transdermal absorption of bupranolol in rabbit skin *in vitro* and *in vivo*, *Biol. Pharm. Bull.*, 24:588–591.

Ogiso, T., Ito, Y., Iwaki, M., and Atago, H. (1986). Absorption of indomethacin and its calcium salt through rat skin: effect of penetration enhancers and relationship between *in vivo* and *in vitro* penetration, *J. Pharmacobiodyn.*, 9:517–525.

Ogiso, T., Iwaki, M., and Paku, T. (1995). Effect of various enhancers on transdermal penetration of indomethacin and urea, and relationship between penetration parameters and enhancement factors, *J. Pharm. Sci.*, 84:482–488.

Ohara, N., Takayama, K., and Nagai, T. (1995). Combined effect of *d*-limonene pretreatment and temperature on the rat skin permeation of lipophilic and hydrophilic drugs, *Biol. Pharm. Bull.*, 18:439–442.

Okabe, H., Obata, Y., Takayama, K., and Nagai, T. (1990). Percutaneous absorption promoting effect and skin irritancy of monocyclic monoterpenes, *Drug. Des. Deliv.*, 6:229–238.

Okabe, H., Takayama, K., and Nagai, T. (1992). Percutaneous absorption of ketoprofen from acrylic gel patches containing D-limonene and ethanol as absorption enhancers, *Chem. Pharm. Bull.*, 40:1906–1910.

Okamoto, H., Muta, K., Hashida, M., and Sezaki, H. (1990). Percutaneous penetration of acyclovir through excised hairless mouse and rat skin: effect of vehicle and percutaneous penetration enhancer, *Pharm. Res.*, 7:64–68.

Patel, R.A. and Vasavada, R.C. (1988). Transdermal delivery of isoproterenol HCl: an investigation of stability, solubility, partition coefficient, and vehicle effects, *Pharm. Res.*, 5:116–119.

Percot, A. and Lafleur, M. (2001). Direct observation of domains in model stratum corneum lipid mixtures by Raman microspectroscopy, *Biophys J.*, 81:2144–2153.

Pershing, L.K., Lambert, L.D., and Knutson, K. (1990). Mechanism of ethanol-enhanced estradiol permeation across human skin *in vivo*, *Pharm Res.*, 7:170–175.

Pilgram, G.S., Van Pelt, A.M., Bouwstra, J.A., and Koerten, H.K. (1999). Electron diffraction provides new information on human stratum corneum lipid organization studied in relation to depth and temperature, *J. Invest. Dermatol.*, 113:403–409.

Pilgram, G.S., Van Pelt, A.M., Spies, F., Bouwstra, J.A., and Koerten, H.K. (1998). Cryo-electron diffraction as a tool to study local variations in the lipid organization of human stratum corneum, *J. Microsc.*, 189:71–78.

Pirot, F., Kalia, Y.N., Stinchcomb, A.L. Keating, G., Bunge, A., and Guy, R.H. (1997). Characterization of the permeability barrier of human skin *in vivo*, *Proc. Natl. Acad. Sci. U S A*, 94:1562–1567.

Ponec, M., Boelsma, E. Weerheim, A., Mulder, A., Bouwstra, J.A., and Mommaas, M. (2000). Lipid and ultrastructural characterization of reconstructed skin models, *Int. J. Pharm.*, 203:211–225.

Ponec, M., Haverkort, M., Soei, Y.L., Kempenaar, J., Brussee, J., and Bodde, H. (1989). Toxicity screening of *N*-alkylazacycloheptan-2-one derivatives in cultured human skin cells: structure-toxicity relationships, *J. Pharm. Sci.*, 78:738–741.

Potts, R.O., Guzek, D.B., Harris, R.R., and McKie, J.E. (1985). A noninvasive, *in vivo* technique to quantitatively measure water concentration of the stratum corneum using attenuated total-reflectance infrared spectroscopy, *Arch. Dermatol. Res.*, 277:489–495.

Priborsky, J. and Muhlbachova, E. (1990). Evaluation of *in-vitro* percutaneous absorption across human skin and in animal models, *J. Pharm. Pharmacol.*, 42:468–472.

Priborsky, J., Takayama, K., Nagai, T., Waitzova, D., and Elis, J. (1987). Combination effect of penetration enhancers and propylene glycol on *in vitro* transdermal absorption of insulin, *Drug. Des. Deliv.*, 2:91–97.

Puglia, C., Bonina, F., Trapani, G., Franco, M., and Ricci, M. (2001). Evaluation of *in vitro* percutaneous absorption of lorazepam and clonazepam from hydro-alcoholic gel formulations, *Int. J. Pharm.*, 228:79–87.

Rastogi, S.K. and Singh, J. (2001). Lipid extraction and transport of hydrophilic solutes through porcine epidermis, *Int. J. Pharm.*, 225:75–82.

Rastogi, S.K. and Singh, J. (2002). Transepidermal transport enhancement of insulin by lipid extraction and iontophoresis, *Pharm. Res.*, 19:427–433.

Rehfeld, S.J., Plachy, W.Z., Hou, S.Y., and Elias, P.M. (1990). Localization of lipid microdomains and thermal phenomena in murine stratum corneum and isolated membrane complexes: an electron spin resonance study, *J. Invest. Dermatol.*, 95:217–223.

Ribaud, C., Garson, J.C., Doucet, J., and Leveque, J.L. (1994). Organization of stratum corneum lipids in relation to permeability: influence of sodium lauryl sulfate and preheating, *Pharm. Res.*, 11:1414–1418.

Riviere, J.E., Qiao, G., Baynes, R.E., Brooks, J.D., and Mumtaz, M. (2001). Mixture component effects on the *in vitro* dermal absorption of pentachlorophenol, *Arch. Toxicol.*, 75:329–334.

Roberts, M.S. and Walters, K.A. (1998). The relationship between structure and barrier function of skin, in M.S. Roberts and K.A. Walters (eds.), *Dermal Absorption and Toxicity Assessment*, New York: Dekker, pp. 1–42.

Rosado, C. and Rodrigues, L.M. (2003). Solvent effects in permeation assessed *in vivo* by skin surface biopsy, *BMC Dermatol.*, 3:5.

Rougier, A., Lotte, C., and Maibach, H.I. (1989). *In vivo* relationship between percutaneous absorption and transepidermal water loss, in R.L. Bronaugh and H.I. Maibach (eds.), *Percutaneous Absorption*, New York: Dekker, pp. 175–190.

Sasaki, H., Kojima, M., Nakamura, J., and Shibasaki, J. (1990a). Acute toxicity and skin irritation of pyrrolidone derivatives as transdermal penetration enhancer, *Chem. Pharm. Bull.*, 38:2308–2310.

Sasaki, H., Kojima, M., Nakamura, J., and Shibasaki, J. (1990b). Enhancing effect of combining two pyrrolidone vehicles on transdermal drug delivery, *J. Pharm. Pharmacol.*, 42:196–199.

Sasaki, H., Kojima, M., Nakamura, J., and Shibasaki, J. (1990c). Enhancing effect of pyrrolidone derivatives on transdermal penetration of phenolsulfonphthalein and indomethacin from aqueous vehicle, *Chem. Pharm. Bull.*, 38:797–799.

Scheuplein, R.J. and Ross, L. (1974). Mechanism of percutaneous absorption. V. Percutaneous absorption of solvent deposited solids, *J. Invest. Dermatol.*, 62:353–360.

Schreiner, V., Gooris, G.S., Pfeiffer, S., Lanzendorfer, G., Wenck, H., Diembeck, W., Proksch, E., and Bouwstra, J. (2000). Barrier characteristics of different human skin types investigated with x-ray diffraction, lipid analysis, and electron microscopy imaging, *J. Inves. Dermatol.*, 114:654–660.

Seki, T., Kawaguchi, T., Sugibayashi, K., Juni, K., and Morimoto, Y. (1989). Percutaneous absorption of azidothymidine in rats, *Int. J. Pharm.*, 57:73–75.

Serban, G.P., Henry, S.M., Cotty, V.F., and Marcus, A.D. (1981). *In vivo* evaluation of skin lotions by electrical capacitance and conductance, *J. Soc. Cosmet. Chem.*, 32:421–435.

Shin, S.C., Shin, E.Y., and Cho, C.W. (2000). Enhancing effects of fatty acids on piroxicam permeation through rat skins, *Drug Dev. Ind. Pharm.*, 26:563–566.

Singh, S. and Singh, J. (2001). Dermal toxicity: effect of jet propellant-8 fuel exposure on the biophysical, macroscopic and microscopic properties of porcine skin, *Environ. Toxicol. Pharmacol.*, 10:123–131.

Singh, S. and Singh, J. (2004). Dermal toxicity and microscopic alterations by JP-8 jet fuel components *in vivo* in rabbit, *Environ. Toxicol. Pharmacol.*, 16:153–161.

Sjogren, F. and Anderson, C. (2000). The spectrum of inflammatory cell response to dimethyl sulfoxide, *Contact Derm.*, 42:216–221.

Smith, J.G., Chalker, D.K., and Wehr, R.F. (1976). The effectiveness of topical and oral tetracycline for acne, *South Med. J.*, 69:695–697.

Southwell, D. and Barry, B.W. (1983). Penetration enhancers for human skin: mode of action of 2-pyrrolidone and dimethylformamide on partition and diffusion of model compounds water, *n*-alcohols, and caffeine, *J. Invest. Dermatol.*, 80:507–514.

Stoughton, R.B. (1982). Enhanced percutaneous penetration with 1-dodecylazacycloheptan-2-one, *Arch. Dermatol.*, 118:474–477.

Sugibayashi, K., Nemoto, M., and Morimoto, Y. (1988). Effect of several penetration enhancers on the percutaneous absorption of indomethacin in hairless rats, *Chem. Pharm. Bull.*, 36:1519–1528.

Takayama, K., Kikuchi, K., Obata, Y., Machida, Y., and Nagai, T. (1991). Terpenes as percutaneous absorption promote, *STP Pharm. Sci.*, 1:83–88.

Tanojo, H., Bouwstra, J.A., Junginger, H.E., and Bodde, H.E. (1994). Subzero thermal analysis of human stratum corneum, *Pharm. Res.*, 11:1610–1616.

Tanojo, H., Boelsma, E. Junginger, H.E., Ponec, M., and Bodde, H.E. (1998). *In vivo* human skin barrier modulation by topical application of fatty acids, *Skin Pharmacol. Appl. Skin Physiol.*, 11:87–97.

Tenjarla, S.N., Kasina, R., Puranajoti, P., Omar, M.S., and Harris, W.T. (1999). Synthesis and evaluation of *N*-acetylprolinate esters—novel skin penetration enhancers, *Int. J. Pharm.*, 192:147–158.

Thiele, F.A. and Malten, K.E. (1973). Evaluation of skin damage. I. Skin resistance measurements with alternating current (impedance measurements), *Br. J. Dermatol.*, 89:373–382.

Touitou, E., Godin, B., Karl, Y., Bujanover, S., and Becker, Y. (2002). Oleic acid, a skin penetration enhancer, affects Langerhans cells and corneocytes, *J. Controlled Release*, 80:1–7.

Vaddi, H.K., Ho, P.C., Chan, Y.W., and Chan, S.Y. (2002). Terpenes in ethanol: haloperidol permeation and partition through human skin and stratum corneum changes, *J. Controlled Release*, 81:121–133.

Vaddi, H.K., Ho, P.C., Chan, Y.W., and Chan, S.Y. (2003). Oxide terpenes as human skin penetration enhancers of haloperidol from ethanol and propylene glycol and their modes of action on stratum corneum, *Biol. Pharm. Bull.*, 26:220–228.

Van Duzee, B.F. (1971). Thermal analysis of human stratum corneum, *J. Invest. Dermatol.*, 65:702–747.

Van Kuijk-Meuwissen, M.E., Mougin, L., Junginger, H.E., and Bouwstra, J.A. (1998). Application of vesicles to rat skin *in vivo*: a confocal laser scanning microscopy study, *J. Controlled Release*, 56:189–196.

Van der Valk, P.G., and Maibach, H.I. (1989). Post-application occlusion substantially increases the irritant response of the skin to repeated short-term sodium lauryl sulfate (SLS). exposure, *Contact Derm.*, 21:335–338.

Wang, M.Y., Yang, Y.Y., and Heng, P.W. (2004). Role of solvent in interactions between fatty acids-based formulations and lipids in porcine stratum corneum, *J. Controlled Release*, 94:207–216.

Warner, R.R., Stone, K.J., and Boissy, Y.L. (2003). Hydration disrupts human stratum corneum ultrastructure, *J. Invest. Dermatol.*, 120:275–284.

Wearley, L. and Chien, Y.W. (1990). Enhancement of *in vitro* permeability of azidothymidine (AZT) via iontophoresis and chemical enhancers, *Pharm. Res.*, 7:34–40.

Weber, C.J., Jicha, D., Matz, S., Siverly, J., O'Doriso, T., Strausberg, L., Laurencot, J., McLarty, A., Norton, J., and Kazim, M. (1987). Passage of somatostatin analogue across human and mouse skin, *Surgery*, 102:974–981.

Wechsler, H.L., Kirk, J., and Slone, J. (1978). Acne treated with a topical tetracycline preparation: results of a one-year multi-group study, *Int. J. Dermatol.*, 17:237–242.

Wester, R.C. and Maibach, H.I. (1989). *In vivo* animal models for percutaneous absorption, in R.L. Bronaugh and H.I. Maibach (eds.), *Percutaneous Absorption, Mechanisms—Methodology—Drug Delivery*, New York: Dekker, pp. 221–238.

Wester, R.C. and Maibach, H.I. (1999). *In vivo* methods for percutaneous absorption measurements, in R.L. Bronaugh and H.I. Maibach (eds.), *Percutaneous Absorption. Drugs—Cosmetics—Mechanisms—Methodology*, New York: Dekker, pp. 215–227.

White, S.H., Mirejovsky, D., and King, G.I. (1988). Structure of lamellar lipid domains and corneocyte envelopes of murine stratum corneum. An x-ray diffraction study, *Biochemistry*, 27:3725–3732.

Wiechers, J.W., Drenth, B.F., Adolfsen, F.A., Prins, L., and de Zeeuw, R.A. (1990). Disposition and metabolic profiling of the penetration enhancer Azone. I. *In vivo* studies: urinary profiles of hamster, rat, monkey, and man, *Pharm. Res.*, 7:496–499.

Wiechers, J.W., Drenth, B.F., Jonkman, J.H., and de Zeeuw, R.A. (1987). Percutaneous absorption and elimination of the penetration enhancer Azone in humans, *Pharm. Res.*, 4:519–523.

Wilhelm, K.P., Surber, C., and Maibach, H.I. (1989). Quantification of sodium lauryl sulfate irritant dermatitis in man: comparison of four techniques: skin color reflectance, transepidermal water loss, laser Doppler flow measurement and visual scores, *Arch. Dermatol. Res.*, 281:293–295.

Wilhelm, K.P., Surber, C., and Maibach, H.I. (1991). Effect of sodium lauryl sulfate-induced skin irritation on *in vivo* percutaneous penetration of four drugs, *J. Invest. Dermatol.*, 97:927–932.

Williams, A.C. and Barry, B.W. (1989). Urea analogues in propylene glycol as penetration enhancers in human skin, *Int. J. Pharm.*,56:43–50.

Williams, A.C. and Barry, B.W. (1991a). The enhancement index concept applied to terpene penetration enhancers for human skin and model lipophilic (oestradiol) and hydrophilic (5-fluorouracil) drugs, *Int. J. Pharm.*, 74:157–168.

Williams, A.C. and Barry, B.W. (1991b). Terpenes and the lipid-protein-partitioning theory of skin penetration enhancement, *Pharm. Res.*, 8:17–24.

Williams, A.C., Edwards, H.G.M., and Barry, B.W. (1992a). Fourier transform Raman spectroscopy: a novel application for examining human stratum corneum, *Int. J. Pharm.*, 81:R11–R14.

Williams, A.C. and Barry, B.W. (1992b). Skin absorption enhancers, *Crit. Rev. Ther. Drug Carrier Syst.*, 94:305–353.

Wilson, D.R. and Maibach, H.I. (1982). A review of transepidermal water loss: physical aspects and measurements as related to infants and adults, in H.I. Maibach and E.K. Bouititis (eds.), *Neonatal Skin*, New York: Dekker, pp. 83–100.

Wong, T.W., Aizawa, K., Sheyhedin, I., Wushur, C., and Kato, H. (2003). Pilot study of topical delivery of mono-L-aspartyl chlorin e6 (NPe6): implication of topical NPe6-photodynamic therapy, *J. Pharmacol. Sci.*, 93:136–142.

Wu, P.C., Chang, J.S., Huang, Y.B., Chai, C.Y., and Tsai, Y.H. (2001). Evaluation of percutaneous absorption and skin irritation of ketoprofen through rat skin: *in vitro* and *in vivo* study, *Int. J. Pharm.*, 222:225–235.

Xu, P. and Chien, Y.W. (1991). Enhanced skin permeability for transdermal drug delivery: physiopathological and physicochemical considerations, *Crit. Rev. Ther. Drug Carrier Syst.*, 8:211–236.

Yamamura, T. and Tezuka, T. (1989). The water-holding capacity of the stratum corneum measured by ^{1}H-NMR, *J. Invest. Dermatol.*, 93:160–164.

Yamane, M.A., Williams, A.C., and Barry, B.W. (1995). Terpene penetration enhancers in propylene glycol/water co-solvent systems: effectiveness and mechanism of action, *J. Pharm. Pharmacol.*, 47:978–989.

Yoshiike, T., Aikawa, Y., Sindhvananda, J., Suto, H., Nishimura, K., Kawamoto, T., and Ogawa, H. (1993). Skin barrier defect in atopic dermatitis: increased permeability of the stratum corneum using dimethyl sulfoxide and theophylline, *J. Dermatol. Sci.*, 5:92–96.

Yu, D., Sanders, L.M., Davidson, G.W., 3rd, Marvin, M.J., and Ling, T. (1988). Percutaneous absorption of nicardipine and ketorolac in rhesus monkeys, *Pharm Res.*, 5:457–462.

Zhao, K. and Singh, J. (1998). *In vitro* percutaneous absorption enhancement of tamoxifen by terpenes: eugenol, D-limonene, and menthone, *J. Controlled Release*, 55:253–260.

Zhao, K. and Singh, J. (1999). *In vitro* percutaneous absorption enhancement of propranolol hydrochloride through porcine epidermis by terpenes/ethanol, *J. Controlled Release*, 62:359–366.

Zhao, K. and Singh, J. (2000). Mechanism(s) of *in vitro* percutaneous absorption enhancement of tamoxifen by enhancers, *J. Pharm. Sci.*, 89:771–780.

Zhao, K., Singh, S., and Singh, J. (1998). Effect of menthone on the *in vitro* percutaneous absorption of tamoxifen and skin reversibility, *Int. J. Pharm.*, 219:177–181.

Zhao, K., Singh, S., and Singh, J. (2001). Effect of menthone on the *in vitro* percutaneous absorption of tamoxifen and skin reversibility, *Int. J. Pharm.*, 219:177–181.

CHAPTER 13

Dermal Blood Flow, Lymphatics, and Binding as Determinants of Topical Absorption, Clearance, and Distribution

Sheree E. Cross and Michael S. Roberts

CONTENTS

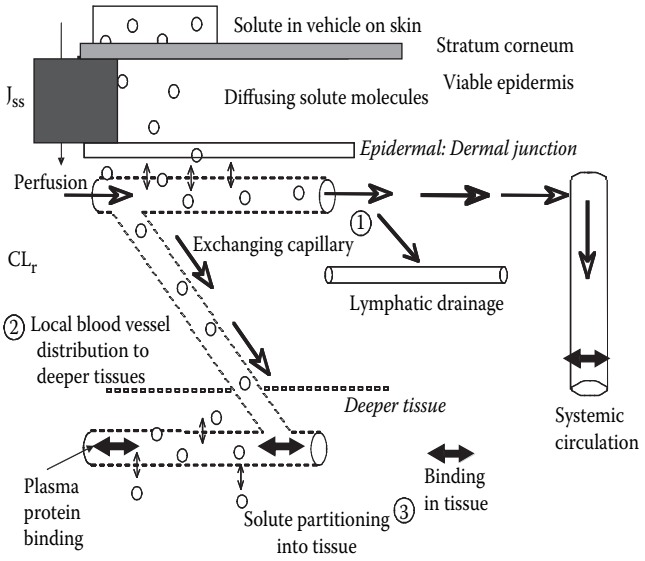

Figure 13.1 Clearance mechanisms determining solute concentrations below topical application sites.

INTRODUCTION

Most studies on percutaneous absorption emphasize the penetration of drugs, toxins, and other solutes into and through the skin as described in this book. Percutaneous absorption is also dependent on the clearance of solutes from the skin and transport into deeper layers of the skin (Figure 13.1). Clearance mechanisms in the avascular viable epidermis, diffusion in the dermis, and export from/within the dermis include solute diffusion and physiological transport by the dermal blood and lymphatic systems. This chapter focuses on the nature of these clearance mechanisms and how they affect the rates of percutaneous absorption and the levels of solute in skin and tissue. We consider first the role of blood flow, followed by the role of binding, transport to deeper tissues, and then the role of lymphatics.

PRINCIPLES OF DERMAL CLEARANCE AND PERCUTANEOUS ABSORPTION

A number of pharmacokinetic models have been used to relate concentrations of drugs in skin tissues and removal from the skin with the various transport determinants. It can be shown that in the simplest, steady-state case, the cumulative amount of a solute penetrating the epidermis $Q_{ss}(t)$ is linearly related to an exposure time t, a steady-state flux J_{ss}, a lag time lag, and the application area A:

$$Q_{ss}(t) = J_{ss}A(t - lag) \quad (13.1)$$

In turn, J_{ss} can be related to the apparent permeability coefficient k_p, the partition coefficient of solute $K_{v\text{-}r}$ between the vehicle v and sampling site r (usually dermis or, if *in vitro*, receptor solution) (note that K_r in Roberts and Anissimov, 2005, equals $1/K_{v-r}$) and the solute concentrations in the donor C_v and sampling site below the epidermis C_{rss} (Roberts and Anissimov, 2005):

$$J_{ss} = k_p (C_v - K_{v-r} C_{rss}) \tag{13.2}$$

where k_p is defined by the resistances ($1/k_p$ = sum of the reciprocals for the permeability coefficients of the stratum corneum *sc*, viable epidermis *ve*, and vehicle *v*; i.e., $1/k_p = 1/k_{p,sc} + 1/k_{p,ve} + 1/k_{p,v}$) (Anissimov and Roberts, 2004). C_{rss} is defined by the relative influx (determined by k_p, C_v, and A) and clearance CL_r from the sampling site and has been expressed as (Roberts and Anissimov, 2004)

$$C_{rss} = \frac{k_p A C_v}{CL_r + K_{v-r} k_p A} \tag{13.3}$$

Siddiqui et al. (1989) applied a reduced form of Equation 13.3 to predict likely steady-state steroid concentrations in the viable dermis using excised skin flux and *in vivo* dermal clearance data. Roberts (1991) used Equation 13.3 to show that when clearance is much less than influx rate, the steady-state tissue or receptor concentration approached that of the donor, that is, $C_{rss} \rightarrow C_v/K_{v-r}$. He suggested that this situation could apply for aqueous solutions of phenolic compounds. In most cases, such as for steroids, varying either influx rate or clearance affects the resulting steady-state concentration (Roberts, 1991).

As is evident by combining Equation 13.2 and Equation 13.3, J_{ss} can also be expressed as a function of clearance CL_r (Anissimov and Roberts, 2004):

$$J_{ss} = k_p C_v \frac{CL_r}{CL_r + K_{v-r} k_p A} \tag{13.4}$$

Thus, two situations arise:

1. When clearance CL_r is sufficiently high to no longer be rate limiting, $C_{ss} \rightarrow 0$, that is, sink conditions, so that $J_{ss} \rightarrow k_p C_v$, the usual equation used by most authors to describe the transport of solutes across the epidermis.
2. When CL_r is a rate-determining step in the transport of drugs through the skin and, in this case, as has been reported with altered vasoconstriction and steroid skin absorption (Siddiqui et al., 1989), a decrease in clearance CL_r will lead first to a decrease in steady-state flux J_{ss} and second an increase in the sampling site concentration C_{rss}. It should be emphasized that, although a significant change in clearance CL_r may not have significantly affected J_{ss}, changes in CL_r may have had substantial effects on the sampling site concentrations C_{ssr} as is evident in Equation 13.3.

The material discussed in this chapter applies to this second case. *In vivo* clearance can be defined by transport into the blood, into the lymphatics, and into deeper tissues and by binding to blood components and tissues as discussed in the section "Direct Deeper Tissue Penetration." The volumes taken and timings of repeated sampling define *in vitro* clearance. Note that if a material is included to increase solute solubility in the receptor solution (for example, protein, surfactant, or cosolvent), K_{v-r} is decreased, sink conditions are promoted, and J_{ss} becomes less dependent on $K_{v-r}C_{ssr}$ (Equation 13.2).

We now consider the first of the *in vivo* determinants, cutaneous blood flow.

CUTANEOUS BLOOD FLOW

Cutaneous blood flow not only serves to remove solutes from the dermal papillary layer immediately below the epidermis into the systemic circulation but also can facilitate the distribution of solutes into tissues below the application site. The role of cutaneous blood flow and blood vessel orientation on the rate of absorption, and subsequent distribution, of topically applied solutes into underlying tissues and the systemic circulation is still a relatively poorly understood area. It remains unclear, for instance, the extent to which solutes reach deeper tissues (such as muscle and joints) after topical application by (1) direct diffusion of solute molecules down to the tissue layers; (2) carriage to deeper tissues by the local cutaneous by the local blood supply; and (3) recirculation, by which solutes cross the epidermal–dermal barrier are then are cleared in the blood capillaries of the upper dermis into the body and then redistributed from the systemic circulation back into the deeper tissues. The mechanism is also likely to be related to site of application and physiological condition at the site. We now consider these factors in more detail.

Skin Microcirculation: Structure and Function

In addition to its barrier function, the skin has a number of functions, including sensory perception, immune activities, metabolism, secretory activities, and thermoregulation. The involvement of dermal microcirculation in body temperature control accounts for much of the observed blood vessel orientation, humoral and nervous control, and large variations in flow capacity (Charkoudian, 2003).

Cutaneous blood supply (arterioles, arterial and venous capillaries), and venules form the two major dermal microcirculatory horizontal plexuses, upper and lower (Figure 13.2). A detailed description of the anatomy and physiology of the cutaneous circulation was presented by Braveman (1995); however, the following summary conceptualizes the main aspects of relevance to this discussion. The upper plexus contains capillary loops that supply each dermal papilla and sits in the upper papillary dermis (1 to 2 μm below the surface of the skin). Within these capillary loops, the diameter of the crest is 1 to 1.5 μm wider than the ascending tube, with a wall thickness measuring only 10 to 30 nm. Bridged fenestrations within capillaries are not normally only found in the skin and are limited to body sites such as the renal glomeruli, in which specific filtration roles exist; however, the review presented by

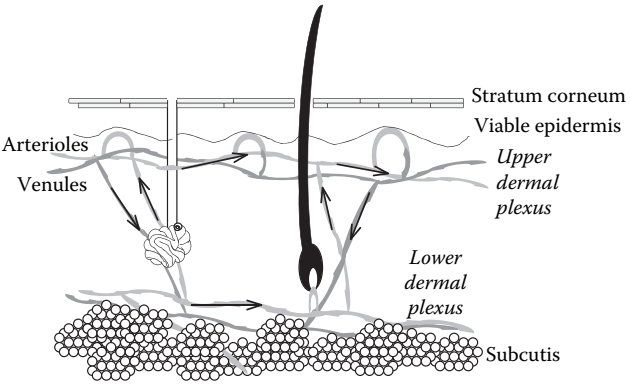

Figure 13.2 Diagrammatic representation of the basic organizational structure of cutaneous microvasculature.

Braveman (1995) suggested that they have been found in capillary loops in psoriatic lesions, although their function in this condition is unclear.

The lower plexus, which is formed by vessels from the underlying muscles and subcutaneous fat, sits in the hypodermis and contains vessels that connect with the upper plexus and connect laterally through the skin to supply hair follicle bulbs and sweat glands. In addition, we also find a number of connections between the arterioles and venules ascending and descending within the dermis between these two main plexuses. In general, the vessels of the upper plexus are smaller in diameter than those of the lower plexus, 10 to 35 μm vs. 40 to 50 μm. The majority of vessels are also postcapillary venules and represent the physiologically most reactive section of the microcirculation for example, the site of inflammatory cell migration into tissues and vascular permeability increases).

Resting blood flow through the skin, in a thermoneutral environment, has been reported to be in the range of 250 ml/min (2.5 to 3 ml/min/100 g tissue), a level capable of dissipating the body's resting metabolic heat production of approximately 80 to 90 kcal/h (Johnson et al., 1986ab; Johnson and Propper, 1996; Brienza et al., 2005). The skin also has a capillary reserve, with, for instance, about half of the capillaries in the human foot being perfused at any time. Vasodilation, as a result of exercising or heat exposure, increases this value manyfold and can involve the redistribution of blood from other regions, such as the spleen, and increases in overall cardiac output. In contrast, on exposure to cold environments, cutaneous vasoconstriction occurs and decreases heat dissipation from the surface and reduces convective heat transfer from the body core (Figure 13.3).

The neural control of cutaneous circulation involves both sympathetic adrenergic vasoconstrictor nerves and sympathetic vasodilator nerves, with the exception of the palms, soles, and lips (glabrous skin), where only vasoconstrictor nerves are found (Johnson and Proppe, 1996). In addition, arteriovenous anastomoses (AVA), which allow high flow rates directly from arterioles to venules, are numerous in glabrous areas, and are richly innervated by the vasoconstrictor nerves yet predominantly absent in other skin areas. Under normal conditions, the vasoconstrictor system is actively maintaining vascular tone, and small changes in activity are able to accommodate necessary adjustments to slight changes in the environmental temperature (Pergola

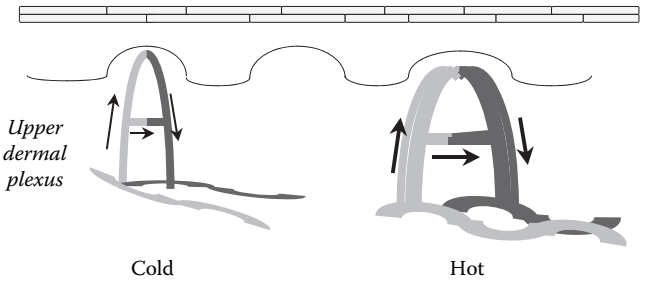

Figure 13.3 Changes in cutaneous blood flow experienced as a result of vasoconstriction to reduce heat dissipation and convective heat transfer from the skin and vasodilation with the opposite effects.

et al., 1994). Vasomotor tone adjustments have been reported to double heat dissipation to the environment with only an increase of 8 ml increase in blood per 100 ml blood volume (i.e., 8% increase in blood flow) over the whole body surface area (Johnson et al., 1986b). The sympathetic vasodilator nerves are not usually tonically active, but when they are can increase skin blood flow to as much as 60% of total cardiac output, equivalent to around 6 to 8 L/min in response to increases in internal body temperature, as experienced during exercise and heat exposure (Hashim and Tadepalli, 1995; Johnson and Proppe, 1996). Cutaneous vasodilation has also been associated with activation of sympathetic cholinergic nerves, although the cotransmitter itself is not thought to be acetylcholine (Shastry et al., 2000; Kellogg et al., 1995), with other candidates investigated contributing to the active vasodilatory effect, including bradykinin (Fox and Hilton, 1958) and nitric oxide (Shastry et al., 2000).

In addition to changes in core body temperature, local warming of the skin causes a direct and significant degree of vasodilation, with a temperature of 42°C reportedly producing maximal dilation of skin blood vessels (Johnson et al., 1986; Pergola et al., 1993). The sensory nerves responsible for this reaction are afferent C fibers that have their effect via release of calcitonin gene-related peptide, substance P, and neurokinin A (Holzer, 1998). Local stimulation of these afferent sensory nerves is also caused by capsaicin (Caterina et al., 1997), an ingredient that can be found in a number of topical sports rubs and creams.

Early Evidence of Changes in Topical Drug Absorption Caused by Altered Perfusion

Scheuplein and Blank (1971) discussed how altered blood flow may affect percutaneous absorption. One of the first experimental studies examining the quantitative effects of perfusion blood flow on percutaneous absorption appears to be by Crutcher and Maibach (1969). They showed increasing the perfusate rate considerably increased the percutaneous absorption rate of testosterone through human skin. Similar results were reported for propionic and butyric acid (Liron and Cohen, 1984).

One of the earlier studies demonstrating the role of blood flow on percutaneous absorption in humans used comparison dermal concentrations after topical application *in vitro* and *in vivo* (Schaefer and Stuttgen, 1978). Perfusion caused by cutaneous microcirculation also affected responses after the topical penetration of the vasodilator methyl nicotinate in humans (Guy et al., 1983). Altered transdermal drug absorption of the vasoactive nonsteroidal antiinflammatory drug (NSAID) methyl salicylate (MeSA) has also been attributed to changes in *in vivo* cutaneous perfusion. Exercise, heat exposure, or both increased MeSA absorption more than three times the control levels in six volunteers (Danon et al., 1986). A later case study reported that skin necrosis and other toxic symptoms occurred when a heating pad was used with a topical MeSA and menthol formulation meant to treat arthritic pain (Heng, 1987).

Experimental Models to Measure Blood Flow Effects on Absorption and Distribution

Determination of the effects of changes in blood flow through the various regions of the cutaneous microvasculature is obviously not possible using traditional Franz-type isolated membrane diffusion cell studies. The ultimate goal of experimental systems is usually to allow quantitative prediction of the absorption and distribution of topically applied solutes that will be applicable to the *in vivo* situation. Therefore, we can deduce that studies examining the effects of changes in cutaneous blood flow are limited to experimental models in which the microvasculature has been preserved and can be effectively perfused and manipulated. Models reported in the literature to date include isolated perfused tissue models, anesthetized animal studies, and more recently human and animal cutaneous microdialysis studies.

Isolated Perfused Tissue Models

Over the years, several isolated perfused organ systems have been described in the literature that have been applied in studies of transdermal absorption kinetics. These have included, but are not limited to, the perfused (1) rabbit ear flap (Celesti et al., 1992; Seki et al., 2004); (2) pig ear flap (De Lange et al., 1992); (3) dorsal flap of hairless rat (Auclair et al., 1991); (4) rat hind limb (Cross et al., 1994, 1996); (5) porcine forelimb (Wagner et al., 2003); (6) cow udder (Kietzmann et al., 1993); and (7) the isolated perfused porcine skin flap (IPPSF) (Riviere et al., 1986), with the last of these the most well characterized. These *in vitro* systems have been developed to maintain the skin physiology as close as possible to the *in vivo* situation and thus generate meaningful quantitative data. The IPPSF possesses both a viable epidermis and an intact functional microcirculation and has been used to investigate the percutaneous absorption of various xenobiotics, including malathion, parathion, diisopropylflurophosphate, benzoic acid, caffeine, testosterone, progesterone, and lidocaine (Williams et al., 1990; Riviere et al., 1991, 1992) and, of more significance to this review, the ability to manipulate the cutaneous circulation by the transdermal administration of vasoactive drugs (Riviere et al., 1991, 1992).

In Vivo *Models*

Rat, a hybrid human and hairless rat model, and human models have been most frequently used to study the effect of altered perfusion on percutaneous absorption. One model used by our group is to examine the effects of percutaneous penetration and dermal clearance. The methodology involves removing the epidermis and examining the rate of disappearance of solutes from solutions applied to the dermis (Siddiqui et al., 1985). The effect of blood flow was shown by repeating the studies in sacrificed animals (Siddiqui et al., 1989) or in the presence of vasoactive drugs (Singh and Roberts, 1994b). Kobayashi et al. (1996) compared permeability coefficients with cutaneous blood flow clearance in hairless rats. The hybrid *in vivo* model consists of a congenitally athymic (nude) rat with a surgically constructed human skin sandwich flap onto which the percutaneous donor cell is placed (Silcox et al., 1990).

A comparison of *in vitro* and *in vivo* dermal levels was used by Schaefer and Stuttgen (1978) to show the importance of blood flow on percutaneous absorption in man. Figure 13.4 shows that much higher levels are observed in the tissues under human skin *in vitro* for topically applied hydrocortisone than *in vivo*. In accordance with Equation 13.2, such a finding emphasizes the role of blood capillaries in facilitating sink conditions to enable faster absorption. A retardation of nicotine transdermal delivery in the presence of intravenous administered nicotine was also used as evidence of blood flow-limited percutaneous penetration (Benowitz et al., 1992). Cutaneous microdialysis has been used to examine the role of vasoconstriction on transport of drugs through human skin (Boutsiouki et al., 2001; Morgan et al., 2003). These authors stripped the stratum corneum before application (analogous to the approach used by Siddiqui and colleagues) and examined transport through normal skin with and without vasoconstriction.

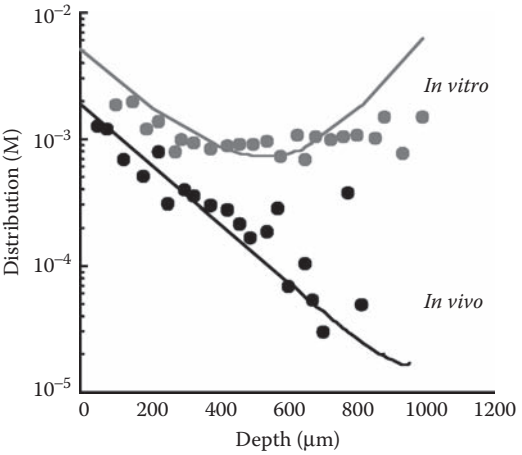

Figure 13.4 Distribution of hydrocortisone in human skin. (Adapted from Schaefer et al., 1996. Used with permission.)

Modeling Effects of Altered Dermal Clearance and Local Distribution Kinetics on Topical Drug Absorption

Blood Flow

Most studies have been concerned with the effect of blood or perfusate flow on absorption. *In vitro* studies are normally defined by equations similar to Equation 13.1 to Equation 13.4 for steady-state conditions and somewhat more complex expressions for finite-dose applications and transient kinetics (Roberts and Anissimov, 2004). Modeling the contribution effect of changes in blood flow through the cutaneous microcirculation on drug disposition in the skin is difficult, particularly as the physiology of the system shows that the vascular network within the skin is not homogeneous. For example, differences in terms of flow rate within the upper and lower plexuses of the dermis and the distribution and number of solute-exchanging capillaries may have significant contributions that are difficult to appreciate from a single blood flow estimation.

As highlighted by Riviere and Williams (1992), one problem with early approaches that applied pharmacokinetics to quantify both drug absorption and distribution in skin after topical application was that they used compartmental (Guy et al., 1982) and physiological (McDougal et al., 1986; McDougal, 1998) concepts that were basically direct extensions of those derived for other organs. The initial simple, physiologically based models that represented the skin as a well-stirred compartment incorporated blood flow Q_{skin} in a manner that had previously been used to describe drug disposition in the liver (Pang and Rowland, 1977; Rowland, 1984). Riviere and Williams (1992) pointed out that the underlying assumptions may not hold for skin because of different vascular physiology in the skin (Riviere and Williams, 1992). Interestingly, hepatic elimination models have evolved to become more physiologically based and better recognize the change in flow-induced changes in vascular volumes (Pang et al., 1988) as well as vascular dispersion in the liver, transport across the sinusoids (hepatic capillaries), binding, organelle sequestration, and diffusion and metabolism (e.g., Siebert et al., 2004). It seems likely that a physiologically based model more consistent with dermal morphology and physiology may eventually enable percutaneous penetration to be better described in terms of the transport mechanisms.

However, it needs to be recognized that thermoregulation in skin adds an additional complexity that needs to be accounted for in any model (Riviere and Williams, 1992). Skin blood flow Q_{skin} consists of skin blood flow through exchanging capillaries $Q_{exchanging\ capillaries}$ and that through shunts Q_{shunts} such that

$$Q_{skin} = Q_{exchanging\ capillaries} + Q_{shunts} \tag{13.5}$$

Shunt transport accounts for approximately 40% of Q_{skin} under resting conditions (Brakkee and Vendrik, 1970). Thermoregulation in the skin predominantly controls the distribution of blood flow through these two pathways, meaning that an increase in Q_{skin} is not necessarily reflected by equal increases in $Q_{exchanging\ capillaries}$ and Q_{shunts}, or that a change in $Q_{exchanging\ capillaries}$ could occur without a change in Q_{skin}. In addition,

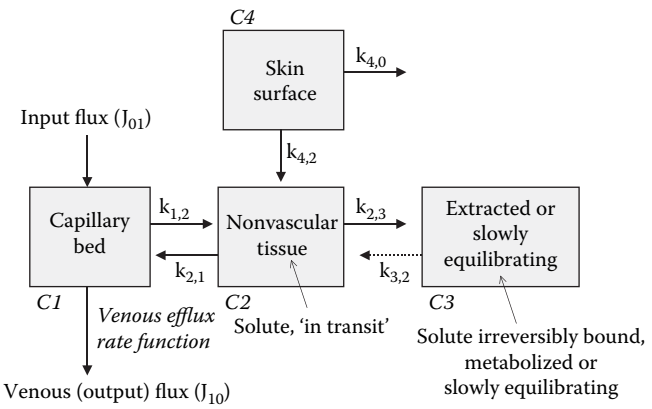

Figure 13.5 Four compartment (C) model used by Williams et al., (1990), to describe drug distribution in the IPPSF, where k, x, and y are transfer rate constants. (Used with permission.)

the distance a solute would have to diffuse through tissue from exchanging capillaries to surrounding target cells, thought generally to be a fixed parameter, would change as different capillary beds within the skin were perfused. Riviere and Williams (1992) also suggested that recruitment of new capillary beds within the skin would increase capillary surface area and tissue volume perfused. Accordingly, the assumption Q_{skin} can be described by an increased flow through existing beds and conventional models (well stirred and parallel tube) is questioned.

To better define the role of blood flow in dermal pharmacokinetics, Williams et al. (1990) represented the skin vasculature as a three-compartment model with a fourth compartment for the skin surface (Figure 13.5). They then examined hypothetical changes in the absorption profile of the organophosphate pesticide malathion in the IPPSF fitted to the model as shown in Figure 13.6 (Riviere and Williams, 1992). The amounts of solute in each compartment of this model are described by the following expressions (Equation 13.6 to Equation 13.9) (Williams et al., 1990):

$$A_1(t) = M_1(t) = V_1 C_{01}(t) \tag{13.6}$$

$$A_2(t) = \frac{M_1 k_{1,2}}{k}(1 - e^{-kt}) + \frac{k_{4,2} A_4(0)}{p - k}(e^{-kt} - e^{-pt}) + A_2(0)e^{-kt} \tag{13.7}$$

$$A_3(t) = k_{2,3}\frac{M_1 k_{1,2}}{k}\left(t - \frac{1 - e^{-kt}}{k}\right) + k_{4,2}A_4(0)\left[\frac{1}{kp} + \frac{e^{-kt}}{k(k-p)} - \frac{e^{-pt}}{p(k-p)}\right] + \frac{A_2(0)(1 - e^{-kt})}{k} + A_3(0) \tag{13.8}$$

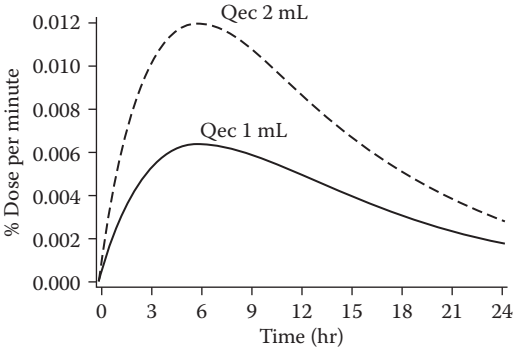

Figure 13.6 Influences of changing exchanging capillary volume (Qec) on the percutaneous absorption profile of topically applied malathion (40 g/cm²) in the IPPSF. (From Riviere and Williams, 1992. Used with permission.)

$$A4(t) = A_4(0)e^{-pt} \tag{13.9}$$

$$\phi_{vitro}(T) = \frac{k_{2,1}k_{4,2}}{p-k}\left[\frac{1-e^{-kt}}{k} - \frac{1-e^{-pt}}{p}\right] \tag{13.10}$$

where $Ai(t)$ is the solute mass in compartment i and time t; $M_i(t)$ is the solute mass in compartment i; $k_{1,2}$ is the transfer rate constant between compartment 1 and compartment 2; V_i is the vascular volume (compartment i); $k = k_{2,1} + k_{2,3}$; $p = k_{4,2} + k_{4,0}$; and $C_{0,1}(t)$ is the incoming solute concentration. Williams et al. (1990) then estimated the cumulative absorption into the systemic circulation with time t [$\phi_{vitro}(T)$] by integrating the flux from the nonvascular tissue compartment into the capillary bed. The resultant expression obtained is shown in Equation 13.10.

Riviere and Williams (1992) suggested that when the exchanging capillary volume was increased from 1 to 2 ml and all other model parameters were kept constant, higher solute absorption rates resulted (Figure 13.6). Hence, they suggested that it was possible that increases in percutaneous absorption could be mistakenly attributed to an increased dermal blood flow when the effect was caused by an increase in the volume of tissue actually perfused.

Blood Flow and Tissue Distribution Kinetics

We used a simpler two-compartment model to describe dermal absorption and efflux of solutes from tissues into a perfused limb preparation (Figure 13.7) (Cross et al., 1994, 1996; Roberts and Cross, 1999). The change dMt/dt in the tissue compartment amount M_T with time t is related to the absorption rate constant k_a and either the initial amount in donor M_{vo} and the elimination rate constant k_{el} or the local perfusate flow Q_p and the perfusate concentration C_p (Roberts and Cross, 1999):

$$\frac{dM_T}{dt} = k_a M_{vo} \exp(-k_a t) - k_{el} M_T = k_a M_{vo} \exp(-k_a t) - Q_p C_p \qquad (13.11)$$

The cumulative amount eluted $Q(t)$ versus time (t) profiles is given by

$$Q(t) = M_0 \left[1 + \frac{k_a}{k_{el} - k_a} \exp\left(-k_{el} t\right) - \frac{k_{el}}{k_{el} - k_a} \exp\left(-k_a t\right) \right] \qquad (13.12)$$

where M_0 is the initial amount applied to the dermis, k_a is the absorption rate constant, and k_{el} is the elimination rate constant. It can be shown that, after some rearrangement, Equation 13.10 is similar to Equation 13.12 (Anissimov and Roberts, 2005). Recognizing that $M_T = V_D C_p$, where V_D is the apparent volume of distribution in tissue, k_{el} is given by its underlying determinants of tissue blood flow Q_p and volume of distribution of the tissue V_D. Hence, from Equation 13.11, the removal term is

$$k_{el} M_T = Q_p \frac{M_T}{V_D}$$

so that an increase in flow rate Q_p or a decrease in V_D will increase this term. V_D can then be further expressed in terms of vascular volume V_p, extravascular tissue space V_{TE}, fraction of solute unbound in the blood fu_b, and fraction unbound in the tissue fu_T (Roberts and Cross, 1999). The overall expression for k_{el} is

$$k_{el} = \frac{Q_p}{V_D} = \frac{Q_p}{V_p + \dfrac{fu_p}{fu_T} V_{TE}} = \frac{Q_p}{\left[\dfrac{V_p}{V_{TE}} + \dfrac{fu_p}{fu_T} \right] V_{TE}} \qquad (13.13)$$

Consistent with the suggestion that removal rate is proportional to flow, Cross et al. (1994) showed that, after dermal application in the perfused rat limb preparation, doubling the perfusate flow rates led to 4, 2.3, and 2.6 times the outflow

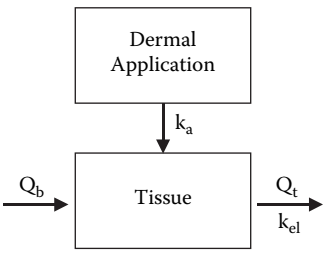

Figure 13.7 Two compartmental model used by Cross et al., 1994, 1996, and Roberts and Cross, 1999, to describe the efflux of solutes from tissues after dermal absorption into a perfused limb preparation.

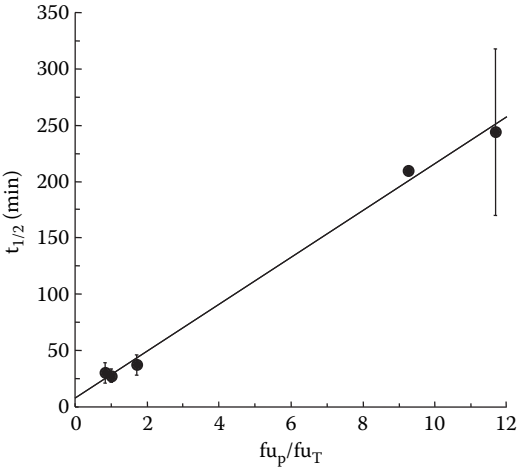

Figure 13.8 Relationship between elimination half-life ($t_{1/2}$) and fraction of solute unbound in the perfusate fu_p and tissue fu_T.

recoveries at 90 min for water, diazepam, and lidocaine, respectively. One reason for the higher-than-expected recoveries was that absorption rates were 1.4, 1.2, and 1.3 times faster than expected at the higher flow rate for water, diazepam, and lidocaine, respectively. Another reason for the greater absorption rate may be because of the better sink conditions in the skin as we have observed that an increase in perfusate flow leads to better limb perfusion and vascular surface area for exchange as is evident by the increases in vascular and extravascular tissue volumes of the perfused leg with increasing flow (Wu et al., 1993).

It is also apparent that the efflux of drug from the tissue and retention in tissue is dependent on the fraction unbound in tissue and in the blood and on blood flow rate. Consequently, Roberts and Cross (1999) showed that the half-life of drugs retained in tissues ($t_{0.5} = 0.693/k_{el}$) could be related to the ratio of the fraction of drug unbound in the plasma and tissue (Figure 13.8). A number of other compartmental and diffusion models have been described and summarized (McCarley and Bunge, 2001; Anissimov and Roberts, 2004).

DIRECT DEEPER TISSUE PENETRATION

It is thought that once penetration of a solute through the epidermis has been achieved, it will either be cleared by the local blood supply on entering the dermis or transported into deeper tissues by diffusion, perfusion, or a combination of both (Roberts et al., 2002). The concept of direct drug delivery to deeper tissues after topical application has been known for some time (Guy and Maibach, 1983). Singh et al. (1998) reviewed later literature, including a number of studies involving application of NSAIDs to human arthritic knees. They concluded that similar synovial drug levels following sampling from arthritic bilateral knee effusions after topical

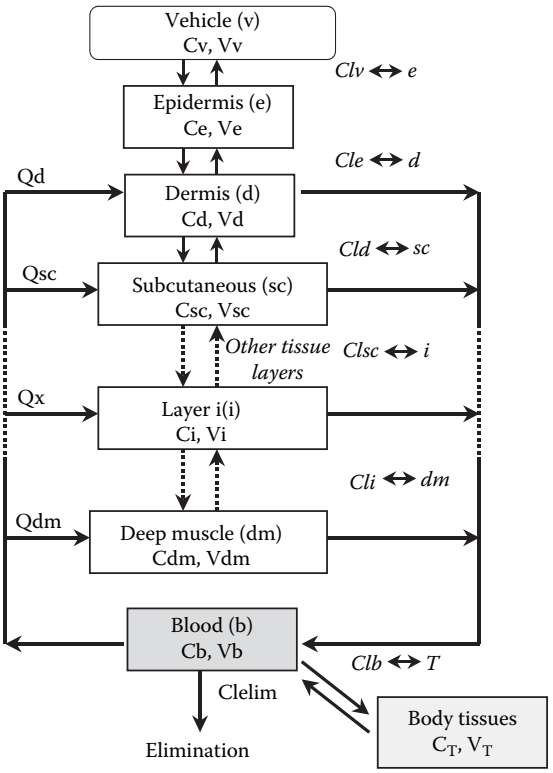

Figure 13.9 Pharmacokinetic model showing the involvement of individual tissue blood flows and systemic blood recirculation on the tissue concentrations of solutes following topical application *in vivo* (adapted from Singh et al., 1998), where Q = blood flow; C = concentration; V = volume; and CL = clearance between the various compartments.

application of drugs to only one knee effusion may be reflecting systemic rather than direct penetration because of the long elapsed time after application. We know that, *in vivo*, topically applied solutes have the ability to penetrate directly into deeper tissue compartments, as shown in the case of lidocaine and salicylic acid applied to the anesthetized rat model used by Singh and Roberts (1993a, 1993b, 1994a), but that the degree of direct penetration may be limited to superficial tissue regions at early (0 to 4 h), with recirculation in the blood supply suggested to be responsible for the levels seen in underlying muscle layers and in other layers at long times (> 8 h). Defining the role of the cutaneous microvasculature in transport of solutes into various tissue layers below a topical application site has been attempted assuming a compartmental representation for each tissue as shown in Figure 13.9, with distribution into the plasma compartment defined by the blood supply to individual tissues. The equations derived to describe this model and the movement of solutes from an applied solution into the exposed dermis and subsequent underlying tissue compartments were presented as follows:

For the solute in the donor solution,

$$-V_s \frac{dC_s}{dt} = Cl_{s,d} C_0 \exp^{-ks,dt} \tag{13.14}$$

For the dermis,

$$V_{ud} \frac{dC_{ud}}{dt} = Vd \frac{dC_d}{dt} = Cl_{s,d} C_0 \exp^{-ks,dt} + Q_d f_{ub} C_b - Q_d f_{ud} C_d + Cl_{d,sc} \left(fu_{sc} C_{sc} - fu_d C_d \right) \tag{13.15}$$

where C_0 and C_s are the concentrations in the solution in contact with the exposed dermis and time 0 and at time t; V_s is the volume of the applied solution, V_{ud} and V_d are the apparent volumes of distribution of unbound solute in the dermis and the total amount in the dermis, respectively; $k_{s,d}$ is the transfer rate constant between the cell solution and the dermis; f_{ud}, f_{ub}, and f_{usc} are the fractions of solute unbound in the dermis, blood, and subcutaneous tissue, respectively; C_b and C_d are the concentration of solute in blood and dermis, respectively; and $CL_{d,sc}$ represents the clearance between the dermis and subcutaneous tissue (Singh et al., 1998). This model was extended to define solute distribution into the underlying (ith) tissue:

$$V_{uTi} \frac{dC_{uTi}}{dt} = Vd \frac{dC_d}{dt} = Cl_{T(i+1),i} (fu_{T(i+1)} C_{T(i+1)} - fu_{Ti} CT_i) + Q_{Ti} (C_b RM_{Ti} - fu_{Ti} C_{Ti}) + Cl_{Ti,(i-1)} \left(fu_{T(i-1)} C_{T(i-1)} - fu_{Ti} C_{Ti} \right) \tag{13.16}$$

where $V_{uT,I}$ and V_T are the apparent volume of distribution of the unbound and total amount of solute in the chosen tissue, respectively; $Cl_{T(i+1),I}$ is the clearance between tissue $i + 1$ and tissue i; C_{Ti}, $C_{T(i+1)}$, and $C_{T(i-1)}$ are the concentrations in the ith tissue, $i + 1$, and $i - 1$ tissue compartments, respectively; fu_{Ti}, $fu_{T(i+1)}$, and $fu_{T(i-1)}$ are the fractions unbound in these same tissue compartments, respectively; Q_{Ti} is the blood flow to tissue i; and RM_{Ti} is the tissue–plasma partition coefficient for tissue i.

Singh and Roberts (1993a, 1993b, 1994a) used this last equation to numerically integrate and fit simultaneously the solute tissue concentration with time data using experimental results collected over a 0.5- to 16-h time interval in anesthetized rats. A sixth-order, polynomial, nonlinear regression of the plasma–time profile was apparently used as the plasma input function at various times into the individual tissue compartments shown in Figure 13.8 and the experimentally determined blood flows (Figure 13.10) and estimated tissue clearances reported for the rat model by the authors (1993b). Of most significant interest in these studies was the identification of two apparent peaks in the tissue concentration–time profiles for salicylic acid

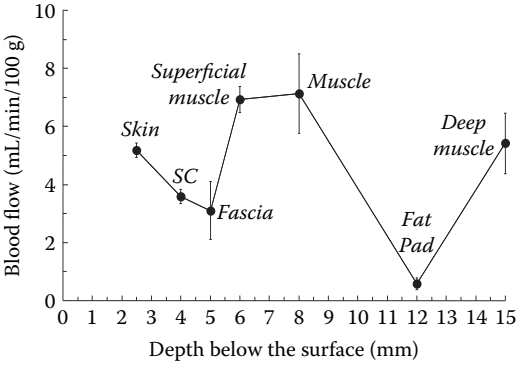

Figure 13.10 Blood flow in skin and underlying tissues determined by Singh and Roberts, 1993a, in their anesthetized rat dermal absorption model. (Adapted from Singh, 1992. Used with permission.)

(Figure 13.11) and to a lesser extent, although still present, for lidocaine following dermal application. The first of these peaks appeared at around 2 to 4 h after dermal application and the second at around 10 h postapplication. The presence of the first peak has been attributed to the direct penetration of solute into the tissue from the application site and the second peak to redistribution from the systemic blood supply as circulating plasma levels increase and contribute a greater mass of solute to the tissue.

It can be seen from the adaptation of their data (Figure 13.11) that superficial tissue levels (dermis and subcutaneous sites) of salicylic acid below the treated site were clearly above circulating plasma levels, indicating that direct penetration had occurred to these tissues. The contralateral site tissues, indicative of tissue salicylic acid distribution solely attributable to recirculation in the systemic blood supply, show a much smaller degree of differentiation between tissue compartments. The treated site levels in each tissue are in fact above their contralateral tissue counterparts, even to the depth of the deeper muscle layers (approximately 15 mm in this model) (Singh and Roberts, 1993a), indicating that a degree of direct penetration or enhanced local redistribution of solute from local overlying tissues must be occurring in addition to the deposition of solute from the systemic blood supply.

This twin-peak phenomenon was also observed following the topical application of piroxicam to the shoulder region of anesthetized rats (Figure 13.12; McNeill et al., 1992). In these studies, the first peak appeared at around 4 h after topical application and the second at around 12 h. The reason for the delay in the appearance of the peaks in McNeill et al.'s study (1992) compared to that of Singh and Roberts (1993a) is attributed to the fact that in the latter study the solute was applied directly to the exposed dermis. As confirmed in the studies of Singh and Roberts (1993b, 1994a), the second peak corresponded to the time at which piroxicam levels were maximal in the plasma, suggesting that drug was entering the muscle sites from the systemic circulation. However, the earlier peak is consistent with penetration from the topical application site, by a more direct route. The concentration of piroxicam found in the contralateral (undosed) tissues was again below that present in the plasma and

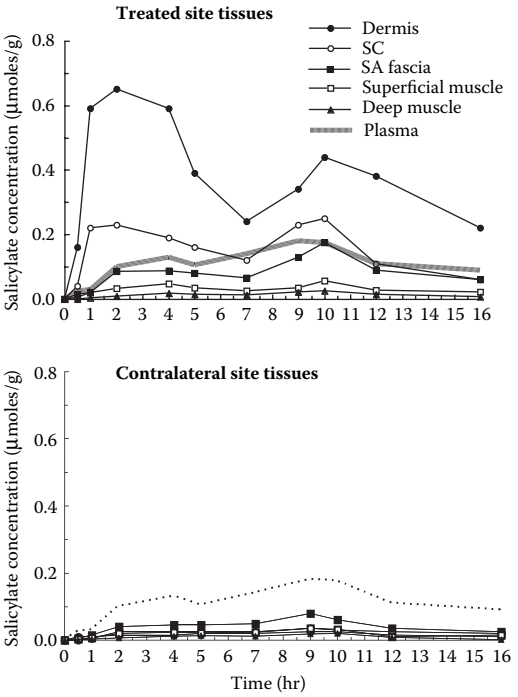

Figure 13.11 Tissue concentration–time profiles of salicylic acid determined in anesthetized rats following dermal application to the abdominal region in their *in vivo* dermal absorption model. (Adapted from Singh, 1992.)

consistent with redistribution from the systemic circulation as the sole source of drug in these areas. McNeill et al. (1992) further stated that the concentrations of piroxicam determined in the subjacent muscles after topical application were impossible to explain on the basis of mass balance and diffusional calculations. The authors suggested the existence of a "convective" physiological force that was capable of transporting significant amounts of drug in a relatively short period of time, naming the cutaneous microvasculature as the most likely candidate.

Later work involving the same author used an anesthetized pig model to reexamine the tissue penetration of topically applied piroxicam to assess the degree of contribution of the systemic circulation on delivery to deeper tissues (Monteiro-Riviere et al., 1993). In support of the previous study, they found that piroxicam penetration occurred into the subcutaneous and muscle tissue only under the dosed sites and not at other more remote sites, therefore ruling out systemic delivery as a prerequisite for local tissue penetration. In addition, the authors found that piroxicam penetration was greater at musculocutaneous sites, areas where skin was overlying large muscle mass, compared to direct cutaneous sites, where skin was overlying more bony sites. *In vitro* penetration studies of piroxicam using skin harvested from each of these sites had shown no significant differences. The study concluded that the orientation of the local vasculature also plays a pivotal role in the deep tissue penetration of topically applied solutes (Monteiro-Riviere et al., 1993). The underlying

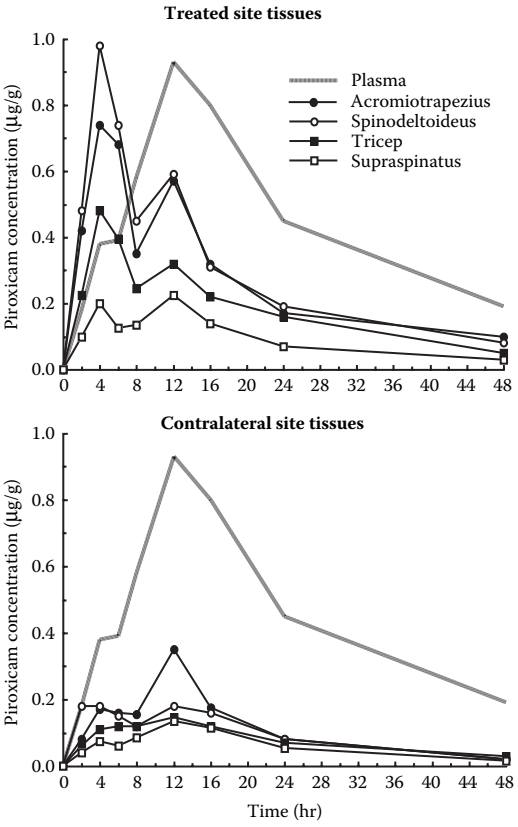

Figure 13.12 Tissue concentration–time profiles of piroxicam determined in anaesthetized young rats following topical application to the shoulder region. (Adapted from McNeill, 1992. Used with permission.)

physiology responsible for this observed effect suggests that, in the first case of penetration through musculocutaneous sites, permeable capillaries that extend from the upper cutaneous region and connect through networks in deeper tissue layers are capable of distributing solute more efficiently than that absorbed into the systemic bloodstream and diluted in the circulating blood volume (Figure 13.2).

Two groups of Japanese workers have further developed the compartmental analysis of deep tissue penetration in treated and contralateral tissues (Nakayama et al., 1999; Hatanaka et al., 2000; Higaki et al., 2002). Figure 13.13 shows the model used in these studies. Figure 13.14 shows the typical profiles for diclofenac and felbinac following application to male Wistar rat abdominal skin that had been treated with thioglycolate gel and was stripped 20 times with tape to reduce the stratum corneum barrier. Also shown in this figure are the predicted contributions of direct penetration and recirculation from the systemic circulation to the treated muscle concentrations. The observed and predicted profiles are similar to those reported previously for salicylate and lidocaine by Singh and Roberts (1993b, 1994a) in that

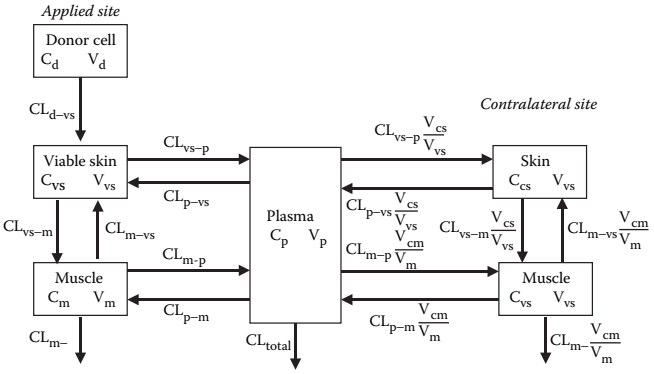

Figure 13.13 Six compartmental model used by Higaki et al. (2002) to describe intradermal kinetics of drugs applied topically. C, concentration; V, distribution volume; d, donor cell; vs, viable skin; m, muscle; p, plasma; cs, contralateral viable skin; cm, contralateral muscle; CL, clearance between the tissue and tissue or plasma as represented by subscripts, where all clearances, except for CL_{total}, were calculated as unit of viable skin or muscle mass. (Used with permission.)

direct penetration into deeper tissues was predominant at early times, and that systemic recirculation only contributes at later times. The relative contributions of direct penetration into muscle layer for this series of drugs studied by Higaki et al. (2002) were antipyrine 90.8%, diclofenac 79.0%, salicylic acid 72.0%, propanolol 86.1%, ketoprofen 69.4%, felbinac 43.3%, and flurbiprofen 62.5%. Higaki et al. (2002) also showed that the direct penetration rate constant could be directly related to the fraction unbound in the viable skin. Interestingly, Singh and Roberts (1993b) had previously suggested that 58% of salicylic acid reached the fascia at early times by direct penetration. They had also suggested that 50% of lidocaine reached the underlying muscle at early times after dermal application (Singh and Roberts, 1994a). Cross and Roberts (1999) used a tissue distribution-blood clearance model to describe the tissue concentration-distance profiles below wounds for a range of growth factors and other solutes after topical application. They showed that solute size was the main determinant of tissue drug concentration *in vivo* at any time. This finding was similar to that reported previously by Singh and Roberts (1996) for the apparent *in vivo* steady-state distribution of a wider range of solutes. Recently, Krestos et al. (2004) used a distributed-clearance model to describe *in vivo* transient drug distribution and applied it to salicylic acid. They obtained parameters which were consistent with those derived by steady-state.

Few studies have examined concentration depth relationships below the topical application site after topical administration in man (Cross et al., 1998; Muller, et al., 1997). In general, studies conducted to date emphasized the use of cutaneous microdialysis and showed a decrease in levels with increasing depth. A key difficulty is the variability in levels with depth, as illustrated by the work or Muller et al. (1997) (Figure 13.15).

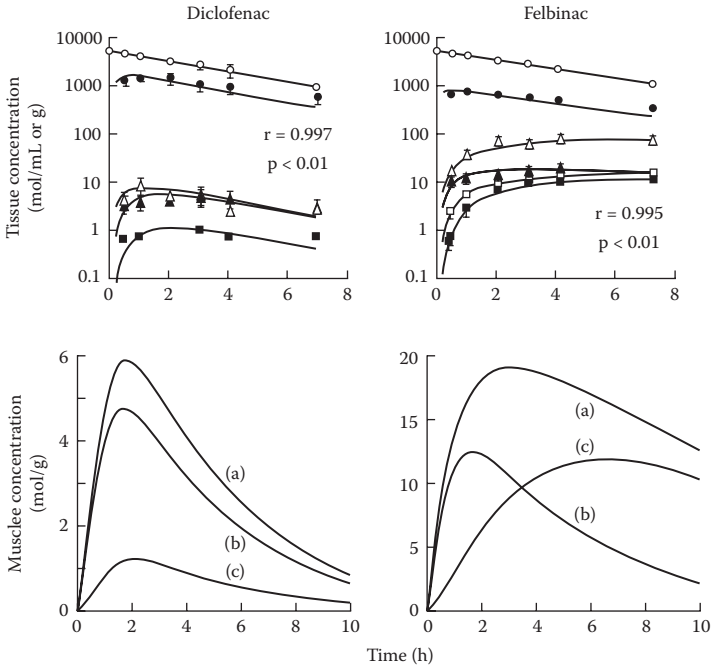

Figure 13.14 Intradermal kinetics of two model drugs (diclofenac and felbinac) after topical application to stripped skin reported by Higaki et al., 2002. The upper panel shows actual mean results from four experiments: ○, donor cell; ●, viable skin; ▲ muscle; △, plasma; □, contralateral viable skin; and ■, contralateral muscle. The lower panel shows simulation curves generated using the parameters obtained by six-compartment model analysis for which (a) is the total concentration, (b) is the concentration caused by direct penetration, and (c) is the concentration caused by systemic circulation.

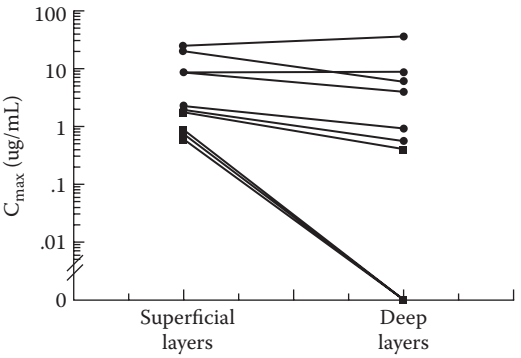

Figure 13.15 Effect of microdialysis probe depth on tissue microdialysate levels below topical application site for diclofenac. (Adapted from Muller et al., 1997. Used with permission.)

EFFECTS OF VASOACTIVE DRUGS ON TRANSDERMAL PENETRATION

As discussed, a number of studies have examined the effect of vasoactive drugs on percutaneous absorption. We therefore limit this discussion to the more detailed investigations. Much of this early work was undertaken using both the IPPSF (Riviere and Williams, 1991) and anesthetized weanling pig model (Riviere et al., 1992). They reported that the vasodilator tolazoline significantly increased lidocaine flux compared to that observed *in vitro*, whereas norepinephrine (a vasoconstrictor) significantly decreased lidocaine flux in the IPPSF (Riviere and Williams, 1991). Tolazoline shortened and norepinephrine increased the mean absorption time. Neither of these effects could be replicated in the *in vitro* model. Their subsequent work in the anesthetized pig model showed that, in tissue samples taken 4 h after a 1-h iontophoretic treatment period, tolazoline had decreased underlying tissue concentrations of lidocaine, and norepinephrine had increased tissue levels compared to those observed when lidocaine was administered alone (Riviere et al., 1992). Subsequently, Williams and Riviere (1993) used a three-compartment pharmacokinetic model to describe these results.

Our group examined the effect of the vasoconstrictor phenylephrine (0 to 0.1%) applied to the dermis on the clearance from the dermal application site and the underlying solute tissue concentration–depth profiles in anesthetized rats and in sacrificed rats (Singh and Roberts, 1994b). The drugs applied to the dermis were salicylic acid, lidocaine, and water following dermal application (Singh and Roberts, 1994b). The results for all three solutes showed that vasoconstriction decreased clearance from the applied solution into the application site (as illustrated in Figure 13.16A) and increased the concentration of solute found in underlying tissues as determined after 2 h of application (as illustrated in Figure 13.16B). The solute concentration–tissue depth profiles were then described using the compartment-in-series model described in Figure 13.9. The increased direct penetration of flurbiprofen in the presence of epinephrine (Sugibayashi et al., 1999) and antipyrine in the presence of phenylephrine (Higaki et al., 2002) is supportive of our findings (Singh and Roberts, 1994b). Overall, these studies highlight that flow through the cutaneous microvasculature and underlying vascular networks can have profound effects on dermal pharmacokinetics and the solute distribution into underlying tissue sites following topical application.

Subsequently, we extended this work with a more in-depth evaluation of the effect of a vasodilator/rubefacient MeSA and a nonvasoactive agent triethanolamine salicylate using multiple serial sampling of tissues at different times in anesthetized rats (Cross et al., 1999). Here, either MeSA or triethanolamine salicylate (TSA) was applied to intact depilated abdominal skin, and groups of treated rats were sacrificed at intervals from 30 min to 6 h; tissue concentrations below the application site and from a contralateral untreated area were determined. The results obtained suggested that faster uptake and distribution of solute occurs with cutaneous vasodilation (Figure 13.17). Significantly higher tissue salicylate concentration–time profiles were observed *in vivo* than were suggested by *in vitro* penetration studies using excised rat skin, particularly at early times (0 to 4 h).

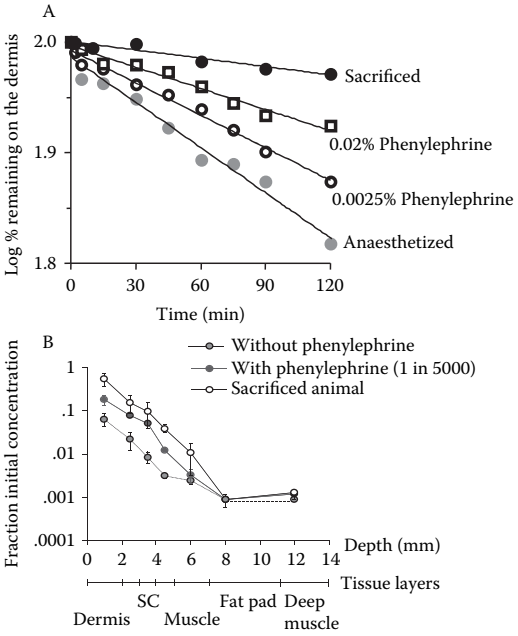

Figure 13.16 A: Effect of vasoconstriction on salicylic acid loss from solution applied to the dermis of rats in the presence of various concentrations of phenylephrine and B: corresponding tissue concentration-depth profiles for salicylic acid 2 h after dermal application.

Studies were also conducted in human volunteers using cutaneous microdialysis to examine dermal and subcutaneous tissue levels. Consistent with the rat observations, dermal and subcutaneous tissue levels of salicylate after methyl salicylate application in human volunteers resulted in much higher salicylate concentrations than were predicted on the basis of *in vitro* human skin penetration data at early time points (Cross et al., 1998). This difference in *in vivo*/*in vitro* outcomes appears to reinforce the work of Schaefer and Stuttgen (1978), in which it was attributed to an *in vivo* functioning capillary system promoting skin absorption. The enhanced tissue distribution of unhydrolyzed MeSA in the animal studies in the first 60 min is also consistent with its known rubefacient (vasodilatory) effect (Cross et al., 1999). The only appearance of unhydrolyzed MeSA in contralateral tissues in this study occurring at the 30-min time point was also indicative of the involvement of this rubefacient effect, which is known to diminish during the first 60 min following application (Cross et al., 1998). These findings are also consistent with the piroxicam studies of McNeill et al. (1992), in which deeper-than-expected tissue penetration of drug was attributed to the orientation of dermal blood vessels.

Cutaneous microdialysis has also been used to examine the role of vasoconstriction on transport of drugs through human skin (Boutsiouki et al., 2001; Morgan et al., 2003). The organophosphorus insecticide malathion is observed following topical application to human volunteers in microdialysate after 30 min, with a steady state reached after 2 h (Boutsiouki et al., 2001). Adding the vasoconstrictor noradrenaline

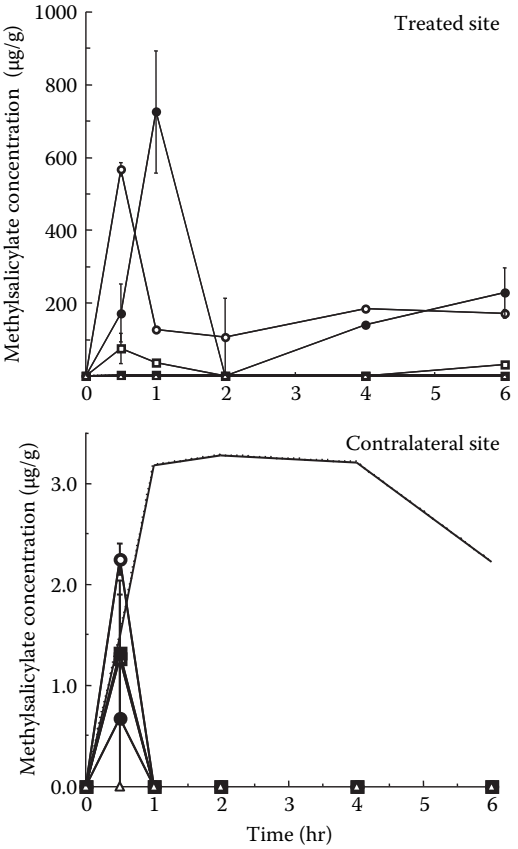

Figure 13.17 Concentration of unhydrolyzed methyl salicylate present in treated and contralateral tissues following application in anesthetized rats (Cross et al., 1999). ○, dermis; ●, subcutaneous tissue; □, superficial muscle; ■, deep muscle; △, fat; dashed line, plasma levels, mean ± SD, $n = 3$. (Used with permission.)

to the microdialysate increased the recovery of malathion eightfold and increased the time to reach steady state to 5 h. Whereas microdialysate concentrations for acyclovir and penciclovir are below the assay threshold (0.05 ng/ml) after topical application to normal skin, mean areas under the microdialysate concentration–time curves of 13.3 ng.h_{0-5}/ml and 27.6 ng.h_{0-5}/ml for acyclovir and penciclovir are observed after noradrenaline-induced local vasoconstriction (Morgan et al., 2003). Much higher microdialysate levels are observed after tape stripping the stratum corneum.

CLEARANCE BY LYMPHATIC FLOW

For drugs and other solutes that reach dermal and subcutaneous tissue sites, clearance into the general circulation can occur either by the blood capillaries or the lymphatics (Figure 13.18). For macromolecules, such as proteins and large sugars, permeability

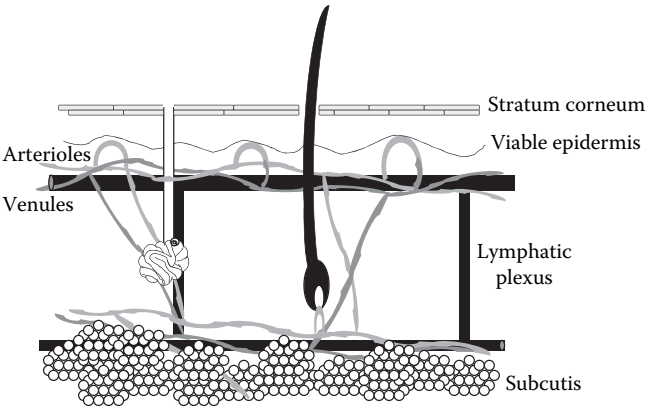

Figure 13.18 Diagrammatic representation of the positioning of the lymphatic plexus in relation to dermal papillary blood vessels and subcutaneous tissue sites.

through the capillary endothelium will be low, and direct movement into the blood will be restricted. These molecules are cleared preferentially by the lymphatics, with their rate of removal even suggested to provide an index of the lymphatic function of the skin (Mortimer et al., 1990). Supersaxo et al. (1990), in a series of studies examining the distribution of various molecular weight solutes injected into the subcutaneous tissue of sheep, suggested that molecules with a molecular weight greater than 16 kDa are mainly cleared by the lymphatics that drain the application site. These results correlated with the earlier work of Bocci et al. (1988), who showed that interferon 2α (molecular weight [MW] approximately 19 kDa) was preferentially absorbed by the lymphatics following intramuscular or subcutaneous administration compared with intravenous dosing, and Yoshikawa et al. (1992), who suggested that MW below 18 kDa were cleared equally well by the blood and lymphatics. Studies by Cross and Roberts (1993), examining the disappearance of interferon γ applied to rat subcutaneous tissue, used vasoconstriction with 10^{-6} *M* noradrenaline to preferentially constrict blood vessels, but not lymphatics, to show that changes could be observed in the clearance of small polar solutes but not of the 17-kDa interferon γ molecule. Interstitial fluid expanders such as albumin and hyaluronidase have been shown to increase the recovery of interferon 2α in the lymphatic system from two- to eightfold, respectively, following subcutaneous injection in rabbits (Bocci et al., 1986). Induction of local edema, following subcutaneous injection of bradykinin or histamine, has also been shown to increase the clearance rate of interferon α in both the lymphatics and capillaries (Pessina et al., 1993).

Lymphatic flow is known to be increased by heat, massage, inflammation, movement of the body part, and increases in hydrostatic pressure within the lumen of lymphatic collecting vessels and decreased by cold, lack of movement, and decreased external pressure (Uren et al., 1999). In addition, the normal lymphatic drainage of the skin has been shown to be highly variable from subject to subject, even when the same region of the body is examined (Uren, 2004). Average flow rates reported by Uren et al. (2004) are shown in Table 13.1. Further, studies have shown that the

Table 13.1 Cutaneous Lymph Flow Rates in Various Regions of the Body Reported by Uren et al. (2004)

Region	Average Flow (cm/min)
Head and neck	1.5
Anterior trunk	2.8
Posterior trunk	3.9
Arm and shoulder	2.0
Forearm and hand	5.5
Thigh	4.2
Leg and foot	10.2

path taken by the lymphatic collecting vessels is unpredictable, as is the ultimate location of draining sentinel nodes (Thompson et al., 1999; O'Toole et al., 2000).

PATHOLOGICAL CONDITIONS THAT AFFECT CUTANEOUS BLOOD FLOW AND CLEARANCE

There are a number of clinical conditions that are known to produce changes in skin blood flow that may be of importance when considering the potential effects of cutaneous blood flow on topical drug absorption and subsequent tissue distribution. For example, skin flushes during menopause represent a dysfunction of the thermoregulatory system that occur because of estrogen, and perhaps other female reproductive hormones, deficiency (Charkoudian and Johnson, 2000). It has been suggested that, in general, estrogens promote cutaneous vasodilation, whereas, although less clear, progesterone appears to inhibit this response (Young and Castellani, 2001; Charkoudian, 2003). A reduced ability of individuals with type 2 diabetes to accommodate elevated environmental temperatures may also be linked to the known local cutaneous vasodilator dysfunction that occurs as a result of this disease (Arora et al., 1998; Veves et al., 1998; Charkoudian, 2003). In addition, evidence from studies showing impaired sympathetic neural control of sweating and blood pressure in these patients (Fealey et al., 1989; Benarroch and low, 1991) has led to the indirect suggestion that sympathetic vasodilator neural function in skin is also impaired, which contributes to the observed impairment in thermoregulatory control (Charkoudian, 2003). Other recognized cutaneous reflex or local thermoregulatory microvascular disorders include Raynaud's phenomenon and erythromelalgia. Raynaud's phenomenon, thought to affect around 3 to 5% of the population, is characterized by excessive vasoconstriction, often accompanied by pain, in response to emotional stimuli or cold (Wigley and Flavahan, 1996) as well as a generally lower finger skin blood flow compared to normal controls (Greenstein et al., 1995) together with evidence significantly impaired endothelium-dependent vasodilation in the fingers (Khan and Belch, 1999). Erythromelalgia, on the other hand, is characterized by intermittent erythema of the extremities, often associated with the sensation of burning pain and thought to involve small nerve fiber neuropathy (Davis et al., 2000). During nonsymptomatic periods, patients often have lower baseline skin perfusion and reduced cutaneous vasoconstrictor responses, with both dysfunc-

tion of reflex sympathetic actions and impairment of local vasodilator responsiveness suggested to be involved (Littleford et al., 1999; Mork et al., 2002).

CONCLUSION

Both the epidermal flux and the viable epidermal concentrations of topically applied solutes are dependent on clearance from the dermis and binding in the dermis. Factors defining this clearance and binding have been considered in this chapter. In addition, examples of altered percutaneous absorption fluxes or tissue levels as a consequence of changes in blood flow, lymphatic flow, and altered binding have been summarized.

ACKNOWLEDGMENTS

We wish to acknowledge the financial support of the National Health and Medical Research Council of Australia, the Lions Kidney and Medical Research Foundation, and the Princess Alexandra Hospital Research Foundation.

REFERENCES

Anissimov, Y.G. and Roberts, M.S., Mathematical models in percutaneous absorption, in H.I. Maibach and R.I. Bronaugh (eds.), *Percutaneous Absorption,* 4th ed., New York: Dekker, 2005, in press.

Arora, S., Smakowski, Fryberg, R.G., Simone, L.R., Freeman, R., Logerfo, F.W., and Veves, A., Differences in foot and forearm skin microcirculation in diabetic patients with and without neuropathy, *Diabetes Care,* 1998, 21, 1339–1344.

Auclair, F., Besnair, M., Dupont, C., and Wepierre, J., Importance of blood flow to the local distribution of drugs after percutaneous absorption in the bipediculated dorsal flap of the hairless rat, *Skin Pharmacol*., 1991, 4, 1–8.

Benarroch, E.E. and Low, P.A., The acetyl choline-induced flare response in evaluation of small fibre dysfunction, *Ann. Neurol.,* 1991, 29, 590–595.

Benowitz, N.L., Jacob, P., Olsson, P., and Johansson, C.J., Intravenous nicotine retards transdermal absorption of nicotine: evidence of blood-flow limited percutaneous absorption, *Clin. Pharm. Ther.,* 1992, 52, 223–230.

Bocci, V., Muscettola, M., Grasso, G., Magyar, Z., Naldini, A., and Szabo, G., The lymphatic route. 1. Albumin and hyaluronidase modify the normal distribution of interferon in lymph and plasma, *Experientia.,* 1986 (April 15), 42(4), 432–433.

Bocci, V., Pessina, G.P., Paulesu, L., and Nicoletti, C., The lymphatic route: VI. Distribution of recombinant interferon α-2 in rabbit and pig plasma and lymph, *J. Biol. Resp. Mod.,* 1988, 7, 390–400.

Boutsiouki, P., Thompson, J.P., and Clough, G.F., Effects of local blood flow on the percutaneous absorption of the organophosphate compound malathion: a microdialysis study in man, *Arch. Toxicol*., 2001, 75, 321–328.

Brakkee, A.J. and Vendrik, A.J., Arterio-venous shunts in peripheral vascular systems, *Pflugers Arch.,* 1970, 314, 170.

Braveman, I.M., Anatomy and physiology of the cutaneous microcirculation, in E. Berardesca, P. Elsner, and H.I. Maibach (eds.), *Bioengineering of the Skin: Cutaneous Blood Flow and Erythema,* Boca Raton, FL: CRC Press, 1995, pp. 3–22.

Brienza, D.M., Geyer, M.J., and Jan, Y.K., A comparison of changes in rhythms of sacral skin blood flow in response to heating and indentation, *Arch. Phys. Med. Rehabil.*, 2005, 86, 1245–1251.

Caterina, M.J., Schmacher, M.A., Tominga, M., Rosen, T.A., Levine, J.D., and Julius, D., The capscaicin receptor: a heat-activated ion channel in the pain pathway, *Nature,* 1997, 389, 816–824.

Celesti, L., Murratzu, C., Valoti, M., Sgaragli, G., and Corti, P., The single-pass perfused rabbit ear as a model for studying percutaneous absorption of clonazepam. I. General characteristics, *Methods Find. Exp. Clin. Pharmacol.,* 1992, 14, 701–709.

Charkoudian, N., Skin blood flow in adult human thermoregulation: how it works, when it does not and why, *Mayo Clinic Proc.,* 2003, 78, 603–611.

Charkoudian, N. and Johnson, J.M., Female reproductive hormones and thermoregulatory control of skin blood flow, *Exerc. Sport Sci. Rev.,* 2000, 28, 108–112.

Cross, S.E., Anderson, C., and Roberts, M.S., Topical penetration of commercial salicylate esters and salts using human isolated skin and clinical microdialysis studies, *Br. J. Clin. Pharmacol.,* 1998, 46, 29–35.

Cross, S.E., Megwa, S.A., Benson, H.A.E., and Roberts, M.S., Self promotion of deep tissue penetration and distribution of methylsalicylate after topical application, *Pharm. Res.,* 1999, 16, 427–433.

Cross, S.E. and Roberts, M.S., Subcutaneous absorption kinetics and local tissue distribution of interferon and other solutes, *J. Pharm. Pharmacol.,* 1993, 45, 606–609.

Cross, S.E. and Roberts, M.S., Defining a model to predict the distribution of topically applied growth factors and other solutes in excisional full-thickness wounds, *J. Invest. Dermatol.*, 1999, 112, 36–41.

Cross, S.E., Wu, Z.-Y., and Roberts, M.S., Effect of perfusion flow rate on the dermal tissue uptake of solutes after dermal application using the isolated perfused rat hindlimb preparation, *J. Pharm. Pharmacol.,* 1994, 46, 844–850.

Cross, S.E., Wu, Z.-Y., and Roberts, M.S., The effect of protein binding on the deep tissue penetration and elution of transdermally applied water, salicylic acid, lignocaine and diazepam in the perfused rat hindlimb, *J. Pharm. Exp. Ther.,* 1996, 277, 366–374.

Crutcher, W.I. and Maibach, H.I., The effect of perfusion rate on *in vitro* percutaneous absorption, *J. Invest. Derm.,* 1969, 53, 264–269.

Danon, A., Ben-Shimon, S., and Ben-Zvi, Z., Effect of exercise and heat exposure on percutaneous absorption of methyl salicylate, *Eur. J. Clin. Pharmacol.,* 1986, 31, 49–52.

Davis, M.D., O'Fallon, W.M., Rogers, R.S., III, and Rooke, T.W., Natural history of erythromelalgia: presentation and outcome in 168 patients, *Arch. Dermatol.,* 2000, 136, 330–336.

De Lange, J., van Eck, P., Elliott, G.R., de Kort, W.L., and Woltuis, O.L., The isolated blood-perfused pig ear: an inexpensive and animal saving model for skin penetration studies, *J. Pharmacol. Toxicol. Methods,* 1992, 27, 71–77.

Fealey, R.D., Low, P.A., and Thomas, J.E., Thermoregulatory sweating abnormalities in diabetes mellitus, *Mayo Clin. Proc.,* 1989, 64, 617–628.

Fox, R.H. and Hilton, S.M., Bradykinin formation in human skin as a factor in heat vasodilation, *J. Physiol.,* 1958, 142, 219–232.

Greenstein, D., Gipta, N.K., Martin, P., Walker, D.R., and Kester, R.C., Impaired thermoregulation in Raynaud's phenomenon, *Angiology,* 1995, 46, 603–611.

Guy, R.H., Hadgraft, J., and Maibach, H.I., A pharmacokinetic model for percutaneous absorption, *Int. J. Pharm.,* 1982, 11, 119–129.

Guy, R.H. and Maibach, H.I., Drug delivery to local subcutaneous structures following topical administration, *J. Pharm. Sci.*, 1983, 72, 1375–1380.

Guy, R.H., Wester, R.C., Tur, E., and Maibach, H.I., Noninvasive assessment of the percutaneous absorption of methyl nicotinate in humans, *J. Pharm. Sci.*, 1983, 72, 1077–1079.

Hashim, M.A. and Tadepalli, A.S., Cutaneous vasomotor effects of neuropeptide Y, *Neuropeptides,* 1995, 29, 263–271.

Hatanaka, T., Manabe, E., Ohtsuki, T., Okuyama K., Mori, M., Okada, H., Katayama, K., and Koizumi, T. Drug targeting efficacy to underlying muscle following topical application. I. Evaluation based on a physiological pharmacokinetic model, *Biol. Pharm. Bull.,* 2000, 23, 860–865.

Heng, M.C., Local necrosis and interstitial nephritis due to topical methyl salicylate and menthol, *Cutis,* 1987, 39, 442–444.

Higaki, K., Asai, M., Suyama, T., Nakayama, K., Ogawara, K., and Kimura, T., Estimation of intradermal disposition kinetics of drugs: II. Factors determining penetration of drugs from viable skin to muscular layer, *Int. J. Pharm.,* 2002, 239, 129–141.

Holzer, P., Neurogenic vasodilation and plasma leakage in the skin, *Gen. Pharmacol.,* 1998, 30, 5–11.

Johnson, J.M., Brengelmann, G.L., Hales, J.R., Vanhoutte, P.M., and Wenger, C.B., Regulation of the cutaneous circulation, *Fed. Proc.,* 1986a, 45, 2841–2850.

Johnson, J.M., O'Leary, D.S., Taylor, W.F., and Kosiba, W., Effect of local warming on forearm reactive hyperaemia, *Clin. Physiol.,* 1986b, 6, 337–346.

Johnson, J.M. and Proppe, D.W., Cardiovascular adjustments to heat stress, in M.J. Fregly and C.M. Blatteis (eds.), *Handbook of Physiology,* New York: Oxford University Press, 1996, pp. 215–243.

Kellogg, D.K.L., Jr., Pergola, P.E., Piest, K.L., et al., Cutaneous active vasodilation in humans is mediated by cholinergic nerve cotransmission, *Circ. Res.,* 1995, 77, 1222–1228.

Khan, F. and Belch, J.J., Skin blood flow in patients with systemic sclerosis and Raynauds phenomenon: effects of L-arginine supplementation, *J. Rheumatol.,* 1999, 26, 2389–2394.

Kietzmann, M., Loscher, W., Arens, D., Maass, P., and Lubach, D., The isolated perfused bovine udder as an *in vitro* model of percutaneous drug absorption. Skin viability and percutaneous absorption of dexamethasone, benzoyl peroxide and etofenamate, *J. Pharmacol. Toxicol. Methods,* 1993, 30, 75–84.

Kobayashi, D., Kawabata, S., Sugibayashi, K., Morimoto, Y., and Kimura, M., *In vitro/in vivo* difference in enhanced skin permeation of nicardipine hydrochloride by the 1-menthol-ethanol system, *Skin Pharmacol.*, 1996, 9, 130–136.

Krestos, K., Kasting, G.B., and Nitsche, J.M., Distributed diffusion-clearance model for transient drug distribution within the skin, *J. Pharm. Sci.,* 2004, 93, 2820–2835.

Liron, Z. and Cohen, S., Percutaneous absorption of alkanoic acids I: a study of operational conditions, *J. Pharm. Sci.*, 1984, 73, 534–537.

Littleford, R.C., Khan, F., and Belch, J.J., Impaired skin vasomotor reflexes in patients with erythromelalgia, *Clin. Sci. (Lond.),* 1999, 96, 507–512.

McCarley, K.D. and Bunge, A.L., Pharmacokinetic models of dermal absorption, *J. Pharm. Sci.*, 2001, 90, 1699–1719.

McDougal, J., Prediction-Physiological Models, in *Dermal Absorption and Toxicity Assessment* (M.S. Roberts and K.A. Walters, eds.), New York: Dekker, 1998, pp.189–202.

McDougal, J.N., Jepsen, G.W., Clewell, H.J., MacNaughton, M.G., and Andersen, M.E., A physiological pharmacokinetic model for dermal absorption of vapours in the rat, *Toxicol. Appl. Pharmacol.,* 1986, 85, 286–294.

McNeill, S.C., Potts, R.O., and Francoeur, M.L., Local enhanced topical delivery (LETD) of drugs: does it truly exist? *Pharm. Res.,* 1992, 11, 1422–1427.

Monterio-Riviere, N.A., Inman, A.O., Riviere, J.E., McNeill, S.C., and Francoeur, M.L., Topical penetration of piroxicam is dependent on the distribution of the local cutaneous vasculature, *Pharm. Res.,* 1993, 10, 1326–1331.

Morgan, C.J., Renwick, A.G., and Friedmann, P.S., The role of stratum corneum and dermal microvascular perfusion in penetration and tissue levels of water-soluble drugs investigated by microdialysis, *J. Invest. Derm.*, 2003, 148, 434–443.

Mork, C., Kalgaard, O.M., and Kvernebo, K., Impaired neurogenic control of skin perfusion in erythromelalgia, *J. Invest. Dermatol.,* 2002, 228, 699–703.

Mortimer, P.S., Simmonds, R., Rezvani, M., Robbins, M., Hopewell, J.W., and Ryan, T.R., The measurement of skin lymph flow by isotope clearance—reliability, reproducibility, injection dynamics and the effect of massage, *J. Invest. Dermatol.,* 1990, 95, 677–682.

Muller, M., Mascher, H., Kikuta, C., Schafer, S., Brunner, M., Domer, G., and Eichler, H.G., Diclofenac concentration in defined tissue layers after topical administration, *Clin. Pharmacol. Ther.*, 1997, 62, 293–299.

Nakayama, K., Matsuura, H., Asai, M., Ogawara, K., Higaki, K., and Kimura, T., Estimation of intradermal disposition kinetics of drugs: I. analysis by compartmental model with contralateral tissues, *Pharm. Res.,* 1999, 16, 302–308.

O'Toole, G.A., Hettiaratchy, S., Allan, R., and Powell, B.W.E.M., Aberrant sentinel nodes in malignant melanoma, *Br. J. Plast. Surg.,* 2000, 53, 415–417.

Pang, K.S., Lee, W.F., Cherry, W.F., Yuen, V., Accaputo, J., Fayz, S., Schwab, A.J., and Goresky, C.A., Effects of perfusate flow rate on measured blood volume, disse space, intracellular water space, and drug extraction in the perfused rat liver preparation: characterization by the multiple indicator dilution technique, *J. Pharmacokinet. Biopharm.,* 1988, 116, 595–632.

Pang, K.S. and Rowland, M., Hepatic clearance of drugs, I. Theoretical considerations of a "well-stirred" model and a "parallel tube" model. Influence of hepatic blood flow, plasma and blood cell binding, and the hepatocellular enzymatic activity on hepatic blood clearance, *J. Pharmacokinet. Biopharm.,* 1977, 5, 625–653.

Pergola, P.E., Kellogg, D.L., Jr., Johnson, J.M., and Kosiba, W.A., Reflex control of active cutaneous vasodilation by skin temperature in humans, *Am. J. Physiol.,* 1994, 266, H1979–H1984.

Pergola, P.E., Kellogg, D.L., Jr., Johnson, J.M., Kosiba, W.A., and Solomon, D.E., Role of sympathetic nerves in the vascular effects of local temperature in human forearm skin, *Am. J. Physiol.,* 1993, 265, H785–H792.

Pessina, G.P., Bocci, V., Carraro, F., Naldini, A., and Paulesu, L., The lymphatic route. IX. Distribution of recombinant interferon-α 2 administered subcutaneously with oedematogenic drugs, *Physiol. Res.,* 1993, 42, 243–250.

Riviere, J.E., Bowman, K.F., Monteiro-Riviere, N.A., Dix, L.P., and Carver, M.P., The isolated perfused porcine skin flap (IPPSF). I. A novel *in vitro* model for percutaneous absorption and cutaneous toxicology studies, *Fundam. Appl. Toxicol.,* 1986, 7, 444–453.

Riviere, J.E., Monteiro-Riviere, N.A., and Inman, A.O., Determination of lidocaine concentrations in skin after transdermal iontophoresis: effects of vasoactive drugs, *Pharm. Res.,* 1992, 9, 211–214.

Riviere, J.E., Sage, B., and Williams, P.L., Effects of vasoactive drugs on transdermal lidocaine iontophoresis, *J. Pharm. Sci.,* 1991, 80, 615–620.

Riviere, J.E. and Williams, P.L., Pharmacokinetic implications of changing blood flow in skin, *J. Pharm. Sci.,* 1992, 81, 601–602.

Roberts, M.S. and Anissimov, Y.G., Mathematical models in percutaneous absorption, in *Percutaneous Absorption Drugs — Cosmetics — Mechanisms — Methodology*, 4th ed., (Bronaugh, R.L. and Maibach, H.I., eds.) New York, Marcel Dekker, 2005, in press.

Roberts, M.S., Cross, S.E., and Pellett, M.A., Skin Transport, in *Dermatological and Transdermal Formulations,* (K.A. Walters, ed.) Marcel Dekker, New York, 2002, pp. 89–195.

Roberts, M.S. and Cross, S.E., A physiological model for solute disposition in tissues below a topical application site, *Pharm. Res.,* 1999, 1392–1398.

Roberts, M.S., Structure-permeability considerations in percutaneous absorption, in *Prediction of Percutaneous Penetration — Methods, Measurement and Modelling,* (R.H. Guy, J. Hadgraft, and M.E. Bodde, eds.), IBC Technical Services, Ltd., 1991, 210–228.

Rowland, M., Physiologic pharmacokinetic models: relevance, experience and future trends, *Drug Metab. Rev.,* 1984, 15, 55–74.

Schaefer, H. and Redelmeier, T.E., *Skin Barrier*, Basel, Switzerland: Karger, 1996, p. 127.

Schaefer, H. and Stuttgen, G., Penetration of a non-steroidal anti-inflammatory drug into human skin *in vitro* and *in vivo*. Tissue concentrations and flow rates of *p*-butoxyphenylacetoxyhydroxamic acid, *Arzneim Forsch.,* 1978, 28, 1021–1023.

Scheuplein, R.J. and Blank, I.H., Permeability of the skin, *Physiol. Rev.,* 1971, 51, 702–747.

Seki, T., Hosoya, O., Yamazaki, T., Sato, T., Saso, Y., Juni, K., and Morimoto, K., A rabbit ear flap perfusion experiment to evaluate the percutaneous absorption of drugs, *Int. J. Pharm.*, 2004, 276, 29–40.

Shastry, S., Minson, C.T., Wilson, S.A., Dietz, N.M., and Joyner, M.J., Effects of atropine and L-NAME on cutaneous blood flow during body heating in humans, *J. Appl. Physiol.,* 2000, 88, 467–472.

Siddiqui, O., Roberts, M.S., and Polack, A.E. Topical absorption of methotrexate: role of dermal transport, *Int. J. Pharm.*, 1985, 27, 193–203.

Siddiqui, O., Roberts, M.S., and Polack, A.E., Percutaneous absorption of steroids: relative contributions of epidermal penetration and dermal clearance, *J. Pharmacokinet. Biopharm.*, 1989, 17, 405–424.

Siebert, G.A., Hung, D.Y., Chang, P., and Roberts, M.S., Ion-trapping, microsomal binding, and unbound drug distribution in the hepatic retention of basic drugs, *J. Pharmacol. Exp. Ther.*, 2004, 308, 228–235.

Silcox, G.D., Parry, G.E., Bunge, A.L., Pershing, L.K., and Pershing, D.W., Percutaneous absorption of benzoic acid across human skin. II Prediction of an *in vivo*, skin-flap system using *in vitro* parameters, *Pharm. Res.,* 1990, 7, 352–354.

Singh, P., Local deep tissue penetration of drugs after topical application, Ph.D. thesis, University of Queensland, Australia, 1992.

Singh, P., Maibach, H.I., and Roberts, M.S., Site of effects, in M.S. Roberts and K.A. Walters (eds.), *Dermal Absorption and Skin Toxicity Assessment,* New York: Dekker, 1998, pp. 353–370.

Singh, P. and Roberts, M.S., Blood flow measurements in skin and underlying tissues by microsphere method—application to dermal pharmacokinetics of polar non-electrolytes, *J. Pharm. Sci.,* 1993a, 82, 873–879.

Singh, P. and Roberts, M.S., Dermal and underlying tissue pharmacokinetics of salicylic acid after topical application, *J. Pharmacokinet. Biopharm.,* 1993b, 21, 337–373.

Singh, P. and Roberts, M.S., Dermal and underlying tissue pharmacokinetics of lidocaine after topical application, *J. Pharm. Sci.,* 1994a, 83, 774–782.

Singh, P. and Roberts, M.S., Effects of vasoconstriction on dermal pharmacokinetics and local distribution of compounds, *J. Pharm. Sci.,* 1994b, 83, 783–791.

Singh, P. and Roberts, M.S., Local deep tissue penetration of compounds after dermal application: structure-tissue penetration relationships, *J. Pharmacol. Exp. Ther.,* 1996, 279, 908–917.

Sugibayashi, K., Yanagimoto, G., Hayashi, T., Seki, T., Juni, K., and Morimoto, Y., Analysis of skin disposition of flurbiprofen after topical application in hairless rats, *J. Controlled Release,* 1999, 62, 193–200.

Supersaxo, A., Hein, W.R., and Steffen, H., Effect of molecular weight on the lymphatic absorption of water-soluble compounds following subcutaneous administration, *Pharm. Res.,* 1990, 7, 167–169.

Thompson, J.F., Uren, R.F., Shaw, H.M., McCarthy, W.H., Quinn, M.J., O'Brien, C.J., and Howman-Giles, R.B., The location of sentinel lymph nodes in patients with cutaneous melanoma: new insights into lymphatic anatomy, *J. Am. Coll. Surg.,* 1999, 189, 195–206.

Uren, R.F., Lymphatic drainage of the skin, *Ann. Surg. Oncol.,* 2004, 11, 179S–185S.

Uren, R.F., Thompson, J.F., and Howman-Giles, R.B., *Lymphatic Drainage of the Skin and Breast, Locating the Sentinel Nodes,* Amsterdam: Harwood, 1999.

Veves, A., Akbari, C.M., Primavera, J., et al., Endothelial dysfunction and the expression of endothelial nitric oxide synthetase in diabetic neuropathy, vascular disease and foot ulceration, *Diabetes,* 1998, 47, 457–463.

Wagner, S.M., Noguiera, A.C., Paul, M., Heydeck, D., Klug, S., and Christ, B., The isolated normothermic hemoperfused porcine forelimb as a test system for transdermal percutaneous absorption studies, *J. Artif. Org*., 2003, 6, 183–191.

Wigley, F.M. and Flavahan, N.A., Raynaud's phenomenon, *Rheum. Dis. Clin. North Am.,* 1996, 22, 765–781.

Williams, P.L., Carver, M.P., and Riviere, J.E., A physiologically relevant pharmacokinetic model of xenobiotic percutaneous absorption utilising the isolated perfused porcine skin flap, *J. Pharm. Sci.,* 1990, 79, 305–311.

Williams, P.L. and Riviere, J.E., Model describing transdermal iontophoretic delivery of lidocaine incorporating consideration of cutaneous vascular state, *J. Pharm. Sci*., 1993, 82, 1080–1084.

Wu, Z., Rivory, L.P., and Roberts, M.S., Physiological pharmacokinetics of solutes in perfused rat hindlimb: characterisation of the physiology with changing perfusate flow, protein content and temperature using statistical moment analysis, *J. Pharmacokinet. Biopharm.*, 1993, 21, 653–688.

Yoshikawa, H., Takada, K., and Muranishi, S., Molecular weight-dependent lymphatic transfer of exogenous macromolecules from large intestine of renal insufficiency rats, *Pharm. Res.,* 1992, 9, 1195–1198.

Young, A.J. and Castellani, J.W., Exertion-induced fatigue and thermoregulation in the cold, *Comp. Biochem. Physiol. A Mol. Integr. Physiol.,* 2001, 128, 769–776.

CHAPTER 14

Chemical Mixtures

Jim E. Riviere

CONTENTS

INTRODUCTION

Drug and chemical dermal absorption typically involves experiments conducted using single chemicals, making the mechanisms of absorption of individual chemicals extensively studied (the subject of most chapters in this volume). Similarly, most risk assessment profiles and mathematical models are based on the behavior of single chemicals. A primary route of occupational and environmental exposure to toxic chemicals is through the skin; however, such exposures are often to complex chemical mixtures. In fact, the effects of coadministered chemicals on the rate and extent of absorption of a topically applied systemic toxicant may determine whether

toxicity is ever realized. This dichotomy between the availability of data and absorption models based on single chemicals with field exposure scenarios dominated by complex mixtures deserves further attention.

It is axiomatic that, for a topically applied chemical to exert systemic toxicity, absorption across the dermal barrier is required. For a topically applied compound to be absorbed into the skin, it must first pass through the stratum corneum, continue through the epidermal layers, and penetrate into the dermis, where absorption into the dermal microcirculation becomes the portal for systemic exposure. For a chemical with direct toxicity to the skin, systemic absorption is not required as the target cells could be any of those comprising the epidermis or dermis.

The application of risk assessment to dermal absorption by U.S. regulatory agencies (U.S. Environmental Protection Agency [EPA], Occupational Safety and Health Administration [OSHA], Agency for Toxic Substances and Disease Registry [ATSDR]) is varied and highly dependent on available data (Poet and McDougal, 2002; EPA, 1995, 2000). A similar concern over lack of data exists for overall risk assessment of chemical mixtures (Bogert et al., 2001; Pohl et al., 1997; EPA, 1986, 1988). The congressional Commission on Risk Assessment and Risk Management (CRARM, 1997) recommended moving beyond individual chemical assessments and focusing on the broader issue of toxicity of chemical mixtures. Current approaches are based on assigning toxicological equivalent units to similar chemical congeners (e.g., dioxins) or assessing toxicity after exposure to the complete mixture. Ideally, dose response curves of individual components of a mixture should be characterized and then a "no interaction" hypothesis tested (Bogert et al., 2001). With complex mixtures of hundreds of components, this approach borders on the impossible. Importantly, interactions that involve modulation of absorption, and thus systemic bioavailability, have not been addressed.

It is impossible to assess all potential combinations of chemicals to determine which has the greatest potential to modulate absorption of a known toxic entity topically exposed in a chemical mixture. The present state of knowledge in this area is particularly weak because the significance of specific interactions has not been quantitated, let alone in many cases identified. In many ways, this same concern continues to define the nature of chemical mixture toxicology. The appreciation of the importance of chemical mixture interactions to effect chemical and drug disposition, biotransformation, pharmacokinetics, and activity has been well recognized for many years and is extensively reviewed elsewhere (see comprehensive reviews by Yang, 1994; Bliss, 1939; Bogert et al., 2001; Groten et al., 2001, Haddad et al., 2000, 2001; Pohl et al., 1997). A large body of literature exists in the field of drug–drug interactions, and a body of work is developing in the area of food additive interactions on drug absorption. Despite this widespread knowledge base of the importance of drug–drug interactions and formulation effects in pharmaceutical science, the potential role of chemical interactions in systemic toxicology has not garnered significant attention. The focus of this chapter is to overview the potential mechanisms operative in topical chemical mixtures as well as present some of our laboratory's efforts to quantitate these effects.

In cases when the potential toxicity of a specific mixture is of concern (for example, at a specific toxic waste site), the complete mixture is often tested

(McDougal and Robinson, 2002). However, how does one quantitate the absorption of a mixture consisting of 50 chemicals? How are markers selected? How are these data expressed? Unfortunately, even after a complete toxicological profile of a specific mixture (such as a "standard" mixture of 50 environmentally relevant compounds, surrogate jet fuels, and so forth) is defined using all the techniques modern toxicology and toxicogenomics has to offer, one cannot define the links between absorption and the effects seen. Was the observed toxicity exerted because a specific toxicant was in the mixture, because two synergistic toxicants were absorbed, or simply because of the presence of a mixture component (such as alcohol, surfactant, or fatty acid) that enhanced the absorption of a normally minimally absorbed toxicant? We have demonstrated (Baynes, Monteiro-Riviere, et al., 2002; Riviere et al., 2002) such an interaction with the putative toxins involved in the Gulf War syndrome (Abou Donia et al., 1996), for which systemic pyridostigmine bromide or coexposure to jet fuel was shown to greatly enhance the dermal absorption of topical permethrin. Would other pesticides have this effect? How does one take into account such critical interactions so that a proper risk assessment may be conducted? An inclusive approach to this problem is to define chemicals on the basis of how they would interact with other components of a mixture as well as with the barrier components of the skin. What are the physical-chemical properties that would significantly modify absorption and potentiate systemic exposure to a toxicant? What are the properties of molecules susceptible to such modulation?

One recently reported approach to address this problem assesses potential interactions in dermal absorption by fractionating the effects of a vehicle on drug penetration onto the two primary parameters describing permeation according to Fick's law: partitioning PC and diffusivity D [Permeability (Kp) = D • PC/Membrane thickness] (Rosada et al., 2003). Although this study only reported on four compounds, one (diazepam) was not predictable using this approach as its physiochemical properties were already optimal for absorption, and only absorption enhancers were investigated. This study illustrated the difficulty of making broad generalizations across compounds solely on physical-chemical properties.

The problem of dermal mixture absorption is conceptually similar to that of dermatological formulations in the pharmaceutical arena. The primary difference is that most pharmaceutical formulation components are added for a specific purpose relative to the delivery, stability, or activity of the active ingredient. In the environmental and occupational scenarios, additives are a function of either their natural occurrence or presence in a mixture for a purpose related to uses of that mixture (e.g., a fuel performance additive, stability) and not for their effects on absorption or toxicity of the potential toxicant. Unlike pharmaceutical formulation additives in a dermal medication, chemical components of a mixture are not classified on how they could modulate percutaneous absorption of simultaneously exposed topical chemicals. They are either present *functionally* for specific purposes (e.g., performance additives, lubricants, modulators of some biological activity), *sequentially* because they were applied to the skin independently at different times for unrelated purposes (cosmetic followed by topical insect repellent, sunscreens), *accidentally* because they were disposed of simultaneously as waste, or *coincidentally* associated as part of a complex occupational or environmental exposure.

MECHANISMS OF INTERACTIONS

Chemical interactions that may modulate dermal absorption can be conveniently classified according to physical location where an interaction may occur. The advantage of this approach is that potential interactions may be defined on the basis of specific mechanisms of action involved as well as by the biological complexity of the experimental model required to detect it.

Surface of skin
- Chemical–chemical (binding, ion pair formation, etc.)
- Altered physical-chemical and solvatochromatic properties (e.g., solubility, volatility, critical micelle concentration [CMC])
- Altered rates of surface evaporation
- Occlusive behavior
- Binding or interaction with adnexial structures or their products (e.g., hair, sweat, sebum)

Stratum corneum
- Altered permeability through lipid pathway (e.g., enhancer)
- Altered partitioning into stratum corneum
- Extraction of intercellular lipids

Epidermis
- Altered biotransformation
- Induction or modulation of inflammatory mediators

Dermis
- Altered vascular function (direct or secondary to mediator release)

The first and most widely studied area of chemical–chemical interactions is on the surface of the skin. The types of phenomena that could occur are governed by the laws of solution chemistry and include factors such as altered solubility, precipitation, supersaturation, solvation, or volatility; as well as physical-chemical effects such as altered surface tension from the presence of surfactants, changed solution viscosity, and micelle formation (Idson et al., 1983; Williams and Barry, 1998; Barry, 2001; Moser et al., 2001). For some of these so-called solvatochromatic effects, chemicals act independent of one another. However, for many the presence of other component chemicals may modulate the effect seen.

Chemical interactions may further be modulated by interaction with adnexial structures or their products, such as hair, sebum, or sweat secretions. The result is that when a marker chemical is dosed on the skin as a component of a chemical mixture, the amount freely available for subsequent absorption may be significantly affected. The primary driving force for chemical absorption in skin is passive diffusion, which requires a concentration gradient of thermodynamically active (free) chemical.

A second level of potential interaction involves the marker or component chemicals with the constituents of the stratum corneum. These include the classic enhancers such as oleic acid, Azone®, or ethanol, widely reviewed elsewhere (Williams and

Barry, 1998). These chemicals alter a compound's permeability within the intercellular lipids of the stratum corneum. Organic vehicles persisting on the surface of the skin may extract stratum corneum lipids that would alter permeability to the marker chemical (Monteiro-Riviere et al., 2001a; Rastogi and Singh, 2001). Compounds may also bind to stratum corneum constituents, forming a depot.

Another level of interaction would be with the viable epidermis. The most obvious point of potential interaction would be with a compound that undergoes biotransformation (Bronaugh et al., 1989; Mukhtar, 1992). A penetrating chemical and mixture component could interact in a number of ways, including competitive or noncompetitive inhibition for occupancy at the enzyme's active site or induction or inhibition of drug-metabolizing enzymes. Other structural and functional enzymes could also be affected (e.g., lipid synthesis enzymes), which would modify barrier function (Elias and Feingold, 1992). A chemical could also induce keratinocytes to release cytokines or other inflammatory mediators (Allen et al., 2000; Luger and Schwarz, 1990; Monteiro-Riviere et al., 2003), which could ultimately alter barrier function in the stratum corneum or vascular function in the dermis. Alternatively, cytokines may modulate biotransformation enzyme activities (Morgan, 2001).

The last level of potential interaction is in the dermis, where a component chemical may directly or indirectly (e.g., via cytokine release in the epidermis) modulate vascular uptake of the penetrated toxicant (Riviere and Williams, 1992; Williams and Riviere, 1993). In addition to modulating transdermal flux of chemical, such vascular modulation could also affect the depth and extent of toxicant penetration into underlying tissues.

The optimal experimental approach to define such interactions is to conduct studies *in vivo* because all potential mechanisms of interactions are present. However, this approach is cost prohibitive and is not amenable to determination of specific permeability parameters that would elucidate basic principles that could then be used to predict interactions in the future. Although the biologically intact skin seen in the *in vivo* setting might seem to be ideal, in reality it is difficult to dissect interactions that occur in the different phases of absorption. This is because of the confounding influence of multiple biological and surface chemical factors, as well as systemic effects, present. This scenario is further aggravated by the high level of interindividual variability typical of *in vivo* studies, which mask the detection of important interactions that might be exerted in other mixtures of slightly different composition. Most important, acute studies or those using extremely toxic chemicals could never be conducted in humans for ethical reasons or even in intact animals because of humane considerations, making an alternative approach such as outlined here a necessity.

EXAMPLES OF DERMAL MIXTURE INTERACTIONS

Our research program has focused on the effects of chemical mixture components on dermal absorption of select "marker" chemicals in the mixture (Qiao et al., 1996; Baynes, Brooks, Mumtaz, et al., 2002; Riviere et al., 2001, 2003). As varied as these potential interactions may be, experimentally isolating them is difficult because of

confounding effects from simultaneously occurring multiple interactions (e.g., enhanced partitioning coupled with decreased diffusivity, solubility, or vascular uptake). To dissect out these processes, our laboratory's approach has been to use different model systems with increasing levels of biological complexity.

Silicone membrane flow-through diffusion cells (SMFT): sensitive to solvatochromatic processes
Porcine skin flow-through diffusion cells (PSFT): also sensitive to changes in lipid permeability
Isolated perfused porcine skin flap (IPPSF): also sensitive to irritation and vascular events

This hierarchy of experimental models allows interactions to be independently studied using efficient and humane *in vitro* model systems. These systems, as well as the basic principles of percutaneous absorption of single chemicals, have been reviewed in chapters 2 and 3 of the present text.

To investigate the nature of mixture interactions on chemical absorption, a series of studies was conducted on 12 diverse chemicals representing three chemical classes (Van der Merwe and Riviere, 2004a, 2004b):

Substituted phenols: nonylphenol, pentachlorophenol (PCP), phenol, ρ-nitrophenol (PNP)
Organophosphate pesticides: chlorpyrifos, ethylparathion, fenthion, methylparathion
Triazines: atrazine, propazine, simazine, and triazine

These compounds have molecular weights ranging from 94 to 350 and log $K_{o/w}$ from −1 to 5. Compounds were studied using a complete factorial experimental design. There were three vehicles and three binary–vehicle combinations: water, ethanol, propylene glycol (PG), water/ethanol, water/PG, and ethanol/PG. For each vehicle combination, a control (no additive) or one or both of two mixture components, the surfactant sodium lauryl sulfate (SLS) or vasodilator methyl nicotinate, were added. This resulted in 24 mixture combinations per chemical, each conducted in two flow-through diffusion cell systems: silastic membrane (SMFT) or porcine skin (PSFT). Porcine stratum corneum partition coefficients (log $K_{SC/MIX}$) across all vehicles were determined. Parameters determined in the diffusion cell studies included permeability and diffusivity. A restricted number of specific vehicles and compound combinations were then selected for study in the IPPSF model. Data were initially analyzed using compass plots to determine mixture interactions. Compass plots have been useful to examine data visually to probe complex mixture interactions (Budsaba et al., 2000; Baynes et al., 2001; Baynes, Brooks, Barlow, et al., 2002; Qiao et al., 1996, Muhammad et al., 2004). Analysis of means (ANOM) is used to visualize statistical significance of effects seen (Budsaba et al., 2000).

The underlying hypothesis in this study was that permeability parameters are a function of log $K_{o/w}$ and molecular weight, which may be affected when a compound is administered in a chemical mixture. This forms the basis of EPA dermal absorption guidelines based on the work of Potts and Guy (1992). Comparisons for which this relationship held confirmed that diffusion processes remain rate limiting. However,

when such relations break down, a significant interaction may be present that is not diffusion limited and thus not directly related to log $K_{o/w}$. This would have an obvious impact on risk assessment procedures as it would affect the mathematical form of any quantitative structure–permeability relationship (QSPR) equation linking log $K_{o/w}$ to dermal absorption. These occurred when extrapolating across solvent systems (e.g., ethanol/water), when surfactant SLS was added to different systems, and occasionally when individual compounds deviated from their predicted fluxes.

Compound Susceptibility to Solvent Interactions

A consistent finding across all mixtures was that, as expected, some compounds behaved differently in specific solvent systems. This interaction tended to be consistent across SMFT and PSFT systems, a finding supporting the hypothesis that the interaction is solvatochromatic and does not involve interaction with other constituents of the stratum corneum or epidermis. Figure 14.1 is a series of compass plots illustrating permeability in PSFT of all 12 study compounds in 12 PG mixtures. Compounds are arranged clockwise around the plot in order of descending log $K_{o/w}$, with the lowest (Triazine, –0.9) at 12 o'clock and the highest (PCP, 5.12) at 11 o'clock. Permeabilities from flow-through diffusion cells are plotted on the radii, which are further demarcated by mean and upper and lower ANOM confidence intervals. These plots illustrate that, in this system, compounds behave similarly except for triazine and phenol, two compounds with the lowest $K_{o/w}$. Exposure to these in PG would not be predicted from a log $K_{o/w}$ relationship. Ethanol modulates these fluxes, especially for phenol. Compass plots across SMFTs (data not shown) and PSFTs were comparable. Absorption in PG was low compared to the other solvents studied (except for low log $K_{o/w}$ compounds), and mixture interactions detected were opposite of those seen in other systems (e.g., water/ethanol). These complex interactions make simple extrapolations difficult.

Mixture Interactions Across Model Systems

Analysis of compass plots detected a series of statistically significant ($p < .05$) interactions in some solvent systems that did not clearly extrapolate across model systems and demonstrated individual compound specificity. Those identified are illustrated in Figure 14.2, which depicts profiles of absorption flux (% Dose/h) vs. time for four compounds in two chemical classes (PNP, PCP, atrazine, and propazine) exposed in water or water plus SLS and studied in SMFT or PSFT models as well as IPPSFs. It must be noted that the shape of the absorption profiles across the three model systems are always different because of differences in model system structure. Flux through the SMFT is an order of magnitude greater than that of the PSFT, making time of peak flux occur earlier in this system. It is the *correlation* of permeability between these systems, and not the absolute magnitude, that is important for assessing mixture effects on absorption. The delayed absorption seen in the PSFT compared to the SMFT reflects the greater lag time, and hence reduced diffusivity, for transport across porcine skin. Similarly, the shorter lag time generally seen in IPPSFs reflects the shorter diffusional distance seen when a model is perfused

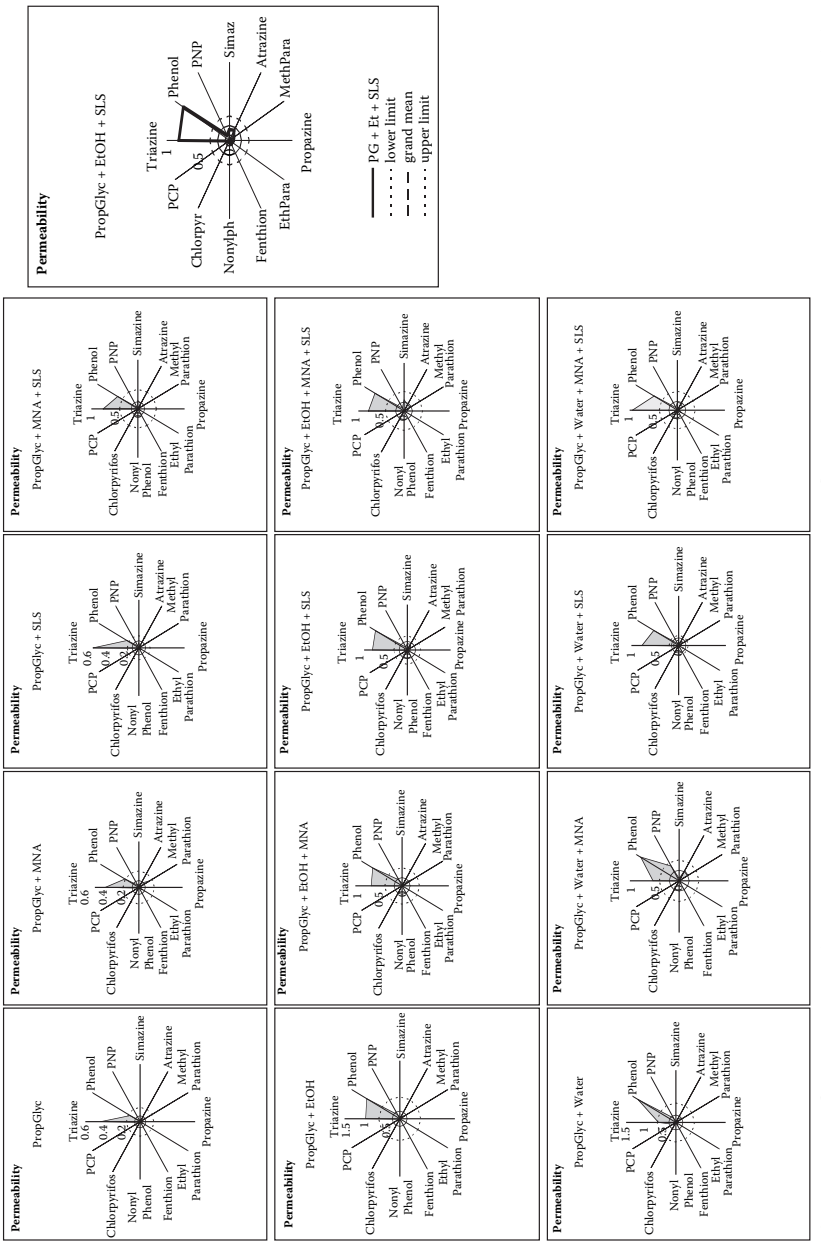

Figure 14.1 Compass plots for penetrants in propylene glycol mixtures in PSFT. The interactions noted in this plot at left for triazine and phenol were positive and outside of the upper confidence interval for significant interactions ($p < .05$). One cell is expanded to illustrate upper and lower bounds.

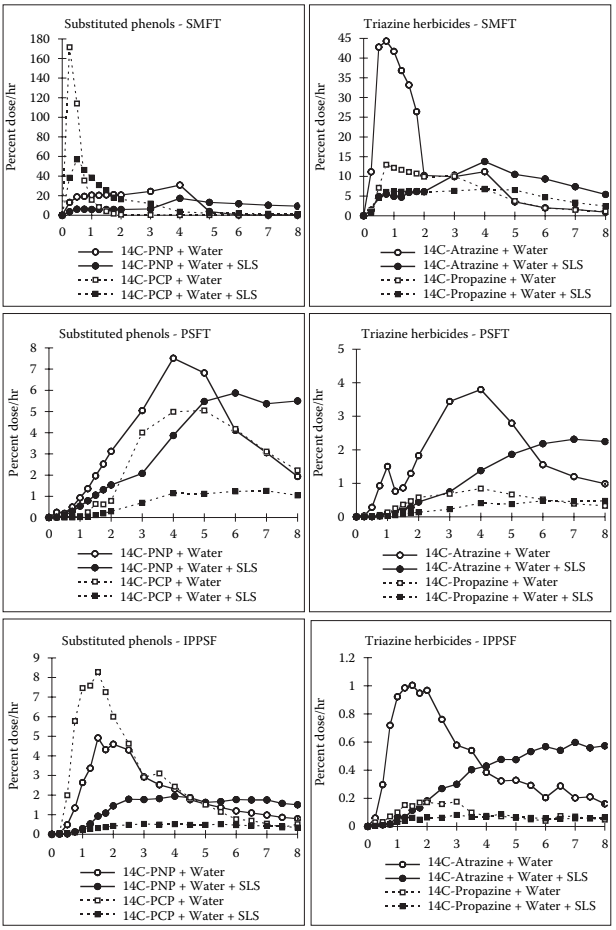

Figure 14.2 Effects of SLS on dermal flux profiles of four model penetrants in SMFT, PSFT, and IPPSF model systems. Open points are control, and solid points are SLS treatments.

by dermal capillaries. Characteristic of these models, compound flux in the PSFT model exceeds those in the IPPSF model, which possesses a more complex membrane.

The first comparison was a relatively consistent SLS effect across compounds and models. The next comparison involved the substituted phenols PCP and PNP in the same solvent systems. In the SMFT system, PCP flux was greater than PNP, as predicted from its greater log $K_{o/w}$ of 5.1 vs. 1.9. However, the fluxes were of a similar order of magnitude in the PSFT experiments, which carried forward into the IPPSF studies, in which the major difference was a slightly earlier peaking of PCP. These compounds have significantly different molecular properties (solubility, H-bonding indices), which could explain these differences both on the basis of stratum corneum penetration and subsequent dermal disposition. Log $K_{o/w}$ alone, used in risk assessment models, would not predict this IPPSF response. Again, in

all systems, SLS reduced flux compared to controls. This suggests that the SLS surfactant effect is detectable in the simplest model system; however, the actual shape of the transdermal flux profile is not directly predictable from the simpler systems. In fact, the broadening of the SLS absorption profiles may reflect modified dermal deposition within the stratum corneum that would be consistent with previously reported enhancing effects of SLS. We would expect the shape of the absorption profile to be a function of the kinetic model parameters describing these flux profiles. Second, it suggests that the SLS effect dominates over any log $K_{o/w}$ QSPR relationship for permeability of a single-compound absorption. This key finding provided the insight into developing the modified linear free-energy relationship (LFER) approaches discussed next.

The mechanism most likely responsible for the flux reduction from SLS at this concentration (10%) under these aqueous solvent conditions may be via reducing the CMC in solution (Baynes, Brooks, Barlow, et al., 2002), an effect that reduces availability of compound for absorption independent of its initial permeability. Mixture interactions modulate CMC, a phenomenon detectable across all model systems; these SLS effects are fully documented in Van der Merwe and Riviere, 2005b. This effect would be present across all model systems. Once the compound is absorbed into the stratum corneum, SLS could affect its structure and further modulate absorption, reflected in the altered shape profiles. It should be noted that, in acetone or dimethyl sulfoxide (DMSO) vehicles, parathion flux had been shown to increase with SLS (Qiao et al., 1996), reflecting a differential response of this mixture additive depending on the solvent system in which it is exposed. This dependency of mixture additive effects on the dosing vehicle was a major finding of this work.

The effects of these mixture interactions on IPPSF kinetic parameters are listed in Table 14.1 as they illustrate the most interesting mixture-specific data (see chapter 3 in this volume for a model description). SLS in water results in a decreased absorption rate (smaller *b,d*) compared to water alone. Ethanol in water reduces *b* for all compounds. Ethanol significantly reduces *d* except for propazine and simazine. These independent changes in rate parameters are consistent with the differently shaped profiles seen under different mixture conditions.

Can a Partition Coefficient Predict Mixture Behavior?

If log *K* is a primary determinant of diffusion, the hypothesis was that disposition from a mixture could be predicted from stratum corneum/mixture partition coefficient $K_{SC/MIX}$. Validation of this relationship would offer strong support for using LFER equations to predict mixture absorption. This was addressed by comparing log $K_{SC/MIX}$ to permeability across SMFT and PSFT models as well as to total IPPSF penetration (absorption plus skin deposition). Figure 14.3 is a histogram of these parameters across all systems using PCP as a model penetrant to illustrate this effect. Chemical mixtures are ordered by decreasing log $K_{SC/MIX}$ (top panel). Permeability in SMFT and PSFT models, as well as IPPSF absorption, generally follow the order of descending log $K_{SC/MIX}$ with a few clear exceptions. SMFT permeability mirrored log $K_{SC/MIX}$ (R^2 = 0.83). A unique mixture was ethanol/water/methyl nicotinate

Table 14.1 Effects of Sodium Lauryl Sulfate or Ethanol on "b"/"d" Mean Isolated Perfused Porcine Skin Flap Kinetic Parameters in Water

	Atrazine	Chlorpyrifos	E-Parathion	M-Parathion	PCP	PNP	Propazine	Simazine
Water	0.45/0.68	0.13/0.29	0.46/0.64	0.57/0.74	0.65/0.77	0.47/0.58	0.39/0.62	0.36/0.69
Water/SLS	0.06/0.11	0.02/0.10	0.11/0.26	0.18/0.31	0.17/0.33	0.16/0.22	0.18/0.38	0.14/0.46
Water/EtOH	0.23/0.46	0.09/0.22	0.15/0.46	0.28/0.65	0.26/0.34	0.36/0.50	0.14/0.72	0.28/1.28

(MNA) in PSFT models, for which permeability was less than predicted from log $K_{SC/MIX}$, an effect that carried into the IPPSF, suggesting a potential interaction with epidermal cells or dermal components, the only consistent factors different between isolated stratum corneum and SMFT compared to PSFT and IPPSF models. This interaction was also seen with other compounds. For PCP, stratum corneum partitioning appears to be the dominant factor. These findings support the hypothesis that a mixture component effect (such as SLS) in a specific solvent system will reduce permeability across penetrants (independent of the compound's specific QSPR relation to log $K_{o/w}$) and can be estimated by partition coefficients in simpler system.

Ethanol–Water Interactions

A significant interaction detected was the different effects seen for absorption across mixtures consisting of water, water/ethanol, and ethanol. Although log $K_{SC/MIX}$ correlated highly to log $K_{o/w}$ in water (system in which most dermal absorption QSPR analyses are defined), there was no clear correlation between log $K_{o/w}$ across these other relatively simple solvents. This mechanism was explored in more detail using log $K_{SC/MIX}$ (Van der Merwe and Riviere, 2005a). Figure 14.4 depicts log $K_{SC/MIX}$ for all 12 compounds ordered by log $K_{o/w}$ as well as the regression analyses for log $K_{SC/MIX}$ vs. log $K_{o/w}$ in the three separate solvent mixtures. As expected, there is a reasonable correlation between these parameters in water. However, the correlation significantly weakened when water/ethanol and ethanol systems were analyzed. Viewed from another perspective, rank order of log $K_{SC/MIX}$ was expected to be water > water/ethanol > ethanol, which held for compounds with log $K_{o/w}$ at the extremes. However, for compounds with midrange *PC*s (for example, atrazine–ethyl parathion), this clear-cut order was lost, suggesting molecular properties not predicted by log $K_{o/w}$ may modulate these relationships. Rosado et al. (2003) showed that diazepam with midrange log $K_{o/w}$ did not respond to chemical enhancement. It is evident that a mixture containing ethanol has a narrower range of altered log $K_{SC/MIX}$ than does a pure water system, potentially reflecting stronger molecular interactions seen with this solvent. Significantly, a 50/50 mixture could not be interpolated from data in the pure solvents. Finally, one must mention that molecular weight was also an important covariate in these analyses; however, they did not add a significant ability to discriminate these interactions or predict absorption over that which partition coefficient already provided.

Modified Quantitative Structure–Permeability Relationship Equations That Predict Chemical Absorption from a Mixture

The above analysis suggested that mixture interactions (for example, vehicles, surfactants) modify the normal correlation seen between a parameter such as log $K_{o/w}$ and absorption. Such correlations are often embedded in the QSPR based on LFERs, fully covered in chapter 7 on QSPR. For individual chemicals, there is often a strong correlation to parameters such as log $K_{o/w}$ and molecular weight (Potts and Guy, 1992) or to multiple molecular descriptors that allow for a wider range of chemicals to be accounted for (Abraham and Martins, 2004). As can be seen from the above

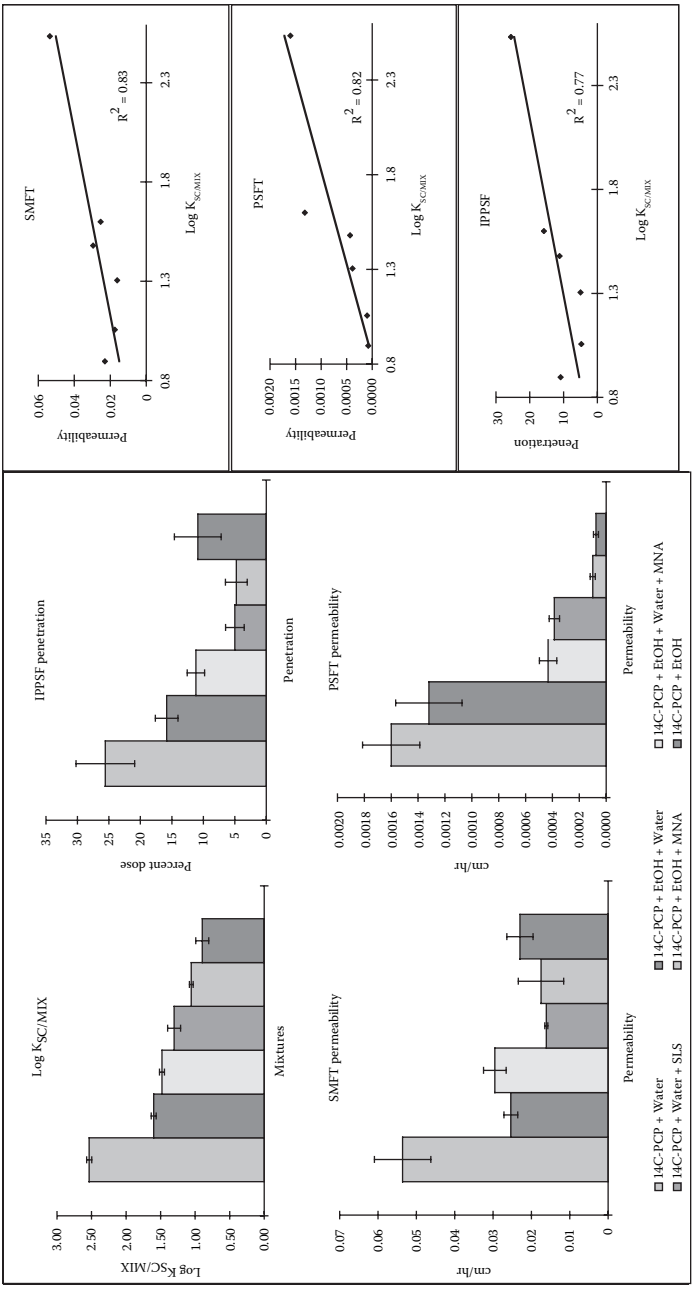

Figure 14.3 Comparative PCP absorption from six mixtures across all model systems.

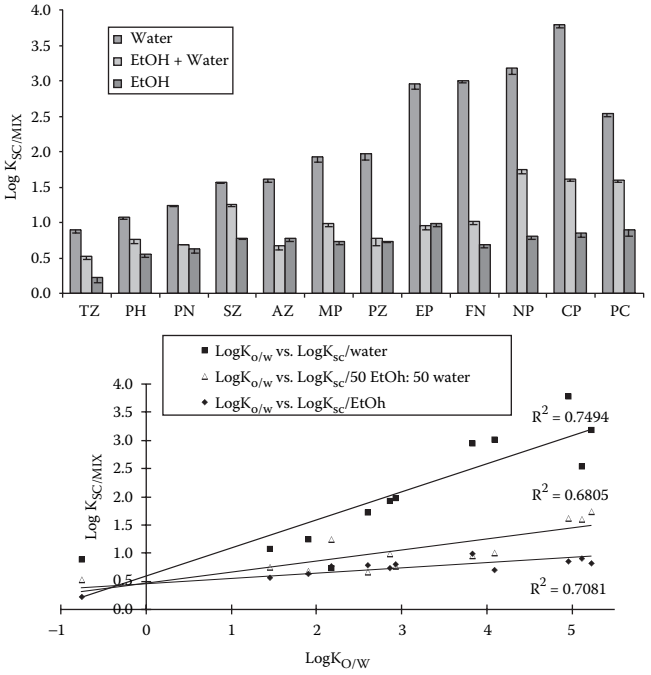

Figure 14.4 Log $K_{SC/MIX}$ in ethanol/water mixtures.

data, addition of SLS or ethanol modified the correlation between absorption and log $K_{SC/MIX}$ or log $K_{o/w}$; however, it did not destroy this relationship. Such mixture effects were often constant across all model systems studied, as was demonstrated with the compass plot analyses. Finally, the fact that mixture effects seen in the IPPSF model somewhat reflected changes in log $K_{SC/MIX}$ suggested that an LFER approach that incorporated both molecular descriptors of the penetrants of interest (classical single chemical approach) and mixture effects described by physical descriptors of the mixture might hold promise.

Our group elected to use Abraham's LFER model as our base equation because it is representative of the dermal QSPR approaches presently available (Abraham and Martins, 2004). Preliminary analyses applying 16 different LFER equations reviewed by Geinoz et al. (2004) to the entire PSFT (288 treatment combinations) and IPPSF data set (32 treatment combinations) demonstrated a superior fit of our data set to the Abraham equation compared to most other models reviewed. It must be stressed that the purpose of this research was not to identify the *optimal* LFER for predicting dermal permeation or to validate that this model is predictive of dermal absorption. Rather, we selected this model because it best described the available data and is widely accepted by the scientific community.

$$\log k_p = c + a\Sigma\alpha^H_2 + b\Sigma\beta^H_2 + s\pi^H_2 + rR_2 + vV_x$$

where k_p is the permeability constant for the PSFT experiments, $\sum\alpha^H_2$ is the hydrogen bond donor acidity, $\sum\beta^H_2$ is the hydrogen bond acceptor basicity, π^H_2 is the dipolarity/polarizability, R_2 represents the excess molar refractivity, and V_x is the McGowan volume. Molecular descriptor values for all of these parameters were calculated for the 12 penetrants studied from ABSOLV® Solute Property Prediction Software (Sirius Analytical Instruments, Ltd., East Sussex, U.K.). The parameters c, m, a, b, s, r, and v are strength coefficients coupling the molecular descriptors to skin permeability in the specific experimental system (for example, PSFT or IPPSF).

To incorporate mixture effects, another term was added, the mixture factor (MF), yielding

$$\log k_p = c + mMF + a\Sigma\alpha^H_2 + b\Sigma\beta^H_2 + s\pi^H_2 + rR_2 + vV_x$$

This concept allows an LFER equation to be defined across data collected from different mixtures. Hostynek and Magee (1997) had used indicator variables embedded in LFER equations to allow analysis across exposures consisting of different vehicles or occlusive conditions. Unlike our approach, their indicator variables did not contain any information concerning the vehicles but were a statistical regression tool to allow the base LFER model to be applied to penetrants dosed under different experimental conditions.

Figure 14.5 depicts the predicted vs. observed permeability constants (log Kp) for all 288 treatment combinations studied without taking into account the specific mixtures at which these chemicals were dosed. The residuals of this model showed no further correlation to penetrant properties. However, when vehicle/mixture component properties were analyzed, trends in residuals became evident. An excellent single parameter explaining some variability of this residual pattern (R^2 of 0.44) was log (1/Henry constant) (1/HC). Figure 14.6 depicts the modified LFER model including an MF = log (1/HC).

The improvement on the prediction of PSFT permeability across all treatments is clearly evident. It must be stressed that an MF related to 1/HC is not the final form of this analysis but was the first property suggestive that this approach might

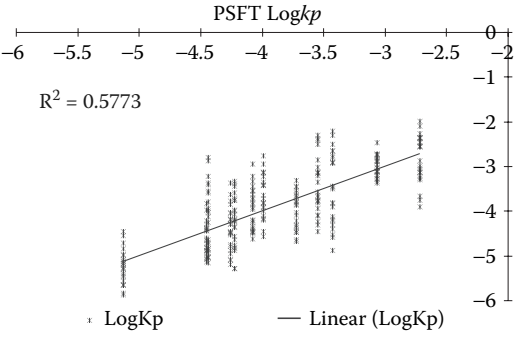

Figure 14.5 Observed vs. predicted log K_p in PSFT without inclusion of a mixture factor.

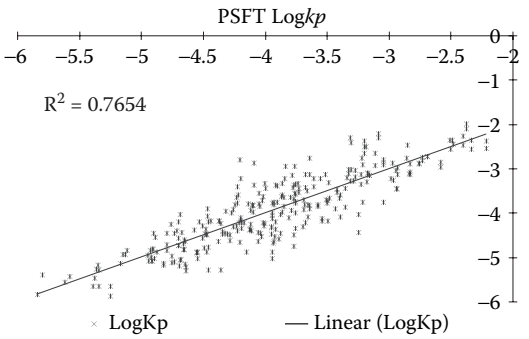

Figure 14.6 Observed vs. predicted log K_p in PSFT taking into account mixture properties.

work. Other physical parameters of the mixture similar to the molecular descriptors of the penetrant have also now been studied (Riviere and Brooks, 2005). A similar approach was used for the smaller data sets available in the IPPSF mixture exposures, and inclusion of an MF improved predictability. The final form of such a modified mixture LFER must await further research. This includes defining which physical chemical property of the mixture best describes the MF. However, the finding that an MF can be used to extrapolate chemical dermal absorption data across different vehicles and mixture combinations is a significant finding that we believe would have an impact on the occupation risk assessment process. It would allow single-chemical data collected in multiple research environments and resulting single-chemical LFER determined in different studies to be modified based on mixture component or vehicle properties. Chapter 5 on the membrane-coated fiber technique should also be consulted on another LFER approach to assess complex mixture interactions.

POTENTIAL IMPACT OF MULTIPLE INTERACTIONS

The complexity occurs when one considers that the above interactions are all independent, making the observed effect *in vivo* a vectorial sum of all interactions. This allows so-called emergent properties of complex systems (Bar-Yum, 1997) to become evident when the individual interactions are finally combined in the intact system, in our case *in vivo* skin. For example, assume that mixture component A decreases absorption of a chemical across skin because of increased binding to skin components. In contrast, mixture component B increases its absorption because of an enhancer effect on stratum corneum lipids. When A and B are administered together, the transdermal flux of the chemical studied may not differ from control. This is illustrated by the effect of two different jet fuel performance additives (MDA, BHT) on dermal absorption of naphthalene administered from the base fuel JP-8 not containing these additives or in combination (Figure 14.7). In this case, we hypothesized that MDA increases surface retention of naphthalene, thereby decreasing its absorption, but BHT functions more like a penetration enhancer within skin.

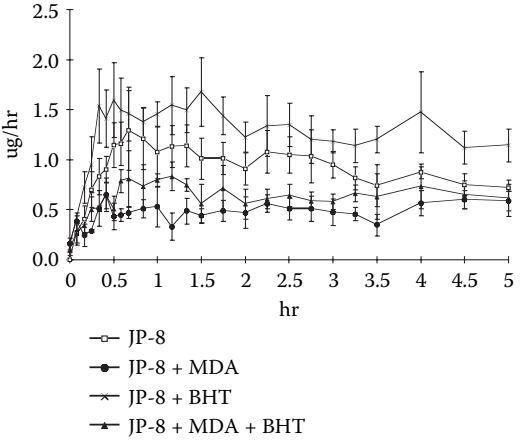

Figure 14.7 Dermal absorption of naphthalene through perfused porcine skin from JP-8 jet fuel administered with additives BHT and MDA alone and in combination.

When both are present, flux returns to base levels (Muhammad et al., 2004). We have previously seen similar effects with other combinations of additives on absorption of jet fuel hydrocarbons (Baynes et al., 2001; Riviere et al., 1999).

It may be a mistake to assume that these opposite effects simply cancel one another out and that the flux of chemical is now equivalent to application of it alone. The mechanisms behind the similarity in fluxes are different. Fick's first law of diffusion can be used to illustrate this. In the base situation ∅, compound flux would equal

$$\text{Flux}_{\varnothing} = (K_p)(\Delta C)$$

where K_p is the permeability coefficient and ΔC is the concentration gradient driving the absorption process. We consider ΔC the effective dermal dose because increasing concentration on the surface of skin effectively increases ΔC. In the presence of additives, we had two scenarios in which additive A decreased absorption by retaining chemical on the surface, effectively reducing ΔC:

$$\downarrow \text{Flux}_{A} = (K_p)(\downarrow \Delta C)$$

and scenario B, in which flux increased because of increased K_p:

$$\uparrow \text{Flux}_{B} = (\uparrow K_p)(\Delta C)$$

When both A and B are present, the flux is now back to base levels but is governed by a fundamentally different set of diffusion parameters:

$$\text{Flux}_{A+B} \cong \text{Flux}_{\varnothing} = (\uparrow K_p)(\downarrow \Delta C)$$

One can appreciate how different factors that would interact with these altered parameters could change dermal disposition patterns within skin compared to the baseline scenario.

CONCLUSION

This chapter reviewed the potential effects that topical exposure to a chemical mixture might produce compared to exposure to a single neat chemical. In fact, most single-chemical exposures are not to neat compound but are rather to a chemical in a defined vehicle such as water, ethanol, or acetone in many toxicological studies. It is clear that there are significant vehicle effects that may overshadow differences between absorption of chemicals with different properties (see Figure 14.2). Such vehicle effects have been previously noted. However, what is just as significant is the phenomenon that chemical interactions may also be vehicle specific depending on the physiochemical properties of both the penetrating chemical as well as the vehicle/mixture in which it is dosed. The ability to dramatically improve the prediction of permeability for 12 diverse chemicals across multiple mixtures when the physical chemical properties of the solvent/mixture are also taken into account presents an approach that may have future utility once fully validated. Even if the flux is similar across mixtures, it is possible that opposing mixture interactions are at work that would alter the toxicological interpretation of this flux compared to control values for which no mixture additives are present.

ACKNOWLEDGMENTS

I would like to acknowledge all of the staff and students in the NCSU/CCTRP for their continued efforts as well as NIOSH grants R01-OH-07555 and AFOSR grant F49620-01-1-0080 for supporting this mixture research.

REFERENCES

Abou-Donia, M.B., Wilmarth, K.R., Jensen, K.F., Oehme, K.W., and Kurt, T.L., Neurotoxicity resulting from coexposure to pyridostigmine bromide, DEET and permethrin, *J. Toxicol. Environ. Health,* 48, 35–56, 1996.

Abraham, M.H. and Martins, F., Human skin permeation and partition: general linear free-energy relationship analyses, *J. Pharm. Sci.,* 93, 1508–1523, 2004.

Allen, D.G., Riviere, J.E., and Monteiro-Riviere, N.A., Induction of early biomarkers of inflammation produced by keratinocytes exposed to jet fuels Jet-A, JP-8, and JP-8(100), *J. Biochem. Molecular Toxicol.,* 14, 231–237, 2000.

Barry, B.W., Novel mechanisms and devices to enable successful transdermal drug delivery, *Eur. J. Pharm. Sci,.* 14, 101–114, 2001.

Bar-Yum, Y., *Dynamic of Complex Systems,* Reading, MA: Addison-Wesley, 1997.

Baynes, R.E., Brooks, J.D., Barlow, B.M., and Riviere, J.E., Physiochemical determinants of linear alkylbenzene sulfonate (LAS) disposition in skin exposed to aqueous cutting fluid mixtures, *Toxicol. Indus. Health,* 18, 237–248, 2002.

Baynes, R.E., Brooks, J.D., Budsaba, K., Smith, C.E., and Riviere, J.E., Mixture effects of JP-8 additives on the dermal disposition of jet fuel components, *Toxicol. Appl. Pharmacol.*, 175, 269–281, 2001.

Baynes, R.E., Brooks, J.D., Mumtaz, M., and Riviere, J.E., Effects of chemical interactions in pentachlorophenol mixtures on skin and membrane transport, *Toxicol. Sci.,* 69, 295–305, 2002.

Baynes, R.E., Monteiro-Riviere, N.A., and Riviere, J.E., Pyridostigmine bromide modulates the dermal disposition of [^{14}C] permethrin, *Toxicol. Appl. Pharmacol.,* 181, 164–173, 2002.

Bliss, C.I., The toxicity of poisons applied jointly, *Ann. Appl. Biol.,* 26, 585–615, 1939.

Bogert, C.J., Price, B., Wells, C.S., and Simon, G.S., Evaluating chemical interaction studies for mixture risk assessment, *Hum. Ecol. Risk Assess.,* 7, 259–306, 2001.

Bronaugh, R.L., Stewart, R.F., and Strom, J.E., Extent of cutaneous metabolism during percutaneous absorption of xenobiotics, *Toxicol. Appl. Pharmacol.,* 99, 534–543, 1989.

Budsaba, K., Smith, C.E., and Riviere, J.E., Compass plots: a combination of star plot and analysis of means (ANOM) to visualize significant interactions in complex toxicology studies, *Toxicol. Methods,* 10, 313–332, 2000.

Commission on Risk Assessment and Risk Management, Risk Assessment and Risk Management in Regulatory Decision-Making, U.S. Congress, Washington, D.C., 1997.

Elias, P.M. and Feingold, K.R., Lipids and the epidermal water barrier: metabolism, regulation, and pathophysiology, *Semin. Dermatol.,* 11, 176–182, 1992.

Environmental Protection Agency, Guidelines for the health risk assessment of chemical mixtures, *Federal Register* 51, 34014–34025, September 1986.

Environmental Protection Agency, *Technical Support Document on Risk Assessment of Chemical Mixtures*, EPA/600/8-90/064, November 1988, Washington, D.C.

Environmental Protection Agency, *Dermal Exposure Assessment: Principles and Applications*, EPA/600/8-91/011B, March 1995, Washington, D.C.

Environmental Protection Agency, *Options for Revising CEB's Method for Screen-Level Estimates of Dermal Exposure*, Chemical Engineering Branch, June 2003, Washington, D.C.

Geinoz, S., Guy, R.H., Testa, B., and Carrupt, P.A., Quantitative structure–permeation relationships (QSPeRs) to predict skin permeation: a critical evaluation, *Pharm. Res.,* 21, 83–92, 2004.

Groten, J.P., Feron, V.J., and Suhnel, J., Toxicology of simple and complex mixtures, *TRENDS Pharmacol. Sci.,* 22, 316–322, 2001.

Haddad, S., Beliveau, M., Tardif, R., and Krishnan, K., A PBPK modeling-based approach to account for interactions in the health risk assessment of chemical mixtures, *Toxicol. Sci.,* 63, 125–131, 2001.

Haddad, S., Charest-Tardif, G., Tardif, R., and Krishnan, K., Validation of a physiological modeling framework for simulating the toxicokinetics of chemicals in mixtures, *Toxicol. Appl. Pharmacol.,* 167, 199–209, 2000.

Hostynek, J.J. and Magee, P.S., Modeling *in vivo* human skin absorption, *Quant. Struct. Activ. Relat.,* 16, 473–479, 1997.

Idson, B., Vehicle effects in percutaneous absorption, *Drug Metab. Rev.,* 14, 207–222, 1983.

Luger, T.A. and Schwarz, T., Evidence for an epidermal cytokine network, *J. Invest. Dermatol.,* 95, 104–110S, 1990.

McDougal, J.N. and Robinson, P.J., Assessment of dermal absorption and penetration of components of a fuel mixture (JP-8), *Science Total Environ.,* 288, 23–30, 2002.

Monteiro-Riviere, N.A., Baynes, R.E., and Riviere, J.E., Pyridostigmine bromide modulates topical irritant-induced cytokine release from human epidermal keratinocytes and isolated perfused porcine skin, *Toxicology,* 183, 15–28, 2003.

Monteiro-Riviere, N.A., Inman, A.O., Mak, V., Wertz, P., and Riviere, J.E., Effects of selective lipid extraction from different body regions on epidermal barrier function, *Pharm. Res.,* 18, 992–998, 2001a.

Morgan, E.T., Regulation of cytochrome P450 by inflammatory mediators: why and how? *Drug Metab. Dispos.,* 29, 207–212, 2001.

Moser, K., Kriwet, K., Kalia, Y.N., and Guy, R.H., Enhanced skin permeation of a lipophilic drug using supersaturated formulations, *J. Controlled Release,* 73, 245–253, 2001.

Muhamad, F., Brooks, J.D., and Riviere, J.E., Comparative mixture effects of JP-8(100) additives on the dermal absorption and disposition of jet fuel hydrocarbons in different membrane systems, *Toxicol. Lett.,* 150, 351–365, 2004.

Mukhtar, H., *Pharmacology of the Skin,* Boca Raton, FL: CRC Press, 1992.

Poet, T.S., and McDougal, J.N., Skin absorption and human risk assessment, *Chem. Biol. Interact.,* 140, 19–34, 2002.

Pohl, H.R., Hansen, H., and Chou, C.H.S.J., Public health guidance values for chemical mixtures: current practice and future directions, *Reg. Toxicol. Pharmacol.,* 26, 322–329, 1997.

Potts, R.O. and Guy, R.H., Predicting skin permeability, *Pharm. Res.,* 9, 663–669, 1992.

Qiao, G.L., Brooks, J.D., Baynes, R.E., Monteiro-Riviere, N.A., Williams, P.L., and Riviere, J.E., The use of mechanistically defined chemical mixtures (MDCM) to assess component effects on the percutaneous absorption and cutaneous disposition of topically-exposed chemicals. I. Studies with parathion mixtures in isolated perfused porcine skin, *Toxicol. Appl. Pharmacol.,* 141, 473–486, 1996.

Rastogi, S.K. and Singh, J., Lipid extraction and transport of hydrophilic solutes through porcine epidermis, *Int. J. Pharm.,* 225, 75–82, 2001.

Riviere, J.E., Baynes, R.E., Brooks, J.D., Yeatts, J.L., and Monteiro-Riviere, N.A., Percutaneous absorption of topical diethyl-*m*-toluamide (DEET): effects of exposure variables and coadministered toxicants, *J. Toxicol. Environ. Health A,* 66, 133–151, 2003.

Riviere, J.E. and Brooks, J.D., Predicting skin permeability from complex chemical mixtures, *Toxicol. Appl. Pharmacol.*, in press, 2005.

Riviere, J.E., Monteiro-Riviere, N.A., and Baynes, R.E., Gulf War illness-related exposure factors influencing topical absorption of ^{14}C-permethrin, *Toxicol. Lett.,* 135, 61–71, 2002.

Riviere, J.E., Monteiro-Riviere, N.A., Brooks, J.D., Budsaba, K., and Smith, C.E., Dermal absorption and distribution of topically dosed jet fuels Jet A, JP-8, and JP-8(100), *Toxicol. Appl. Pharmacol.,* 160, 60–75, 1999.

Riviere, J.E., Qiao, G., Baynes, R.E., Brooks, J.D., and Mumtaz, M., Mixture component effects on the *in vitro* dermal absorption of pentachlorophenol, *Arch. Toxicol.,* 75, 329–334, 2001b.

Riviere, J.E. and Williams, P.L., Pharmacokinetic implications of changing blood flow to the skin, *J. Pharm. Sci.,* 81, 601–602, 1992.

Robinson, P.J., Prediction: simple risk models and overview of dermal risk assessment, in *Dermal Absorption and Toxicity Assessment* (M.S. Roberts and K.A. Walters, eds.), New York: Dekker, pp. 203–229, 1998.

Rosado, C., Cross, S.E., Pugh, W.J., Roberts, M.S., and Hadgraft, J., Effect of vehicle pretreatment on the flux, retention, and diffusion of topically applied penetrants *in vitro*, *Pharm. Res.,* 20, 1502–1507, 2003.

Van der Merwe, D. and Riviere, J.E., Comparative studies on the effect of water, ethanol and water/ethanol mixtures on chemical partitioning into porcine stratum corneum and silastic membrane, *Toxicol.* In Vitro*,* 19, 69–77, 2005b.

Van der Merwe, D. and Riviere, J.E., Effect of vehicles and surfactants on xenobiotic permeability and stratum corneum partitioning in porcine skin, *Toxicology,* 206, 325–335, 2005b.

Williams, A.C. and Barry, B.W., Chemical penetration enhancement, in *Dermal Absorption and Toxicity Assessment*. (M.S. Roberts and K.A. Walters, eds.), New York: Dekker, pp. 297–312, 1998.

Williams, P.L. and Riviere, J.E., Model describing transdermal iontophoretic delivery of lidocaine incorporating consideration of cutaneous microvascular state, *J. Pharm. Sci.,* 82, 1080–1084, 1993.

Yang, R.S.H. (ed.), *Toxicology of Chemical Mixtures*, San Diego, CA: Academic Press, 1994.

CHAPTER 15

Animal Models: A Comparison of Permeability Coefficients for Excised Skin from Humans and Animals

Brent E. Vecchia and Annette L. Bunge

CONTENTS

INTRODUCTION

Because of its availability, excised animal skin has been used extensively to model percutaneous absorption of drugs and other chemicals in humans. Percutaneous absorption of toxic compounds can be measured satisfactorily with excised skin (*in vitro*), but adequate supplies of human skin are not always available. When

available, sometimes samples have been stored for lengthy periods, which can alter their barrier function. Except for a few animals (such as primates), it is usually possible to obtain animal skin that is excised shortly before use. Although we consider only *in vitro* results here, it is worth mentioning that *in vivo* experiments are usually restricted to animals. The toxicity of many compounds limits their testing in humans *in vivo* as does the cost and time required for approvals and experiments.

The relevance of permeability coefficient measurements made using animal skins to dermal absorption in humans can be examined by histological or empirical comparisons. An animal's skin is considered to be more relevant when certain physiological features (such as skin morphology, thickness, and capillary perfusion) and chemical factors (such as lipid composition, enzymes, and water content) are similar to human skin. For example, the skin of rodents lacks sweat glands and abounds in hair and hair follicles (not true in the hairless and nude strains); human skin does not, making rodents potentially less relevant than animal species possessing sweat glands and less hair. Usually, the higher terrestrial mammals (for example, the rhesus monkey) have skin that is physiologically and chemically more similar to human skin than nonmammals (for example, the black rat snake). However, some researchers have found that snake skin, although chemically and structurally quite different from terrestrial mammalian skin (Rigg and Barry, 1990), reproduces closely permeability coefficients measured in human skin (Itoh, Magavi, et al., 1990; Itoh, Xia, et al., 1990; Takahashi et al., 1993). This demonstrates that assessing the relevancy of an animal skin purely from the histological approach might be misleading.

Alternatively, an animal skin can be judged as more relevant when permeability coefficients measured in animal skins compare meaningfully with those measured in human skin. By this standard, the skin of a relevant substitute animal must behave at least qualitatively, if not quantitatively, like human skin (Durrheim et al., 1980). In practice, both measures of relevance should be used in combination to infer human absorption with animal skin measurements. The empirical method is most useful for establishing quantitative relationships for permeability coefficients from animal and human skins; while histological comparisons are useful for anticipating potential departures from these relationships.

The relationships between animal and human permeability coefficients have been studied from the histological (Bronaugh et al., 1982) and empirical (Bronaugh et al., 1982; Marzulli et al., 1969; Wester and Noonan, 1980) perspectives. Most investigations reported that the skins of animals are different, usually more permeable, than human skin. In Appendix C , we review nine prior investigations or reviews of the relationship of permeability coefficients for animal and human skins. With one exception (Sato et al., 1989), none of these studies recommended a quantitative approach for adjusting permeability coefficients from animal skins to represent human skin.

Several investigations present relative rankings of permeability coefficients observed for several different animal species (for example, Marzulli et al., 1969; Wester and Noonan, 1980). Although these rankings agree that skin from most of the animal species studied are more permeable than human skin, the relative order of the various species and the quantitative results are often inconsistent. Many rankings are derived from permeability coefficients measured *in vivo*, from different

vehicles, at different temperatures, with compounds at different extents of ionization, using skin from different locations. That is, there are a number of reasons for differences in these permeability coefficients that are external to the fact that they were measured in different species. Significantly, these investigations are based on permeability coefficients for only a few chemicals. As shown by Vecchia and Bunge (Vecchia and Bunge, 2002b), permeability coefficients measured in human skin by different laboratories for the same chemical can differ by an order of magnitude or more. Thus, the experimental uncertainties in the measurements themselves are so large that conclusions drawn from only a few chemicals may be meaningless.

The nine studies reviewed in Appendix C (and like them others) have examined only a small fraction of the permeability coefficient data available for animal skins. By utilizing many more of the available measurements and by restricting comparisons of skins from different species to data from a standardized experiment and analysis, it should be possible to improve our understanding of the relationships between measurements in human skin with those from animals. The study described here was a limited investigation designed to demonstrate this strategy.

We have previously presented a large set of *fully validated* permeability coefficient data, all measured in human skin using a single type of experiment and meeting certain quality criteria (Vecchia and Bunge, 2002b). Specifically, all data designated as fully validated were *in vitro* measurements on human skin from aqueous solutions for which (1) the temperature was specified and between 20 and 40°C, (2) the penetrating chemical was at least 10% unionized with a known validated or calculable octanol–water partition coefficient K_{ow}, and (3) the calculated permeability coefficients probably represent the steady-state value. Here, we describe several new databases of measurements from animals that meet these same criteria. The goal is to use these databases of permeability coefficients for human and animal skins from comparable experiments to identify the similarities and differences in the penetration of chemicals in human, mammalian, and other (primarily shed snake) skins. We also examine two strategies for developing methods to quantitatively extrapolate measurements from one species to another.

THEORY

The steady-state permeability across the stratum corneum (SC) from an aqueous vehicle P_{cw} into an infinite sink depends on the diffusivity of the chemical in the SC (D_c), the SC thickness (L_c), and the equilibrium partition coefficient between the SC and the water vehicle K_{cw}:

$$P_{cw} = \frac{K_{cw} D_c}{L_c} \tag{15.1}$$

where K_{cw} is defined as the concentration of chemical in the SC (mass/volume of SC at absorbing conditions) divided by the equilibrium concentration in the vehicle (mass/volume) (Parry et al., 1990). As defined here, D_c is an effective diffusivity

based on the SC thickness rather than the true diffusivity based on the actual molecular diffusion path length, which is not known.

Equation 15.1 is the basis for several common semitheoretical models of SC permeability coefficients (Potts and Guy, 1992). In many of these, the SC–water partition coefficient is assumed to be related to K_{ow} through a power function:

$$K_{cw} = K_{ow}^{d} \tag{15.2}$$

where the exponent d accounts for differences in lipophilic character of the SC lipids (Potts and Guy, 1992). However, for many organic solvents, the relationship is offset by a constant, and an equation of the form

$$K_{cw} = a\ K_{ow}{}^{f} \tag{15.3}$$

or

$$\log K_{cw} = \log(a) + f\ \log K_{ow} \tag{15.4}$$

is more appropriate (Lyman et al., 1982). The diffusion of small molecules in membranes such as skin is generally considered to be an activated process that varies exponentially with the size of the penetrant:

$$D_c = D_o \exp\left(-\hat{\beta}\ MV\right) \tag{15.5}$$

where D_o is the diffusion coefficient of a hypothetical molecule having zero molecular volume (MV), and $\hat{\beta}$ is a constant. Because it is more readily available, the molecular weight (MW) is often used instead of the MV in the following modification of Equation 15.5:

$$D_c = D_o \exp\left(-\tilde{\beta}\ MW\right) \tag{15.6}$$

where $\tilde{\beta}$ is a constant but with a different value from $\hat{\beta}$. Substituting Equation 15.3 and Equation 15.6 into Equation 15.1, followed by logarithmic transformation and rearrangement, yields

$$\log P_{cw} = \left[\log\left(a\right) + \log\left(D_o\ /\ L_c\right)\right] + f\ \log K_{ow} + \beta\ MW \tag{15.7}$$

where $\beta = \tilde{\beta}\ \log\ (e) = 0.434\ \tilde{\beta}$. Thus, linear regressions of logarithmically transformed skin permeability measurements with Equation 15.7 will provide values for [log (a) + log (D_o/L_c)], f, and β, which have attributable physicochemical meaning. Relationships between permeability coefficients measured in human and animal

skins can be deduced by comparing regressions of Equation 15.7 from human and the different animal skins.

Occasionally, permeability coefficients have been measured in the skin of different species for the same compound. In this case, the ratio of the animal and human skin permeability coefficients can be modeled with an equation of the form

$$\log\left(\frac{P_{cw,animal}}{P_{cw,human}}\right) = \Delta\left[\log(a) + \log\left(D_o / L_c\right)\right] + \Delta f \quad \log K_{ow} + \Delta\beta \quad MW \qquad (15.8)$$

where Δy represents $y_{animal} - y_{human}$ for y equal to [log (a) + log (D_o/L_c)], f, or β. Linear regression of logarithmically transformed skin permeability coefficient ratios with Equation 15.8 will provide values for Δ[log (a) + log (D_o/L_c)], Δf, and $\Delta\beta$, which have attributable physicochemical meaning allowing for relationships with human permeability coefficients to be developed.

Permeability coefficients may be affected by chemical properties other than log K_{ow} and *MW*. For example, steric interactions, limitations of *MW* as a representation of molecular size, and unidentified factors that cause some compounds to act as penetration enhancers may affect permeability coefficients but would not be conveyed entirely by log K_{ow} and *MW*. Equation 15.7 will not account for these additional influences on permeability coefficients. However, the error in Equation 15.8 may be reduced compared with Equation 15.7, because Equation 15.8 is based on the animal-to-human ratio of permeability values. Equation 15.7 implicitly assumes that permeability coefficients are affected by log K_{ow} and *MW* only, which is a more restrictive assumption than the assumption built into Equation 15.8 that all unexplored factors have quantitatively the same effect in all species. That is, with the same amount of data, analysis with Equation 15.8 is preferable to analysis with Equation 15.7 as long as these additional factors influence permeability coefficients the same way in both human and animal skins.

DATABASE COLLECTION AND VALIDATION

All permeability coefficients presented in this chapter were measured *in vitro* through animal skin from aqueous vehicles. Prior to developing regression equations, a critical review process was used to remove data that were unable to meet a set of quality criteria. Permeability coefficients reported without pertinent details are reserved for future analysis, allowing time for contact with the authors, but are excluded for purposes of data regressions described in the conclusion. Two collectively exhaustive (taken together, they contain all permeability measurements we have considered) and mutually exclusive (measurements appearing in one database do not appear in others) databases are presented: (1) the fully validated database (containing the measurements used to develop structure–activity regression equations) and (2) an excluded database (containing data that did not meet the validation criteria). Details about how the permeability coefficients were extracted from the original references are described in Appendix B.

The fully validated database contains only measurements that satisfy the following five criteria:

1. The temperature must be in the range of 20 to 40°C.
2. More than 10% of the penetrating compound must be in an unionized form.
3. A valid log K_{ow} must be available for the penetrating compound (obtained from the Star list of Hansch and colleagues, 1995, or else calculated consistently with this database using Daylight software [PC Models, 1995]).
4. The measurement must have been determined with data that reasonably approximate steady state.
5. The donor and receptor fluids do not compromise (more than water does) the barrier of the skin.

Permeability coefficients were adjusted for ionization using the procedure described by Vecchia and Bunge (2002b). We assume that penetration is attributed to the unionized species alone and divide the observed permeability coefficients ($P_{cw,obs}$, based on the total concentration) by the fraction unionized f_{ui}. That is, $P_{cw} = P_{cw,obs}/f_{ui}$ where f_{ui} is calculated from the pH and the acid dissociation constant pK_a as given by

$$f_{ui} = \frac{1}{\left(1 + 10^{g}\right)} \tag{15.9}$$

where the exponent g = (pH – pK_a) for acids and (pK_a – pH) for bases. SPARC (SPARC Performs Automated Reasoning in Chemistry; SPARC, 1995) was used to calculate pK_a values at 25°C. We adjusted all pK_a values to the experimental temperature using an integrated form of the van't Hoff equation (Smith and Van Ness, 1987) with enthalpies of ionization (defined for the direction of the pK_a) from (Sober, 1968) 0.0 for carboxylic acids, 5.0 for phenolic compounds, 10 for amines (primary, secondary, or tertiary), 7.5 for aniline (or amines attached directly to an aromatic ring system), 5 for aromatic nitrogen (pyridine derivatives and isoquinoline). Multiple pK_a values for the same molecule were adjusted independently for effects of temperature. When more than one pK_a was important, the fraction unionized was determined by writing dissociation reactions for all relevant species.

When buffer solutions were not used and the pH was not reported, we calculated the pH using the solution concentration and pK_a values for all dissociation reactions and assuming that the pH was 7.0 prior to solute addition. A general treatment of simultaneous equilibrium involving equations for all linearly independent reactions, the water dissociation reaction ($K_a = 1.0 \times 10^{-14}$), a molecular balance on the active species, and an equation requiring solution electroneutrality is required to calculate the natural pH (Brescia et al., 1975). A more detailed discussion of the adjustment for ionization and associated calculations is presented in Vecchia and Bunge (2002b).

Except for temperature adjustments in pK_a for estimating f_{ui}, no other adjustments were made for temperature. In a previous analysis of permeability coefficient data from human skin, we observed that temperature affected the data by a factor between 2 and 5 for temperatures varying between 25 and 40°C (Vecchia and Bunge, 2002b).

Despite this, predictions by regression equations that included temperature were minimally better than equations that did not include temperature (Vecchia and Bunge, 2002b). This was probably because the majority of measurements were made at 30 to 35°C and contributions from other sources of variability were not insignificant. For the databases provided here of permeability coefficients in animal skins, the number of measurements are too few and the temperature variation too limited for reliable evaluation of the effect of temperature.

RESULTS AND DISCUSSION

Inspection of the Data

The reported observed permeability coefficients $P_{cw,obs}$ and the ionization-adjusted coefficients P_{cw}, log K_{ow}, MW and other experimental details (temperature, pH, skin type, and animal strain) are tabulated in Appendix A. Tables A1 through A4 list data from hairless mouse, hairless rat, rat, and shed snake skin, respectively. Table A5 contains permeability coefficient values measured in the skins from various animals, for which the number of measurements collected for each species was small (that is, a dog, guinea pig, marmoset, mouse, nude mouse, nude rat, pig, or rabbit). Excluded measurements are labeled with an E in the left-hand margin, identifying them as failing one or more of the validation criteria. Excluded measurements are not included in the development of regression equations described in the next subsection. Several excluded measurements have the potential for validation provided that additional relevant information can be obtained from the original investigators. Table A6 contains SC–water partition coefficients measured in animal skins. Although useful, the data listed in Table A6 were not one of the main objectives of this study, and this table is not discussed further.

Ionized species are identified by the different formal charges using (–) to represent each formal negative charge and (+) to represent each formal positive charge. For example, alanine is represented as (+–) to designate that it is a zwitterion with one formal positive charge and one formal negative charge. The identifications are consistent with pK_a values calculated by SPARC and may not be consistent with the reported formal charges on the chemical. Adjustment of the pK_a values for temperature, calculation of the naturally attained pH (when a pH was not specified), and calculation of the fraction of the compound that was unionized are summarized in Table A7.

Figure 15.1 through Figure 15.6 show skin permeability coefficient measurements from hairless mouse, hairless rat, rat, shed snake, and the lesser-studied animals (guinea pig, marmoset, rabbit, pig, dog, mouse, nude rat) plotted as a function of log K_{ow}. In Figure 15.1 to Figure 15.4 and Figure 15.6, compounds that were more than 90% ionized are identified by the form of the dominant ionic species (that is, cation, anion, or zwitterion) and labeled as excluded. Ionized species with undetermined log K_{ow} are plotted to the left of the dashed vertical line located at log K_{ow} = –6.0. Cations are plotted at log K_{ow} = –6.5, anions at log K_{ow} = –7.0, and zwitterions at log K_{ow} = –7.5. A few permeability coefficient measurements that are

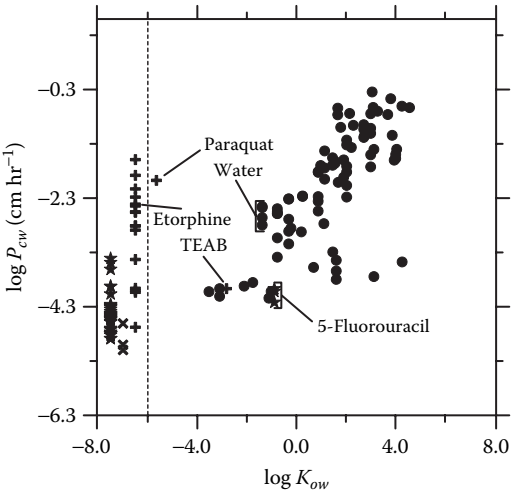

Figure 15.1 Permeability coefficients from hairless mouse plotted as a function of log K_{ow}: •, fully validated; +, excluded cation; ×, excluded anion; ★, excluded zwitterion. Ionized species without an appropriate log K_{ow} are plotted to the left of the vertical dashed line: cations at log K_{ow} = –6.5, anions at log K_{ow} = –7.0, zwitterions at log K_{ow} = –7.5.

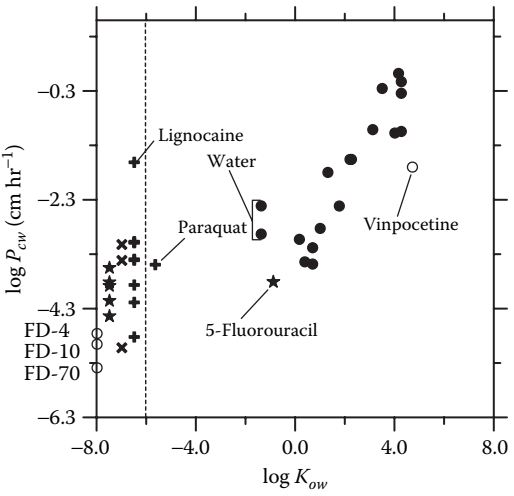

Figure 15.2 Permeability coefficients from hairless rat plotted as a function of log K_{ow}: ●, fully validated; ○, excluded nonionized; +, excluded cation; ×, excluded anion; ★, excluded zwitterion. Ionized species without an appropriate log K_{ow} are plotted to the left of the vertical dashed line: cations at log K_{ow} = –6.5, anions at log K_{ow} = –7.0, zwitterions at log K_{ow} = –7.5.

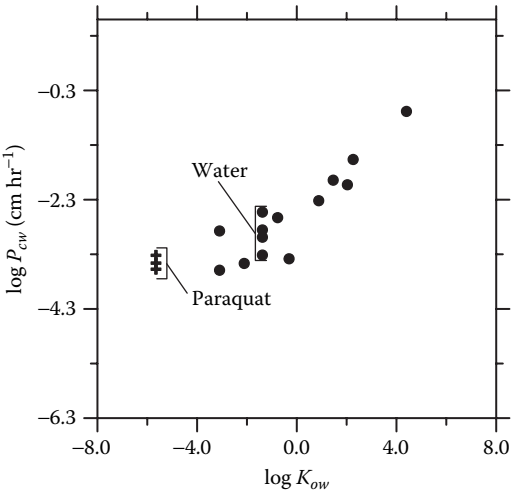

Figure 15.3 Permeability coefficients from rat plotted as a function of log K_{ow}: •, fully validated; +, excluded cation.

referenced in the text or excluded for reasons other than ionization are identified on these plots.

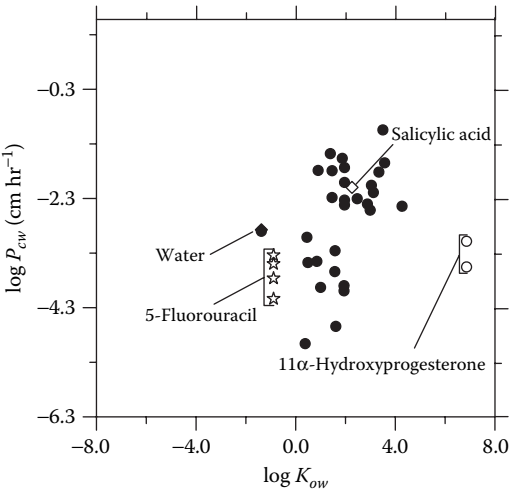

Figure 15.4 Permeability coefficients from shed snake skin plotted as a function of log K_{ow}: •, *Elaphe obsoleta*; ◇, *Python molurus* or *reticulatus*; ○, excluded *Elaphe obsoleta* for invalid K_{ow}; ★, excluded zwitterion *Elaphe obsoleta*; ☆, excluded zwitterion Python molurus.

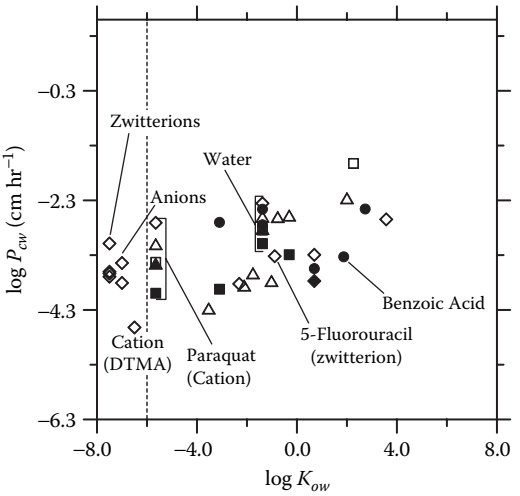

Figure 15.5 Permeability coefficients from various animal skins plotted as a function of log K_{ow} identified by animal species and including valid and excluded measurements: •, pig; ♦, dog; ◇, guinea pig; ■, marmoset; □, mouse; ▲, nude rat; △, rabbit. Ionized species without an appropriate log K_{ow} are plotted to the left of the vertical dashed line: cations at log K_{ow} = –6.5, anions at log K_{ow} = –7.0, zwitterions at log K_{ow} = –7.5.

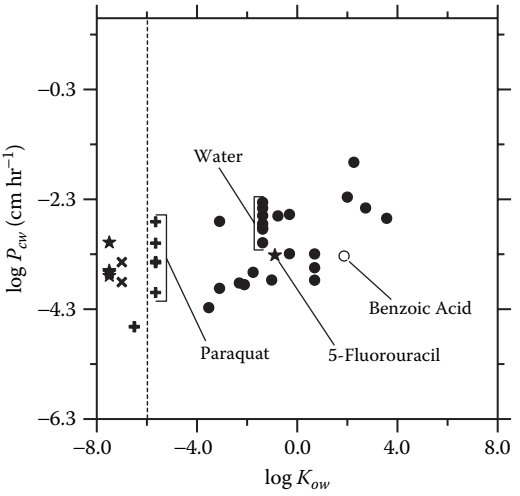

Figure 15.6 Permeability coefficients for various animal skins from Figure 15.5 plotted as a function of log K_{ow} with validated and excluded data points identified: •, fully validated; ○, excluded nonionized; +, excluded cation; ×, excluded anion; ★, excluded zwitterion. Ionized species without an appropriate log K_{ow} are plotted to the left of the vertical dashed line: cations at log K_{ow} = –6.5, anions at log K_{ow} = –7.0, zwitterions at log K_{ow} = –7.5.

Table A1 lists and Figure 15.1 shows 144 permeability coefficient values for 83 compounds (83 fully validated and 61 excluded data points; 45 fully validated compounds) measured in hairless mouse skin. All of the measurements excluded from this database were more than 90% ionized. Etorphine is distinguished on this figure because Vecchia and Bunge (2002b) used the fact that the human permeability coefficient is larger than the hairless mouse permeability coefficient to support exclusion of the measurement from the fully validated database for human skin. Notice that the hairless mouse permeability coefficient of etorphine is consistent with measurements for other cations, which was not the case with the human permeability coefficient for etorphine (Vecchia and Bunge, 2002b).

The permeability coefficients shown in Figure 15.1 span approximately four orders of magnitude. Notice that log P_{cw} varies almost linearly with log K_{ow}, and as we soon show in the next subsection, a portion of the variance can be explained by differences in *MW*. Even after adjustment for ionization, the permeability coefficients for anionic and zwitterionic species are generally lower than for the unionized species. Permeability coefficients for cationic species are highly variable. Based on pK_a values calculated in SPARC, all but 4 of the 40 permeability coefficients from the Ruland and Kreuter (1991) investigation of amino acids are shown as zwitterions (at pH 7.4, aspartic acid and glutamic acid are calculated to be anions and lysine and arginine are calculated to be cations). Ruland and Kreuter concluded that charged and net neutral species permeate skin at the same rates (i.e., penetration rates were not statistically significantly different). However, this conclusion may not be general because their claim was tested with only 4 charged species compared to 36 zwitterionic species.

Figure 15.1 is similar to a comparable figure for the human skin database (see Figure 2 in Vecchia and Bunge, 2002b), suggesting that the underlying mechanism of dermal absorption is similar for both species. Several specific comparisons with the human permeability coefficients are noteworthy:

1. There are fewer extremely low (i.e., log $P_{cw} < -4.0$) permeability coefficient values in hairless mouse skin than in human skin.
2. Both species have a similar linear dependence on log K_{ow}.
3. The largest permeability coefficient values are similar in both species ($-0.7 <$ log $P_{cw} < -0.9$).
4. The permeability coefficients of zwitterions are similar in magnitude in both species.
5. In both species, permeability coefficients for anions and zwitterions are lower than permeability coefficients for cations.
6. Cations have highly variable rates of penetration.
7. Hairless mouse skin is more permeable to water than human skin (i.e., 2.67×10^{-3} cm h^{-1} in hairless mouse compared to 1.18×10^{-3} cm h^{-1} in humans). Notably, there is only one measurement for paraquat in hairless mouse (1.07×10^{-2} cm h^{-1}), and it is more than 1000 times larger than the average value reported for human skin (8.70×10^{-6} cm h^{-1}). By comparison, the measurement for 5-fluorouracil is only about two times larger in hairless mouse (8.76×10^{-5} cm h^{-1}) compared to humans (4.02×10^{-5} cm h^{-1}).

Table A2 tabulates and Figure 15.2 shows 41 permeability coefficient values of 33 different compounds (18 fully validated and 23 excluded data points; 14 fully validated compounds) measured in hairless rat skin. The database contains permeability coefficients for structurally diverse compounds, predominantly pharmaceutically active compounds, with varied chemical properties. Vinpocetine was excluded because (1) the concentration was not reported, and as a result the fraction unionized could not be determined; and (2) K_{ow} could not be reliably calculated (vinpocetine has structural fragments that are not adequately represented in Daylight software; PCModels, 1995). Vinpocetine is plotted at the calculated value for log K_{ow}.

We also excluded permeability coefficient values for three macromolecular dextrans (fluorescein isothiocyanate-labeled dextrans) from Ogiso et al. (1994): FD-4 (average MW = 4400), FD-10 (average MW = 9,600), and FD-70 (average MW = 69,000). These macromolecules probably penetrate through a pathway (for example, appendageal structures such as hair follicles and sweat glands) that is not built into the solution-diffusion model of permeability for which Equation 15.1 was derived. Because K_{ow} values were not available for these compounds, they are plotted arbitrarily at log K_{ow} = −8.0. Permeability coefficients for these dextrans are lower but not significantly lower than those of highly ionized species. This may suggest that large molecules and highly polar molecules penetrate skin by the same pathway. Permeability coefficients for these three macromolecules decrease less with MW than the other, much smaller, chemicals in the database. This is consistent with penetration through a pathway with a large enough free volume that even these large molecules were not size segregated. The permeability coefficients of water (2.79×10^{-3} cm h^{-1}) and 5-fluorouracil (1.71×10^{-4} cm h^{-1}) measured in hairless rat are only slightly larger than those measured in human skin (1.18×10^{-3} cm h^{-1} and 4.02×10^{-5} cm h^{-1} for water and 5-fluorouracil, respectively). Similar to the hairless mouse, the permeability coefficient of paraquat measured in hairless rat (3.55×10^{-4} cm h^{-1}) is much larger than that measured in human skin (8.70×10^{-6} cm h^{-1}). However, the ratio of the paraquat permeability coefficient was about 40 for the hairless rat as compared with 1150 for the hairless mouse.

Table A3 tabulates and Figure 15.3 shows 17 permeability coefficient values for 11 compounds (14 fully validated and 3 excluded data points; 10 fully validated compounds) measured in rat skin. This database is small and consists mainly of phenols, alcohols, and water. Because all chemicals in this database are of relatively low MW and many are structurally related (meaning that MW and log K_{ow} are correlated), log P_{cw} is more clearly linear with log K_{ow} than in Figure 15.1 and Figure 15.2. Water permeability coefficients are similar to human skin (i.e., 1.47×10^{-3} cm h^{-1} in rats compared to 1.18×10^{-3} cm h^{-1} in humans). However, the permeability coefficient for paraquat in the rat is significantly higher than in humans (i.e., 3.07×10^{-4} cm h^{-1} in rats compared to 8.70×10^{-6} cm h^{-1} in humans, a ratio of about 35). Paraquat permeability was similar in the haired and hairless rat.

Table A4 lists and Figure 15.4 shows 37 permeability coefficient values for 28 compounds (31 fully validated and 6 excluded data points; 28 fully validated compounds) measured in shed snake skin. Although the database is small, it is diverse and consists of compounds, predominantly pharmaceutically active compounds, spanning a wide range of molecular structures and properties. These permeability

coefficient measurements were determined in three species of snake: *Elaphe obsoleta* (black rat snake), *Python molurus*, and *Python reticulatus*; *Elaphe obsoleta* was used most commonly. As shown, differences between permeability coefficients measured in the shed skin of different snake species appears to be minor. For example, the water permeability coefficients measured in *Elaphe obsoleta* and *Python molurus* skin are nearly identical. The permeability coefficients for 11α-hydroxyprogesterone have been excluded because the log K_{ow} calculated for this compound using the Daylight software (PCModels, 1995) was not valid. However, 11α-hydroxyprogesterone is plotted at the calculated log K_{ow} value of 6.86. It is possible that these permeability coefficients would not be significant outliers if a valid log K_{ow} were available. Permeability coefficients for water are close but slightly higher in snake than in human (i.e., 1.30×10^{-3} cm h^{-1} in snake compared to 1.18×10^{-3} cm h^{-1} in humans), and 5-fluorouracil is more permeable in snake than human (i.e., 2.50×10^{-4} cm h^{-1} in snake compared to 4.02×10^{-5} cm h^{-1} in humans). We did not have values for paraquat in snake.

Figure 15.5 and Figure 15.6 show 38 permeability coefficient values for 21 compounds (24 fully validated and 14 excluded data points; 13 fully validated compounds) measured in seven other animal species (guinea pig, marmoset, rabbit, pig, dog, mouse, or nude rat) from Table A5. Among the permeability coefficient measurements with pigskin, those made by Bhatti and colleagues (1988) were made on pig ear skin, and those made by Sato and colleagues (1989) were made with skin from the backs of immature pigs. The measurement for benzoic acid was determined at an unknown level of ionization and was therefore excluded. It is labeled in Table A5 with a P, indicating that this is a provisional exclusion that could be removed if the experimental pH could be learned from the authors.

There is not enough data on any individual species in Figure 15.5 and Figure 15.6 to develop empirical relationships with human permeability coefficients. However, relational analysis can be informative until more data are assembled. Among the compounds investigated in more than one species, some relationships in Figure 15.5 are notable:

1. Ethanol is less permeable in marmoset than in rabbit.
2. Mannitol is less permeable in marmoset than in pig.
3. For nicorandil, the order of increasing permeability is dog, pig, guinea pig.
4. For paraquat, the order of increasing permeability is marmoset, nude rat, mouse, rabbit, guinea pig.
5. For water, the order of increasing permeability coefficients is marmoset, mouse, nude rat, rabbit, guinea pig, with pig being somewhere between guinea pig and nude rat.

It is interesting, and perhaps not surprising, that the species ordering observed for water and paraquat is similar. However, drawing definitive conclusions from this database is clearly inappropriate because relationships may be strongly influenced by a single investigation (for example, most of the interspecies measurements of the same compounds were made by Walker et al. in 1983, and all marmoset permeability coefficients were measured by Scott et al. in 1991). More data are required before

reliable conclusions can be made regarding relative rates of penetration in these animals and humans.

Figure 15.1 to Figure 15.6 bear many similarities to comparable plots of human skin permeability coefficient data (Vecchia and Bunge, 2002b). It is not surprising that skin from different terrestrial species has similar characteristics of dermal penetration. Several mechanistic trends are consistently observed and also make good chemical sense:

1. The permeability coefficient of lipophilic compounds clearly increases linearly with increasing log K_{ow} of the penetrant.
2. Hydrophilic compounds and ions (at least anions and zwitterions) penetrate through the SC with rates that are lower and perhaps less dependent on log K_{ow} than rates of lipophilic compounds.
3. Permeability coefficients for water have remarkably similar magnitude in all of the species studied.
4. Anions and zwitterions appear to penetrate more slowly than cations.
5. The penetration of cations appears to be significantly more variable than the penetration of other ionized compounds (i.e., anions or zwitterions).

Regressions of the Validated Data to Structure–Activity Parameters

The valid permeability coefficient measurements for each species were examined in terms of log K_{ow} and MW as represented by Equation 15.7 and then compared with a similar regression equation developed for human skin (Vecchia and Bunge, 2002b). The results are listed in Table 15.1. In the case of multiple values for a single compound, each value was entered independently into the regression analysis.

Uncertainties in the regression coefficients are quantified by the standard error of the coefficients and are contained within parenthesis in the regression equations shown in Table 15.1. In addition to the squared correlation coefficient r^2, an adjusted squared correlation coefficient r^2_{adj} is provided to allow for more relevant comparisons between models with different numbers of fitted parameters (JMP User's Guide, SAS Institute, 1995). Specifically, $(1 - r^2)$ = Error sum of squares/Total sum of squares and $(1 - r^2_{adj}) = (1 - r^2)(n - 1)/(n - k)$ where n is the number of data points and k is the number of parameters. RMSE is the root-mean-square error of the model, which is zero when the model perfectly correlates the data. When presented alone, the F ratio is the model F ratio (the sum of squares for the model divided by the degrees of freedom for the model)/(the sum of squares for the error divided by the degrees of freedom for the error). When presented with a parameter (i.e., log K_{ow} or MW), the F ratio is the effect F ratio (the sum of squares for the effect divided by the degrees of freedom for the effect)/(the sum of squares for the error divided by the degrees of freedom for the error). The model F ratio = 1 when there is zero correlation with the parameters and is large for correlations with good predictive power. Because the number of fitted parameters is in the denominator of the F ratio, changes in the model F ratio with an increase in the number of parameters should reflect the effect on predictive power relative to the number of fitted parameters. Thus, a regression with a larger number of parameters might give a higher r^2 (or r^2_{adj}) but a lower F ratio than a regression with fewer parameters. This would indicate

Table 15.1 Comparison of Data Regressions on Log K_{ow} and MW Derived from Data Sets of the Various Animal Types

No.	Data Set[a]	n/m[b]	Log P_{cw} (cm h−1)[c,d]	r^2	r^2_{adj}	*RMSE*	F Ratio[e]	K_{ow} F Ratio[f]	*MW* *F* Ratio[f]	*MW* *p*[g]
T15.1-1	Human[h]	170/127	–2.44 (0.12) + 0.514 (0.04) log K_{ow} – 0.0050 (0.0005) *MW*	0.551	0.546	0.803	102.6	—	—	—
T15.1-2	HLMouse	84/45	–2.27 (0.13) + 0.47 (0.05) log K_{ow} – 0.0024 (0.0007) *MW*	0.580	0.570	0.681	55.9	110	13.3	0.0005
T15.1-3	HLRat	18/14	–2.07 (0.37) + 0.742 (0.108) log K_{ow} – 0.0050 (0.0021) *MW*	0.815	0.791	0.550	33.1	46.9	5.7	0.0304
T15.1-4	HLRat	18/14	–2.83 (0.21) + 0.545 (0.080) log K_{ow}	0.745	0.729	0.625	46.7	—	—	
T15.1-5	Rat	14/10	–2.70 (0.16) + 0.31(0.05) log K_{ow} – 0.002 (0.001) *MW**	0.846	0.818	0.350	30.1	41.3	2.6	0.134
T15.1-6	Rat	14/10	–2.49 (0.10) + 0.336 (0.047) log K_{ow}	0.809	0.793	0.373	50.8	—	—	
T15.1-7	Snake	31/28	–2.20 (0.20) + 0.76 (0.08) log K_{ow} – 0.0098 (0.001) *MW*	0.776	0.760	0.475	48.5	80.6	74.8	0.0000

[a] HLMouse, hairless mouse; HLRat, hairless rat.
[b] *n*, number of data points; *m,* number of different compounds.
[c] The uncertainties expressed within parentheses are reported as standard error in the coefficients (i.e., the standard deviation in the coefficient divided by the value of the coefficient).
[d] Coefficients indicated with an asterisk (*) are not meaningfully different from zero at the 95% confidence level. For all equations, the probability that the coefficient multiplying log K_{ow} is zero was < 0.0001.
[e] Model *F* ratio.
[f] Parameter *F* ratio.
[g] Probability that the coefficient multiplying the *MW* is zero.
[h] The equation for human skin and the data set from which it was derived are described in Vecchia and Bunge (2002b).

that the improvement in predictive power (as indicated by a larger r^2) was not as large per parameter as for the equation with fewer parameters.

The probability p that each of the regression coefficients was equal to zero was calculated. In all cases, the probability was less than 0.0001 that the coefficient multiplying log K_{ow} was zero. However, the coefficient multiplying *MW* was not always significantly different from zero. Based on a 95% confidence level, the *MW* coefficient for the hairless rat was only slightly significant ($p = 0.0304$); for the rat, it was not meaningfully different from zero ($p = 0.134$). The regression for both the hairless rat and rat were repeated for an equation that did not include the *MW,* and these results are listed in Table 15.1 also. In the hairless rat data set, the range of *MW* values was limited: Only two compounds (18 and 188) had $MW < 200$, and two compounds (339 and 346) had $MW > 300$. The rat database was small and consisted of chemicals for which log K_{ow} is correlated with *MW*. It would be presumptuous and probably incorrect to conclude that molecular size, represented by *MW* or another suitable descriptor, does not affect permeability in the hairless rat or rat. Comparing the equations listed in Table 15.1, we see that, for the data sets studied here, only shed snake skin depended more strongly on *MW* than does human skin.

Figure 15.7 shows the permeability coefficient regression equations for skin from human (Equation T15.1-1), hairless mouse (Equation T15.1-2), hairless rat (Equation T15.1-3), rat (Equation T15.1-6), and shed snake (Equation T15.1-7) plotted as a function of log K_{ow} for relatively small molecules ($MW = 100$) and larger molecules ($MW = 300$). The regression equations for human, hairless mouse, and shed snake skin are most relevant because these databases are the largest and most diverse. Permeability coefficients in all species increase linearly with log K_{ow}.

As illustrated in Figure 15.7, differences between species in the K_{ow} dependence of permeability coefficients can cause the relative order of penetration rates to change with K_{ow}. For example, for a chemical with $MW = 100$ and log $K_{ow} = 4$, the predicted order for the permeability coefficients is snake > hairless mouse > human; for a chemical with $MW = 100$ and log $K_{ow} = -2.0$, the predicted order is hairless mouse > human > snake. However, when $MW = 300$, the relative order among these three species is predicted to be independent of log K_{ow}. These plots show clearly that relative rankings of permeability coefficients in different species may depend on chemical properties of the penetrant.

Figure 15.8 shows the permeability coefficient regression equations plotted as a function of *MW* when log $K_{ow} = 2.0$. Similar to Figure 15.7, Figure 15.8 illustrates dramatically that the relative order of permeability coefficients between species could depend on chemical properties of the penetrating compound. Based on the regression equations derived here, a chemical with log $K_{ow} = 2.0$ and $MW = 75$ would penetrate slightly more rapidly through snake skin than through either hairless mouse or human skin, and a chemical with log $K_{ow} = 2.0$ and $MW = 300$ would penetrate much more rapidly through hairless mouse skin than through either human or snake skin.

Table 15.2 lists the logarithmically transformed ratio of the various animal data to human skin permeability coefficients [i.e., log ($P_{cw,Animal}/P_{cw,Human}$) derived by subtracting the regression of log P_{cw} developed from the human skin database from the regression equation for log $P_{cw,Animal}$]. The standard error listed in Table 15.2 for

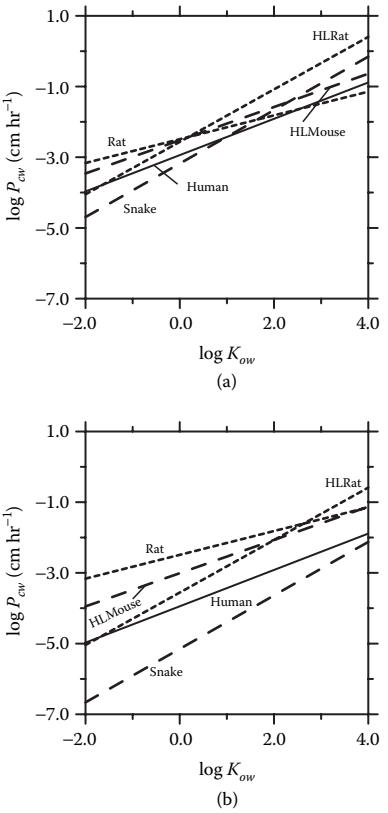

Figure 15.7 Permeability coefficient regressions for human, hairless mouse (HLMouse), hairless rat (HLRat), rat, and shed snake skin plotted as a function of log K_{ow} at (a) MW = 100 and (b) MW = 300: human (solid), satisfactory correlation (long dashes), limited correlation (short dashes).

a each coefficient in equation for log ($P_{cw,Animal}/P_{cw,Human}$) was calculated as the square root of the sum of the squared standard errors for the corresponding coefficients in the animal and human regression equations.

Comparing Compounds Common to the Animal and Human Databases

New databases were created consisting of chemicals for which fully validated measurements appeared in both the animal and human skin data sets. For compounds with multiple measurements, each measurement was independently adjusted for ionization (if necessary), and then all adjusted measurements for that compound were averaged. The ratio of the average animal and average human permeability coefficients was then calculated for each compound in the database of common chemicals. The logarithm of the ratios of the animal-to-human permeability coefficients were then linearly regressed as a function of MW and log K_{ow} using Equation 15.8. For all the databases studied here, the effects of both MW and log K_{ow} were

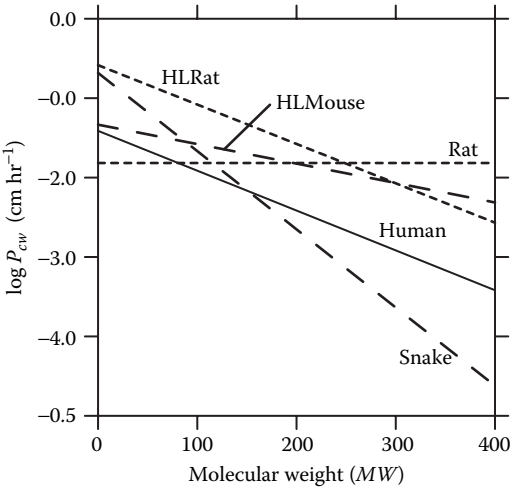

Figure 15.8 Permeability coefficient regressions for human, hairless mouse (HLMouse), hairless rat (HLRat), rat, and shed snake skin plotted as a function of *MW* at log K_{ow} = 2: human (solid), satisfactory correlation (long dashes), limited correlation (short dashes).

insignificant at the 95% confidence level, and mean values and confidence intervals of the permeability ratios were determined. These results are summarized in Table 15.3.

Figure 15.9 shows the ratio of permeability coefficients for 31 compounds common to the hairless mouse and human databases compared with the prediction plotted as a function of log K_{ow} and *MW*. Several of the labeled data are clear outliers (such as cortisone, hydrocortisone, indomethacin, and progesterone) for unknown reasons. However, in most cases these measurements were also outliers in either the human or hairless mouse databases (for example, the permeability coefficient for indomethacin [Morimoto et al., 1992] was an outlier in human skin). The solid line is the mean value of the permeability coefficient ratio. Equation T15.2-1 is designated by the dashed lines for *MW* of 100 and 300 in Figure 15.9a and for log K_{ow} of 2 and 4 in Figure 15.9b. Predictions based on the entire valid databases for hairless mouse and human skins (i.e., Equation T15.2-1) and the subset of measurements for compounds common to both databases are in relative agreement that the ratio of permeability coefficients in hairless mouse and human skin is essentially insensitive to K_{ow} of the penetrants. However, according to Equation T15.2-1, the hairless mouse-to-human ratio increases as *MW* increases. This effect is not evident in the data shown, although only a few chemicals with $MW > 300$ are common to the two databases. It may be that the dashed lines, which were developed from data with a larger range of *MW*, more accurately represent the effect of *MW*.

Figure 15.10 shows the ratio of permeability coefficients for the 14 compounds common to the snake and human databases compared with predictions plotted as a function of log K_{ow} and *MW*. The two steroids deoxycorticosterone (DC, called deoxycorticosterone in the animal investigation and cortexone in the human investigation)

Table 15.2 Estimated Permeability Coefficient Ratios Derived from Equations Listed in Table 15.1

No.	Data Set[a]	Basis Eq.[b]	Log ($P_{cw,Animal}/P_{cw,Humans}$)[c]	r^2	r^2_{adj}	RMSE	F Ratio
T15.2-1	HLMouse	T15.1-2	0.17 (0.18) – 0.044 (0.06) log K_{ow} + 0.0026 (0.0008) *MW*	0.551	0.546	0.803	102.6
T15.2-2	HLRat	T15.1-3	0.37 (0.39) + 0.23 (0.12) log K_{ow} – 0 (0.002) *MW*	0.580	0.570	0.681	55.9
T15.2-3	Rat	T15.1-6	–0.05 (0.16) – 0.18 (0.06) log K_{ow} + 0.0050 (0.0005) *MW*	0.815	0.791	0.550	33.1
T15.2-4	Snake	T15.1-7	0.24 (0.23) + 0.25 (0.09) log K_{ow} – 0.0048 (0.001) *MW*	0.745	0.729	0.625	46.7

[a] HLMouse, hairless mouse; HLRat, hairless rat.
[b] The presented equation was derived by subtracting Equation T15.1-1 from the equation number listed here.
[c] The uncertainties expressed within parentheses are reported as standard error in the coefficients calculated as the square root of the sum of the square standard errors for the coefficients in the animal and human equation. For example, the standard error listed for the coefficient multiplying log K_{ow} in Equation T15.2-1 was calculated from $\sqrt{0.04^2 + 0.05^2} = 0.06$.

Table 15.3 Mean Values and Confidence Intervals of the Animal-to-Human Permeability Coefficient Ratios for Compounds Common to the Animal and Human Data Sets

Data Set[a]	Number of Common Compounds	Number of Measurements		Log ($P_{cw,Animal}$ /$P_{cw,Humans}$)[b]	$P_{cw,Animal}$/$P_{cw,Humans}$
		Human	Animal		
HLMouse	31	64	67	0.491 (0.134)	3.10 (1.64/5.82)[c]
Snake	14	31	18	–0.371 (0.196)	0.426 (0.16/1.13)[c]
HLRat	12	28	15	0.365 (0.122)	2.32 (1.15/4.79)[d]
Rat	10	32	14	0.272 (0.436)	1.87 (0.89/3.24)[d]

[a] HLMouse, hairless mouse; HLRat, hairless rat.
[b] The uncertainty expressed within parentheses is the standard error (i.e., the standard deviation divided by the mean value of the logarithm of the permeability coefficient ratio).
[c] Mean value of the permeability coefficient ratio. Values in parentheses are the lower and upper values of the ratio at the 95% confidence interval.
[d] Mean value of the permeability coefficient ratio. Values in parentheses are the lower and upper values of the ratio at the 75% confidence interval.

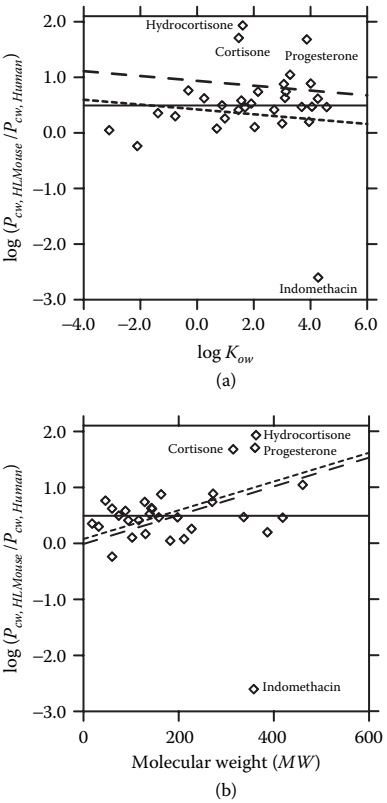

Figure 15.9 Ratios of average permeability coefficients for 31 compounds common to the validated hairless mouse and human databases compared to the average ratio of 3.1 (solid horizontal line) and to the difference between the regressions developed from the hairless mouse database and the fully validated human databases: (a) plotted as a function of log K_{ow} for MW = 100 (short dashes) and MW = 300 (long dashes); (b) plotted as a function of MW for log K_{ow} = 2 (short dashes) and log K_{ow} = 4 (long dashes).

and hydrocortisone (HC) are outliers. The solid line is the average value of the permeability coefficient ratios that are shown, which is consistent with the finding that both MW and log K_{ow} do not significantly influence the permeability coefficient ratio for compounds common to the human skin and shed snake skin databases. Equation T15.2-4, indicated by the dashed lines, is shown at a MW of 100 and 300 in Figure 15.10a and at log K_{ow} of 2 and 4 in Figure 15.10b. According to Equation T15.2-4, the permeability coefficient ratios should increase with increasing K_{ow}; this is not indicated by the measurements that are common to both databases.

With respect to the effect of MW, Equation T15.2-4 predicts a significant decrease in the permeability coefficient ratio as MW increases, a trend that is supported by the measurements common to both databases except DC and HC. However, the database of compounds common to both databases has a narrower range of MW than the individual databases for human skin and snakeskin, and this could conceal

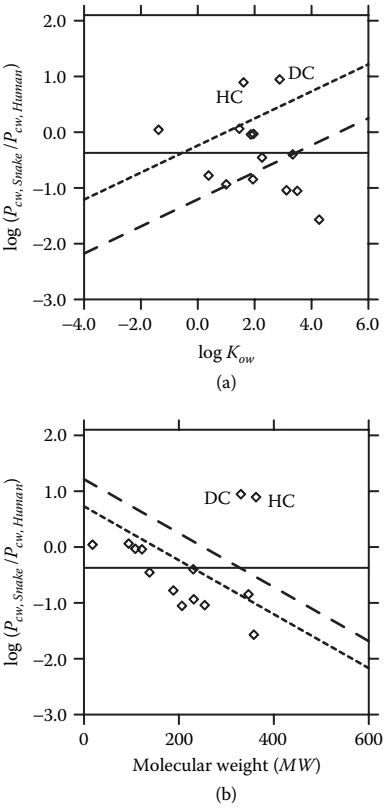

Figure 15.10 Ratios of average permeability coefficients for 14 compounds common to the validated snake and human databases compared to the average ratio of 0.4 (solid horizontal line) and to the difference between the correlations developed from the snake database and the fully validated human databases: (a) plotted as a function of log K_{ow} for MW = 100 (short dashes) and MW = 300 (long dashes); (b) plotted as a function of MW for log K_{ow} = 2 (short dashes) and log K_{ow} = 4 (long dashes).

trends within the uncertainty of the data. It is important to remember that the full databases contain measurements for many more compounds with a broader range of properties than in the data for compounds common to both databases. Thus, it could be that the dashed lines provide the more credible prediction of the effects of K_{ow} and MW. Certainly, meaningful conclusions about the relationship between snake and human skin measurements await an expansion of the snakeskin database.

The number of compounds that are common to the rat (hairless and with hair) databases and the fully validated human skin database are too small and the range of chemical properties too narrow for meaningful conclusions. However, as a starting place we have linearly regressed the permeability ratios of those two databases. The results from this extremely limited analysis, included in Table 15.3, are similar to those for the hairless mouse.

CONCLUSION

Dermal absorption in different animal species has many qualitative similarities to dermal absorption in humans that can be observed through examination of permeability coefficients. However, for the purpose of estimating dermal absorption in humans, the large numbers of permeability coefficient values determined in animal skins are of limited use until quantitative relationships to human skin are established. Based on the data collected so far, we have developed regression equations of permeability coefficients as functions of log K_{ow} and MW for several animal species (hairless mouse, hairless rat, rat, and snake). The regression equation from hairless mouse skin is similar to an equation of the same form for human skin. On average, hairless mouse skin is 3.1 times more permeable than human skin; this ratio appears to be independent of K_{ow} but may increase weakly for higher MW compounds.

Based on the analysis of the small data sets examined here, the permeability coefficient ratio may not be constant for other species of animals. In particular, there is some evidence that the ratio may depend on MW or K_{ow} for some species. For example, for the shed snake skin data examined here, the permeability coefficient in snake was affected more by MW and log K_{ow} than human skin; thus, the permeability coefficient ratio for snake and human skins appears to vary with MW and log K_{ow}. Based on our present data sets, the ratio of permeability coefficients for hairless rat and rat skin compared with human skin also may depend on log K_{ow} and MW. However, the data sets for these animal species are so small that this conclusion cannot be supported with confidence. Until more data are compiled to better define these relationships, we recommend using the average ratios of 2.3 for hairless rat skin and 1.9 for rat skin.

Historically, many researchers have ranked penetration rates measured in different animals and implied that the same relative rankings would apply for other penetrants. This assumption is clearly inappropriate when snakeskin is considered and may also be inappropriate when hairless rat or rat skin is considered. Data such as those presented here demonstrate that the general application of relative penetration rates in various animal species would be careless. The variability in measurements of permeability coefficients are sufficiently large for both animal and human skin that conclusions based on only a few measurements may be misleading. Hence, relationships of penetration rates in animal skins relative to human skins need to be determined from large numbers of measurements on many chemicals with varied properties. In this regard, the results presented here illustrate a strategy for quantitatively assessing relationships between skin permeability values in animal and human skins. Many more measurements in animal skins are available in the literature than were assembled here. The collection of these data presents an opportunity to improve substantially our ability to extrapolate reliably permeability coefficient measurements in various animal skins to the skin of other animals and humans.

ACKNOWLEDGMENTS

This work was supported in part by the National Institute of Environmental Health Sciences (ES06825), the U.S. Environmental Protection Agency (CR824053, R826684, R830131), and the U.S. Air Force Office of Scientific Research (F49620-95-1-021).

NOTATION

a	Parameter in Equation 15.3
d	Parameter in Equation 15.2
D_c	Effective diffusivity of the absorbing chemical in the SC
D_o	Diffusion constant of hypothetical chemical having zero *MV*
f	Parameter in Equation 15.3
f_{ui}	Fraction of the total chemical dose that is unionized in the vehicle
g	Parameter in Equation 15.9 = (pH − pK_a) for acids and (pK_a − pH) for bases
K_a	Acid dissociation constant for the absorbing chemical
K_{cw}	Equilibrium partition coefficient between the SC and water for the absorbing chemical
K_{ow}	Octanol–water partition coefficient of the penetrating chemical
L_c	Effective thickness of the SC
MV	Molecular volume of the absorbing chemical
MW	Molecular weight of the absorbing chemical
P_{cw}	Steady-state permeability of the SC from water
$P_{cw,i}$	Steady-state permeability of the SC from water for species *i*
pH	Negative logarithm of the hydrogen ion molarity = $-\log_{10}[H^+]$
pK_a	Negative logarithm of the acidity equilibrium constant = $-\log_{10}[K_a]$
SC	stratum corneum

GREEK

β	0.434 $\tilde{\beta}$
$\hat{\beta}$	Parameter in Equation 15.5 describing the effect of *MV* on D_c
$\tilde{\beta}$	Parameter in Equation 15.6 describing the effect of *MW* on D_c

REFERENCES

Ackermann, C. (1983). Percutaneous absorption of selected hydrophilic compounds—an *in vitro* study on hairless mouse skin, Ph.D. thesis, Potchefstroom University for Christian Higher Education, Potchefstroom, South Africa.

Ackermann, C. and Flynn, G.L. (1987). Ether–water partitioning and permeability through nude mouse skin *in vitro*. I. Urea, thiourea, glycerol and glucose, *International Journal of Pharmaceutics,* 36:61–66.

Ackermann, C., Flynn, G.L., and Smith, W.M. (1987). Ether–water partitioning and permeability through nude mouse skin in vitro. II. Hydrocortisone 21-n-alkyl esters, alkanols and hydrophilic compounds, *International Journal of Pharmaceutics,* 36:67–71.

Ackermann, C., Flynn, G.L., and Van Wyk, C.J. (1985). Percutaneous absorption of urea, *International Journal of Cosmetic Science,* 7:251–264.

Aguiar, A.J. and Weiner, M.A. (1969). Percutaneous absorption studies of chloramphenicol solutions, *Journal of Pharmaceutical Sciences,* 58:210–215.

Ahmed, S., Imai, T., and Otagiri, M. (1995). Stereoselective hydrolysis and penetration of propanolol prodrugs: *in vitro* evaluation using hairless mouse skin, *Journal of Pharmaceutical Sciences,* 84:877–883.

Andersen, K.E., Maibach, H.I., and Anjo, M.D. (1980). The guinea-pig: an animal model for human skin absorption of hydrocortisone, testosterone and benzoic acid? *British Journal of Dermatology,* 102:447–453.

Aspe, E., Guy, R.H., Lee, W.A., Kennedy, J.A., Visor, G.C., and Ennis, R.D. (1995). Optimization of *in vitro* flux through hairless mouse skin of cidofovir, a potent nucleotide analog, *Journal of Pharmaceutical Sciences,* 84:750–754.

Barber, E.D., Teetsel, N.M., Kolberg, K.F., and Guest, D. (1992). A comparative study of the rates of *in vitro* percutaneous absorption of eight chemicals using rat and human skin, *Fundamental and Applied Toxicology,* 19:493–497.

Bartek, M.J. and LaBudde, J.A. (1976). Metabolism of (14c)-quazodine in the rat, dog, and man, *Toxicology and Applied Pharmacology,* 36:307–322.

Bartek, M.J., La Budde, J.A., and Maibach, H.I. (1972). Skin permeability *in vivo*, comparison in rat, rabbit, pig and man, *Journal of Investigative Dermatology,* 58:114–123.

Behl, C.R. and Barrett, M. (1981). Hydration and percutaneous absorption II: influence of hydration on water and alkanol permeation through Swiss mouse skin; comparison with hairless mouse, *Journal of Pharmaceutical Sciences,* 70:1212–1215.

Behl, C.R., El-Sayed, A.A., and Flynn, G.L. (1983). Hydration and percutaneous absorption IV: influence of hydration on *n*-alkanol permeation through rat skin; comparison with hairless and Swiss mice, *Journal of Pharmaceutical Sciences,* 72:79–82.

Behl, C.R., Flynn, G.L., Kurihara, T., Harper, N., Smith, W., Higuchi, W.I., Ho, N.F., and Pierson, C.L. (1980). Hydration and percutaneous absorption I: influence of hydration on alkanol permeation through hairless mouse skin, *Journal of Investigative Dermatology,* 75:346–352.

Behl, C.R., Flynn, G.L., Linn, E.E., and Smith, W.M. (1984). Percutaneous absorption of corticosteroids: age, site, and skin-sectioning influences on rates of permeation of hairless mouse skin by hydrocortisone, *Journal of Pharmaceutical Sciences,* 73:1287–1290.

Behl, C.R., Linn, E.E., Flynn, G.L., Pierson, C.L., Higuchi, W.I., and Ho, N.F. (1983). Permeation of skin and eschar by antiseptics I: baseline studies with phenol, *Journal of Pharmaceutical Sciences,* 72:391–397.

Bhatti, A.S., Scott, R.C., and Dyer, A. (1988). *In-vitro* percutaneous absorption: pig epidermal membrane as a model for human skin, *Journal of Pharmacy and Pharmacology,* 40:45P.

Bond, J.R. and Barry, B.W. (1988a). Hairless mouse skin is limited as a model for assessing the effects of penetration enhancers in human skin, *Journal of Investigative Dermatology,* 90:810–813.

Bond, J.R. and Barry, B.W. (1988b). Limitations of hairless mouse skin as a model for *in vitro* permeation studies through human skin: hydration damage, *Journal of Investigative Dermatology,* 90:486–489.

Brescia, F., Arents, J., Meislich, H., and Turk, A. (1975). *Fundamentals of Chemistry,* New York: Academic Press.

Bronaugh, R.L., Stewart, R.F., and Congdon, E.R. (1982). Methods for *in vitro* percutaneous absorption studies. II. Animal models for human skin, *Toxicology and Applied Pharmacology,* 62:481–488.

Campbell, P., Watanabe, T., and Chandrasekaran, S.K. (1976). Comparison of *in vitro* skin permeability of scopolamine in rat, rabbit, and man, *Federation Proceedings,* 35:639.

Chowhan, Z.T. and Pritchard, R. (1978). Effect of surfactants on percutaneous absorption of naproxen I: comparisons of rabbit, rat, and human excised skin, *Journal of Pharmaceutical Sciences,* 67:1272–1274.

Dick, I.P. and Scott, R.C. (1992). Pig ear skin as an *in-vitro* model for human skin permeability, *Journal of Pharmacy and Pharmacology,* 44:640–645.

Durrheim, H., Flynn, G.L., Higuchi, W.I., and Behl, C.R. (1980). Permeation of hairless mouse skin I: experimental methods and comparison with human epidermal permeation by alkanols, *Journal of Pharmaceutical Sciences,* 69:781–786.

Fleeker, C., Wong, O., and Rytting, J.H. (1989). Facilitated transport of basic and acidic drugs in solutions through snakeskin by a new enhancer-dodecyl *N,N*-dimethylamino acetate, *Pharmaceutical Research,* 6:443–448.

Flynn, G.L., Durrheim, H., and Higuchi, W.I. (1981). Permeation of hairless mouse skin II: membrane sectioning techniques and influence on alkanol permeabilities, *Journal of Pharmaceutical Sciences,* 70:52–56.

Galey, W.R., Lonsdale, H.K., and Nacht, S. (1976). The *in vitro* permeability of skin and buccal mucosa to selected drugs and tritiated water, *Journal of Investigative Dermatology,* 67:713–717.

Ghosh, T.K., Chiao, C.S., and Gokhale, R.D. (1993). *In-vitro* permeation of some β-blockers across the hairless mouse skin, *Journal of Pharmacy and Pharmacology,* 45:218–219.

Hansch, C., Leo, A., and Hoekman, D. (1995). *Exploring QSAR: Hydrophobic, Electronic, and Steric Constants,* Washington, D.C.: American Chemical Society.

Harada, K., Murakami, T., Kawasaki, E., Higashi, Y., Yamamoto, S., and Yata, N. (1993). *In vitro* permeability to salicylic acid of human, rodent, and shed snake skin, *Journal of Pharmacy and Pharmacology,* 45:414–418.

Hatanaka, T., Inuma, M., Sugibayashi, K., and Morimoto, Y. (1990). Prediction of skin permeability of drugs. I. Comparison with artificial membrane, *Chemical and Pharmaceutical Bulletin* (Tokyo), 38:3452–3459.

Hawkins, G.S. and Reifenrath, W.G. (1986). Influence of skin source, penetration cell fluid, and partition coefficient on *in vitro* skin penetration, *Journal of Pharmaceutical Sciences,* 75:378–381.

Hayashi, T., Sugibayashi, K., and Morimoto, Y. (1992). Calculation of skin permeability coefficient for ionized and unionized species of indomethacin, *Chemical and Pharmaceutical Bulletin* (Tokyo), 40:3090–3093.

Huq, A.S., Ho, N.F.H., Husari, N., Flynn, G.L., Jetzer, W.E., and Condie, L. (1986). Permeation of water contaminative phenols through hairless mouse skin, *Archives of Environmental Contamination and Toxicology,* 15:557–566.

Itoh, T., Magavi, R., Casady, R.L., Nishihata, T., and Rytting, J.H. (1990). A method to predict the percutaneous permeability of various compounds: shed snake skin as a model membrane, *Pharmaceutical Research,* 7:1302–1306.

Itoh, T., Xia, J., Magavi, R., Nishihata, T., and Rytting, J.H. (1990). Use of shed snake skin as a model membrane for *in vitro* percutaneous penetration studies: comparison with human skin, *Pharmaceutical Research,* 7:1042–1047.

Jepson, G.W., Hoover, D.K., Black, R.K., McCafferty, J.D., Mahle, D.A., and Gearhart, J.M. (1994). A partition coefficient determination method for nonvolatile chemicals in biological tissues, *Fundamental and Applied Toxicology,* 22:519–524.

Jetzer, W.E., Huq, A.S., Ho, N.F., Flynn, G.L., Duraiswamy, N., and Condie, L. (1986). Permeation of mouse skin and silicone rubber membranes by phenols: relationship to *in vitro* partitioning, *Journal of Pharmaceutical Sciences,* 75:1098–1103.

Jolicoeur, L.M., Nassiri, M.R., Shipman, C., Choi, H.K., and Flynn, G.L. (1992). Etorphine is an opiate analgesic physicochemically suited to transdermal delivery, *Pharmaceutical Research,* 9:963–965.

Katayama, K., Takahashi, O., Matsui, R., Morigaki, S., Aiba, T., Kakemi, M., and Koizumi, T. (1992). Effect of l-menthol on the permeation of indomethacin, mannitol and cortisone through excised hairless mouse skin, *Chemical and Pharmaceutical Bulletin* (Tokyo), 40:3097–3099.

Kikkoji, T., Gumbleton, M., Higo, N., Guy, R.H., and Benet, L.Z. (1991). Percutaneous penetration kinetics of nitroglycerin and its dinitrate metabolites across hairless mouse skin *in vitro*, *Pharmaceutical Research,* 8:1231–1237.

Kim, Y.-H., Ghanem, A.-H., and Higuchi, W.I. (1992). Model studies of epidermal permeability, *Seminars in Dermatology,* 11:145–156.

Kobayashi, D., Matsuzawa, T., Sugibayashi, K., Morimoto, Y., and Kimura, M. (1994). Analysis of the combined effect of 1-menthol and ethanol as skin permeation enhancers based on a two-layer skin model, *Pharmaceutical Research,* 11:96–103.

Liu, P., Higuchi, W.I., Ghanem, A.-H., and Good, W.R. (1994). Transport of β-estradiol in freshly excised human skin *in vitro*: diffusion and metabolism in each skin layer, *Pharmaceutical Research,* 11:1777–1784.

Lyman, W.J., Keehl, W.K., and Rosenblatt, D.H. (1982). *Handbook of Chemical Property Estimation Methods,* New York: McGraw-Hill.

Maitani, Y., Coutel-Egros, A., Obata, Y., and Nagai, T. (1993). Prediction of skin permeabilities of diclofenac and propranolol from theoretical partition coefficients determined from cohesion parameters, *Journal of Pharmaceutical Sciences,* 82:416–420.

Marzulli, F.N., Brown, D.W.C., and Maibach, H.I. (1969). Techniques for studying skin penetration, *Toxicology and Applied Pharmacology,* Supplement 3:76–83.

McGreesh, A.H. (1965). Percutaneous toxicity, *Toxicology and Applied Pharmacology,* 2:20–26.

Morimoto, Y., Hatanaka, T., Sugibayashi, K., and Omiya, H. (1992). Prediction of skin permeability of drugs: comparison of human and hairless rat skin, *Journal of Pharmacy and Pharmacology,* 44:634–639.

Ogiso, T., Paku, T., Iwaki, M., and Tanino, T. (1994). Mechanism of the enhancement effect of *n*-octyl-β-*d*-thioglucoside on the transdermal penetration of fluorescein isothiocyanate-labeled dextrans and the molecular weight dependence of water-soluble penetrants through stripped skin, *Journal of Pharmaceutical Sciences,* 83:1676–1681.

Okamoto, H., Hashida, M., and Sezaki, H. (1988). Structure–activity relationship of 1-alkyl- or 1-alkenylazacycloalkanone derivatives as percutaneous penetration enhancers, *Journal of Pharmaceutical Sciences,* 77:418–424.

Okamoto, H., Hashida, M., and Sezaki, H. (1991). Effect of 1-alkyl- or 1-alkenylazacycloalkanone derivatives on the penetration of drugs with different lipophilicities through guinea pigskin, *Journal of Pharmaceutical Sciences,* 80:39–45.

Okamoto, H., Yamashita, F., Saito, K., and Hashida, M. (1989). Analysis of drug penetration through the skin by the two-layer skin model, *Pharmaceutical Research,* 6:931–937.

Okumura, F., Sugibayashi, K., Ogawa, K., and Morimoto, Y. (1989). Skin permeability of water-soluble drugs, *Chemical and Pharmaceutical Bulletin* (Tokyo), 37:1404–1406.

Parry, G.E., Bunge, A.L., Silcox, G.D., Pershing, L.K., and Pershing, D.W. (1990). Percutaneous absorption of benzoic acid across human skin. I. *In vitro* experiments and mathematical modeling, *Pharmaceutical Research,* 7:230–236.

PCModels. (1995). PCModel, 4.2, Mission Viejo, CA: Daylight Chemical Information Systems.

Potts, R.O. and Guy, R.H. (1992). Predicting skin permeability, *Pharmaceutical Research,* 9:663–669.

Rigg, P.C. and Barry, B.W. (1990). Shed snake skin and hairless mouse skin as model membranes for human skin during permeation studies, *Journal of Investigative Dermatology,* 94:235–240.

Roberts, M.S. and Anderson, R.A. (1975). The percutaneous absorption of phenolic compounds: the effect of vehicles on the penetration of phenol, *Journal of Pharmacy and Pharmacology,* 27:599–605.

Roy, S.D., Hou, S.-Y., Witham, S.L., and Flynn, G.L. (1994). Transdermal delivery of narcotic analgesics: comparative metabolism and permeability of human cadaver skin and hairless mouse skin, *Journal of Pharmaceutical Sciences,* 83:1723–1728.

Ruland, A. and Kreuter, J. (1991). Transdermal permeability and skin accumulation of amino acids, *International Journal of Pharmaceutics,* 72:149–155.

SAS Institute. (1995). JMP Statistical Discovery Software, 3.1, Cary, NC: SAS Institute.

Sato, K., Sugibayashi, K., and Morimoto, Y. (1991). Species differences in percutaneous absorption of nicorandil, *Journal of Pharmaceutical Sciences,* 80:104–107.

Sato, K., Sugibayashi, K., Morimoto, Y., Omiya, H., and Enomoto, N. (1989). Prediction of the *in-vitro* human skin permeability of nicorandil from animal data, *Journal of Pharmacy and Pharmacology,* 41:379–383.

Scala, J., McOsker, D.E., and Reller, H.H. (1968). The percutaneous absorption of ionic surfactants, *Journal of Investigative Dermatology,* 50:371–379.

Scott, R.C., Corrigan, M.A., Smith, F., and Mason, H. (1991). The influence of skin structure on permeability: an intersite and interspecies comparison with hydrophilic penetrants, *Journal of Investigative Dermatology,* 96:921–925.

Smith, J.M. and Van Ness, H.C. (1987). *Introduction to Chemical Engineering Thermodynamics,* New York: McGraw Hill.

Sober, H.A. (ed.). (1968). *Handbook of Biochemistry,* Cleveland, OH: Chemical Rubber Company.

SPARC. (1995). *SPARC Performs Automated Reasoning in Chemistry: An Expert System for Estimating Physical and Chemical Reactivity*, Windows Prototype Version 1.1, Athens, GA: U.S. EPA (Ecosystem Research Division) and University of Georgia.

Stoughton, R.B. (1975). Animal models for in vitro percutaneous absorption, in H. Maibach (ed.), *Animal Models in Dermatology Relevance to Human Dermatopharmacology and Dermatotoxicology*, Edinburgh, U.K.: Churchill Livingstone, pp. 121–132.

Surber, C., Wilhelm, K.P., Maibach, H.I., Hall, L.L., and Guy, R.H. (1990). Partitioning of chemicals into human stratum corneum: implications for risk assessment following dermal exposure, *Fundamental and Applied Toxicology,* 15:99–107.

Takahashi, K., Tamagawa, S., Katagi, T., Rytting, J.H., Nishihata, T., and Mizuno, N. (1993). Percutaneous permeation of basic compounds through shed snake skin as a model membrane, *Journal of Pharmacy and Pharmacology,* 45:882–886.

Tojo, K., Chiang, C.C., and Chien, Y.W. (1987). Drug permeation across the skin: effect of penetrant hydrophilicity, *Journal of Pharmaceutical Sciences,* 76:123–126.

Tregear, R.T. (1966). *Physical Functions of the Skin,* New York: Academic Press.

Treherne, J.E. (1956). The permeability of skin to some non-electrolytes, *Journal of Physiology,* 133:171–180.

U.S. Environmental Protection Agency. (1992). *Dermal Exposure Assessment: Principles and Applications*, EPA/600/8-91/011B, Washington, D.C.: Exposure Assessment Group, Office of Health and Environmental Assessment, Office of Research and Development.

Vecchia, B.E. (1997). Estimating the dermally absorbed dose from chemical exposure: data analysis, parameter estimation, and sensitivity to parameter uncertainties, M.S. thesis, Colorado School of Mines, Golden.

Vecchia, B.E. and Bunge, A.L. (2002a). Partitioning of chemicals into skin: results and prediction, in J. Hadgraft and Guy, R.H. (eds.), *Transdermal Drug Delivery Systems*, New York: Dekker, pp. 143–198.

Vecchia, B.E. and Bunge, A.L. (2002b). Skin absorption databases and predictive equations, in J. Hadgraft and Guy, R.H. (eds.), *Transdermal Drug Delivery Systems*, New York: Dekker, pp. 57–141.

Walker, M., Dugard, P.H., and Scott, R.C. (1983). *In vitro* percutaneous absorption studies: a comparison of human and laboratory species, *Human Toxicology,* 2:561–562.

Wearley, L.L., Tojo, K., and Chien, Y.W. (1990). A numerical approach to study the effect of binding on the iontophoretic transport of a series of amino acids, *Journal of Pharmaceutical Sciences,* 79:992–998.

Wester, R.C. and Maibach, H.I. (1975a). Percutaneous absorption in the rhesus monkey compared to man, *Toxicology and Applied Pharmacology,* 32:394 –398.

Wester, R.C. and Maibach, H.I. (1975b). Rhesus monkey as an animal model for percutaneous absorption. in H.I. Maibach (ed.), *Animal Models in Dermatology*, New York: Churchill Livingstone, pp. 133–137.

Wester, R.C. and Maibach, H.I. (1976). Relationship of topical dose and percutaneous absorption in rhesus monkey and man, *Journal of Investigative Dermatology,* 67:518–520.

Wester, R.C. and Maibach, H.I. (1977). Percutaneous absorption in man and animal: a perspective, in V.A. Drill and P. Lazar (eds.), *Cutaneous Toxicity*, New York: Academic Press, pp. 111–126.

Wester, R.C. and Maibach, H.I. (1986). Dermatopharmacokinetics: a dead membrane or a complex multifunctional viable process? in J.W. Bridges and L.F. Chasseaud (eds.), *Progress in Drug Metabolism*, London: Taylor and Francis, pp. 95–109.

Wester, R.C. and Noonan, P.K. (1980). Relevance of animal models for percutaneous absorption, *International Journal of Pharmaceutics,* 7:99–110.

Williams, P.L., Brooks, J.D., Inman, A.O., Monteiro-Riviere, N.A., and Riviere, J.E. (1994). Determination of physicochemical properties of phenol, *p*-nitrophenol, acetone and ethanol relevant to quantitating their percutaneous absorption in porcine skin, *Research Communications in Chemical Pathology and Pharmacology,* 83:61–75.

Appendix A: Permeability Coefficients and Input Parameters

Table A1 Hairless Mouse Skin Permeability Coefficient Measurements

	Compound[a]	Log K_{ow}[b]	*MW*	T (°C)	$P_{cw,obs}$[c] (cm h^{-1})	P_{cw} (cm h^{-1})	f_{ui}[d]	pH[e]	Skin[f]	Strain	Reference
E	Alanine (+ –)	–2.96	89.1	37	5.50E-05	Ion	<0.1	7.4	FULL	hr/hr-c_3H/Tif Bom	Ruland and Kreuter, 1991
E	Alanine (+ –)	–2.96	89.1	37	3.70E-05	Ion	<0.1	6	FULL	hr/hr-c_3H/Tif Bom	Ruland and Kreuter, 1991
E	Arginine (+ – +)	–4.20	174.2	37	1.00E-04	Ion	<0.1	7.4	FULL	hr/hr-c_3H/Tif Bom	Ruland and Kreuter, 1991
E	Arginine (+ –)	–4.20	174.2	37	3.26E-04	Ion	<0.1	10.8	FULL	hr/hr-c_3H/Tif Bom	Ruland and Kreuter, 1991
E	Asparagine (+ –)	–3.41	132.1	37	3.50E-05	Ion	<0.1	7.4	FULL	hr/hr-c_3H/Tif Bom	Ruland and Kreuter, 1991
E	Asparagine (+ –)	–3.41	132.1	37	4.10E-05	Ion	<0.1	5.4	FULL	hr/hr-c_3H/Tif Bom	Ruland and Kreuter, 1991
E	Aspartic acid (– + –)	N/A	133.1	37	8.00E-06	Ion	<0.1	7.4	FULL	hr/hr-c_3H/Tif Bom	Ruland and Kreuter, 1991
E	Aspartic acid (+ –)	N/A	133.1	37	8.60E-05	Ion	<0.1	2.8	FULL	hr/hr-c_3H/Tif Bom	Ruland and Kreuter, 1991
E	Bevantolol (+)	[2.64]	345.4	37	1.32E-02	Ion	<0.1	7.4	FULL	Skh:Sr-1	Ghosh et al., 1993
	Butanol	0.88	74.1	37	1.46E-02	1.50E-02	1	ND	FULL	HRS/J or SKH-hr-1[g]	Durrheim et al., 1980
	Butanol	0.88	74.1	37	5.35E-03[L]	5.35E-03	1	ND	FULL	SKH-hr-1	Behl et al., 1980
	Butanol	0.88	74.1	20	2.90E-03	2.90E-03	1	ND	FULL	HRS/J	Durrheim et al., 1980
	Butanol	0.88	74.1	25	4.40E-03	4.40E-03	1	ND	FULL	HRS/J	Durrheim et al., 1980
	Butanol	0.88	74.1	37	1.54E-02	1.54E-02	1	ND	SC[h]	HRS/J	Flynn et al., 1981
	Chloramphenicol	1.14	323.1	31	1.12E-02	1.12E-02	1	ND	FULL	HR/HR	Aguiar and Weiner, 1969
	Chloramphenicol	1.14	323.1	37	1.81E-02	1.81E-02	1	ND	FULL	HR/HR	Aguiar and Weiner, 1969
	Chloramphenicol	1.14	323.1	45	3.72E-02	3.72E-02	1	ND	FULL	HR/HR	Aguiar and Weiner, 1969
	4-Chloro-3-cresol	3.10	142.6	37	2.35E-01	2.35E-01	1	ND	SC[h]	SKH-hr-1	Huq et al., 1986
	2-Chlorophenol	2.15	128.6	37	1.82E-01	1.82E-01	1	ND	SC[h]	SKH-hr-1	Huq et al., 1986
E	Cidofovir (– + –)	N/A[i]	279.0	35	2.47E-05	Ion	<0.1	7	FULL	N/A	Aspe et al., 1995
	Cortisone	1.47	360.5	30	5.11E-04	5.11E-04	1	7.4	FULL	N/A	Katayama et al., 1992
E	Cyclopropanoyl propranolol (+)	[3.94]	327.0	37	1.29E-03	Ion	<0.1	4	FULL	N/A	Ahmed et al., 1995
E	Cysteine (+ –)	–2.49	121.2	37	1.90E-05	Ion	<0.1	7.4	FULL	hr/hr-c_3H/Tif Bom	Ruland and Kreuter, 1991
E	Cysteine (+ –)	–2.49	121.2	37	3.40E-05	Ion	<0.1	5.2	FULL	hr/hr-c_3H/Tif Bom	Ruland and Kreuter, 1991
	Decanol	4.57	158.3	37	2.33E-01	2.33E-01	1	ND	EPID	HRS/J	Flynn et al., 1981
	2,4-Dichlorophenol	3.06	163.0	37	4.53E-01	4.53E-01	1	ND	SC[h]	SKH-hr-1	Huq et al., 1986
	2,4-Dimethylphenol	2.30	122.2	37	1.10E-01	1.10E-01	1	ND	FULL	SKH-hr-1	Huq et al., 1986
	2,4-Dinitrophenol	1.67	184.1	37	2.28E-01	2.28E-01	1	ND	SC[h]	SKH-hr-1	Huq et al., 1986
	2,4-Dinitrophenol	1.67	184.1	37	1.72E-01	1.72E-01	1	ND	FULL	SKH-hr-1	Jetzer et al., 1986
	β-Estradiol	4.01	272.4	37	[2.70E-02]	2.70E-02	1	ND	FULL	N/A	Kim et al., 1992
	β-Estradiol	4.01	272.4	37	3.20E-02	3.20E-02	1	ND	SC	SKH-HR1	Liu et al., 1994
	Estrone	3.13	270.4	37	[3.96E-02]	3.96E-02	1	ND	FULL	N/A	Kim et al., 1992

	Estrone ammonium sulfate	3.13[J]	270.4[J]	37	[1.80E-04]	1.80E-04	1	ND	FULL	N/A	Kim et al., 1992
	Ethanol	–0.31	46.0	37	4.80E-03	4.80E-03	1	ND	FULL	HRS/J or SKH-hr-1[g]	Durrheim et al., 1980
	Ethanol	–0.31	46.0	N/A	2.05E-03[L]	2.05E-03	1	ND	FULL	SKH-hr-1	Behl et al., 1980
	Ethanol	–0.31	46.0	20	7.20E-04	7.20E-04	1	ND	FULL	HRS/J	Durrheim et al., 1980
	Ethanol	–0.31	46.0	25	1.23E-03	1.23E-03	1	ND	FULL	HRS/J	Durrheim et al., 1980
	Ethanol	–0.31	46.0	37	4.88E-03	4.88E-03	1	ND	SC[h]	HRS/J	Flynn et al., 1981
E	Etorphine (+)	[1.41]	411.5	37	3.60E-03	Ion	<0.1	7.3	FULL	SKH-hr-1	Jolicoeur et al., 1992
	Fentanyl	4.05	336.5	37	2.90E-02	3.97E-02	0.73	7.4	FULL	SKH-HR1	Roy et al., 1994
E	5-Fluorouracil (+ – + –)	–0.89	130.1	31	1.07E-04	Ion	<0.1	4.75[k]	FULL	CBA/HL	Bond and Barry, 1988a
E	5-Fluorouracil (+ – + –)	–0.89	130.1	31	9.56E-05	Ion	<0.1	4.75[k]	FULL	CBA/hl	Rigg and Barry, 1990
E	5-Fluorouracil (+ – + –)	–0.89	130.1	31	6.03E-05	Ion	<0.1	4.75[k]	FULL	CBA/hl	Rigg and Barry, 1990
	Glucose	[–3.53]	180.2	N/A	9.50E-05	9.50E-05	1	N/A	N/A	SKH-hr-1	Ackermann and Flynn, 1987
E	Glutamic acid (– + –)	–3.69	147.1	37	1.00E-05	Ion	<0.1	7.4	FULL	hr/hr-c_3H/Tif Bom	Ruland and Kreuter, 1991
E	Glutamic acid (+ –)	–3.69	147.1	37	4.90E-05	Ion	<0.1	2.8	FULL	hr/hr-c_3H/Tif Bom	Ruland and Kreuter, 1991
E	Glutamine (+ –)	–3.15	146.2	37	5.00E-05	Ion	<0.1	7.4	FULL	hr/hr-c_3H/Tif Bom	Ruland and Kreuter, 1991
E	Glutamine (+ –)	–3.15	146.2	37	3.20E-05	Ion	<0.1	5.6	FULL	hr/hr-c_3H/Tif Bom	Ruland and Kreuter, 1991
	Glycerol	–1.76	92.1	N/A	1.40E-04	1.40E-04	1	N/A	N/A	SKH-hr-1	Ackermann and Flynn, 1987
	1,2-Glyceryl dinitrate	[–0.22]	183.0	N/A	1.40E-03	1.40E-03	1	7.4	FULL	SKH:HR-1	Kikkoji et al., 1991
	1,3-Glyceryl dinitrate	[0.20]	183.0	N/A	1.20E-03	1.20E-03	1	7.4	FULL	SKH:HR-1	Kikkoji et al., 1991
E	Glycine (+ –)	–3.21	75.1	37	3.80E-05	Ion	<0.1	7.4	FULL	hr/hr-c_3H/Tif Bom	Ruland and Kreuter, 1991
E	Glycine (+ –)	–3.21	75.1	37	1.19E-04	Ion	<0.1	6	FULL	hr/hr-c_3H/Tif Bom	Ruland and Kreuter, 1991
	Heptanol	2.72	116.0	37	9.30E-02	9.30E-02	1	ND	FULL	HRS/J or SKH-hr-1[g]	Durrheim et al., 1980
	Heptanol	2.72	116.0	N/A	6.59E-02[L]	6.59E-02	1	ND	FULL	SKH-hr-1	Behl et al., 1980
	Heptanol	2.72	116.0	37	1.13E-01	1.13E-01	1	ND	EPID	HRS/J	Flynn et al., 1981
	Hexanol	2.03	102.2	37	4.80E-02	4.80E-02	1	ND	FULL	HRS/J or SKH-hr-1[g]	Durrheim et al., 1980
	Hexanol	2.03	102.2	N/A	1.94E-02[L]	1.94E-02	1	ND	FULL	SKH-hr-1	Behl et al., 1980
	Hexanol	2.03	102.2	31	1.52E-02	1.52E-02	1	ND	FULL	CBA/HL	Bond and Barry, 1988b
	Hexanol	2.03	102.0	20	5.25E-03	5.25E-03	1	ND	FULL	HRS/J	Durrheim et al., 1980
	Hexanol	2.03	102.0	25	8.60E-03	8.60E-03	1	ND	FULL	HRS/J	Durrheim et al., 1980
	Hexanol	2.03	102.2	37	5.88E-02	5.88E-02	1	ND	SC[h]	HRS/J	Flynn et al., 1981
E	Histidine (+ –)	–3.56	155.2	37	2.00E-05	Ion	<0.1	7.4	FULL	hr/hr-c_3H/Tif Bom	Ruland and Kreuter, 1991
E	Histidine (+ –)	–3.56	155.2	37	1.60E-05	Ion	<0.1	7.6	FULL	hr/hr-c_3H/Tif Bom	Ruland and Kreuter, 1991
	Hydrocortisone	1.61	362.5	37	1.60E-04	1.60E-04	1	N/A	FULL	SKH-hr-1	Ackermann et al., 1987
	Hydrocortisone	1.61	362.5	37	2.28E-04	2.28E-04	1	ND	FULL	SKH-hr-1	Behl et al., 1984
	Hydrocortisone	1.61	362.5	37	[3.60E-04]	3.60E-04	1	ND	FULL	N/A	Kim et al., 1992

Table A1 (continued) Hairless Mouse Skin Permeability Coefficient Measurements

	Compound[a]	Log K_{ow}[b]	*MW*	T (°C)	$P_{cw,obs}$[c] (cm h^{-1})	P_{cw} (cm h^{-1})	f_{ui}[d]	pH[e]	Skin[f]	Strain	Reference
	Hydrocortisone-21-acetate	1.11	404.0	37	1.70E-03	1.70E-03	1	N/A	N/A	SKH-hr-1	Ackermann et al., 1987
	Hydrocortisone-21-butyrate	[2.22]	432.0	37	4.30E-02	4.30E-02	1	N/A	N/A	SKH-hr-1	Ackermann et al., 1987
	Hydrocortisone-21-heptanoate	[3.81]	474.0	37	3.40E-01	3.40E-01	1	N/A	N/A	SKH-hr-1	Ackermann et al., 1987
	Hydrocortisone-21-hexanoate	[3.28]	460.6	37	2.00E-01	2.00E-01	1	N/A	N/A	SKH-hr-1	Ackermann et al., 1987
	Hydrocortisone-21-pentanoate	[2.75]	446.0	37	7.10E-02	7.10E-02	1	N/A	N/A	SKH-hr-1	Ackermann et al., 1987
	Hydrocortisone-21-propionate	[1.69]	418.5	37	9.80E-03	9.80E-03	1	N/A	N/A	SKH-hr-1	Ackermann et al., 1987
	Indomethacin	4.27	357.8	30	3.25E-04	3.35E-04	0.97	3	FULL	N/A	Katayama et al., 1992
E	Isoleucine (+ –)	–1.72	131.2	37	1.30E-05	Ion	<0.1	7.4	FULL	hr/hr-c_3H/Tif Bom	Ruland and Kreuter, 1991
E	Isoleucine (+ –)	–1.72	131.2	37	5.20E-05	Ion	<0.1	6	FULL	hr/hr-c_3H/Tif Bom	Ruland and Kreuter, 1991
E	Isovaleryl propranolol (+)	[5.04]	343.3	37	2.80E-03	Ion	<0.1	4	FULL	N/A	Ahmed et al., 1995
E	Leucine (+ –)	–1.52	131.2	37	2.90E-05	Ion	<0.1	7.4	FULL	hr/hr-c_3H/Tif Bom	Ruland and Kreuter, 1991
E	Leucine (+ –)	–1.52	131.2	37	1.60E-05	Ion	<0.1	6	FULL	hr/hr-c_3H/Tif Bom	Ruland and Kreuter, 1991
E	Levobunolol (+)	2.40	291.0	37	1.55E-03	Ion	<0.1	7.4	FULL	Skh:Sr-1	Ghosh et al., 1993
E	Lysine (+ – +)	–3.05	146.2	37	2.10E-05	Ion	<0.1	7.4	FULL	hr/hr-c_3H/Tif Bom	Ruland and Kreuter, 1991
E	Lysine (+ –)	–3.05	146.2	37	3.89E-04	Ion	<0.1	9.8	FULL	hr/hr-c_3H/Tif Bom	Ruland and Kreuter, 1991
	Mannitol	–3.10	182.2	30	7.80E-05	7.80E-05	1	7.4	FULL	N/A	Katayama et al., 1992
	Mannitol	–3.10	182.2	37	[1.08E-04]	1.08E-04	1	ND	FULL	N/A	Kim et al., 1992
	Methanol	–0.77	32.0	37	2.60E-03	2.60E-03	1	ND	FULL	HRS/J or SKH-hr-1[g]	Durrheim et al., 1980
	Methanol	–0.77	32.0	37	2.81E-03[L]	2.81E-03	1	ND	FULL	SKH-hr-1	Behl et al., 1980
	Methanol	–0.77	32.0	37	3.20E-03[L]	3.20E-03	1	ND	SC[h]	SKH-hr-1	Behl, Linn, et al., 1983
	Methanol	–0.77	32.0	20	4.10E-04	4.10E-04	1	ND	FULL	HRS/J	Durrheim et al., 1980
	Methanol	–0.77	32.0	25	9.30E-04	9.30E-04	1	ND	FULL	HRS/J	Durrheim et al., 1980
	Methanol	–0.77	32.0	37	2.62E-03	2.62E-03	1	ND	SC[h]	HRS/J	Flynn et al., 1981
E	Methionine (+ –)	–1.87	149.2	37	3.10E-05	Ion	<0.1	7.4	FULL	hr/hr-c_3H/Tif Bom	Ruland and Kreuter, 1991
E	Methionine (+ –)	–1.87	149.2	37	1.70E-05	Ion	<0.1	5.6	FULL	hr/hr-c_3H/Tif Bom	Ruland and Kreuter, 1991
E	Metoprolol (+)	1.88	267.4	37	2.75E-03	Ion	<0.1	7.4	FULL	Skh:Sr-1	Ghosh et al., 1993
E	Morphine (+)	0.76	285.3	37	1.10E-04	Ion	<0.1	7	FULL	SKH-HR1	Roy et al., 1994

E	Nadolol (+)	0.71	309.4	37	3.89E-03	Ion	<0.1	7.4	FULL	Skh:Sr-1	Ghosh et al., 1993
	Nicorandil	[0.69]	211.2	37	2.66E-04	2.66E-04	1	[8.0]	FULL	WBN/kob	Sato et al., 1991
	Nitroglycerine	[0.98]	227.1	N/A	2.00E-02	2.00E-02	1	7.4	FULL	SKH:HR-1	Kikkoji et al., 1991
	2-Nitrophenol	1.79	139.1	37	1.01E-01	1.01E-01	1	ND	FULL	SKH-hr-1	Huq et al., 1986
	4-Nitrophenol	1.91	139.1	37	2.54E-02	2.54E-02	1	ND	SC[h]	SKH-hr-1	Huq et al., 1986
	4-Nitrophenol	1.91	139.1	37	1.22E-02	1.22E-02	1	ND	FULL	SKH-hr-1	Jetzer et al., 1986
	Nonanol	4.26	144.0	37	2.48E-01	2.48E-01	1	ND	EPID	HRS/J	Flynn et al., 1981
	Octanol	3.00	130.2	37	9.70E-02	9.70E-02	1	ND	FULL	HRS/J or SKH-hr-1[g]	Durrheim et al., 1980
	Octanol	3.00	130.2	37	7.82E-02[L]	7.82E-02	1	ND	FULL	SKH-hr-1	Behl et al., 1980
	Octanol	3.00	130.0	20	1.89E-02	1.89E-02	1	ND	FULL	HRS/J	Durrheim et al., 1980
	Octanol	3.00	130.0	25	3.15E-02	3.15E-02	1	ND	FULL	HRS/J	Durrheim et al., 1980
	Octanol	3.00	130.2	37	1.80E-01	1.80E-01	1	ND	EPID	HRS/J	Flynn et al., 1981
E	Oxprenolol (+)	2.10	265.3	37	5.25E-03	Ion	<0.1	7.4	FULL	Skh:Sr-1	Ghosh et al., 1993
E	Paraquat Dichloride (++)	[–5.65]	257.3	N/A	1.07E-02	Ion	<0.1	N/A	FULL	N/A	Walker et al., 1983
E	Penbutolol (+)	4.15	291.0	37	2.57E-02	Ion	<0.1	7.4	FULL	Skh:Sr-1	Ghosh et al., 1993
	Pentanol	1.56	88.0	37	2.20E-02	2.20E-02	1	ND	FULL	HRS/J or SKH-hr-1[g]	Durrheim et al., 1980
	Pentanol	1.56	88.0	37	2.38E-02	2.38E-02	1	ND	SC[h]	HRS/J	Flynn et al., 1981
	Phenol	1.46	94.1	37	2.78E-02[L]	2.78E-02	1	ND	SC[h]	SKH-hr-1	Behl, Linn, et al., 1983
	Phenol	1.46	94.1	37	2.02E-02	2.02E-02	1	ND	SC[h]	SKH-hr-1	Huq et al., 1986
E	Phenylalanine (+ –)	–1.52	165.2	37	3.00E-05	Ion	<0.1	7.4	FULL	hr/hr-c$_3$H/Tif Bom	Ruland and Kreuter, 1991
E	Phenylalanine (+ –)	–1.52	165.2	37	2.44E-04	Ion	<0.1	5.4	FULL	hr/hr-c$_3$H/Tif Bom	Ruland and Kreuter, 1991
	Progesterone	3.87	314.5	37	[7.20E-02]	7.20E-02	1	ND	FULL	N/A	Kim et al., 1992
E	Proline (+ –)	–2.50	115.1	37	2.70E-05	Ion	<0.1	7.4	FULL	hr/hr-c$_3$H/Tif Bom	Ruland and Kreuter, 1991
E	Proline (+ –)	–2.50	115.1	37	3.30E-05	Ion	<0.1	6.3	FULL	hr/hr-c$_3$H/Tif Bom	Ruland and Kreuter, 1991
	Propanol	0.25	60.0	37	5.40E-03	5.40E-03	1	ND	FULL	HRS/J or SKH-hr-1[g]	Durrheim et al., 1980
	Propanol	0.25	60.0	37	5.49E-03	5.49E-03	1	ND	SC[h]	HRS/J	Flynn et al., 1981
E	Propranolol (+)	2.98	259.3	37	9.25E-05	Ion	<0.1	4	FULL	N/A	Ahmed et al., 1995
E	Propranolol (+)	2.98	259.3	37	7.41E-03	Ion	<0.1	7.4	FULL	Skh:Sr-1	Ghosh et al., 1993
E	Serine (+ –)	–3.07	105.1	37	3.00E-05	Ion	<0.1	7.4	FULL	hr/hr-c$_3$H/Tif Bom	Ruland and Kreuter, 1991
E	Serine (+ –)	–3.07	105.1	37	3.60E-05	Ion	<0.1	5.6	FULL	hr/hr-c$_3$H/Tif Bom	Ruland and Kreuter, 1991
E	Sotalol (+)	[0.23]	272.4	37	3.72E-04	Ion	<0.1	7.4	FULL	Skh:Sr-1	Ghosh et al., 1993
	Sufentanil	3.95	386.5	37	2.40E-02	2.53E-02	0.95	7.4	FULL	SKH-hr-1	Roy et al., 1994
E	Tetraethylammonium bromide (+)	–2.82	210.2	37	[1.08E-04]	Ion	<0.1	ND	FULL	N/A	Kim et al., 1992
	Thiourea	–1.02	76.1	N/A	9.60E-05	9.60E-05	1	N/A	N/A	SKH-hr-1	Ackermann and Flynn, 1987
E	Threonine (+ –)	–2.94	119.1	37	1.30E-05	Ion	<0.1	7.4	FULL	hr/hr-c$_3$H/Tif Bom	Ruland and Kreuter, 1991

Table A1 (continued) Hairless Mouse Skin Permeability Coefficient Measurements

	Compound[a]	Log K_{ow}[b]	*MW*	T (°C)	$P_{cw,obs}$[c] (cm h^{-1})	P_{cw} (cm h^{-1})	f_{ui}[d]	pH[e]	Skin[f]	Strain	Reference
E	Threonine (+ –)	–2.94	119.1	37	1.18E-04	Ion	<0.1	6.2	FULL	hr/hr-c_3H/Tif Bom	Ruland and Kreuter, 1991
E	Timolol (+)	1.83	316.4	37	1.55E-03	Ion	<0.1	7.4	FULL	Skh:Sr-1	Ghosh et al., 1993
	2,4,6-Trichlorophenol	3.69	197.5	37	1.74E-01	1.74E-01	1	ND	FULL	SKH-hr-1	Huq et al., 1986
E	Tryptophan (+ –)	–1.06	204.2	37	1.50E-05	Ion	<0.1	7.4	FULL	hr/hr-c_3H/Tif Bom	Ruland and Kreuter, 1991
E	Tryptophan (+ –)	–1.06	204.2	37	1.90E-05	Ion	<0.1	5.7	FULL	hr/hr-c_3H/Tif Bom	Ruland and Kreuter, 1991
E	Tyrosine (+ –)	–2.26	181.2	37	1.60E-05	Ion	<0.1	7.4	FULL	hr/hr-c_3H/Tif Bom	Ruland and Kreuter, 1991
E	Tyrosine (+ –)	–2.26	181.2	37	2.60E-05	Ion	<0.1	5.6	FULL	hr/hr-c_3H/Tif Bom	Ruland and Kreuter, 1991
	Urea	–2.11	60.1	N/A	1.20E-04	1.20E-04	1	N/A	N/A	SKH-hr-1	Ackermann and Flynn, 1987
E	Valine (+ –)	–2.26	117.2	37	1.30E-05	Ion	<0.1	7.4	FULL	hr/hr-c_3H/Tif Bom	Ruland and Kreuter, 1991
E	Valine (+ –)	–2.26	117.2	37	4.50E-05	Ion	<0.1	6	FULL	hr/hr-c_3H/Tif Bom	Ruland and Kreuter, 1991
E	Vidarabine	–1.11	285.3	37	[7.20E-05]	7.66E-05	0.94	>[7]	FULL	N/A	Kim et al., 1992
	Water	–1.38	18.0	N/A	1.60E-03	1.60E-03	1	ND	FULL	SKH-hr-1	Behl et al., 1980
	Water	–1.38	18.0	31	3.36E-03	3.36E-03	1	ND	FULL	CBA/HL	Bond and Barry, 1988b
	Water	–1.38	18.0	31	2.19E-03	2.19E-03	1	ND	FULL	CBA/hl	Rigg and Barry, 1990
	Water	–1.38	18.0	N/A	3.51E-03	3.51E-03	1	ND	FULL	N/A	Walker et al., 1983

[a] The compound investigated. Measurements indicated at left by an E are excluded measurements. All positive (+) and negative (–) ionic charges (for the chemical at experimental conditions) are indicated. For example, zwitterionic alanine with one positive and one negative charge is indicated as (+ –).
[b] Reported log K_{ow} are taken from the Hansch Starlist (Hansch et al., 1995) unless contained within brackets (e.g., for bevantolol [2.64]), in which case they were calculated using the Daylight program (PCModels, 1995).
[c] Permeability coefficients contained within brackets were digitized from figures in the publication.
[d] Fraction unionized determined from pK_a values calculated in SPARC (1995) at 25°C and adjusted to the experimental temperature as listed in Table A7.
[e] Reported solution pH unless contained within brackets (e.g., for nicorandil [8.0]), in which case the pH was calculated from the reported concentration and calculated pK_a values (see Table A7). Compounds that are essentially undissociated are indicated by ND (not dissociated) when no pH was reported.
[f] Type of skin used in the study: isolated stratum corneum (SC), epidermal membranes (EPID), or full-thickness skin (FULL).
[g] According to Durrheim et al. (1980), these data were measured using the HRS/J hairless mouse strain. However, Ackermann et al. (1987) stated that these measurements were made on the SKH-hr-1 hairless mouse. See Appendix B for more details.
[h] SC permeability coefficient was estimated from measurements made with other skin layers.
[i] The log K_{ow} of –1.29 calculated using the Daylight program (PCModels, 1995) is invalid (structural fragments of this molecule are not adequately represented by Daylight software).
[J] The parameters log K_{ow} and *MW* are for estrone, which was the penetrating species.
[k] Information obtained through personal communication from Barry (1996).
[L] The permeability coefficients for this chemical and a different copenetrating chemical were measured simultaneously (also see Appendix B).

Table A2 Hairless Rat Skin Permeability Coefficient Measurements

	Compound[a]	Log K_{ow}[b]	*MW*	T (°C)	$P_{cw,obs}$[c] (cm h^{-1})	P_{cw} (cm h^{-1})	f_{ui}[d]	pH[e]	Skin[f]	Strain	Reference
E	Alanine (+ −)	−2.96	89.1	37	1.68E-04	Ion	<0.1	6	FULL	N/A	Wearley et al., 1990
	Aminopyrine	1.00	231.3	37[g]	[1.65E-03]	1.65E-03	1	7.94[h]	SC[i]	WBN/ILA-Ht	Hatanaka et al., 1990
	Antipyrene	0.38	188.2	37[g]	[4.00E-04]	4.00E-04	1	7.6[h]	SC[i]	WBN/ILA-Ht	Hatanaka et al., 1990
	Atenolol	0.16	266.3	37	1.04E-03	1.06E-03	0.98	[10.9]	FULL	WBN/ILA-Ht	Kobayashi et al., 1994
	Cyclobarbitone	1.77	236.3	37[g]	[4.26E-03]	4.26E-03	1	3.58[h]	SC[i]	WBN/ILA-Ht	Hatanaka et al., 1990
E	Diclofenac (−)	4.40	260.7	37[g]	[8.34E-04]	Ion	<0.1	7.96[h]	SC[i]	WBN/ILA-Ht	Hatanaka et al., 1990
E	Diclofenac (−)	4.40	260.7	37	4.25E-04	Ion	<0.1	7.7	FULL	WBN/kob	Okumura et al., 1989
E	Diltiazem (+)	[3.55]	414.5	37	[1.66E-05]	Ion	<0.1	3.3	FULL	WBN/kob	Okumura et al., 1989
E	Disodium Cromoglycate (− −)	1.92	468.4	37	[1.05E-05]	Ion	<0.1	5.7	FULL	WBN/kob	Okumura et al., 1989
E	Dopamine (+)	[−0.05]	153.2	37[g]	[9.40E-04]	Ion	<0.1	3.26[h]	SC[i]	WBN/ILA-Ht	Hatanaka et al., 1990
E	Dopamine (+)	[−0.05]	153.2	37	9.04E-04	Ion	<0.1	3.7	FULL	WBN/kob	Okumura et al., 1989
	Estradiol (beta)	4.01	272.4	37[g]	[9.40E-02]	9.40E-02	1	ND	SC[i]	WBN/ILA-Ht	Hatanaka et al., 1990
E	FD-4 (FITC dextran)[J]	N/A	4400[k]	37	1.92E-05	1.92E-05	1	7.4	FULL	N/A	Ogiso et al., 1994
E	FD-10 (FITC dextran)[J]	N/A	9600[k]	37	1.22E-05	1.22E-05	1	7.4	FULL	N/A	Ogiso et al., 1994
E	FD-70 (FITC dextran)[J]	N/A	69000[k]	37	4.50E-06	4.50E-06	1	7.4	FULL	N/A	Ogiso et al., 1994
E	5-Fluorouracil (+ − + −)	−0.89	130.1	37[g]	[1.71E-04]	Ion	<0.1	4.66[h]	SC[i]	WBN/ILA-Ht	Hatanaka et al., 1990
	Flurbiprofen	4.16	244.3	37[g]	[3.80E-01]	1.17E+00	0.32	4.7[h]	SC[i]	WBN/ILA-Ht	Hatanaka et al., 1990
E	Glycine (+ −)	−3.21	75.1	37	3.99E-05	Ion	<0.1	6	FULL	N/A	Wearley et al., 1990
	Ibuprofen	3.50	206.3	37[g]	[3.60E-01]	6.21E-01	0.58	4.44[h]	SC[i]	WBN/ILA-Ht	Hatanaka et al., 1990
	Indomethacin	4.27	357.8	37[g]	[1.49E-01]	8.28E-01	0.18	5.15[h]	SC[i]	WBN/ILA-Ht	Hatanaka et al., 1990
	Indomethacin	4.27	357.8	37	1.00E-01	1.00E-01	1[L]	Range	FULL	WBN/ILA-Ht	Hayashi et al., 1992
	Indomethacin	4.27	357.8	37	1.54E-01	5.06E-01	0.30	4.9	FULL	WBN/kob	Okumura et al., 1989
E	Isoproterenol (+)	[0.08]	211.2	37[g]	[9.10E-04]	Ion	<0.1	2.75[h]	SC[i]	WBN/ILA-Ht	Hatanaka et al., 1990
E	Isoproterenol (+)	[0.08]	211.2	37	4.46E-04	Ion	<0.1	3.8	FULL	WBN/kob	Okumura et al., 1989
	Isosorbide dinitrate	1.31	236.1	37[g]	[1.77E-02]	1.77E-02	1	ND	SC[i]	WBN/ILA-Ht	Hatanaka et al., 1990
	Ketoprofen	3.12	254.3	37[g]	[8.57E-02]	1.08E-01	0.79	3.72[h]	SC[i]	WBN/ILA-Ht	Hatanaka et al., 1990
E	Leucine (+ −)	−1.52	131.2	37	1.45E-04	Ion	<0.1	6	FULL	N/A	Wearley et al., 1990
E	Levodopa (+ −)	−2.74	197.0	37[g]	[3.10E-04]	Ion	<0.1	5.42[h]	SC[i]	WBN/ILA-Ht	Hatanaka et al., 1990
E	Lignocaine (+)	2.26	234.3	37[g]	[2.72E-02]	Ion	<0.1	6.82[h]	SC[i]	WBN/ILA-Ht	Hatanaka et al., 1990
E	Morphine (+)	0.76	285.3	37	1.50E-04	Ion	<0.1	[4.9]	FULL	WBN/ILA-Ht	Kobayashi et al., 1994
E	Morphine (+)	0.76	285.3	37[g]	[4.30E-04]	Ion	<0.1	4.22[h]	SC[i]	WBN/ILA-Ht	Hatanaka et al., 1990
	Nicorandil	[0.69]	211.2	37[g]	[3.64E-04]	3.64E-04	1	[8.0]	SC[i]	WBN/ILA-Ht	Hatanaka et al., 1990

Table A2 (continued) Hairless Rat Skin Permeability Coefficient Measurements

	Compound[a]	Log K_{ow}[b]	*MW*	T (°C)	$P_{cw,obs}$[c] (cm h^{-1})	P_{cw} (cm h^{-1})	f_{ui}[d]	pH[e]	Skin[f]	Strain	Reference
	Nicorandil	[0.69]	211.2	37	7.27E-04	7.27E-04	1	[8.0]	FULL	WBN/kob	Sato et al., 1989
	Nifedipine	[2.20]	346.3	37	3.06E-02	3.06E-02	1	ND	FULL	WBN/ILA-Ht	Kobayashi et al., 1994
E	Papaverine (+)	[3.00]	339.4	37	[7.18E-05]	Ion	<0.1	3	FULL	WBN/kob	Okumura et al., 1989
E	Paraquat dichloride (+ +)	[–5.65]	257.3	N/A	3.55E-04	Ion	<0.1	ND	FULL	N/A	Walker et al., 1983
	Salicylic acid	2.26	138.1	25	1.50E-02	3.07E-02	0.49	3	FULL	N/A	Harada et al., 1993
E	Valine (+ –)	–2.26	117.2	37	7.68E-05	Ion	<0.1	6	FULL	N/A	Wearley et al., 1990
E	Vinpocetine	N/A[m]	350.5	37	2.22E-02	N/A	N/A	>[7]	FULL	WBN/ILA-Ht	Kobayashi et al., 1994
	Water	–1.38	18.0	37	4.28E-03	4.28E-03	1	ND	FULL	WBN/kob	Okumura et al., 1989
	Water	–1.38	18.0	N/A	1.30E-03	1.30E-03	1	ND	FULL	N/A	Walker et al., 1983

[a] The compound investigated. Measurements indicated at left by an E are excluded measurements. All positive (+) and negative (–) ionic charges (for the chemical at experimental conditions) are indicated. For example, zwitterionic alanine with one negative charge and one positive charge is indicated by (+ –).
[b] Reported log K_{ow} are taken from the Hansch Starlist (Hansch et al., 1995) unless contained within brackets (e.g., for dopamine [–0.05]), in which case they were calculated using the Daylight program (PCModels, 1995).
[c] Permeability coefficients contained within brackets were digitized from figures in the reference.
[d] Fraction unionized determined from pK_a values calculated in SPARC (1995) at 25°C and adjusted to the experimental temperature as listed in Table A7.
[e] Reported solution pH unless contained within brackets (e.g., for atenolol [10.9]), in which case they were calculated from the concentration and calculated pK_a values (see Table A7). Compounds that are essentially undissociated are identified with ND (not dissociated) when no pH was reported.
[f] Type of skin used in the study: isolated stratum corneum (SC), epidermis (EPID), split (SPLIT), or full-thickness skin (FULL).
[g] The temperature was not provided. We assumed 37°C, which is the temperature at which the K_{ow} was reported.
[h] The pH of saturated solutions at this temperature were reported by Morimoto et al. (1992).
[i] Permeability coefficients of the SC membrane were calculated from measurements made on full-thickness skin and stripped full-thickness skin.
[J] Fluorescein isothiocyanate-labeled dextrans.
[k] The average *MW* of a polydispersed mixture.
[L] The unionized permeability coefficient was determined from measurements covering a range of pH (i.e., fraction ionized).
[m] The log K_{ow} of 4.72 calculated using the Daylight program (PCModels, 1995) is invalid (structural fragments of this molecule are not adequately represented by Daylight software).

Table A3 Rat Skin Permeability Coefficient Measurements

	Compound[a]	Log K_{ow}[b]	*MW*	T (°C)	$P_{cw,obs}$[c] (cm h^{-1})	P_{cw} (cm h^{-1})	f_{ui}[d]	pH[e]	Skin[f]	Strain	Reference
	Butanol	0.88	74.1	37	4.80E-03[L]	4.80E-03	1	ND	FULL	Sprague-Dawley	Behl, El-Sayed, et al., 1983
	Diclofenac	4.40	260.7	37[g]	2.07E-01	2.07E-01[h]	0.92	3	N/A	N/A	Maitani et al., 1993
	Ethanol	–0.31	46.0	30	4.15E-04	4.15E-04	1	ND	FULL	Alpk/AP	Scott et al., 1991
	Hexanol	2.03	102.2	37	9.40E-03[L]	9.40E-03	1	ND	FULL	Sprague-Dawley	Behl, El-Sayed, et al., 1983
	Mannitol	–3.10	182.2	30	[2.56E-04]	2.56E-04	1	ND	EPID	Alpk:APfSD	Dick and Scott, 1992
	Mannitol	–3.10	182.2	30	1.34E-03	1.34E-03	1	ND	FULL	Alpk/AP	Scott et al., 1991
	Methanol	–0.77	32.0	37	2.35E-03[L]	2.35E-03	1	ND	FULL	Sprague-Dawley	Behl, El-Sayed, et al., 1983
E	Paraquat dichloride (+ +)	[–5.65]	257.3	30	[4.81E-04]	Ion	<0.1	ND	EPID	Alpk:APfSD	Dick and Scott, 1992
E	Paraquat dichloride (+ +)	[–5.65]	257.3	30	3.46E-04	Ion	<0.1	ND	FULL	Alpk/AP	Scott et al., 1991
E	Paraquat dichloride (+ +)	[–5.65]	257.3	N/A	2.67E-04	Ion	<0.1	ND	FULL	N/A	Walker et al., 1983
	Phenol	1.46	94.1	37	1.14E-02	1.14E-02	1	ND	FULL	Wistar	Roberts and Anderson, 1975
	Salicylic acid	2.26	138.1	25	2.73E-02	2.73E-02	1[i]	Range	FULL	Wistar	Harada et al., 1993
	Urea	–2.11	60.1	37	3.41E-04	3.41E-04	1	7.1[J]	SC[J]	CD(SD)BR	Barber et al., 1992
	Water	–1.38	18.0	30[J]	2.97E-03	2.97E-03	1	ND	SC[J]	CD(SD)BR[k]	Barber et al., 1992
	Water	–1.38	18.0	30	[1.40E-03]	1.40E-03	1	ND	EPID	Alpk:APfSD	Dick and Scott, 1992
	Water	–1.38	18.0	30	4.85E-04	4.85E-04	1	ND	FULL	Alpk/AP	Scott et al., 1991
	Water	–1.38	18.0	N/A	1.03E-03	1.03E-03	1	ND	FULL	N/A	Walker et al., 1983

[a] The compound investigated. Measurements indicated at left by E are excluded measurements. All positive (+) and negative (–) ionic charges (for the chemical at experimental conditions) are indicated. For example, paraquat with two positive charges is indicated by (+ +).
[b] Reported *log* K_{ow} are taken from the Hansch Starlist (Hansch et al., 1995) unless contained within brackets (e.g., for paraquat [–5.65]), in which case they were calculated using the Daylight program (PCModels, 1995).
[c] Permeability coefficients contained within brackets were digitized from figures in the publication.
[d] Fraction unionized determined from pK_a values calculated in SPARC (1995) at 25°C and adjusted to the experimental temperature as listed in Table A7.
[e] Reported solution pH. Compounds that are essentially undissociated are indicated by ND (not dissociated) when no pH was reported.
[f] Type of skin used in the study: isolated stratum corneum (SC), epidermal membranes (EPID), or full-thickness skin (FULL).
[g] The temperature was not reported. Solubilities of these compounds were determined at 37°C.
[h] The permeability coefficient of the unionized species was reported by Maitani et al. (1993).
[i] Permeability coefficient has been corrected for the fraction unionized for measurements made over a range of pH.
[J] Information obtained through personal communication from Barber (1996).
[k] In addition to this Sprague-Dawley strain [CD(SD)BR], Fisher 344 CDF(F-344)/CrlBR rats were used.
[L] Permeability coefficients for this chemical and a different copenetrating chemical were measured simultaneously (see discussion in Appendix B).

Table A4 Shed Snakeskin Permeability Coefficient Measurements

	Compound[a]	Log K_{ow}[b]	*MW*	T (°C)	$P_{cw,obs}$[c] (cm h^{-1})	P_{cw} (cm h^{-1})	f_{ul}[d]	pH[e]	Strain	Reference
	Acetanilide	0.45	135.2	32	9.77E-04	9.77E-04	1	7	Elaphe obsoleta	Takahashi et al., 1993
	Aminopyrine	1.00	231.3	32	1.18E-04	1.18E-04	1	7	Elaphe obsoleta	Takahashi et al., 1993
	Aniline	0.90	93.1	32	1.64E-02	1.64E-02	1	7	Elaphe obsoleta	Takahashi et al., 1993
	Antipyrine	0.38	188.2	32	1.10E-05	1.10E-05	1	7	Elaphe obsoleta	Takahashi et al., 1993
	Benzoic acid	1.87	122.1	37	2.43E-02	2.73E-02	0.89	3	Elaphe obsoleta	Itoh, Xia, et al., 1990
	Butylparaben	3.57	194.2	37	2.26E-02	2.26E-02	1	7.2	Elaphe obsoleta	Itoh, Xia, et al., 1990
	Clonidine	1.57	230.1	32	2.30E-04	2.30E-04	1[f]	4.6, 7	Elaphe obsoleta	Fleeker et al., 1989
	Corticosterone	1.94	346.5	25	1.02E-04	1.02E-04	1	7.2	Elaphe obsoleta	Itoh, Xia, et al., 1990
	Corticosterone	1.94	346.5	37	1.27E-04	1.27E-04	1	7.2	Elaphe obsoleta	Itoh, Magavi, et al., 1990
	m-Cresol	1.96	108.1	25	9.88E-03	9.88E-03	1	7.2	Elaphe obsoleta	Itoh, Xia, et al., 1990
	m-Cresol	1.96	108.1	37	1.85E-02	1.85E-02	1	3	Elaphe obsoleta	Itoh, Xia, et al., 1990
	Deoxycorticosterone	2.88	330.5	37	3.98E-03	3.98E-03	1	7.2	Elaphe obsoleta	Itoh, Magavi, et al., 1990
	Diazepam	2.99	284.8	32	3.07E-03	3.07E-03	1	7	Elaphe obsoleta	Takahashi et al., 1993
	Ethylparaben	2.47	166.2	37	4.97E-03	4.97E-03	1	7.2	Elaphe obsoleta	Itoh, Xia, et al., 1990
E	5-Fluorouracil (+ − + −)	−0.89	130.1	31	3.18E-04	Ion	<0.1	4.75[g]	Elaphe obsoleta	Rigg and Barry, 1990
E	5-Fluorouracil (+ − + −)	−0.89	130.1	31	4.59E-04	Ion	<0.1	4.75[g]	Elaphe obsoleta	Rigg and Barry, 1990
E	5-Fluorouracil (+ − + −)	−0.89	130.1	31	1.73E-04	Ion	<0.1	4.75[g]	Python Molurus	Rigg and Barry, 1990
E	5-Fluorouracil (+ − + −)	−0.89	130.1	31	7.30E-05	Ion	<0.1	4.75[g]	Python Molurus	Rigg and Barry, 1990
	Hydrocortisone	1.61	362.5	37	2.28E-05	2.28E-05	1	7.2	Elaphe obsoleta	Itoh, Magavi, et al., 1990
	p-Hydroxybenzoic acid	1.58	138.1	37	5.10E-04	5.54E-04	0.92	3	Elaphe obsoleta	Itoh, Xia, et al., 1990
	m-Hydroxybenzyl alcohol	0.49	124.1	37	3.37E-04	3.37E-04	1	3	Elaphe obsoleta	Itoh, Xia, et al., 1990
	m-Hydroxyphenylacetic acid	0.85	152.1	37	3.40E-04	3.54E-04	0.96	3	Elaphe obsoleta	Itoh, Xia, et al., 1990
E	11a-Hydroxyprogesterone	N/A[h]	330.0	25	2.80E-04	2.80E-04	1	7.2	Elaphe obsoleta	Itoh, Xia, et al., 1990
E	11a-Hydroxyprogesterone	N/A[h]	330.0	37	8.26E-04	8.26E-04	1	7.2	Elaphe obsoleta	Itoh, Magavi, et al., 1990
	Ibuprofen	3.50	206.3	37	8.81E-02	9.05E-02	0.97	3[i]	Elaphe obsoleta	Itoh, Magavi, et al., 1990
	Indomethacin	4.27	357.8	32	3.62E-03	3.62E-03	1[f]	2.9, 7	Elaphe obsoleta	Fleeker et al., 1989
	Ketoprofen	3.12	254.3	37	6.22E-03	6.46E-03	0.96	3	Elaphe obsoleta	Itoh, Magavi, et al., 1990
	Methylparaben	1.96	152.1	25	4.69E-03	4.69E-03	1	7.2	Elaphe obsoleta	Itoh, Xia, et al., 1990
	Methylparaben	1.96	152.1	37	3.82E-03	3.82E-03	1	7.2	Elaphe obsoleta	Itoh, Xia, et al., 1990
	Naproxen	3.34	230.3	37	1.48E-02	1.53E-02	0.97	3	Elaphe obsoleta	Itoh, Magavi, et al., 1990
	Phenol	1.46	94.1	25	5.23E-03	5.23E-03	1	7.2	Elaphe obsoleta	Itoh, Xia, et al., 1990
	Phenol	1.46	94.1	37	1.62E-02	1.62E-02	1	3	Elaphe obsoleta	Itoh, Xia, et al., 1990
	Propylparaben	3.04	180.2	37	8.75E-03	8.75E-03	1	7.2	Elaphe obsoleta	Itoh, Xia, et al., 1990

Salicylic acid	2.26	138.1	25	8.00E-03	8.00E-03	1[f]	Range	Python reticulatus	Harada et al., 1993
p-Toluidine	1.39	107.2	32	3.33E-02	3.33E-02	1	7	Elaphe obsoleta	Takahashi et al., 1993
Water	−1.38	18.0	31	1.26E-03	1.26E-03	1	ND	Elaphe obsoleta	Rigg and Barry, 1990
Water	−1.38	18.0	31	1.34E-03	1.34E-03	1	ND	Python molurus	Rigg and Barry, 1990

[a] The compound investigated. Measurements indicated at left by an E are excluded measurements. All positive (+) and negative (−) ionic charges (for the chemical at experimental conditions) are indicated. For example, 5-fluorouracil with two negative charges and two positive charges is indicated by (+ − + −).
[b] Reported log K_{ow} are taken from the Hansch Starlist (Hansch et al., 1995).
[c] Permeability coefficients contained within brackets were digitized from figures in the reference.
[d] Fraction unionized determined from pK_a values calculated in SPARC (1995) at 25°C and adjusted to the experimental temperature as listed in Table A7.
[e] Reported solution pH unless contained within brackets in which case the pH was calculated from the reported concentration and calculated pK_a values (see Table A7). Compounds that are essentially undissociated are indicated by ND (not dissociated) when no pH was reported.
[f] Unionized species permeability coefficient was determined from measurements covering a range of pH (i.e., fraction unionized).
[g] Information obtained through personal communication from Barry (1996).
[h] The log K_{ow} of 6.86 calculated using the Daylight program (PCModels, 1995) is not valid.
[i] The pH used in studying ibuprofen was not reported. We assumed a pH of 3.0, which is the same pH at which penetration of the other carboxylic acids (indomethacin, ketoprofen, naproxen) and the distribution coefficients were measured.

Table A5 Permeability Coefficient Measurements for Skin of Various Animals

	Compound[a]	Log K_{ow}[b]	*MW*	T (°C)	$P_{cw,obs}$[c] (cm h^{-1})	P_{cw} (cm h^{-1})	f_{ui}[d]	pH[e]	Skin[f]	Strain	Reference
	Acyclovir	[−2.31]	225.0	37	1.50E-04	1.56E-04	0.96	[9.8]	FULL	Guinea pig (Hartley)	Okamoto et al., 1991
P	Benzoic acid	1.87	122.1	N/A	4.66E-04	N/A	N/A	N/A	EPID	Pig (ear)	Bhatti et al., 1988
	Butyl paraben	3.57	194.2	37	2.26E-03	2.26E-03	1	ND	FULL	Guinea pig (Hartley)	Okamoto et al., 1991
E	DTMA[g] chloride (+)	N/A	263.8	N/A	2.40E-05	Ion	<0.1	7	FULL	Guinea pig	Scala et al., 1968
	Ethanol	−0.31	46.0	30	5.12E-04	5.12E-04	1	ND	FULL	Marmoset	Scott et al., 1991
	Ethanol	−0.31	46.0	33	2.66E-03	2.66E-03	1	ND	FULL	Rabbit	Treherne, 1956
	Ethyl iodide	2.00	156.0	33	5.50E-03	5.50E-03	1	ND	FULL	Rabbit	Treherne, 1956
E	5-Fluorouracil (+ − + −)	−0.89	130.1	37	4.80E-04	Ion	<0.1	[4.1]	FULL	Guinea pig (Hartley)	Okamoto et al., 1991
	Glucose	[−3.53]	180.2	33	5.34E-05	5.34E-05	1	ND	FULL	Rabbit	Treherne, 1956
	Glycerol	−1.76	92.1	33	2.35E-04	2.35E-04	1	ND	FULL	Rabbit	Treherne, 1956
	Mannitol	−3.10	182.2	N/A	1.99E-03	1.99E-03	1	ND	EPID	Pig (ear)	Bhatti et al., 1988
	Mannitol	−3.10	182.2	30	1.20E-04	1.20E-04	1	ND	FULL	Marmoset	Scott et al., 1991
E	6-Mercaptopurine (+ −)	0.01	152.2	37	2.32E-04	Ion	<0.1	[4.6]	FULL	Guinea pig (Hartley)	Okamoto et al., 1988
E	6-Mercaptopurine (+ −)	0.01	152.2	37	2.03E-04	Ion	<0.1	[4.6]	SC[h,i]	Guinea pig	Okamoto et al., 1989
E	6-Mercaptopurine (+ −)	0.01	152.2	37	2.50E-04	Ion	<0.1	[4.6]	FULL	Guinea pig (Hartley)	Okamoto et al., 1991
	Methanol	−0.77	32.0	33	2.50E-03	2.50E-03	1	ND	FULL	Rabbit	Treherne, 1956
	Nicorandil	[0.69]	211.2	37	5.08E-04	5.08E-04	1	[8.0]	FULL	Guinea pig (Hartley)	Sato et al., 1989
	Nicorandil	[0.69]	211.2	37	2.85E-04	2.85E-04	1	[8.0]	FULL	Pig (immature, LWD)	Sato et al., 1989
	Nicorandil	[0.69]	211.2	37	1.69E-04	1.69E-04	1	[8.0]	FULL	Dog	Sato et al., 1989
E	Nicotinic acid (−)	[0.77]	123.1	N/A	3.60E-04	Ion	<0.1	7	FULL	Guinea pig	Scala et al., 1968
E	Paraquat dichloride (+ +)	[−5.65]	257.3	30	1.01E-04	Ion	<0.1	ND	FULL	Marmoset	Scott et al., 1991
E	Paraquat dichloride (+ +)	[−5.65]	257.3	N/A	7.99E-04	Ion	<0.1	ND	FULL	Rabbit	Walker et al., 1983
E	Paraquat dichloride (+ +)	[−5.65]	257.3	N/A	1.96E-03	Ion	<0.1	ND	FULL	Guinea pig	Walker et al., 1983
E	Paraquat dichloride (+ +)	[−5.65]	257.3	N/A	3.53E-04	Ion	<0.1	ND	FULL	Nude rat	Walker et al., 1983
E	Paraquat dichloride (+ +)	[−5.65]	257.3	N/A	3.72E-04	Ion	<0.1	ND	FULL	Mouse	Walker et al., 1983
	Salicylic acid	2.26	138.1	25	1.16E-02	2.38E-02	0.49	3	FULL	Nude mouse	Harada et al., 1993
E	Sulfanilic acid (+ −)	[−0.94]	173.8	37	8.20E-04	Ion	<0.1	[3.4]	FULL	Guinea Pig (Hartley)	Okamoto et al., 1991
	Thiourea	−1.02	76.1	33	1.70E-04	1.70E-04	1	ND	FULL	Rabbit	Treherne, 1956
	Toluene	2.73	92.1	N/A	3.49E-03	3.49E-03	1	ND	EPID	Pig (ear)	Bhatti et al., 1988
E	TPBS[J] sodium salt) (−)	N/A	N/A	N/A	1.56E-04	Ion	<0.1	7	FULL	Guinea pig	Scala et al., 1968
	Urea	−2.11	60.1	33	1.40E-04	1.40E-04	1	ND	FULL	Rabbit	Treherne, 1956
	Water	−1.38	18.0	N/A	3.46E-03	3.46E-03	1	ND	EPID	Pig (ear)	Bhatti et al., 1988
	Water	−1.38	18.0	30	1.80E-03	1.80E-03	1	ND	FULL	Pig	Galey et al., 1976

Water	−1.38	18.0	30	8.12E-04	8.12E-04	1	ND	FULL	Marmoset	Scott et al., 1991
Water	−1.38	18.0	N/A	2.53E-03	2.53E-03	1	ND	FULL	Rabbit	Walker et al., 1983
Water	−1.38	18.0	N/A	4.42E-03	4.42E-03	1	ND	FULL	Guinea pig	Walker et al., 1983
Water	−1.38	18.0	N/A	1.52E-03	1.52E-03	1	ND	FULL	Nude rat	Walker et al., 1983
Water	−1.38	18.0	N/A	1.44E-03	1.44E-03	1	ND	FULL	Mouse	Walker et al., 1983

[a] The compound investigated. Measurements indicated at left by E are excluded measurements and those indicated by a P are provisional measurements. All positive (+) and negative (–) ionic charges (for the chemical at experimental conditions) are indicated. For example, 5-fluorouracil with two negative charges and two positive charges is indicated by (+ – + –).

[b] Reported log K_{ow} are taken from the Hansch Starlist (Hansch et al., 1995) unless contained within brackets (e.g., for nicorandil [0.69]), in which case they were calculated using the Daylight program (PCModels, 1995).

[c] Permeability coefficients contained within brackets were digitized from figures in the reference.

[d] Fraction unionized determined from pK_a values calculated in SPARC (1995) at 25°C and adjusted to the experimental temperature as listed in Table A7.

[e] Reported solution pH unless contained within brackets in which case the pH was calculated from the reported concentration and calculated pK_a values (see Table A7). Compounds that are essentially undissociated are indicated by ND (not dissociated) when no pH was reported.

[f] Type of skin used in the study: isolated stratum corneum (SC), epidermal membranes (EPID), or full-thickness skin (FULL).

[g] Dodecyltrimethylammonium.

[h] SC permeability coefficient is calculated from measurements with intact full-thickness and stripped full-thickness skin.

[i] Permeability coefficient obtained by combining an SC–water partition coefficient, SC diffusion coefficient, and SC thickness, which are consistent with measured penetration data.

[J] Sodium tetrapropylenebenzenesulfonate.

Table A6 Stratum Corneum–Water Partition Coefficients Determined for Skin from Various Animals

Compound[a]	Log K_{ow}[b]	*MW*	T (°C)[c]	K_{cw}[c]	Basis[d]	f_{ui}[e]	pH[f]	t_{equil}[g]	Species	Reference
Acetamidophenol	0.51	151.2	25	5.0	Dry mass	1	ND	24	RhMonkey	Surber et al., 1990
Acetamidophenol	0.51	151.2	25	4.5	Dry mass	1	ND	24	HLGuinea pig	Surber et al., 1990
Atenolol[h]	0.16	266.3	37	0.2	N/A	0.98	[10.9]	8	HLRat[i]	Kobayashi et al., 1994
Butanol	0.88	74.1	37	5.3	Excised mass[J]	1	ND	Overnight	HLMouse	Flynn et al., 1981
Cyclopropanoyl propranolol[k] (+)	[3.94]	327.0	37	0.6	Excised mass	<0.1	4	6	HLMouse	Ahmed et al., 1995
Ethanol	−0.31	46.0	37	4.5	Excised mass[J]	1	ND	Overnight	HLMouse	Flynn et al., 1981
Heptanol	2.72	116.0	37	24.1	Excised mass[J]	1	ND	Overnight	HLMouse	Flynn et al., 1981
Hexanol	2.03	102.2	37	14.0	Excised mass[J]	1	ND	Overnight	HLMouse	Flynn et al., 1981
Isovaleryl propranolol[k] (+)	[5.04]	343.3	37	1.5	Excised mass	<0.1	4	6	HLMouse	Ahmed et al., 1995
Lindane (C_w = 4 μg/ml)	[3.72][L]	291.0	37	160.0	Excised volume[m]	1	ND	18	Fisher rat	Jepson et al., 1994
Lindane (C_w = 8 μg/ml)	[3.72][L]	291.0	37	235.0	Excised volume[m]	1	ND	18	Fisher rat	Jepson et al., 1994
6-Mercaptopurine (+ −)	0.01	152.2	37	1.3	Wet mass	<0.1	[4.6]	24	Guinea pig	Okamoto et al., 1989
Morphine[h] (+)	0.76	285.3	37	0.0	N/A	<0.1	[4.9]	8	HLRat[i]	Kobayashi et al., 1994
Nicorandil	[0.65]	211.2	37	10.4	Dry mass	1	[7–8]	24	HLRat	Sato et al., 1989
Nicorandil	[0.65]	211.2	37	8.6	Dry mass	1	[7–8]	24	Guinea pig	Sato et al., 1989
Nicorandil	[0.65]	211.2	37	4.5	Dry mass	1	[7–8]	24	Dog	Sato et al., 1989
Nicorandil	[0.65]	211.2	37	7.9	Dry mass	1	[7–8]	24	Pig	Sato et al., 1989
Nifedipine[h]	[2.20]	346.3	37	3.9	N/A	1	ND	8	HLRat[i]	Kobayashi et al., 1994
p-Nitrophenol	1.91	139.1	25	12.4	Dry mass	1	4.2	>24	Pig	Williams et al., 1994
Nonanol	4.26	144.0	37	118.0	Excised mass[J]	1	ND	Overnight	HLMouse	Flynn et al., 1981
Octanol	3.00	130.2	37	68.5	Excised mass[J]	1	ND	Overnight	HLMouse	Flynn et al., 1981
Parathion (C_w = 3.5 μg/ml)	[3.83][L]	291.0	37	160.0	Excised volume[m]	1	ND	18	Fisher rat	Jepson et al., 1994
Parathion (C_w = 7 μg/ml)	[3.83][L]	291.0	37	180.0	Excised volume[m]	1	ND	18	Fisher rat	Jepson et al., 1994
Pentanol	1.56	88.0	37	5.1	Excised mass[J]	1	ND	Overnight	HLMouse	Flynn et al., 1981
Pentyloxyphenol	3.50	180.2	25	153.0	Dry mass	1	ND	24	RhMonkey	Surber et al., 1990
Pentyloxyphenol	3.50	180.2	25	140.0	Dry mass	1	ND	24	HLGuinea pig	Surber et al., 1990
Phenol	1.46	94.1	25	11.7	Dry mass	1	7.1	>24	Pig	Williams et al., 1994
Propanol	0.25	60.0	37	4.4	Excised mass[J]	1	ND	Overnight	HLMouse	Flynn et al., 1981
Propranolol[k] (+)	2.98	259.3	37	0.1	Excised mass	<0.1	4	6	HLMouse	Ahmed et al., 1995
Vinpocetine[h]	N/A[n]	350.5	37	9.5	N/A	N/A	>[7]	8	HLRat[i]	Kobayashi et al., 1994

[a] The compound investigated. All positive (+) and negative (–) ionic charges (for the chemical at experimental conditions) are indicated. For example, 6-mercaptopurine with one negative and one positive charge is indicated by (+ –).
[b] Reported log K_{ow} are taken from the Hansch Starlist (Hansch et al., 1995) unless contained within brackets (e.g., for nicorandil [0.69]), in which case they were calculated using the Daylight program (PCModels, 1995).
[c] Reported SC–water partition coefficients prior to any adjustment.
[d] Basis on which the unadjusted SC–water partition coefficient was reported. SC concentration expressed relative to a gram of dry SC (dry mass), a gram of hydrated SC (wet mass), or a unit volume or mass of freshly excised SC (excised volume or excised mass). See Vecchia (1997) or Vecchia and Bunge (2002a).
[e] Fraction unionized determined from pK_a values calculated in SPARC (1995) at 25°C and adjusted to the experimental temperature as listed in Table A7.
[f] Reported solution pH unless contained within brackets in which case the pH was calculated from the reported concentration and calculated pK_a values (see Table A7). Compounds that are essentially undissociated are indicated by ND (not dissociated) when no pH was reported.
[g] Time allowed for the absorbing chemical to equilibrate with the SC.
[h] Partition coefficients calculated as the ratio of concentrations in full-thickness skin and vehicle at the end of the penetration experiments.
[i] Full-thickness skin of WBN/ILA-HT hairless rats.
[J] SC–water partition coefficients have units of milliliters/(gram freshly excised epidermis).
[k] The average partition coefficient of two stereoisomers.
[L] This log K_{ow} is a calculated value taken from the U.S. Environmental Protection Agency interim report (1992) on dermal exposure assessment.
[m] Partition coefficients are relative to the skin volume. Freshly excised full-thickness skin weighing 0.3 mg was used in the partitioning experiment.
[n] The log K_{ow} of 4.72 calculated using the Daylight program (PCModels, 1995) is not valid (structural fragments of this molecule are not adequately represented by Daylight software).

Table A7 Temperature Effects on f_{ui} and Calculation of Unmeasured pH

Compound[a]	pK_a (25°C)[b]	T (°C)	ΔH (kcal mol^{-1})[c]	pK_a (T)[d]	C_w (mol L^{-1})[e]	pH[f]	f_{ui}[g]	Reference
Acyclovir	8.69	37	10	8.40	0.002	[9.8]	0.96	Okamoto et al., 1991
Atenolol	9.52	37	10	9.23	0.038	[10.9]	0.98	Kobayashi et al., 1994
Benzoic acid	3.91	37	0	3.91		3	0.89	Itoh, Xia, et al., 1990
Diclofenac	4.07	37	0	4.07		3	0.92	Maitani et al., 1993
Fentanyl	7.25	37	10	6.96		7.4	0.73	Roy et al., 1994
5-Fluorouracil (– +– → +– +–)	5.59	37	5	5.45	0.002	[4.1][h]	<0.1	Okamoto et al., 1991
5-Fluorouracil (– – → +– –)	11.95	37	5	11.81	0.002	[4.1][h]	<0.1	Okamoto et al., 1991
5-Fluorouracil (– – → – +–)	12.63	37	5	12.49	0.002	[4.1][h]	<0.1	Okamoto et al., 1991
Flurbiprofen	4.38	37	0	4.38		4.7	0.32	Hatanaka et al., 1990
p-Hydroxybenzoic acid	4.05	37	0	4.05		3	0.92	Itoh, Xia, et al., 1990
m-Hydroxyphenylacetic acid	4.41	37	0	4.41		3	0.96	Itoh, Xia, et al., 1990
Ibuprofen	4.55	37	0	4.55		4.44	0.58	Hatanaka et al., 1990
Ibuprofen	4.55	37	0	4.55		3	0.97	Itoh, Magavi, et al., 1990
Indomethacin	4.54	37	0	4.54		5.15	0.18	Hatanaka et al., 1990
Indomethacin	4.54	37	0	4.54		4.9	0.30	Okumura et al., 1989
Ketoprofen	4.41	37	0	4.41		3.72	0.79	Hatanaka et al., 1990
Ketoprofen	4.41	37	0	4.41		3	0.96	Itoh, Magavi, et al., 1990
6-Mercaptopurine (+– → –)	6.3	37	10	6.16	0.001	[4.6]	<0.1	Okamoto et al., 1988[i]
Morphine HCl (– → +–)	10.56	37	10	10.27	0.031	[4.9][J]	<0.1	Kobayashi et al., 1994
Morphine HCl (N → +)	9.40	37	10	9.11	0.031	[4.9][J]	<0.1	Kobayashi et al., 1994
Morphine HCl (N → –)	9.51	37	5	9.37	0.031	[4.9][J]	<0.1	Kobayashi et al., 1994
Naproxen	4.49	37	0	4.49		3	0.97	Itoh, Magavi, et al., 1990
Nicorandil	2.87	37	5	2.72	0.188[k]	[8.0]	1	Hatanaka et al., 1990[l]
Sufentanil	6.44	37	10	6.15		7.4	0.95	Roy et al., 1994
Sulfanilic acid (– → +–)	3.44	37	10	3.15	0.002	[3.4]	<0.1	Okamoto et al., 1991
Sulfanilic acid (N → +)	3.98	37	10	3.69	0.002	[3.4]	<0.1	Okamoto et al., 1991
Sulfanilic acid (N → –)	2.39	37	0[m]	2.39	0.002	[3.4]	<0.1	Okamoto et al., 1991
p-Toluidine	5.20	32	7.5	5.07		7	1	Takahashi et al., 1993
Vidarabine	5.91	37	5	5.77	N/A	>[7]	0.94	Kim et al., 1992
Vinpocetine	8.49	37	10	8.20	N/A	>[7]	N/A	Kobayashi et al., 1994

[a] The compound investigated. Cations are indicated with (+), anions with (–), and zwitterions with (+ –).
[b] pK_a values calculated in SPARC (1995) at 25°C using methods described in Vecchia (1997) or Vecchia and Bunge (2002b).
[c] These heats of ionization are approximate values obtained from Sober (1968). See also Vecchia (1997) or Vecchia and Bunge (2002b).
[d] Calculated using an integrated form of the van't Hoff equation [see Equation 3 in Vecchia and Bunge (2002b)].
[e] Solution concentration provided only when it was needed to calculate the pH.
[f] The pH was reported in the original article unless contained within brackets (e.g., for acyclovir [9.8]), in which case it was calculated from pK_a(T) and the solution concentration assuming that pH was 7.0 prior to chemical addition.
[g] The fraction unionized was calculated using Equation 15.8 when one pK_a was dominant. Otherwise, it was determined from a more rigorous solution of simultaneous equilibrium as described in Vecchia (1997) or Vecchia and Bunge (2002b).
[h] The pH of 5-fluorouracil was calculated assuming that the drug was added to solution in its net-neutral form.
[i] This result also applies to the investigations reported in Okamoto et al. (1989, 1991).
[J] Morphine hydrochloride (protonated morphine) was initially added to solution.
[k] The concentration of a saturated solution of nicorandil was reported by Morimoto et al. (1992).
[L] The calculated natural pH and fraction unionized were the same for Sato et al. (1989, 1991).
[m] This dissociation for sulfanilic acid was not adjusted for effects of temperature.

Appendix B: Documentation of Permeability Coefficient Data

This appendix contains specific information about the permeability coefficient data included in the database, arranged alphabetically by the last name of the first author of the investigation. Unless stated otherwise, conclusions about the ionization of chemicals are based on calculations made in SPARC (1995).

Ackermann and Flynn, 1987

Permeability coefficients were taken without alteration from Table 2 for full-thickness skin of the SKH-hr-1 hairless mouse (although the authors referred to this strain as a nude mouse). This article does not specify temperature, although other citations by the same authors indicated that the temperature was 37°C (Ackermann, 1983; Ackermann et al., 1985).

Ackermann et al., 1987

Permeability coefficients for hydrocortisone and 21-*n*-alkyl ethers of hydrocortisone were taken without alteration from Table 1. According to this article, these measurements were made on the SKH-hr-1 hairless mouse (although the authors referred to this strain as a nude mouse). As in Ackermann and Flynn (1987), the temperature was not specified. Nevertheless, it seems likely that the temperature was 37°C (Ackermann, 1983; Ackermann et al., 1985; Durrheim et al., 1980).

Aguiar and Weiner, 1969

The permeability coefficients of chloramphenicol at three temperatures were taken from Table II.

Ahmed et al., 1995

Permeability coefficients were taken directly from Table 4. The R- and S-stereoisomer permeability coefficients were averaged. These compounds were essentially all ionized.

Aspe et al., 1995

The permeability of cidofovir was taken as the average of three permeability coefficients, from a solution at pH 7.0, reported in Table 1.

Barber et al., 1992

The permeability coefficients of water and urea in rat were taken without modification from Table 1. Urea was more than 10% unionized in the vehicle. The exposure time was 8 h, which was sufficient for steady state to be obtained. We learned the following from personal communication with Barber (1996): (1) The temperature used in the water permeation studies was 30°C; (2) urea was delivered in a vehicle with pH 7.1; (3) the membrane was isolated SC; and (4) the authors are not aware of any inaccuracies in the document. The authors also listed permeability coefficient values for six other compounds that could be added to this database. These compounds are 2-ethoxypropionzte, diethylene glycol monobutyl ether, di(2-ethylhexyl) phthalate, 2-ethylhexanol, ethyl 3-ethoxypropioniate, and 2-propoxyethanol.

Behl et al., 1980

Behl et al. studied the effect of prolonged contact of hairless mouse skin with water on permeability coefficients. The authors showed that permeability coefficients increase after extended periods of hydration. Because other permeability coefficients in the database we have assembled were measured on previously unhydrated skins or skins that were hydrated for short periods, the permeability coefficients with the shortest hydration time (0.3 to 0.8 h) from Table I were selected for the validated database. Permeability coefficients were determined with either water or ethanol as a copenetrant. The concentrations were dilute (alcohol concentrations less than 10^{-4} *M*) and probably were not damaging. Six reported measurements were averaged for methanol, two for ethanol, and two for butanol, and permeability coefficients were reported singly for hexanol, heptanol, and octanol. Although this article did not specify the diffusion cell temperature, subsequent articles by the same authors describing similar data indicated that the temperature was 37°C (e.g., Behl and Barrett, 1981; Behl, El-Sayed, et al., 1983; Behl, Linn, et al., 1983). It seems likely that the temperature was also 37°C in the experiments described in this article.

Behl, El-Sayed, et al., 1983

The permeability coefficient for methanol was taken from Table 1. The average of permeability coefficients measured in skin without prior hydration from sets 1 and

2 were used (see discussion of hydration time in documentation of Behl et al., 1980). The average permeability coefficient, for zero hydration time, was taken from Table II for butanol and from Table III for hexanol. Permeability coefficients of butanol and hexanol were determined with methanol as a copenetrant, and the methanol permeability coefficient is the average of one permeability coefficient for which butanol was the copenetrant (set 1) and one for which hexanol was the copenetrant (set 2). The concentrations were dilute (alcohol concentrations less than 10^{-4} *M*) and probably were not damaging.

Behl, Linn, et al., 1983

The SC permeability coefficients of methanol and phenol were taken from Table IX. The abdominal skin and dorsal skin measurements were not statistically different and were averaged. Phenol and methanol were copenetrants. The concentrations were dilute (alcohol concentrations less than 10^{-4} *M*) and were probably below damaging concentrations.

Behl et al., 1984

The permeability of hydrocortisone was taken from Table I. The phase I, combined site (C) permeability coefficients for mice of aged 35, 516, and 657 days were averaged. (Permeability coefficient data for mice 5, 15, and 20 days old were larger and less certain and not added to the database.) The phase I permeability is the permeability coefficient observed for periods less than that required for hydration damage of skin (see discussion of hydration time in documentation of Behl et al., 1980).

Bhatti et al., 1988

The permeability coefficients through epidermal membranes were taken from Table I. The permeability coefficient for paraquat was not included in these databases because the membrane was reported to be damaged.

Bond and Barry, 1988a

The permeability coefficient of 5-fluorouracil was taken unaltered from Table I.

Bond and Barry, 1988b

Hexanol and water permeabilities were taken from text on page 488.

Dick and Scott, 1992

Permeability coefficient values for water, mannitol, and paraquat were digitized from Figure 4. The discrepancy in values shown in Figure 4 and Table 1 appear to be an error in the typesetting of Table 1. We were unsuccessful at contacting the authors,

so we included the values we thought were most likely correct. Water and mannitol were not ionized in the unbuffered vehicle. Paraquat (corresponding anion not specified) exists naturally as a divalent cation and was placed in the provisional database. Paraquat was likely applied as a dichloride salt because this was the form used by Scott et al. (1991). The exposure times were not specified, but it was likely that steady state was reached for these hydrophilic chemicals.

Durrheim et al., 1980

Permeabilities of methanol, ethanol, butanol, hexanol, heptanol, and octanol were taken from Table III at the temperatures 20, 25, and 37°C. In this article, the membrane is listed as the HRS/J strain of hairless mouse. However, the data at 37°C are also listed in Table 1 by Ackermann et al. (1987), which states that these measurements were conducted using the SKH-hr-1 hairless mouse.

Fleeker et al., 1989

The permeability coefficients of the unionized form of clonidine was taken from Table I, and the permeability coefficient of the unionized form of indomethacin was taken from Table IV.

Flynn et al., 1981

Permeability coefficients for normal alcohols (C_1 through C_{10}) were reported for full-thickness skin, heat-separated epidermis and dermis, and tape-stripped full-thickness skin. Data for methanol through hexanol were reported in Table IV as resistances through the SC calculated from the difference of resistances in the full-thickness skin and heat-separated dermis. Data for heptanol through decanol were taken from the values for heat-separated epidermis reported in Table 3.

Galey et al., 1976

The permeability of full-thickness pigskin to water was taken from Table II.

Ghosh et al., 1993

Permeability coefficients were taken without alteration from Table 1.

Harada et al., 1993

Salicylic acid permeability coefficients for all species were obtained from measurements reported in Table 1. Unionized permeability coefficients were calculated from reported flux values reported by dividing by a concentration of 500 $\mu g/mL^{-1}$ and then adjusting by the fraction unionized. We judged that the solution at pH 2.0 may be damaging to the SC and excluded this measurement. All other pH levels, for which the compound was less than 90% ionized as estimated from pK_a values

calculated by SPARC (i.e., 3.0, 3.5), were equally weighted in this average. For the hairless rat and the nude mouse, the pH 3.5 measurement was not reported, so the value was based only on measurements made at pH 3.0.

Hatanaka et al., 1990

All permeability coefficients were digitized from Figure 13. Measurements were made on intact full-thickness and stripped full-thickness skin. According to the authors, the effect of permeation resistance in the dermis was corrected by calculating the permeability coefficient of the SC from the permeation data of stripped skin. These same data also appeared in an article comparing these data with permeability coefficients measured in human skin (Morimoto et al., 1992).

Hayashi et al., 1992

The permeability coefficient for the unionized from of indomethacin was converted from the value given (in cm/sec) in Table I.

Huq et al., 1986

These authors calculated the SC permeability coefficient from the differences in resistances presented by whole skin and tape-stripped (no SC) skin. The permeability coefficients in the database were taken from the SC permeability values reported in Table 4. SC permeability values were not calculated for three chemicals (2-nitrophenol, 2,4-dimethylphenol, and 2,4,6-trichlorophenol) because the permeability coefficient from tape-stripped skin was not available. The permeability coefficient values for these three chemicals were taken from the whole skin values in Table 1.

Itoh, Xia, et al., 1990

Permeability coefficients for black rat snake were taken directly from Table II for ibuprofen, naproxen, ketoprofen, deoxycorticosterone, 11α-hydroxyprogesterone, corticosterone, and hydrocortisone. Permeability coefficients for indomethacin and progesterone were not included because they were not measured from aqueous solution. Permeability coefficients for the parabens were not included because they are identical to those reported by Itoh, Xia, et al. (1990).

Itoh, Magavi, et al., 1990

The permeability coefficients at 25°C of phenol, *m*-cresol, methylparaben, 11α-hydroxyprogesterone, and corticosterone were taken from Table II. The 37°C permeability coefficients of ethylparaben, propylparaben, butylparaben, phenol, benzoic acid, *p*-hydroxybenzoic acid, *m*-cresol, *m*-HBAl (*m*-hydroxybenzyl alcohol), and *m*-hydroxyphenyl acetic acid were taken from Table III. The 37°C permeability coefficient of methylparaben was not taken from Table III, but from Table VI (in which the values reported in Table III are averaged with several additional values).

Jepson et al., 1994

Skin–saline partition coefficients for parathion and lindane in Fisher rats are listed in Table 2. Whole skin from the back was used after the subcutaneous fat and muscle were removed using a razor blade. Tissue was equilibrated for 18 h in solutions, which were subsequently filtered and analyzed. Partitioning into the skin was determined by change in the solution concentration.

Jetzer et al., 1986

Permeation of 2,4-dinitrophenol and 4-nitrophenol, which was different from that reported by Huq et al. (1986), were taken from Table I. The value for 4-nitrophenol is the average value of permeability coefficients determined at two concentrations.

Jolicoeur et al., 1992

The permeability coefficient of etorphine was taken from Table I. Three measurements on hairless mouse skin were averaged.

Katayama et al., 1994

Permeability of mannitol, cortisone, and indomethacin (data at pH 3.0 were used) were taken directly from Table 1.

Kikkoji et al., 1991

Permeability coefficients for full-thickness skin were reported in Table II.

Kim et al., 1992

Permeability coefficients through whole skin are digitized from Figure 3. These data were originally reported in three other articles (references 3, 4, and 5 in the reference list of this article).

Kobayashi et al., 1994

Permeability coefficients presented in Table II (in cm/sec) from an aqueous vehicle were converted from centimeters/second to centimeters/hour.

Liu et al., 1994

A SC permeability coefficient for β-estradiol was reported in the text on page 1781. The permeability coefficient was originally reported in another article (reference 1 in this article).

Maitani et al., 1993

The permeability coefficient of diclofenac was taken from Table II, with unit conversion from centimeters/second to centimeters/hour. The 0% v/v ethanol value was selected.

Ogiso et al., 1994

The permeability coefficients for three high *MW* compounds were reported in Table 1: FITC dextrans FD-4 (*MW* = 4400), FD-10 (*MW* = 9600), and FD-70 (*MW* = 69,000).

Okamoto et al., 1988

The permeability coefficient of 6-mercaptopurine was taken directly from Table II. The control value (guinea pigskin without pretreatment) was selected.

Okamoto et al., 1989

In this article, partition coefficients between SC and vehicle and stripped skin and vehicle were directly determined. Then, the penetration profile of 6-mercaptopurine through the stripped skin was regressed to the solution of the one-membrane differential mass balance to determine the diffusion coefficient and thickness of the stripped skin. The diffusion coefficient and thickness of the SC were then determined by fitting the penetration profile of 6-mercaptopurine through intact (unstripped) skin to the solution of the two-membrane differential mass balance to which the previously determined parameters (partition coefficients, diffusion, and thickness for the stripped skin) were applied. They reported their results as the SC–water partition coefficient, an SC diffusion coefficient, and SC thickness. The permeability coefficient was then calculated from $D_c K_{cw}/L_c$.

Okamoto et al., 1991

The authors determined (D_c/ L_c^2) and ($K_{cw}L_c$) by analyzing the cumulative appearance of penetrating chemical in the receptor fluid using the complete solution of the one-membrane differential material balance equation. Permeability coefficients included in the database were calculated by multiplying the parameters reported in Table III (i.e., D_c/ L_c^2 times $K_{cw}L_c$). The measurements in this article are different from those reported in their other two articles (Okamoto et al., 1988, 1989).

Okumura et al., 1989

Permeability coefficients in this article are different from permeability coefficients in another related article (Hatanaka et al., 1990) because different hairless rat strains were used. The permeability coefficients for diclofenac sodium, dopamine hydrochloride, isoproterenol hydrochloride, indomethacin, and water were reported in the

text on page 1406 in centimeters/second. Permeability coefficients for disodium cromoglycate, diltiazem hydrochloride, and papaverine hydrochloride were digitized from Figure 3a and converted into centimeters/hour.

Rigg and Barry, 1990

Water and 5-fluorouracil permeability coefficients are reported for hairless mouse skin and the shed skin of two different snakes (*Python molurus*, *Elaphe obsoleta*). Water permeability coefficient values were determined by diffusion cell experiments lasting about 6 h. These investigators studied the effect of pretreatment of skin with water for 1 to 8 days, which did affect permeability coefficients in hairless mouse, although apparently not for snake skin. The water permeability coefficient in hairless mouse was taken from Table 1 for the 1-day pretreatment with water (the shortest pretreatment time studied). The water permeability coefficients for snake skin were calculated as the average of the permeability coefficients reported in Table 1 for water pretreatment times of 1 to 8 days. The permeability coefficient values for the dorsal and ventral skin from the *Python molurus* were reported separately and were different. The values for dorsal skin were arbitrarily chosen for the database. The normal saline and control permeability coefficients of 5-fluorouracil were taken, respectively, from Table 2 and Table 3 for all species. Again, the dorsal skin of *Python molurus* was used. These two 5-fluorouracil permeability coefficients were not averaged because the Table 2 (normal saline control) permeability coefficient was pretreated with saline for 12 h, and the Table 3 permeability coefficient (control) was not pretreated with water.

Roberts and Anderson, 1975

The permeability coefficient of phenol from a water vehicle was taken from Table 2 and converted to appropriate units.

Roy et al., 1994

The permeability of fentanyl, sufentanil, and morphine were taken directly from Table 1.

Ruland and Kreuter, 1991

The permeability coefficients of 20 amino acids at physiological pH (7.4) and at the pH of the isoelectric point were taken without alteration from Table 2. Based on pK_a values calculated by SPARC and the pH reported in this article, we calculated that the ionic condition of the amino acids was zwitterionic for all but four measurements. The exceptions were aspartic acid at pH 7.4 and glutamic acid at pH 7.4 (which were both net anionic) and lysine at pH 7.4 and arginine at pH 7.4 (which were both net positive).

Sato et al., 1989

Permeability coefficients for nicorandil in hairless rat, guinea pig, dog, and pigskin were taken directly from Table 1.

Sato et al., 1991

The permeability coefficient of nicorandil in hairless mouse given in Table 1 was not reported previously (Sato et al., 1989).

Scala et al., 1968

Permeability coefficients measured using whole skin were presented in Table II and converted to consistent units. The permeability coefficients are based on penetration over 10 to 15 h.

Scott et al., 1991

Permeability coefficients for rat skin were taken directly from Table I. Permeability coefficients for marmoset skin were calculated as the average for measurements made with abdomen, back, thigh, and thorax skin of the marmoset.

Surber et al., 1990

The mean values of $K_{cw,rep}$ (based on dry SC mass) for two chemicals (acetomidol and penyloxyphenol) were taken from Table 4, which compared results from human skin, rhesus monkey, and hairless guinea pig.

Takahashi et al., 1993

Permeability coefficients were taken directly from Table 1.

Tojo et al., 1987

The authors calculated SC permeability coefficients from the measurements on full-thickness skin and from stripped full-thickness skin (no SC) reported in Table II by assuming a bilaminate model.

Treherne, 1956

Permeability coefficients through whole skin were taken from Table II with conversion from centimeters/minute to centimeters/hour.

Walker et al., 1983

Permeability coefficients were taken without alteration from Table 1.

Wearley et al., 1990

Permeability coefficients for the amino acids alanine, glycine, leucine, and valine were calculated from the flux measurements reported in Table III divided by the concentration (10 m*M*).

Williams et al., 1994

Partition coefficients for *p*-nitrophenol and phenol in isolated pig SC are listed on page 70. There were no significant differences in partition coefficients determined in 24, 48, or 72 h.

Appendix C: Review of Prior Comparisons of Animal Skin Permeability Coefficient Data (in Chronological Order)

Marzulli et al., 1969

Marzulli and colleagues (unpublished results of Marzulli that are reviewed in Marzulli et al., 1969) reported that the back skin of weanling pigs most closely approximates human forearm skin regarding its resistance to penetration of several classified chemical warfare agents and agent stimulants. The forearm of the chimpanzee was less permeable than that of humans, whereas the back skins of monkey, dog, cat, horse, rabbit, goat, guinea pig, and mouse, in that order, were increasingly more permeable than the forearm skin of humans. The more permeable skins also showed a greater enhancement effect of vehicles and agent stimulants. The type of vehicle and other details of these, probably *in vitro*, experiments were not provided.

Bartek et al., 1972

Bartek and colleagues determined *in vivo* dermal absorption by analyzing chemical in the urine from rats, rabbits, miniature swine, and humans. Five chemicals were studied (haloprogin, *N*-acetylcysteine, cortisone, testosterone, caffeine, and butter yellow) by depositing the chemical on the skin using acetone, which then evaporated (Bartek et al., 1972). The skin permeability for the different animal species increased in the following order: human, pig, rat, and rabbit. The authors also referenced Tregear (Tregear, 1966) as determining that the skins of pig, guinea pig, rat, and rabbit were increasingly more permeable than human skin *in vitro* to organic solutes and ions. The Tregear results were not available for our analysis.

Chowhan and Pritchard, 1978

Chowhan and Pritchard (1978) studied the penetration of naproxen from oil-in-water cream vehicles through human, rat, and rabbit skins. If naproxen in the oil-in-water cream, which was adjusted to pH 7.5, ionizes the same as it would in aqueous solution, then essentially all of the naproxen would be ionized. Based on the *in vitro*

mean flux measured in the control experiments on naproxen, human skin was the least permeable (mean flux = 1.66 μg cm^{-2} h^{-1}), rat skin was more permeable (mean flux = 3.75 μg cm^{-2} h^{-1}), and excised rabbit skin was the most permeable (mean flux = 5.86 μg cm^{-2} h^{-1}). The lag time for naproxen penetrating through human skin was approximately 100 h; the lag time for naproxen penetrating through rat and rabbit skin was approximately 14 h. These lag times suggest, at least in the conventional interpretation, that species differences arise from differences in the skin thickness or the diffusion coefficient. Other data in this study suggested that the effect of surfactants on the penetration of compounds similar to naproxen can be quite different in human and animal skins.

Wester and Noonan, 1980

Wester and Noonan (1980) reviewed several *in vivo* and *in vitro* experimental investigations of the relationship of animal and human skin permeability coefficients. An analysis by Wester and Maibach (1986) is so similar to this study that it will is not discussed separately.

The authors reviewed several *in vivo* investigations of dermal absorption of acetone-deposited chemicals: (1) the Bartek and colleagues investigation already discussed (Bartek et al., 1972); (2) an experimentally similar investigation by Bartek and La Budde, 1976, which found that DDT, lindane, parathion, and malathion penetrated much more rapidly in rabbit than in pig or in squirrel monkey or humans (which were similar); (3) an investigation of the dermal absorption of hydrocortisone, testosterone, and benzoic acid that showed the rhesus monkey and humans have similar barriers to penetration for these compounds (Wester and Maibach, 1975a, 1975b, 1976, 1977); and (4) an investigation of the dermal absorption of neat hydrocortisone and benzoic acid that showed that guinea pig and human skin were similar and analogous measurements for testosterone that showed that guinea pig skin was more permeable than human skin (Andersen et al., 1980). The authors summarized these results with a recommendation that percutaneous absorption in the pig and monkey (rhesus or squirrel) is in most cases similar to humans, whereas in the rat and especially in the rabbit, skin penetration is greater than that observed in humans. The amount of absorption in the guinea pig was similar to humans for hydrocortisone and benzoic acid but higher for testosterone.

The authors also reviewed three *in vitro* rankings of skin permeability in different species, two of which we have already discussed: (1) experiments performed by Tregear (1966) provided the following ranking of permeability coefficient values: rabbit > rat > guinea pig > humans; (2) Marzulli and colleagues (1969) observed the following ranking of permeability coefficient values: mouse > guinea pig > goat > rabbit > horse > cat > dog > monkey > weanling pig > humans > chimpanzee; and (3) McGreesh (1965) observed the following ranking of permeability coefficient values: rabbit > rat > guinea pig > cat > goat > monkey > dog > pig. Also reviewed was the study of Campbell and others (1976), who found that human skin was less permeable than rat or rabbit to scopolamine, and the relative order of rat and rabbit skin permeability coefficient values depends both on skin location (back and side) and the method used to remove the hair. They concluded that, considering the

different compounds used in each study to rank the species and the differences in origin of the skin sample (back, forearm), the studies generally showed the skins of common laboratory animals (rat, rabbit, and guinea pig) are more permeable than the skin of humans. They also cited notable discrepancies to this trend. For example, the *in vitro* findings of Stoughton, who observed that human skin and hairless mouse skin have similar absorption for several compounds, disagreed with the large differences observed by other researchers (e.g., Marzulli et al., 1969).

Bronaugh et al., 1982

Bronaugh and colleagues (1982) compared the percutaneous absorption of three chemicals (benzoic acid, acetylsalicylic acid, and urea) through the skin of four animals (Hormel miniature pigs, Osborne-Mendel rats, NIH hairless mice, and Swiss mice) and human skin using an *in vitro* diffusion cell technique. The compounds were delivered in a petrolatum vehicle. They concluded that the animal model of choice depends on the compound. For benzoic acid and acetylsalicylic acid, permeability coefficients measured in pig and rat were similar to those in human skin; hairless mouse and mouse skins were much more permeable than human skin. These investigators recommended that slowly absorbed (hydrophilic) compounds such as urea should be investigated with animals that are not densely haired because the haired species (mouse and rat) absorbed urea more readily than either of the lesser haired species (pig, human, hairless mouse). They also compared several different studies that we discussed in this appendix (i.e., Andersen et al., 1980; Bartek et al., 1972; Chowhan and Pritchard, 1978; Stoughton, 1975; Tregear, 1966). Based on their comparison, which was also published in the U.S, Environmental Protection Agency's interim report on dermal absorption (1992), they observed that values for even the most permeable animal skins are often well within an order of magnitude of values for human skin. However, this data comparison combines observations with different experimental techniques, which might not be appropriate. The authors also presented results of measured skin layer thickness and hair follicle density in these different species.

Hawkins and Reifenrath, 1986

Hawkins and Reifenrath made *in vitro* percutaneous absorption measurements using neat compounds applied to skin and allowed to evaporate to air circulated over the applied dose. For studies on benzo(a)pyrene absorption without sodium azide (NaN_3), they found that mouse skin (6% of dose absorbed) was more permeable than human skin (1% of dose absorbed), which was more permeable than pig skin (0.6% of dose absorbed). In a similar study using 11 compounds [DDT, benzo(a)pyrene, fluocinonide acetonide, progesterone, lindane, testosterone, parathion, diisopropyl fluorophosphonate, malathion, benzoic acid, and caffeine], they found that there was no statistically significant difference between human and pig skin.

Sato et al., 1989

Sato and others (1989) investigated the *in vitro* permeability of nicorandil from saturated aqueous solution into several species and found that penetration rates had the following order: hairless rat > guinea pig > pig > dog. They calculated D/L^2 and KL, in each species by curve fitting the *in vitro* permeation data to a solution of the differential mass balance equation describing the drug permeation through a homogeneous membrane. From these results, the diffusion coefficient D and partition coefficient from the drug donor compartment to skin of the drug K were calculated using the measured thickness of the SC for L. The species differences in the diffusion coefficient for nicorandil were small. As a result, they concluded that K was the main factor for the species differences in the skin permeability. They also measured SC–water partition coefficients in a separate experiment. Although these experimentally determined partition coefficients differed from the values of K, there was a linear relationship between the two values.

Based on these observations, Sato and colleagues proposed one of the few quantitative methods for inferring human permeability coefficients from animal data. They recommend calculating cumulative penetration through human skin using estimates of K, D, and L for human SC. The SC thickness is measured for human SC. They recommended estimating D as the average of the D values determined with skin from the different animal species. In their scheme, four steps are required to estimate K for human SC. First, partition coefficients between skin and the vehicle are measured for the SC from various animals. Second, these experimental partition coefficient values are linearly regressed against values of K determined from skin permeation data for the same animal species. Third, the partition coefficient between human SC (they used callus) and the vehicle is measured. Last, this measured human partition coefficient value is used along with the regression equation developed in step 2 to obtain an estimated K for human SC. Because this procedure requires skin permeation and partition coefficient experiments for the skin from two or more animals and a partition coefficient measurement in human skin (although the authors substituted callus for a skin membrane), it is useful only when excised human skin is not available, but human callus and animal can be obtained. Many fewer experiments are needed if there is access to human skin.

Dick and Scott, 1992

Dick and Scott (1992) measured skin permeability of several lipophilic (aldrin, carbaryl, and fluaziflop-butyl) and hydrophilic (water, mannitol, and paraquat) compounds in pig ear skin, rat dorsal skin, and human abdominal skin. Although different concentrations and vehicles make a comparison of the compounds difficult, all the data can be used for interspecies comparison because the vehicle and penetrant concentration were the same for all species studied. There is a discrepancy between values shown in Figure 4 and Table 1 that appears to be an error in the typesetting of Table 1 (see discussion in Appendix B). The qualitative conclusion that pig ear skin and rat dorsal skin are both more permeable than human abdominal skin is not affected by this error.

U.S. Environmental Protection Agency, 1992

The panel of authors who wrote the interim report on dermal absorption (U.S. Environmental Protection Agency, 1992) reviewed several earlier experimental studies comparing permeability coefficients of human and animal skin, especially the review by Bronaugh et al. (1982), which was discussed separately in this appendix. No new data were presented in this report. The opinion of this panel was that the numerical differences between human skin and animal skin permeability coefficients vary with the test compound. Thus, they concluded that it was not possible to find a constant factor for adjusting the permeability coefficient from a specified animal to reliably represent the permeability coefficient for human skin. Major conclusions of this report were that animal skins are generally more permeable than human skin, and that dermal absorption data from animals could be used as a conservative estimate of absorption in humans.

Index

E

F

G

H

I

J

K

L

M

N

O

P

Q

R

S

T

V

W

X